AIC 2003

BANGKOK

"Color Communication and Management"

MIDTERM MEETING AIC
Grand Hyatt Erawan Hotel
4-6 August 2003
Bangkok Thailand

Proceedings

AIC 2003 Bangkok

Color Communication and Management

Grand Hyatt Erawan Hotel
Bangkok, Thailand
4-6 August 2003

Aran Hansuebsai

Editor

Organized by

Chulalongkorn University

The Color Group of Thailand

Supported by

The Federation of Thai Industries

Thai Airways International

Tourism Authority of Thailand

The papers appearing in this book compose the proceedings of the technical conference cited on the cover and title page of this volume. They reflect the authors' opinions and are published as presented, in the interests of timely dissemination. Their inclusion in this publication does not necessarily constitute endorsement by the editor. Papers were selected by the conference program committee to be presented in oral or poster format, and were subject to review by volume editors or program committees.

Please use the following format to cite material from this book:

Author(s), "Title of paper," in Proceedings of AIC 2003 Bangkok: Color Communication and Management, page numbers (2003).

ISBN 974-13-2516-9

Published by
The Color Group of Thailand (CGT)
58 Napasap 5, Sukhumvit 36, Klongton, Klongtoey, Bangkok 10110, Thailand
Tel: 66-2-2185588-9 Fax: 66-2-218-5583
http://www.colorgroupthai.com

Printed by DocuTech6135 and Docucolor6060

Thai Fuji Xerox Co., Ltd.
Bangkok, Thailand

THE DOCUMENT COMPANY

FUJI XEROX

FOREWORD

Thailand continues to be committed to steadily increase its participation in world cultural and scientific events and will be hosting and international meeting of the AIC in the year 2003. The theme, like all AIC meetings, is the constantly changing and increasingly complex problems involved with the management of color in all disciplines. Imaging technology has undergone dramatic changes over the past decade. Our goal is to prepare a number of basic and advanced instructive seminars that examine the impact of this evolution. Digital technology has had an enormous influence on color communication and continues to grow in importance. Virtually every area of color management will feel the dramatic effects of the digital world. Psychologists have been aware for years that color has profound effects of human emotions and indeed human wellbeing. More sophisticated tools are rapidly becoming available to help industrial designers and commercial artists of all types to utilize the multiple disciplines that include physiology, biology, chemistry and physics in the world of quantitative sciences while psychologists continue to refine their understanding of human emotional responses to color in all cultures. Constructive management of these challenges will determine not only how and what we teach and study but most importantly improve workflow and ultimately customer satisfaction. Not too many years ago, color was limited to carefully defined and relatively narrow areas in the world of printing and photography. Efforts to make color control a factor in other areas whether subjective or objective were dismissed as irrelevant. This is no longer true.

Thailand is endowed with a superlative background of natural resources which make the country and ideal venue for business and leisure visitors. There are interesting places to see and comfortable accommodations at reasonable prices. We are honored to host the AIC Midterm Meeting in Bangkok from August 4-6, 2003. It will be a unique and attractive opportunity for the color community to come together to explore present developments and future trends.

Professor Sakda Siripant,
Chairman of AIC 2003 Bangkok

President's Address

I will begin my address with a quote from Thomas Kinkade, "When I filter the sunshine in my life, I bask in the light of a transforming and inspiring reality." When I think of the AIC Midterm 2003 Bangkok Meeting on Color Communication and Management, I see all of our AIC color colleagues from around the world gathering in Thailand filtering the sunshine from around the world as we bask together in an inspiring forum to share the latest state-of-the-art color technology, communication and management concepts.

We are proud to have this meeting organized by The Color Group of Thailand, especially since they are very new members to our AIC family. Our former president, Professor Mitsuo Ikeda, brought The Color Group of Thailand into the AIC family during his 1998-2001 quadrennial term. Almost immediately after joining AIC, The Color Group of Thailand enthusiastically invited AIC to their country for a meeting in 2003. They chose a topic, Color Communication and Management, that is very relevant to the rapidly changing technology-filled world in which we live. My sincere thanks goes out to Chulalongkorn University and The Color Group of Thailand, with special thanks to the Local Organizing Committee, for planning this very high caliber meeting paying close attention to every last detail in order to insure perfection.

Again, a quote from Thomas Kinkade is appropriate. "To live a truly joyful, light-filled life, the filtering process must be internal as well as external." Our AIC Executive Committee colleague, Associate Professor Dr. Aran Hansuebsai, has brought together presentations from fellow Thai countrymen, our Asian AIC colleagues, as well as AIC color experts from around the world to give oral and poster presentations that will enrich our knowledge as we share this experience together in Bangkok, Thailand. The main topics of:

- Color Management
- Colorimetry and Color Vision
- Color Imaging
- Color Communication
- Color Environmental Design
- Color Emotion
- The Perception of the Elderly (as a symposium)

provide a unique backdrop for formal and informal interactions between color scientists, designers, engineers, artists, and psychologists. The exhibition displays allow participants to experience the most modern and up-to-date color equipment available.

It is our distinct honor to be experiencing this unique meeting in Bangkok, Thailand, one of the most exciting, beautiful and exotic cities in the world. The Color Group of Thailand is graciously sharing their culture with us by providing us excursion opportunities to see museums, temples, and shopping areas while riding one of the most advanced public transportation services in the world; the light rail system.

This AIC 2003 Midterm Bangkok Meeting would not have been possible without the support of The Federation of Thai Industries, The Federation of Thai Printing Industry, Thai Airways International and the Tourism Authority of Thailand. Many thanks for their support in the entire organization and planning process.

I will close my address with yet another quote from Thomas Kinkade. “Properly maintained filters will actually bring you closer in touch with the deepest form of reality.” After all of our AIC colleagues from around the world have come to experience the AIC 2003 Bangkok Midterm Meeting, they will have been touched with increased knowledge in the areas of color communication and management while meeting their AIC friends to enrich their personal relationships as they share in learning the customs and culture of our gracious hosts, The Color Group of Thailand.

With My Sincere Thanks for a Smashing Success at the AIC 2003 Midterm Bangkok Meeting,

Paula J. Alessi,
AIC President

AIC 2003 Organizing Committee

Chairman:	Professor Sakda Siripant
Vice Chairman:	Associate Professor Pontawee Pungrassamee
	Mr. Santi Songsermsawas
Technical Program:	Associate Professor Dr. Aran Hansuebsai
Exhibition:	Mr. Prasit Klongngooluerm
Publicity:	Mr. Trisorn Vorayankosol
Poster:	Dr.Suchitra Sueeprasarn
Social Program:	Dr. Pitchayada Katemake
	Ms. Soraphat Bunnak
	Lecturer Worawadee Chiangtong
Audio Visual:	Dr. Chawan Koopipat
Finance:	Mr. Prasat Veerakul
Publications:	Lecturer Dhamrongruchana Hoontrakool
Secretariat:	Associate Professor Dr. Aran Hansuebsai

Advisory Board

President of Chulalongkorn University
Vice president for Science and Technology Affair, Chulalongkorn University
Professor Dr. Mitsuo Ikeda
Dean of Faculty of Science, Chulalongkorn University
Head of Department of Imaging and Printing Technology, Chulalongkorn University
President of the Federation of Thai Printing Industry
Chairman of the Federation of Thai Industries (FTI)

International Advisory Committee

Professor Dr. Hirohisa Yaguchi	Chiba University, Japan
Professor Dr. Shoji Tominaga	Osaka Electro-Communication University, Japan
Professor Dr. Miyoshi Ayama	Utsunomiya University, Japan
Professor Dr. Mituo Kobayasi	The University of Electro-Communications, Japan
Professor Dr. Lee Jin-Sook	Chungnam National University, Korea
Professor Dr. Ronnier Luo	Derby University, UK
Dr. James Nobb	Leeds University, UK
Professor Dr. Javier Romero	University of Granada, Spain
Professor Lucia Ronchi	Institute of Optics, Florence, Italy
Professor Dr. John S. Werner	University of California, USA
Dr. Berit Bergstrom	Scandinavian Colour Institute AB., Sweden
Professor Dr. Jose' Luis Caivano	Buenos Aires University, Argentina
Dr. Leonhard Oberascher	Psychology of Architecture and Design, Austria

Schedule

Monday, August 4

8.15 am. **Opening Ceremony** ***(Grand Ballroom)***

Report Address by Chairman of AIC 2003 Bangkok Organizing Committee

Opening Remark by the President of Chulalongkorn University

Welcome Address by the President of AIC

8.30-9.00 am. **Open Session and Special Lecture**

Color in Thai Small Puppet Art : Epic Story of Ramayana

"Hanuman captures Nang Benjakai" Episode

by Mr. Teerawuth Kittisurin, Joe Louis Theater

9.00-10.30 am. **Session I : Color Management**

M.R. Luo, Colour & Imaging Institute, University of Derby, Session Chair

S. Bruees, Color management on the fly-embedding color control in printing devices **(Keynote Speaker)**

P. Juntarawatt, CxF – Color Exchange Format

Y.P. Tanaka, Fundamental theory of advanced CMS software, PD System Pro

M. Kobayasi and K. Yosiki, Mathematical distance between color values in NCS color space

11.00-12.00 am. **Session I (Continued)**

H. Yaguchi, Chiba University, Session Chair

A. Ohta and S. Tominaga, Color coordinate conversion using neural networks and its application

G. Minah, Blackness, whiteness, chromaticness: Formulas for high visibility in the modern city

Y.J. Kim, H.S. Kim and S.O. Park, A study on the designation of Munsell notation for Korean color names

12.00-1.00 pm. **Lunch**

1.00-2.30 pm. **Session II : Colorimetry and Color Vision**

V. Pogacar, University of Maribor, Slovenia, Session Chair

J.H. Xin, C.C. Lam and M.R. Luo, Investigation of texture effect on CRT color difference evaluation

H. Shinoda and M. Ikeda, Spectral luminous efficiency functions measured in real environments

T. Eda, M. Ayama, D. Kon, S. Kanaya and K. Mukai, Effect of white surface on achromatic perception in different visual environments

Y. Mizokami, J.S. Werner, M.A. Crognale and M.A. Webster, Unique hue and spectral bandwidth

A. Fujita, K. Ando, M. Arai, N. Kawabe and R.D. Saxena, The optical characteristic of luminescence pavement material

2.30-4.00 pm. **Poster Presentation**

4.00-5.30 pm. **Session II (Continued)**

S. Tominaga, Osaka Electro-Communication University, Session Chair

S. Sueeprasan and M.R. Luo, Colorimetric tolerances for D50 simulators

M. Arai, X. Liu and A. Fujita, The usage of luminescent particle for measuring the particle settling velocity in hydraulic laboratory

K. Suzuki and G. Baba, Geometric conditions for reflectance factor measurement

R. Yamauchi, H. Shinoda and M. Ikeda, Importance of enclosing a space by walls for constructing the recognized visual space of illumination

P. Cunthasaksiri, H. Shinoda and M. Ikeda, Space recognition: New account for simultaneous color contrast on a center-surround configuration

7.00-9.30 pm. **Welcome Dinner Banquet** ***(Grand Ballroom)***

Tuesday, August 5

8.00-9.00 am. **AIC General Assembly** ***(Rajdamri Room)***

9.00-10.30 am. **Session III : Color Imaging** ***(Grand Ballroom)***

H. Shinoda, Ritsumeikan University, Session Chair

M.R. Luo, Development of colour appearance models **(Keynote Speaker)**

A.N. Chalmers and S. Soltic, Colour image quality assessment using the CIECAM97s model

C. Li, G.H. Cui and M.R. Luo, The accuracy of polynomial models for characterising digital cameras

J. Duan, G. Hong, J. Morovic and P.L. Sun, Calculating image difference: A study based on the use of gamut mapped images

11.00-12.00 am. **Session III (Continued)**

P. Green-Armytage, Curtin University of Technology, Session Chair

B. Han, G.H. Cui and M.R. Luo, Texture effect on evaluation of colour difference

M.C. Lo, Y.L. Chen, P.L. Sun and Y.H. Chiang, The color rendering between a color proofer and a printing press

L. Yang, M. Akimoto and M. Miyakawa, Development of an imaging colorimeter for skin color measurement and its clinical application

T. Suzuki and M. Kobayasi, Measurement of gonio-spectral reflectance of a figured satin ---An examination of the color recording method for Japanese KIMONO (1) ---

12.00-1.00 pm. **Lunch**

1.00-2.30 pm. **Session IV : Color Communication**

J.L. Caivano, University of Buenos Aires, Session Chair

H.J. Suk, H. Irtel, K.J. Lee and Y.J. Kim, Color namings as brand identity

H. Ohno and S. Shibano, Interior and exterior colors used by one home building company in new houses in the Kyoto and Osaka region

C. Udagawa, Research on appearance rate of "Trendy colors" and "Regularly-used colors"

S. Iijima and T. Inagaki, The relation between stone color and streetscape color on various blocks in a city-A case study at Ghent in Flanders, Belgium

K. Maki, Color composition features of magazine advertisements

2.30-4.00 pm. **Poster Presentation**

4.00-5.45 pm. **Session IV (Continued)**

M. Billger, Chalmers University of Technology, Session Chair

C.M. Burton, An AIC international color research survey for divers disciplines

M. Kobayasi, T. Yamaguchi and Y. Ogawa, An analysis of color features of Japanese traditional robes "Kimono" in Edo-era

J.S. Lee and M.J. Lee, Making exterior color line of residential area through sensibility evaluation method

B. Bergstrom, How to teach colour and encourage colour communication

V. Pogacar and V. Golob, Application of geometrical system for harmonious color selection

O. Da Pos, S.S. Bergstrom and C. Cernuschi, Desaturation of the perceived illumination in the ambegujas display

7.00-8.30 pm. **Special Thai Dinner at Koopkam Restaurant** ***(Siam Square)*** **hosted by Network Consulting Group**

Wednesday, August 6

8.00-9.30 am. **Session V : Color Environmental Design** ***(Grand Ballroom)***

L. Oberascher, Psychology of Architecture and Design, Session Chair

L. Luzzatto and R. Pompas, Artificial environment, cyber space and new colours projects

M. Billger, Experience of light, colour and space in reality compared to visual reality

T. Inagaki and S. Iijima, A study on evaluation of the interior atmospheres and the choice of behavior with effects of lighting, color and gloss

K. Sakahara, A color image in a shopping street: The case of "Tanuki-Koji" in Sapporo

J.L. Caivano and M.A. Lopez, The Rhethoric of Black, White and Red: Reasonability and aesthetics to persuade with color

9.30-10.15 am. Special Lecture by Judd Awardee ***(Grand Ballroom)***

10.30-12.30 am. Session VI : Color Emotion ***(Grand Ballroom)***

J.H. Xin, The Hong Kong Polytechnic University, Session Chair

T. Sato, J.H. Xin, J. Nobbs and A. Hansuebsai, Numerical expression of colour emotion and its application **(Keynote Speaker)**

L. Oberascher and M. Gallmetzer, Colour and emotion

I. Satake, A. Hansuebsai, J.H. Xin, T. Tianming, T. Sato, K. Ando, K. Kuwano and K. Kajiwara, Sensory words for describing automotive exterior colors in Japan, Hongkong, China and Thailand

L.C. Ou and M.R. Luo, Factors affecting colour harmony for two-colour combinations

W.Y. Lee and M.R. Luo, A study on the image of colour-shape combinations

H.S. Lee-Niinioja, Goethe in me (Goethe's esthetic and visual impact on my emotional art)

10.30-12.30 am. Study Group Symposium : Color Perception of the Elderly ***(Ploenchit Room)***

K. Okajima, Tokyo Institute of Technology, Session Chair

J.S. Werner, P. Delahunt, L. Ma and M.A. Webster, Renormalization of color mechanisms across the life span **(Keynote Speaker)**

K. Okajima, Color perception of the elderly: Basic researches and applications

M. Ikeda, T. Obama, A. Kusumi and H. Shinoda, Color appearance of color charts observed with a cataract experiencing goggle

A. Kusumi, M. Ikeda and H. Shinoda, Duality of color perception with colored eyeglasses for different color appearance modes

K. Shinomori, Age-related changes in temporal characteristics of achromatic and chromatic channels

K. Sagawa, Age-related luminanceand span of categorical colours for designing visual signs for older people

M. Ayama, K. Narisada and N. Suda, Change of color appearance of elderly observer through human lens and intraocular lens

1.30-5.00 pm. Excursion

Type A : Emerald Buddha Temple and Grand Palace

Type B : City Tour

6.00-10.00 pm. AIC EC Meeting ***(Business Center)***

List of Poster Presentation

Color Management

P1 **Test of the additivity of a color impression from colored texture pattern**
S. Sunaga and Y. Yamashita, Kyushu Institute of Design (Japan)

P2 **RGB color data compensation for illumination change**
P. Rattanasakornchai and Y. Hoshino, Nippon Institute of Technology (Japan)

P3 **Spectral based color reproduction compatible with standard system for mixed illumination conditions**
K. Cherdhirunkorn, N. Tsumura and Y. Miyake, Chiba University (Japan)

P4 **Selection of the optimum offset ink set for colour digital image reproduction by gamut matching**
P. Sukkaew, P. Katemake, Chulalongkorn University (Thailand)
and M. Pozzi, Sirindhorn International Institute of Technology (Thailand)

P5 **Simulating the colour gamut of ink-jet ink systems on coated and uncoated substrates**
N. Kasadesinchai, P. Katemake, Chulalongkorn University (Thailand)
and H. Noguchi, Canon Inc. (Japan)

Colorimetry and Color Vision

P6 **Effects of three dimensional stimulus configuration on simultaneous color contrast**
S. Nakamura, Nihon Fukushi University (Japan)

P7 **The physiological and psychological effects of color in the interior space**
H. Sakai, A. Enami, T. Shimonaka, K. Yamashita and M. Sato,
Osaka City University (Japan)

P8 **Cognitive aspects of color vision in natural scenes**
L.R. Ronchi, S. Villani and M. Abbozzo, Associazione Ottica Italiana (Italy)

P9 **The manner of viewing in lightness contrast - assimilation**
M. Takashima, Nihon University (Japan)

P10 **Colorimetry: Colorfastness to light and changes in fluorescence of paper and textiles**
H.H. Epps, The University of Georgia (USA)

P11 **Recognition of the space illumination as the main determinant of the border of the color mode change**
Y. Thiangthangtum, M. Ikeda and H. Shinoda, Ritsumaikan University (Japan)

Color Imaging

Color Communication

Table of Contents

Poster Papers

Colorimetry and Color Vision

Oral Papers

Poster Papers

Color Imaging

Oral Papers

Poster Papers

Color Communication

Oral Papers

Poster Papers

Color Environmental Design

Oral Papers

Poster Papers

Color Emotion

Oral Papers

Poster Papers

Study Group Symposium : Color Perception of the Elderly

Oral Papers

Poster Paper

Citation for 2003 Deane B. Judd – AIC Award

Miyoshi Ayama
Information and Control Systems Science
Graduate School of Engineering
Utsunomiya University

The Judd AIC Award is one of the most honorable awards in the fields of color vision, color science, and color technology. This award was created in 1975 to honor the memory of Deane B.Judd. Every two years since, the AIC has carried out a laborious process of selection of the recipients for this award.

It is with great pleasure that I announce Prof. Mitsuo Ikeda as the recipient of the 2003 Judd Award, at this AIC Meeting in Bangkok, Thailand. Among the great accomplishments Prof. Mitsuo Ikeda has made throughout his career, his dedicated educational and research contribution to the field of vision and color psychophysics should be addressed first.

In 1971, nearly a decade after he got his Ph.D. from the University of Rochester, New York, he moved to the Department of Information Processing, Tokyo Institute of Technology, TIT, Japan, to become an associate professor and start his educational career. In 1976 he became a professor in his early forties. Before him, there were no professors in Japan who specialized in visual psychophysics on the basis of a science and engineering point of view. He needed colleagues, and thus he brought up his students zealously to let them become mature scientists. Many students were encouraged by Prof. Ikeda to choose visual psychophysics as their career work, and they responded to his tough education. During the TIT period, more than twenty of his students won their degree in Dr. of Engineering. He has collaborated with all of his students to publish invaluable papers on visual psychophysics.

In the early to middle part of the TIT period, his interest was on eye movements for pattern recognition, functional visual field, color vision, and photometry. One of his landmark works then was the publication of a technical report of CIE for spectral sensitivity functions for brightness. In the last part of the TIT period, he became interested in color appearance mode, which led to further investigations on Recognized Visual Space of Illumination in which he is still carrying out research.

In 1990, Prof. Mitsuo Ikeda was invited to become a professor at the School of Architecture, Kyoto University. There he introduced a new concept of Recognized Visual Space of Illumination, RVSI to explain various phenomena related to color appearance in visual environments, blowing a new wind to people in the field of architecture.

In 1996, he became a professor of the Department of Photonics at Ritsumeikan University. There he developed the concept of RVSI extensively through many interesting experiments including the field studies of illumination using a living room in his house.

During the Kyoto University and Ritsumeikan University periods, about ten students got their doctorates, and some of those students, including two from Thailand, are continuing to study in the doctorate course at Ritsumeikan University.

Prof. Ikeda published five books, all in Japanese. One is “Visual psychophysics” which is an excellent textbook and is unique in a sense that the readers can follow the way Prof. Ikeda learned visual psychophysics from previous studies. It has been well read not only by many experts on psychophysics but also by professors and/or engineers of other fields, as well as students. Two books are purely on color; “Fundamentals of color engineering” and “Science of color and color vision”. These books played an important role to advance education and research on color science and color vision in Japan. The other two books are written with his wife, an ophthalmologist, Dr. Fusako Ikeda.

It is often said that a good researcher is not necessarily a good educator at the same time, but Prof. Mitsuo Ikeda is an exception to the rule. Splendid research ideas always came to his mind and then he constructed ingenious and precise apparatuses to realize the ideas with his students. He taught them psychophysical procedures in a bottle-fed manner doing the experimental sessions together. He always stimulated, encouraged and inspired students, who came to have a strong interest and pleasure in studying human sensory and cognitive processes. Now all of his former students are very active in related fields in Japan, and many of them are also active internationally, especially in the AIC.

Another fact worth noting here is his dedicated contribution to the AIC activities especially to an expansion of the AIC in Asian countries.

He was the chairman of the steering committee of the 8th AIC Congress held in Kyoto in 1997 and led the congress to a great success. He served as the Vice-President of AIC from 1993 to 1997 to help Prof. Ronchi, the AIC President. He became the President in 1998 and completed his term at the end of 2001. He took it as his mission to evangelize about AIC in Asian countries as the president coming from Asia.

By that time, his mission in Japan was already accomplished. The Japanese organization of the AIC is the Color Science Association of Japan, CSAJ. Prof. Ikeda served as a board member of the CSAJ many times and contributed a great deal to the development and evolution of the association. There have been many papers presented by Prof. Ikeda's former students and their students, i.e. Ikeda's grand children, in every annual meeting of CSAJ. Some of his former students play important roles in the CSAJ. On the present board of CSAJ, there are four members coming from his school beside Prof. Ikeda himself.

During his vice presidency and presidency of the AIC, he often visited Korea and encouraged colleagues in that country to join the AIC as members. He succeeded, and Korea sponsored the AIC Interim Meeting of 2000 in Seoul. It was a fruitful and precious conference. He then started to visit Thailand and encouraged their people to organize a national committee of color. They organized the Color Group of Thailand and joined the AIC. The group is now organizing the AIC Midterm Meeting in Bangkok where Prof. Ikeda will receive the gold medal.

Prof. Ikeda published about two hundreds of scientific papers. The following list is only a selection of his papers related to color.

1) M. Ikeda; Study of interrelations between mechanisms at threshold. J. Opt. Soc. Am. 53, 1305-1313 (1963).
2) M. Ikeda; Further use of the summation index for the study of color vision. J. Opt. Soc. Am. 54, 89-94 (1964).
3) R. M. Boynton, M. Ikeda and E. S. Stiles; Interactions among chromatic mechanisms as inferred from positive and negative increment thresholds. Vis. Res. 4, 87-117 (1964).
4) M. Ikeda and M. Urakubo; Flicker HTRF as test of color vision. J. Opt. Soc. Am. 58, 27-31 (1968).
5) M. Ikeda and T. Uetsuki; Interrelations among Stiles □ mechanisms. J. Opt. Soc. Am. 60, 406-415 (1970).
6) M. Ikeda and H. Shimozono; Luminous efficiency functions determined by successive brightness matching. J. Opt. Soc. Am. 68, 1767-1771 (1978).
7) M. Ikeda and H. Uchikawa; Functional visual fields for detecting a colored target. Acta Chromatica, 3, 141-146 (1979).
8) M. Ikeda and M. Ayama; Additivity of opponent chromatic valence. Vis. Res. 20, 995-999 (1980).
9) H. Yaguchi and M. Ikeda; Luminous efficiency functions by heterochromatic brightness matching for a wide range of retinal illuminance. J. Light & Vis. Evn. 4, 14-17 (1980).
10) M. Ikeda and Y. Nakashima; Wavelength difference limit for binocular color vision. Vis. Res. 20, 693-697 (1980).
11) M. Ikeda and H. Shimozono; Mesopic luminous efficiency functions. J. Opt. Soc. Am. 71, 280-284 (1981).
12) M. Ayama and M. Ikeda; Chromatic valence curves; Alternative interpretation derived by the direct matching method. Science 215, 1538-1539 (1982).
13) H. Yaguchi and M. Ikeda; Nonlinear nature of the opponent-color channels. Col. Res. & Appl. 7, 187-190 (1982).
14) M. Ikeda, M. Ayama and M. Ohmi; Additivity failure of chromatic valence in the opponent-color theory. Col. Res. & Appl. 7, 197-200 (1982).
15) M. Ikeda and H. Yaguchi; Brightness luminous efficiency functions for 2 and 10 degrees fields. J. Opt. Soc. Am. 72, 1660-1665 (1982).
16) H. Yaguchi and M. Ikeda; Subadditivity and supraadditivity in heterochromatic brightness matching. Vis. Res. 23, 1711-1718 (1983).
17) H. Yaguchi and M. Ikeda; Mesopic luminous-efficiency functions for various adapting levels. J. Opt. Soc. Am. A. 1, 120-123 (1984).
18) H. Yaguchi and M. Ikeda; A phtometric sysytem for brightness perception. Kogaku (Optics)13, 140-145 (1984) (in Japanese).
19) K. Uchikawa and M. Ikeda; Wavelength discrimination with a chromatically alternating stimulus. Col. Res. & Appl. 10, 204-209 (1985).
20) M. Ayama and M. Ikeda; Additivity of yellow chromatic valence. Vis. Res. 26, 763-769 (1986).
21) Y. Nakano and M. Ikeda; Visual model for brightness perception at mesopic level. Kogaku (Optics) 15, 296-302 (1986) (in Japanese).
22) M. Ikeda and Y. Nakano; Spectral luminous efficiency functions obtained by direct heterochromatic brightness matching for point sources and for 2 and 10 degrees fields. J. Opt. Soc. Am. A. 3, 2105-2108 (1986).
23) Y. Nakano, M. Ikeda and P. K. Kaiser; Contributions of opponent mechanisms to brightness and nonlinear models. Vis. Res. 28, 799-810 (1988).
24) K. Okajima, M. Ayama, K. Uchikawa and M. Ikeda; Comparison of luminous efficiency for brightness in a light source color mode and asurface color mode. Kogaku (Optics) 17, 582-592 (1988) (in Japanese).
25) S. Ashizawa and M. Ikeda; Change of color conspicuity for various illuminance levels: Derivation of empirical formula. J. Illum. Engng. Inst. Jan. 72, 79-84 (1988).
26) M. Ikeda and I. Uehira; Unique hue loci and implications. Col. Res. & Appl. 14, 318-324 (1989).
27) M. Ikeda, C. C. Huang and S. Ashizawa; Equivalent lightness of colored objects at illuminances from the scotopic to the photopic level. Col. Res. & Appl. 14, 198-206 (1989).

28) M. Ayama and M. Ikeda; Dependence of the chromatic valence function on chromatic standards. Vis. Res. 29, 1233-1244 (1989).
29) T. Tamura and M. Ikeda; Relation between blue cone response and brightness. Kogaku (Optics) 18, 572-576 (1989) (in Japanese).
30) K. Okajima and M. Ikeda; Relation of corresponding color in a surface color mode and a luminous color mode. Kogaku (Optics) 20, 363-368 (1991) (in Japanese).
31) M. Ikeda and S. Ashizawa; Equivalent lightness of colored objects of equal Munsell Chroma and of equal Munsell Value at various illuminances. Col. Res. & Appl. 16, 72-80 (1991).
32) M. Ayama and M. Ikeda; Hue and saturation of colored lights in the whole area of the u'v' charomaticity diagram. J. of Col. Sci. Assoc. Jpn. 18, 186-199 (1994) (in Japanese).
33) M. Ikeda, K. Motonaga, N. Matsuzawa and T. Ishida; Threshold determination for unnatural color appearance with l ocal illumination. Kogaku (Optics) 22, 289-298 (1993) (in Japanese).
34) N. Matsuzawa, M. Ikeda and T. Ishida; Temporal properties of changing color appearance mode studied by changing stimulus onset asynchrony between a test and surrounding stimuli. Kogaku (Optics) 22, 512-517 (1993) (in Japanese).
35) M. Ikeda and S. Ashizawa; Color conspicuity at different retinal positions. J. of Col. Sci. Assoc. Jpn. 16, 140-147 (1993) (in Japanese).
36) M. Ikeda, S. Fukumura, N. Matsuzawa and T. Ishida; Influence of surrounding visual informations on the recognition threshold of local illumination. Kogaku (Optics) 23, 42-49 (1994) (in Japanese)
37) M. Ikeda, S. Ashizawa and H. Kobayashi; Hue coefficient of equivalent lightness formulas. J. Illum. Engng. Inst. Jpn. 78, 511-515 (1994) (in Japanese).
38) H. Shinoda and M. Ikeda; Color matching repeatability as a function of time interval in successive presentation. J. Illum. Engng. Inst. Jpn. 78, 560-567 (1994) (in Japanese).
39) T. Ishida, T. Shimizu and M. Ikeda; Identification of surface colors at various illuminances. J. of Col. Sci. Assoc. Jpn. 19, 121-129 (1995) (in Japanese).
40) H. Yoon and M. Ikeda; Interaction between two recognized visual space of illumination as a function of illuminance of the observer's room. J. Illum, Engng. Inst. Jpn. 80, 69-75 (1996) (in Japanese).
41) M. Ikeda and F. Kaneko; Effect of initial visual information on the recognized visual space of illumination - The case of lightness and saturation. J. Illum. Engng. Inst. Jpn. 80, 319-323 (1996) (in Japanese).
42) H. Yoon, M. Ikeda and H. Shinoda; Tolerable range of illuminance of a room to yield continuity perception to outside in presence of color temperature difference in the two spaces. J. Illum. Engng. Inst. Jpn. 81, 621-627 (1997) (in Japanese).
43) H. Yoon, M. Ikeda and T. Ishida; Tolerable range of illuminance and color of illumination for providing a sense of continuity between two rooms. J. Illum. Engng. Inst. Jpn. 82, 523-529 (1998) (in Japanese).
44) M. Ayama and M. Ikeda; Brightness-to-luminance ratio of colored light in the entire chromaticity diagram. Col. Res. & Appl. 23, 274-287 (1998).
45) H. Shinoda, M. Ikeda and M. Niimoto; J. Illum. Engng. Inst. Jpn. 81, 695-699 (1997) (in Japanese).
46) Y. Mizokami, M. Ikeda and H. Shinoda; Apparent lightness influenced by the size of the recognized visual space of illumination. J. Illum. Engng. Inst. Jpn. 82, 91-96 (1998) (in Japanese).
47) M. Ikeda, H. Shinoda and Y. Mizokami; Three dimensionality of the recognized visual space of illumination proved by hidden illumination. Opt. Rev. 5, 200-205 (1998).
48) Y. Mizokami, M. Ikeda and H. Shinoda; Lightness change as perceived in relation to the size of recognized visual space of illumination. Opt. Rev. 5, 315-319 (1998).
49) M. Ikeda, H. Shinoda and Y. Mizokami; Phenomena of apparent lightness interpreted by the recognized visual space of illumination. Opt. Rev. 5, 2380-386 (1998).
50) Y. Mizokami, M. Ikeda and H. Shinoda; Color property of the recognized visual space of illumination controlled by interior color as the initial visual information. Opt. Rev. 7, 358-363 (2000).
51) M. Ikeda, A. Kusumi and H. Shinoda; Color appearance seen through a colored filter of various sizes. Opt. Rev. 8, 480-486 (2001).
52) M. Ikeda, Y. Mizokami, S. Nakane and H. Shinoda; Color appearance of a patch explained by RVSI for the conditions of various colors of room illumination and of various luminance levels of the patch. Opt. Rev. 9, 132-139 (2002).

(Selection of paper is laboriously prepared by Prof. T.Ishida)

Color appearance explained, predicted and confirmed by the concept of recognized visual space of illumination, RVSI.

Mitsuo Ikeda

Ritsumeikan University

1. INTRODUCTION

To understand how the 3D space is illuminated in front of us is one of the most important actions of our brain when we open our eyes because we live and have to live in the 3D world throughout our life. The illumination changes constantly and light coming from objects in the space varies accordingly. In order to perceive the objects correctly we should be able to understand about the illumination and adapt ourselves to the illumination without any time loss and all the time, and we indeed do as the phenomenon called the color constancy indicates. We called the understanding the recognized visual space of illumination RVSI[1-7]. To construct a RVSI we use any visual information available in the space and we call it the initial visual information.

One property of the RVSI is the recognition about the brightness of the space, namely whether the space is illuminated brightly or dimly. We call the property the brightness size of the space and show it by the size of a sphere that represents RVSI as illustrated in Fig. 1. We express the color property of the RVSI by the angle from the fundamental axis FX, the clockwise direction for red and the anticlockwise green, for example. Any object in the space is plotted on a radius with a proper direction that is determined by the color and at a proper distance from the center that is determined by the reflectance or the lightness of the object. O_1 represents a reddish object with low lightness and O_2 the same reddish object but with high lightness. If the illuminance level is increased the size of the circle to represent the new RVSI increases accordingly, but the relative positions of the two objects in the circle remains unchanged because the luminance of the objects also increases with the same ratio

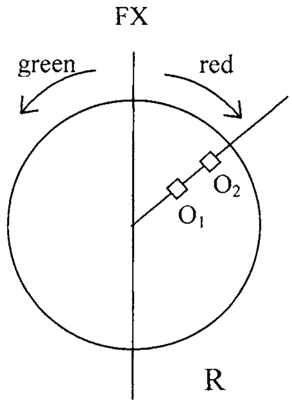

Fig. 1 Scheme of RVSI. FX, fundamental axis; O_1 and O_2 represent objects in the space.

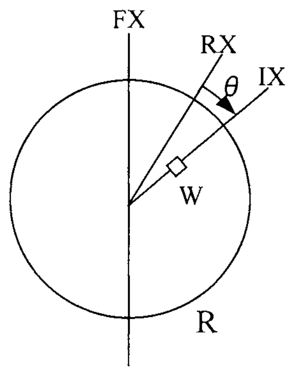

Fig. 2 Scheme of RVSI to show illumination axis IX and recognition axis RX. W represents physically an achromatic object.

as the increase of the circle. Their lightness remains same as before. This is the lightness constancy. If the color of the illumination changes from the daylight to the incandescent light, the illumination axis IX changes from the vertical position to the reddish direction as shown in Fig. 2. A physically achromatic object W, so to say, in the space is plotted on the illumination axis IX. The recognition axis RX defines the axis of the achromatic color appearance and the color appearance of any object in the space is determined by the angle from the RX to the object point in the RVSI. Its position is determined by the illumination axis IX and the angle from RX to IX, θ is small as we know from the color constancy.

The concept RVSI developed above can explain many color appearance phenomena reported in the past[8] and can propose new experiments with definite prediction. In the present lecture some of the experiments that we did will be introduced to demonstrate the power of the RVSI in the research of color appearance.

2. COLOR SEEN IN THE OTHER SIDE OF A COLORED FILTER

When we see a white paper by putting a small red filter directly on it in a room illuminated by the daylight type of fluorescent lamps, the color of the paper appears very reddish. But when we see the same white paper by holding the filter just in front of our eyes, the color now returns to white. These phenomena can be understood by the scheme of RVSI shown in Fig. 2. The white paper can be positioned at W if the color through the red filter is at the direction IX. In the former situation of the above two cases the RVSI of the observer is for the room illuminated by the daylight type of lamps and the recognition axis RX coincides with the fundamental axis FX. When he sees W, its color should appear very reddish as the angle from RX to IX is large. When the red filter is pulled toward his eyes so that the entire room is now seen through the filter the room is equivalent to the situation when it is illuminated by the color of the filter and the recognition axis RX comes close to IX just as illustrated in Fig. 2. The angle θ is small and the white paper appears almost white again.

A new experiment can be proposed to ask where the color of the white paper changes from red to white, or in our way of expression how the axis RX rotates toward the axis IX when the color filter is moved from the white paper to the eyes? The experiment was done[9, 10]. Fig. 3 shows the experimental arrangement. T is the white color chart of N8 to serve as the test stimulus and F the color filter. The subject sees T and judges its color by the elementary color naming method. T is moved back and forth on an optical bench to change the visual field size seen through the filter. Four color filters, red, yellow, green and blue, are employed. The room was illuminated by daylight type fluorescent lamps of 6500K at 660 lx. Two sizes of the test stimulus were employed, 9 x 9 cm and 18 x 18 cm.

Fig. 3 Apparatus to investigate the effect of field size for color appearance. T, test stimulus; F, colored filter.

The result of chromaticness is shown in Fig. 4 for the larger test stimulus and red and yellow filters as a function of the visual field size. Three curves correspond to subjects. The chromaticness is very large when the visual field through the filter is small to cover only the central part of the test stimulus, but it is very small when the visual field is large to cover the entire front view of the room to confirm our experience. The most interesting result is a sudden drop of the chromaticness at the fifth point from the left. All the three subjects showed the property. At the fourth point the visual field just covered the entire test stimulus and the subject saw only the test stimulus within the filter. At the fifth point the visual field became a bit larger than the test stimulus and he could see the wall of the room surrounding the test stimulus though only narrow area. The reason for the sudden drop is clear. The subject could see another world through the filter and was able to construct a new RVSI with RX rotated closer to IX of the colored filter.

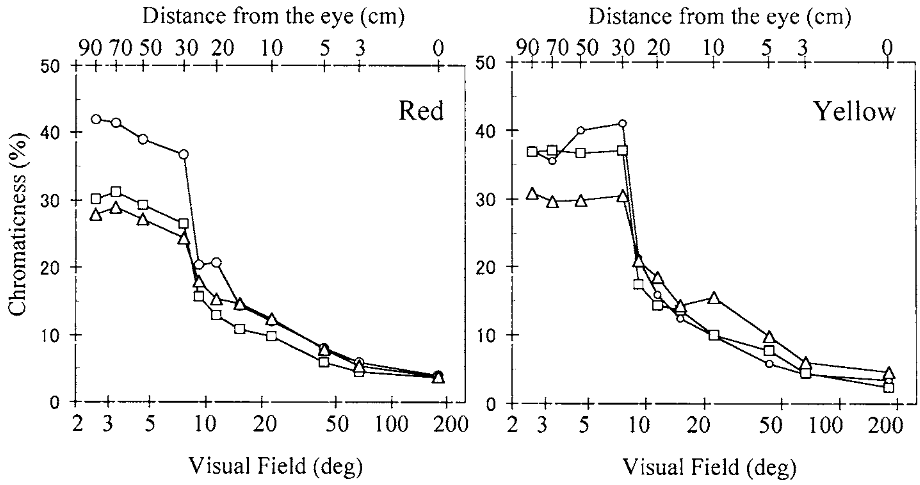

Fig. 4 Chromaticness judged for the achromatic chart through colored filters, red and yellow, at different positions of the filters.

3. ADAPTATION TO COLOR OF ILLUMINATION

We live in environment of changing illumination from place to place and from time to time. Light coming from objects changes accordingly and our visual system must discount the change instantly and without any break. Indeed our system does so. In our RVSI concept it means that the recognition axis RX almost instantly rotates toward and close to the illumination axis IX. We can then propose another experiment. Let us suppose that there is an achromatic test stimulus of which physical property does not change in spite of the change in illumination. Its location in RVSI circle comes at W_F of Fig. 5. The angle from RX to W_F is θ_F in the direction to green. The test stimulus should appear a very vivid green. We did an experiment to confirm this prediction[11].

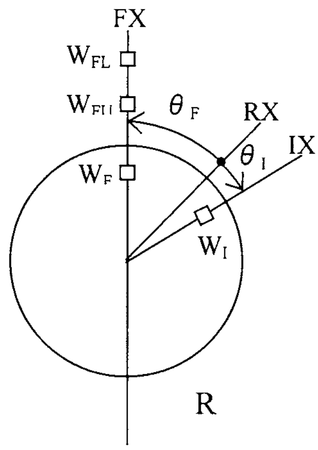

Fig. 5 Illustration to explain the color appearance of W_F whose physical property is kept constant regardless the room illumination. W_{FU} and W_{FL} are to illustrate the unnatural object color and the light source color, respectively.

Fig. 6 shows an experimental room simulating a normal room with decorations. Color of the ceiling fluorescent lamps can be changed. A is a small circular aperture and S is a rear screen. A white light is projected on the screen by a slide projector P. When a subject looked at the aperture she felt as if a round paper is pasted on the front wall. When the subject first entered the room she felt the entire room was illuminated very colorfully, but she quickly became unnoticed with the color. Walls and objects appeared normal to her in color. This is nothing but the adaptation to the new environment. In Japanese there are two words for adaptation, teki-oh 適応 and jun-nou 順応. If we distinguish the two words as the teki-oh to mean a positive adaptation to environment and the jun-nou a passive adaptation, it is the teki-oh that we do when we come to a new environment. The action should be very quick and it is. At the same time with the teki-oh the color of the test stimulus appeared very vivid.

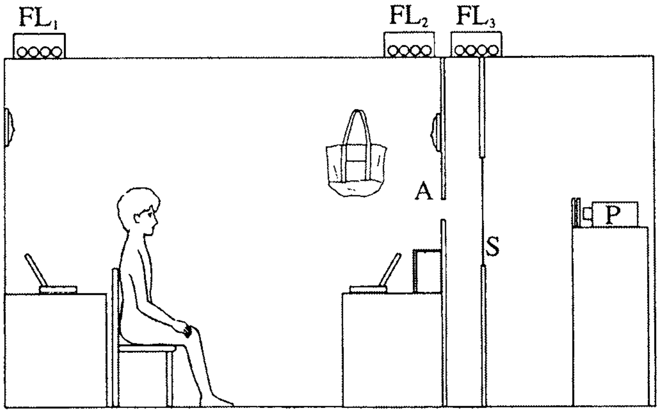

Fig. 6 Experimental room to present a test stimulus A independently from the subject's room.

In the experiment seven colors were employed for the illumination and the elementary color naming was carried out for the test stimulus. Two examples of the results are shown in Fig. 7 by the NCS polar diagram for the red illumination on the left and the blue illumination on the right. The outer edge of the circle represents 100 % chromaticness. Filled signs indicate the color appearance for the ceiling illumination judged by five individuals and open signs indicate the color appearance for the achromatic test stimulus. As predicted the apparent color of the test stimulus changed to a vivid color roughly opposite to the illumination color. It is interesting to note that the vivid color is not exactly opposite to the color of illumination, a unexpected result in view of the opponent colors theory.

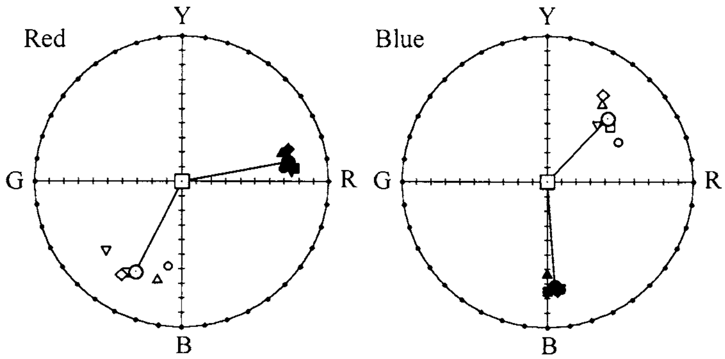

Fig. 7 Color appearance of the room illumination shown by filled signs, and that of the test stimulus shown by open signs. Large sings are the averages of five subjects.

4. COLOR OF PICTURES TO PRESENT THE EXACT COLOR IMPRESSION

Our visual system does "teki-oh" or adapt to the environment of which illumination changes from time to time, and this is a splendid nature of our eyes. But in this modern age it brings us problems some time. We enjoy taking photograph of scenes by a camera. We may take a picture in a room lit with incandescent lamps. When we see the printed picture in a room illuminated by the daylight type of illumination we are surprised to see a very reddish picture than that we experienced for the real scene at the time of taking the picture. This is explained by the RVSI concept. When we took the picture in the room our eyes did teki-oh to the room illumination and RX was very close to IX having an angle θ as illustrated in Fig. 5. Every color looked normal to us. The camera reproduced physically exact color of the scene on the print without doing teki-oh to the room illumination and achromatic objects were reproduced same as the illumination axis IX. When we saw the picture displayed in the different room illuminated by the daylight type RX coincided with FX and the achromatic objects appeared very reddish as the angle from RX to IX is large. In order to see the same color on the print as the real scene the picture should be modified so that its color comes at the direction with the angle θ from FX. The modification differs depending on the combination of both illuminations at the time of taking a photograph and of observing the print. We did an experiment to investigate that point[12].

The same apparatus as Fig. 6 was used by some modifications. The aperture A was changed to a larger rectangular aperture, 25.5 cm wide and 20.5 cm high, and the projector P was used to project picture slides on the rear screen S. The pictures were a series of the left side wall in the figure which were prepared beforehand for different color temperature of the ceiling fluorescent lamps FL_1. In the experiment the subject first looked at the left side wall for five minutes to get color impression of the scene. The room was illuminated by FL_1 with a certain color temperature. Then the subject turned around to see the right side wall to observe a picture appeared on the aperture A. The room was illuminated by FL_2 with another color temperature. The subject operated the slide projector to decide which picture was closest to the color that she experienced minutes ago for the left side wall. One example of the results is shown in Fig. 8 on the xy diagram. A large open circle indicates the color of FL_1 and a large filled circle the color of FL_2. There are seven symbols representing subjects and a large open diamond is the average. It is clear that the color of printed picture should be modified from the exact reproduction shown by the large open circle toward the displaying illumination shown by the large filled circle. The result shows that a careful choice of illumination must be conducted in displaying photographs so that an observer can experience the same color impression on the photographs that the photographer experienced.

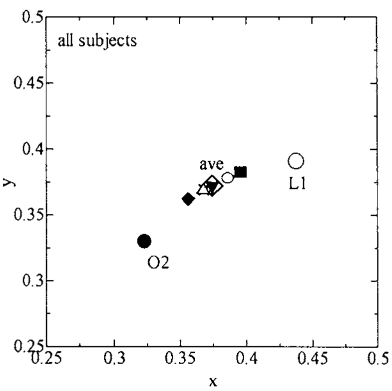

Fig. 8 The color of a picture print to present the exact color impression as experienced at the time of observing a real scene.

5. COLOR APPEARANCE MODE

Color appearance of a small portion changes depending on the observing condition and the CIE defines seven names, object color, surface color, aperture color, related color, unrelated color, luminous color and non luminous color. The Japanese Industrial Standards, JIS defines four, object color, surface color, light source color and aperture color. I like to add two, illumination color and light color. How these colors are related to RVSI?

Suppose a small grey patch placed in a lit room is additionally and locally illuminated by a white spotlight. Its luminance increases gradually and its position in the RVSI moves upper ward from the original position expressed by W_F if we use Fig. 5 again. It finally goes beyond the edge of the circle as shown by W_{FU}. It is outside the RVSI and its appearance is too bright and unnatural as an object in the room, although it is still the object color. For a further increase of the additional illumination the position separates further from the RVSI such as shown by W_{FL} and it begins to appear to shine itself to present the light source color. Three phases are seen here, the object color natural as an object in the room, the object color unnatural as an object in the room, and the light source color. The color appearance is determined in relation to the brightness size of RVSI. The aperture color and the luminous color can be demonstrated by keeping the room dark and making the luminance of the grey patch high. These demonstrations become different if the spotlight is increased in area so that there can be included other objects than the grey patch. As shown in the first experiment the appearance of the grey patch returns to its original grey if the observer can construct a new RVSI for the spotlight beside the

RVSI for the subject's room[9, 13]. The related and unrelated colors differ only in the sense that in the case of the related color the grey patch was judged in relation to the RVSI to which it belonged and in the case of the unrelated color the grey patch did not have the RVSI to which it belonged.

If the above explanation is correct an experiment can be proposed about the color appearance of the light source color. We illuminate the subject's room in Fig. 6 by a red light for example. The situation is expressed by a RVSI with its IX and RX at red directions just as shown by Fig. 5. If a white light is projected by P on the rear screen at a moderate intensity, its position in the RVSI comes at W_F and its color appearance is a vivid green as shown by the previous experiment. Let us increase the luminance of the test stimulus by simply increasing the intensity of the slide projector. The position goes beyond the edge of the circle to locate at W_{FU} or at W_{FL} and as the consequence the stimulus is released from the RVSI and becomes out of control of the RVSI so to speak. Its color appearance is no longer determined by the RX, but by the fundamental axis FX which is the achromatic axis recognized at dark or the inherent recognition axis from birth. The appearance of the test stimulus should return to its original color, achromatic. The experiment was carried out to confirm this prediction using the apparatus shown in Fig. 6 by keeping the red ceiling light constant at about 100 lx and increasing the luminance of the achromatic test stimulus[11]. The result is shown in Fig. 9 for two subjects. Along the abscissa the luminance of the test stimulus is taken and along the ordinate the percentage of chromaticness by shadowed area, blackness by black area and whiteness by clear area. The test stimulus appeared very vivid blueish green at low luminance, but it changed gradually to white at high luminance. The prediction was confirmed. The light source color gives its original color to us whatever the color of environmental illumination is.

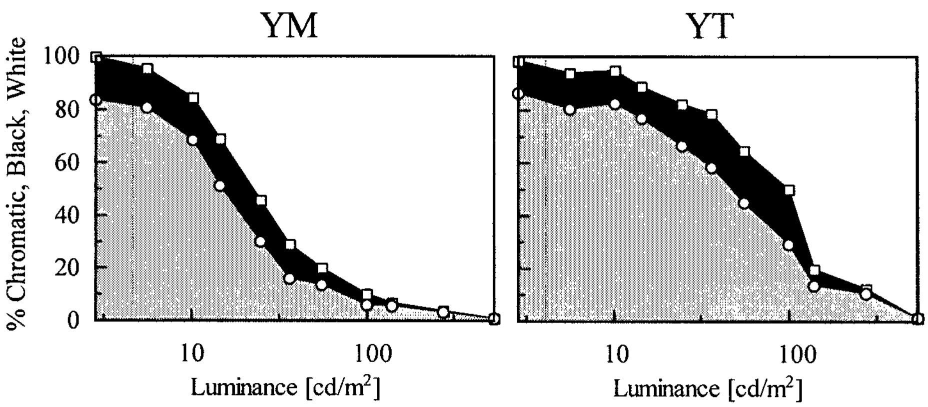

Fig. 9 Color appearance change for luminance of test stimulus. The vertical line shows the border from natural object color to unnatural object color. Shadowed area, chromaticness; black, blackness; clear, whiteness. Left, subject YM; right, YT.

6. RVSI FOR 2D PICTURES

The first action of our brain when we open our eyes is to see a 3D space in front of us and to grasp all about the space. This action is continued throughout our life. The brain receives only a 2D image from the retina and it must reconstruct the corresponding 3D space from the 2D image even when the image is abstract such as a grating pattern shown in Fig. 10 if it is only the image that the brain receives. If a 3D space is constructed the RVSI for the space is also constructed. We showed that really happened[14].

When one sees the grating pattern shown in Fig. 10 he recognizes a bright space in the front and a dark space in the back of the white gratings. Four short gray bars are drawn differently only at their ends so that the left two gray bars appear to lie in the bright space and the right two in the dark space. If these four bars are made of a same lightness the left two bars should appear darker than the right two according to the theory of RVSI.

We presented this pattern to subjects with a view limiting box that limited the subjects' view only to the pattern so that they can perceive three dimensional space more easily and asked subjects to report "yes" if the left two bars appeared brighter than the right two bars. The measurement was repeated for different lightness of the left two bars. The results are shown by open circles in Fig 11, where the lightness of the left two bars is taken along the abscissa and the yes percentage along the ordinate. The measurement was also done for another similar pattern where the depth relation of the left and right bars was reversed. The results are shown by filled circles. The prediction is confirmed.

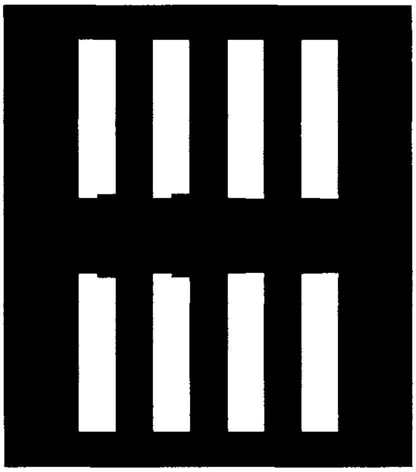

Fig. 10 Grating pattern to demonstrate the construction of RVSIs for the 2D picture.

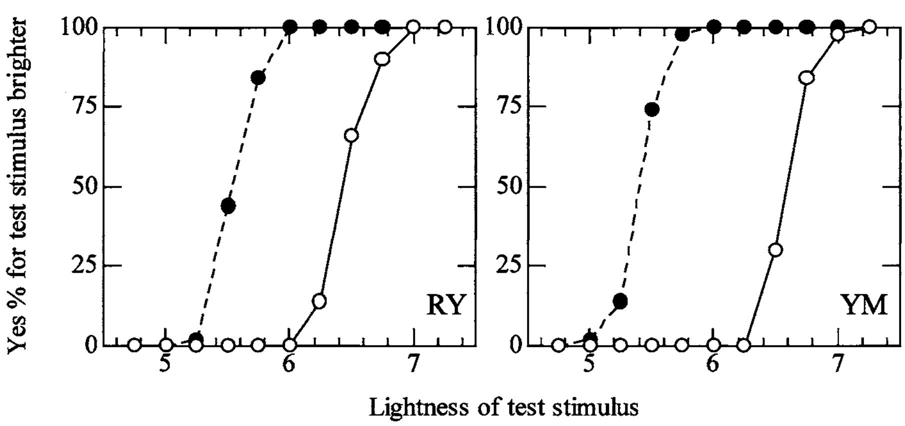

Fig. 11 Yes percentage for the left two bars brighter than the right two bars in the pattern shown in Fig. 10 (open circles) and in the reversed pattern as to the depth of the bars (filled circles). Subjects, RY and YM.

7. REMARKS

The concept of RVSI emphasizes the recognition of space illumination when color appearance is studied. When one does any experiment on color appearance there exists always a space in which the test stimulus is presented whether the researcher is conscious or not, and the color appearance is determined in relation to the subject's RVSI for the space whether he/she is conscious or not. I believe that many experimental results reported in the past can be reinterpreted by RVSI, differently and more neatly from the authors. I believe that the attention should be definitely paid to the environment illumination when one does experiment on the color appearance.

ACKNOWLEDGMENT

The present lecture is based on the experiments that I did with my students at Tokyo Institute of Technology, Kyoto University and Ritsumeikan University. I thank all of them, and particularly students at Ritsumeikan University with whom I carried out most of the RVSI experiments. They were not only my students but also my colleagues with whom I could discuss on research and from whom I could get many valuable comments and ideas.

REFERENCES

1) M. Ikeda; Appearance of colours in environment and their use in life, Proc. AIC Colour 93 Budapest 1 (1993) 123.
2) M. Ikeda, K. Motonaga, N. Matsuzawa and T. Ishida; Threshold determination for unnatural color appearance with local illumination, Kogaku (Optics) 22 (1993) 289 (in Japanese).
3) M. Ikeda and S. Fukumura; Formation of a recognized visual space of illumination with increasing initial visual information, J. Illum. Engng. Inst. Jpn. 79 (1995) 392 (in Japanese).
4) Y. Mizokami, M. Ikeda and H. Shinoda; Lightness judgment in relation to the size of the recognized visual space of illumination controlled by lightness and color saturation of objects, Proc. AIC Color 97 Kyoto 1 (1997) 167.
5) M. Ikeda, H. Shinoda and Y. Mizokami; Three dimensionality of the recognized visual space of illumination proved by hidden illumination, Opt. Rev. 5 (1998) 200.
6) Y. Mizokami, M. Ikeda and S. Shinoda; Color appearance not explained by x and y but by the recognized visual space of illumination, Proc. AIC Color 99 Warsaw (1999) 69.
7) R. Yamauchi, M. Ikeda and H. Shinoda; Color change in the construction process of the recognized visual space of illumination for a new environment, Proc. AIC Color 2000 Seoul (2000) 89.
8) M. Ikeda, H. Shinoda and Y. Mizokami; Phenomena of apparent lightness interpreted by the recognized visual space of illumination, Opt. Rev. 5 (1998)380.
9) M. Ikeda, A. Kusumi and H. Shinoda; Color appearance seen through a colored filter of various sizes, Opt. Rev. 8 (2001) 480.
10) A. Kusumi, M. Ikeda and H. Shinoda; Color constancy and color appearance mode in relation to the visual field size, Proc. AIC Color 2001 Rochester (2001) 595.
11) M. Ikeda, Y. Mizokami, S. Nakane and H. Shinoda; Color appearance of a patch explained by RVSI for the conditions of various colors of room illumination and of various luminance levels of the patch, Opt. Rev. 9 (2002) 132.
12) M. Ikeda, Y. Hattori and H. Shinoda; Color modification of pictures requiring same color impression as real scene, Opt. Rev. 9 (2002) 282.
13) R. Yamauchi, M. Ikeda and H. Shinoda; Walls surrounding a space work more efficiently to construct a recognized visual space of illumination than do scattered objects, Opt. Rev. 10 (2003) 166.
14) M. Ikeda, R. Yamauchi and H. Shinoda; Effect of space recognition on the apparent lightness of gray patches demonstrated on printed patterns, Opt. Rev. (accepted).

Color Management on the fly - Embedding Color Control in Printing Devices

Stefan Bruees
University of Wuppertal, Germany

GretagMacbeth

Color Management on the fly - Embedding color control in printing devices

Prof. Dr. Stefan Brües,
University of Wuppertal, Germany

AIC 2003, Bangkok — GretagMacbeth

Content

- Color Management approaches for printers
- Embedding CM technology in printers
  - Off-line solutions
  - Internal RIP/controller concepts
  - Performance and precision
- Outlook

Output Profiling

GretagMacbeth

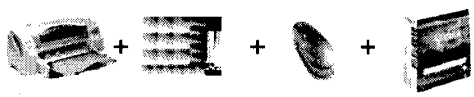

Printer + Characterization chart + Measurement Device + Profiling Software

↓

ICC Profile
Standardized, multidimensional description of device rendering capabilities

Color management system

GretagMacbeth

Printer + Characterization chart + Measurement Device + Profiling Software

↓

ICC Profile + Smart CMM
(Color Management Module) performs actual color transformation, provides advanced features

Getting components smaller

GretagMacbeth

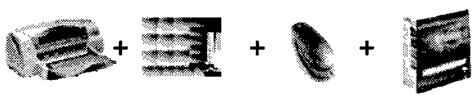

Printer + Characterization chart + Measurement Device + Profiling Software

Characterization chart ↓ Dedicated charts

Measurement Device ↓ Spectral mini sensor

Profiling Software ↓ Hardware optimized profiling libraries

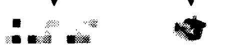

Characterization targets

GretagMacbeth

No need for big testcharts in dedicated environments

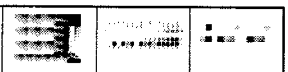

Number of Patches	1485	80	36 or less
Preferred Use	Universal	Dedicated for offset	Dedicated for printer

Smaller sensors

GretagMacbeth

Advanced Sensor Designs

- Small, getting even smaller...
- Typically multispectral
- Mass market products
- Density and spectral sensors for different applications

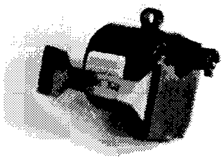

Profiling Libs and CMMs

GretagMacbeth

Optimized profiling and CMM libraries

- Small and fast hardware dedicated code
- Getting ICC functionality to controller level
- Links to applications available (e.g. downloading new profiles to controller embedded solutions)

GretagMacbeth ProfileMaker and LogoSync SDK

Color control modules

GretagMacbeth

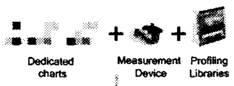

Smart CMM

ICC Profile ↓ | Technology ↓

Color control embedded in printer/controller

Implementation

GretagMacbeth

Color control embedded in printer/controller

Software components | Sensor components

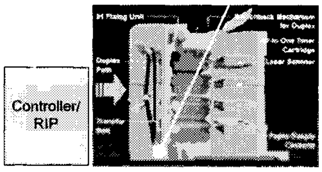

Embedded solutions

GretagMacbeth

Embedded color management strategies

- Re-Scanning (e.g. Efl, Canon)
- Static device profile plus density control
- Dynamic device profile, controlled by dedicated control element
- Dynamic device profile, detecting control data from printed images

Embedded solutions

GretagMacbeth

RGB-Scanner as 'colorimeter'

- Using build-in image scanning device
- RGB-based, no colorimetric measurement device
- Reduced color matching quality
- Lower end markets

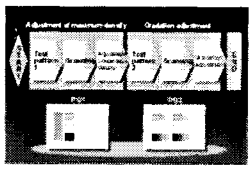

Embedded solutions

GretagMacbeth

Static profile plus densitometry control

- Standard profile sets or downloadable individual ICC device profiles
- Densitometric sensor built in printing device
- Re-linearizing the profile by modifying TRC values within the ICC profile
- 'Out of tolerance' indication requires new ICC device profile to be downloaded

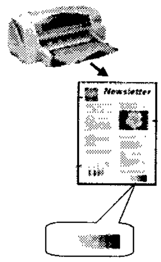

Embedded solutions

GretagMacbeth

Dynamic device profile, controlled by dedicated control wedge

- Standard profile to be individualized in printer (e.g by abstract profiles)
- Optional: Dedicated profiling step in printer set-up process
- Fully automated, integrated profiling and re-profiling
- Internal 'Out of tolerance' indication generates new ICC device profile
- Requires spectral sensor
- Dedicated calibration procedure and testpatches required

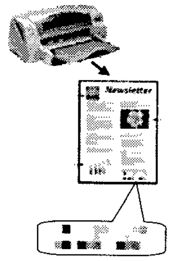

Embedded solutions

GretagMacbeth

Dynamic device profile, detecting control data from image data

- Standard profile to be individualized in printer (e.g by abstract profiles)
- Optional: Dedicated profiling step in printer set-up process
- Fully automated, integrated profiling and re-profiling
- Internal 'Out of tolerance' indication generates new ICC device profile
- Requires spectral sensor
- Dedicated profiling procedure or profile downloading
- No dedicated testpatches required

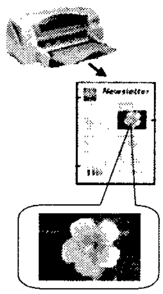

Embedded solutions

GretagMacbeth

Embedded color management at GretagMacbeth

- Real multichannel color transformations, independent of number and kind of primary colors
- Advanced, empirical modelling of 'separation processes'
- Implemented as 'add on' features in ICC standard environments (Smart CMMs)
- Minimizing testchart pattern

Future trend: Spectral technology

GretagMacbeth

Why will spectral solutions dominate the future?

- Illuminant independent color management
- Detecting paper and ink characteristics
- Compensating for metamerism, flourescency and other effects
- Most precise and controllable color management technology

CxF – Color Exchange Format

P. Juntarawatt
Gretag Macbeth, Hong Kong

The universal language to communicate colors digitally

Abstract: In a global world, communicating electronically the color data of spot colors is a hot (and not yet solved) issue. Global workflows and value chains, whether they are found in a B2B or B2C process, as well as an in-house digital workflow from designer to press, are demanding adequate and effective means to communicate (spot) colors. CxF is a new standard allowing seamless, worldwidedigital communication of all commercially significant aspects of spot colors. Furthermore, CxF is defined in a completely open way so that all aspects of a color can be communicated, even when the application and the color communication features required are unknown. For example, every software vendor implementing / supporting CxF is able to extend the basic feature set to the needs of a new application without affecting the general usability. Wherever color communication is mission critical, CxF should be considered to be the solution to the problem!

How to communicate color?

Background and history of color communication

The best way to do standardized color communications has been in discussion for years and many different approaches have been tried. Typically, color communication is done today using colorimetric measurement values such as CIE-Lab, XYZ, RGB, density, CMYK or spectral measurement values. Today, the new economy is based on a worldwide digital workflow. The evolving use of Internet technology in distribution and logistics creates an even greater demand for a standardized color communication method. A new universal language to communicate colors would simplify the process to communicate colors greatly.

Device dependent versus device independent color spaces

An important aspect in color communications is to differentiate whether device dependent or device independent color spaces are used. For a long time, the way to communicate colors has been to exchange CMYK, (Scanner-) RGB values or to use named colors like Pantone®, Toyo or HKS.

When device dependent color spaces are used to communicate, color profiles (ex. ICC-profiles) assigned to those color coordinates must be used, to ensure accurate color communications. The appropriate algorithms, procedures and data exchange standards therefore have been defined by the ICC (International Color Consortium; http://www.color.org). Device dependent color spaces are specified therein by so called device profiles. The detailed specifications can be found in the ICC document “Spec ICC.1: 1998-09”.

Named color spaces

Other approaches to communicate colors are "named color spaces". This approach is used by companies and organizations like Pantone®[1], RAL, NCS, Toyo or HKS. In this approach, colorimetric values / spectral values are assigned to color names. The assigned color name is then used to communicate the color.

Appearance effects

Human perception of colors is not defined ultimately by a colorimetric measurement value of the sample. As important as the colorimetric value itself, are surrounding colors, or the absolute brightness (light level). One possible approach to that problem can be found in the CIE publication CIE 131-1998 ("The CIE 1997 interim colour appearance model (simple version) CIECAM 97s"). Other mathematical models are known as well.

Further effects affecting the appearance of colors, are angular dependencies of the emission or reflectance, as typically seen on metallic surfaces. This effect is measured using a gonio spectrophotometer. The color has to be defined in that situation by a set of, angular dependent, reflectance curves.

In many situations the appearance / perception of the color is affected not only by the color itself. As important as the color is the substrate the color is printed / applied on. Fluorescence effects, implied by the use of optical brighteners affect the color significantly. Appropriate measures to quantify those effects are white and yellow indexes or as a preferred alternative substrate measurements done with a double monochromatic spectrophotometer in a wavelength range from 360 nm to 730 nm. This data must be communicated as well, to communicate those colors.

In many applications, homogeneousity and structure of the sample are important in color communications. A possible way to solve that problem is to communicate pictures of spot colors in combination with the colorimetric / spectral information.

Other effects affecting the perception of colors are surface effects of the color sample (gloss effects of the color and or the substrate). These are effects typically measured by a gloss meter built according to DIN 16357. A universal color communication language should support such appearance effects.

Other important aspects in color communication are size, position and shape of color patches. There are several papers published defining appearance effects based on the simultaneous contrast of color patches.

---

[1] Pantone®, is a registered Trademark of Pantone Inc., Carlstadt, New Jersey

Commercial aspects

Commercially used colors have to be within a certain colorimetric tolerance field. This tolerance is often defined as a dE tolerance using the CIE-Lab, CMC or FMCII color space. To communicate the color, dE implies the communication of the acceptable color tolerance field as well.

Other factors, such as light resistance, resistance against chemicals, or other physical, chemical, biological aspects of a color matter may also need to be communicated, depending on the application.

Mathematical and optical conditions

Absolute colorimetric values depend further on the physical / optical configuration used to do the measurement. Measurements done on the same sample using a 45/0° optical system versus a sphere will not match. Other well-known optical setups affecting the measured results include polarization filters and the physical light source used to illuminate the sample (ie. D65-flash or A-Tungsten halogen). In general it is not possible to convert spectrophotometer readings, done with different optical setups. Therefore, to compare and communicate those spectrophotometer readings, the physical optical setup conditions used to do the measurements must be communicated as well.

Another important aspect, as far as colorimetric values are used to communicate, are the mathematical conditions used to do the calculations (observer 2°/10°, light sources D65, D50, A, C, F1...F11). Depending on the illuminating light source, the colorimetric values will differ. Therefore all commercially known color measurement devices, define these conditions. It may be useful in some conditions, to do the above-mentioned calculations on the spot. A universal data communication standard must therefore be able to include physical light sources or emissions standards as well.

ANSI standard to communicate colors

One possible way to communicate colors (especially useful to communicate colorimetric values of device profiling charts) using absolute colorimetric values is explained in detail in the ANSI Standard IT 8.7/2-1993. ("Graphic technology - Color reflection target for input scanner calibration"). Therein especially, the aspect is explained how colorimetric and spectral measurement values, can be serialized into an ASCII data stream.

Summary

In general, it is not sufficient to communicate a reflectance curve or a CIE-Lab value. Depending on the application, there are specific needs in the way a color should be communicated. A universal color communication language must be open – to describe and communicate such known and even new, not yet defined effects.

Depending on the application, further attributes need to be assigned to spot colors. Among the infinite list of possible attributes assigned to spot colors are, serial numbers, part numbers, color mixtures, price of pigments, light resistance of the color, descriptions, application notes, comments and many more.

To define and communicate a color, dependent on the application, an open set of selected attributes of a color has to be communicated. Today's existing color exchange formats, such as the IT8 format, use a table-based approach to store colorimetric and or reflectance values. Every record / line in the file will therefore contain a sample name and the colorimetric or spectral values to be communicated in columns. This approach to store the attributes of a sample has severe limitations. As soon as you store different samples with different attributes, a table-based approach will lead to large tables containing a column for every attribute to be stored. And many of these cells will end up being left blank. Every application that required a new attribute to be stored would require the table to be extended with a new column and therefore an established color data communication standard would have to be changed.

The CxF solution to color communications

Aim of CxF

The Aim of CxF is to define a procedure to communicate all aspects of spot colors in a global value chain by electronic means. To achieve that goal, all relevant attributes affecting the appearance or any other important aspect of the colors needs to be stored (serialized) using a suitable form. Furthermore it must be possible to specify every color in a different way. The specifications have to be open to all software applications dealing with colors. The user or the software application package has to have the choice, to choose the attribute of interest to be used in the application. In general, depending on the application, CxF must support the communication of all further aspects as color recipes, price, weight or any other information that can be helpful. CxF must be a container to store any kind of information assigned to a spot color as well.

CxF must be built in a way, allowing soft- and hardware vendors, to extend the definition, to their specific needs. These extensions, must not affect the backward compatibility, i.e. the new extended attributes should simply be ignored by applications that don't recognize them.

A modern color communication standard has to be Internet aware. The data format chosen should follow standards used today in Internet applications and must therefore seamlessly integrate into existing standards.

Support of color management is a must. Therefore embedding of device profiles must be supported, to allow true color visualization / print out of colors on the remote site and therefore guarantee a seamless workflow.

The CxF design approach

XML based design

The design approach chosen to implement CxF is to define an XML based language featuring a basic set of attributes used in color communications. This XML based data format must be chosen for the following reasons:

- CxF can be seamlessly integrated into an Internet-based workflow.
- A color communication language must be defined platform and programming language independent.
- XML is a widely accepted standard in the Internet world. There are already many tools available supporting the XML standard.
- Using an XML based approach provides for an ASCII data stream. An ASCII stream will simplify the communication.
- It is easy to embed an XML data stream into objects.
- The ASCII stream can be read and understood by human beings as well. An ASCII capable editor is therefore the only tool required to do the first steps in composing / editing CxF files.
- XML is perfectly suited to define and serialize a set of hierarchically structured data objects – each data object having an open set of attributes.
- XML is a perfect tool, to achieve persistency of objects found in OO programming languages.

Support of ICC profiles

Today color communication software packages must be aware of the ICC approach. CxF allows a set of device ICC profiles to be assigned to every sample. These profiles can be used to either transform a device dependent color value into a device independent one, or to simulate a color on an output device.

Links

Often there is a need to assign the same information to a set of samples. Typical examples are measuring conditions or ICC profiles. To avoid encoding recurrent / redundant information CxF allows a link to an object inside the CxF compatible file to be defined. In this way, ICC profiles or measuring conditions only need to be stored once in a file. The profile or measuring conditions can then be referenced by this link – thus greatly reducing the required size to store the information.

A typical CxF compatible system

A CxF compatible system is built of the following components:

- A spectrophotometer or any other device capable of doing colorimetric or spectral readings.
- An application software, (CxF composer) that allows spot colors to be measured or entered (using reflectance data, RGB, CIE-Lab...) and defines or adds additional attributes (pictures, text strings...) to the sample. This software is capable of serializing this data with the help of a CxF library.
- A CxF library. The CxF library is capable of reading and writing spot colors according to the CxF standard. In addition the CxF library will give the application access to the CxF type of data structures and interfaces to colorimetric and color management functions. The data stream produced by the library can be embedded in other data formats.
- A viewer software (CxF viewer) that can load, display and print spot colors found in CxF files in true color. In addition, the CxF viewer can export CxF color patches to different application specific formats, such as Adobe® Photoshop palette files or similar palettes. (**i1Share** is a **free** CxF composer / viewer.
  The application can be downloaded at http://www.i1color.com/freeware/).
- An ICC based color management system, that can synchronize all involved input / output devices. In addition ICC profiles allow device dependent color definitions to be translated into device independent color definitions.
- An optional print device, to get a hard copy of the color patches in true colors as well as to get a printout of the text and picture attributes assigned to colors.
- An appearance modeling system, to visualize the appearance effects of the samples.

The system components interact as follows:

A user will enter the colors to communicate with help of the graphical interface of the CxF composer. Typically the user will do a measurement with an attached spectrophotometer. The CxF composer will then add the new sample to the existing sample set. An alternative way to add a color is to enter the color manually. After the color is defined by colorimetric or spectral data, the user can add additional attributes to the color, such as ICC profiles, pictures or any other attribute required by the application. Typically these attributes will be added using either a drag-and-drop style user interface (specifically suited to add profiles and pictures) or the user will add additional attributes in text form using a ASCII editor or a specialized input mask. The colors added will be immediately visualized in true color using ICC compatible color management. Once the full sample set is defined, the information is serialized into an ASCII compatible data stream. This stream can be stored into a file, or as an alternative solution, can be embedded into a parent object. The file is transmitted afterwards to the recipient. The recipient will then use a CxF compatible viewer, to open and visualize the file in true colors. In addition the user may choose to print out the sample set in true colors. Because of the capability of the CxF viewer to write color data files compatible with the most important applications as Photoshop, Quark Express or similar applications, the user may want to export the color data into a data format compatible with those applications.

CxF tree

An alternative way to visualize the defintions above, is to use a tree like structure:

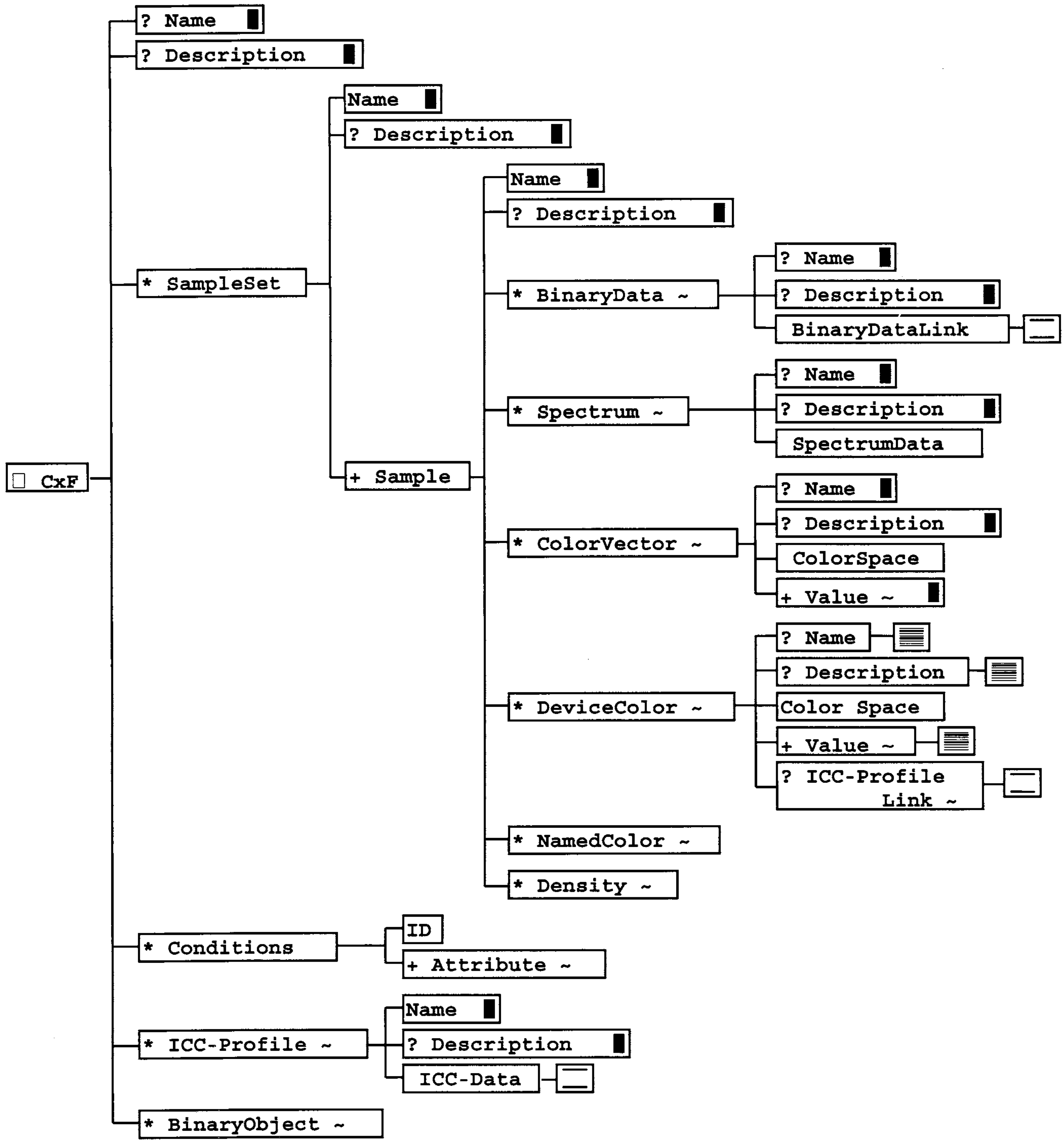

CxF SDK

To support the use of CxF compatible data files, GretagMacbeth has developed a CxF software development kit (SDK). The functionality of a CxF compatible application may be structured into 5 layers. On top is the CxF application layer. A CxF application will access layer 1 to 3 for colorimetric or spectral sample definitions. Layer 4 serves to apply color management or appearance modeling functions to this information.

CxF compatible application		
color management	appearance modeling	... ...
layer 3		
layer 2		
layer 1		

Going a little bit more into the details of the CxF SDK we can assign the following functionality to the main CxF layers:

Layer 4: CxF – appearance / perception / color management layer C++ Software Development Kit (SDK) Access to color management, appearance information
Layer 3: CxF – colorimetric data layer C++ Software Development Kit (SDK) high level C++ access to colorimetric data
Layer 2: CxF – data structure layer C++ Software Development Kit (SDK) low level C++ access to CxF data structures
Layer 1: CxF – file layer File-format: XML

Layer 1: CxF file layer. Layer 1 is a representation of the tools / methods and data structures used to load and store CxF compatible data files to / from disk or to / from a memory stream.

Layer 2: CxF data structure layer. Layer 2 will parse the basic IO / memory stream defined in layer 1 and transform the attributes and objects found in the stream into a tree like data structure in memory. In addition layer 2 will give the application access to this data structures. All objects and attributes are stored as ASCII strings on layer 2. No conversion to binary data structures is done on layer 2.

Layer 3: CxF – colorimetric layer: Layer 3 does provide access to all kinds of colorimetric information found in a CxF compatible file. Tools are provided to iterate through the tree to find the appropriate colorimetric values. Output of layer 3 is binary formatted data.

Layer 4: CxF – appearance / perception / color management layer: Once colorimetric values are extracted using layer 3 functionality, depending on the application, the colorimetric values must be adapted / transformed into a visual representation of the (spot) colors. To achieve this goal, layer 4 functionality of CxF is used to apply the rules of color management and appearance management to the sample.

The Future of CxF

In former times, to communicate a Pantone® number or a CMYK value was enough. Today we know that we need to communicate much more information to get the color right the first time.

CxF can be the base that can be added to any digital workflow to provide the ability to communicate spot colors electronically. In a digital workflow from prepress to press, no standardized ways to communicate all aspects of spot colors in the whole value chain is known. CxF will open new opportunities to automate and simplify the color communication of spot colors in a digital workflow.

In a world moving from analog proofs to electronic proofs, we need to extend the capabilities of our workflow tools. They must be extended to allow proofing of all appearance effects of the color. The more electronic the workflow becomes, the more significant the aspect to control color and appearance of a spot color becomes.

PDF and PostScript allow electronic proofing of pictures – to a certain extent. However, the exact specification and communication of spot color has not been implemented so far. CxF can do in the future for spot colors, what PDF and PostScript has done for documents in the past.

The CxF committee

As a matter of fact, because of the open definition of the CxF standard, CxF will never be finally defined. All attributes stored in a CxF compatible file, used to communicate between software packages of different vendors, needs, of course, to be identified. To simplify and organize this task, the CxF committee will be set up. Every organization or company interested in color communications can become a member of the CxF committee.

Questions and Answers about CxF Technology

- What do I need to build my own CxF compatible application?
  We recommend licensing the free CxF SDK from GretagMacbeth to write CxF compatible applications.

- Where do I get the free CxF SDK (software development kit)?
  You can get the CxF SDK from GretagMacbeth AG. Send an email to:
  mailto:cxf@gretagmacbeth.ch

- How do I get the free CxF viewer / composer?
  A free CxF compatible viewer / composer "(i1Share") can be downloaded from the GretagMacbeth Web site. http://www.i1color.com/freeware/. A CxF compatible composer will also be bundled with select GretagMacbeth instruments. In addition, all Gretag-Macbeth soft- and hardware products will support CxF as a color communication standard. Check http://www.gretagmacbeth.com for an update of your application and/or firmware.

- How do I embed a CxF compatible data stream into my application?
  We recommend using the free GretagMacbeth CxF SDK. The SDK has functionality to redirect a CxF compatible data stream into a memory stream.

- How to participate in future CxF development?
  Any organization interested in CxF can become a member of the CxF committee. Contact mailto:cxf@gretagmacbeth.ch to get additional information.

- How do I become member of the CxF consortium?
  To become a member of the CxF consortium send an email to mailto:cxf@gretagmacbeth.ch

Fundamental Theory of Advanced CMS Software, PD System Pro

Yasuyuki P. Tanaka
FUJIFILM Regional Services (Singapore)

Fundamental Theory of Advanced CMS Software,

PD System Pro

- How to achieve the precise color -

FUJIFILM Regional Services (Singapore)
Yasuyuki P Tanaka

<Digital Direct Color Proof>

- High End DDCP→ High Quality but High Cost
- Inkjet Printer → Low cost, but Poor color matching

↓

Inkjet Printer with Color Management System (CMS) become trend.

CMS Software in the market

CMS software based on ICC Profile become popular in the market.
But
The market is still not satisfied with its color matching level.

The Problem of CMS Software based on ICC Profile

1. Insufficient color reproduce quality on RGB->CMYK conversion.
2. Insufficient color matching accuracy
3. Black change to CMY during the color matching procedure.

PD System Pro

Precise Color Matching

- Average ? E < 2.0

<Key Point for precise color matching>
- Standardization of colorimetric condition
- Automatic feedback correction
- Elimination of fluorescent effect
- Keep black separation

Compare to other CMS software based on ICC profile

Quality of CMS profile

PD System Pro Average ? E = 1.6

(Other ICC profile base CMS software)

CMS software A	= 6.0
CMS software B	=16.6
CMS software C	= 9.1
CMS software D	= 7.3

Obtained from the customer data.

Key Point - 1

Standardization of colorimetric condition

Eliminate deviations in Colorimetric Measurements

- •Differences in Background Color
- •Differences of Spectrophotometer Performance

↓

Device Profile/Target Profile are created under identical, standardized condition, generating device link profiles.

Key Point-2

Auto Feedback Correction

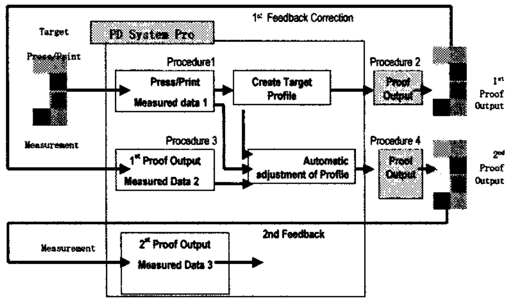

Key Point-3

Elimination of fluorescent effect

Fluorescent dye in the paper affect to the color measurement result.

- Fluorescent dye generate the short wavelength light by UV light.
- Spectrum difference between spectrophotometer light source and the observation light makes different fluorescent effect.

↓

New algorithm and dedicated spectrophotometer with UV filter minimize the effect.

Key Point-4

Keep black separation

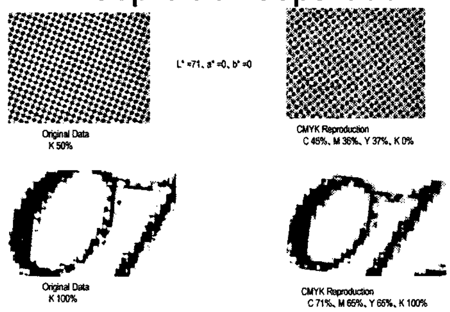

Key Point-4

Keep black separation

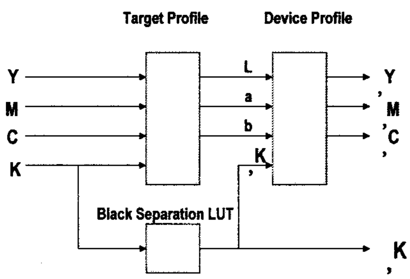

Summary of PD System Pro

- Precise Color Matching -

	PD System Pro	ICC profile base CMS software
Profile Format	ICC + Original format	ICC only
Profile Accuracy	Standardization ->High accuracy	Depend on spectrophotometer and software
Profile Making Skill	Eliminate the fluorescent effect	Depend on spectrophotometer and software
Link Function	Keep black separation ->Eliminate noises	Noise in the primary and secondary color
Color Matching Adjustment	Auto feedback correction	Manual correction

Mathematical Distance between Color Values in NCS Color Space

KOBAYASI, Mituo* and YOSIKI, Kayoko*
The University of Electro-Communications

1. INTRODUCTION

NCS(Natural Color System)[1] is a color specification system constructed by means of phenomenological analysis and psychophysical experiments. NCS is especially valuable for theoretical consideration on color perception and for practical evaluation of color design in any environment, since the idea of Color Gestalt is reflected in the development of the system.

Based on NCS, some formulae to calculate color difference between a pair of juxtaposed colors, e.g., "distinctness of border", are proposed.[2] An idea to introduce a kind of distance to a perceptual color space has proposed by Y.Nayatani,[3] however, measures of color difference between an arbitrary pair of colors in NCS color space are not yet provided, since the color space is not uniform.

This study is an attempt to introduce a new concept of color distance in NCS. The proposed color distance, slightly similar to but essentially different from Nayatani's distance, is derived naturally and mathematically from the structure of NCS.

2. DEFINITION OF THE COLOR DISTANCE IN NCS

2.1. The Distance on the Color Triangle

Typical attributes of a color in NCS, whiteness w, blackness s, and chromaticness c, satisfy the relation :

$$w + s + c = 100[\%]. \tag{1}$$

A triplet (w, s, c), called "nuance", is a barycentric coordinate defined by a triangle, called "color triangle", whose apices represent two elementary colors, white W and black S, and one arbitrary full color C. For simplicity of explanation, the color triangle is usually drawn as a equilateral triangle, but it is not necessarily equilateral because a barycentric coordinate does not depend on the shape of a triangle.

The "nuance difference" between two colors in a color triangle should not be represented by Euclidean distance. If the shape of a color triangle varies, the nuance difference should keep the same value, while the Euclidean distance between two points, representing two nuances, varies. Moreover the Euclidean distance is difficult to interpret as a perceptual difference of two colors.

Define d_n by the amount of move from a nuance to the other nuance along the shortest route, on which any one of the elements of nuance are fixed and the other two are varied. The quantity d_n represents the nuance distance on the color triangle. It can be calculated in several cases, finally reduced to the following simple form:

$$d_\mathrm{n} = \max(|\Delta w|, |\Delta s|, |\Delta c|) \tag{2}$$

$$= \frac{1}{2}(|\Delta w| + |\Delta s| + |\Delta c|), \tag{3}$$

where Δw, Δs, and Δc are the difference of whiteness, the difference of blackness, and the difference of chromaticness respectively.

This idea of distance can be applied to any other color specification system having a barycentric coordinate, e.g., Ostwald system and the xy chromaticity coordinate system. Although xy chromaticity coordinate is usually represented as an orthogonal coordinate, it is not appropriate to use the Euclidean distance between two xy coordinates.

* phone 81 424 43-5324; fax 81 424 43-5334; The University of Electro-Communications, 1-5-1 Chofugaoka, Chofu-shi, Tokyo 182-8585, JAPAN

2.2. The Distance on the Color Circle

A pair (c, ϕ) composed of chromaticness c and hue ϕ is a polar coordinate on a circle, called the "color circle". In order to consider a distance on the color circle, it will be necessary to make hue steps uniform on the whole circle. In NCS, however, the uniformity of hue is restricted within each quadrant of the color circle.

We will first try to modify NCS hue steps and then construct a distance on the color circle.

2.2.1. modification of hue steps

Hård et al.[2] said that on the color circle of NCS straight lines connecting the pair of perceived hues of complementary colors intersect approximately at the point X (20, R75B), a slightly eccentric point from the center of the circle (Figure 1).

Modifying the position of original hue, we can make new color circle, so that the opposite position of any new hue coincide with the position of its complementary hue (Figure 2).

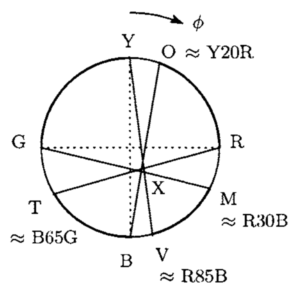

Figure 1. position of complementary hues of afterimage

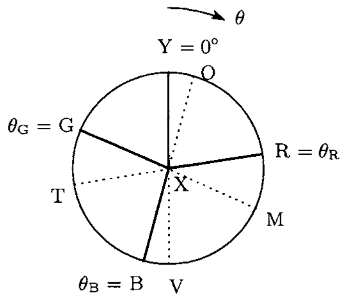

Figure 2. modified hue (θ) and modified NCS color circle

The obtained transformation from the original hue ϕ (numerical representation) to the new hue θ (angle in degree) is defined by

$$\theta = \begin{cases} \theta_R \dfrac{\phi - 100}{100}, & 100 \le \phi < 200, \\ (\theta_B - \theta_R)\dfrac{\phi - 200}{100} + \theta_R, & 200 \le \phi < 300, \\ (\theta_G - \theta_B)\dfrac{\phi - 300}{100} + \theta_B, & 300 \le \phi < 400, \\ (360^\circ - \theta_G)\dfrac{\phi - 400}{100} + \theta_G, & 400 \le \phi < 500, \end{cases} \tag{4}$$

where $\theta_R = 82.0^\circ$, $\theta_B = 196.9^\circ$, and $\theta_G = 296.7^\circ$.

In Figure 3, a relation of the modified NCS hue θ and the Munsell hue H are shown. (Here the chroma $C = 10$ and the value $V = 5$ are fixed.) The right graph of the correspondence between H and θ is almost a straight line, which suggests the modified NCS hue has good uniformity.

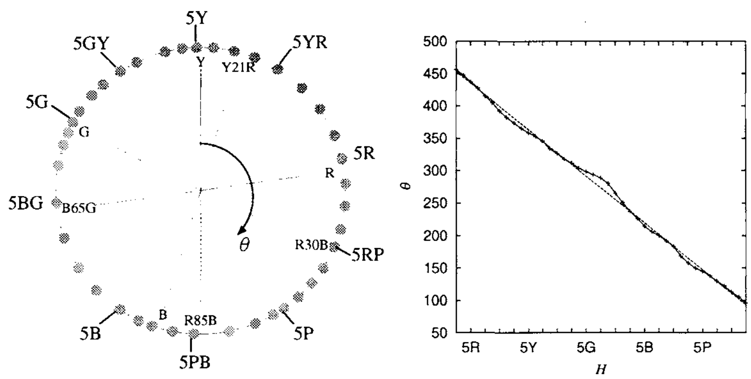

Figure 3. relation between Munsell hue(H) and modified NCS hue(θ)

2.2.2. construction of the distance

The method of constructing a distance between two points on the modified color circle is the same method of "shortest route" as used in the case of nuance distance (§2.1). The calculation is rather complex than in the case of nuance. However, the resultant form of the distance d_{ch} is simple:

$$d_{\mathrm{ch}} = |\Delta c| + d_{\mathrm{h}}, \tag{5}$$

$$d_{\mathrm{h}} = \begin{cases} \min(c_1, c_2)|\Delta\theta|(\pi/180^\circ), & |\Delta\theta|(\pi/180^\circ) \le 2, \\ 2\min(c_1, c_2), & |\Delta\theta|(\pi/180^\circ) > 2, \end{cases} \tag{6}$$

where c_1 and c_2 are the chromaticness of two colors and $\Delta\theta$ is the difference of hue angle.

The component d_{h} of d_{ch} is so-called "hue difference".

2.3. The Distance in the Color Space

The color distance in NCS color space is finally defined by the following expression:

$$d_{\mathrm{NCS}} = d_{\mathrm{n}} + d_{\mathrm{h}}. \tag{7}$$

Figure 4 illustrates the relation among several kinds of NCS color distances. The distances d_{n}, d_{ch}, and d_{NCS} are regarded as a kind of city block distance. All of these quantity satisfy the mathematical axiom of distance, however the proof is omitted due to limitation of space.

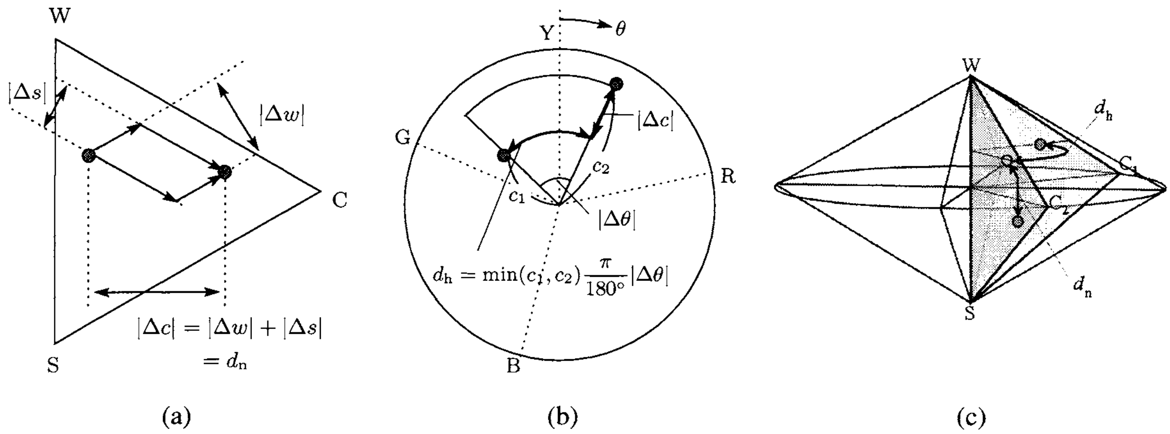

Figure 4. NCS Color Distances (a) on the color triangle, (b) on the color circle, and (c) in the color space

3. EQUIDISTANT LOCUS

In order to examine the characteristics of the distance defined above, equidistant loci will be plotted in several color spaces.

Figure 5(a) shows the loci of $d_{\mathrm{n}} = 10, 20, \ldots, 80$ distant from a point $(w, s, c) =$ (30,20,50) on the color triangle. Figure 5(b) shows the loci of $d_{\mathrm{ch}} = 20, 40, \ldots, 140$ distant from a point $(c, \theta) =$ (50,0) on the modified color circle. Figure 5(c) shows the loci of $d_{\mathrm{ch}} = 10$ distant from several points on the modified color circle. Figure 5(d) shows the loci of $d_{\mathrm{ch}} = 10$ on the original NCS color circle.

Transferring these equidistant loci to a uniform color space, it will be able to compare qualitatively the color distance in NCS with the color difference in the uniform color space.

The loci of $d_{\mathrm{ch}} = 10$ shown in Figure 5(d) are transfered to the uniform color spaces, CIELAB, CIELUV, and Munsell, keeping the whiteness constant $w = 10$ (Figure 6). As $\Delta w = 0$ in this case, $d_{\mathrm{n}} = |\Delta c|$ is derived from the equation (2), and $d_{\mathrm{ch}} = d_{\mathrm{NCS}}$ is derived from the equation (5) and (7). Consequently, the loci of $d_{\mathrm{ch}} = 10$ in Figure 6 is also the loci of $d_{\mathrm{NCS}} = 10$.

A locus of equal color difference forms a circle in a uniform color space. However, in Figure 6, each of the loci is not a circle, and becomes larger as the chromaticness increase. It tells that the distance in NCS is quite different from the color difference in a uniform color space. This color distance in NCS does not correspond to a sensual color difference but corresponds to a perceptual color difference.

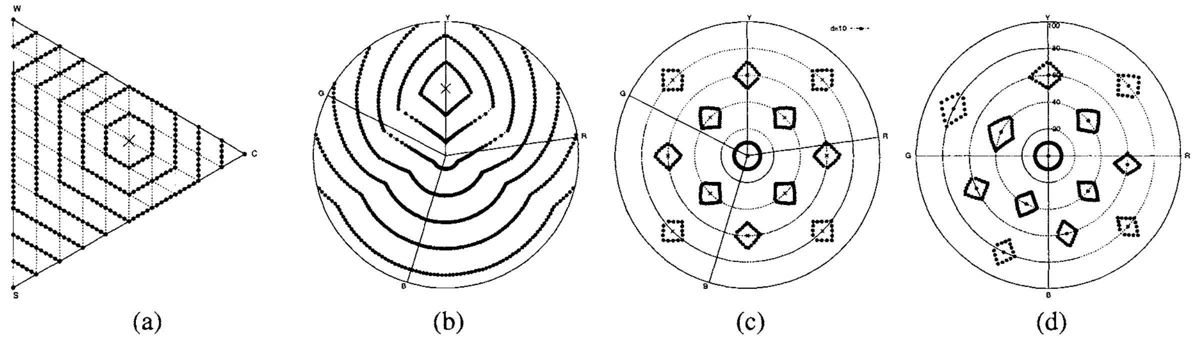

Figure 5. equally distant locus (a)on the color triangle ($d_n = 10, 20, \ldots, 80$), (b)on the modified color circle ($d_{ch} = 20, 40, \ldots, 140$), (c)on the modified color circle ($d_{ch} = 10$), and (d)on the original color circle ($d_{ch} = 10$)

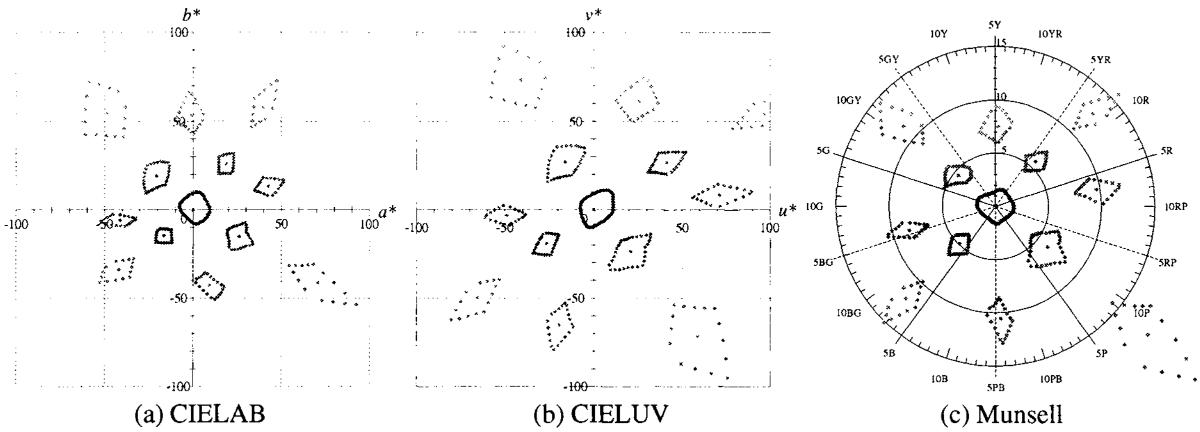

Figure 6. equally distant locus on the uniform color spaces ($d_{ch} = 10$)

4. RELATION TO THE SIMILAR MEASURES IN NCS

Hård et al.[2] introduced some measures expressing the size of difference between two colors in NCS. Two of them will be compared with the above-defined color distance.

4.1. comparison with the "interval size"

A color in NCS is originally represented by six elementary attributes, whiteness, blackness, yellowness, redness, blueness, and greenness. Each of these attributes is a degree of resemblance of the color to each of elementary colors respectively. The "interval size(IS)", which was introduced to express the specific color contrast, is defined by the mean of two largest differences of elementary attributes divided by 100.

Using the concept of color distance, the same quantity as IS can not be constructed but the maximum of d_n and d_h will be analogous to IS. So, $\max(d_n, d_h)$ and the IS for 13 color pairs listed in the literature [2, Table 3] are plotted in Figure 8 (the scale of IS is multiplied by 100). The abscissa of the graph indicates a color pair, whose elements are selected from 10 colors (Figure 7). In case d_n is chosen as the maximum, $\max(d_n, d_h)$ is similar to IS, on the other hand, if d_h is chosen $\max(d_n, d_h)$ is larger than IS. For any color pair the value of IS does not exceed 1, while d_h becomes larger as two colors are far from each other.

Thus the concept of the color distance and IS are not the same, nevertheless our color distance seems to be useful instead of IS as a measure of color contrast.

4.2. comparison with the "distinctness of border"

The "distinctness of border (GT)" is defined as follows:

$$GT = 1.5\{[\Delta s_v - 0.3] + 0.2[\Delta c - 0.5] \\ +0.3[\Delta\phi(c_1 + c_2)/200 - 0.3]\}^{0.4}, \quad (8)$$

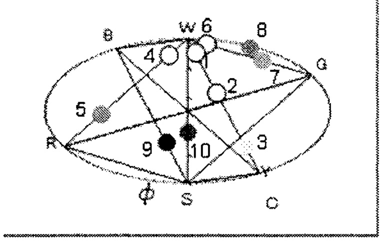

no.	NCS values	no.	NCS values
1	0010-Y	6	0015-G
2	0040-Y	7	0060-G
3	0080-Y	8	0080-B70G
4	0015-R	9	7030-B
5	0070-R	10	6500

Figure 7. 10 colors used in section 4.1 and 4.2

where Δs_v is the "correlated blackness difference" actually representing the difference Δv of NCS lightness v, $\Delta\phi$ is the difference of original hue ϕ, and the brackets [ ] represents a function to take out the positive value of the arguments.

In our terms of color distance, GT will be represented by

$$GT^* = 10 \times \{\max(|\Delta v|, (1/4)d_{\mathrm{NCS}}/100)\}^{0.4} \quad (9)$$

(One may adopt $\{|\Delta v| + (1/4)d_{\mathrm{ch}}/100\}^{0.4}$ for GT^* instead of the above expression.)

In the definition of GT^* the coefficient (1/4) in front of d_{NCS} comes from Godlove's evaluation of the scales of the chromatic difference and the lightness difference, and the factor 10 before the brace and the divisor 100 behind d_{NCS} is for adjustment of the scale.

Figure 9 shows good correspondence between GT and GT^* for the same color pairs referred in the previous section. It is noted that GT is derived from experiments while GT^* is a theoretical result. Furthermore, GT^* has clear perceptual meaning that "the distinctness of border between juxtaposed regions is determined by the larger value of the lightness difference or the NCS color distance."

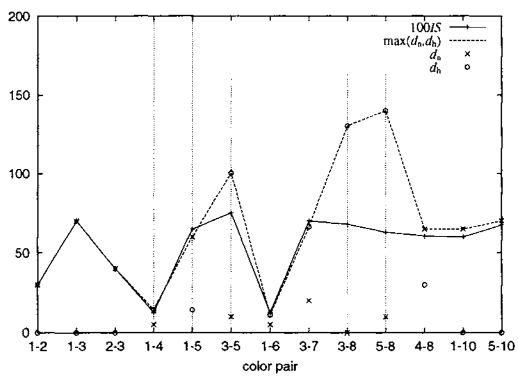

Figure 8. comparison with IS

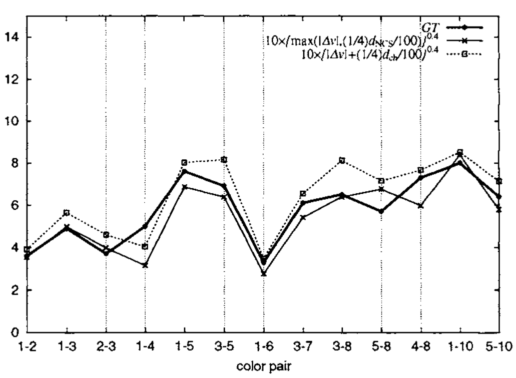

Figure 9. comparison with GT

5. CONCLUSION

Some mathematical distances between color specification values of NCS are constructed. The distance, a kind of city block distance, does not corresponds to color difference in uniform color spaces but expresses a perceptual color difference. Using the concept of color distance, the distinctness of border, which is an experimental measure, can be theoretically represented. The proposed color distance will be useful for any application that requires a perceptual color difference in NCS.

REFERENCES

1. Swedish standard SS 01 91 00E, colour notation system, 1990.
2. A.Hård and L.Sivik: A theory of colors in combination – a descriptive model related to the NCS color-order system, *Color Res.Appl.*, Vol. **26**, No. 1, pp. 4–28 (2001).
3. Y. Nayatani: A hue rectangle and its color metrics in a modified opponent-colors system, *Color Res.Appl.*, Vol. **27**, No. 3, pp. 171–179 (2002).

Color Coordinate Conversion Using Neural Networks and Its Application

Atsushi OHTA* and Shoji TOMINAGA*
Osaka Electro-Communication University
Department of Engineering Informatics, Neyagawa, Osaka 572-8530, Japan

ABSTRACT

We describe a color management system for displaying color-notation systems on a calibrated monitor based on the neural network technique. First, we discuss two color-notation conversions between the Munsell and CIE color systems, and between the NCS and CIE color systems. The conversion algorithms using neural networks are developed for both directions of Munsell-to-L*a*b* and L*a*b*-to-Munsell, and then for both directions of NCS-to-L*a*b* and L*a*b*-to-NCS. The performance of the algorithms is examined using the databases of Munsell and NCS colors. Next, images of the color systems from arbitrary viewing directions are rendered as 3D images by using computer graphics techniques. The images of a color system are represented with a set of 3D color patches, which are displayed on a calibrated monitor. Color reproduction on a CRT monitor is done with a look-up table and a color conversion matrix. An interactive rendering system is developed based on Open GL for displaying three-dimensional images of the color systems in real time.

1. INTRODUCTION

Color coordinate conversion among a variety of color systems is crucial for color image processing and color management. The color conversion often requires a complicated nonlinear mapping between two color spaces. For instance, no equations have been defined for specifying a direct mapping between Munsell and CIE color systems, but a data table has been published that indicates the relationship between the two color spaces [1][2]. The conversion was usually carried out by a three-dimensional interpolation technique to the table data [3]. Recently we proposed a neural network method, which takes an advantage of small amount of data storage instead of the table data [4]. The neural network technique was then extended to the problem of color management including conversion between a color specification system and device coordinate system [5].

The present paper describes a color management system for displaying color-notation systems on a calibrated monitor based on the neural network technique. First, we discuss two color-notation conversions between the Munsell and CIE color systems, and between the NCS and CIE color systems. The conversion algorithms using neural networks are developed for both directions of Munsell-to-L*a*b* and L*a*b*-to-Munsell, and then for both directions of NCS-to-L*a*b* and L*a*b*-to-NCS. The performance of the algorithms is examined using the databases of Munsell and NCS colors.

Next, the color-notation systems are rendered as 3D images by using computer graphics techniques. For this rendering, we represent the color spaces by arranging a set of color patches in a 3D space, and determine the color values of the respective color patches. The 3D color patches are then displayed on a calibrated CRT monitor. The color reproduction on the monitor is done with a look-up table and a color conversion matrix. The 3D color spaces can be rendered under the arbitrary condition of viewing direction. A system for interactively manipulating the computer graphics images is developed by using OpenGL.

2. STRUCTURE OF COLOR SYSTEMS

2.1 NCS Color System

The Natural Colour System (NCS) is a logical color coordinate system developed in Sweden. The display algorithm is based on the opponent-color theory proposed by Hering. NCS has the six primary colors of W (white), S (black), Y (yellow), R (red), B (blue), and G (green). The color notation is determined based on the composite ratio of these primaries for a given color from a perceptual point of view. For instance, the hue of composite ratio Y=30% and R =70% is expressed as ϕ=Y70R. ***Figure 1*** depicts the hue circle of NCS.

Arbitrary color is defined by the hue ϕ and the three attributes of whiteness W, blackness S, and chromaticness C. ***Figure 2*** depicts the color triangle by W, S, and C. It is a vertical section cut through the sphere. The vertical center core is the gray scale from W (at the top) to S (at the bottom). The height of this triangle is 100. For any inner point of the triangle, a sum of distances (w+s+c) to three sides from the point becomes 100. We have always $w+s+c=100$. So, if s and c is decided, then w is automatically decided. Thus usually w is omitted. For example, then w=30, s=20 and c=50, the coordinate is expressed as sc=2050. Moreover when ϕ=Y70R, the NCS notation is expressed as sc-ϕ=2050–Y70R. The color sphere of NCS forms a rotated double-cone, where W and S are the two tops of cones. The circumference of the cone has the maximal c.

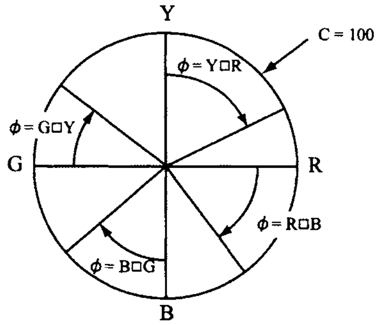

Figure 1 *Hue circle in NCS.*

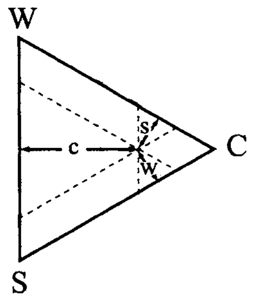

Figure 2 *Color triangle in NCS.*

2.2 Munsell Color System

This color system is defined in terms of three perceptual attributes of Hue, Value, and Chroma. It uses cylindrical coordinates. Hue is structured by ten sectors R, YR, Y, GY, G, BG, B, PB, P and RP. Any sectors are furthermore divided to 10 sectors. Thus Munsell Hue (H) is divided into100 sectors. A chromatic color is expressed with N. Value indicates the lightness of color. The scale of value ranges from 0 for pure black and 10 for pure white. Chroma is the degree of departure of a color from the neutral color of the same value. Colors of high chroma are called to be highly saturated. ***Figure 3*** shows an example of a hue sector. Note that the maximal chroma value differs at different hue and value. The Munsell system is related with the CIE 1931 color specification system in a table data. This table is used for conversion between Munsell HVC and CIE xyY.

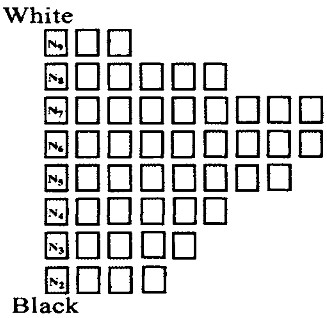

Figure 3 *Example of hue sector.*

2.3 CIE-L*a*b* Color System

This color system provides a perceptually uniform color system specified by CIE. The details of this system are described in many textbooks on color science. The three-dimensional color space is defined as a rectangular coordinate system of three quantities L*, a*, and b*. The three quantities are transformed from the tristimulus values in the following equations.

$$L^* = 116\left(\frac{Y}{Y_n}\right)^{1/3} - 16, \quad a^* = 500\left[\left(\frac{X}{X_n}\right)^{1/3} - \left(\frac{Y}{Y_n}\right)^{1/3}\right], \quad b^* = 200\left[\left(\frac{Y}{Y_n}\right)^{1/3} - \left(\frac{Z}{Z_n}\right)^{1/3}\right], \qquad (1)$$

where $X_0Y_0Z_0$ are the tristimulus values for reference standard white.

3. NEURAL NETWORK CONVERSION

3.1 Network Structure

A multilayer feedforward neural network is used at the heart of color coordinate conversion. ***Figure 4*** depicts the network structure. The present network consists of an input layer, three hidden layers, and an output layer. Every unit sends its output to higher layers than its own, and receives its input from lower layers than its own. Therefore signals always pass forward.

Given an input vector, a unit computes a simple nonlinear function to produce an output that represents a level of activation for the unit. Let o_i be the output of the unit i in the prior layer, w_i be the weighting coefficient of connection from unit i to next unit, and *offset* be the bias term of the unit. The input to next unit is then described as the sum of the weighted outputs from the prior layer

$$X = \sum_i (o_i \cdot w_i) + offset \qquad (2)$$

The nonlinear output of next unit is

$$o_j = f(X) \qquad (3)$$

where f is an activation function . In this study we use the sigmoidal activation function $f(X) = (1 + \exp(-4\alpha X))^{-1}$. This function takes any real number in the interval [0,1], and the positive constant α represents the slope of f at $X = 0$.

The number of two hidden layers is determined empirically. The knowledge of mapping from input to output color space is stored in the network in the form of weights in all the connecting links. For simplicity we normalize all the input/output signals of the network. Concerning the input signals, the original data are transformed into the interval [-1, 1]. On the other hand the output signals are normalized into [0,1].

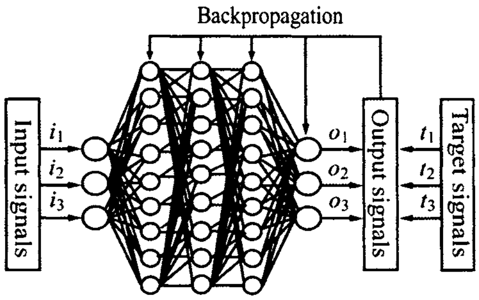

Figure 4 *Neural network structure and learning.*

3.2 Network Learning

Learning is the process of determining a set of weights and biases that produces a desired response to an input color vector. We adopt the learning rule of Error Back-Propagation [6]. In the present learning rule, the error is propagated backward through the network from the output layer to the input layer, in order to minimize the overall error.

We use the two tables given by Newhall et al. [7] as the original data of the Munsell renotations and the table by the Swedish Standard Institution [8] as the original data of NCS. Half the original data were used training the networks. We sample the original tabulated data at every other point so that the samples are distributed uniformly in the Munsell space and NCS space. The numbers of training data are 2089 for Munsell with C<36 and 1585 for NCS. For the purpose of effective network conversion, all the table data of (x, y, Y) are transformed into the equivalent CIE-L*a*b* coordinates, so that the color conversion by neural networks are carried out between Munsell and L*a*b* spaces and between NCS and L*a*b* spaces. One period of presenting the entire training data is defined as an epoch. Training is iterated for as many epochs as are necessary to decrease the mean squared error to an acceptable level.

The color differences between the estimated coordinates and the originals are calculated for all the test data where training was continued for 40000 iterations (epochs). Data for testing the reliability of the network conversion are chosen from the remaining original data set after removing the training data.

3.3 Pre-Processing

The Munsell coordinate system uses cylindrical coordinates in Munsell Hue (H), Value (V), and Chromaticness (C) as in the notation HV/C. For computational convenience, we describe this space in rectangular coordinates of (V, A, B) defined by

$$V = V, \quad A = C \cdot \cos(2\pi H/100), \quad B = C \cdot \sin(2\pi H/100), \qquad (4)$$

where the hue H is denoted as a real number ranging $0 \le H \le 100$. The NCS coordinate system is a type of cylindrical coordinate system in Hue (ϕ), Blackness (s), and Chromaticness (c) as in the notation Sc-ϕ. Therefore, in the same way as Munsell, we describe the NCS system in rectangular coordinates of (S, a, b) defined by

$$S = s, \quad a = c \cdot \cos(2\pi\phi/400), \quad b = c \cdot \sin(2\pi\phi/400), \qquad (5)$$

where ϕ is denoted as a real ranging $0 \le \phi \le 400$. Thus, all the network conversions are done between (V, A, B) and (L*, a*, b*) and between (S, a, b) and (L*, a*, b*).

3.4 Performance

Figure 5 shows the learning behavior of the networks in the Munsell-to-L*a*b* conversion. The curve represents the rate of decrease of the mean squared error (system error) on L*, a*, and b* as the iteration (epoch) increases. The system error converges around 40,000 iterations. So all the network trainings were continued for 4000 iterations. Data for testing the conversion by the networks are chosen from the remaining original data set after removing the training data. The numbers of test data are 1770 for Munsell and 1499 for NCS. The conversion accuracy is evaluated using the CIE-L*a*b* color difference. ***Table 1*** list the test results of conversion accuracy in the average value of ΔEab for all conversions of Munsell-to-L*a*b*, L*a*b*-to-Munsell, NCS-to-L*a*b* and L*a*b*-to-NCS. In the table, the α values denote the most proper values for the slope of the sigmoidal function.

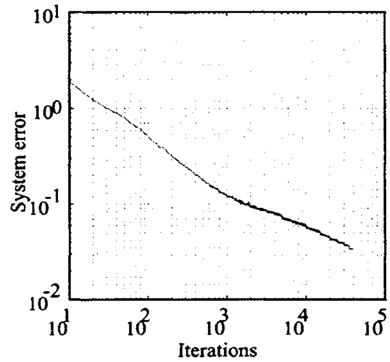

***Figure 5** Learning behavior in Munsell-to-L*a*b*.*

***Table 1** Conversion accuracy*

type	α	ΔEab
Munsell-to-L*a*b*	0.64	0.839
L*a*b*-to-Munsell	0.61	0.810
NCS-to-L*a*b*	0.40	1.465
L*a*b*-to-NCS	0.54	0.227

4. 3D GRAPHICS OF COLOR SPECIFICATION SYSTEMS

4.1 Display Calibration

We use a CRT monitor for displaying three-dimensional images of color specification systems. The characteristics of the CRT monitor are expressed in the triplet of the CIE chromaticity coordinates (x, y) and the luminance Y for three primaries of RGB phosphors. Color reproduction on the monitor consists of two steps of (1) color coordinate transformation and (2) Gamma correction. First, the target tristimulus values XYZ are transformed into the monitor RGB values at a resolution of 8 bits (256 levels). This transformation is represented as $[R \quad G \quad B]^{\mathrm{T}} = \mathbf{M}^{-1} \cdot [X \quad Y \quad Z]^{\mathrm{T}}$ with a conversion matrix $\mathbf{M}$,

$$\mathbf{M} = \begin{bmatrix} x_R/y_R & x_G/y_G & x_B/y_B \\ 1 & 1 & 1 \\ (1-x_R-y_R)/y_R & (1-x_G-y_G)/y_G & (1-x_B-y_B)/y_B \end{bmatrix} \cdot \begin{bmatrix} Y_{R\max}/255 & 0 & 0 \\ 0 & Y_{G\max}/255 & 0 \\ 0 & 0 & Y_{B\max}/255 \end{bmatrix}, \qquad (6)$$

where $(Y_{R\max}, Y_{G\max}, Y_{B\max})$ are the maximal luminances of three primaries. Next, these RGB values are corrected into the practical monitor RGB digital values by a lookup table. We examined the performance of color reproduction for many color patches and evaluated the accuracy in the average L*a*b* color difference. We have ΔEab of about 2.0.

4.2 Rendering Color Systems

We have developed an interactive rendering procedure based on Open GL for displaying three-dimensional images of the color systems in an arbitrary viewing direction. OpenGL is useful as graphics library for real-time rendering [9]. It is an application program interface (API) to access directly graphics hardware. A set of functions in the OpenGL library are used for creating three-dimensional geometric models in a 3D virtual space, and determining color value at each pixel on an image plane.

The images of a color system viewed from an arbitrary direction can be rendered in real time. We can create a variety of image by operating a mouse. Simple mouse operations can execute several image operations such as expansion, reduction, movement, and change in viewing direction. This system provides a browsing system for understanding the color system. The Z-buffer algorithm is used as 3D rendering including detection of hidden surfaces. Each coordinate point in the color system is represented by a small color cube. The input data for these color cubes are the 3D coordinate values in the rectangular system of (V, A, B) and (S, a, b). These data are transformed into the calibrated monitor (R, G, B) values. ***Figure 6*** demonstrates some of computer graphics images of NCS created by the above procedure. Moreover ***Figure 7*** demonstrates the two images in top and side views for the Munsell color system. These images are helpful in understanding the features of the respective color order systems.

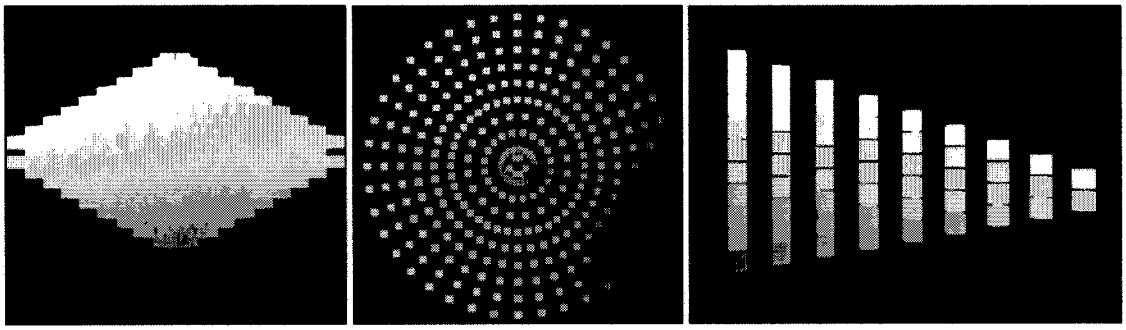

(a) Side view *(b) Top view* *(c) Color triangle for Y10R*

***Figure 6** Computer graphics images of NCS*

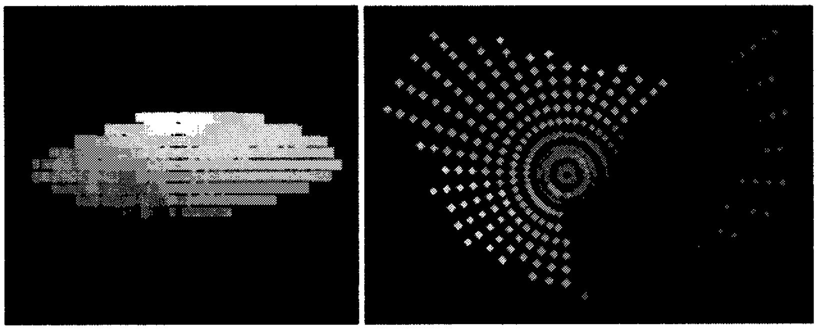

(a) Side view *(b) Top view*

***Figure 7** Computer graphics images of Munsell.*

5. CONCLUSION

A color management system was described for displaying color-notation systems on a calibrated monitor based on the neural network technique. First, we have developed the conversion algorithms using neural networks for both directions of Munsell-to-L*a*b* and L*a*b*-to-Munsell, and then for both directions of NCS-to-L*a*b* and L*a*b*-to-NCS. Next, images of the color systems from arbitrary viewing directions were rendered using computer graphics techniques. An interactive rendering system was developed based on OpenGL for displaying 3D images of the color systems in real time.

6. REFERENCE

[1] G. Wyszecki and W.S. Stiles, *Color Science*, 2nd edn. Wiley, 1982.
[2] Swedish Standard Institution, *Colour Atlas SS 01 91 02*, NCS, 1982
[3] N.S. Smith, T.W.A. Whitfield, and T.J. Wiltshire, A colour notation conversion program, *Color Res. Appl.*, **15**, pp.338-343, 1990.
[4] S. Tominaga, Color notation conversion by neural networks, *Color Res. Appl.*, **18**, pp.253-259, 1993.
[5] S. Tominaga, Color coordinate conversion via neural networks, In L.W. MacDonald and M.R. Luo (eds.), *Color Imaging*, Wiley, Ch.9, 1999.
[6] D.E. Rumelhart, G.E. Hinton, and R.J. Williams, Learning internal representations by error propagation, in *Parallel Distrihbute Processing*, D.E. Rumelhart and J.E. McClelland, Eds., MIT Press, Vol.1, Ch.8, 1986
[7] S.M.Newhall, D. Nickerson, and D.B. Judd, Final report of the OSA Subcommittee on spacing of the Munsell colors, *J. Opt., Soc. Am.*, 33, pp385-418, 1943.
[8] Swedish Standard Institution, *CIE tristimulus values and chromaticity coordinates for the colour samples in SS 01 91 02*, 1982.
[9] D.Rogelberg, *OpenGL Reference Manual*, Addison-Wesley, 1992.

* Correspondence: oota@tmlab.osakac.ac.jp; shoji@tmlab.osakac.ac.jp: phone +81-72-820-4562; fax +81-72-824-0014; Tominaga lab., Osaka Electro-Communication Univ., Neyagawa, Osaka 572-8530, Japan.

BLACKNESS, WHITENESS, CHROMATICNESS: FORMULAS FOR HIGH VISIBILITY IN THE MODERN CITY

Galen Minah, College of Architecture and Urban Planning, University of Washington, Seattle, Washington, U.S.A.

"If you want to know all about Andy Warhol, just look at the surface: of my paintings and films and me, and there I am. There's nothing behind it." Andy Warhol

INTRODUCTION

In most cities of the world, particularly those associated with western culture, buildings which had significance to their society, were treated architecturally as figural elements in contrast to their background urban fabric. These buildings were those that expressed the values of the civic realm and included the main center of worship, the center of government, and often other civic institutions. As monuments, these structures had meaning to their societies and cultural values were expressed in the architectural design. Since the late middle ages in Europe these buildings were usually the largest and tallest, the most richly ornamented, and sited in strategic locations within the city to ensure high visibility and prominence. These sites were at the end of major axes, on top of hills within the city, and dominant structures on major piazze, or significant public places. These structures were often the organizing elements within the city, and often created a strong hierarchical symbolism that was characteristic of the political structure of these urban centers. In modern cities, the most visible structures are commercial office towers, which express values associated with our consumer culture. They do not express the civic realm as significant institutions, but, like the earlier civic architecture, their power is carried by their image. They strive to be visually dominant in cityscapes where there is fierce competition for this dominance, and they must use a range of visual design tools to achieve this goal.

Historical Context

Color has always played a role in the figural status of these structures. Since the 13th century, two significant structures dominated the cityscape of Sienna, Italy. The main cathedral, clad in alternating bands of white and dark green marble, had a tall campanile and was sited at the highest elevation in the city. This structure appeared otherworldly within the context of darker brick and stone city, and symbolized the spiritual realm. The city hall was also dominated by an impressive tower and located on the main piazza. The materials, however, were brick and gray stone, similar to the rest of the city, symbolizing the temporal realm. The two towers were highly visible and they represented the core of this society.

The Industrial Revolution brought cultural upheaval to cities. New materials, advances in engineering and, particularly the growth of new institutions were changing the appearance of cities. The values associated with significance in architecture were also changing. Most architects were looking to historical precedents for the physical expression of these new institutions, but others, such as the Italian Futurists, were seeking new forms of expression which had no connection to the past, and saw the future of architecture in the dynamism of engineering and industry.

Modern Movement

The Modern Movement envisioned architecture as universal – built of mass-produced materials such as steel and glass, and based upon an aesthetic that expressed function and structure, free of ornament, and stripped of any reference to historical precedents or cultural symbolism. This architecture became known as the 'International Style', which has dominated the architecture of the 20th century. It celebrated the primacy of form and function, structural expression, and the unadorned use of natural materials, which determined the color palette for most of these structures. Significant architecture within the urban fabric achieved its status through plastic form and scale. The critical institutions, usually lost in the grid planned cities, were hard to distinguish from other public structures. The most figural buildings were the corporate office towers.

Postmodernism

A change occurred when Robert Venturi, *Complexity and Contradiction in Architecture*, 1966, and *Leaning from Las Vegas*, 1972, attacked the elitist position of mainstream modern architecture. He advocated pluralism and eclecticism. His quote 'messy vitality over obvious unity' became the theme for postmodernism in art as well as architecture. Venturi's interest in such phenomena as the Las Vegas strip, billboard cluttered arterials, and 'main street', inspired him to find in this garish display all of the symbolism and richness eliminated in cities by the Modern Movement. This was the beginning of Postmodernism in architecture, as well as art. Historical precedents, pluralism, local and regional identity, as well as color and ornament, returned to the architecture of the modern city. This began new attitudes toward architectural expression, and fit the values of post-industrial societies driven by consumerism and capitalism. Mass media and advertising recognized the power of image in architecture, and through their influence the appearance of big buildings, as well as cities, began to change.

In the decades since the 1960's, postmodern theories have called into question the role of significance in architecture of the city. Visibility and recognizable imagery are the principal characteristics of figural urban structures. In both art and architecture, this imagery can be experienced more effectively in visual media than viewing the object in real life. The potential of this photographic imagery can be seen in the effect the Sydney Opera House has had upon the marketing of Sydney, and Australia, as a major tourist destination. The potential for color in this imagery was demonstrated by the artists Christo and Jeanne Claude whose large scale work in the environment is known throughout the world by the photography of this work. In earlier work, white fabric was used to wrap large-scale objects, but in 'Surrounded Islands in Biscayne Bay, 1980, they used a pink fabric which was presented in aerial photography. The power of this color in the landscape was very apparent.

INVESTIGATION

This study investigates other major urban centers throughout the world, and identifies structures in these cities that achieve high visibility through the use of color. These observations were recorded from aerial and eye-level photographic images of these cities. Most occur in conditions of daylight at midday in clear atmosphere, but represent a context, which display color in a manner envisioned by the architects of these buildings. It was noted that the color in these structures was similar to figural colors in the Seattle cityscape, and, like Seattle, tended toward whiteness, blackness, or chromaticness. Within each city, however, there were variations in the background colors within the urban environment, and by measuring this color context it is possible to predict what color values might achieve figural status in this context. In an earlier investigation, *Figural Color in the Seattle Cityscape*, Minah, 1997, colors of significant figural structures were studied in Seattle, Washington. The change in these colors due to the varying light and atmosphere in the predominantly overcast skies of the Pacific Northwest was recorded. Colors observed were those that demonstrated strong light-dark contrast within their color field, and those that achieved high figural status through hue contrasts. Within this group the relationship between figural status and the level of chromaticness was observed.

Urban Context

The most important factor affecting high visibility through the use of color in modern cities is that the vast majority of larger buildings, which dominate these cities, were designed and built in the late 20th century and are, therefore, strongly influenced by the restrictive attitudes toward color of the Modern Movement. The large buildings demonstrated the primacy of architectural tectonic form displayed in materials in neutral colors of low blackness (s =10-30) and low chromaticness (c =10-40). Visibility is commanded by sculptural presence rather than by color juxtaposition with its surrounding context. Figural structures in these urban environments are, therefore, the largest or tallest structures. Buildings of lower status, and budgets, often use color as a means of competing for visibility. To achieve high visibility in cities today, however, form alone will not create figural dominance. Architects must combine form with color, pattern, and texture.

Methodology

This study identified parts of a number of cities, which represented typical urban contexts. The mean hue and nuance was approximated by mounting photographs on a spinning disc and measuring the most dominant blended color. Photographs of this context were made purposefully out-of-focus to create a blurred color field that could also be measured. This was compared to the previous measurement. These nuances give an approximation, which, for this study, were adequate. Locating the nuance of this hue on an NCS color triangle, and inscribing a circle by using this nuance as the center (x), and the distance to the nearest leg of the color triangle as the radius, a circular 'context area' (Ax) can be identified. Colors in the context area will appear as background. If (x) is the center of the color triangle (S3333), the inscribed circle will have the maximum radius, and be tangent to three sides of the triangle. For context areas with a smaller radius, drawing lines parallel to the remaining sides, tangent to the circle representing the context area (Ax), a smaller triangular figure is produced. This study predicts that colors located between the context area (Ax) and the three apexes of the triangle will be figural color (F) in the areas of whiteness (Fw), blackness (Fs), and chromaticness (Fc). Context areas (Ax) in Seattle, San Francisco, and Rome show different ranges of figural colors. A smaller context area will define a closer range of context colors, and, therefore, figural colors can be achieved within a smaller range of nuance. (Figures 1-3).

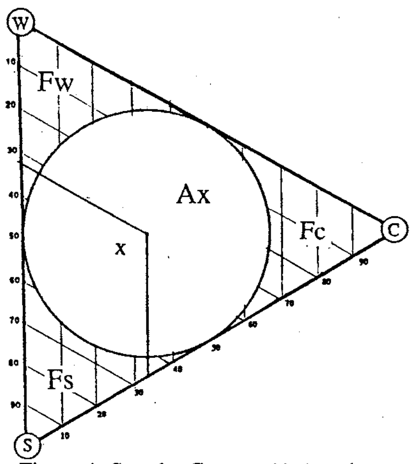

Figure 1. Seattle. Context (Ax) and figural colors (F). Context center (x) 3333 Y80R.

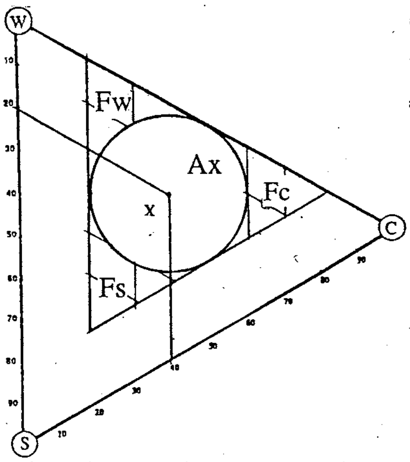

Figure 2. Rome. Context (Ax) and figural colors (F). Context center (x) 2040 Y20R.

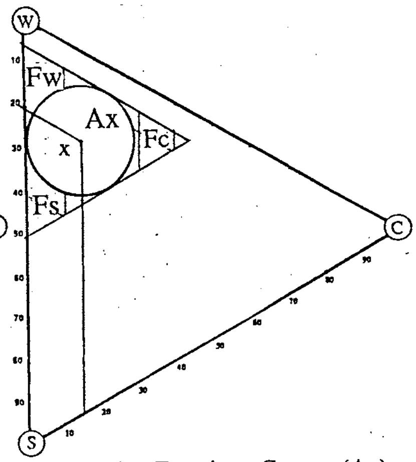

Figure 3. San Francisco. Context (Ax) and figural colors (F). Context center (x) 2015 R.

FIGURAL PHENOMENA

Color Constellations

In a view of Sao Paulo, Brazil, one of the densest cities in the world, there are many dark towers in hues of s = 70 and above. Other clusters of buildings show a repetition of red (1030 – 1040 R), and still other color clusters are visible in this cityscape. These clusters often form color constellations where the group of these similar colored surfaces forms a dominant figure. The color constellation is a powerful tool in creating high visibility within an urban environment. In a previous study, *Color Constellations in the Seattle Cityscape*, Minah, 2001, it was observed that the higher the chroma of similar hues in a color constellation, the more distinct it became. These colors advanced and appeared to float in a plane removed from the objects they were part of. Hue variations in color constellations were 20% or less, and nuance variations were 10% or less. Large cities have many buildings of similar figural colors and they tend to group in these clusters, thus reducing their figural status. Based upon visual observation, in order for one element of a color constellation to become dominant, it must be approximately twice the combined area of all other elements in the constellation. Constellations formed by vertical elements, the dominant element must be approximately twice as high as the next tallest structure.

Figural Texture, Figural Pattern

As one experiences an urban environment from the view of a pedestrian within the city, color becomes less of a factor in figural dominance. Characteristics of form, texture, and pattern usually prevail. Design that accentuates the continuity of the building skin and minimizes the texture of windows, or spatial characteristics of the facade (i.e. Disney Concert Hall, Los Angeles, Frank Gehry, 2001) (Figure 4), will usually become visually dominant from this perspective. Tall buildings in a number of cities have used large scale patterns of intersecting lines, or giant frames to create a new sense of scale in the cityscape that appears larger than that of the urban context. The patterns are the visual element that give theses buildings their figural dominance. In visually complex settings such as a Tokyo streetscape, white horizontal stripes on a black surface can be figural (Figure 5).

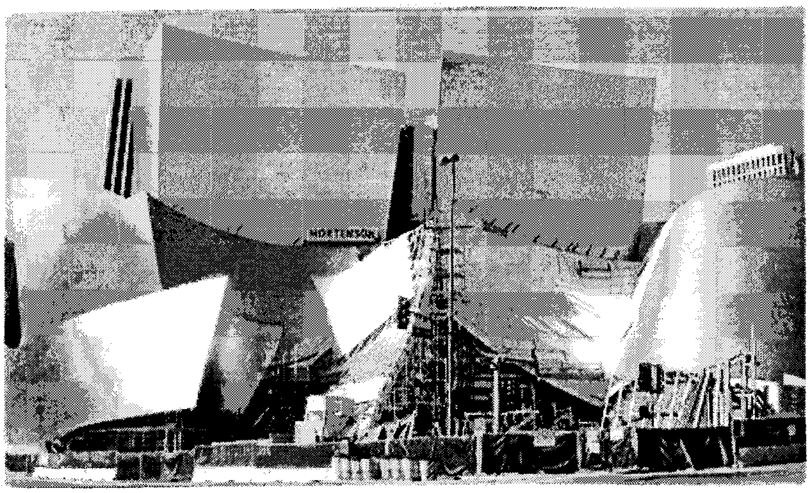

Figure 4. Figural texture. Disney Concert Hall, Los Angeles, by Frank Gehry.

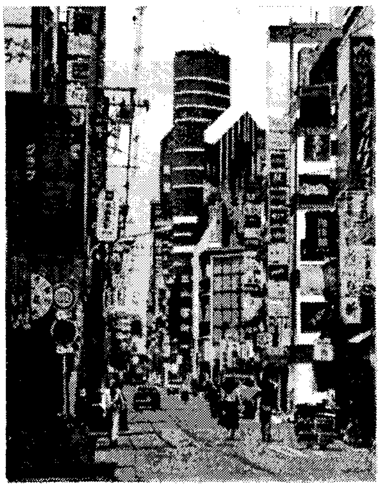

Figure 5. Figural pattern. Ichiban-kan in the Shinjuku district, Tokyo.

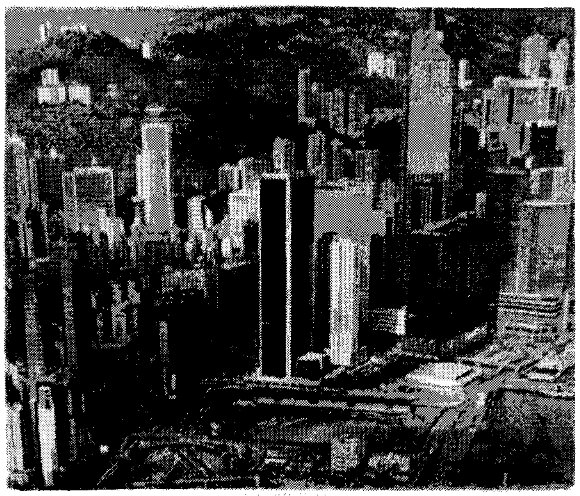

Figure 6. Superfigure in Downtown Hongkong.

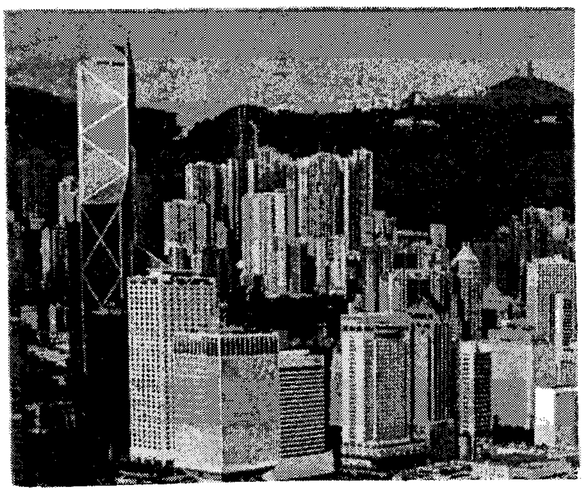

Figure 7. Superfigure. Bank of China Tower, Hong Kong.

Superfigure

A 'superfigure' is a structure in an urban environment that becomes a dominant figure in a field of other figural structures. These buildings are so effective in their visual dominance that other figural buildings appear as background. Superfigures are present in many cities, although some require the right vantagepoint in optimum light conditions. Superfigures achieve their dominance by 1) using figural colors (Fw, Fs, and Fc) in combination, and 2) combining figural color with figural pattern. These characteristics in concert with building form create objects that stand alone in their dominance as seen in the cityscape of Hong Kong (Figures 6, 7).

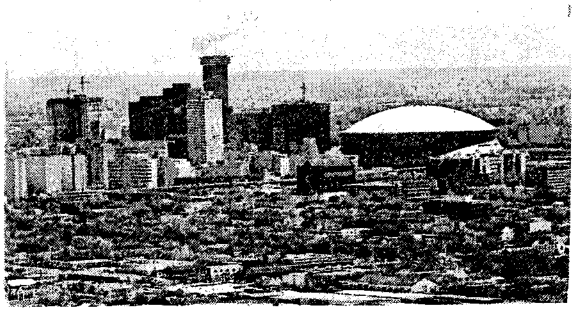

Figure 8. White dome as figure, New Orleans.

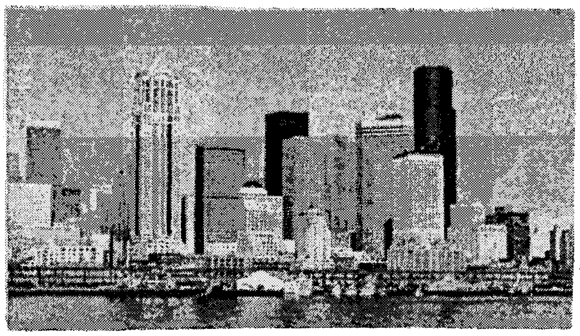

Figure 9. Black tower as figure. Seattle.

CONCLUSIONS

Colors approaching whiteness, blackness, and chromaticness are the most effective in creating high visibility in modern cities. The choice of which figural color from the three areas will create maximum visibility is determined by other contextual factors including site, building type, light, and atmospheric conditions. General considerations are as follows: **Whiteness.** Whiteness has been used to create high visibility since the period of Neoclassicism, particularly in monuments and significant architecture. White achieves its figural status primarily through its light reflectance and is most visible when seen against a darker ground – which in cities is the context of the urban environment. Since many lighter hues appear in modern cities, the most visible architecture must have large, continuous areas. Shade, shadow, and window texture will diminish the power of white as a figural color. In modern cities the most visible white structures are the roofs of white domed stadiums (Figure 8), being large horizontal unbroken surfaces facing the sky, reflecting maximum light. Whiteness is the most effective figural color in lower light conditions, such as overcast sky, fog, or haze, and is particularly dominant in low angle sun light at dawn or sunset. **Blackness.** Black and hues low in (s) are best seen against lighter color fields. Towers, seen against sky, are most effective. Black is relatively unchanged by shade, shadow, and window patterns and textures. At a distance black towers appear as giant monoliths without scale (Figure 9). In lower light levels and overcast sky, fog, or haze, and by atmospheric perspective at a distance they tend to appear lighter and lose their figural status. **Chromaticness.** From studies in the Seattle cityscape, and in observing images from many cities throughout the world, chromaticness is usually the variable, which achieves the highest figural status in an urban context. This is due to the paucity of high chroma (c) in large structures in most modern cities. High values of (c) are seen to a large extent in smaller building surfaces, signs, billboards, vehicles, and on parts of buildings in retail and commercial streetscapes where graphics and advertising are prominent. When used in larger buildings, high (c) values of are extremely effective in creating figural dominance (i.e. Pacific Design Center, 'Blue Whale', 1971, Los Angeles). The use of high chroma on the surfaces of skyscrapers is used rarely, but has great potential for high visibility.

References

Bognar, B., The New Japanese Architecture, Rizzoli, N.Y., 1990.

Gleason, D., Over New Orleans, Cameron and Co., San Francisco, 1985.

Kjurokawa, K., New Wave Japanese Architecture, Academy Editions, London, 1993.

Minah, G., Figural Color in the Seattle Cityscape. AICColor 97, CSA, Kyoto,1997.

Minah, G., Color Constellations in the Seattle Cityscape, AIC 2001, SPIE, Rochester, 2001.

Roberts, D., Over Hong Kong, Pacific Century Publishing, Hong Kong, 1996.

Sandler, I., Art of the Postmodern Era, Icon Editions, N.Y., 1996.

Toy, M., World Cities: Los Angeles, Academy Editions, London, 1994.

A STUDY ON THE DESIGNATION OF MUNSELL NOTATION FOR KOREAN COLOR NAMES

Youn Jin Kim, Hong-Suk Kim, Seung-Ok Park
Department of Physics, Daejin University, Korea

Principal Contact: Youn Jin Kim
Phone: +82-31-539-1832 Fax: +82-31-539-1830
e-mail:younkim2003@yahoo.co.kr

ABSTRACT

The psychophysical experiment was carried out to designate Munsell notation for Korean color names. Twenty Korean university students who consist of nine males and eleven females took part in the experiment. Munsell color chips were displayed on a calibrated CRT monitor and the subjects were asked to answer which ones are matched to the given color names. Eight color names were selected from the names of non-luminous object color in Korean Industrial Standard KS A 0011. The results were compared with the Munsell notation designated in KS A 0011 and ISCC-NBS system of color names.

INTRODUCTION

This study aimed to designate the Munsell notation for Korean color names. Color can be described in many ways due to the cultural differences. Many studies have been carried out to investigate the differences in color naming between the different languages. For example, Lin[1, 2] researched the cross-cultural color naming study between the English and Mandarin. Jiyima[3] also did study the cultural factors of color naming in Japanese. It is important to standardize the description of Korean color names. This study was carried out to find the Munsell notation corresponding to Korean eight color names and those were compared with KS A 0011[4], color regions of the CIE chromaticity diagram (from Judd DB) and ISCC-NBS Color Names.

EXPERIMENTAL DESIGN

The eight Korean color names selected for this study are; Bbalgansaek, Noransaek, Noksaek, Paransaek, Boraseak, Pink, Olive, and Brown. Those color names were translated to English color names; red, yellow, green, blue, purple, pink, olive and brown, respectively in Korean Industrial Standard KS A 0011.

The images were processed on a Windows operating PC equipped with an NVIDIA GeForce series video graphics adapter. A Samsung CRT monitor of model number Sync Master 750p(T) was used for displaying the images. The monitor resolution was set to 1024x768 pixels at 80Hz frequency, and 24 color bits per pixel. Using monitor on screen display controls, the brightness and contrast were initially set to 50 and 90, respectively. The monitor was calibrated daily and the white point was set to 6500K. Other monitor characteristics were controlled following the sRGB reference conditions. More than two hours were taken for warming up and stabilizing the monitor. The viewing conditions were the daylight office situation. The sRGB input values for 1181 Munsell color chips were calculated using color space transformation software, and then 40 constant hue pages of Munsell color chips were displayed on the calibrated CRT monitor in random order. The Munsell hue of each page was not known to subjects. The surround of the color chips on the monitor screen was filled with neutral gray having the RGB DAC count of (127, 127, 127). They were asked to answer which ones are matched to the given color names. The subjects consisted of nine males and eleven females and were all students of the Daejin University in Korea. They were an average of 25 years old. It took approximately 30 seconds to choose each color, and the whole process lasted about 5 minutes for each subject.

The Munsell hue, value, and chroma of color chips checked by subjects were transformed to x, y, Y and their mean values for twenty subjects were calculated and retransformed to HV/C using the Color Space Conversion Program[5].They were compared with KS A 0011, color regions of the CIE chromaticity diagram (from Judd DB), and ISCC-NBS Color Names.

RESULTS AND DISCUSSION

Table 1 shows the experimental results for eight Korean color names. The first column of Table1 shows the color names and the next three columns show the mean Munsell notation for males, females, and total subjects, respectively. There was not large discrepancy in the results of males and females. However, especially for olive, 7 males did have no idea about it. The mean of Munsell value and chroma obtained from 2 males was lower than that of females. Besides, for brown, there was some discrepancy in Munsell hue between males and females.

Table 1 also shows an interesting result for basic Korean color names. Red, yellow, and purple color names were matched closely to 5R, 5Y, and 5P Munsell hue. However, green and blue color names were matched to 1G and 2PB Munsell hue, not 5G and 5B Munsell hue.

Table 1. Experimental result for eight Korean color names

Color Name (Korean/English)	Munsell Notation (Mean)		
	Males (9)	Females (11)	Total (20)
Bbalgansaek / Red	6.7R 4.0/15.0	7.0R 3.8/15.3	6.9R 3.9/15.2
Noransaek / Yellow	3.8Y 8.1/13.4	3.2Y 7.9/13.4	3.5Y 8.0/13.4
Noksaek / Green	1.3G 4.5/9.7	9.4GY 4.6/9.7	0.3G 4.5/9.6
Paransaek / Blue	3.6PB 3.8/11.3	1.2PB 4.0/11.3	2.2PB 3.9/11.3
Boraseak / Purple	3.9P 3.5/11.0	2.9P 3.5/11.0	3.3P 3.5/11.0
Pink / Pink	2.2RP 7.3/7.9	3.3RP 7.6/7.6	2.8RP 7.5/7.7
Olive / Olive	1.9GY 3.5/5.8	2.5GY 5.6/7.3	2.4GY 5.3/7.1
Brown / Brown	7.5YR 3.1/6.4	4.4YR 3.7/5.8	5.4YR 3.4/5.9

Table 2 shows the comparison of the experimental results to KS A 0011. The Korean color names are standardized with the range of Munsell Hue, value, and chroma in KS A 0011. The third column of Table 2 shows the values of centroid colors in each range. Some discrepancy was found between experimental results and KS A 0011. In KS A 0011, Red, Yellow, and Brown color names are designated with the lesser Munsell chroma and green and purple color names were more greenish and purplish Munsell hue. All data of color names except olive in the experiment were very close to that of them in KS A 0011.

Table 2. Comparison of experimental result to KS A 0011

	Experimental result	KS A 0011			
	(Mean value)	Centroid Color	Range		
			Hue	Value	Chroma
Red	6.9R 3.9/**15.2**	3.5R 5/10	1R~6R	4~6	8~12
Yellow	3.5Y 8.0/**13.4**	4Y 7.7/10.3	2Y~6Y	7~8.3	8.3~12.3
Green	**0.3G** 4.5/9.6	4G 5.5/10.1	1G~7G	4.5~6.5	8~12.2
Blue	2.2PB 3.9/11.3	1PB 4.8/10.5	7B~4PB	3.7~5.8	8.5~12.5
Purple	**3.3P** 3.5/11.0	7.5P 4.5/10.5	6P~9P	3.5~5.5	8.5~12.5

Table 2. Comparison of experimental result to KS A 0011

	Experimental result	KS A 0011			
	(Mean value)	Centroid Color	Range		
			Hue	Value	Chroma
Red	6.9R 3.9/15.2	3.5R 5/10	1R~6R	4~6	8~12
Yellow	3.5Y 8.0/13.4	4Y 7.7/10.3	2Y~6Y	7~8.3	8.3~12.3
Green	0.3G 4.5/9.6	4G 5.5/10.1	1G~7G	4.5~6.5	8~12.2
Blue	2.2PB 3.9/11.3	1PB 4.8/10.5	7B~4PB	3.7~5.8	8.5~12.5
Purple	3.3P 3.5/11.0	7.5P 4.5/10.5	6P~9P	3.5~5.5	8.5~12.5
Pink	2.8RP 7.5/7.7	2.5R 7/7	2.5R	7	7
Olive	2.4GY 5.3/7.1	7.5Y 3.5/4	7.5Y	3.5	4
Brown	5.4YR 3.4/5.9	5YR 3.5/4	5YR	3.5	4

Fig. 1 shows the experimental data and the color labels applied to various regions of the CIE chromaticity diagram (from Judd DB). The eight large sized symbols present the mean values of all subjects for eight color names. For most color names, the areas of experimental data are consistent with the same name's region of Judd DB. However, the area of green color name located at yellowish green region, and the area of pink color name located at purplish pink region on the CIE x, y chromaticity diagram.

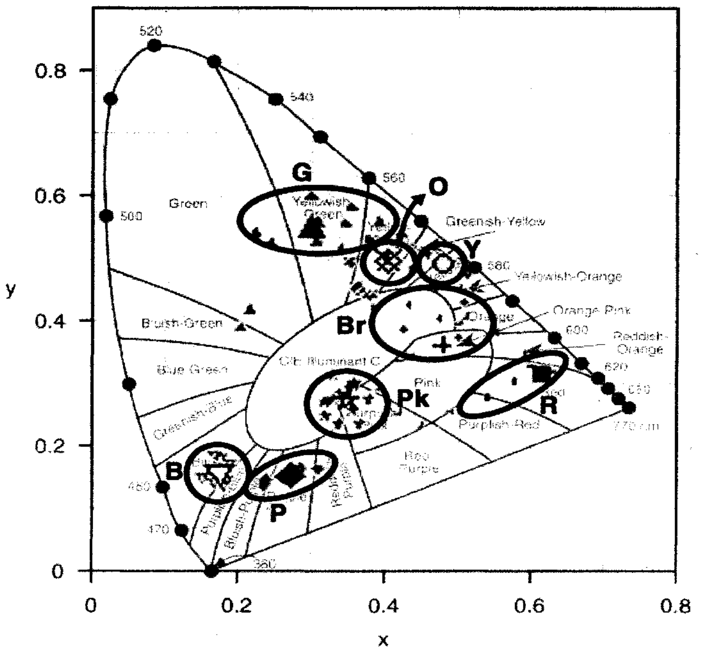

Fig. 1. The experimental data and the color labels applied to various regions of the CIE chromaticity diagram (from Judd DB).

Table 3. Comparison of region

Experiment	Judd DB
Red	Red
Yellow	Yellow
Green	Yellowish Green
Blue	Blue
Purple	Purple
Pink	Purplish Pink
Olive	-
Brown	

Table 4 shows the comparison of the experimental results to ISCC-NBS Color Names. ISCC-NBS Color Names resulted from a comprehensive project designed to apply popular color names to the Munsell colors and thus generated a standard verbal designation for color.

The similar colors to the experimental result of this study are as follows. Red and yellow Korean color

	HV/C	HV/C	No, Color Name
Red	6.9R 3.9/15.2	5R 3.9/15.4	11, vivid red
Yellow	3.5Y 8.0/13.4	3.3Y 8.0/14.3	82, vivid yellow
Green	0.3G 4.5/9.6	1.1G 5.9/11.2	129, vivid yellowish green
Blue	2.2PB 3.9/11.3	2.9PB 4.1/10.4	178, strong blue
Purple	3.3P 3.5/11.0	6.5P 4.3/9.2	218, strong purple
Pink	2.8RP 7.5/7.7	5.6RP 6.8/9.0	247, strong purplish pink
Olive	2.4GY 5.3/7.1	5.4GY 6.0/8.7	117, strong yellowish green
Brown	5.4YR 3.4/5.9	4.6YR 3.5/7.6	55, strong brown

CONCLUSION

The Munsell notation for Korean color names was designated by twenty Korean subjects who consist of nine males and eleven females. The first interesting result is that Green and Blue Korean color names were matched to 1G and 2PB Munsell Hue, not 5G and 5B Munsell Hue.

By comparing the experimental result to KS A 0011, large discrepancy was found in Munsell notation for most color names except blue. Especially, there were some shifts in green and pink Korean color names. Those were located in the yellowish green area and purplish pink area on the CIE chromaticity diagram. Besides, the experimentally designated Munsell notations for Eight Korean color names were compared to ISCC-NBS Color Names. For red, yellow, blue, purple, and brown Korean color names, there were some differences in adjectives of tone. However, for green, pink, and olive Korean color name, there were differences in adjectives both of hue and tone.

REFERENCES

1. Lin H, Luo MR, Macdonald LW, Tarrant AWS. A cross-cultural colour-naming study. Part I – Using an unconstrained method. Color Res Appl 2001; 1:40-60
2. Lin H, Luo MR, Macdonald LW, Tarrant AWS. A cross-cultural colour-naming study. Part II – Using a constrained method. Color Res Appl 2001; 3:193-208
3. Jiyima T, Wenning W, Zollinger H. Cultural factors of color naming in Japanese: naming tests with Japanese children in Japan and Europe. Anthro Linguist 1982; 24:245-262.
4. Names of non-luminous object colours(KS A 0011). 2002
5. J. W. Kim. Development of color space conversion program. Color science laboratory, Dept. of Physics, Daejin University, Korea. MSc thesis. 2001

Test of the Additivity of a Color Impression from Colored Texture Pattern

Shoji Sunaga and Yukio Yamashita
Department of Visual Communication Design, Kyushu Institute of Design, Fukuoka, Japan

INTRODUCTION

When the scene consisting of many small patches of some similar colors is observed, it may be experienced that the impression of one color is received as a whole [1]. If the sizes of the patches are sufficiently small, the received color seems to be the additively mixed color of patch colors. When the sizes of the patches increase to the distinguishable degree, it may be decided by the general appearance of patch colors juxtaposed to each other. The purpose of this study was to investigate the mechanism underlying the determination of the whole color impression received from a multi-colored scene. We examined by what kind of characteristics of patch colors the impression of general color was made.

We used colored random-dot textured patterns consisting of many patches of two colors which had an identical unique hue and different saturations as stimuli and measured the apparent single colors sensed for those patterns with a color matching method.

Since unique red and unique blue loci were generally known not to be on straight lines on the chromaticity diagram [2, 3], the chromaticity loci of the colors which were made by additively mixing two patch colors seems to deviate from the unique hue loci. If the color impression of the colored textured pattern has been decided by additively mixing the patch colors, the measured color must be located on the straight line that connects the loci of two unique patch colors on the chromaticity diagram. On the other hand, if it decided by apparent colors of the patch colors, it must be located on the curved unique loci.

METHOD

Apparatus

Stimuli were presented on a color CRT display with VSG 2/4 (Cambridge Research). Subjects observed them from the distance of 80 cm in a dark room.

Stimuli

A stimulus pattern was an square extent of 4 deg of the side filled by colored square patches whose size was 4 min and consisted of colored patches which had a unique color, different saturations, and an equal brightness (Fig.1). The brightness of each patch color was equated previously with a unique white of 7.0 cd/m^2 measured by each observer with the method of brightness matching.

Procedure

Experiment was carried out in next order for each subject.

1. Settings of unique loci and equal brightness
2. Estimation of saturation for colored texture pattern
3. Color matching of the whole color impression for colored texture pattern made by two colors

On male and two females were served as subjects. They had normal color vision and normal acuity or corrected-to –normal acuity. Their acuity was enough to resolve the texture pattern.

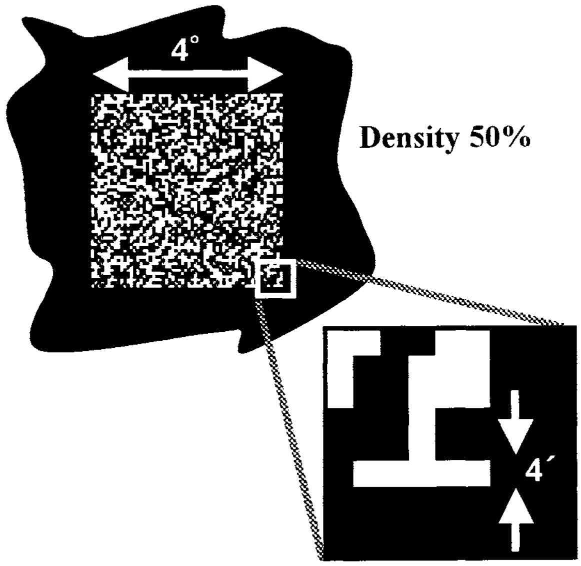

Fig.1 Stimulus Pattern of single color. The color of the patch had a unique hue and an equal brightness.

Settings of unique loci and equal brightness

To determine the unique loci of red, yellow, green, and blue for each observer, a single colored texture pattern in which single color and black patches occupied each 50%. Two of such patterns were presented in pair comparison: One was a reference, which had a unique white patch of 7.0 cd/m^2 previously obtained by each observer. The other was a test which had patches whose color and brightness were adjustable by observers, who varied the patch color to become a unique color under one of six saturation conditions and equal brightness to the reference unique white pattern. The unique loci obtained by Subj. SS, shown in Fig.2, on CIE u'v' UCS indicate a typical feature that the loci are bent particularly in red and blue.

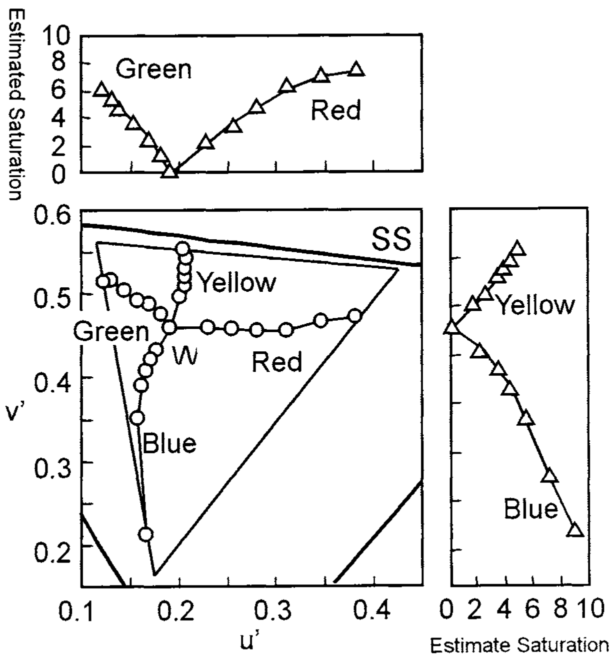

Fig.2 Results of unique hue loci and the saturation estimation for SS. The loci of unique red and blue are curved.

Estimation of saturation for colored texture pattern

On each unique hue, Subjects estimated the apparent saturation of each of the six unique colors obtained by the previous setting with the ten point method. Fig.2 shows the chromaticity loci of those unique colors and estimated saturations.

Color matching of the whole color impression for colored texture pattern

As shown in Fig.2, the estimated saturations of colors were extended to 7.4 for unique red, to 4.3 for unique yellow, to 6.0 for unique green, and to 8.8 for unique blue. The highest saturated color and the lower saturated color (the point of the saturation estimation was 3.0) of an identical unique hue were combined at the seven different proportions (1.00:0.00, 0.84:0.16, 0.32:0.68, 0.50:0.50, 0.68:0.32, 0.16:0.84, 0.00:1.00) to make colored texture patterns, which consist of two colors and appear different saturation as a whole. Fig.3 shows the test stimulus pattern. Subjects matched the color impression of the test pattern with the color of a reference texture pattern juxtaposed in the neighbor. The chromaticity and the luminance of the patch color in the reference, which was identical to the pattern used in the setting procedure of the unique loci, were adjustable by subjects.

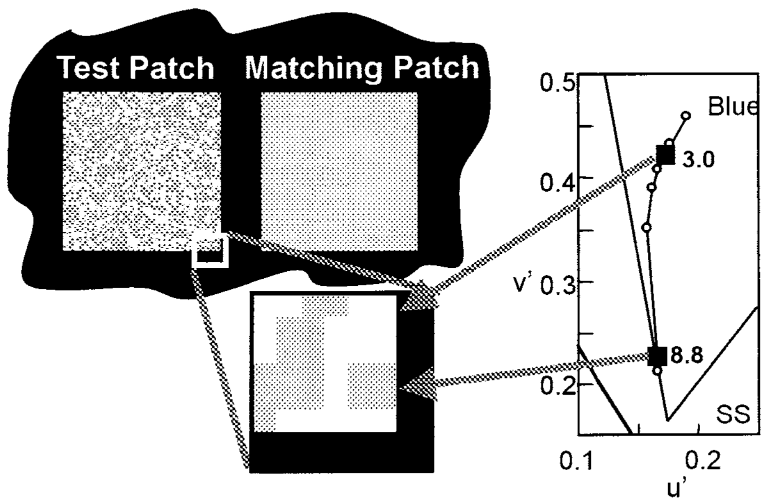

Fig.3 Stimulus used for color matching of the whole color impression for the colored texture pattern.

RESULTS AND DISCUSSION

Additivity of the patch colors in determination of whole color impression

Fig.4 shows the results of subject SS. Closed squares indicate the u'v' chromaticity loci of the patch colors in the test pattern and open circles represent those of matched colors with color impression for the patterns textured with various proportion of the highest and the lowest saturation color. With the change of the proportion of two colors, the matched color changed on the unique hue locus (dashed lines in Fig.4), not on the traight line connecting the loci of the two colors. This suggested that the appearance of opponent colors was underlying the determination of impression of whole color, that is, the additivity of patch colors was not established in determination of whole color impression.

Enhanced apparent saturation in colored texture pattern

To examine the relationship of the apparent saturation of the colored texture pattern to the saturation of colorimetric additive mixture of patch colors, Fig.5 shows the apparent saturations obtained with data in Fig.2 as a function of saturations of colorimetric mixtures predicted by the proportion of two colors.

The apparent saturations are higher than the saturations colorimetrically predicted, that is, linear summations of the patch colors do not predict the color impression of the pattern.

CONCLUSION

We indicated the following findings: In the determination of color impression sensed as a whole in a multi-colored scene, color appearance of the color elements involving in the scene plays an important role than colorimetric loci of them. The colors impressed appear as being more saturated than those predicted by additive color mixture of element colors.

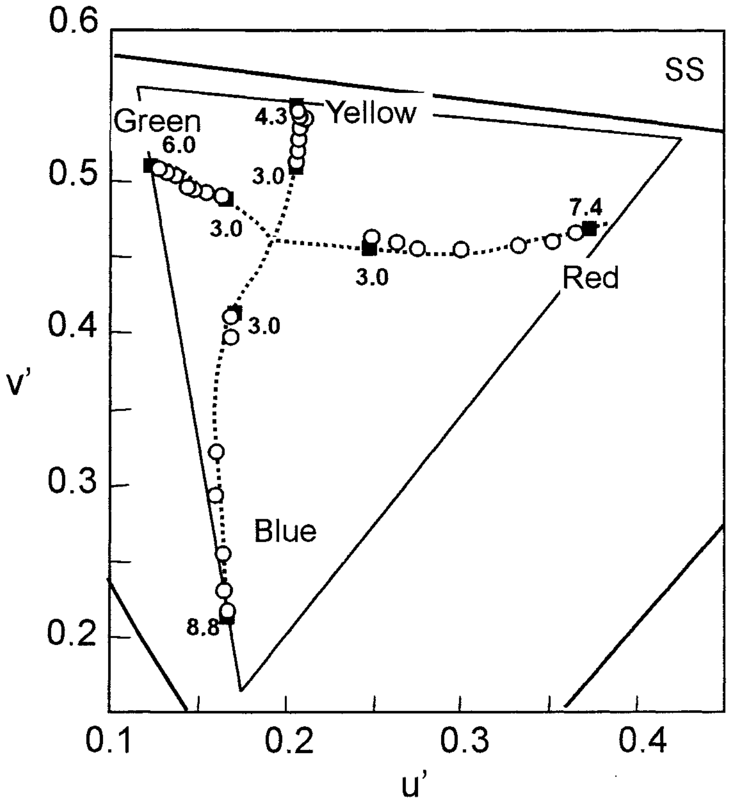

Fig.4 The chromaticity coordinates of the color impression for colored texture pattern the colored texture pattern.

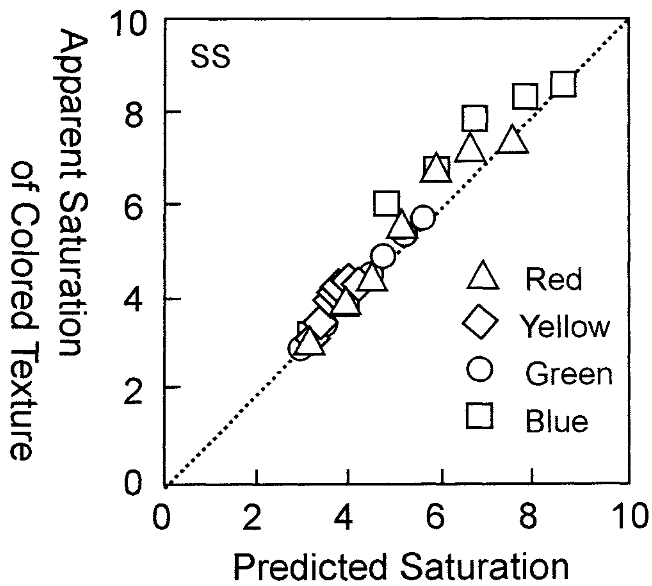

Fig.5 The relationship of the apparent saturation of the colored texture and the saturation predicted by the linear summation of the patch colors.

REFERENCE

1) S.Sunaga and Y.Yamashita, "Apparent color impressed by colored texture pattern", Investigative Ophthalmology and Visual Science, Vol.41, S238, 2000
2) S.A.Burns, A.E.Elsner, J.Pokorny and V.C.Smith, "The abney effect : Chromaticity coordinates of the unique and other constant hues", Vision Research, Vol.24, 479-489, 1984
3) M.Ayama and M.Ikeda, "Hue and saturation of colored lights in the whole area of the u'v' chromaticity diagram", Journal of the Color Science Association of Japan, Vol.18, 186-199, 1994 *(in Japanese)*

RGB Color Data Compensation for Illumination Change

Pranchalee Rattanasakornchai Yasushi Hoshino

Department of Systems Engineering, Nippon Institute of Technology

4-1 Gakuendai, Miyashiro, Minamisaitama, Saitama 345-8501, Japan

E-mail: s2004021@stu.nit.ac.jp

ABSTACT

Our researches have been interesting in human tracking for a variety of applications such as surveillance, activity monitoring and motion analysis. Human motion is traced by using a digital interface camera. Since a digital camera converts light into RGB image data with RGB filters, the illuminant directly affects the RGB image data of the human images. We have focused on reducing effect of illumination change on the images. In this paper, the compensation model of RGB color data for illumination change is proposed. The samples are taken by using a digital interface camera and a checkerboard array of 24 scientifically prepared colored squares, ColorChecker color rendition chart. The lighting environment of our experiment system is a fluorescent indoor space and an indoor space that is indirectly illuminated by sunlight. A new color model, m x n transformation, is used for changing RGB color data of camera to compensated color data. Regarding to the result, the error due to illumination change is decreased when using the compensation model.

1. INTRODUCTION

One of our research works which is continuing studied is to detect real-time human's motion in room by using RGB information. We employ the background subtraction method to separate the human figure from the captured image [1]. Background subtraction is an efficient method to discriminate moving objects move in. The human motion tracking system for this approach is shown in Fig. 1. Nevertheless, we still find an important problem is the changing of light condition. As shown in Fig. 1, two main light sources will illuminate into our system. One is the light source from fluorescent lamp and the other is sunlight which penetrates through windows. To simulate and test the experimental system as real application which we want to detect the human motion for all day, the system was continuously tested for a long period at different time of days. We found that the illumination condition cannot be kept constant because the varying illumination condition will depend on the direction and volume of sunlight and the status of fluorescent lamp ("ON" or "OFF") in the room. Therefore the major problem in this research is the varying illumination condition which effect to the RGB information from camera, and this cause error in human's motion detection algorithm.

Therefore, we are interested in finding solution to compensate the effect of varying illumination for RGB data. The method to control overall illumination at constant value may be considered to correct this problem however this method is not suitable because more equipments and hardware were required. This paper propose the method to compensate RGB information which effect by varying illumination condition, then these normalized RGB information will be used in the application called "Tracking human motion in real-time".

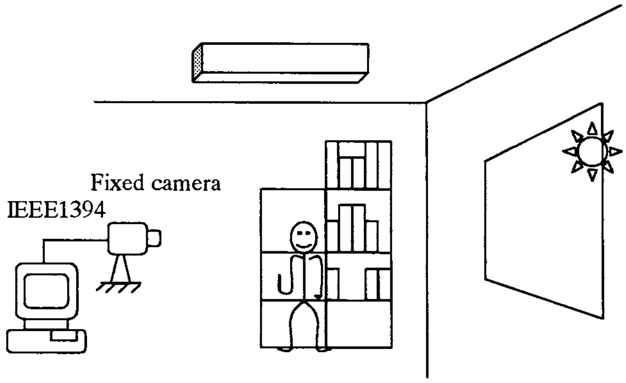

Fig.1: The human motion tracking system.

2. PROPOSED MODEL

We employ a simple model of image formation in which the response of an image device to an object depends on three factors: the light by which the object is lit, the surface reflectance properties of the object, and the properties of the device's sensors. Its response is defined as:

$$q_k = \int E(\lambda) S(\lambda) Q_k(\lambda) d\lambda, \qquad k = 1, \cdots, m \tag{1}$$

where $E(\lambda)$: the light spectrum
$S(\lambda)$: the reflectance properties of a surface
$Q_k(\lambda)$: the sensor's spectral sensitivity function.

The subscript k denotes that this is the k^{th} sensor. In what follow we assume that our devices have three sensors (m=3) so that the response of a values: (q_1, q_2, q_3). It is common to denote these triplets as R, G, and B. Accounting for a change in illumination is more difficult because, as is clear from Eq.(1), the interaction between light, surface, and sensor is complex.

2.1. Linear Model

To reduce the complexity of equation, we try to construct the easy model which can be used to compensate the varying illumination condition as shown in Fig. 2. At the first step, we suppose that the effect due to varying illumination is the relation in the form of linear equation. This linear equation can be expressed in the term of RGB relation as:

$$\begin{bmatrix} R' \\ G' \\ B' \end{bmatrix} = \begin{bmatrix} a_{11} & a_{12} & a_{13} \\ a_{21} & a_{22} & a_{23} \\ a_{31} & a_{32} & a_{33} \end{bmatrix} \bullet \begin{bmatrix} R \\ G \\ B \end{bmatrix} \tag{2}$$

where R, G, and B are information from camera and R', G', and B' are the compensated value.

Subsequently, the least square error is employed to find the suitable "a_{mn}" for compensation of varying illumination in experimental system. The dimension of Matrix A is 3x3. The method of least squared error is one common choice of the best estimate. The squared error is the sum of the squared differences between each sample and the expected value as predicted by the function. The parameter values that minimize this error are considered the best estimates.

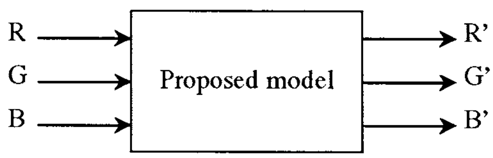

Fig.2: Proposed model.

$$
\begin{aligned}
S_r &= \sum \{R' - (a_{11}R + a_{12}G + a_{13}B)\}^2 \\
S_g &= \sum \{G' - (a_{21}R + a_{22}G + a_{23}B)\}^2 \\
S_b &= \sum \{B' - (a_{31}R + a_{32}G + a_{33}B)\}^2
\end{aligned}
\tag{3}
$$

This function will have a minimum where the first derivatives with respect to a_{mn} are zero.

$$
\begin{aligned}
\frac{\partial S_r}{\partial r} &= 0 \\
\frac{\partial S_g}{\partial g} &= 0 \\
\frac{\partial S_b}{\partial b} &= 0
\end{aligned}
\tag{4}
$$

Matrix 3x4 is used instead of Matrix 3x3 to decrease the overall error.

$$
\begin{bmatrix} R' \\ G' \\ B' \end{bmatrix} = \begin{bmatrix} a_{11} & a_{12} & a_{13} & a_{14} \\ a_{21} & a_{22} & a_{23} & a_{24} \\ a_{31} & a_{32} & a_{33} & a_{34} \end{bmatrix} \bullet \begin{bmatrix} R \\ G \\ B \\ 1 \end{bmatrix}
\tag{5}
$$

where *R*, *G*, and *B* are information from camera and *R'*, *G'*, and *B'* are the compensated value.

2.2. Quadratic Model

From the equation (1), the complexity of the equation express that the linearity is not suitable to calculate the effect of varying illumination. Hence, the quadratic equation is applied to solve this problem. An equation where the variable has an exponent of 2 somewhere in the equation as called quadratic equation is employed to increase matrix's size. This quadratic equation can be expressed in the term of RGB relation as:

$$
\begin{bmatrix} R' \\ G' \\ B' \end{bmatrix} = \begin{bmatrix} a_{11} & \cdots & a_{110} \\ \vdots & \ddots & \vdots \\ a_{31} & \cdots & a_{310} \end{bmatrix} \bullet \begin{bmatrix} R \\ G \\ B \\ R^2 \\ G^2 \\ B^2 \\ RG \\ RB \\ GB \\ 1 \end{bmatrix}
\tag{6}
$$

The suitable "a_{mn}" for compensation of varying illumination is found by using the least square error. The dimension of the matrix is 3x10.

3. EXPERIMENTS

The experimental system is composed of IEEE1394 Digital Interface Camera (DFW-VL500 : Sony), IEEE1394 PCI Card (PFW41 : Techno Scope) and personal computer. The image data is taken by using a digital interface camera and a checkerboard array of 24 scientifically prepared colored squares, ColorChecker color rendition chart. To detect Human's motion in room, the lighting environment of our experimental system is a fluorescent indoor space and an indoor space that is indirectly illuminated by sunlight.

The above illumination compensation was applied to the images of 320×240 pixels. Sample images are taken by using a digital interface camera within the configured room. The configuration of room can be classified into 2 types according to the light source,

- the light source is sunlight which penetrate through windows
- the light source is fluorescent lamp.

4. EXPERIMENTAL RESULTS

In our experiments, we applied the three compensation models to sample images:

- the linear model, 3x3
- the linear model, 3x4
- the quadratic model, 3x10.

The absolute error of R value of our proposed model and auto white balance in both type of light source are shown in Table 1.

Regarding to the model which the effect of varied illumination is linear, this compensation approach still have a numerous error. This large scale of error expresses the sign that the effect of varied illumination is not in linearity. The results of experiment as shown in the Fig. 3 and 4 show that varied illumination model in quadratic model gives the good result than linear model and auto white balance. The results of quadratic model have reduced the error over 76% for sunlight and over 91% for fluorescent illuminated condition. And we think it is not too complex to run in real-time system for human motion tracking.

5. CONCLUSION

We have developed a new algorithm for RGB color data compensation for illumination change. The least square error method is employed to find the suitable matrix for linear model and quadratic model. The linear model, 3x3 and 3x4 matrix's size, is very simple model but it can not solve the problem under the illumination change. Then we proposed the quadratic model, 3x10 matrix's size to reduce the compensated error. Consequently, this model is acceptable to compensate the effect of illumination change for tracking the human motion work.

REFERENCES

[1] P. Rattanasakornchai and Y. Hoshino, "Extraction of The Characteristic Points for Motion Detection by Using Color Information",pp.141-148, Proceedings of SPIE Real-Time Imaging, 2002.

[2] A. Kimachi and S. Tominaga, "A Study on Scene Estimation Using Controlled Illumination", A-9, General VIR Group Lecture, 2002.

[3] S.D. Hordley, G.D. Finlayson, G. Schaefer, and G.Y. Tian, "Illuminant and Device Invariant Colour Using Histogram Equalisation", UEA Technical Report No. SYS-C02-16, 2002.

[4] K. Barnard, V. Cardei, and B. Funt, "A Comparison of Computational Color Constancy Algorithms; Part One: Methodology and Experiments with Synthesized Data", pp.972-984, IEEE Transactions in Image Processing, 2002.

[5] G.D. Cubber, H. Sahli, H. Ping, and E. Colon,"A color Constancy Approach for Illumination Invariant Color Target Tracking", pp.63-68, IARP Workshop on Robots for Humanitarian Demining, 2002.

[6] G.D. Finlayson, "Color in Perspective", pp.1034-1038, IEEE Transactions on Pattern Analysis and Machine Intelligence, 1996.

Table 1: Average Absolute Error of R value in Sunlight and Fluorescent light source.

Illumination Condition	Non Process	White Balance	Matrix Size (proposed model)		
			3x3	3x4	3x10
Sunlight	35.67	29.33	14.00	11.25	8.25
Fluorescent	92.21	23.25	18.29	18.29	7.917

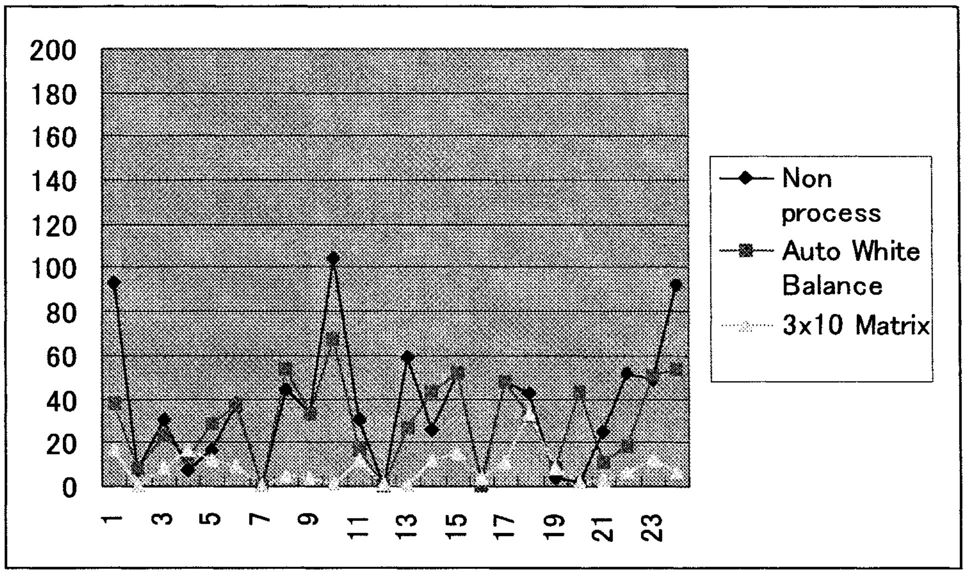

Fig.3: The absolute error of R value in the sunlight.

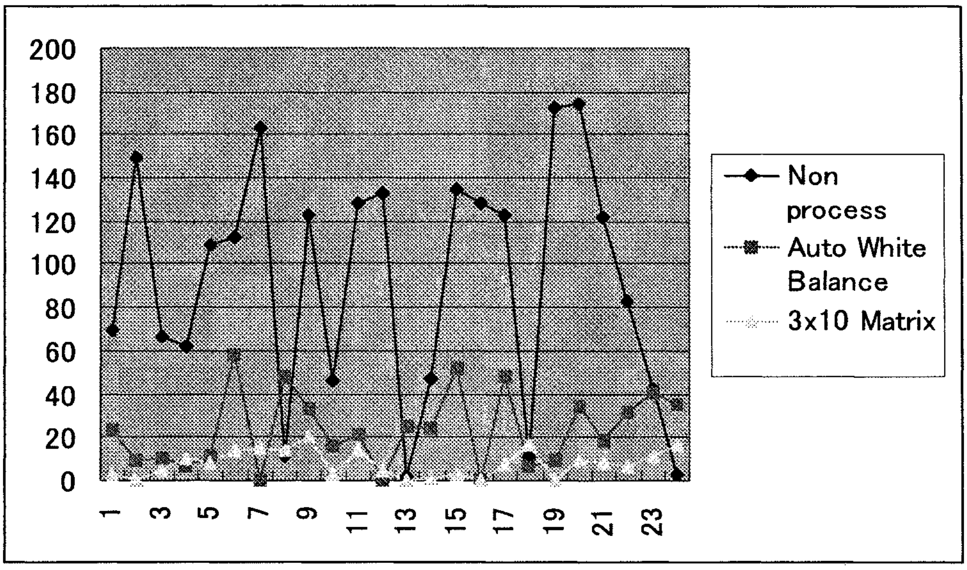

Fig.4: The absolute error of R value in the fluorescent light.

Spectral Based Color Reproduction Compatible with standard System for Mixed Illumination Conditions

Kunlaya Cherdhirunkorn, Norimichi Tsumura *,**and Yoichi Miyake**
**Department of Information and Imaging Sciences, Chiba University, Japan*
***PRESTO, Japan Science and Technology Corporation, Japan*

Abstract

A standard color space, sRGB, has been widely used for reproducing the accurate color in the internet system. However, this color is accurate only under the sRGB reference viewing environment. In practice, the customers viewing environments are not always standard conditions. It is known that the multispectral color reproduction can be used to obtain highly accurate colors which are independent of device and viewing conditions. However, since the recent color reproduction system is based on conventional RGB or CMYK imaging technology, it is a huge task to change resources and devices in the market to be those in the multispectral technology. In our previous research, the spectral turn technique was proposed to achieve the spectral based color reproduction in the E-commerce with a high compatibility to the sRGB system. However the haploscopic method, used to compare colors on monitor and an object, was not compatible with the exact viewing conditions in real life. In this paper we propose more practical spectral turn technique using the revised mixed chromatic adaptation model, S-LMS(2001) applied with simultaneous binocular (SMB) matching method for more correct color appearance matching between softcopy and hardcopy under the practical viewing conditions.

Introduction

The recent advancements in broadband technology became possible to buy products from the Internet from home or office conveniently. Color is the one of the most important factors in making the purchasing decision when the customer purchases the products by browsing the pictures of those products displayed on the monitor. The product purchased through the E-commerce system will be physically sent to the customer's office or home. After that the customer can compare the color of the product's image displayed on the monitor to the delivered product. In this case the comparison or matching the color will occur in the customer's environment. Therefore the accurate color reproduction under the customer's light source in his/her environment is very important in the E-commerce system.

In the recent imaging technology, device independent color reproduction based on ICC-profile [1] or RGB-color space [2] are widely used for the color reproduction. However, the accurate color reproduction is only guaranteed in the decided standard environment. This is not practical for the general customer. Viewing condition independent color reproduction based on color appearance model is expected to reproduce the color under different viewing conditions. In this reproduction, however, the reproduced appearance of color is that of color under taken illuminants. The color of the object under the customer's viewing condition cannot be reproduced by this technique.

It is known that the multispectral color reproduction is used to obtain highly accurate device independent and viewing condition independent colors. Therefore, the color reproduction techniques based on an estimation of reflectance spectra were proposed to reproduce correct color under an arbitrary environment [3-10]. However, they are not used practically in the E-commerce, since almost all of the resources and devices traded in the recent market are based on the conventional RGB or CMYK imaging technology. It is difficult to change them into those of the multi-spectral imaging technology.

Spectral turn method [11] was proposed as the spectral based color reproduction technique, which is compatible with sRGB-system for E-commerce. In the spectral turn method the values of sRGB is inversely transformed into the spectral reflectance. The process of chromatic adaptation is also inversely processed in the method. A chromatic adaptation in RLAB model is used in the previous experiments. Therefore, the haploscopic matching method was used in the experiment for comparing the color of the images displayed on the monitor with the original objects. However in practice when the customer compares the color of the purchased product with the color of the image of product, which is displayed on the monitor, they used both of their eyes simultaneously for matching the color. This is similar to the simultaneous binocular matching method (SMB) method in the experimental level. Therefore the haploscopic matching method and RLAB chromatic adaptation model used in the previous experiment was impractical for the E-commerce.

In this paper, the spectral turn method applied with the revised mixed chromatic adaptation model: S-LMS (2001) [15] is proposed to achieve more accurate color appearance and more practically match the color using the SMB matching method for the usual office conditions. The revised S-LMS model is used for the color comparison under the mixed illumination condition. Under this condition the human visual system partially adapts to the monitor's white point and to the ambient light (mixed adaptation), since the observer's eyes are not fixed to the monitor all the time, but they also look to the surrounding area. Therefore we need to apply mixed adaptation to the chromatic adaptation transformation in the spectral turn method to improve the prediction of color appearance of CRT monitor viewed under mixed illumination.

In the next section we will briefly introduce the previously proposed spectral turn method and the previous experiments. After that the new spectral turn method applied with the revised S-LMS model, experiment using SMB matching method, results and conclusion will be described respectively.

Spectral Turn method

The spectral turn technique compatible with the conventional RGB or CMYK imaging technology was proposed to achieve a highly accurate color reproduction for E-commerce[11]. In this technique, the process of the camera system is assumed to be based on the sRGB system and the spectral based technique is applied into the conventional system.

Figure 1 shows the process of spectral based processing for sRGB system. The sRGB system is assumed to be designed to reproduce the appearance of color under the taken illuminant on the sRGB display under the standard sRGB viewing conditions. Based on the process of the spectral based color reproduction, the process in the camera is assumed as the process surrounded by broken lines in Figure 1. From the camera, the sRGB values were transformed to tristimulus values, $\mathbf{x} = [X, Y, Z]^t$ with the consideration of the chromatic adaptation and color appearance transformation.

Then, to match the color under illuminant #2, it is necessary to process the color inversely into the spectral reflectance. The estimation of the spectral reflectance, $r(\lambda)$, can be obtained by using the following equation.

$$r = (TL_1)^- x \qquad (1)$$

where L_1 is the diagonal matrix with spectral radiance of illuminant #1, T is the matrix of color matching function. The samples of the reflectance spectra, which were measured previously, are used to make the $(TL_1)^-$ by the multiple regression method. After this we return the spectral reflectance values to the sRGB values after the exchange of the illuminants.

In the previously proposed spectral turn method, the taken image is reproduced on sRGB display under sRGB environment, and confirmed that the color is reproduced correctly on sRGB display by simultaneous haploscopic (SMH) matching method. Then the processed image assumed to be taken under the observer's illumination was reproduced by using spectral turn technique for matching the color to the original object placed under the observer's illuminant. The single state chromatic adaptation model of RLAB model, which was developed for matching the color under single illuminant condition [3], was used. To precisely match between the color of softcopy images on the self-luminous display and the object under the observer's ambient illuminant by using this model, the observer's eyes should not be adapted to the monitor and the ambient light in the same time. Therefore the haploscopic method was used in the previous method. Figure 2 shows the simultaneous haploscopic matching method used in the previous spectral turn experiment.

The results of the previous experiment showed that most of the color was reproduced well by the spectral turn method. We concluded that the proposed spectral turn technique has a high compatibility to the conventional imaging technology and the spectral band color reproduction can be implemented. However, the haploscopic matching method applied in the previous spectral turn experiment was used only for the fixed state of single adaptation. That is impractical for general use in the usual office or home environment. In the next section, the revised mixed chromatic adaptation model, S-LMS (2001) [16] is applied into in the spectral turn method for using more practical simultaneous binocular (SMB) matching method. Since this SMB matching method can be used to simulate the practical viewing situation when the customer uses his/her both eyes simultaneously to compare the color of digital picture on the monitor and the delivered product under the ambient light.

Spectral Turn applied with the mixed chromatic adaptation model: (Revised S-LMS)

In the usual office or home environments there are mainly 2 kinds of illuminants that affect the customer's eyes when the product and its image are viewed or compared simultaneously. Those illuminants are the monitor or self-luminous display and the ambient light as shown in Figure 3. This viewing condition is called mixed illumination condition. Under this condition the human eyes adapt partially to each illuminant called unfixed state of mixed chromatic adaptation.

Therefore, to achieve more accurate color appearance matching between the softcopy and the hardcopy (the image of product and the product in the E-commerce system) under the practical viewing conditions the mixed chromatic adaptation model: S-LMS (2001) is newly applied to the spectral turn method, as shown in figure 4.

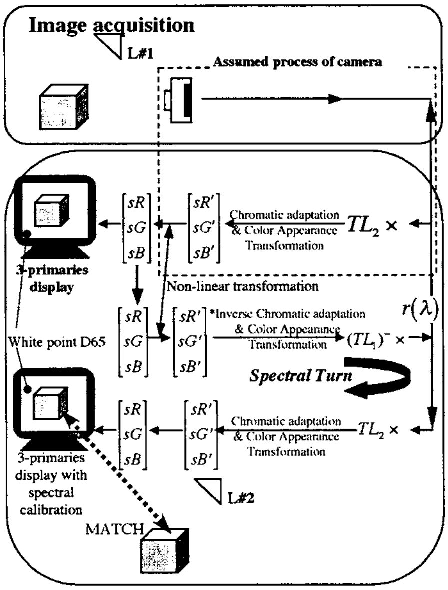

Figure 1. The process of spectral based processing for sRGB system.

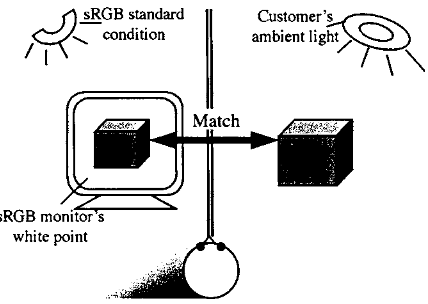

Figure 2. Haploscopic matching method used in the previous experiment for the spectral turn technique applied with the single chromatic adaptation model in RLAB model

The device independent sRGB values of the image taken under the illuminant $L_{\#1}$ are transformed to the tristimulus values. Then the revised S-LMS model is used inversely to calculate the tristimulus values which are used in the next spectral transformation step. The inverse matrix of color matching function and the diagonal matrix with spectral radiance of illuminant #1, L_1, are used to estimate the spectral reflectance, $r(\lambda)$. After that, we transform these spectral reflectance values back to the tristimulus values corresponded to illuminant $L_{\#2}$ by using the matrix functions T and L_2. The revised S-LMS is used to transform the tristimulus values corresponded to the mixed illumination viewing condition. Finally these values are converted to the digital counts of sRGB values to display on the sRGB monitor under the observer's ambient light.

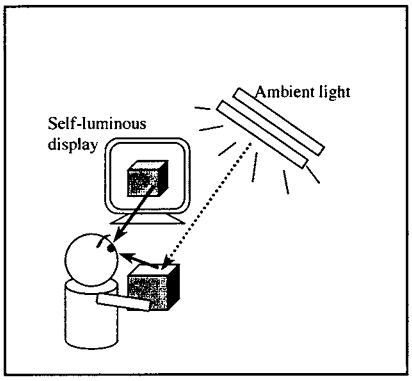

Figure 3. Human visual system adapted partially under the mixed illumination condition (as in the simultaneous binocular matching method).

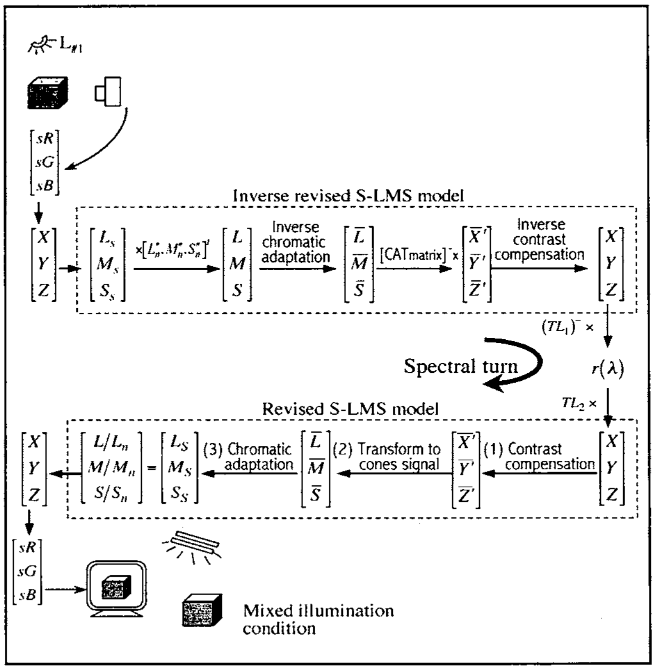

Figure 4. The spectral turn method applied with the mixed chromatic adaptation model: revised S-LMS model.

There are three essential stages used in the revised S-LMS model as shown in figure 4. For the first stage, the contrast variation for the soft copy images caused by the reflection of the ambient light must be compensated. The second stage is the transformation from tristimulus values to cone signals. And the final stage is the compensation for chromatic adaptation.

In addition, to apply this model with the spectral turn technique, we need to inverse the model before transform the tristimulus values to the spectral reflectance values, as shown in figure 4. The inverse S-LMS step can be achieved by calculating inversely of the revised S-LMS model.

Following the whole proposed process of the spectral turn technique applied with the revised S-LMS model, we will be able to achieve more practical spectral based color reproduction compatible with sRGB system under mixed illumination conditions for E-commerce. In the next section we will describe the experiment used for this technique.

Experiment

Figure 5 shows the steps of the experiment using the spectral turn method applied with the mixed chromatic adaptation: revised S-LMS model. The object's original image was taken under the first illuminant (In this experiment, the standard daylight D65 was used). Then, the processed image was reproduced from the original image by using the proposed mixed illumination spectral turn method to be compatible with the mixed illumination condition, which is the usual user's viewing condition. To compare or match the color of the object's images and original object or product, the simultaneous binocular matching method was applied. The original images taken by the digital camera and the processed images were placed on the sRGB display simultaneously. The observers compared the color of both images with the color of the original object, and then chose the best matched image, as shown in figure 5.

The room where the experiments were performed simulated a typical office or home environment. In the preliminary experiment we set the room to be illuminated by the standard A light source. For the original object, we used the standard Gretag-Macbeth color checker in the first step.

For the color-matching step, 15 observers participated. Before the experiments, all of the observers took a color-blind test to confirm that they had color-normal vision. The observers were given approximately five minutes to adapt to the viewing conditions of the room and they were instructed to sit approximately 50-60 cm from the screen and to identify and to match the original object to the softcopy image on the monitor. Every observer was allowed to move the original object anywhere he/she desired, but not on the screen next to the softcopy image, so that the observer had to move his/her eyes at some distances to make comparisons. Also no time restriction was placed to the observers.

Each color in the Gretag-Macbeth color checker was compared to that color in both original image and processed image. The number of the observers who chose processed images was counted to calculate the processed images preferring rate (%). For example, after the observers compared the green patch in Macbeth color checker, there were 10 observers from all 15 participants who chose the processed color image to be the best matched to the original object. In this case the processed images preferring rate was 67%. We used this preferring rate to determine the results.

In the next step of experiments we used the real products (for example cloths, accessories, postcards, etc.) instead of Macbeth Color Checker for color matching under varied illuminants (around 3000K~7000K). It should be noted that to obtain the best results in the experiment, a proximal field should not be distinguished when the images are shown on the monitor (the proximal field is the immediate environment of the stimulus extending for about 2 degrees from the edge of the stimulus in all, or most, directions [18]).

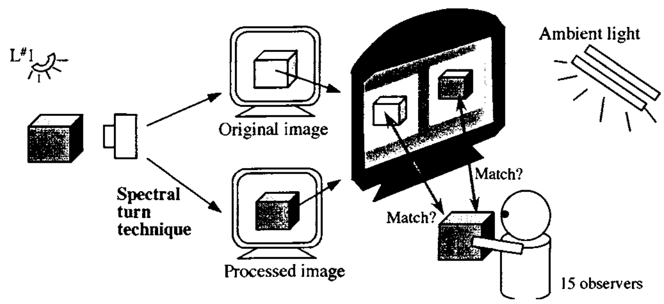

Figure 5. The experiment using the spectral turn method applied with the mixed chromatic adaptation: revised S-LMS model.

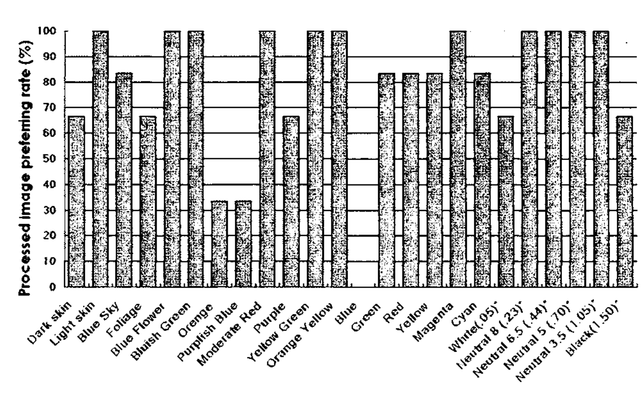

Figure 6. The graph of the processed images preferring rate (%) of each color in Macbeth Color Checker

Results and Discussion

Figure 6 shows the results of the preliminary experiment by a bar graph of the processed images preferring rate (%) of each color in Macbeth Color Checker. This graph indicates that almost all of the processed color obtained by using the spectral turn method applied with revised S-LMS model was preferred by more than 50% of the observers. This means that the color of the processed image matched to each color of Macbeth color checker more than the original image obtained from the sRGB camera.

However, the blue, purplish blue and orange colors could not be matched well by this experiment. These errors might be either occurred from the experimental errors or the limitation for reproducing the blue color of the CRT monitor.

For the next experiments, which used the variety color objects and variety ambient lights instead of Macbeth color checker and A light source, the results indicated that 90% of the observers preferred the processed images of those products. In addition, the reproduced colors matched very well under the yellowish light sources. However, the processed images could not be matched well under the bluish illuminants (6000K~7000K).

Conclusion

The proposed spectral turn technique has a high compatibility to the conventional imaging technology and this technique can be implemented to spectral based color reproduction. The mixed chromatic adaptation revised S-LMS model (2001) applied within this spectral turn technique can be used to improve this technique for more practical use. Especially the applied revised S-LMS model could provide highly accurate color matching under warm color illuminants. However, the inadequate results from the color matching under the bluish lights need to be corrected.

References

1. ICC (International Color Consortium), *Spec ICC.1: 1998-09, File Format for Color Profiles*, (1998).
2. IEC 61966-2-1, *Multimedia systems and equipment - Colour measurement and management - Part 2-1: Colour management - Default RGB colour space –sRGB*, (1999).
3. B.A. Wandell, *IEEE Trans. PAMI PAMI*, **9**, 2-13. (1987).
4. M.J. Vrhel and H.J. Trussell, *J. Color Res. Appl.*, **17**, 328 (1992).
5. T. Shiobara, S. Zhou, H. Haneishi, N. Tsumura and Y. Miyake, *J. Imag. Sci. and Tech.*, **40**, 494-501. (1996).
6. H. Maitre, F. Schmitt, J.-P. Crettez, Y. Wu and J.Y. Hardeberg, *Proc. IS&T/CIC 4th CIC*, pg. 50. (1996).
7. F. H. Imai, N. Tsumura, H. Haneishi, Y. Miyake, *J. Image Science and Technology*, **41**, 2, 166-173 (1997).
8. Y. Yokoyama, N. Tsumura, H. Haneishi, and Y. Miyake, J. Hayashi, M. Saito, A new color management system based on human perception and its application to recording and reproduction of art printing, *Proc. IS&T/SID's 5th CIC*, pg. 169-172. (1997).
9. M. Yamaguchi, R. Iwama, Y. Ohya, T. Ohyama, Y. Komiya, Natural color reproduction in the television system for telemedicine, *Proc. SPIE 3031*, pg. 482-489. (1997).
10. F. H. Imai and R. S. Berns, High-Resolution Multi-Spectral Image Archives, *Proc. IS&T/SID's 6th CIC*, 224-227 (1998).
11. N. Tsumura, K. Cherdhirunkorn, Y. Miyake, Spectral based color reproduction for e-commerce with high compatibility, *Proc. CIC10*, pg. 246-249 (2002).
12. D. Nakao, N. Tsumura et al., Developing Java SDK for spectral image delivering based on generalized color matching, *Proc. ICIS01*, (Tokyo, 2002).
13. T. Kawaguchi, N. Tsumura, H. Haneishi, M. Kouzaki and Y. Miyake, Vector Error Diffusion Method for Spectral Color Reproduction, *Proc. IS&T PICS99*, pg. 394-397. (1999).
14. Th. Keusen, Multispectral color system with an Encoding Format Compatible with the conventional tristimulus model, *JIST* pg. 510-515 (1996).
15. N. Katoh, K. Nakabayashi, Applying mixed adaptation to various chromatic adaptation transformation (CAT) models, *Proc. PICS*, pg. 299-305 (2001).
16. N. Katoh, *Corresponding color reproduction from softcopy images to hardcopy images*, Dissertation, 2002, pg. 89-121.
17. Nathan Moroney, Usage guidelines for CIECAM97s, *Proc. PICS*, pg. 164-168. (2000).
18. M.D. Fairchild, Color Appearance Models, Addison-Wesley, Mass., 1998, 161-172.
19. N. Katoh, K. Nakabayashi, M. Ito, J. Elec. Imaging, **7(4)**, 794-806 (1998).
20. M.D. Fairchild, *Color Research and Application*, **26**, 418-427 (2001

Selection of the Optimum Offset Ink Set for Colour Digital Image Reproduction by Gamut Matching

*Pattamas Sukkaew, *Pichayada Katemake and **Michele Pozzi
*Department of Imaging and Printing Technology
Faculty of Science, Chulalongkorn University, Bangkok 10330, Thailand
** Mechanical Engineering Program, SIIT, Thammasat University, Rangsit Campus, Pathumthani 12121, Thailand

ABSTRACT

A quantity of original paintings with artistic colours, and several photos with colours produced by dyes, cannot be matched with only four-colour process inks. This difficulty has been solved, to a certain extent, by using High-Fidelity colour printing. Nevertheless, not many coloured inks are added for halftone printing at present. This research was concerned with the introduction of a method for the selection of custom inks, in any combination and number, to provide a colour gamut with shape and size similar to the original. Calibration prints of three sets of four-colour process inks and twenty-one special inks were prepared on glossy paper so as to determine their optical properties using the two-constant method of Kubelka-Munk theory. Spreadsheet tools were used to calculate the optical properties and to obtain colour gamuts for any combination of inks. A selection of SHIPP standard digital images were used as testbed of the method. The ink formulation was optimized to produce a colour gamut as close as possible to the original; the two criteria were volume matching and shape matching. The tool showed that while some SHIPP images can be faithfully reproduced with only four-inks, the most colourful ones require a greater number of inks. The tools developed permit the investigation of the ink-set that is most suitable for the reproduction of any given image.

INTRODUCTION

The offset printing using four-process colours has played an important role in the printing industry for a long time. Since the available colour gamut could only produce the prints with limited satisfaction, every aspect of the technology for four colour halftone printing including devices, substrates, and software has been continually developed. However, the brilliant colours in the original, which could be recorded with the drum scanner, could not be reproduced by the use of the four-process colour printing. This is because of the limitations of the process-colour inks, which have a deficiency in absorbing the light spectrum.

Halftone printing with more than four colours has been developed in order to expand the printing colour gamut. There are six and seven colour printings, which can provide a wide colour gamut. This results in saturated colours and colourful prints, which is suitable for the printing of packaging, annual reports, and advertisement. Although halftone printing with more than four colours can produce high quality colour prints, it may not be necessary when the original image has a limited colour gamut. The most important requirement is that the chosen custom inks be suitable for the colours of the original image:printing with only four or three colours may still produce high quality colour prints. Besides the expansion of the printing colour gamut, the matching of colours between an original and a reproduction is an important topic in this research.

The development of the method presented here involves determination of the optical properties of 4 sets of lithographic inks by using the Kubelka-Munk equation to predict the printing colour gamut. Katemake developed the method of determination of the optical properties systematically using a spreadsheet [1,2]. The determination of colour gamut using the predicted reflectance spectrum of mixed inks and single ink printed on coated paper was also developed [1,2]. The printable gamuts obtained from different colour ink-sets is not the same since each ink has its own reflectance that is unique. This results in different ink-sets producing different colour gamuts.

This research developed a method to guide in the selection of the custom inks that suits the prints. This could enable the system to produce the highest colour quality job and consume the least amount of inks. A database of the offset inks was developed. By using it together with the tools for simulating the colour gamut of the selected custom inks, the desired colour gamut, which corresponds to the colour of the original image, can be achieved.

THEORETICAL BACKGROUND

Kubelka – Munk theory.

The Kubelka-Munk (KM) theory based on the consideration of the interaction of light within the layers in terms of two fluxes of energy, travelling in opposite directions. The interaction of light within the layers can be described by an absorption coefficient *K* and a scattering *S*. An application of the theory to the prediction of the reflectance presented here was reviewed by Nobbs [3]. Nobbs gave a description of how the theory can be used to relate the reflectance of a transparent layer to *K* and *S*.

K and S coefficients of semitransparent layers [2].

This theory provides a solution for semitransparent layers and it can be developed by first establishing the optical properties of a layer in isolation. From this idea, it can calculate the value of *K* and *S* by Equation 1 and Equation 2.

$$K = \frac{Z}{D}\left[\frac{1-R_\infty}{1+R_\infty}\right] \qquad (1)$$

$$S = \frac{Z}{D}\left[\frac{2R_\infty}{1-R_\infty^2}\right] \qquad (2)$$

where R_∞ is the reflectance of the ink film that is sufficiently thick to be opaque and D is the thickness of the layer. The value of *Z* is the function of β as shown in Equation 3.

$$Z = \frac{1}{2}\ln(\beta+1) \qquad (3)$$

β is independent of the substrate of the semitransparent layer.

Since R_∞ is the reflectance of an opaque layer of the ink. Determination of R_∞ seems to be difficult because the layer of the printing ink is not a fully opaque layer. Therefore, a value of R_∞ may be determined from the reflectance of prints over a white and over a black substrate. Assuming that R_w and R_b are the reflectance of the layer over the white substrate and over the black substrate respectively and $R_{g,w}$ and $R_{g,b}$ are the reflectance of the white and black substrates, then the value of β can be obtained by Equation 4. The value of β from the print over black and white substrate is the same.

$$\beta = \left[\frac{R_{g,b}-R_b}{R_b-R_\infty}\right]\left[\frac{1-R_\infty^2}{1-R_{g,b}\cdot R_\infty}\right] = \left[\frac{R_{g,w}-R_w}{R_w-R_\infty}\right]\left[\frac{1-R_\infty^2}{1-R_{g,w}\cdot R_\infty}\right] \qquad (4)$$

Equation 4 is rearranged to obtain R_∞:

$$R_\infty = B - \sqrt{B^2-1} \qquad (5)$$

where B is defined by Equation 6:

$$B = \frac{(1+R_bR_w)(R_{g,w}-R_{g,b})-(1+R_{g,b}R_{g,w})(R_w-R_b)}{2(R_bR_{g,w}-R_{g,b}R_w)} \qquad (6)$$

Saunderson correction [2].

However, the Kubelka-Munk theory is limited in the sense that it does not take the partial effect at the air to layer bounding into account, therefore the Saunderson correction is needed to correct the measured reflectance ρ to the true or body reflectance R before applying the Kubelka-Munk theory. The true reflectance can be calculated by equation 7.

$$R = \frac{\rho - r_e}{t_e t_i + r_i(\rho - r_e)} \qquad (7)$$

where r_e : is the fraction of the incident flux I reflected by the interface,
t_e : is the fraction of the incident flux I transmitted by the interface,
r_i : is the fraction of the incident flux J reflected by the boundary,
t_i : is the fraction of the incident flux J transmitted by the boundary.

OVERVIEW OF PROCEDURE

Preparation of Printed Calibration Panels.

Three types of four-colour ink-sets were used in this research: DIC Geos-GZQRTZ inks, Fresh & Fast inks and Hostmann inks including 21 DIC HIZ-GT special inks. Each coloured ink was mixed with a tint medium to produce 7 levels of dilution and then applied onto 120 g/m^2 glossy paper.

Determination of R_∞, K and S from Semitransparent layers.

The true reflectance of the substrate and that of the sample at every concentration level were obtained by the Saunderson correction equation and then R_∞, K and S were computed. For match prediction, the values of *K* and *S* derived from the Kubelka-Munk theory were not used directly. The coefficients derived from a least squares method fit of the non-linear dependence of K on C (colour ink volume) were used instead. The general form adopted for the non-linear dependence was a cubic approximation, as in Equation 8.

$$K = a_1C_1 + a_2C_1^2 + a_3C_1^3 \tag{8}$$

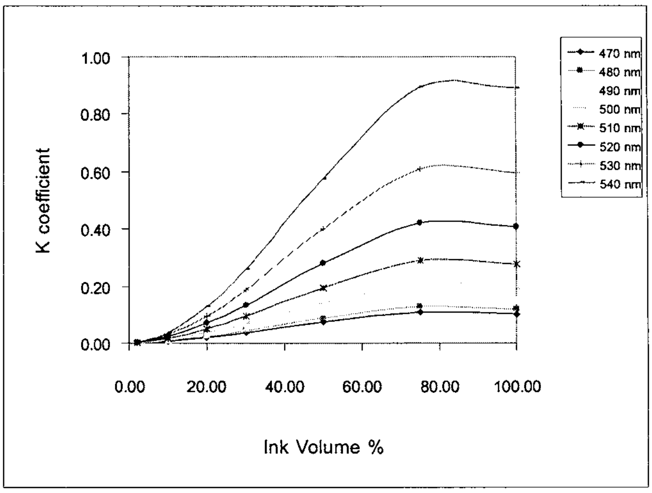

Figure 3: Plot of absorption coefficient of prints of Fresh & Fast four – colour process cyan ink mixed with clear tint medium on glossy paper against coloured inkconcentration.

Colour Gamut of a Custom Combination of Inks.

The input data contained the values of K/S, a_1, a_2 and a_3, which can be used in the recipes. In this research, each recipe contained several inks, each of which was present with a concentration of 100, 75, 50, 25 or 0 %. The aim of the tool was to determine the colour of the print of the ink mixtures by determining the reflectance spectrum and the tristimulus values. Therefore, a calculation of the reflectance spectrum of the semi-transparent layer of the mixture was carried out. Finally the tristimulus values XYZ and CIE L*a*b* coordinates were derived and employed for a gamut plot. The steps of calculation can be defined as follows:

1. Select the number and type of inks to be used in the formulation.
2. Calculate the absorption, K_A (Equation 8) and scattering S_A (Equation 9) coefficients of all inks in the formulation.

$$S_A = \frac{K_A}{\omega} \tag{9}$$

where $\omega = \frac{(1-R_\infty)^2}{2R_\infty}$)

3. Calculate the total absorption, K_M and the total scattering S_M coefficients by summing the contributions from each component in the formulation at each wavelength in the spectrum (Equation 10)

$$\omega = \frac{K_1 + K_2 + \ldots + K_n}{S_1 + S_2 + \ldots + S_n} \tag{10}$$

4. Calculate the reflectance of the layer R_M which depends on K_M, S_M and the reflectance of the substrate R_g via Equation 11.

$$R_M = \frac{\alpha.R_g + \beta.R_\infty}{\alpha + \beta} \tag{11}$$

where α is a function of both the opaque reflectance R_∞ and R_g. R_∞ is given by Equation 12:

$$R_\infty = 1 + \omega - \left[(1+\omega)^2 - 1\right]^{1/2} \tag{12}$$

where $\omega = K_M/S_M$ is a function of both the K_M and S_M values of the layer and the thickness D of the layer relative to that used for the calibration print.

5. Correct the R_M value by taking into account the effect of the coating-to-air interface.
6. Calculate the colour coordinates from the recipe reflectance spectrum.

Obtaining the Colour Gamut of a Digital Image.

In this experiment, SHIPP Images, standard high precision picture data from IIEEJ (The Institute of Image Electronics Engineers of Japan) were used as the standard digital images. Three images were selected, namely P1rgb (Bride), P3rgb (Wool), P4rgb (bottles).

MATLAB was used to read the RGB values of every pixel of each standard digital image and to transform them into XYZ and CIE L*a*b* coordinates.

The algorithm used for the conversion from SHIPP-Calibrated RGB to XYZ is available in [4].

Gamut Matching

After obtaining the colour gamut of the combination of inks and of the digital image, they were compared in order to determine the best combination of inks that matches the digital image. The criteria of comparison were as follows.

1. Size and shape of gamut.

The best combination of inks was the one in which boundaries of its colour gamut covered all colour gamuts of the digital image.

2. Gamut volume

A dedicated software program was used to calculate the gamut volume of the combination of inks and of the digital image. Then, the ink combination having a gamut volume closer to the gamut volume of the digital image was selected.

RESULTS AND DISCUSSION

Using the tool, the theoretical L*a*b* coordinates of any formulation of ink were computed. To verify the validity of the tool, the L*a*b* coordinates predicted for 100% single inks were compared with the measured L*a*b* coordinates. The average colour difference between predicted L*a*b* and measured L*a*b* of the single colours of Geos ink-set, FF ink-set and Hostmann ink-set are 3.86, 4.07 and 4.55 respectively.

A spreadsheet for the determination of K and S was developed. The correction coefficients that are appropriate for the lithographic ink layer and coated substrate were $r_e = 0.025$ for print, $r_e = 0.040$ for substrate, $r_i = 0.600$ for print, $r_i = 0.600$ for substrate, $t_e = 0.975$ for print, $t_e = 0.960$ for substrate, $t_i = 0.400$ for print and $t_i = 0.400$ for substrate when an integrating sphere instrument was used.

The colour gamut volume of the FF ink-set is 7550 which is the highest value compared to those of the Hostmann and the Geos ink-sets, which have a gamut volume of 7220 and 7110, respectively. The colour gamut volumes of the images used, Bride, Wool and Bottles are 1860, 8830 and 1150, respectively.

Figures 4 to 6 compare the gamut of the selected combination of inks selected for each of the the digital images considered with the gamut of the images themselves. Figure 4 shows the comparison of the FF ink-set with the P1rgb (Bride) digital image. The P1rgb image has a large yellow and red area but small green and blue area. The boundary of the four-colour process ink-set can cover the colour of this digital image.

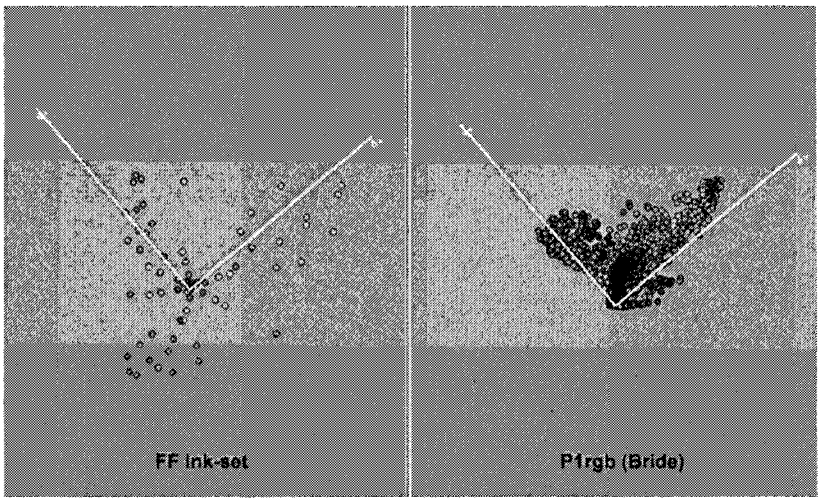

Figure 4: The colour gamut of FF ink-set compared to SHIPP image P1rgb (Bride).

Figure 5 shows the comparison of the Hostmann ink-set plus five HIZGT special inks consisting of bronze red 30, dark blue 69, reddish yellow 40, green, and violet 68 with P3rgb (Wool) digital image. The P3rgb image has a large gamut which makes it difficult to find the combination of inks that covers it all, especially in the pink, violet and dark blue areas. The P3rgb (Wool) image has a larger gamut than any combination of inks. The Hostmann ink-set plus five HIZGT special inks mentioned above is the best selected combination of inks that covers almost all colours of the Wool image.

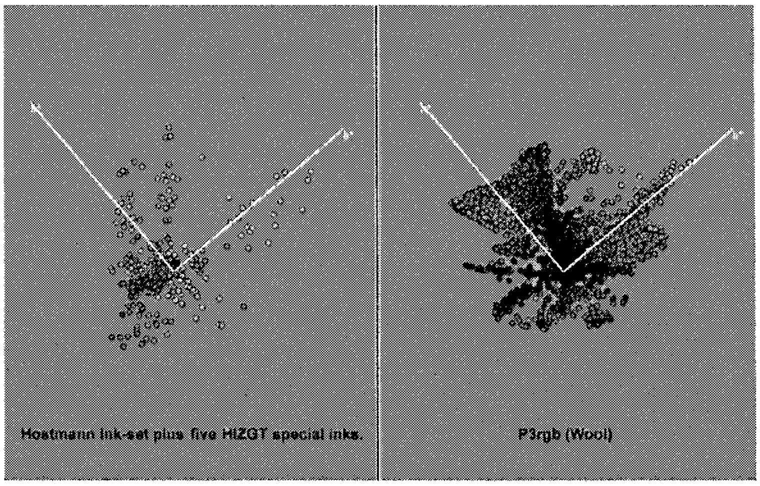

Figure 5: The colour gamut of the Hostmann ink-set plus five HIZGT special inks consists of bronze red 30, dark blue 69, reddish yellow 40, green, and violet 68 compared to the SHIPP image P3rgb (Wool).

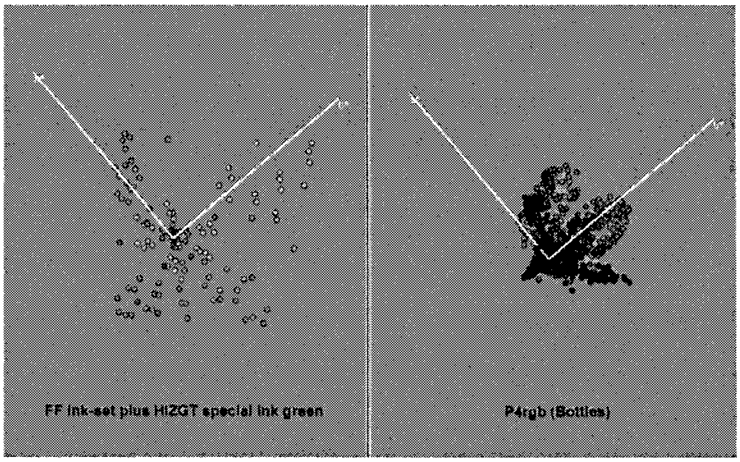

Figure 6: The colour gamut of FF ink-set plus HIZGT special ink green compared to SHIPP image P4rgb (Bottles).

Figure 6 shows the comparison of the FF ink-set plus HIZGT special ink green with the P4rgb (Bottles) digital image. The Bottles image gives large green, yellow and brown areas but small blue and red areas. The FF ink-set plus HIZGT special green ink is the best ink combination that covers all colours of the Bottles image.

CONCLUSIONS AND FUTURE WORK

A user-friendly tool was developed as a spreadsheet that permits to perform gamut mapping as well as the analysis of the K and S coefficients. In this way, users can investigate the colour gamut of their own combination of inks, which simplifies the process of selecting an optimal ink formulation for each print job.

In this study, the reflectance values were obtained from spectrophotometer measurements made with integrating sphere geometry. For further studies, it is suggested that bi-directional spectrophotometers be used to investigate the difference of the correction coefficients in the Saunderson model for the lithographic ink layer printed on the glossy substrate.

In this research, the colour gamut of a given digital image was computed using MATLAB. The method used to convert RGB values into X, Y, Z and L*, a*, b* coordinates is specific to the SHIPP standard pictures. Therefore, if images from other sources are used, the method of obtaining the tristimulus values must be modified accordingly. Then the tristimulus values will be encoded to the same standard of the SHIPP pictures. The MATLAB code should be developed further to handle different kinds of images according to the process mentioned above.

References

1. Katemake P., Color matching in printing ink systems, Ph.D Thesis, University of Leeds, Leeds, UK, (2001).
2. Nobbs J.H., Colour-Match Prediction for pigment material, *Colour Physics for industry,* 2nd ed, ed. R. McDonald, Society of Dyers and Colourists, (1997), pp.229-338.
3. Nobbs J.H., Kubelka-Munk theory and prediction of reflectance, Rev. Prog. Coloration, Vol.15, (1985), pp.66-79.
4. Sakamoto, K., and Urabe H., "Standard High Precision Pictures : SHIPP," *Proceedings of 5th the IS&T/SID Colour Imaging Conference*, Scottsdale, Arizona, November, 1997, pp. 240-244.

Simulating the Colour Gamut of Ink-Jet Ink Systems on Coated and Uncoated Substrates

*Niramol Kasadesinchai, *Pichayada Katemake and **Hiromichi Noguchi
*Department of Imaging and Printing Technology
Faculty of Science, Chulalongkorn University, Bangkok, Thailand
**Canon Inc., 16-1 Shimonoge 3-Chome, Takatsu-ku, Kawasaki-shi, Kanagawa 213-8512, Japan

ABSTRACT

Nowadays, research and development in colorants has led to a number of new colorants with a wider colour gamut. It is important to select the widest gamut of colorants at the lowest cost. This study is intended to simulate the colour gamut of inkjet inks printed on coated and uncoated substrates using the two-constant Kubelka-Munk theory to obtain the optical properties of the inks: absorption coefficients (K) and the scattering coefficients (S). The K and S values were determined independently. Fourteen dye-based inks, supplied by Canon, were employed for the calibration of prints to determine their optical properties on coated and uncoated substrates. Spreadsheets and the Visual Basic codes were developed to make the calculations much easier. The nonlinear relationship between absorption coefficients and concentration of inkjet ink (C) was characterised by a power series of the equation $K = aC+bC^2+cC^3$ for all wavelengths. The correction coefficients for coated paper (PR-101) found as $r_{e,sub}$, $r_{i,sub}$, $r_{e,print}$ and $r_{i,print}$ were 0.021, 0.600, 0.007 and 0.600, respectively. This resulted in an average colour difference, ΔE_{ab}^*, between the predicted reflectance and the measured reflectance of 4 when the single colour of fourteen dyes was investigated. The application of gamut simulation gave a good performance. The inkset giving the largest gamut was the one that contained Direct Blue 199, Acid Magenta 1, Direct Yellow 86, and Direct Black (reddish).

INTRODUCTION

Four-colour inkjet printing is a non-impact printing technology that has been rapidly developed with respect to both printing and material technology. In terms of materials, the developments are two-fold, the development of inks and the development of substrates. Various different types of inks have been developed and used in inkjet applications. Generally, they are composed of two main components, ink bases and colorants.

In the colorant component, there are a number of pigments or dyes that are used to produce inkjet ink. The pigment-based inkjet ink has been developed by several companies, such as 3M, Dupont, and Kodak. One significant advantage of pigment-based ink is its superior to dyes in colour durability in terms of waterfastness and lightfastness. However, dyes are mostly used for production of inkjet printed on paper because of small particles and water-soluble dyes. The selection of dyes is dependent on their physical properties such as water solubility, waterfastness and lightfastness, and optical properties such as colour strength, absorption coefficient (K) and scattering coefficient (S). These properties will be optimised to obtain the appropriate dyes so as to use for a four-colour ink set: cyan, magenta, yellow and black or for six-colour in a printer. These inks provide an optimum size of colour gamut. However, it takes some time to obtain the properties of a large number of dye-base inks and in making the best decision. Nowadays, not only the four-colour ink set is used but also High-fidelity colour printing using more than four coloured inks is employed to provide the widest colour gamut. This research investigated a faster and simpler way of achieving the desired colour gamut from the minimum number of inks. The simulation of colour gamut of inkjet ink systems was carried out by developing tools based on the optical properties of inks. These tools were developed from Katemake's tools [1]. The optical properties of inks are determined by using the two-constant Kubelka-Munk (KM) model. The method used in this study involves the calibration of the set of inkjet printing inks to determine the optical properties. The investigation method concerns the development of a spreadsheet application that determines the colour gamut that is obtained from the selected number of inks from the database.

THEORY

Applying Kubelka-Munk Theory to Semitransparent Layers [2].

The KM theory was used to describe the interaction of light with the layers in terms of two fluxes of energy. This theory provides a solution for semitransparent layers and it can be developed by first establishing the optical properties of a layer in isolation. From this idea, it can calculate the value of K and S by Equation 1 and Equation 2.

$$K = \frac{Z}{D}\left[\frac{1-R_\infty}{1+R_\infty}\right] \tag{1}$$

$$S = \frac{Z}{D}\left[\frac{2R_\infty}{1-R_\infty{}^2}\right] \tag{2}$$

where R_∞ is the reflectance of the ink film that is sufficiently thick to be opaque and D is the thickness of the layer. The value of Z is the function of β as shown in Equation 3.

$$Z = \frac{1}{2}\ln(\beta + 1) \tag{3}$$

β is independent of the substrate of the semitransparent layer.

Since R_∞ is the reflectance of an opaque layer of the ink. Determination of R_∞ seems to be difficult because the layer of the printing ink is not a fully opaque layer. Therefore, a value of R_∞ may be determined from the reflectance of prints over a white and over a black substrate. Assuming that R_w and R_b are the reflectance of the layer over the white substrate and over the black substrate respectively and $R_{g,w}$ and $R_{g,b}$ are the reflectance of the white and black substrates, then the value of β can be obtained by Equation 4. The value of β from the print over black and white substrate is the same.

$$\beta = \left[\frac{R_{g,b}-R_b}{R_b-R_\infty}\right]\left[\frac{1-R_\infty^2}{1-R_{g,b}\cdot R_\infty}\right] = \left[\frac{R_{g,w}-R_w}{R_w-R_\infty}\right]\left[\frac{1-R_\infty^2}{1-R_{g,w}\cdot R_\infty}\right] \tag{4}$$

Equation 4 is rearranged to obtain R_∞:

$$R_\infty = B - \sqrt{B^2 - 1} \tag{5}$$

where B is defined by Equation 6:

$$B = \frac{(1+R_bR_w)(R_{g,w}-R_{g,b}) - (1+R_{g,b}R_{g,w})(R_w-R_b)}{2(R_bR_{g,w}-R_{g,b}R_w)} \tag{6}$$

Saunderson Correction.

The measured reflectance is corrected by Equation 7 before it is used to calculate K and S in the KM theory,

$$R = \frac{\rho - r_e}{t_e t_i + r_i(\rho - r_e)} \tag{7}$$

where r_e and t_e are the fractions of the incident flux I are reflected and transmitted by the interface respectively. r_i and t_i are the fractions to the incident flux J that are reflected and transmitted by the boundary respectively. ρ is the measured reflectance. R is true reflectance. This equation is often known as the Saunderson equation.[2]

EXPERIMENTAL

Ink Calibration.

Fourteen dyes: Black (reddish), Black (bluish), Acid Red 289, Basacid Red 510, Acid Magenta 1, Acid Yellow 23, Direct Yellow 132, Direct Yellow 86, Direct Blue 199, Acid Blue 9, Orange, Green, Violet were used to formulate dye-based inks for use with the BJ F850 Canon printer. Fourteen dye-based inks were employed for calibration of prints to determine their optical properties on coated and uncoated paper. They were diluted with water in order to produce 7 levels of calibration inks which were 2%, 10%, 20%, 30%, 50%, 75% and 100%. Subsequently, each level of inkjet ink concentration was filtered before it was injected into an ink tank. The ink was printed one by one as a colour patch on black and white substrate, Canon PR-101 for coated paper and photocopying paper for uncoated substrate, using a yellow printing head for all dye-base inks. The reflectance spectra, of the printed patches were measured by using the Gretag Macbeth Color Eye 7000 spectrophotometer with an illumination/observation of D65/10 and specular component included. The measured reflectances are corrected by using the Saunderson equation (Equation 7). The R_∞, K and S then were calculated using equations 5, 1 and 2 respectively. K obtained were plotted against the volume concentration, C, to check the degree of the linearity of water-based inkjet ink. Then the non-linearity that appeared was characterised by fitting the data to a power series. The coefficients of the power series equation of the relationship of K and C, and then were stored as a database.

Colour Gamut Prediction.

The colour gamut of the printed colour patch containing different amount of coloured inks mixed together can be predicted when the set of inks was selected. The amounts of the inks mixing in this research were varied from 100, 75, 50, 25 and 0 percent with the condition that the total amount in each recipe was 100. The tristimulus values XYZ and CIE L*a*b* coordinates were calculated from the predicted reflectance of colour patches. The steps of calculation can be defined as follows:

1. Select the number of inks and type of inks to be used in the formulation.
2. Calculate the absorption, K using the power series equation and scattering S (Equation 8) coefficients of all inks in the formulation.

$$S_A = \frac{K_A}{\omega} \tag{8}$$

where $\omega = \frac{(1-R_\infty)^2}{2R_\infty}$

3. Calculate the total absorption, K_M and total scattering S_M coefficients of the mixture by summing the contributions from each component in the formulation at each wavelength in the spectrum (Equation 9)

$$\omega = \frac{K_1 + K_2 + ... + K_n}{S_1 + S_2 + ... + S_n} \tag{9}$$

4. Calculate the reflectance of the layer R_M which depends on K_M, S_M and the reflectance of the substrate R_g via (Equation 11).

$$R_M = \frac{\alpha.R_g + \beta.R_\infty}{\alpha + \beta} \tag{11}$$

where α is a function of both the opaque reflectance R_∞ and R_g,
when R_∞ is given by (Equation 12).

$$R_\infty = 1 + \omega - \left[(1+\omega)^2 - 1\right]^{1/2} \tag{12}$$

where $\omega = K_M/S_M$. ω is a function of both the K_M and S_M values of the layer and the thickness D of the layer relative to that used for the calibration print.

5. Correct the R_M value by taking into account the effect of the coating-to-air interface.
6. Calculate the colour coordinates from the recipe reflectance spectrum.

RESULTS AND DISCUSSION

Absorption of the ink

The water dye-based inkjet ink was printed on the substrates that are the coated and uncoated papers. The coated paper has a receiving layer, which is absorbed layer, and a base. The ink penetrates into the receiving layer as shown in Figure 1.

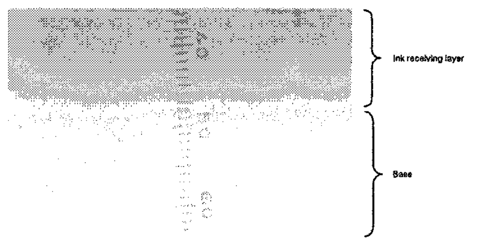

FIGURE 1 The cross-section of coated paper printed using Direct Blue 199 ink.

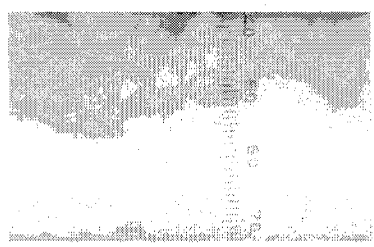

FIGURE 2 The cross-section of uncoated paper printed using Direct Blue 199 ink.

Figures 1 and 2 were taken at a magnification of 50 by the light microscope. The scale of the ruler was equal 0.0038 mm. The receiving layer was filled with the ink. It was distributed homogeneously since the coated paper used was a micro-porous paper. The characteristics of micro-porous paper affect the speed of ink absorption. The ink is absorbed into the ink receiving layer so fast that it does not leave an unsmooth gradation. Figure 2, the ink penetrates into the fiber of paper that is not homogeneous. This may affect the scattering of light entering and the two-constant KM model may be not able to explain this phenomenon very well.

Concentration dependence of K and S

The reflectance spectrums obtained were subsequently used to determine the opaque reflectance, absorption coefficients and scattering coefficients. The absorption coefficients of the dyes have a nonlinear relationship with the volume concentrations as shown in an example in Figure 3. The degree of nonlinearity of the plots for water-based inkjet ink is similar to that of the plots for lithographic ink. The nonlinearity then can be characterised by fitting the data to a power series. The nonlinear dependence of K on C of water-based inkjet ink can be characterised by the following equation:

$$K = aC + bC^2 + cC^3 \qquad (8)$$

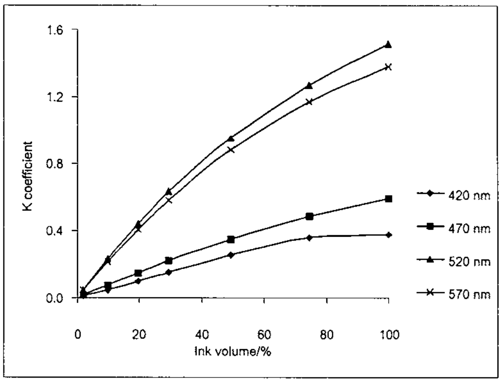

FIGURE 3 Concentration dependence of K for an acid magenta 1 inkjet ink printed on coated paper (PR 101).

The R_∞, K and S determined and were carried out after the surface correction. The correction coefficients suitable for inkjet layer printed on Canon PR-101 paper and uncoated photocopying paper were found as shown in Table 1. In this case an integrating sphere spectrophotometer was used.

TABLE 1 The corrected coefficients for inkjet ink on Canon PR-101 and photocopying paper.

Type of substrates		r_e	r_i	t_e	t_i
Canon PR-101	Print	0.007	0.600	0.993	0.400
	Subtrate	0.021	0.600	0.979	0.400
Photo copying Paper	Print	0.020	0.625	0.980	0.375
	Subtrate	0.025	0.600	0975	0.400

The average colour difference between the predicted R and the measured R on the Canon PR-101 was 4. The coloured inks that gave a high colour difference were the single colour inks or the mixture of the inks that contained fluorescent dyes. These dyes were the Acid Red 289 and the Basonyl Red 540 which appeared the fluorescent effect in the 590 to 700 nm. This caused a high dE_{ab}* because KM theory does not take into account for fluorescence.

The two-constant KM theory is not suitable for prediction of the optical property on uncoated paper because the average colour difference between the predicted R and the measured R on uncoated paper was high.

Gamut Simulation

The colour gamut was simulated using different inks in the set. It was found that the ink set consists of four inks (Direct Blue 199, Acid Magenta 1, Direct Yellow 86 and Black (reddish)) gave the widest colour gamut on coated paper as shown in Figure 4.

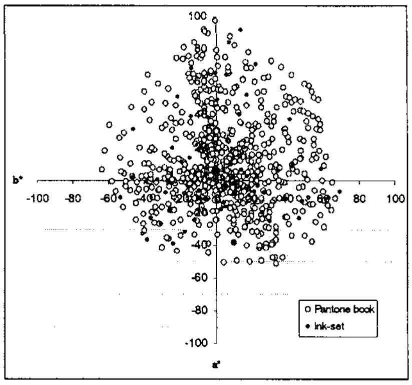

*FIGURE 4 The CIE L*a*b* colour gamut of four inks: Direct Blue 199, Acid Magenta 1 Direct Yellow 86 and Black (reddish), D65/10.*

Seven inks consist of four inks from the best set shown above, and orange, green as well as violet inks. It is obvious that using the extra inks extends the colour gamut significantly. The colour gamut of seven inks extends the gamut in the orange region, the green region and the violet region greatly which can covered the gamut of the Pantone book completely (Figure 5).

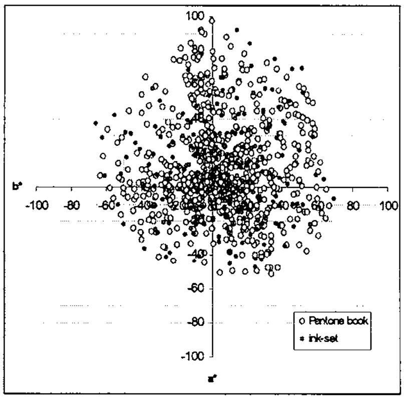

FIGURE 5 The colour gamut of seven inks: Direct Blue 199 ink, Acid Magenta 1 ink, Direct Yellow 86 ink, Black (reddish) ink, Orange ink, Green ink and Violet ink, printed on coated paper, D65/10.

CONCLUSIONS

This study investigated the possibility of applying the two-constant Kubelka-Munk theory to the inkjet ink systems. The two-constant Kubelka-Munk theory can be applied in inkjet ink with a good performance only for coated paper. The nonlinearity of K against concentration was characterised by fitting data to the power series of $K = ac+bc^2+cC^3$. The correction coefficients, r_e of 0.007 for print, r_e of 0.021 for substrate, r_I of 0.600 for print, r_I of 0.600 for substrate, t_e of 0.993 for print, t_e of 0.979 for substrate, t_I of 0.400 for print and t_I of 0.400 for subtrate can minimise the colour difference between the predicted R and the measured R on coated paper to when an integrating sphere instrument was used.

The four colour of inkjet ink set that give the widest colour gamut includes inks containing Direct Blue 199, Acid Magenta 1, Direct Yellow 86 and Black (reddish) ink. Adding orange, green and violet ink can extend the gamut in the orange, green region and violet region that covered the gamut of the Pantone book greatly.

REFERENCES

1. Katemake, P. *Colour matching in printing ink systems.* Ph.D. Thesis, Department of Colour Chemistry and Dyeing, University of Leeds, Leeds, 2001.
2. Nobbs, J. H. Colour-match prediction for pigmented materials. In R.Mcdonald (ed.), *Colour Physics for Industry.* pp. 292-372. West Yorkshire: Society of Dyers and Colourists, 1997.
3. Kang, H. R. Kubelka-Munk modeling of ink-jet ink mixing. *J. Imaging Technology.* 17(1991): 76-83.
4. Parton, K. H., and Berns, R. S. Color modeling of ink-jet ink on paper using Kubelka-Munk theory: *Proceedings of IS&T 7th International Congress on Advanced Non-impact Printing Technologies.* Virginia: IS&T, 1991. pp. 271-280.

Investigation of Texture Effect on CRT Colour Difference Evaluation

John H. Xin[1], Chuen Chuen Lam[1], M. Ronnier Luo[2]

1. Institute of Textiles and Clothing, the Hong Kong Polytechnic University, Hong Kong.
2. Colour & Imaging Institute, University of Derby, UK

ABSTRACT

The effect of the texture and the level of the texture pattern of the textile woven fabrics on the visual colour difference evaluation were studied in this work. The texture images were captured by high performance scanner and simulated on CRT for colour difference evaluation. 15 different textures were used in the colour difference evaluation. The mapping of the textures to the solid colours was according to a work conducted in the same Institute. The colour difference values for the pairs with texture patterns are around 5.0 CIELAB units. The level of texture was expressed using the measure of the distribution of the luminosity. In comparison with the solid colour pairs, the texture mapped pairs showed a reduction in visual colour difference around 35% to 43%. The performance of the various colour difference formulae were also tested and it was found that CIELAB performed the best with the medium magnitude colour difference samples used in this study(around 5.0 CIELAB value).

1. INTRODUCTION

With the advances in information and electronic technologies, more and more colour information exchanges in areas of product design and product quality rely on electron means, which greatly shortened the exchange lead-time. To visualise the colour information, cathode ray tube (CRT) devices have been widely used by many commercial companies. It is also common in many textile companies to visually evaluate the colour samples mapped with texture patterns. Although the influence of texture on colour difference evaluation is known, as a parametric factor to the colour difference equation, few reports on quantitative analysis of the influence have been published. A lightness tolerance thresholds experiment was performed using the stimuli with a simulated texture of thread wound on a card by Montag and Berns [1]. The suprathreshold lightness tolerances were investigated around neutral colour centres at CIELAB L* equalling 10, 20, 40, 60, 80 and 100. The tolerances were compared among simulated full-textured samples, uniform samples, and samples with a simulated texture in between the two. Comparing to the uniform stimuli, the textured stimuli had an effect of increasing the tolerance thresholds by a factor of almost 2.

In this study, the influence of the texture on the visual colour difference assessment was investigated. Various colour difference equations were also tested against the visual data. The texture patterns used in this study were scanned from fifteen differently woven fabrics. These textures were then mapped to the pre-determined colours and simulated on a 21' Sony Trinitron CRT display. Totally 150 colour difference pairs were evaluated in this study. The method of simulation and visual evaluation are discussed in details in the following sections.

2. SYNTHESIS OF TEXTURE IMAGES WITH PRE-DETERMINED DEFIEND COLOURS

Before displaying a synthesized texture image on the CRT display, it was characterized using the Gain, Offset, and Gamma method with the consideration of the inter-reflections [2]. The selected woven patterns included various plain, twill, rib, jacquard and rhomb(fig 2). The textures were scanned using an EPSON EPX-10000 scanner. The histogram of the Y channel was used to represent the texture strength in this study since the textures of textile fabrics are regular in general. A "coarse" texture has a wide spread in its luminance distribution while a "fine" texture has a narrow spread. The half-width W was used to approximately represent the distribution of the histogram. It is defined as the distance between the left and right half values of the peak of the histogram distribution. For a woven textile fabric with spatially homogeneous texture pattern, W can be used to represent the texture strength. A schematic diagram of the Y channel histogram is given in Figure 1. The luminance was calculated using Y of the FCC RGB (Federal Communication Commission, USA) colour space [3]. The calculation of Y is given as the following:

$$Y = 0.299\,R + 0.587\,G + 0.114\,B \qquad (1)$$

Fifteen textures were selected from 80 scanned fabric images with different texture strength. The W of these fifteen textures ranged from 5 to 81 with an interval of around 5. The Y channel histograms of the fifteen textures are shown in Figure 2 and the images of those fabric samples with different texture strength are given in Figure 3.

As it was intended to use coloured texture samples in the colour difference evaluation, textures were required to map to solid colours. The grey (Y channel) to colour mapping was performed, which meant to deduce three-dimensional information of red, green and blue channels from the existing one-dimensional spatial distribution of the Y channel. Suppose $Y(p)$ is the luminance at pixel p, the deviation of spatial distribution of pixel p of the image can be written as:

$$\Delta Y(p) = Y(p) - \bar{Y} \qquad (2)$$

where, $\bar{Y}$ is the mean luminance of the texture image. Once we select a target colour S_n, we can map this colour to grey texture images. The channel output at pixel p is computed according to the following:

$$M_n(p) = S_n + \Delta Y\ (p) \qquad (3)$$

where n represents red, green, or blue channels. For instance, when $\Delta Y\ (p) = 10$, a target colour with R = 100, G = 150, and B = 200 is used to map to pixel p, the new colour becomes R' = 60, G' = 160 and B' = 210.

3. COLOUR DIFFERENCE PAIRS AND THE VISUAL ASSESSMENT

Five colour centres selected are listed in Table 1. These colour centres are the same as the ones in reference [4]. For each colour centre, thirty texture mapped colour difference pairs were generated, two pairs for each of the fifteen textures. A spectroradiometer (Photo Research model PR704) was used to measure the colour difference of the texture mapped colour difference pairs. The input colour values were adjusted until the synthesized texture pairs having a colour difference of around 5.0 ΔE^*_{ab} units in lightness direction. The arrangement of the synthesized texture colour difference pairs and the grey scale pairs on the CRT screen for visual assessment is shown in Figure 4. Observers were asked to rate the colour difference using the uniform grey scale generated. In order to evaluate the texture effect, a reference experiment using solid colour difference pairs with the same colour difference corresponding to the texture mapped pairs measured using the Photo Research spectroradiometer were also conducted under the same viewing conditions.

Table 1. Colour center used in the colour difference evaluation

Colour Centre	Orange	Yellow	Grey	Green	Blue
L*	48.33	69.28	68.25	28.69	28.96
a*	13.14	4.48	3.21	-17.83	4.43
b*	16.87	19.11	0.29	-0.50	-9.13

4. RESULTS AND DISCUSSION

The grey scale results were firstly converted to the visual difference ΔV according to a 3rd-polynomial conversion equation derived using grey scales[4]. The visual colour difference results from texture and solid colour difference pairs were then compared directly. The K value is defined as the ratio of ΔV of texture pairs to the ΔV of the solid pairs. K value deviates from 1.0 indicates a parametric effect.

For each colour centre, the average K value for the 30 colour difference pairs was given in Table 2. The K values vary from 0.57 to 0.65 with an overall average around 0.61 indicating a 39% decrease in the magnitude of colour difference evaluation for the textured pairs, which is very significant. Comparing the average K values of those five different colour centres, the K for yellow colour centre is the lowest, which indicate the highest parametric effect. However, the different among the average K values are not very significant.

Table 2. The average K value indicating the texture effect for the five colour centres.

Orange	Yellow	Grey	Green	Blue
0.6	0.57	0.62	0.65	0.63

The effect of the magnitude of texture strength on the visual colour difference evaluation is shown in Figure 5. When the half-width of the Y channel *W* is very low, which indicates a low texture strength, the K value is closer to 1.0. However, when *W* increases, the K value becomes smaller, indicating a stronger parametric effect. The spread of the K values is from 0.33 to 0.82. This trend is very similar for the five colour centres studied.

5. CONCLUSION

The influence of the texture on the visual colour difference of textile fabrics was investigated in this study. The results clearly showed that the visual colour difference evaluation is strongly influence by the texture of the sample pairs. The ratio between the visual colour difference of the texture sample pairs to the solid colour sample pairs varies from 0.33 to 0.82 for the fifteen texture patterns studied, the higher the texture strength, the lower the visual colour difference result. The texture effect is therefore a very important parametric effect. Further studies are necessary to quantify this effect and build it into the instrumental colour difference assessment to make the instrumental assessment more reliable.

ACKNOWLEDGMENT

The Authors wish to acknowledge the funding support from the Hong Kong Polytechnic University.

REFERENCE

[1]. ED Montag, RS Berns, Lightness dependencies and the effect of texture on suprathreshold lightness tolerances, *Color. Res. Appl.*, 2000:25, 241-249.
[2]. R S Berns, Methods for characterizing CRT displays, Displays, Vol. 16 No. 4, 1996.
[3]. S J Sangwine and REN Horne, The Color Image Processing Handbook, London: Chapman & Hall, 1998, pp.67-92
[4]. J H Xin, CC Lam, MR Luo, Investigation of Parametric Effects Using Medium Colour Difference Pairs, *Color. Res. Appl. 2001*:26, 376-383.

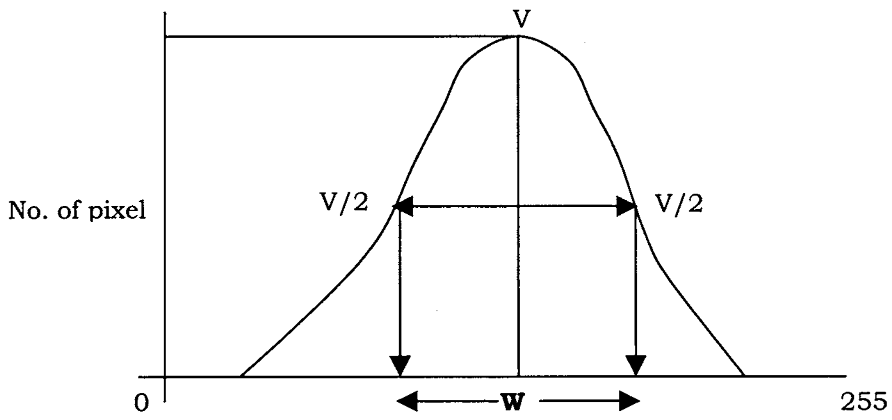

Figure 1. Illustration of the half-width of the Y channel histogram.

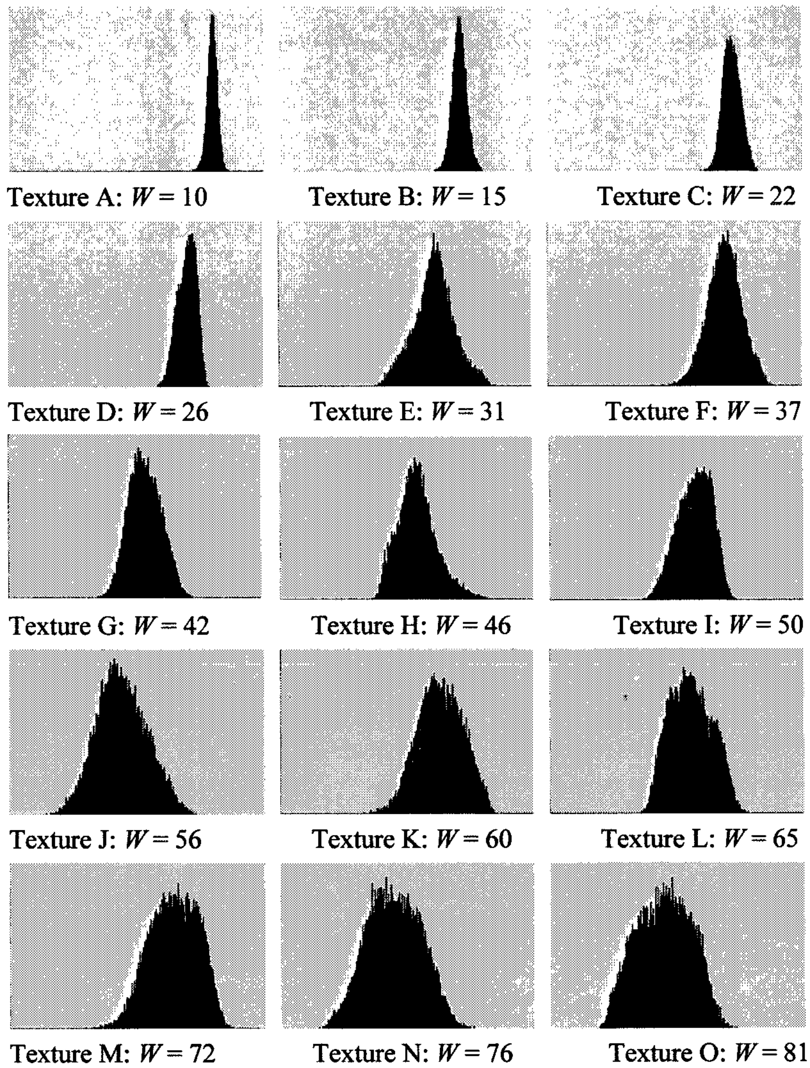

Figure 2. The Y channel histograms of the fifteen selected textures.

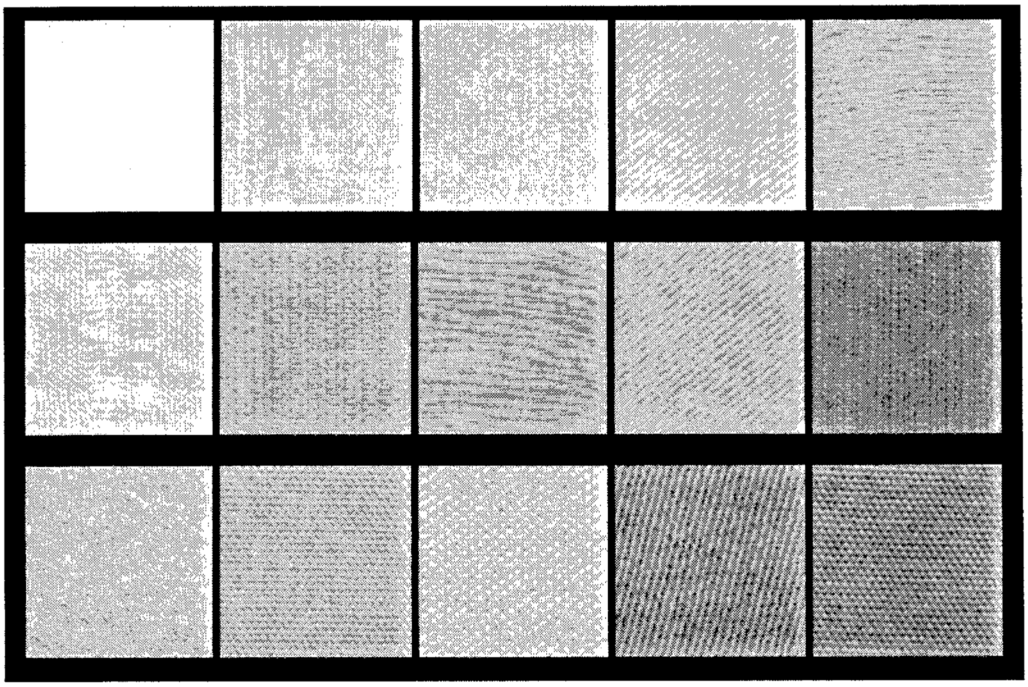

Fig. 3. The fabric samples with different texture strength used in the colour difference evaluation.

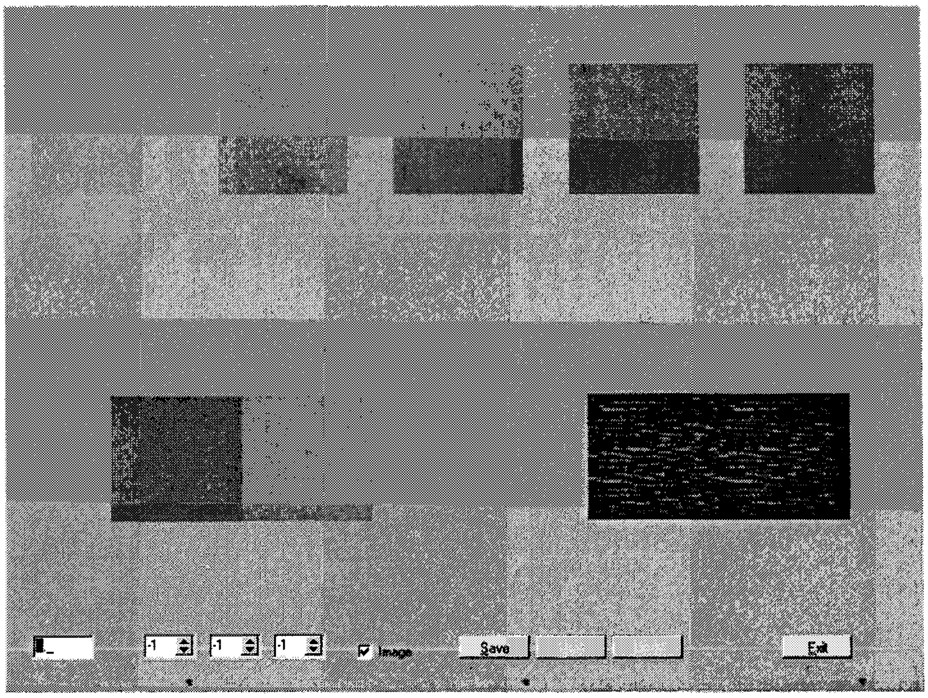

Fig. 4 The arrangement of sample pair and grey scales on a CRT monitor.

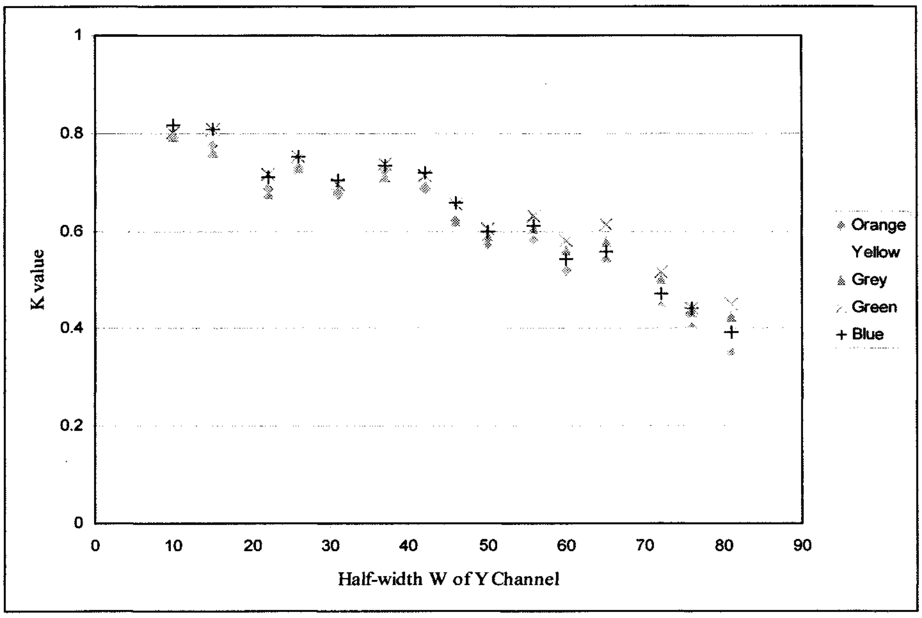

Figure 5. The relationship between K value and the half-width of Y channel.

Spectral luminous efficiency functions measured in real environments

Hiroyuki Shinoda and Mitsuo Ikeda
Dept. of Photonics, Ritsumeikan University
1-1-1 Nojihigashi, Kusatsu, Shiga, 525-8577 Japan

ABSTRACT

The spectral sensitivity varies depending on conditions. Though many luminous efficiency curves have been measured for various levels, it is quite difficult to select the most suitable one to a given practical situation. Since real environments have complex luminance distributions and retinal stimulation is changed by eye-movement, the level cannot be defined by any single quantity such as retinal illuminance, luminance, or illuminance. Here, we introduced a practical method for measurement of the luminous efficiency curve. Assuming the curve to be expressed by a linear combination of $V(\lambda)$ and $V'(\lambda)$, we tried to determine a coefficient defining these relative contributions. In this method, the heterochromatic flicker photometry HFP was carried out with a few color stimuli in real environments, using a small gray patch spotlighted by a projector. The results show that the method can track the coefficient shift as an environment or a target changed.

Keywords: luminous efficiency function, mesopic vision, flicker photometry, complex visual environment

1. INTRODUCTION

To calculate the luminance or brightness, you have to use the luminous efficiency function defined by the heterochromatic flicker photometry HFP or the heterochromatic brightness matching HBM. In the CIE photometric system, two luminous efficiency functions $V(\lambda)$ and $V'(\lambda)$ are used for photopic and scotopic luminance calculation. In mesopic range, the spectral sensitivity of our visual system changes its shape gradually from $V(\lambda)$ to $V'(\lambda)$ as the level goes down. Plenty of data has been accumulated from experiments of HFP and HBM in the mesopic range under a very simplified experimental condition, such as a dark surround or a uniform surround. The various functions are now ready to be applied as a function of retinal illuminance, or luminance. The problem is, however, to select the most appropriate function to a real and complex environment. In everyday lives, we see an object or a light in a complex surrounding consisting of objects and lights of various luminance and chromaticities. Furthermore the retinal stimulation rapidly changes as our eyes move. It is difficult to define the adaptational level in a practical situation with a single measure such as retinal illuminance or luminance.

In the present report, we propose a easy method for measuring luminous efficiency function in a real environments. The mesopic function $V_{\text{mesopic}}(\lambda)$ is known to be expressed by a combination of the photopic $V_{\text{photopic}}(\lambda)$ and the scotopic $V_{\text{scotopic}}(\lambda)$ functions. We first employed the most simply model, a linear combination, as shown by the following formula.

$$V_{\text{mesopic}}(\lambda) = a \cdot V_{\text{scotopic}}(\lambda) + (1-a) \cdot V_{\text{photopic}}(\lambda) \quad (1)$$

where a is called an adaptation coefficient or a weighting factor, which gives a relative contribution of rod system to the luminance channel. Here measuring a luminous efficiency function corresponds to determining the adaptation coefficient. In the experiment, equiluminous settings for several colors were obtained using the heterochromatic flicker method HFP. Supposing the minimum flicker was obtained between two colors whose spectral radiance distribution are $Le_m(\lambda)$ and $Le_n(\lambda)$, the following equation holds.

$$\int_{\text{visible light}} Le_m(\lambda)\cdot V_{\text{mesopic}}(\lambda)d\lambda = \int_{\text{visible light}} Le_n(\lambda)\cdot V_{\text{mesopic}}(\lambda)d\lambda \qquad (2)$$

By substituting (1) into (2), a function $F(a)$ is defined as follows. The coefficient a is analytically given by solving the equation $F_{mn}(a) = 0$.

$$F_{mn}(a) = \int_{\text{visible light}} \left[Le_m(\lambda) - Le_n(\lambda)\right]\cdot\left[a\cdot V_{\text{scotopic}}(\lambda) + (1-a)\cdot V_{\text{photopic}}(\lambda)\right]d\lambda \qquad (3)$$

Ideally any color pairs give the same coefficient a, when they are all balanced through HFP. In practical situation, however, they do not necessarily give the same a mainly because of deviation of subjects' spectral sensitivity function from that for the standard observer. In the present method here, the least square method is applied. The sum of squared $F_{mn}(a)$ is introduced as follows.

$$S(a) = \sum_{m,\,n}^{\text{all flicker pairs}} \left[F_{mn}(a)\right]^2 \qquad (4)$$

The value of a that gives the minimum $S(a)$ is obtained when its differential, d$S(a)$/da, becomes zero. The resulted a is given by the following formula.

$$a = \frac{\sum_{m,\,n}^{\text{all fliker pairs}} \left(I_{mn} - J_{mn}\right)\cdot I_{mn}}{\sum_{m,\,n}^{\text{all fliker pairs}} \left(I_{mn} - J_{mn}\right)^2} \qquad (5)$$

where $\boldsymbol{I}_{mn}$ and $\boldsymbol{J}_{mn}$ are defined by the following formulae.

$$I_{mn} = \int_{\text{visible light}} \left[Le_m(\lambda) - Le_n(\lambda)\right]\cdot V_{\text{photopic}}(\lambda)d\lambda$$
$$J_{mn} = \int_{\text{visible light}} \left[Le_m(\lambda) - Le_n(\lambda)\right]\cdot V_{\text{scotopic}}(\lambda)d\lambda \qquad (6)$$

Instead of the integrals over wavelength of visible light, summations with a certain wavelength interval Δλ are calculated. We developed a portable apparatus for HFP consisting a gray patch and a projector of variable intensity. In the experiment, the coefficient was measured through HFP in complex visual environments and the performance of the method was evaluated. The CIE1924 $V(\lambda)$ and the CIE1951 $V'(\lambda)$, shown in Fiqure 1, were employed as $V_{\text{photopic}}(\lambda)$ and $V_{\text{scotopic}}(\lambda)$.

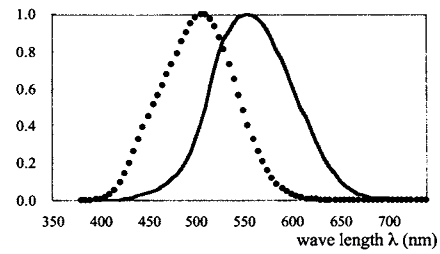

Figure.1 The CIE1924 photopic *V(λ)* and the CIE1951mesopic *V'(λ)*.

2. EXPERIMENT

The experiment was conducted in a enclosed booth equipped with fluorescent lamps on the ceiling. Inside the booth many objects were put to simulate a normal and complex visual environment as shown in Figure 1. The room illuminance was monitored with an illuminometer on the table in front of the wall. An N5.5 mat gray patch of 7cm x 7cm square was spotlighted by a small DLP projector, PLUS U2-1130, driven by an Apple PowerBookG4. The patch subtended 5 degree for the subject 80 cm away. This was large enough to surpass the rod free region on the retina. The patch was tilted so as to be illuminated by the projector but not by the ceiling light. Appropriate neutral density filters were inserted in a light path to attenuate the intensity of projecting light.

The spectral radiance distribution ($W/sr{\cdot}m^2{\cdot}nm$) was measured with a spectroradiometer, Minolta CS-1000. The spectral radiance for each phosphors without filters were shown in Figure 2.

Colors were controlled by input values for each phosphor (r, g, b) with 8 bit depth, namely 0 through 255. The reference and the test colors were presented alternately with a frequency of 15 Hz. Given a certain intensity of the reference color, a subject adjusted the intensity of the test color until the perceived flicker would disappear or be the minimum. The intensity of colors on the patch was varied while keeping the ratio of (r, g, b). A neutral color N (r:g:b=1:1:1) was employed as the reference and three colors R (r:g:b = 1:0:0), G (r:g:b = 0:1:0), and B (r:g:b = 0:0:1) as the test colors. So there were three flicker pairs R-N, G-N, and B-N to be used for the calculation of the coefficient.

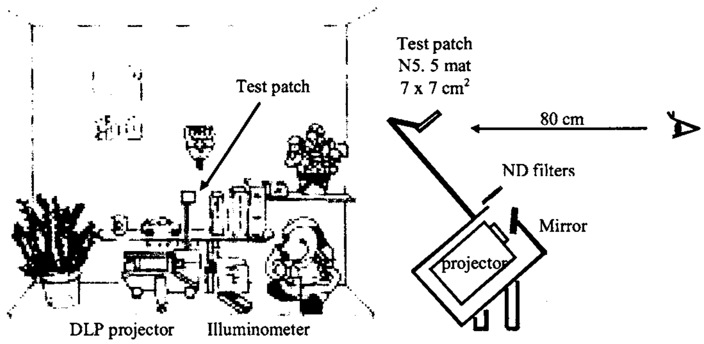

Figure.2 Experimental booth, the left, and the portable HFP apparatus, the right. The illuminometer and the apparatus were put on the front table. The N5.5 gray patch was spotlighted by a DLP projector controlled through an Apple's PowerBookG4. To attenuate the intensity ND filters were inserted in the projecting light path.

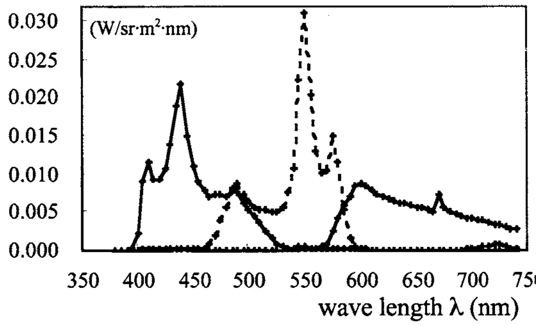

Figure.3 Spectral radiance ($W/sr{\cdot}m^2{\cdot}nm$) on the gray patch of three test colors without ND filters.

The HFP experiment was done under five different illuminance levels, 0.1, 1.0, 15, 250, 500 lx, which were achieved by the light dimmer and black covers with many holes over the ceiling light. The experiment started after the 5 minutes dark adaptation. The subject adjusted the intensity of the test colors through a mouse or a trackball until the minimum flicker is obtained. The level of the neutral reference was selected from (70, 70, 70) through (110, 110, 110) randomly.

3. RESULTS

As examples, the sum of squared $F(a)$ and three $F(a)$ for each flicker pair are shown as functions of a in Figure 4. Here the formula (3) for $F(a)$ was obtained from a subject HS's minimum flicker settings with the reference of 0.31 $W/sr{\cdot}m^2$ under the iluuminance 500 lx. These three functions do not become zero at the exact same a. The best suited coefficient a is given by the minimum $S(a)$, the sum of squared $F(a)$, instead. Here we did just three pairs of flicker adjustments. More flicker pairs, however, might improve the accuracy in determination of a.

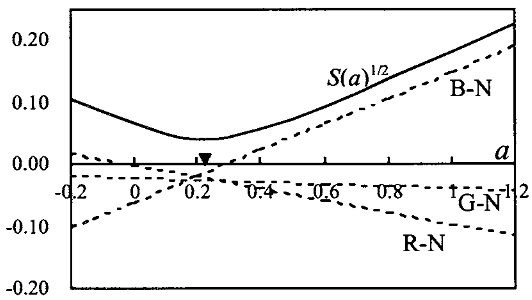

Figure.4 The square root of $S(a)$, a solid line, and $F(a)$ for each flicker pair, dashed lines. Subject HS, illuminance 500 lx, reference radiance 0.31 $W{\cdot}sr^{-1}{\cdot}m^{-2}$. Minimum $S(a)$ gives the best suited coefficient as shown by the arrow.

In figure 5, the root square of $S(a)$ are shown for different reference radiance levels. The curves were calculated from flicker settings done by the

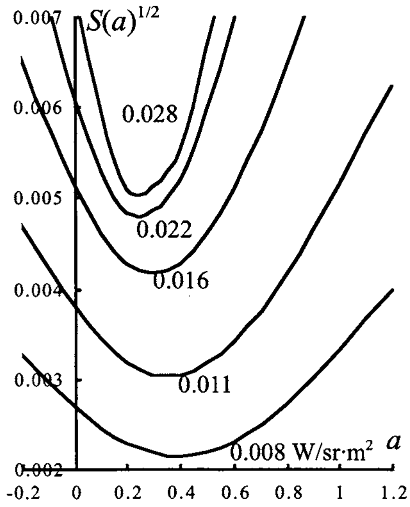

Figure.5 The square root of $S(a)$ for different radiance levels of reference. The subject HS, the illuminance of 15 lx. The minimum point in $S(a)$ shifts leftward with the reference level.

same subject HS under the illuminance of 15 lx. As the radiance of reference increase, $S(a)^{1/2}$ itself increase. In addition to that, the curve shifts toward the left, indicating that the coefficient a become smaller with the radiance level. It implicates the method can track the coefficient change.

In figure 6, the coefficient a is plotted for all illuminance and reference conditions. The coefficient was analytically obtained by putting the spectral radiance distributions for the minimum flicker setting of the three pairs R-N, G-N, and B-N, into the formulae (5) and (6). As mentioned, the summations with $\Delta\lambda$=5nm from 380 through 740 nm were calculated instead of the integrals.

The coefficient varies in a range from 0.2 to 0.7. Every lines show negative slope, indicating a as a decreasing function with reference level. However the reference level does not solely determine the coefficient. The illuminance of a room is also an important factor. Even with the same reference, the coefficient became high under higher illuminance level.

Small coefficient for high radiance of reference is quite reasonable even under low illuminance. Since adaptation of the cone system proceeds more quickly than the rod system, brighter stimuli in a visual field may predominant in determination of adaptation level.

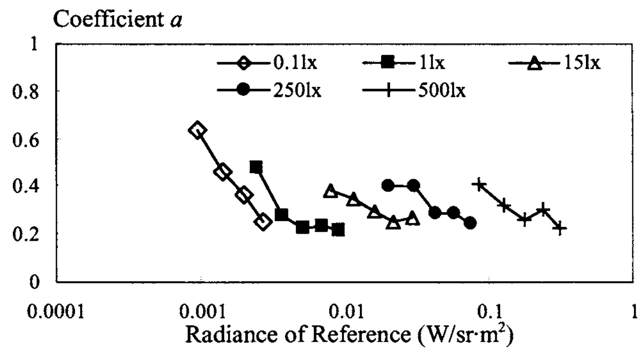

Figure.6 Coefficient a as a function of the radiance level of reference for the subject HS. Five curves correspond to different illuminance levels.

On the other hands, large coefficient was unexpected at high illuminance levels for the same reason. Here, however, even at high illuminance such as 250 lx, the coefficient reached around 0.4. Because of our fitting for the relation between input value and radiance in each RGB channel, calibration was not accurate for lower input values. The leftmost points of each curves might have larger errors. The another possible error might be caused by an added illumination from the ceiling light. The relative amount of illumination by the ceiling light is large for the reference of low radiance. The result suggests that accuracy of the method should to be improved for low radiance level of reference.

The method should be improved in many ways. Here just three pairs were matched through HFP. More flicker pairs might improve the accuracy of the method. Instead of the linear combination model, the linear combination of logarithmic functions might be better. Or employing the photopic and scotopic functions for standard observer may set a limit. That might be why the range where the coefficient varied did not cover the whole range from 0 to 1. The subject was instructed not to make rigid fixations onto the patch but to look around the room as much as possible during the adjustment. Even so, if the task requires long time enough to eliminate the effect from the prior retinal stimulation, the measurement itself would change the adaptational state and the radiance level of reference would be dominant. If it is true, instead of adjustment, another procedure should be employed which does not require long fixation.

Acknowledgements

We acknowledge Mr. Y. Harada and Mr. T. Hashimoto at Ritsumeikan University for their cooperation and participation in the experiment.

Effect of white surface on achromatic perception in different visual environments

Tetsuya Eda*, Miyoshi Ayama*, Daisuke Kon*
Sueko Kanaya**, Kenji Mukai***

* Utsunomiya University, Japan

** Kanazawa Institute of Technology, Japan

*** Matsushita Electric Industrial, Lighting Company, Japan

ABSTRACT

In this study, we conducted the experiment to investigate whether the perceptually achromatic point observed in a chromatically biased room is influenced by existence of white surface there. Perceptually achromatic region was determined using grayish Munsell chips (Value is 5.0, Chroma is 0, 0.5 or 1.0) under the fluorescent lamps of correlated color temperatures of 3000K and 6700K in either reddish or bluish room with and without white surfaces.

The resulting achromatic regions do not show stark difference between the conditions with and without white surfaces, suggesting that white surface does not play a role of anchor for the achromatic perception. It seems that perceptually achromatic point is determined by the chromatic adaptation to a given environment where the light source and the color of the environment are effective factors.

Keywords: White surface, Fluorescent lamp, Reddish or Bluish room, Achromatic point

1. INTRODUCTION

In everyday life, there exit a lot of white surfaces around us. White surface seems to play a role of anchor when we judge color appearance of objects in a visual environment. We might judge the lightness of a certain surface by comparing it with apparent brightness of white surface, and we might judge the chromaticness of an object by comparing it to the perceived whiteness of white surface existed in the same environment. White surface reflects the spectral radiant distribution of the light source most directly. So we have been considering that properties of white surface in various illumination conditions could be used as some indices to evaluate the quality of illumination.

In previous studies, we have conducted several experiments to investigate the whiteness perception under a variety of fluorescent lamps [1], [2]. The results of our studies showed that ranking of the perceived whiteness of white and nearly white chips changes with the correlated color temperature of the lamps.

In this study, we carried out the experiment to examine whether the existence of white surface affects the perceptually achromatic point in strongly chromatically biased visual environments.

2. EXPERIMENT

Two chromatically biased observation booths were constructed. One room is reddish, and the other is bluish. In the reddish one, the floor was covered by a dark red carpet and walls were covered by various reddish cloths with medium to low lightness (See Fig.1). The bluish room was made in a similar way, such as using navy carpet, and bluish cloths. Fig. 2 is a side view of experimental booth. The size of one booth was 210cm cubic. Using these booths, we set the conditions with and without white surfaces. A white shirt and four sheets of blank copy papers were used as familiar white surfaces. Two kinds of fluorescent lamps, correlated color temperature of 3000K and 6700K, were employed as light sources. Therefore total of eight conditions (2 lamps × 2 booths × 2 settings with and without white surfaces) were employed.

In each condition, we tried to determine the perceptually achromatic point. Forty-one grayish Munsell chips framed by a black paper, the size of 4 cm × 4 cm, were prepared. Munsell values of them are 5.0, and the Munsell chroma is either 0, 0.5, or 1.0. Illuminance was set at 500lx on the upper surface of the low table.

Chromaticity coordinates of the Munsell chips used as test stimuli in each condition were measured. We were carefully controlled the amount of white surfaces not to change the chromaticities of the Munsell chips from those without white surface condition under the same fluorescent lamps in the same booth.

The observer wore a hat with a wide brim not to look at the light source directly and a gray cloth to avoid effects of their colored cloths. The observer also wore an eye mask when he/she entered the booth so that they could not recognize quality or kind of illumination in the booth from the outside. After they sat down in front of the low table, they took out the eye mask and adapted to the illumination in the booth for 5 minutes. Then, the observer looked at the test chip which was placed on the table at an angle of 45 degrees to the table surface.

In the first step, he/she was instructed to answer whether the chip appears chromatic or achromatic. In the case of chromatic, he/she should response the monolexemic color name for the chip. In the case of achromatic, the chip was put into the "achromatic basket" in the side of the low table. This procedure was repeated for 41 chips. In the second step, the observer placed all the chips judged as achromatic in the first step on the low table, and looked at them simultaneously and then chose the most achromatic one among them. For each observer, four sessions were done for each of the eight conditions.

One female and two male students participated as observer. All of them were in their early twenties confirmed to have normal color vision as determined by the Farnsworth-Munsell 100 Hue Test.

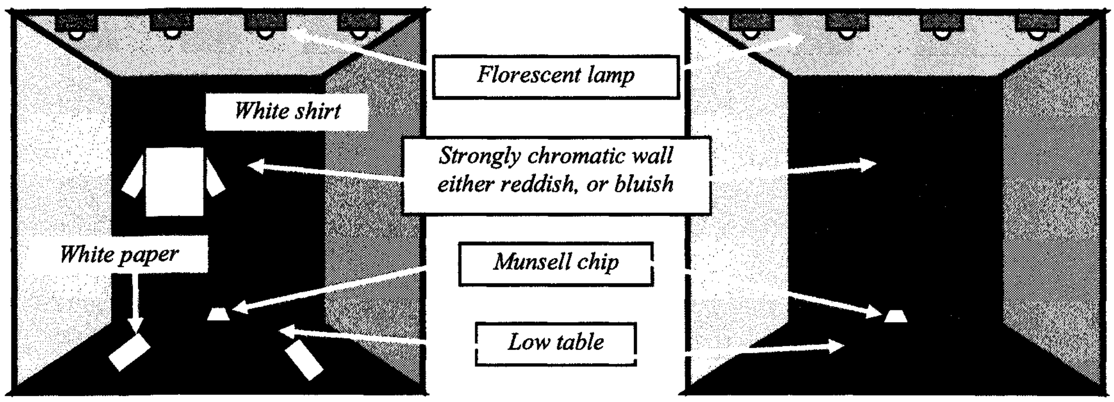

Figure 1. Experimental booth with left and without right white surfaces. A white shirt and four sheets of blank copy papers are used as white surfaces.

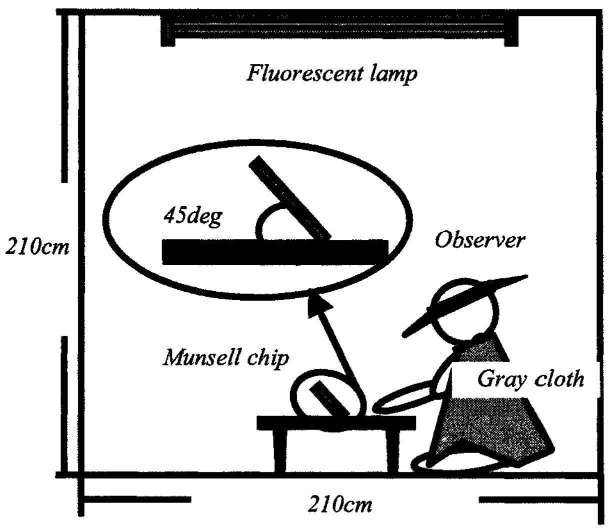

Figure 2. Inside of the booth at the time of an experiment

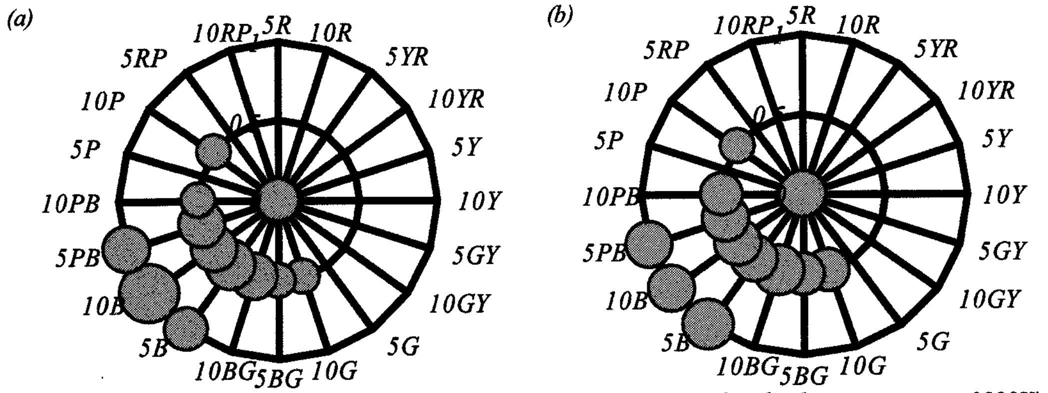

In the reddish booth with (a) and without (b) white surface (Correlated color temperature: 3000K)

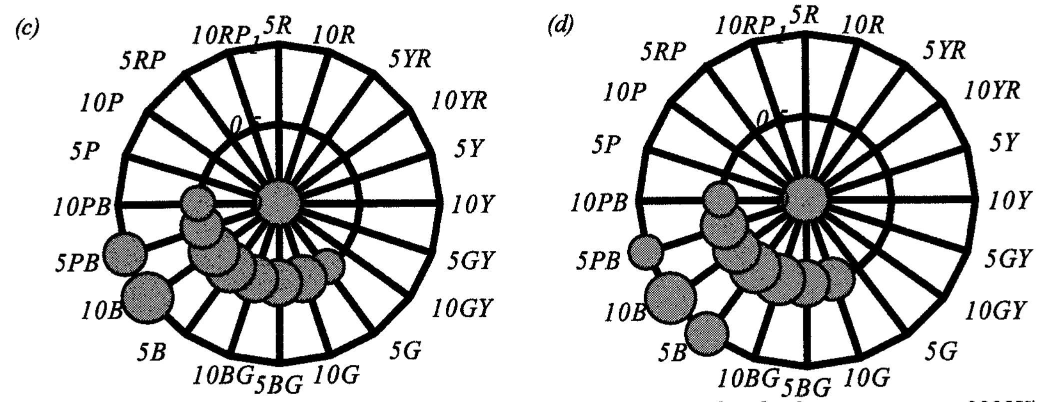

In the bluish booth with (c) and without (d) white surface (Correlated color temperature: 3000K)

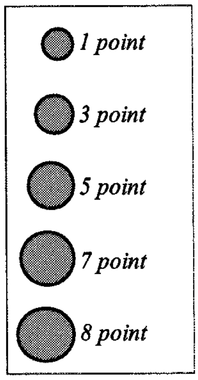

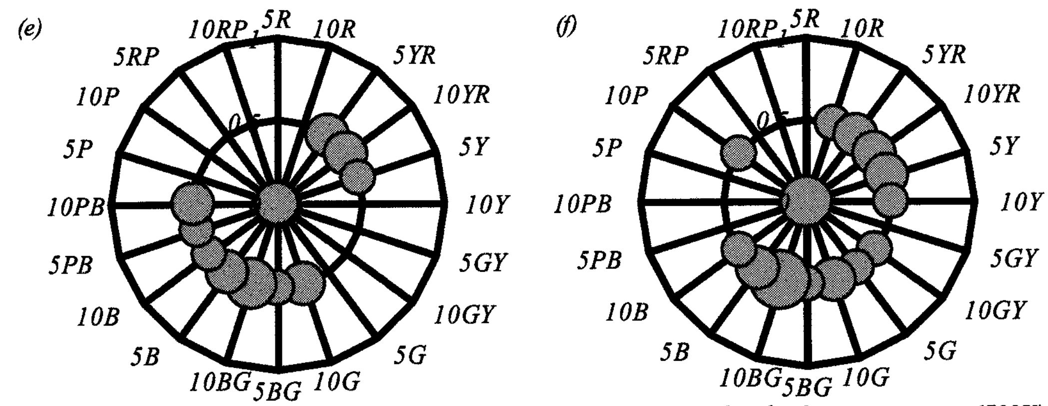

In the reddish booth with (e) and without (f) white surface (Correlated color temperature: 6700K)

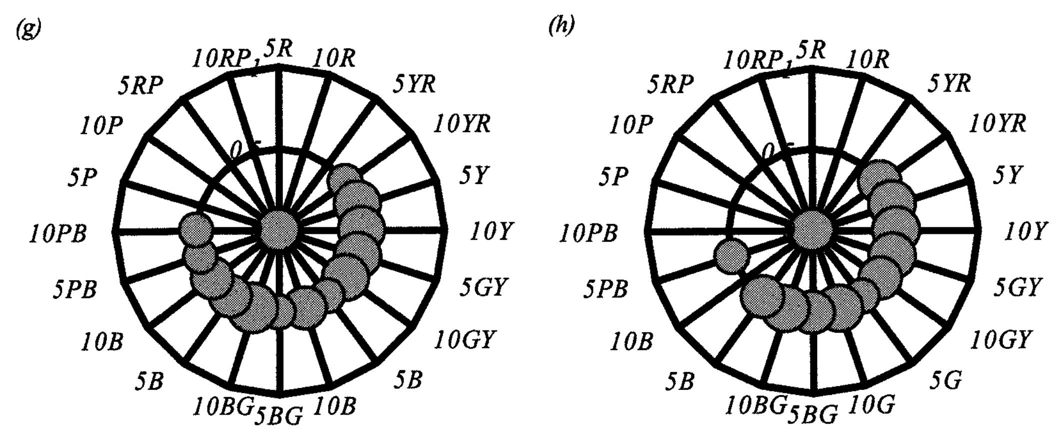

In the bluish booth with (g) and without (h) white surface (Correlated color temperature: 6700K)

Figure 3. Result of achromatic region in various conditions

3. RESULTS

For the results of each session, two points were assigned to the chip which was selected as the most achromatic one in the second step of the procedure, whereas one point was given to the chips that were selected as achromatic one in the first step. These points were summed up for four sessions for each observer, and then mean value of three observers was calculated. Therefore the maximum value is eight. The results are plotted on the Munsell hue circle as shown in Fig. 3.

Fig.3 indicates that, in all the conditions, to determine the perceptually achromatic point seems quite difficult, and instead of a 'point', achromatic region was determined. As shown in Fig.3, the existence of the white surface does not affect the perceptually white region under strongly chromatic environment. The results obtained in the reddish and bluish booths do not show significant difference. Correlated color temperature of the lamp is the most effective factor on the achromatic region. In 3000K lamp conditions (Fig.3 (a) to (d)), the achromatic region extends over from G to P. Particularly from 5B to 5PB, the Munsell chips of chroma 1.0 are selected as achromatic in most of the cases. In 6700K lamp conditions (Fig.3 (e) to (h)), the achromatic region spreads over from 10PB to YR through G and GY. Under the 6700K lamp, the Munsell chips of chroma 1.0 is never included in an achromatic region. Difference between the reddish and bluish booths are more obvious than the case of 3000K lamp condition. In the results of the reddish booth with white surfaces (Fig.3 (e)), the chips of 5G to 10Y were not selected as achromatic at al. In the case of Fig.3 (f), the reddish booth without white surface, 5GY is not included in the achromatic range, while the chips of 5G to 10Y show very low scores. On the other hand, the results in the bluish booth (Fig.3 (g) to (h)), the chips of G to GY are in the achromatic region and do not necessarily indicate low scores. This suggests that achromatic perception under 6700K lamp is more easily influenced by the colors in the environment than that under the 3000K lamp.

4. SUMMARY

In this study, we conducted the experiment to investigate whether the perceptually achromatic point observed in a chromatically biased room is influenced by existence of white surface there. Perceptually achromatic region was determined using grayish Munsell chips (Value is 5.0, Chroma is 0, 0.5 or 1.0) under the fluorescent lamps of correlated color temperatures of 3000K and 6700K in strongly chromatic environments of either reddish or bluish room with and without white surfaces.

The resulting achromatic regions do not show stark difference between the conditions with and without white surface, suggesting that white surface does not play a role of anchor for the achromatic perception. It seems that perceptually achromatic point is determined by the chromatic adaptation to a given environment where the light source is the most effective factor while the color of the environment is also a factor to be taken into consideration.

REFERENCES

[1] Takao Akatsu, Eiichiro Toriumi, Miyoshi Ayama, Kenji Mukai, Sueko Kanaya., "Effects of color temperature of fluorescent lamp on the whiteness perception", CIE, Warsaw, 1999, pp. 48-51.

[2] Miyoshi Ayama, Takao Akatsu, Eiichiro Toriumi, Kenji Mukai, Sueko Kanaya, "Whiteness Perception under Different Types of Fluorescent Lamps", Color Res. Appl., 2003, 28, pp. 96-102.

Authors

Tetsuya Eda, Miyoshi Ayama, and Daisuke Kon,
Information and Control Systems Science, Graduate School of Engineering, Utsunomiya University
7-1-2 Yoto, Utsunomiya 321-8585 Japan
Phone: +81-28-689-6264, e-mail: eda@hawk.is.utsunomiya-u.ac.jp

Sueko Kanaya,
Division of Architecture, Kanazawa Institute of Technology
7-1 Ohgigaoka, Nonoichi, 921-8501 Japan

Kenji Mukai,
Matsushita Electric Industrial, Lighting Company
1-1 Saiwai-chou, Takatsuki, 569-1193 Japan

Unique hue and spectral bandwidth

Yoko Mizokami[1], John S. Werner[2], Michael A. Crognale[1] and Michael A. Webster[1]

[1]Department of Psychology, University of Nevada, Reno
[2]Departments of Ophthalmology, and Neurobiology, Physiology & Behavior, University of California, Davis

ABSTRACT

A central question in color vision is: to what extent are the unique hues tied to properties of the environment versus properties of observers? We are exploring this by asking how the unique hues vary with changes in the spectral bandwidth of the stimuli, for which environmental and physiological accounts make different predictions. Selective filtering by the lens and macular pigment differentially biases the spectrum of broader bandwidth lights relative to narrower bandwidths. We examined the extent to which these biases influence differences in perceived hue both across individuals and within the same individuals at different retinal eccentricities. Differences across observers were compared to two possible models of the unique hues (based on assuming a common set of cone ratios or a common stimulus in the environment) which differ in predicting either a decrease or increase in interobserver differences as the spectrum narrows. The results did not clearly support either model implying the unique hues are relatively unaffected by the filtering effects of screening pigments and that differences between observers may reflect different weightings of the cone signals or normalization to different stimuli in the environment.

1. INTRODUCTION

The color appearance of any aperture light can be described by combining different pairs of the four unique hues: red, green, blue, and yellow. The unique hues themselves appear as pure and irreducible sensations, and are thus important to models of human color appearance (Abramov and Gordon, 1994). Observers vary widely in the specific spectral stimuli that they choose for unique hues, but the bases for these individual differences remain uncertain (Schefrin and Werner, 1990; Webster et al., 2000). One suggestion is that the unique hues isolate postreceptoral channels that draw on specific combinations of the cone signals (Kaiser and Boynton, 1996), so that individual differences arise from physiological factors such as, for example, differences in the relative numbers of cone receptors (e.g. Cicerone and Nerger, 1989). An alternative is that they correspond to learned properties of the visual environment (Pokorny and Smith, 1977), so that interobserver differences reflect the nature of our experience with color signals. We tested whether the unique hues are consistent with a fixed rule for weighting the cone signals, by asking how unique hues vary as the spectral bandwidth of the light changes from narrow (e.g. monochromatic) to broadband. Selective filtering by the lens and macular screening pigments reduces sensitivity at shorter wavelengths, and is a major factor contributing to individual differences in color matching (Webster and MacLeod, 1988). This screening differentially biases the spectrum of broader bandwidth lights relative to narrower bandwidths, and thus alters the dominant wavelength of the light reaching the receptors. To maintain a fixed cone ratio, the dominant wavelength of the stimulus must shift toward shorter wavelengths as the stimulus bandwidth increases. Thus a fixed weighting – whether innate or learned – predicts that the dominant wavelength chosen for the unique hues will vary with bandwidth. On the other hand, environmental and physiological accounts make different predictions about how the unique hues should vary across individuals (who might vary in ocular pigment density) and within the same individuals at different retinal eccentricities (which differ in macular pigment density). If the unique hues are determined by a fixed ratio of the cone signals, then individual differences should be smaller for narrowband stimuli than broadband. This is because the stimuli required to maintain this ratio should diverge as the spectrum is broadened and as individual differences in ocular density come to play a larger role. That is, narrowing the spectrum removes one potential source of physiological variation, and thus should lead to greater consensus across observers. However, if the unique hues instead reflect learned stimuli in the environment, then differences in the hue settings should instead be larger for narrowband stimuli. In this case, this is predicted to occur because natural color signals are very broadband while narrowband stimuli are rare (Maloney, 1999). Suppose that observers learn to agree about the natural color signals they label as pure green, even though these signals are filtered in different ways by their individual eyes (Jordan and Mollon, 1995). As the spectrum is artificially narrowed, each observer might choose a stimulus that preserves the cone ratio they learned from the broadband stimulus, and these will diverge as the screening pigments now become less important in shaping the spectrum. Thus the experiential account predicts that learned consensus for broadband stimuli will break down for narrower spectra. Note that similar predictions also apply to the color judgments of a single observer for stimuli viewed at different retinal eccentricities, since the macular screening pigment is limited to the central retina. We therefore compared the predictions for physiologically and environmentally determined models of the unique hues both for different observers and for the same observer in foveal and peripheral viewing, and asked to what extent either model could account for actual measurements of the changes in unique hues between narrow and broadband stimuli.

2. MODEL METHODS

Predictions were based on calculating the unique hue loci for a set of simulated color-normal observers who differed in lens and macular pigment density and in the spectral peaks of the long, medium, and shortwave (L, M, and S) cones. The spectral sensitivities for individual observers were reconstructed from a factor analysis of the 49 observers in the Stiles and Burch 10 deg field color matches (Webster and MacLeod, 1988), following procedures described in Webster et al. (2000). For the common LMS ratio model, we calculate for each observer the stimulus required to produce the same angle relative to white (Illuminant C) within an LvsM and SvsLM chromatic plane. The chosen angle corresponded to the mean unique hue settings for the set of observers tested by Webster et al. (2000). As the spectral bandwidth varied each observer was assumed to vary the stimulus to preserve the same LvsM and SvsLM ratio. For the common environmental stimulus, observers were assumed to all choose the same broadband stimulus. This corresponded to the spectrum of a moderately saturated Munsell chip again with a chromatic angle equal to the mean unique green settings of the Webster et al. (2000) observers. As the spectral bandwidth varied each observer again had to vary the stimulus to preserve the same LvsM and SvsLM ratio. The resulting predictions are shown in Figure 1. Note that both models predict that blue and green settings should shift toward shorter wavelengths for broader spectra. However, the common ratio model predicts large increases in interobserver variations as the spectrum is broadened, while the common environmental stimulus predicts modest decreases in individual differences for broader spectra.

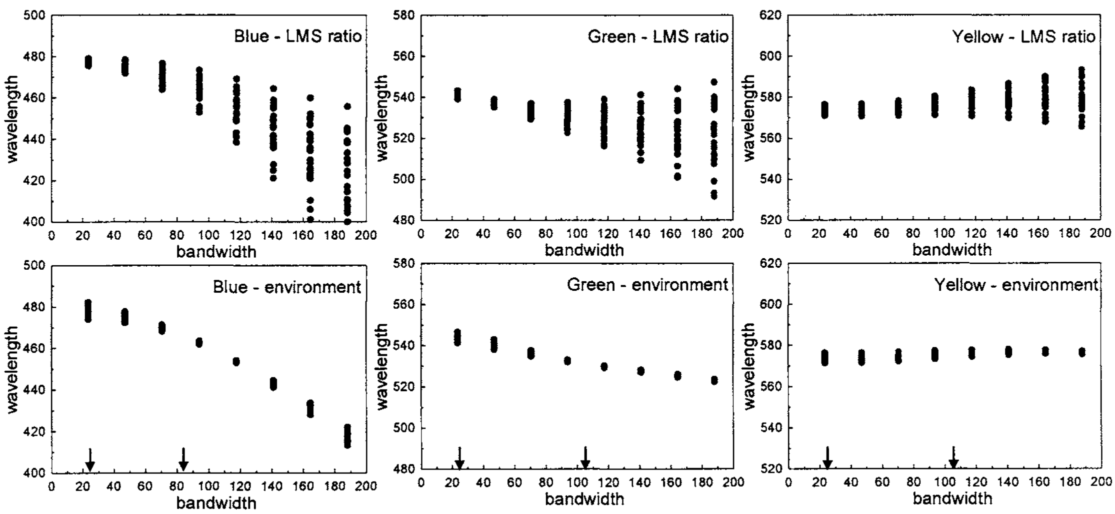

Fig. 1. Predicted individual differences in unique hues as a function of spectral bandwidth, assuming a common LMS ratio (upper) or a common environmental stimulus (lower) for unique blue, green and yellow. Arrows show bandwidths examined in the following experiments.

3. EXPERIMENT

Unique hue settings were measured with the apparatus shown in Figure 2. Light generated by a 200W Xenon lamp is collimated by a lens, L. The collimated light illuminates an interference wedge, IF, which gives a continuous spectrum that is linear in wavelength units. The light then passes through an LCD panel placed directly after the interference wedge. Spatial patterns generated on the LCD panel mask the light from different parts of IF and thus control the spectrum reaching an integrating sphere, IS, which forms a uniform 2 deg stimulus (Bonnardel et al., 1996). Subjects viewed the stimulus binocularly on a dark background in a dark room.

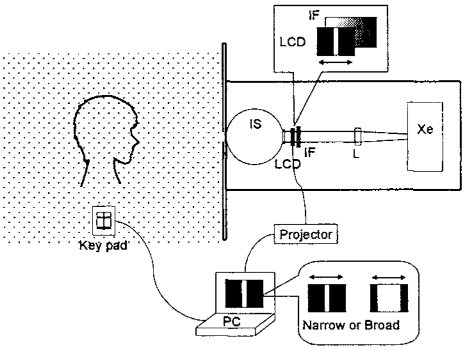

Fig. 2. Experimental apparatus. L, lens; IF, interference wedge; LCD, LCD panel; IS, integrating sphere.

Stimuli were roughly Gaussian spectral distributions. Two different bandwidth conditions were prepared for test stimuli: 25 nm at half height for the narrow stimulus and 105 nm for broad in the case of unique green and yellow, or 85 nm in the case of unique blue. These ranges were limited by available light (at the narrow end) and spectral limits (at the broad end). The stimuli were generated by changing the slit size on the LCD panel as shown in Figure 2. The luminance of test stimuli was set near 2.0 cd/m^2 and matched for brightness to an achromatic adaptation light. Stimulus spectra were measured with a PR650 spectroradiometer.

In the 2-deg field, the test stimulus was shown for 1.5 sec following adaptation for 30 sec to an achromatic light, and then followed again by the achromatic light. Observers used a keypad to rate the color of the test as either reddish or greenish for unique blue or yellow settings, or as yellowish or bluish for unique green. A staircase method was used to vary subsequent stimuli and the average of ten reversals was taken as the unique hue setting. Observers made unique hue settings for narrow and broad stimuli in the fovea or at 10 deg in the periphery. Each observer made six settings for each condition in random order. The same procedures were conducted for blue, green and yellow judgments. Because unique red is an extraspectral stimulus, we did not carry out measurements for red. Thirty or more subjects with normal color vision participated in the foveal fixation condition and nine of these made settings for both foveal and peripheral viewing for each unique hue condition.

4. RESULTS AND DISCUSSION

Figure 3 shows the results of unique blue, green and yellow settings for all observers on the CIE 1931 chromaticity diagram and dominant wavelength according to bandwidth of the test stimuli, respectively. These dominant wavelengths were determined with respect to CIE standard Illuminant C. Means and standard deviations are shown in the third and fourth column in Table 1. There are a number of ways in which the results deviate from the predictions of both models. First, the range of observed variation is much larger than the ranges predicted by either model we considered. This indicates that there are important factors contributing to interobserver differences that were not incorporated in the models. For example, we did not attempt to model known physiological differences such as the relative numbers of cones since these differences are not given by the Stiles and Burch color matches, nor a possible influence of rods. Moreover, we assumed that all observers would choose the same LMS ratio (for the physiological model) or the same physical stimulus (for the environmental model). The larger observed variability could suggest that these assumptions are wrong. For example, if the unique hues are learned then it is plausible to expect that observers will have different experiences and thus would learn to associate them with different stimuli. Consequently there may be no single physiological rule that is common for all observers and no environmental stimulus for which all observers would agree.

How the unique hues varied with bandwidth also differed from the predictions of both models. First, as Table 1 shows, the mean dominant wavelengths for all three hues show little systematic shift across bandwidth, in contrast to the short-wavelength shifts predicted for blue and green by either model. Second, the range of observed variation also remained similar for narrow and broadband stimuli. Thus there is no clear sign of convergence at narrower bandwidths as predicted by a fixed physiologically-defined weighting. The results also

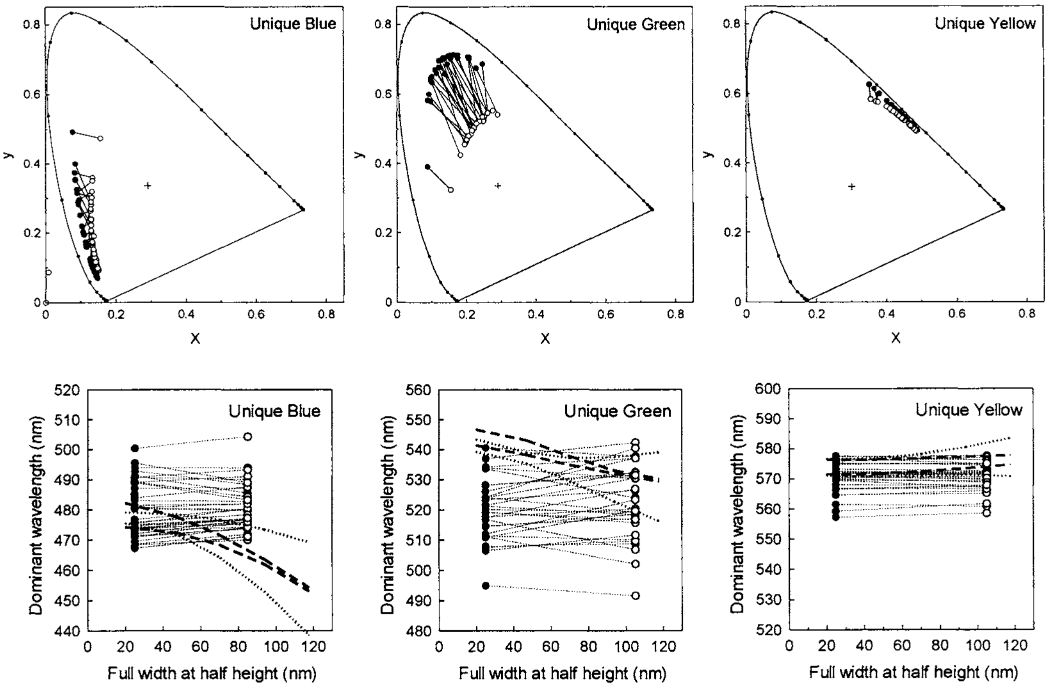

Fig. 3. Unique blue, green and red for foveally viewed stimuli shown by the CIE 1931 chromaticity coordinates (upper) and dominant wavelength (lower), respectively. Solid and open symbols indicate narrowband and broadband conditions, respectively. Crosses on chromaticity diagrams indicate the chromaticity of the achromatic adaptation. Dotted and dashed lines show the ranges of individual difference predicted by a common LMS ratio or a common environmental stimulus, respectively.

Table 1. Mean and standard deviations among subjects (dominant wavelength)

		Narrow (fovea)	Broad (fovea)		Narrow (fovea)	Broad (fovea)	Narrow (peripheral)	Broad (peripheral)
Blue	mean(38)	479.44	480.72	mean(8)	475.46	476.79	472.84	476.57
	SD(38)	8.99	7.42	SD(8)	3.37	2.44	5.29	4.31
Green	mean(30)	520.05	521.92	mean(9)	520.30	519.33	512.95	517.66
	SD(30)	10.23	12.07	SD(9)	13.50	14.89	10.60	13.98
Yellow	mean(33)	570.59	570.68	mean(9)	569.40	569.48	560.42	561.72
	SD(33)	5.11	4.83	SD(9)	6.10	5.87	7.25	4.99

do not hint at a convergence toward a common broadband environmental stimulus, though the expected changes in this case are less pronounced.

Finally, Figure 4 also shows the average results of nine observers in both foveal and peripheral viewing conditions. Means and standard deviations are given in the right hand columns of Table 1. The effects of peripheral viewing were not consistent across observers. There was a slight overall trend for the peripheral settings to shift toward shorter wavelengths for yellow and green but not blue, a pattern roughly comparable to previous reports (Nerger et al., 1995; Volbrecht et al., 2000). However, these shifts were most evident for unique yellow, whereas the change in macular density would be expected to have larger effects on the blue and green settings. The relative stability of the hue settings at the two eccentricities is consistent with an environmental account of the unique hues, because it predicts that observers would learn to compensate for the variations in their own retinas. However, normalization for a fixed broadband color signal predicts that there should be greater constancy for the broadband stimuli. There is some suggestion of this pattern for the unique green settings, but not for blue and yellow.

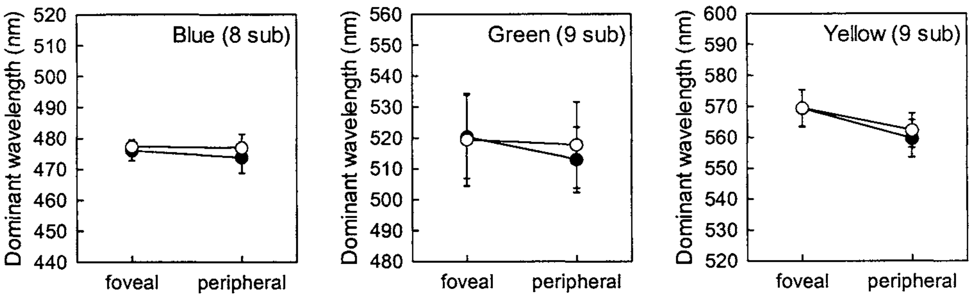

Fig. 4. Results of unique blue, green and red in foveal and peripheral condition shown dominant wavelength. Solid and open symbols indicate narrowband and broadband condition, respectively. Vertical bars show standard deviations.

In conclusion, neither of the specific models we tested adequately accounts for the observed variations in the unique hues. Both models share the assumption that changing the spectral bandwidth should require subjects to choose different stimuli in order to compensate for changes in the spectrum introduced by ocular screening pigments, but differ in the pattern these compensations take. The fact that these effects are not manifest suggests that the unique hues are relatively independent of individual differences in lens and macular pigment. Webster et al. (2000) previously found that unique hue settings between different observers could not be accounted for by differences in ocular screening, and Schefrin and Werner (1990) showed that unique hues remain stable across the lifespan despite the fact that lens density increases with age. The current results suggest that even within a single observer at a single time, the unique hues are not closely tied to the filtering properties of their eyes. This could in part be because other factors are more important and perhaps mask this influence, or because the processes subserving color appearance already include some compensatory adjustment for the effects of screening pigments (for example, calibrating for the differences in macular density with retinal eccentricity). In either case, our results suggest that individual differences in color appearance cannot be readily traced to normal physiological variation in the spectral sensitivity of the visual system.

Supported by EY10834 and AG04058

REFERENCES

I. Abramov and J. Gordon: Color appearance: on seeing red – or yellow, or green or blue, Annu. Rev. Psycol. 45, pp. 451-485 (1994)

B. Schefrin and J. S. Werner: Loci of spectral unique hues throughout the lifespan, J. Opt. Soc. Am. A 7, pp.305-311 (1990)

M. A. Webster, E. Miyahara, G. Malkoc, and V. E. Raker: Variations in normal color vision. II. Unique hues, J. Opt. Soc. Am. A 17, pp.1545-1555 (2000)

P. Kaiser and R. M. Boynton: *Human color vision* (Optical Society of America, Washington, D.C., 1996)

C. M. Cicerone and J. L. Nerger: The relative numbers of long-wavelength-sensitive to middle-wavelength-sensitive cones in the human fovea centralis, Vision Res. 29, pp.115-128 (1989)

J. Pokorny and V. C. Smith: Evaluation of single-pigment shift model of anomalous trichromacy, J. Opt. Soc. Am. 67, pp.1196-1209 (1977)

M. A. Webster and D. I. A. Macleod: Factors underlying individual differences in color matches of normal observers, J. Opt. Soc. Am. A 5, pp.1722-1735 (1988)

L. T. Maloney: Physics-based approaches to modeling surface color perception, in *Color Vision: From Genes to Peceptiom* (Cambridge U. Press, Cambridge, UK, 1999) pp.387-416

G. Jordan and J. D. Mollon: Rayleigh Matches and Unique Green, Vision Res. 35, pp.613-620 (1995)

V. Bonnardel, H. Bellemare, and J. D. Mollon: Measurements of human sensitivity to comb-filtered spectra, Vision Res. 36, pp.2713-2720 (1996)

J. L. Narger, V. J. Volbrecht, and C. J. Ayde: Uniquehue judgments as a function of test size in the fovea and at 20-deg temporal eccentricity, J. Opt. Soc. Am. A 12, pp.1225-1232 (1995)

V. J. Volbrecht, J.L. Nerger, S. M. Imhoff, and C. J. Ayde: Effect of the short-wavelength-sensitive-cone mosaic and rods on the locus of unique green, J. Opt. Soc. Am. A 17, pp.628-634 (2000)

THE OPTICAL CHARACTERISTIC OF LUMINESCENCE PAVEMENT MATERIAL

Akihiro Fujita[1)], Kazuyoshi Ando[1)] , Muneyuki Arai[1)] , Noritaka Kawabe[2)] , R.D.Saxena[3)]
Meijo University[1)] , EZ-BRIGHT Co,Ltd[2)] .,Aichigakuin University[3)]

1. INTRODUCTION

These days, traffic safety is more necessary than ever before because of the increases in volume and variety. Of special importance is the problem of traffic safety deterioration due to the low visibility of the road at night or when raining. In order to improve the level of safety, we studied luminous polymer mortar cement (hereinafter LPMC) as a means to contribute to improved visibility and visual navigation. We succeeded in developing a new road paving material, LPMC, which combines inorganic luminescent pigment and polymer (an agent to improve the adhesive strength of mortar) with white cement. This report details the luminous and dynamic properties of the thin luminous paving road material, which is quite a different type of material compared to ordinary paved roads.

2. DETAILS OF THE EXPERIMENT

2.1 Materials used and their ratios

The materials used and their combination for these tests are described in Tables [1] and [2].

Table [1] - Polymer material table

kind	material	specific gravity
Cement	Usually porto land cement(White)	3.10
Thin aggregate	Silica sand No. 6	2.60
Polymer	SBR system	1.00
	EVA system	1.00
	Acrylics system	1.02
Fluorescence pigment	Luminescence color(G, R, W, Y, B)	1.00

Table [2] - Polymer combination table

Combinati \ Polymer kind			Plain	SBR	EVA	Acrylics
Water cement ratio		W/C (%)	52	33	42	40
Polymer cement ratio		P/C (%)	0	15	15	15
The ameount of units (kg/m³)	Water	$W+P_w$	323	210	253	244
	Cement	C	620	636	602	609
	Thin aggregate	s	1240	1272	1204	1218
	Polymer	P_k	0	93	90	91

As we believe that actual roads should be thinly paved, the various tests were measured under conditions that simulated the surface of thinly paved roads. Consideration was given to how lowering the cost of the luminescent pigment would affect the luminousness of the materials used. As LPMC must have enough strength and adhesion, the affinity and the dynamic properties for polymer mortar cement and luminescent pigment were examined using three different kinds of polymer.

2.2 The methods of examination

(1) Dynamic properties examination

Five different strength tests required for the thinly paved roads (1. Bending strength, 2. Compression strength, 3. Adhesive strength, 4. Strain strength, 5. Shock strength) were conducted on LPMC, polymer and inorganic luminescent pigment (10% of Green) added to white cement.

(2) Optical properties examination

The test materials were chosen depending on their classification for emitting color and adding ratio. The two tests were conducted under environmental conditions simulating different strengths of ultraviolet and illumination states. Measurements were taken with a device that checks color difference. Additionally, visibility tests were conducted by a number of people to gauge the emitting state of the LPMC test materials.

3. DYNAMIC PROPERTIES TEST RESULTS

Table [3] describes the test results of the dynamic properties.

Table [3]: Dynamic properties results

Examination / The rate of added pigment / Polymer kind		Plain		SBR	EVA	Acrylics	Quotation standard
		0%	10%	10%	10%	10%	
bending strength	(N/mm2)	8.53	8.41	10.52	8.34	4.7	JIS A 1171
compressive strength	(N/mm2)	48.2	48.9	39.3	33.9	10.1	JIS A 1171
bond strength	(N/mm2)	1.82	1.88	3.02	2.22		
Contraction distortion	(×10-6)	486	465	309	330		JIS A 1129
shock resistance	(cm)	30	32	57	52		JIS A 1129
General comment		△		◎	○	×	

The results show that Plain has the strongest properties in bending and compression strength among the three, but we found that the properties in shock and adhesion strength, which are required for making a thinly paved coating, are weak.

SBR and EVA, the test material used, have good properties in floating and maintaining water, which we can expect from a good coating. We could get a lot of results that showed an increase in the overall stability. SBR type polymer showed an especially excellent strength property in overall tests. It has a high adhesion property, which is required for making a thin coating pavement. After examination of the tests, we decided to use SBR as a strengthening agent for mortar.

4. OPTICAL TEST RESULT

4.1 Relation of luminous and ultraviolet intensity

Measurement results are shown in Fig [1].

The luminous intensity increases in proportion to the ultraviolet intensity. The rate of increase changes according to the luminous colors. The luminous colors of Green＞Yellow＞white＞Red＞Blue shows, in order, high luminous intensity. Green is exceedingly high in intensity. It showed five times higher luminous intensity than the lowest, blue.

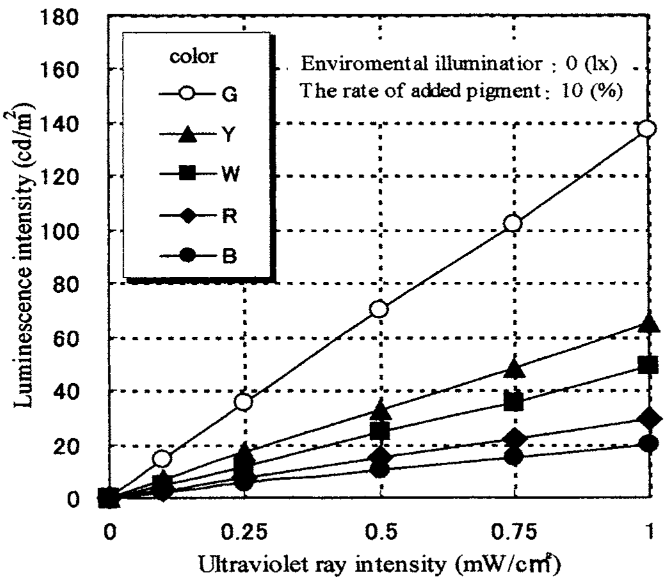

Fig [1]: Relation between luminescence intensity and ultraviolet ray intensity

4.1.1 Relation of luminous intensity and the rate of added pigment

Fig [2] shows the measurement results.

The luminous intensity increases as the rate of added pigment is increased. The rate of increase of the luminous intensity of each color lowered after 30% and remained in a stable condition. We found that there is a limitation in which the luminous intensity is effect by the rate of added pigment. The luminous property of LPMC is thought to consist of an outside factor, the intensity of ultraviolet and an inside factor, the added pigment.

4.2 Visual evaluation test

4.2.1 Test method for the visual evaluation

The visual evaluation test was done in cooperation with seven young men and women who were in their twenties. Five different evaluation levels were used to evaluate the color luminous of the supplied test materials under each environmental illumination.

We collected the evaluation data from the seven people. We set up the maximum value as 70, which meant that the seven people agreed that they could see the supplied samples well. Those numbers were converted into our own evaluation points. We examined those value numbers very carefully.

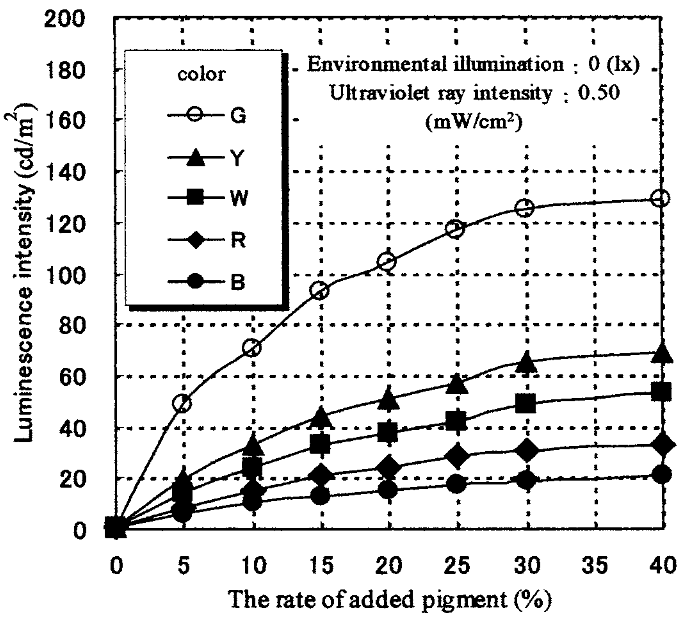

Fig [2]: Relation between luminescence intensity and the rate of added pigment

4.2.2 Visual evaluation test results

The test results are shown in Fig [3].

According to the results, it is possible to get enough visibility in each case when the environmental illumination value is 0(lx). However, when the environmental illumination value increases as 25(lx) or 100(lx) we can see that the evaluation value and luminous percentage disperse, even when there is a difference in luminous colors.

This result means that the absolute visibility improves, as the environmental illumination increases and the luminous visible level will change. Therefore, it is very important to find a method to determine the rate of added pigment and ultraviolet intensity to get the desired luminous intensity. The proper environmental illumination value will depend on the place where you are going to apply the materials.

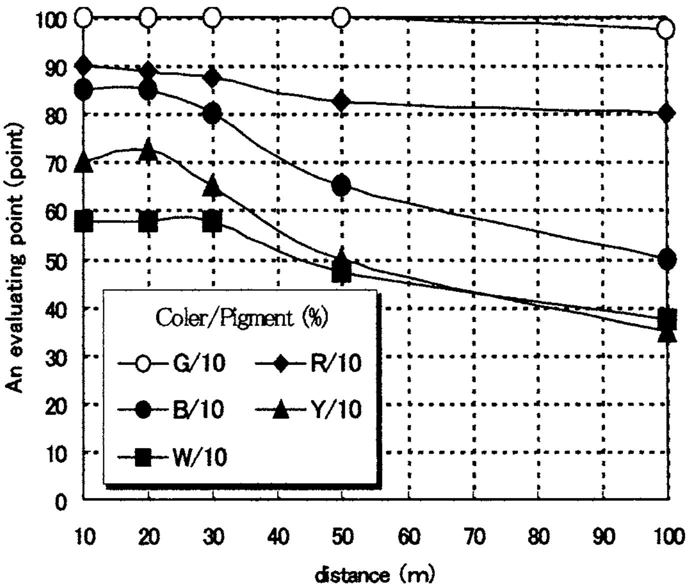

Fig [3] Visual evaluation examination results

5 Multiple regression model of the luminous intensity and Visual evaluation

Multiple regression models were made based on the data attained by the measurement results of luminous intensity.

The result is the luminous intensity multiple regression model (formula [1]) and the Visual evaluation multiple regression model (formula [2]). And, the results calculated from the models are shown in Table [4]. The heavy correlations R^2 of luminous intensity is higher than 0.85.

$$y_{i1}=\beta_1 x_{i1}+\beta_2 \times x_{i2}+\beta_3 \times x_{i3}+\varepsilon_i \quad [1]$$

$$y_{i2}=\beta_1 x_{i1}+\beta_2 \times x_{i2}+\beta_3 \times x_{i3}+\beta_4 \times x_{i4}+\varepsilon_i \quad [2]$$

y_{i1} : luminous intensity (cd/m^2) , y_{i2} : visual evaluation (point)

β_1 : the rate of added pigment as a coefficient, x_{i1} : the rate of added pigment (%)

β_2 : environmental illumination as a coefficient, x_{i2} : environmental illumination (lx)

ß3 : ultraviolet intensity as a coefficient, xi3 : environmental illumination (mW/cm^2)
ß4 : distance as a coefficient, xi4 : distance (m), εi : a fixed number

Table [4] Coefficient and Heavy correlation R^2

test	color	β1	β2	β3	β4	εi	Heavy correlation R^2
Luminescence intensity	Green	1.35	0.01	185.35	—	-26.87	0.9079
	Red	0.42	0.01	42.05	—	-8.55	0.8763
	Yellow	1.16	0.00	85.39	—	-19.43	0.9123
	Blue	0.29	0.03	25.31	—	-5.49	0.9035
	White	0.62	0.03	65.63	—	-12.56	0.8525
Visual evaluation	Green	0.08	-0.05	17.23	-0.06	29.09	0.5000
	Red	0.12	-0.07	21.40	0.01	23.69	0.6270
	Yellow	0.18	-0.08	19.80	-0.10	22.35	0.7021
	Blue	0.12	-0.06	23.40	-0.05	23.90	0.6544
	White	0.02	-0.09	22.20	-0.08	20.07	0.7251

6 CONCLUSION

We found that when the luminescent pigment is added to the polymer mortar cement, it hardly affects the dyna mic property.
The Measurement results of The luminous intensity are by the order of colors.The luminous colors of Green>Yellow>white>Red>Blue shows, in order, higher luminous in tensity.
Luminescent pigment is emitted when luminescent particles are irradiated on the surface of the mortar cement. Therefore, even though the rate of luminous intensity increases with the rate of added pigment, the amount of pigment that can be added to the surface space of the polymer mortar is limited.
Tnrough the cooperation of present cooperatiag group. We could get high visibility results of LPCM and in gererel various opinions also. In future we plan to measure the visibility for higher age peoples and other persons than the present cooperating group. We wish to measure the visibility for handi capped persons also. Such data can be used for barrier free develop ments.

Reference

1.Takayuki Kitao, Akihiro Fujita, Takeo Iisaka, Hiromitsu Nakanishi, Hideki Fujii : "Study on Optical Characteristic and Visibility for Fluorescent White Cement" , ⅢInternational Conference on High-performance Concrete, and Performance and quality of concrete structures, Proceedings Third International Conference Recife, PE,Brazil,2002,pp.1～11,2002

2.Akihiro Fujita, Kazuyoshi Ando: " The unigue charaetristics of Lumini scent Mortar Cement research for visibilily could be continued. " , Association of Civil Engineering pauement journal, No7, pp32-1~32-8, (2002-12)

3.Akihiro Fujita、Hiromitu Nakanishi、Hidehiko Maruyama : VAR10US USE OF FLOURESCENT RESIN CONCRETE , INTERNATIONAL CONGRESS CREATING WITH CONCRETE Edited by R.K.Dhir pp.553～558, (1999-9)

4.Hideki Tubouti, Kazuyoshi Ando, Akihiro Fujita: "Characteristic of Luminescence pavement material. " , Civil Engiaeering Chubu branch. Abstract of Lecture in 2002 research meeting, □-15, pp.551~552, (2003-3)

Colorimetric Tolerances for D50 Simulators

Suchitra Sueeprasan and Ronnier Luo*
Department of Imaging and Printing Technology
Chulalongkorn University, Thailand
*Colour & Imaging Institute
University of Derby, United Kingdom

ABSTRACT

Printed complex images were simulated on a CRT monitor to investigate perceptibility and acceptability tolerances when the same images were viewed under a number of D50 simulators having different chromaticities and luminances. These simulators were distributed around the colour centre simulating CIE D50 illuminant and along eighteen vector directions in the u' v' L (cd/m^2) space. Three standard images were used. The simulated images were assessed against the standard images by a panel of 20 observers in terms of perceptibility and acceptability criteria. Probit analysis was used to estimate the threshold of frequency-perceived difference responses. Colorimetric tolerances were represented in terms of ellipsoids. It was found that there was little tilting of ellipsoids with respect to the L axis. Acceptability tolerances were larger than the T65 and T50 perceptibility ellipsoids by a factor of 2.3 and 4.3, respectively. The major axis of the ellipse in u' v' plane pointed along the v' (yellow/blue) direction, but was only slightly longer than the minor axis. All tolerances found in this study were larger than the tolerance specified by ISO Standard 3664, *Viewing conditions for Graphic Technology and Photography.*

INTRODUCTION

The quality of light sources in terms of chromaticity and luminance are crucial factors influencing the colour appearance of an image. The same image can appear considerably different in colour when viewed under different light sources and/or at different luminance levels. In the graphic arts industry, images are typically reproduced through a lengthy production chain. Colour images are often viewed in many places where viewing conditions may not be well controlled. Even though it is claimed that the same type of daylight simulator is used, variations in chromaticities and luminances may still occur and alter colour appearance of the images. This could cause mistaken rejection of satisfactory colour images in some cases. Hence it is essential to establish the colorimetric tolerance for daylight simulators in which a colour image will look the same or be acceptable.

Many organisations endeavour to standardise viewing conditions for colour image assessments[1]. The tolerance for specified simulators should not only be tight enough to achieve colour matches, but also be large enough for lamp manufacturing purposes. ISO 3664: *Viewing conditions – for Graphic Technology and Photography*[2], standardises the viewing conditions for image comparisons in the graphic arts industry. For practical appraisal of prints, illuminant D50 is specified. Colorimetric tolerances for the deviation of chromaticity from the illuminant D50 in the u' v' chromaticity diagram are defined by a circle with a radius of 0.005. The proposed illuminance is 500 lux with a tolerance of ± 125 lux, i.e. 25% variation. This study aimed to investigate colorimetric tolerances of D50 simulators used in colour-image comparisons. Two aspects were taken into consideration: perceptibility and acceptability.

EXPERIMENTAL DESIGN

A situation where a printed image was assessed under different illumination conditions was simulated. The aim was to define tolerances where the colour appearance of the same image viewed under different illumination conditions will show a just noticeable-difference (perceptibility) and where the differences are within an acceptable limit (acceptability). Instead of having a variety of physical D50 simulators, the CAM97s2[3] colour appearance model, an improvement of the CIE 1997 colour appearance model, CIECAM97s[4], was used to predict the colour appearance of the printed images viewed under D50 simulators having different chromaticities and luminances. The CIECAM97s model has been proven to give outstanding performance for predicting the change of colour appearance of images under different illuminants[5]. A flowchart of image processing is shown in Figure 1. First, the printed images were digitised using an Agfa StudioCam digital camera. Then, via a camera characterisation model, the camera RGB data were converted to CIE XYZ tristimulus values according to CIE D50 Illuminant and 2° Standard Observer. These XYZ images were used as originals for the simulation purpose. After predicting colour appearance of printed images using the CAM97s2 model, the X'Y'Z' images were then converted to RGB data for displaying on a calibrated monitor using the GOG model[6]. The precision of the monitor characterisation model was 0.27 ± 0.19 ΔE^*_{ab} units (average ± standard deviation) based on 27 test colours. The monitor white point was set closely to an illuminant D50 with luminance level of 40 cd/m^2. The images generated using the white point of the monitor were used as standard images while the test images were processed using slightly different white points chosen as described later.

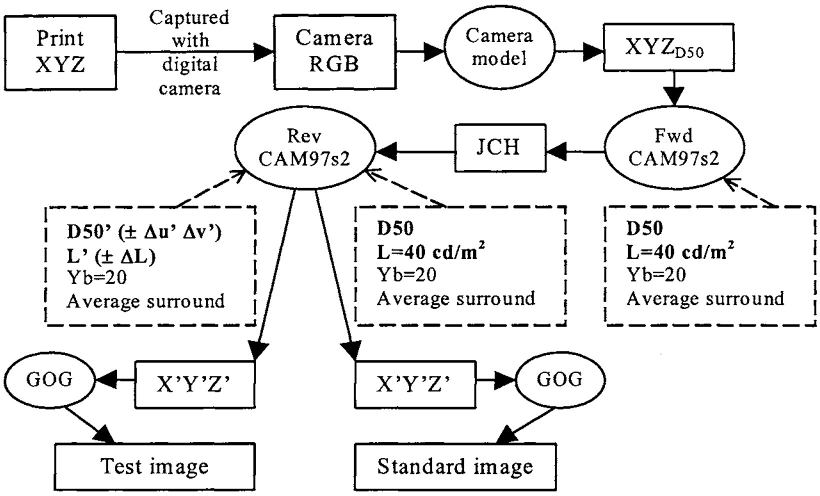

Figure 1. A flowchart of image processing.

The white point of the test images varied from the illuminant D50 along nine directions in u' v' L (cd/m^2) space. Four of these were in the u' v' plane as shown in Figure 2a. One direction was along L axis. The sampled points were determined based on a pilot experiment such that each direction gave a good coverage of a range of pairs between the centre and each extreme data point. Finally, the u', v' and L values were simultaneously varied along four additional directions, i.e. mixtures of L in the four existing directions in u' v' plane. These directions were included to reveal any interaction between u' and L, and v' and L.

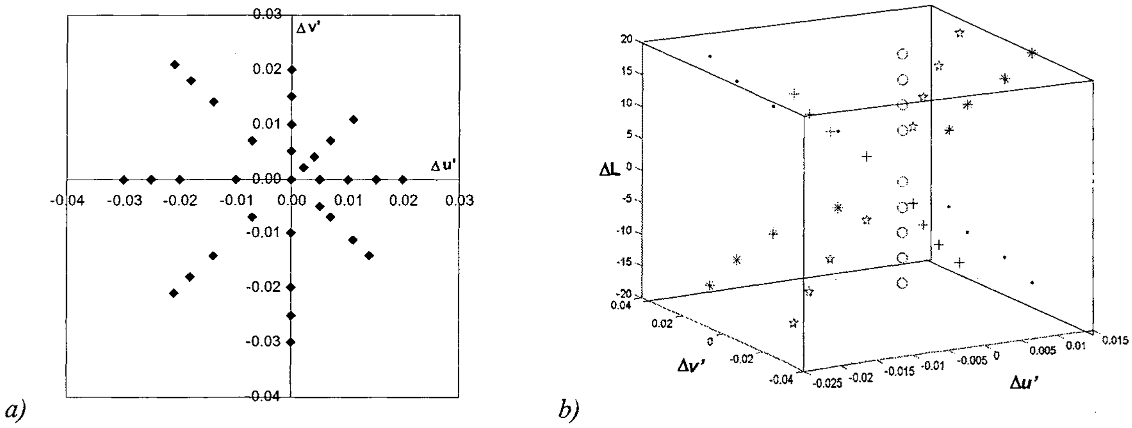

Figure 2. Sampled points relative to the centre white point along four vector directions on the u' v' plane (a) and five vector directions on the u' v' L (cd/m^2) plane (b).

Three complex images were used in the study: Picnic, Party and Bottle, as shown in Figure 3. Picnic was an outdoor scene containing three ladies of different race, green grass and a blue sky. Party was a picture of a lady shot indoors against a greyish background. Bottle contained metallic objects with a neutral background.

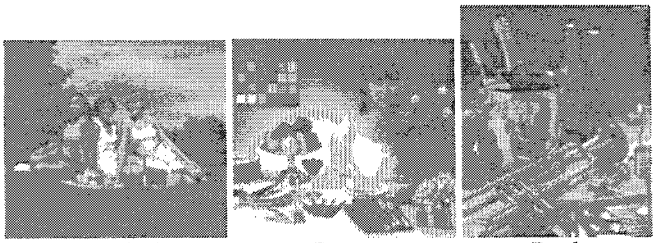

Picnic Party Bottle

Figure 3. Experimental images

The method of constant stimuli[7] was used in the psychophysical experiment. Observers compared each test image to the standard image and were asked *whether they perceived colour differences between the two images*. If so, *would they regard them as acceptable match to each other?* They did not know which image of a given pair was the standard image and all test images were presented following a random order. The experiment was conducted in a darkened room. A series of pairs of images were displayed on the centre of the monitor and observers could see one image at a time. Each image was surrounded by a 5-mm white border and displayed against a grey background having the same chromaticity as its input illuminant/white border, but only 20% of the luminance of the white. Before displaying each image, the grey background was presented for 12 seconds, allowing adaptation to take place. There was no time restriction for an observer viewing an image. They were asked to memorise colours of the image and compare them with the next image of the given pair. A black background was presented for 3 seconds before the next background/image was displayed. This was designed to minimise observers' prejudice about making judgements based on a noticeable change of background rather than colour differences between the images. The whole experiment was divided into three sessions according to image content. Each session contained 72 test images and lasted about 45 minutes. Twenty observers participated in the experiments and completed all three sessions. In total, 4320 assessments were made.

EVALUATION OF DATA

Probit analysis[8,9] was employed to determine threshold limits, along each direction, where probability of positive/negative responses equals to 0.50 (denoted as T50, median tolerance), i.e. 50% of observers perceive or accept the difference and 50% do not. However, for threshold perceptibility, 30% of observers judged two identical images as "perceptible difference" which causes a negative threshold in the u' direction for the Party image. To avoid this, a false alarm rate[10] was introduced. Threshold perceptibility is denoted as T65, i.e. 65% of observers responded that they perceived a difference.

Tolerances in colour space are commonly presented by an ellipsoid. The general form is defined as follows:

$$\Delta E^2 = g_{11}(\Delta u')^2 + g_{22}(\Delta v')^2 + g_{33}(\Delta L)^2 + 2g_{12}\Delta u'\Delta v' + 2g_{13}g\Delta u'\Delta L + 2g_{23}\Delta v'\Delta L \quad (1)$$

where ΔE represents colour differences around the colour centre. The g_{ik} coefficients are estimated to minimise the sum of the square of the difference (S^2) between the visual difference (ΔV) and ΔE calculated from the threshold data points of each direction. The ΔV of unity corresponds to perceptibility and acceptability tolerances, i.e. T65 and T50, respectively.

If the ellipsoid is not tilted appreciably with respect to the L axis, the g_{13} and g_{23} coefficients in Equation 1 can be taken to be zero and the ellipsoid is defined by 4 coefficients. Both 4 and 6 coefficients (designated as *4 gs* and *6 gs*, respectively) ellipsoids were computed to investigate the significance of any tilting.

The measure of PF/3[11] was used to indicate how well the ellipsoids fitted the visual data. For perfect agreement, the PF/3 value should be zero. It can also be used to compare differences between two ellipsoids. Five hundred randomly distributed sets of Δu' Δv' and ΔL were generated. Two sets of ΔE values can be calculated for a pair of ellipsoid equations. The PF/3 measure can therefore be calculated to indicate the difference between two ellipsoids.

RESULTS AND DISCUSSION

Ellipsoids calculated from 4- and 6-coefficient equations corresponding to perceptibility and acceptability tolerances were derived. For the perceptibility tolerances, both T50 and T65 threshold values were used to derive the ellipsoids. The agreement between visual results and ellipsoids are given in Table 1. For perceptibility tolerances, the ellipsoid derived from T65 gave a better fit to the visual data than that from T50, especially for the Party image where a negative threshold was found. It can be seen that the PF/3 values for the

4 gs and *6 gs* ellipsoid equations are quite similar in most cases. This is particularly true for the results for the combined 3 images (All); both *4 gs* and *6 gs* equations fit equally well to the visual data. The tilt of the ellipsoid in the u' L and v' L planes is not significant. For the perceptibility ellipsoid, the tilted angles of 'All' data in u' L and v' L planes are 89.68° and 89.33°, respectively, less than 1° away from the normal axis (90°). The largest tilt of any ellipsoid was found for the Bottle image, i.e. 89.22° in the u' L plane and 87.20° in the v' L plane. This resulted in the 4-coefficient equation for perceptibility giving a slightly poorer fit to the visual data. Nevertheless, there was only 3% between the two equations. Table 2 shows the differences between *4 gs* and *6 gs* ellipsoid equations directly in terms of PF/3 values. For the acceptability ellipsoids, the differences were very small. For the perceptibility ellipsoids, the differences were higher but still considered to be reasonable. As expected, the T50 ellipsoids had a larger difference than the T65 ellipsoids. Again, the Bottle image showed a relatively high percentage difference between the two different equations due to somewhat larger-tilt of the ellipsoids as mentioned earlier.

Table 1. Measures of fit between threshold-data points and ellipsoids.

PF/3(%)	Perceptibility				Acceptability	
	T50		T65		T50	
	4 gs	6 gs	4 gs	6 gs	4 gs	6 gs
Picnic	24	22	23	22	23	23
Party	41	40	19	19	15	14
Bottle	29	26	25	23	20	20
All	21	20	17	17	19	19

Table 2. Agreements between 4- and 6-coefficient ellipsoids.

PF/3	Perceptibility		Acceptability
(%)	T50	T65	T50
Picnic	9	6	2
Party	10	3	5
Bottle	15	11	3
All	6	3	2

As discussed above, the tilting of ellipsoids seems not to be important; therefore, only 4 coefficients should be sufficient to define an ellipsoid. Further investigation was carried out to identify whether the perceptibility and acceptability tolerances are dependent on image content. The PF/3 results indicating differences between the ellipsoids calculated from the different images are summarised in Table 3. It can be seen that for both the perceptibility and acceptability results the Picnic image shows the largest differences form the other two images. One possible explanation is that the content of the Picnic image was somewhat different from the other two. It contained saturated colours while the Party and Bottle images were mainly middle-tone images. In addition the Picnic image contained several colours (on faces, grass and sky) which the observers would be expected to recognise. Generally, the variation between the images was quite small. In addition, the results from the combined data for the 3 images (All) against each individual image were smaller than those of the individuals against one another. Hence, the ellipsoids from 'All' results are taken to represent the perceptibility and acceptability tolerance ellipsoids of the three images.

Table 3. Variations between 4 coefficient ellipsoids of different images.

PF/3	Perceptibility (T65)			Acceptability (T50)		
(%)	Picnic	Party	Bottle	Picnic	Party	Bottle
Party	10			7		
Bottle	9	4		5	5	
All	6	4	3	5	4	2

The cross sections of the ellipsoids for perceptibility and acceptability tolerances are shown in Figure 4. The full and broken lines represent perceptibility and acceptability tolerances, respectively. The innermost ellipses correspond to the T50 tolerance for the perceptibility ellipsoids. The ellipses in the u' v' plane were slightly larger along the v' (yellow/blue) axis. Figure 4 also shows that acceptability tolerances are about two and four times as large as the T65 and T50 perceptibility tolerances, respectively. Note that ISO defined the chromaticity tolerance by a circle with a radius of 0.005 in the *u' v'* diagram. The illuminance is defined with a tolerance of ± 125 lux for the specified illuminance of 500 lux, i.e. 25% variation; thus this corresponds to a range of ± 10 cd/m^2 with a mean of 40 cd/m^2 in this study. It was found that the T50 perceptibility tolerances agree quite well with that specified by ISO Standard 3664 compared with the other two tolerances.

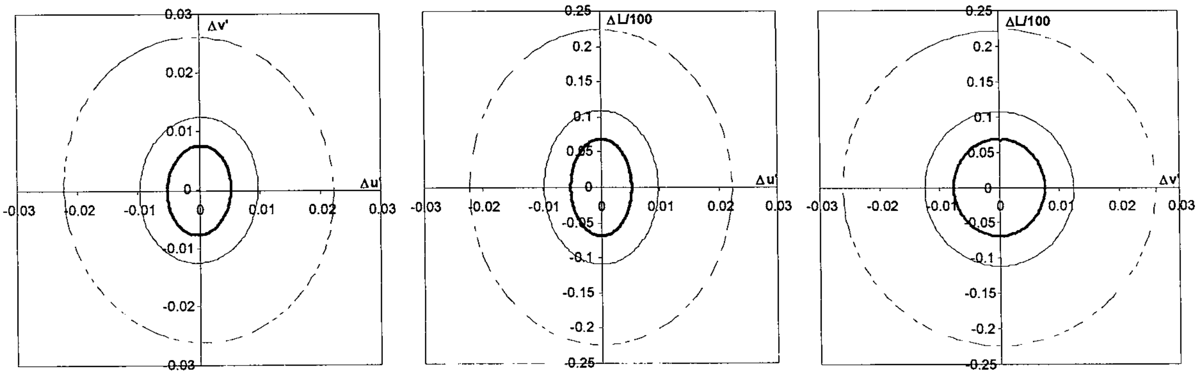

a) *b)* *c)*

Figure 4. Perceptibility (—T50, —T65) and Acceptability (----) ellipses for 'All' in a) u' v', b) u' L/100, and c) v' L/100 planes.

CONCLUSIONS

A series of simulated colour prints corresponding to different D50 simulators with different chromaticities and luminances were generated on a CRT. CAM97s2 was used to simulate the images as if viewed under different illumination conditions. Three complex images were used in the study. Psychophysical experiments were carried out involving the observers comparing the standard image (under CIE illuminant D50) with test images (rendered around the illuminant D50) and answering two questions: a) do you perceive differences between the two images, and b) do you accept these differences? The test illuminants varied along 9 directions in u' v' L space. Probit analysis was employed to estimate the threshold where the probability of a positive response was equal to 0.50 or 0.65 when false alarm rate was included. Ellipsoids fitting the threshold results were used to represent results. The results show that the tilting of the ellipsoids in the u' L or v' L planes was insignificant. Therefore it was adequate to fit the ellipsoid with the 4-coefficient equation. The variations between the ellipsoids derived from different images were also investigated. Some differences were found between images, especially for the perceptibility experiments. The results showed that image content has some impact on perceptibility tolerance but not much for acceptability. The semi-major axes of perceptibility and acceptability ellipsoids were slightly orientated along the v' (yellow/blue) direction. However, ISO 3664 specifies the tolerance by a circle. The T50 perceptibility tolerance agrees quite well with the specification while the T65 and acceptability tolerances are about twice and four times as large as that defined by ISO 3664, respectively.

ACKNOWLEDGEMENTS

We thank Professor Tony Johnson for his technical advice on experimental design and to those who spared their precious time to complete the massive experiments.

REFERENCES

1. T. Johnson and M. Scott-Taggart, Guidelines for choosing the correct viewing conditions for colour publishing, revised edition, Pira International, Surrey, 1998.
2. ISO 3664: Viewing conditions – for Graphic Technology and Photography, UK (2000).
3. C. Li, M.R. Luo, and R.W.G Hunt, The CAM97s2 model, *Proc. IS&T/SID Color Imaging Conference* **7**, 262-263 (1999).
4. M.R. Luo and R.W.G. Hunt, The structures of CIE1997 colour appearance model (CIECAM97s), *Color Res. Appl.* **23**, 138-146 (1998).
5. S. Sueeprasan, M.R. Luo and P.A. Rhodes, Investigation of colour appearance models for illumination changes across media, *Color Res. Appl.* **26**, 428-435 (2001).
6. R.S. Berns, Methods for characterizing CRT displays, *Display* **6**, 173-182 (1996).
7. C.J. Bartleson, Optical radiation measurement –Visual measurements, Vol. 5, Academic Press, 1984.
8. D.H. Alman, R.S. Berns, G.D. Snyder, and W.A. Larsen, Performance testing of color-difference metrices using a color tolerance dataset, *Color Res. Appl.* **14**, 139-151 (1989).
9. D.J. Finney, Probit Analysis, 3rd ed., Cambridge U. Press, Cambridge, 1971.
10. K. Witt and G. Döring, Parametric variations in a threshold color-difference perceptibility ellipses for surface-color samples, *J. Opt. Soc. Am.* **65**, 956-959, 1389 (1975).
11. M.R. Luo and B. Rigg, BFD(l:c) colour-difference formula: Part 1-Development of the formula, *JSDC* **103**, 86-94 (1987).

The Usage of Luminescent Particle for Measuring the Particle Settling Velocity in Hydraulic Laboratory

Muneyuki Arai[1)], Xuelan Liu[2)] and Akihiro Fujita[1)]
1)Faculty of Science and Technology of Meijo University, 1-501 Shiogamaguti, Tenpaku-ku, Nagoya, Japan
2)Graduate School of Meijo University, 1-501 Shiogamaguti, Tenpaku-ku, Nagoya, Japan

ABSTRACT

It takes less than 2 seconds for the sand particles with diameter of about 2mm to settle in water till the steady status. For measuring the settling velocity of sand particles in water, it needs the more expensive high speed CCD camera than the standard ones. It is kind of difficult for a university to do so in purpose of education. However, limited by using common CCD digital camera, it is possible to use the luminescent particles which the visibility of the particles is fair to observe and measure the whole settling process from the still state to steady state. Herein, it is shown that luminescent particles can be used in hydraulic laboratory for the educational purpose.

1. INTRODUCTION

In this paper, the experiments of luminescent particles settling in water are mentioned. Since the study on fluid mechanics and behaviors of mixtures of sediment and water is very important in fields of river engineering, Sabo engineering, coastal engineering and so on, it is one of the fundamental educational items in university and graduate school in these areas. In particular, the settling of particles in water is one of the basic particle behaviors; it is related to many research fields like what mentioned above. Generally speaking, it needs some costly and special man-made equipment for measuring the process of particle settling in water. Herein, from the view point of education on process of particle settling into the liquid, the possibility of usage of luminescent particles in this kind of experiments is discussed.

2. SETTLING OF PARTICLES IN WATER

When the Reynolds number is high, and the resistance of flow is in proposition to the square of velocity, it is well known that the kinetic equation of a single particle settling in water can be considered as following

(*Komura, S.,1982*):

$$M\frac{dw}{dt} = (M-m)g - \frac{1}{2}m\frac{dw}{dt} - \frac{1}{8}\pi d^2 \rho C_D w^2 \quad (1)$$

Here, $M = \pi d^3 \sigma / 6$: mass of the particle, $m = \pi d^3 \rho / 6$: mass of water with the same volume of particle, σ: density of the solid particle, ρ: density of water, d :diameter of solid particle, C_D : resistance coefficient, w : settling velocity of solid particle, g: acceleration due to gravity , t: time.

The left side of equation (1) shows the force via the change of momentum of the solid particle; the first item of the right side implies the gravity on the particle in water; the second item is called "additional" mass, which is apparent mass of the solid particle; and the third item indicates the resistance force on the particle. Taking the settling velocity as w_0 when $t \to \infty$, with initial condition of $t = 0$ and $w = 0$, the settling velocity w after a period of time t can be calculated with the following equation:

$$\frac{w}{w_0} = \tanh(\eta t) \quad (2)$$

Where

$$w_0 = \left\{\frac{4}{3}\left(\frac{\sigma}{\rho} - 1\right)\frac{gd}{C_D}\right\}^{\frac{1}{2}} \quad (3), \eta = \frac{\left(\frac{\sigma}{\rho} - 1\right)g}{\left(\frac{\sigma}{\rho} + \frac{1}{2}\right)w_0} \quad (4)$$

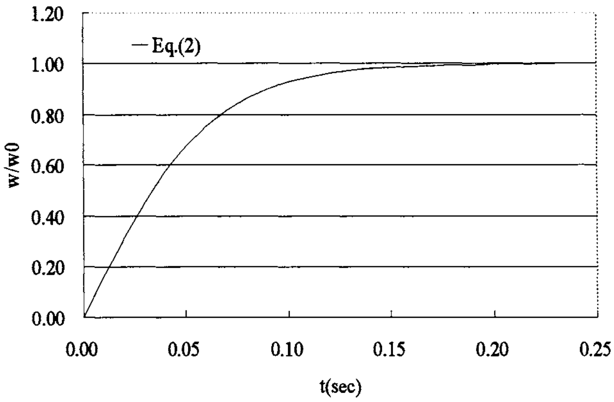

Figure 1. The settling velocity of particle

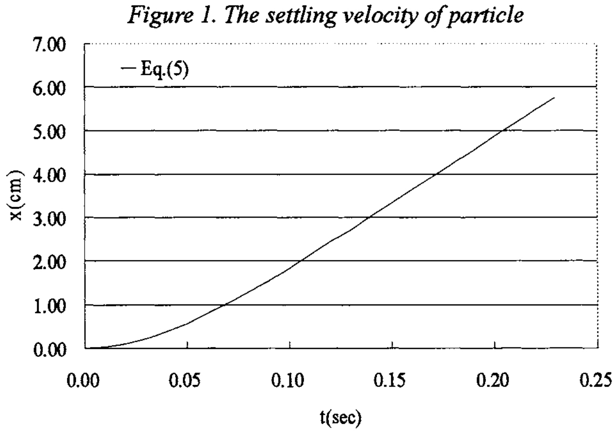

Figure 2. The settling position of particle

From equation (2), in initial condition of $t = 0$ and $x = 0$, the settling position x of the particle can be written as following after period of time t:

$$x = \frac{1}{\eta}\ln(\cosh \eta t) w_0 \quad (5)$$

In case of the glass bead with the diameter of $d = 2.4$ mm, density of $\sigma = 2.63$ g/cm^3 settling in 23 °C water, the change of settling velocity can be calculated with equation (2). As shown as in Figure 1, the vertical axis shows the relative settling velocity w / w_0, the horizontal axis indicates the time (sec), the calculation result is illustrated as the solid line. It can be seen that $w / w_0 \approx 0.99$ which means the settling velocity is almost equal the "ending" velocity when $t = 0.15$ second. Figure 2 illustrates the relation between the settling position x from the start point and the period of time t (sec) by equation (5). The settling velocity becomes almost uniform after time period of 0.2 sec. These results are simple but necessary for students to understand the settling process.

3. EXPERIMENTS AND RESULTS

The particle settling experiments were done with the transparent glass beads. The density of particles are same as the assume condition when calculated as above. Figure 3 shows the luminescent particles and ultraviolet rays' irradiation equipment. The luminescent particles are made-up with the glass beads by half-transparent and water-resistant luminous paint. The colors are red, blue, yellow, green and orange in respectively.

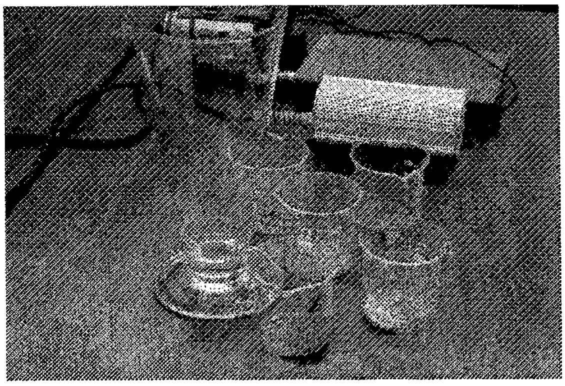

Figure3. Equipments and material of Experiments

Visibility of Particles

The visibility of transparent glass beads is very bad in water (Figure 4). In case of teaching experiments, the container for particle settling is 1.0m wide and 1.5m high. It is made of steel, and one side with glass. The processes of particle settling are observed through the glass side. Usually, it is very difficult to recognize the particle with diameter of about 2mm settling in the water in the container. For the good experiment results, it is necessary to improve the visibility of the particle in water by using the well-lit illumination. Figure 4 and 5 show the difference between the transparent glass beads with indoors illumination and luminescent particle with ultraviolet rays, respectively. The pictures are taken from the distance of 0.8m from the object. Both photos show the results in the same glass vessel. The arrows show the positions of particles. As shown as in Figure 4, it is very difficult to distinguish the particle from the background under the indoor illumination. It would be more difficult for tracing the bigger size particles in water for the faster settling velocity. As a comparing, the luminescent particle is very distinct by applying the ultraviolet rays, which is shown in Figure 5. As a result, blue luminescent particles are the most distinct ones than other colors. However, the focus of CCD camera is clear under the common indoor illumination, but blurry in case of ultraviolet rays.

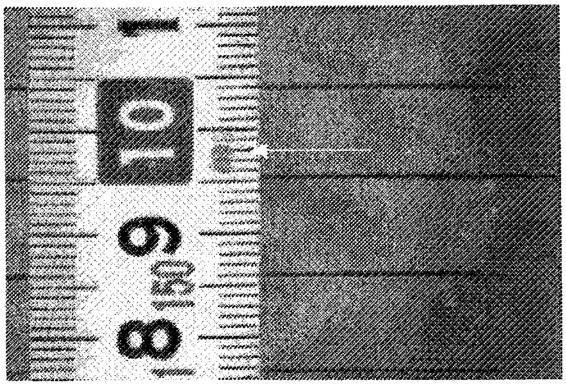

Figure4. Transparent particle in water

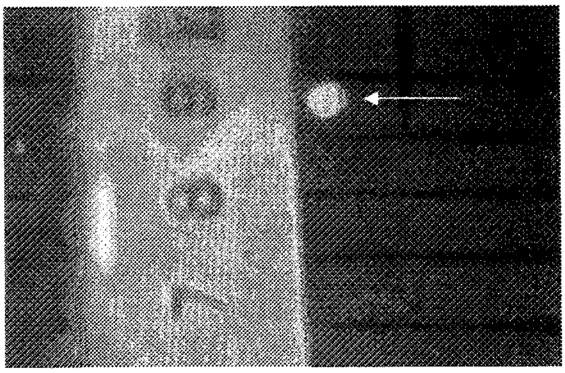

Figure5. Luminescent particle with ultraviolet rays

Settling of Particles

The ordinary digital CCD video camera is used to record and measure the settling processes of particles (Figure 6).

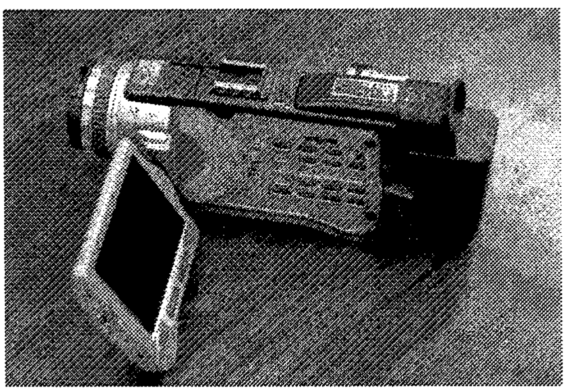

*Figure6. Digital video camera, resolution (640*480)*

The resolution of the images is 640*480 pixels, and the flame rate is 1/30sec (30fps). Generally, the images recorded by digital video camera can be replayed more stable than those recorded by analog cameras such as VHS and so on. The real distance of one pixel is around 0.2mm/pixel in this experiment. Equation (2) and (5) show the settling velocity and position respectively in case of a particle settles from the still to steady status, herein, the settling velocity and position are analyzed from the recorded video.

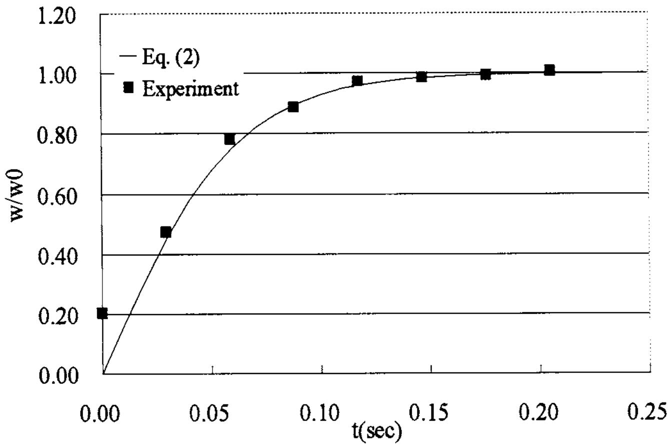

Figure 7. The settling velocity of particle

4. DISCUSSIONS AND CONCLUSIONS

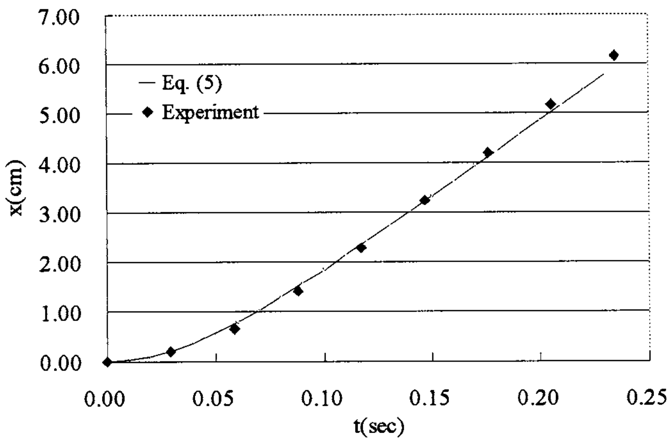

Figure 8. The settling position of particle

Figure 7 shows the change of relative settling velocity of w/w_0 with time t, in conditions of diameter of particle $d = 2.4$ mm, $\rho = 2.63$ g/cm^3, and x=0, when t=0.
Here, w_0 is taken as the almost steady settling velocity in the experiment. This steady settling velocity is fitting to the one when the resistance coefficient $C_D = 0.53$. The solid line indicates the calculation result, and shows the good agreement with the experiment results which are illustrated as the mark(■). Furthermore, Figure 8 implies the relation between the theoretical and experimental results of settling positions of a single particle starting from the still status. Similar as in Figure 7, the solid line illustrates the calculation result, which has good agreement with experiments results which are shown as mark (◆).

As mentioned above, it is possible to measure the particle movement which is shown with equation (1) with those simple equipments and material in laboratory. Certainly, more accuracy results could be obtained by using high speed CCD cameras, but it is limited to be used in the laboratory for the purpose of education due to the high cost and the complex setup procedure. The simple method mentioned in this paper is very useful for education in a university. Besides, the luminescent particles what are used in this experiment can be applied to some other experiments and environment, such as low illumination environment, low contrast between the particles and the background, unclear flow and so on. Moreover, the looking of luminescent particle settling in water is very beautiful.

REFERENCE

Komura, S.: Sediment Hydraulics, Morikita Shuppan, 1982,(in Japanese)

Geometric Conditions for Reflectance Factor Measurement

Kenichi Suzuki and Gorow Baba
MURAKAMI Color Research Laboratory, Tokyo, JAPAN

ABSTRACT

At first, spatial reflected light characteristics of white and chromatic samples were measured by gonio-spectrophotometer, and colorimetric values were calculated. Generally spectral reflectance factor changes with receiving angle, then measured colorimetric values are strongly affected by viewing angle[1). Secondly, effects of light trap size of integrating sphere were studied. Colorimetric values of nearly uniform diffuse samples are not affected by light trap size, but that of glossy or semi-glossy samples are fairly affected by light trap size[2). Finally, directionality of textile color samples were measured by three-dimensional gonio-spectrophotometry. Color of textile samples is able to assume by principal component analysis of three-dimensional spectral reflectance factor distribution.

1. EXPERIMENTS

1.1 Instruments

For this study, two instruments were used.

a) Murakami Model GCMS-3B, Gonio-Spectrophotometric Color Measurement System.

Geometric conditions	Incident angle: -70° to 70° (anormal designation)
	Receiving angle: -70° to 70°
	Azimuthal angle: changeable by rotating the sample stage in specimen plane
	Source and receiver aperture: ca. 2°, circular
Spectral conditions	Wavelength range: 390nm to 730nm, 10nm interval
	Bandpass: ca. 10nm
	Polychromatic illumination

b) Murakami CMS-35SP, Spectrophotometer.

Geometric conditions	Polychromatic diffuse illumination, 7° viewing
	Integrating sphere: 200mm in dia.
	Cone half-angle of light trap: changeable from 0° to 11°
Spectral conditions	Wavelength range: 390nm to 730nm, 10nm interval
	Bandpass: ca. 10nm

1.2 Measurement of directional spectral reflectance factor

Using GCMS-3B Gonio-Spectrophotometer, directional spectral reflectance factor for -45° incidence of white and chromatic samples were measured. Samples were as follows;

1) White surfaces - Matt surfaces - Pressed $BaSO_4$, Coated $BaSO_4$, PTFE, Roughened porcelain.

Glossy surfaces - Polished porcelain, White ceramic tile.

Paint surfaces - White paint, glossy, semi-glossy and matt.

2) Chromatic surfaces - Matt surfaces - Spectralon, blue, green yellow and red.

Glossy surfaces - Polished porcelain, Evercolor, blue, green, yellow and red.

Glazed ceramic tile, BCRA tiles.

Paint surfaces - Green paint, glossy, semi-glossy and matt.

Yellow paint, glossy, semi-glossy and matt.

As an example, spectral reflectance factor at 560nm of white surfaces for -45° incidence are shown in Fig. 1.

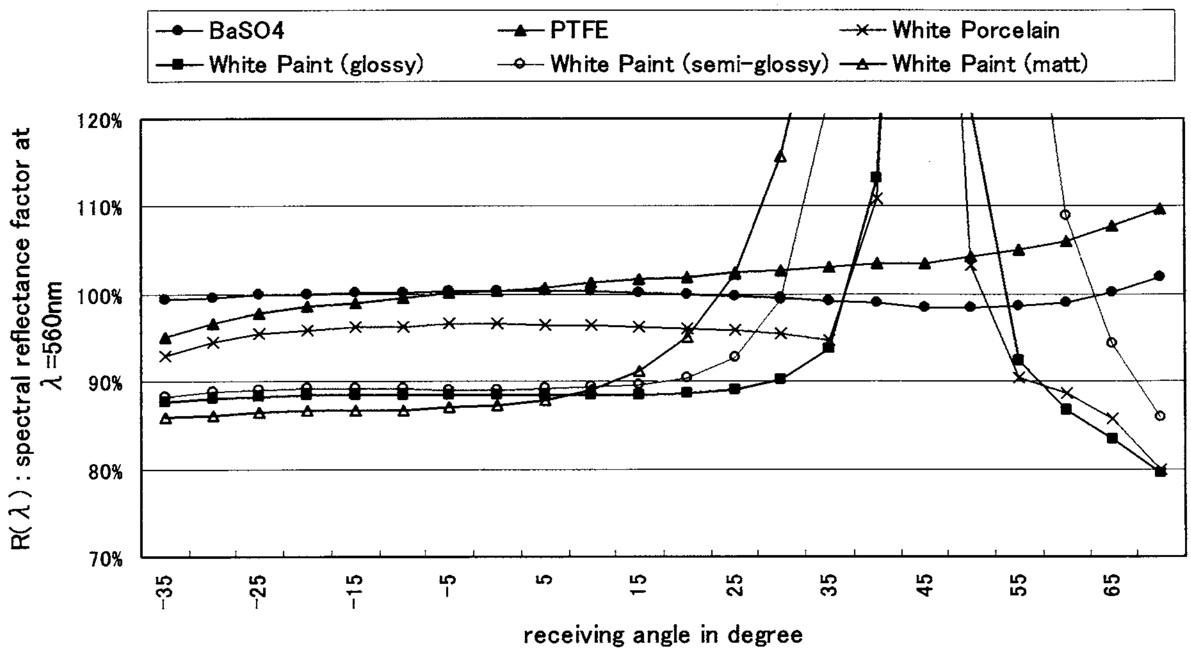

Fig. 1 Angular dependence of spectral reflectance factor at 560nm of white surfaces for -45° incidence.

1.3 Effects of light trap size of integrating sphere.

Using CMS-35SP Spectrophotometer with integrating sphere, effects of light trap size were examined, changing cone half-angle (κ) of light trap from 0° to 11°. From spectral reflectance factor for each measurement, tristimulus values for CIE 1931 standard observer and CIE standard illuminant D65, and colorimetric values (L*a*b*, L*C*h*) were calculated. Samples were as follows;

1) Achromatic samples - Pressed $BaSO_4$, Pasted $BaSO_4$, White porcelain (polished and roughened),

PTFE (white, gray and black), White ceramic tiles (60°Gs - 80, 60, 40, 20 and 10)

2) Chromatic samples - PTFE (blue, green, yellow and red), 12 BCRA tiles, Paint panels (with various color And gloss), Ink-jet printings, Textiles, Colored paper.

As an example, effects of cone half-angle of light trap for L* and C* are shown in Fig. 2

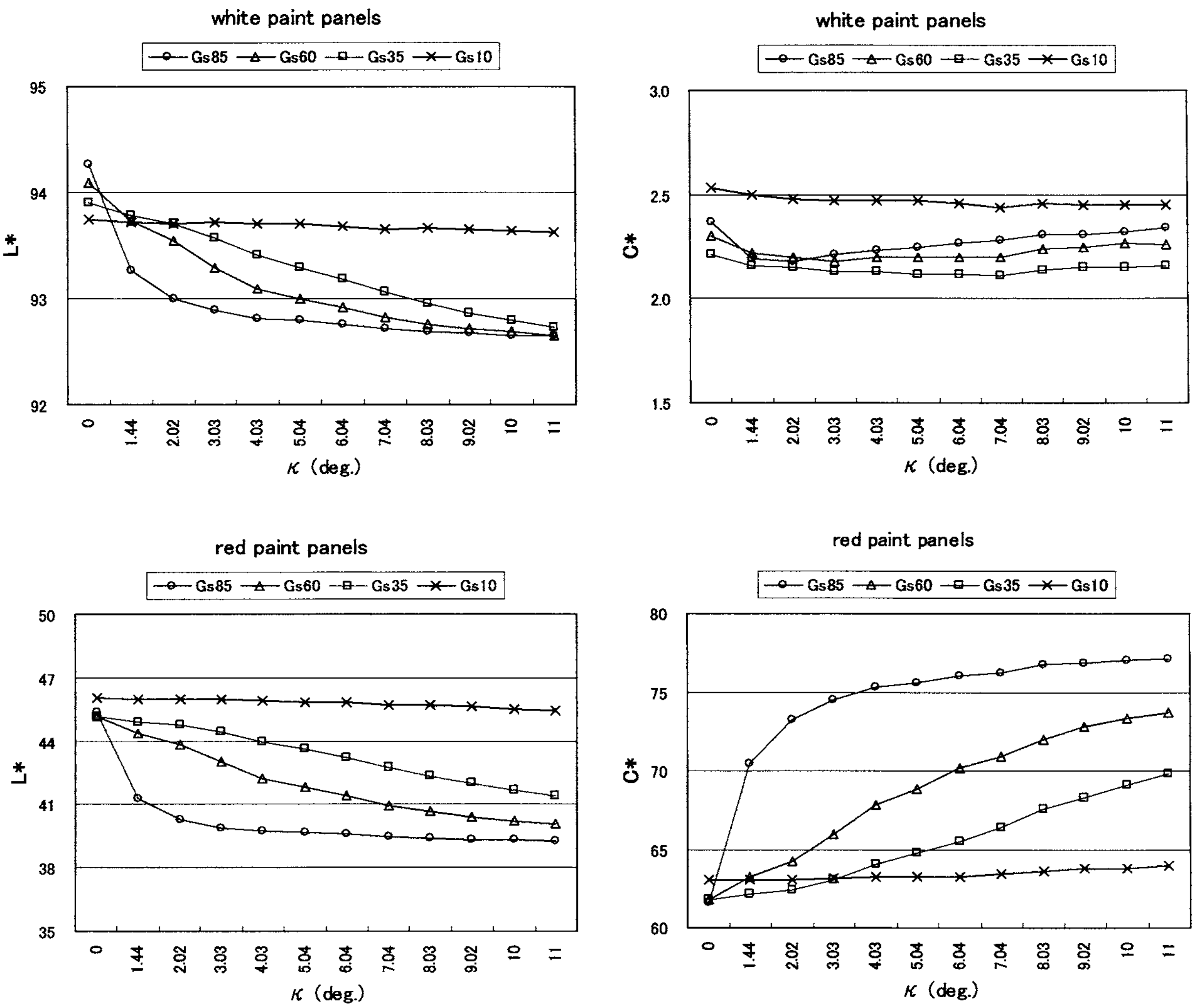

Fig. 2 Effects of cone half-angle of light trap for lightness and chroma for white and red paint samples.

1.4Directional color of textile samples.

Using GCMS-3B Gonio-Spectrophotometer, three-dimensional spectral reflectance factor distributions of textile samples were measured. Geometric conditions were,

Incident angle: 0°

Receiving angle: 15°, 30°, 45° and 60°.

Azimuthal angle: 0° to 360°, 15° step, by rotating the sample stage in specimen plane.

As an example, C* (chroma) changes with azimuthal angle, for each receiving angle were shown in Fig. 3.

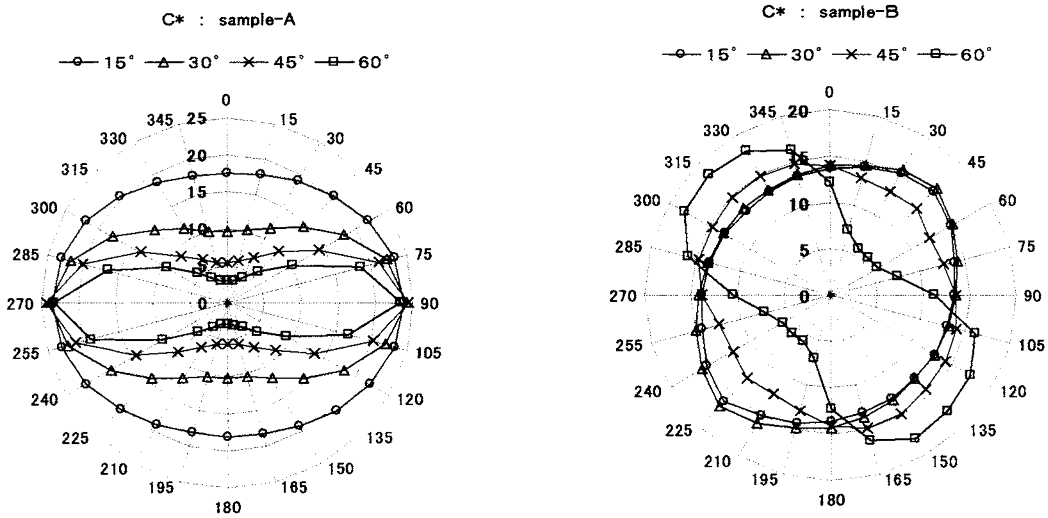

Fig. 3 Three-dimensional C changes of textile samples.*

2. CONSIDERATIONS

1) As shown in Fig. 1, the angular dependence of directional spectral reflectance factor of white surfaces for -45° incidence is not always uniform. In many cases, these white surfaces are used as reference or working standards. When spatial distribution of reflected light from a reference material and that from a sample is similar, the geometric conditions are not so important. But usually, spatial distributions from samples are different, therefore , for precise color measurement, geometric conditions should be strictly specified.
2) As shown in Fig. 2, the reflected light distribution from matt, white surface is nearly uniform, then lightness L* or metric chroma C* have no relation to light trap size. But, in case of glossy or semi-glossy chromatic surfaces, lightness or metric chroma is affected by light trap size, because elimination of specularly reflected light is different.
3) Generally speaking, color or appearance of textile is different with the viewing direction, as shown in Fig. 3. For precise color measurement of textiles, three-dimensional gonio-spectrophotometry may be suitable. Color of textiles, when viewed from one direction, may be assumed from product of color and effective area of warp and woof, and for these purposes, statistical analysis of directional spectral reflectance factor distribution by three-dimensional gonio-spectrophotometry.

REFERENCES

1) Baba,G. and Suzuki, K.: Gonio-spectrophotomeric analysis of white and chromatic reference materials, *Analytica Chimica Acta,* **380**, 1999, pp 173-182.

Baba, G. and Suzuki, K.: Study on geometric conditions for reflection measurement (2). Effect of light trap size of integrating sphere, 9th Congress of AIC, Proceedings of SPIE Vol. 4421 (2002) pp 769-772.

Importance of enclosing a space by walls for constructing the recognized visual space of illumination

Rumi Yamauchi, Hiroyuki Shinoda and Mitsuo Ikeda
Department of Photonics, Faculty of Science and Engineering, Ritsumeikan University

ABSTRACT

This is an experiment conducted based on the concept of the recognized visual space of illumination RVSI, which is defined as the understanding about the illumination state of a space[1]. To construct a RVSI one first observes objects in the space and we call them the initial visual information, IVI. A gray test patch was placed in an actual room illuminated at 60 lx by a ceiling light and a small area around the patch was additionally illuminated by a white, red, yellow, green or blue spotlight. The eight different combinations of four planes, namely a back wall, a floor and side walls, were introduced around the test patch to serve as IVI for the spotlight and the apparent color of the patch in terms of whiteness and chromaticness was measured to quantify the efficiency of the planes that enclose the space of the spotlight in constructing the RVSI. The apparent lightness or chromaticness was judged largest when no planes were introduced but was judged smallest when the test patch was enclosed by all the four planes. The efficiency of walls to construct the RVSI was highest when all the four were used to enclose the space. When individual walls were compared, the back wall was most efficient, and the floor and the sidewalls followed in that order.

KEYWARDS: apparent lightness, color, color naming, perceived illumination, recognized visual space of illumination, initial visual information

1. INTRODUCTION

When we enter a room we can immediately understand how the room is illuminated brightly or dimly and yellowish or bluewish. We express this situation that we construct in our brain the recognized visual space of illumination, RVSI for the room based on the appearance of all the objects in the room, which work as the initial visual information, IVI. The appearance of the object in the room is determined by the RVSI.

The RVSI has two properties; the brightness size, which expresses how an observer feels the brightness of a space, and the color. The RVSI is schematically illustrated by a circle as shown in Fig.1. Its radius represents the brightness size and axes express the color property. Let us consider an achromatic object O in a room dimly illuminated by, say, a ceiling light. It is additionally illuminated by a spotlight without being noticed by an observer. The observer constructs only the RVSI, R_{room} for the dimly illuminated room as shown in Fig.1(a) and its radius is small. The object O is plotted along the radius near to the circumference of the circle as its luminance is higher than its original luminance because of the additional illumination. Its apparent lightness is judged high. If the observer comes to know the existence of the spotlight by being increased with IVI for the spotlight, he/she will construct another RVSI, $R_{spotlight}$, of which brightness size is larger than R_{room} as illustrated by Fig.1(b). The luminance of the object O does not change and its relative position along the radius comes closer to the center of the RVSI. The apparent lightness should be judged low returning to its original lightness.

Let us now employ a colored light, red for example, for the spotlight, again without being noticed by an observer. The achromatic object O is illuminated by the red spotlight and its position rotates in R_{room} toward right as Fig. 1(c). Its apparent color is determined in relation to the recognition axis RX and it is red in this case because the RX still remains vertical as the ceiling light is white. In Fig. 1(c) FX represents the fundamental axis and IX the illumination axis. When the observer comes to notice the existence of the red spotlight by being increased with IVI for the spotlight, he will construct another RVSI, $R_{spotlight}$, of which RX is rotated toward and near to IX with angle θ as shown in Fig.1 (d). As the angle θ is small the color of the object should be judged almost achromatic. The apparent color returns to its original color.

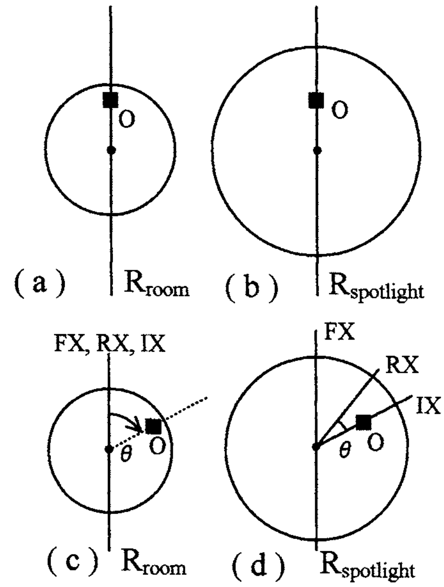

Fig.1 The scheme of the RVSI.

The recovery of the original lightness and color is expected to be greater as the IVI for the spotlight is increased. In previous experiments number of objects placed in the spotlight was varied and walls to surround them were introduced gradually to investigate the effect of IVI to construct $R_{spotlight}$[2,3,4]. It was suggested through these experiments that walls to surround a space are most effective in constructing a RVSI. We will systematically investigate which walls are more effective, sidewalls, back wall, floor, or their combinations in constructing $R_{spotlight}$ by measuring the apparent lightness and color of a test patch.

2. EXPERIMENT

2.1 Experimental Conditions

We employed an actual room to carry out the experiment as shown in Fig.2. The entire room had the width, length and height of 2m and was divided to the test and the subject room with a wall having a rectangular aperture of the size 40 x 50 cm at the subject's eye level. Both rooms were decorated with books, dolls, flowers and others with various colors to simulate an actual room. The test patch T of the size 4 x 4 cm was supported by a pole projected from the back wall and the subject could not see the pole. Its position from the floor was 105 cm high. The test size became about 2.2 x 2.2 degrees in visual angle when viewed by the subject at the distance 105 cm. The surface of the test patch was slightly tilted upward so that it can receive the spotlight coming from the above. The color chart of the Munsell Value of N4 was used for the test patch. Both test and subject rooms were illuminated by the fluorescent lamps FL_t and FL_s of the daylight type. The spotlight was provided by a slide projector SP placed at the roof via a mirror. The subject could not notice the existence of the spotlight if only the test patch was illuminated by it, thus becoming a hidden illumination.

We employed eight different combinations of four planes as the condition of the initial visual information as shown in Fig.3. Central gray small squares indicate the test patch T. The condition C0 had no planes to surround the test patch, C1 only back wall, C2 only floor, and so on. The condition C7 used all the four planes. The shape and size of each plane were same as those of C7, where the sidewalls and the back wall were slightly opened upward so that they could receive the spotlight coming from the above, and the sidewalls were slightly opened toward the subject so that their surfaces could be seen by the subject. The front side of the floor was 44 cm length, the back side 34 cm, the depth 30 cm, the upper side of the back wall 40 cm and the height 30 cm.

The illuminance level was fixed for both test and subject rooms at 60 lx when measured on the tables 67 cm high from the floor. In the apparent lightness experiment a white spotlight was employed with illuminance fixed at 400 lx. The total illuminance was 460 lx. In the color experiment the same room illumination was used and four different spotlights, red, yellow, green and blue were employed. The total illuminace was 120, 220, 120 and 100 lx, respectively. The chromaticity coordinates at the test patch are shown in Fig.4, W denoting the illumination in the apparent lightness experiment, and R, Y, G and B in the color experiment.

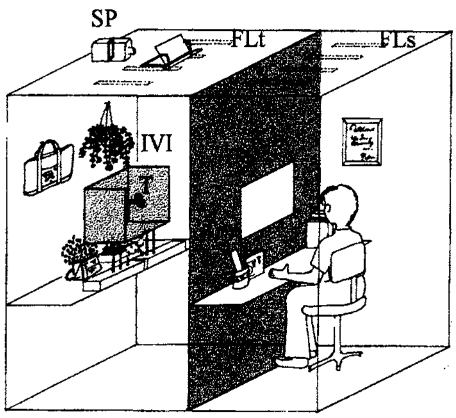

Fig.2 The experimental booth. T, test patch; IVI, initial visual information; FL_t and FL_s, fluorescent lamps; SP, slide projector.

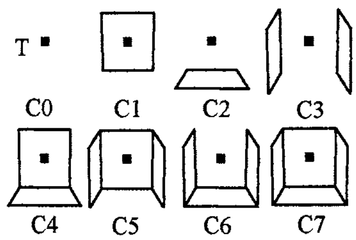

Fig.3 The eight different combinations of the planes as IVI.

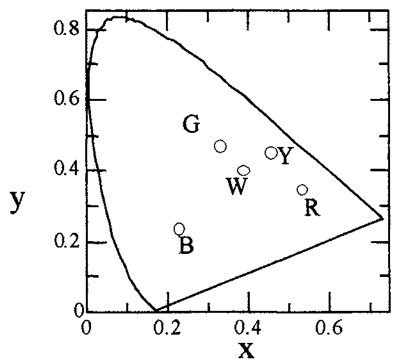

Fig.4 The xy chromaticity coordinates of the test patch N4 under five different colors of spotlight.

2.2 Procedure

In the apparent lightness experiment eight combinations of the planes were randomly presented and the subject judged the percentage of blackness and whiteness perceived in the test patch. Ten such sessions were conducted. In the color experiment eight combinations and four spotlights were randomly presented and the subject judged the percentage of chromaticness, blackness and whiteness, and then the hue by using four unique colors. Ten such sessions were conducted. The subject used both eyes. He was asked to look around the test room without staring only at the test patch so that he always recognized the test patch as an object in the test room.

Four subjects participated in the apparent lightness experiment and five subjects in the color experiments. They all had the normal color vision as tested by the Ishihara plates.

3. Results and Discussion

For the condition C0 when only the test patch was presented in the spotlight, all the subjects did not recognize the existence of the spotlight. They reported in the lightness experiment that the test patch was a mere bright object and in the color experiment a mere colored object.

Results from the lightness experiment are shown in Fig.5, sections corresponding to the subjects. The IVI conditions are taken along the abscissa and the percentage of whiteness along the ordinate. Each point shows the average of ten judgments and vertical bar the standard deviation. All the subjects judged the highest amount of whiteness for the condition C0 where only test patch was in the spotlight, and the lowest for the C7 where the test patch was surrounded by four planes all illuminated by the spotlight. They judged intermediate amount of whiteness for other conditions between C0 and C7.

Based on the RVSI theory the result for C0 is interpreted that the subjects judged the lightness of the test patch in relation to a small RVSI for the test room illuminated at 60 lx as illustrated in Fig.1(a). On the other hand, the result for C7 is interpreted that the subjects judged the lightness of the test patch in relation to a large RVSI as illustrated in Fig.1(b).

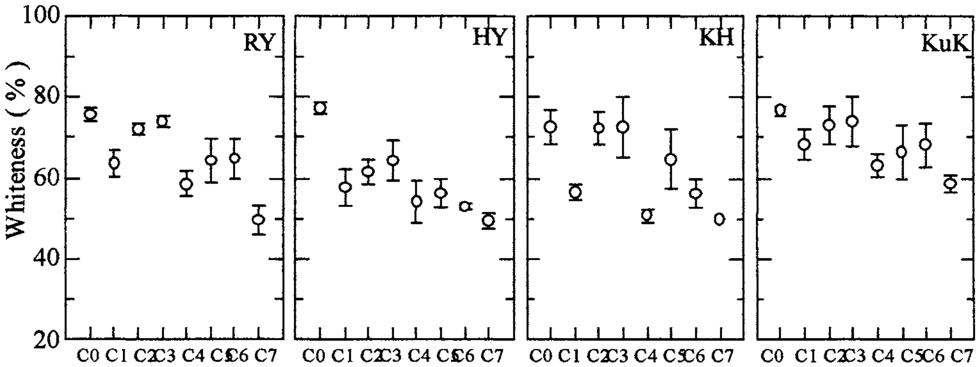

Fig.5 The results for the lightness condition.

The results from the color experiment are shown in Fig. 6 for all the five subjects but for the red spotlight condition only. The upper figures are for the chromaticness and the lower for the hue. Each point shows the average of ten judgments and vertical bar the standard deviation. All the subjects judged the highest chromaticness in the condition C0 and the lowest in the C7. There were almost no hue shift for all IVI conditions except for the subject HYu, who expressed a difficulty to discriminate the blackness from the blueness. The tendency of no hue shift also obtained for other three colors.

In the RVSI theory the condition C0 corresponds to the case illustrated by Fig.1(c) and the prediction is confirmed here that subjects would perceive a large amount of red color. The condition C7 corresponds to Fig. 1(d) and the prediction is also confirmed that they would perceive a small amount of red color.

To see the efficiency of planes to construct the RVSI for the spotlight the amount of whiteness or chromaticness was plotted simply in the order for each illumination condition as shown in Fig. 7. Each point is the average of all the subjects. The points from a same IVI condition are connected by a line to see if the efficiency is same for all the illumination conditions. There is no crossing in the lines for the combinations C0, C3, C2, C4 and C7 and the efficiency increases in this order. The efficiencies of the conditions C1, C5 and C6 come between those of C2 and C4, but there are found crossings of their lines. If we neglect the crossing having

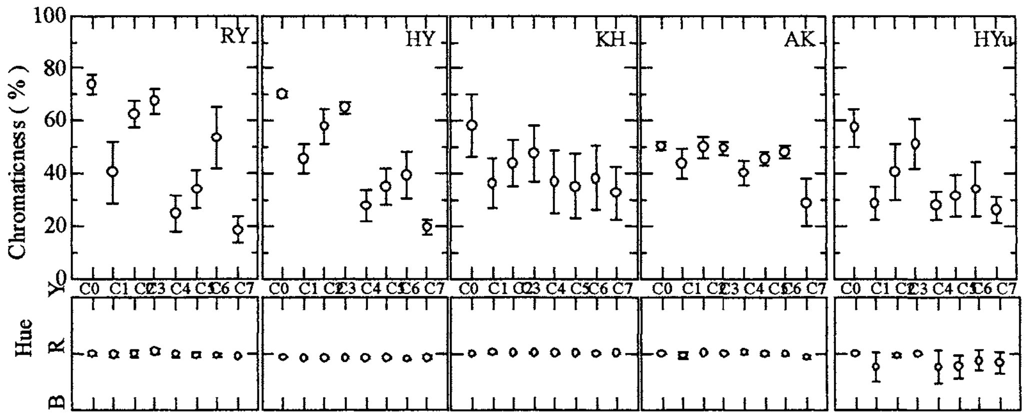

Fig.6 The results for the red spotlight. Top law indicates the chromaticness and the bottom the shift of hue.

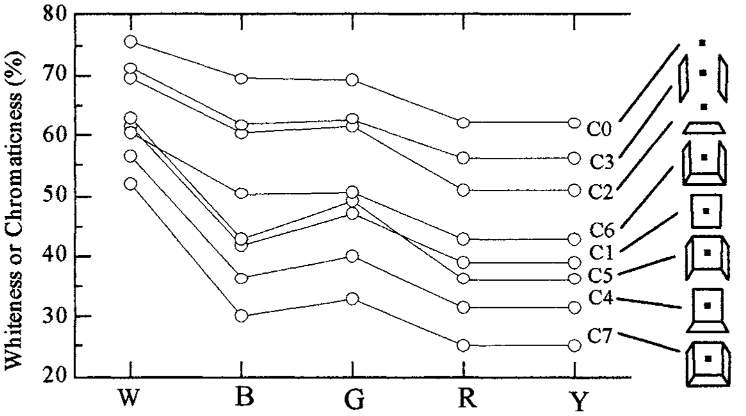

Fig.7 The average from all subjects for five different colors.

similar value, C5, C1, C6 in W, C5, C1 in B and C 6, C5 in G we can conclude that the efficiency increases in the order C0, C3, C2, C6, C1, C5, C4 and C7 as indicated at the right of the figure. Number of planes in these combinations is 0, 2, 1, 3, 1, 3, 2 and 4, respectively, which suggests that the number alone can not be a decisive factor for the efficiency. The common feature in the last four conditions, C1, C5, C4 and C7, is the existence of the back wall, and the common feature in the first four conditions is the lack of the back wall. The condition C2 is more efficient than C3 in spite of only one plane compared to two, which suggests the floor is more efficient than two sidewalls for constructing RVSI. The order can be expressed by giving points to the planes, for example, 1 point for two sidewalls, 3 points for the floor, and 5 points for the back wall, and additing them for combinations. The final points become 0, 1, 3, 4, 5, 6, 8 and 9 for C0, C3, C2, C6, C1, C5, C4 and C7. It is seen in Fig. 7 that the difference is rather large between C2 and C6, and C4 and C7 and can not be explained by the points alone. A common feature in these four conditions is the existence of the floor, and the difference in the feature between these two pairs is whether the sidewalls exist to enclose the space of the test patch.

To conclude the back wall is most important in constructing a RVSI, and then the floor. The construction improves greatly by enclosing the space by two sidewalls.

Reference

1) M. Ikeda: Abstract of the 7th Congress of AIC,Budapest, pp 257-258, 1993.
2) R. Yamauchi, M. Ikeda, H. Shinoda: KOGAKU, Japanese Journal of Optics, Vol.30, pp41-48, 2001. [in Japanese]
3) R. Yamauchi, M. Ikeda, H. Shinoda: Proc. of AIC, midterm meeting,Seoul, pp89-93,2000.
4) R. Yamauchi, M. Ikeda, H. Shinoda: Optical Review Vol.10, pp166-173,2003.

Space recognition: New account for simultaneous color contrast on a center-surround configuration

Prasit Cunthasaksiri*, Hiroyuki Shinoda, and Mitsuo Ikeda
Department of Photonics, Faculty of Science and Engineering,
Ritsumeikan University

* *Department of Photonics, Faculty of Science and Engineering, Ritsumeikan Univ., 1-1-1 Noji-higashi, Kusatsu, Shiga, 525-8577 JAPAN Tel: +81-77-566-1111 email: gr024013@se.ritsumei.ac.jp*

Keywords: simultaneous color contrast, color induction, space recognition, RVSI, center-surround

ABSTRACT

Appearances of object color in a space are determined by a cortical representation of illuminant for the space, or the recognized visual space of illumination, "RVSI". The simultaneous color contrast phenomenon on a simple center-surround configuration can be explained by RVSI. It is hypothesized that our visual system constructs RVSI for the surround, then that RVSI determines color appearance of center test. If this is correct, the color contrast can be quite strong when the surround is enlarged and finally make an enclosed space. To prove the hypothesis, color appearance of physically gray test was measured in a colored surround of various sizes. Subjects matched appearance of the test with Munsell color chart placed in a gray box. Four major colors R, G, Y, and B were examined as the surround. The results show same tendency for all surrounding colors; once the surround is extended to walls, a ceiling, and a floor of a box, apparent chromaticness abruptly increases. In other words, three-dimensional surround evoked strong simultaneous color contrast. The well-known color contrast is thought to be a weak version of this color change. It suggests that RVSI plays an important roll in the well-known color contrast demonstration on 2D plane.

INTRODUCTION

Simultaneous color contrast is an apparent deviation of a color due to its immediate color. A well known stimulus is a center gray field surrounded by another chromatic surround field that is observed under typical white illumination [a]. The gray field appears as if it was chromatic. A large number of experiment has been conducted to explore this phenomenon, however, each experimental scheme has been carried in various aspects respect to their purpose and hypothesis. Herein, the consideration is at the stimulus which appears as an object in daily life environment. Given example can be found easily in any text book about color vision as a printout which is illustrated, mostly, a gray patch within a chromatic surround. Under typical room circumstance, the patch appears as if it was chromatic. However this effect is *weak*. Term *weak* here refers to the fact that human visual system responds very well to the room illumination rather than the chromatic surround which is an object within scene[(1), (2)].

Based on this inspiration, present work will show that underneath mechanism of the phenomenon is a weak effect of which the visual system attempts to recognize a state of illumination over the surround of stimulus field.

The recognized visual space of illumination

A visual system is very essential for us to be aware state of environment and to correctly take response. The state of environment is physically originated by three dimensional space filled with illumination. Therefore these properties are very mutual. However, to achieve daily life task, the visual system utilizes information that purely obtains from its retina. Simply, it sees out side three dimensional world through two dimensional retinal screen as if we saw out side of a room through its window. Thus it must always interpret these information, called *initial visual information*, to recover the out side state. The interpretation, or construction, results in a recognition called *recognized visual space of illumination*, *"RVSI"*, which is a representative state of a real environment that consequently serves as a base for its perception[(3), (4)]. For instance, if a chromatic attribute of a constructed RVSI is reddish, a reddish spectral ray that comes from the scene would appear as if it was whitish, and also a whitish spectral ray would appear as if it was greenish[(5)]. It should be emphasized here that the

(a) Term gray, chromatic and white here mean, physically, spectral reflectance and power distribution.

constructed RVSI may or may not represent physical space of illumination because it is what the visual system is understood how a space is illuminated due to provided initial visual information which is the combination of physical objects and illumination. This also implies that the RVSI could be controlled by modifying the initial visual information. For example, Mizokami[6] attempted to allure the visual system to recognize that the illumination is chromatic, despite physically being achromatic, by mean of introduction chromatic objects into the scene as controlled initial visual information. Brainard[7] also showed that by mean of altering objects in the scene, the understanding of illumination is deviated in range of 11% to 83% as index of constancy refer to the physical illumination; the interpretation based on RVSI is that altering object is controlling initial visual information.

Simultaneous color contrast explained by the RVSI

Why does the center gray patch appear as if it was chromatic when it is surrounded by the chromatic surround? Our hypothesis is that the light, reflected from the surround, acts as initial visual information to for the visual system to construct a RVSI over the stimulus[8]. Consequently the patch is perceived in relation to that constructed RVSI; in other hand its appearance acts as a probe that how attribute of constructed RVSI is[9]. Why is the effect, in this case, weak? The explanation is that it depends on how the visual system interprets; whether the chromatic content of the incoming light reflected from the surround is due to the surround itself or illumination. If the visual system interprets in a manner that the chromatic content belongs to the illumination then the gray patch would be perceived as being strong chromatic. Nonetheless, the given example is not in the case because, the simple surround is not adequate to persuade the visual system.

If the underneath mechanism of this phenomenon is as described it must be able to evoke the visual system a strong effect despite the fact that the physical chromatic content belongs to the surround.

Pre-experiment

An employed method to test the hypothesis is, thus, modifying the surround to lead the visual system to construct a chromatic RVSI even though the actual illumination is achromatic. Under the above circumstance, the attracted initial visual information, which is modifiable, is a size of the surround. If the surround is expanded from a typical small size in the text book to a large one in order to dominate a visual field, it is possible that the visual system might be persuaded. Thus we put two pieces of green paper, one is 106.0x80.0 and another is 37.0x45.0 degree^2 of visual angle on the wall of corridor in a building. At the center of them was attached with Munsell gray patches size 1.4x1.4 degree^2. The illumination of corridor was household fluorescent. However, from an observation, there is no noticeable difference of chromatic appearance between the patches on the large and the small surround. It suggested that, in this circumstance, the larger size of surround did not strongly evoke the visual system a greenish RVSI. Therefore, in consideration of characteristic of RVSI, we went further to modify the surround by altering the plane surround to be three dimensional.

Important of three dimensionality

According to the concept of RVSI, important initial visual information that the visual system utilizes to recognize the state of illumination is physical three dimensional. It is asked which aspect that three dimensionality strongly affect the construction of RVSI. We believed that physical enclosed space would strongly persuade the visual system because it is the space we are familiar with. Thus, we expected that if the surround is altered to be three dimensional, the visual system perhaps recognize that the greenness belongs to the illumination over that particular space. To achieve that, an observation should be performed in the three dimensional enclosed space. We, therefore, made an enclosed surround which is big enough to solely cover the visual field as shown in figure 1 (a). A test patch, which was kept achromatic constant, was at the center of the front panel consequently the room behaved as its immediate surround. The properties of stimuli were still on the same basis; green paper surround, Musell gray test patch, and fluorescent illumination. The green surround paper was step by step introduced, beginning from the edge of the test stimulus in place of the gray surround as shown at the figure 1 (b). Successively, each step the surround was increased, chromatic appearance of the test was observed. The surround was increased till it covers all of two dimensional front panel and then all of visual field which were three dimensional. It should be noted here that the reason we designed the method of change surround size is that it can be later compared the appearance of the test in each surround size condition; if three dimensionality significantly affect the construction of RVSI then the simultaneous color contrast effect should be significantly different when the surround is changed from being two dimensional to three dimensional. Pre-observation indicated the significant difference of chromatic appearance between those two conditions. Hence we quantitatively investigated the effect according to the introduction of three dimensional surround.

Experiment

Stimuli and Apparatus

As shown in figure 2, the apparatus was composed of an observer room and a stimulus box. Inside the room was decorated by a gray paper. At the front panel, there is a 1.6-degree square hole when observed at 80cm distance. Surround of this hole, there was a chromatic paper which it could be replaced, or taken off, to alter its size. The room is illuminated by two fluorescent lamps, FL, from behind observing position. The stimulus box was a diffuse surface contained Munsell paper N7.25 illuminated by same type fluorescent lamp used in the observer room. All of the lamp could be controlled their intensity separately. When binocularly observed from the room through the hole the Munsell paper appeared as if it was a paper pasted on the front panel. A control box, which is not shown in the figure, was decorated with same gray paper and illuminated by same type fluorescent lamp. At the box observer could select a Munsell patch by moving a mask. This box was placed adjacent to the room therefore observer can move out from the room to select a match color in the control box. All of these apparatus were in a complete dark room; light from each source do not interfere.

Task and procedure

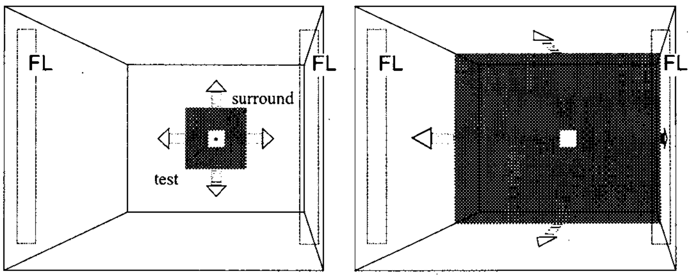

Figure 1 a (left) and b (right) are observer' view. The experiment composed of 7 sizes on 4 color surround. The color surround, represented with gray area in the figure, was replaced to alter its size in each condition; starting with "no surround", 4.5x4.5-degree, 14x14-degree, 42x34-degree, 48x41-degree, 52x44-degree and cover whole room; the 2nd to 5th conditions were physical two dimensional and the 6th to 7th were three dimensional.

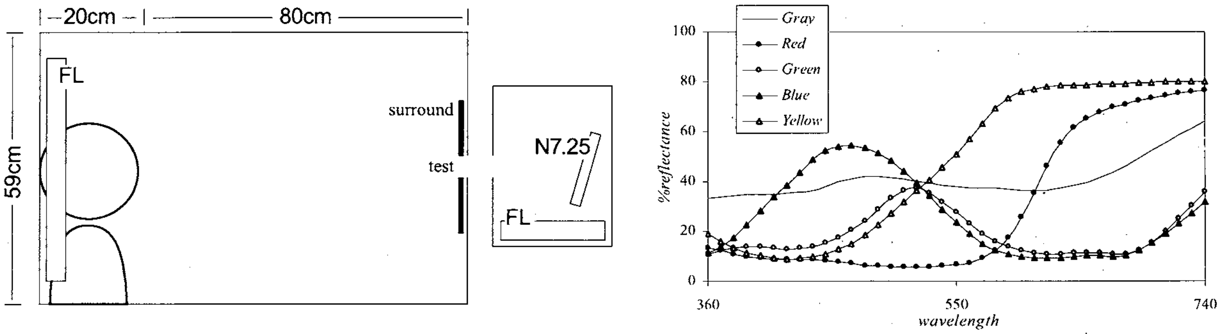

Figure 2 (left) is side view of the apparatus. The fluorescent lamp was 4500K type. Figure 2 (right) shows a reflectance index of the gray and color papers used as surround in the experiment. These papers were matt and arbitrarily chosen therefore the gray paper was not perfect gray as Musell gray paper. Through the experiment conditions, the room illumination was set by keeping a measure of luminance at the area (around 1-degree) adjacent to the hole as constant at 27.5 cd/m^2 and the test stimulus was kept its measure of luminance at 22.18 cd/m^2; both were measured from observing position. Their chromaticity coordinates under each experimental condition were; (0.364, 0.383) in reference condition, (0.535, 0.346) for red, (0.306, 0.445) for green, (0.242, 0.316) for blue, (0.482, 0.442) for yellow in condition 2nd to 6th, and (0.602, 0.332) for red, (0.293, 0.475) for green, (0.209, 0.273) for blue, (0.566, 0.408) for yellow in condition 7th. The 7th condition was not same in chromaticity coordinate due to mutual reflectance light caused by the apparatus arrangement. Those luminance setting ratio between the test and surround were obtained from observer PC who was required to adjust the luminance level to get a strongest simultaneous color contrast effect.

The experiment was conducted for seven sizes on four colors surround. In each surround color, the experiment was run to vary its size. The first condition was the room that totally decorated by gray paper without any color surround as a reference condition. Then at the second condition, the smallest color surround was introduced with 4x4-degree^2 size, 13x13-degree^2 size and so on, till it was decorated all in seventh condition. For each condition, observers were asked to select a Munsell color patch, in the control box, that matches to the appearance of the test patch. One session composed of these seven conditions; their series were randomly presented. Each observer was asked to repeat the experiment ten sessions.

Four observers were, with normal color vision, participated. Observers were allowed to freely look around and their head was not fixed. There was no intention to have them an adaptation before each judgment[(10)]. The instruction was that "When you get into the room you will see a test in front of you. Please select a Munsell color patch in the control box that matches appearance of the test. You are neither asked to fix your head nor gaze the test patch. You can look back and forth between the room and the control boxes till you are sure to select the Munsell color patch."

In trial session, because the effect was chromatic and hue deviation, each observer was firstly asked to choose a Munsell hue chart that can be match the appearance of the test in those seven conditions; later each observer use their own Munsell hue chart through the experiment.

RESULT

Figure 3 shows results of three observers which presents a relation between an area of visual field occupied by the surround and a Munsell chroma of the test. Along the abscissa each surround condition is plotted in logarithmic scale of area of visual field (square-degree) and along the ordinate the Munsell chroma is plotted. The judgment of each condition is averaged from those ten sessions and presented by each symbol which includes its standard deviation. All symbols are connected with a line which its slope indicates a degree of a change in Munsell chroma score corresponded to a change of surround size.

The result of the 2nd condition, where the smallest color surround was presented, is indicated by the first left symbol and the next is the result of the next condition where the bigger color surround was presented. The arrow point at the abscissa divides the results into two groups; the left part is results where the surrounds are physical two dimensional plane meanwhile the right part is results where the surround are physical three dimensional. The apparent hue of the test is not presented here since there was no significant difference through the conditions except reference condition where the color surround was removed. In condition that color surround was presented, the hue appeared to be approximate complementary; for instance the test appeared reddish within green surround condition.

The results show following tendency. The reference condition of all observer resulted in following Munsell chroma number; 1.32 for PC, 2.14 for AK and 1.48 for SP. From 2nd to 3rd condition, where the surround was flatly enlarged from 4x4 to 13x13 degree^2 area, all results show gentle slope. Then at 3rd to 4th (42x34 degree^2) condition, where the surround was enlarged to almost cover the two dimensional front wall of the room, the slope becomes a little bit steeper. Consequently at 4th to 6th condition, where the surround was enlarged to cover the front two dimensional wall of the room (48x41 degree^2) and turned to be three dimensional (52x44 degree^2), the slope become abrupt. Finally at 7th condition, where the surround covered all the room, the slope turned to be gentle again.

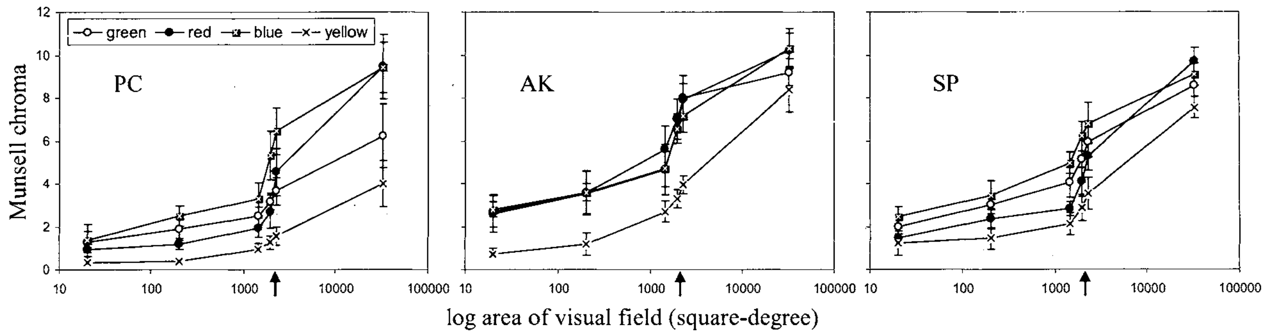

Figure 3 shows results of three observer PC, AK and SP.

DISCUSSION

The major question of this experiment is whether the recognition of three dimensionality affects the simultaneous color contrast. Since the immediate area of the test was kept its physical properties as constant along the 2nd to 6th condition then the abrupt slope, at 4th to 6th condition, indicates a high degree of change in Munsell chroma caused by contribution of the three dimensionality. This implies that when the surround was altered to be three dimensional enclosed space the recognition of visual space of illumination become more chromatic which resulted in stronger simultaneous color contrast effect.

The gentle slope at 2nd to 3rd condition shows a little influence of surround size which was not shown in the pre-experiment. However, both surround sizes in the pre-experiment, perhaps, was at their extremes of contribution therefore there was no different in appearance. The slope at 3rd to 4th condition was raised despite flat expansion. This perhaps at 4th condition, there was a mutual reflection light occurred due to the peripheral edge of the surround which was close to the side wall. This light was not observed by observers because of adaptation which may cause this raised slope.

This mutual reflection light still occurred at 5th and 6th condition and it was strongest at 7th condition when the reflection light filled the area of the surround which was adjacent to the test. Nonetheless, the slope from 4th through 7th condition appeared in contrast; the steepest slope occurred where the surround was changed to be three dimensional in 6th condition but consequently the slope dropped at 7th condition even though the mutual reflection light was strongest. It could be interpreted that even though enlarged surround or mutual reflection light influenced the effect, the recognition of the space constructed due to the three dimensionality was stronger contribution.

REFERRENCE

1. A. Valberg and B. Lange-Malecki: Vision Res. **30** (1990) 371.
2. D. H. Brainard: J.Opt. Soc. Am. A **15** (1998) 307.
3. M. Ikeda, H. Shinoda and Y. Mizokami: Opt. Rev. **5** (1998) 200.
4. M. A. Changeizi and D. M. Widders: Perception **31** (2002) 1241.
5. M. Ikeda, S. Nakane, Y. Mizokami and H. Shinoda: Opt. Rev. **9** (2002) 132.
6. Y. Mizokami, M. Ikeda and H. Shinoda: Opt. Rev. **7** (2000) 358.
7. D. H. Brainard: Proc. Natl. Acad. Sci. 96 (1999) 307.
8. M. Ikeda, H. Shinoda and Y. Mizokami: Opt. Rev. **5** (1998) 380.
9. M. Ikeda, S. Nakane, Y. Mizokami and H. Shinoda: Opt. Rev. **9** (2002) 132.
10. M. Ikeda, H. Shinoda and Y. Mizokami: Opt. Rev. **5** (1998) 200.

Effects of Three Dimensional Stimulus Configuration on Simultaneous Color Contrast

Shinji Nakamura
Nihon Fukushi University, Faculty of Information and Social Sciences

The effects of the three-dimensional configuration of visual stimulus on simultaneous brightness or hue contrast using Koffka-ring pattern were investigated. Subjects reported perceived color of Test Figure (TF) surrounded by Inducing Field (IF) with two distinct colors (red-green or black-white) by using magnitude estimation method. Depth distances between stimulus components, such as subregions of TF and IF, or dividing line which bisects TF, were manipulated as experimental conditions. Results of the psychophysical experiments show that magnitude of contrast is not affected by depth distances between TF and IF. On the other hand, depth separation between TF and dividing line affects color appearance of TF, that is, magnitude of contrast decreases with increasing depth distance between these two stimulus components. These results suggest that post-retinal information processing, as well as retinal image processing, play very important role in human color vision including contrast, assimilation and integration between these phenomena.

INTRODUCTION

When a gray test figure (TF) overlaps a red or green background, the figure appears to change its hue as a result of a simultaneous hue contrast, and be perceived more reddish in the condition with green background and more greenish with red background. On the other hand, when the gray TF overlays across an inducing filed (IF) which consists of red and green subregions, perceived hue of the TF remains to be achromatic regardless of local hue contrast. It can be considered that induced hues generated in both subregions are cancelled with each other. Thus, when the TF is divided by a line placed along demarcation of the IF, divided parts of the TF appear to have chromaticities (i.e., red against green subregion and green against red subregion). This phenomenon, called "Wertheimer-Bennusi's pattern" or "Koffka-ring", provides evidence for strong effects of configurations (or Gestalts) of visual stimulus on simultaneous color contrast (Koffka, 1935).

Many researchers investigated the effects of the division in Koffka-ring patterns (e.g., Anderson et al., 1975). Furthermore, our previous studies indicated that figural unity manipulated by dividing line and separation of the TF itself affect magnitude of simultaneous hue contrast in Koffka-ring type pattern strongly (Ito et al., 1993; Takahashi et al., 1996). However, previous investigations of figural factors on Koffka-ring have been executed only in two-dimensional patterns, and effects of three-dimensional configurations of the visual stimulus have been still unresolved. Thus, the purpose of this study is to analyze effects of depth separations between the TF and the IF (experiment 1), or between the TF and the dividing line (experiment 2). Two psychophysical experiments were carried out with magnitude estimation method in order to address this question.

It has been indicated that simple brightness contrast is a monocular phenomena and not affected by binocular disparities (Sugita, 1995). Furthermore, brightness and hue contrasts in Koffka-ring pattern share very similar tendencies against various stimulus factors, suggesting that both types of contrast share same underlying perceptual mechanism (Takahashi et al., 1996). Thus it can be supposed that simultaneous color contrast in Koffka-ring pattern is not affected by the depth distances between the TF and the IF. Experiment 1 is carried out to address this issue. On the other hand, cancellation of induced color components within the TF (I'd like to refer this process as assimilation in Koffka-ring) is supposed to be rather cognitive process (Goto et al., 1995), and affected by perceived depth structure of the figure (Wist & Susen, 1973; Ito et al., 1993). Therefore, it can be hypothesized that depth discrepancies between the TF and the dividing line, which is inhibitor of assimilative process, would affect magnitude of hue or brightness contrast in Koffka-ring pattern. Experiment 2 tests this hypothesis. Furthermore, differences between the effects of three-dimensional stimulus configuration in simultaneous hue and brightness contrast are investigated. In the hue contrast experiments (experiments 1-a and 2-a), the IF consisted of red and green subregions, while in the brightness contrast experiments (experiments 1-b and 2-b), the IF is black and white.

METHODS

Visual Stimulus

Visual stimuli consisted of three components, namely Inducing Field (IF), Test Figure (TF), and fixation cross. IF was divided left and right subregions. In experiments 1-a and 2-a in which hue contrast was examined, the left subregion was red (x=.5896, y=.3347, 40.49cd/m^2) and the right subregion was green (x=.2811,y=.5564, 32.92cd/m^2), while brightness contrast experiments (experiments 1-b and 2-b), the left and right subregions were black (x=.3492,y=.3757, 4.62cd/m^2) and white (x=.3529,y=.3808, 187.0cd/m^2). Size of each half of the IF was 15.2 deg in height and 11.3 deg in width in visual angle. The IF was placed on gray background (46.0cd/m^2). TF was a diamond shaped ring with the size of 11.8 deg in height and width. Width of the ring was 0.76 deg. Color of TF was bright gray (109.0cd/m^2). Fixation cross had a size of 1.9 deg in height and width, and its color was dark gray (23.74 cd/m^2). Furthermore, in experiment 2, dividing line bisecting the TF was added. The dividing line was placed along the border between the left and right subregions of the IF. Color of the dividing line was white (187.0 cd/m^2) and its width was 0.38 deg. Figure 1 schematically indicated the visual stimulus. The visual stimulus was printed on the cardboard specialized for fine color printing by inkjet printer. In a real stimulus, visual patterns for left and right eyes were printed in an isolated fashion for stereoscopic observation, and binocular disparities were set in accordance with stimulus conditions described below.

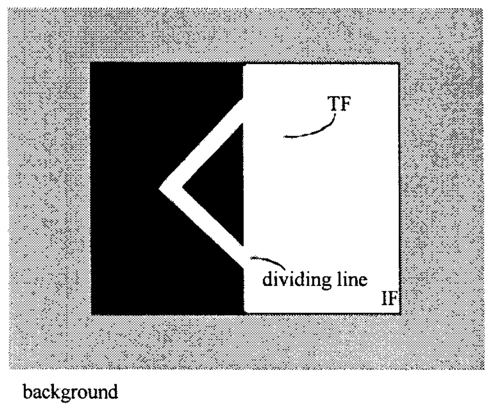

Figure 1 Schematical illustration of the visual stimuli used in the experiments

Procedure

Five naïve subjects (male, undergraduate students) who had normal visual acuity and color and stereoscopic vision participated in the experiments. Subjects observed visual stimulus with using binocular scope under illumination of a fluorescent lamp with their eyes fixating on the fixation cross. Observation distance was 15 cm.

Subjects estimated perceived color of the TF, hue for experiments 1-a and 2-a, and brightness for experiments 1-b and 2-b. For a modulus of the estimation, comparison stimulus was presented in a different sheet from the visual stimulus. The comparison stimulus had three squares with different color. For the hue estimation, the color of the squares were gray (109.0cd/m^2, same as the TF) , reddish gray (x=0.3783, y=0.3863, 111.5cd/m^2) and greenish gray (x=0.3437, y=0.4015, 118.5cd/m^2), while for the brightness estimation, the squares were gray of different brightness (88.51, 109.0, 132.5cd/m^2). Subjects estimated perceived hue of the TF with a scale from -100 (same hue as reddish comparison square) via 0 (same as gray square), to 100 (greenish square). Similarly, brightness estimation was executed with comparison squares (-100 for dark, 0 for middle and 100 for bright square). Subject reported estimated hue or brightness for both left and right halves of the TF separately.

Trials for each experimental condition were repeated five times in a randomized order. All experimental trials were executed after five minutes adaptation for illumination level and training trials (it took about 5 minutes).

Stimulus Conditions

In experiment 1, depth distance between the IF and the TF was manipulated as an experimental condition, and had four levels (crossed binocular disparities 0, 14, 23 and 46 min; 0 disparity means that the TF and IF were presented in the same depth plane). Separation of the TF was also introduced as a second experimental factor, separated and united TF. In separated TF condition, annular diamond was separated into left and right parts resulting two bracket-like shapes (separation distance was 1.9 deg). United TF was standard annular diamond.

In experiment 2, experimental condition was depth separation between the TF and the dividing line, and there were four different distances (crossed binocular disparities 0, 14, 23 and 46 min). Furthermore, control condition was added with no dividing line.

RESULTS & DISCUSSION

Magnitudes of hue and brightness contrast were calculated by differences between estimated values for left and right halves of the TF. Figure 2 indicates magnitude of hue (2-a) and brightness contrast (2-b) as a function of binocular disparity attached by the TF (which correspond to the depth distance between the TF and the IF) under each separated and united TF condition (experiment 1). Magnitudes of hue and brightness contrasts were larger in the separated TF and smaller in the united TF. It can be considered that local color contrasts invoked by hue or brightness difference between the TF and the IF in the left and right subregions of TF are cancelled with each other through the united TF. However, it was indicated that small but significant contrast was still remained in the united TF. This result indicated that the cancellation of local contrast

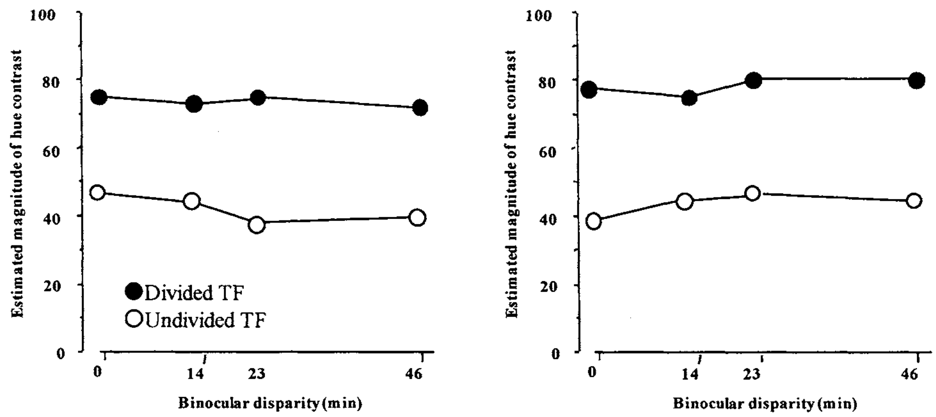

(a) (b)

Figure 2 Estimated magnitudes of hue (a) or brightness(b) contrast as a function of binocular disparity of the TF (Experiment 1). Closed circles indicate the divided TF and Open Circles indicate the undivided TF

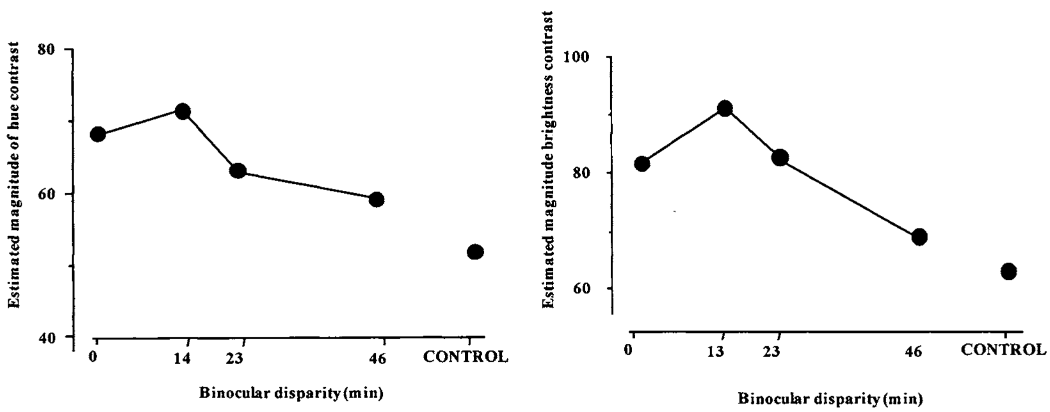

(a) (b)

Figure 3 Estimated magnitudes of hue (a) or brightness(b) contrast as a function of binocular disparity of the dividing line (Experiment 2)

throughout united (and undivided) TF is not accomplished perfectly, and consistent with our previous study (Ito et al., 1993). Furthermore, it was indicated that both hue and brightness contrasts were not changed by the depth separation between the TF and the IF. Two-way analysis of variance indicated that there was significant main effect of TF separation (hue contrast: $F(1,4)=36.42$ $p<.01$; brightness contrast $F(1,4)=25.45$ $p<.01$), but main effect of the depth distance between the TF and the IF, nor the interaction between these two factors, are not significant ($F(3,12)=1.92$, n.s. for main effect of the disparity in hue contrast; $F<1$ for the other items). The non-significant effect of the depth separation suggested that local color contrast derived by hue or brightness difference between the TF and the IF is processed by monocular system in early stage in the visual information processing. This is consistent with the previous study which investigated the effect of stimulus depth structure on simultaneous color contrast (e.g., Sugita, 1995).

Figure 3 indicates magnitude of hue (3-a) and brightness contrast (3-b) as a function of binocular disparity attached to the dividing line (experiment 2). It was indicated that magnitudes of contrast varied with the depth distances between the TF and the dividing line. When the dividing line was presented with the same depth plane with the TF, or near it, the magnitude of contrast was larger. With growing the depth separation between the dividing line and the TF, the magnitude of the contrast decreased. In the control condition where there was no dividing line, the magnitude of contrast was quite lower. Analysis of variance indicated that significant effect of the depth separation of the dividing line (hue contrast: $F(4,16)=14.61$, $p<.01$; brightness contrast: $F(4,16)=18.18$, $p<.01$). The results of the experiment 2 suggested that the dividing line inhibits propagation of the cancellation of the local color contrast in Koffka-ring pattern and its effect is stronger when the dividing line is presented three dimensionally adjacent to the TF. Thus, cancellation, or assimilative, process in Koffka-ring pattern is executed higher stage in visual information processing, at least after binocular fusion. This consideration is consistent with our previous discussion in which we assumed that cognitive factors such as perceived depth structure of the visual pattern or subject's set for observing the stimulus might affect color perception in Koffka-ring pattern, especially its assimilative process (Ito et al., 1993; Goto et al., 1995).

Finally, I can propose tentative hypothesis on perceptual process of simultaneous color contrast in Koffka-ring pattern as follows. Hue and brightness contrasts in Koffka-ring are transacted in two successive processes. First, local color contrast is derived by the differences of hue or brightness between two adjacent regions. This process is dealt with monocular system early in the visual information processing. Then, local contrast is propagated throughout in united visual figures, especially in the case of Koffka-ring pattern, canceling color components induced by the local contrast. Perceptual process responsible for this assimilative stage is binocular, and perhaps affected by cognitive factors.

References

Anderson, N. S., Pine, S. M. & Rosenfeld, A., 1975, Derived scales for degree of simultaneous contarast in six Benussi ring figures. *Bulletin of Psychonomic Society*, **6**, 289-292

Goto, T., Hanari, T., Ohnuma, S., Kobari, H., Shinoda, N., Sugiura, J., Tamoto, K. & Hishnuma, Y., 1995, Effects of grasping-form attitude on brightness contrast in Koffka-ring type patterns. *Psychologia*, **38**, 192-198

Ito, M., Takahashi, S., Hanari, T., Tanaka, S., Nakamura, S., Nonami, H., Homma, H., Fuku'uchi, Y. & Goto, T., 1993, Effects of separation and division of test figure on simultaneous hue contrast in Koffka-ring type patterns. *Psychologia*, **36**, 103-108

Koffka, K., 1935, *Principles of Gestalt Psychology*. Harcoust, Brace

Sugita, Y., 1995, Contrast and assimilation on different depth planes. *Vision Research*, **35**, 881-994

Takahashi, S., Ito, M., Hanari, T., Nakamura, S., Nonami, H., Fuku'uchi, Y. & Goto, T., 1996, Effects of form in Koffka-ring type patterns (1): Comparison between hue and brightness contrasts. *Psychologia*, **39**, 126-133

Wist, E. R. & Susen, P. 1973, Evidence for the role of post-retinal processes in simultaneous contrast. *Psychologishe Forshung*, **36**, 1-12

The Physiological and Psychological Effects of Color in the Interior Space

Hideki Sakai, Aya Enami, Tomomi Shimonaka, Kuniko Yamashita, and Masako Sato

Graduate School of Human Life Science, Osaka City University, Japan

1.INTRODUCTION

Radiant energy of color would more or less affect the human body and mind, because it should stimulate the autonomic nervous system of human[1]. For example, the concept of warm and cool colors is very common in designing and painting[2,3]; it is said that a warm-colored space will give us warmer impression and a cool-colored space will give us cooler impression than a neutral-colored space.

The purpose of this paper is to investigate how colors affect the human body and mind. The physiological parameters of subjects, heart rate, brain waves, bloodstream, and body temperature, were measured using a male subject sitting in the model room painted with a single color. After the task, the subject was asked some questionnaires. The relations between the physiological effects and the psychological evaluation were discussed. The examined interior colors were yellow-red (typical warm color), blue (typical cool color), and two achromatic colors, gray and white. In this study, the experiment was conducted under strictly well-defined condition as described below.

2.METHODS

Subjects

Fourteen healthy males in their twenties participated in this experiment as subjects. All subjects were clothed in T-shirts and long trousers, controlled to be nearly equal to 0.4 clo.

Experimental setup

The experiment was conducted in a small room as shown in Fig.1. Four experimental rooms (HWD= 2160mm × 800mm × 1100mm) were constructed in an artificial climate chamber controlled to a temperature 25℃

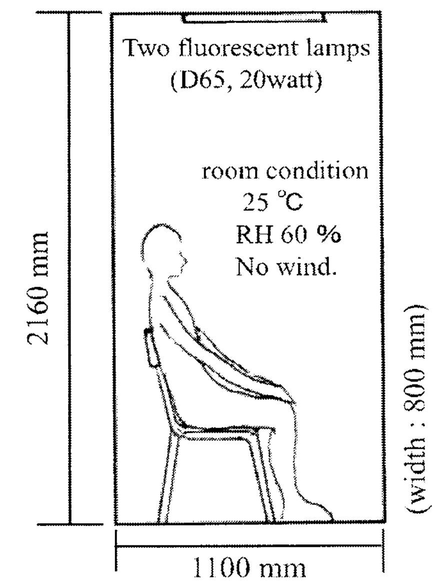

Fig.1 The setup and the condition of four experimental rooms. All inner surfaces of each room were painted with single color; yellow-red(7.1R 4.8/13.3), blue(4.3PB 5.5/9.5), gray(N5.4), or white(N9.5).

and a relative humidity of 60 % with no wind (less than 0.1 m/s). Two straight tube fluorescent lamps (D65 20-watt Toshiba Light and Technology FL20S.D-EDL-D65) were put on the center of the ceiling of each room. All inner surfaces of each room were painted only single color, yellow-red(7.1R 4.8/13.3), blue(4.3PB 5.5/9.5), gray(N5.4), or white(N9.5); Munsell notations, HV/C, were measured by Minolta Spectrophotometer CM-2600d under the condition of D65/2 degrees. Here, the lightness of yellow-red and blue was selected to be nearly equal to the lightness of N5 gray to avoid the influence caused by the lightness. This is because the lightness itself affects the central nervous system[4]. In this study, we concentrated our attention on the effects caused by Munsell Hue of color. The measured value of horizontal illuminance at the center of each room was 641 lx for the yellow-red, 665 lx for the blue, 645 lx for gray, and 1106 lx for the white room.

Procedure

The experimental schedule: After some electrodes and an eye mask blindfold were attached, the subject was lead into the experimental room of a certain color and sat on the chair put at the center of the room (Fig.1). After five minutes, the blindfold was removed. Then, the subject continued at rest another five minutes. At 10-17 minutes, the subject was set the task of one-digit addition. At 17-22 minutes, the subject kept rest another five minutes and then finished the first half of the experiment. When coming out of the experimental room, the subject was asked to guess the elapsed time of stay in the room. The subject was not informed of the time schedule.

After ten-minute recess, the subject was lead into the experimental room of different color, wearing the eye mask blindfold, and repeated the above 22-minute procedure. After the latter half of the experiment, the subject was asked to fill in the questionnaire. Question 1: Which room made you feel more spacious? Question 2: Which room made you feel warmer? Question 3: Which room made you feel more comfortable? Question 4 (free-answer question): How did you feel in each room?

The two colors compared by 14 subjects were listed at the second and third columns in Table 1. The color combination was planned appropriate for the pair comparison among yellow-red, blue, and gray.

Table 1 The examined colors and the resutls of pair comparison

Subject No.	former room	latter room	estimated time for former (min)	estimated time for latter (min)	more spacious	warmer	more comfortable
1	yellow-red	blue	15	20	blue	yellow-red	blue
2	yellow-red	blue	20	15	blue	yellow-red	blue
3	yellow-red	gray	25	22	gray	yellow-red	gray
4	yellow-red	gray	20	15	gray	yellow-red	gray
5	blue	yellow-red	20	15	blue	yellow-red	blue
6	blue	yellow-red	30	15	blue	yellow-red	blue
7	blue	gray	30	15	gray	blue	gray
8	blue	gray	30	25	gray	blue	gray
9	gray	yellow-red	30	20	gray	yellow-red	yellow-red
10	gray	yellow-red	15	20	gray	yellow-red	yellow-red
11	gray	blue	15	20	blue	blue	blue
12	gray	blue	20	30	gray	blue	gray
13	gray	white	25	30	white	white	gray
14	white	gray	20	17	white	gray	gray

Measurements

Electroencephalogram(EEG), heart rate, heart rate variability(HRV), bloodstream and tympanic temperature were measured as physiological indices. EEG was recorded by electrodes from the Cz and Fz locations according to the international 10/20 method system[4]. The α-wave proportion, $\alpha/(\alpha+\beta)$, was calculated and this served as a central nervous activity index. Here, α is the α-wave component (8-13 Hz) and β is the β-wave component (13-30Hz) in the EEG spectrum. HF/(LF+HF) was calculated from the frequency spectrum of HRV, this was taken as a relative activity level index for parasympathetic nerves in autonomic nervous activity[5,6]. The low frequency(LF) component of HRV provided a quantitative index of the sympathetic and parasympathetic activities, and the high frequency(HF) component of HRV relates to parasympathetic activity. In recent applications to evaluate the changes in autonomic activities, HRV has been employed in physiological assessment of living environmental factors such as thermal condition and lighting[5].

Physiological measurements were made at 2-4 minutes (session 1, before visual stimulation, before removal of blindfold), 5-7 minutes (session 2, immediately after visual stimulation, immediately after removal of blindfold), and 19-21 (session 3, after one-digit addition tasks).

3.RESULTS

Psychological evaluation

The estimated elapsed time spent in the experimental rooms, and the answers of three pair-comparison questions between the former and the latter rooms (Question 1: Which room made you feel more spacious? Question 2: Which room made you feel warmer? Question 3: Which room made you feel more comfortable?) are listed in Table 1. Answers for free-answer question (Question 4: How did you feel in each room?) are as follows:

For the yellow-red room: "irritating eyes", "glitter", "feel pressure", "feel eye ache".

For the blue room: "favorable impression", "good feeling", "feel comfortable", "feel at ease".

For the gray room: "dull and depressing", "dark".

For the white room: "strong impression", "extremely bright", "irritating eyes".

Although the illuminance level was almost the same for the yellow-red (641 lx), blue (665 lx) and gray (645 lx) rooms, most of the subjects who examined the gray room replied that the gray room made them feel darker than the yellow-red or blue room. This was probably the Helmholtz-Kohlrausch effect[7], that is, a chromatic stimulus appears brighter than the achromatic stimulus of the same luminance.

Physiological measurements

The results for the α-wave proportion, $\alpha/(\alpha+\beta)$, are shown in Fig.2(a), and the results for the HF/(LF+HF) in Fig.2(b). The absolute values of α-wave proportion and HF/(LF+HF) depend on the individual. Thus, their initial values at session 1(before visual stimulation) were adjusted to the origin in the figures. With regard to heart rate, bloodstream, and tympanic temperature, the variations of these parameters between sessions were less than a few percent; There was no significant change in them.

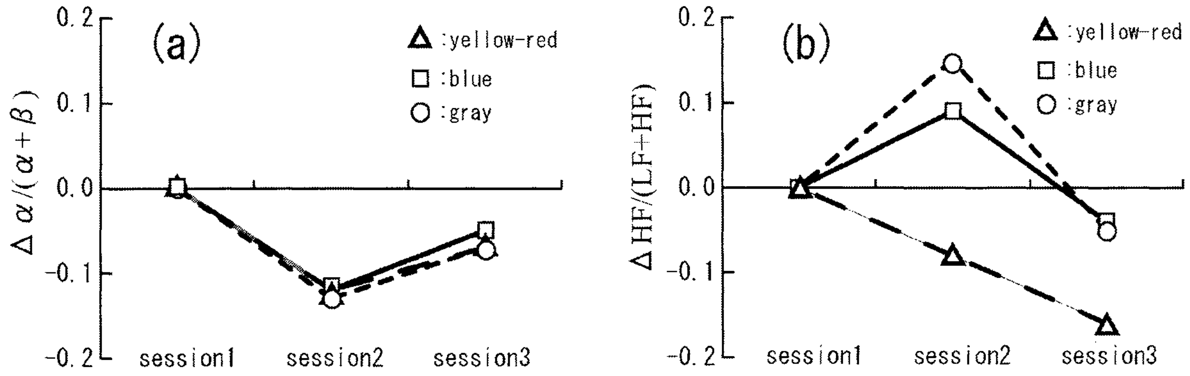

Fig.2 (a) The variation of the α-wave proportion, $\Delta\alpha/(\alpha+\beta)$. (b) The variation of $\Delta HF/(LF+HF)$.
In the figure, session1: before visual stimulation, session2: immediately after visual stimulation, session3: after one-digit addition task. Note that the initial values at session1 (before visual stimulation) were adjusted to the origin. Open triangles (△) represent the mean values of data of eight subjects who examined the yellow-red room. Open squares (□) are those of eight subjects who examined blue. Open circles (○) are those of ten subjects who examined gray.

4.DISCUSSION

About the spacious interior color: Four subjects examined the combination of yellow-red and blue (cf. Table1); All of them replied the blue room was more spacious than the yellow-red room, abbreviated to "spacious: blue>yellow-red". (We will use this abbreviated notation below.) For the combination of yellow-red and gray, all four subjects replied "gray>yellow-red". For blue and gray, three out of four subjects replied "gray>blue". Thus, we conclude that "spacious: gray>blue>yellow-red" (gray is the most spacious color). Here, we except white in the discussion because the experiment was planned appropriate for the comparison among yellow-red, blue, and gray.

Next about the warm interior color: All of the subjects examined the combination of yellow-red and blue replied "warm: yellow-red>blue". For yellow-red and gray, all of them replied "yellow-red>gray" and for gray and blue, "blue>gray". Thus, we conclude that "warm: yellow-red>blue>gray" (yellow-red is the warmest color). These agreements among subjects show that color impressions, such as advancing-receding and warm-cool, are universal.

About the comfortable color: "comfortable: gray>blue>yellow-red", though the evaluations were a bit fluctuated. This is because that whether it is comfortable or not is higher-level judgement in mind and they will depend strongly on the individual.

Estimated elapsed times spent in the experimental room are listed on Table 1. The mean estimated time spent in the yellow-red room is 18.8 minutes (standard deviation $\sigma=3.5$). It is 19.4 minutes ($\sigma=5.4$) for gray, and 24.4 minutes ($\sigma=6.2$) for blue. The difference between yellow-red and blue is statistically significant ($p<0.05$). The exact time spent in the experimental rooms is 22.0 minutes. Thus, the yellow-red-colored environment seems to reduce time whereas the blue-colored environment seems to slow time. This result is contrary to common belief (It is usually said that a warm environment will slow time.) This discrepancy suggests that sense of elapsed time is related to not only Hue but also Value and Chroma in more complicated manner. Further systematic studies are needed to reveal the relationship between sense of time and color.

As for the physiological resutls as shown in Fig.2, there was no difference in the variations of α-wave proportion among colors. Irrespective of color, the values of α-wave proportion decrease 0.12 point immediately after the removal of blindfold at session 2. This shows that the subjects' central nervous systems were activated by visual stimulus and magnitude of activation did not depend on the Hue of color. At session 3, the α-wave proportion recovered about 0.05 point. This shows that the subjects would adapt to the visual stimulus after 10-minuite exposure to the same color.

In contrast to the variations of α-wave proportion, there are significant differences in the variations of HF/(LF+HF) among colors. The values of HF/(LF+HF) of blue and gray increase at session 2. However, it decreases monotonically for yellow-red. The decrease in HF/(LF+HF) indicates the enhanced sympathetic nervous activity, which is caused by a physiological burden or stress. Thus, to conclude, the monotonic decrease in HF/(LF+HF) for yellow-red reflects stress caused by feeling of pressure specific to an advancing color. The fact that most subjects complained of eye ache and feeling of pressure in the yellow-red room supports this conclusion. However, with regard to heart rate, bloodstream, and tympanic temperature, there was no significant change; our 22-minute experiment may be too short to take effect in them. A long time experiment is needed to make sure whether color affect them or not.

REFERENCES

[1] H.Ohno and N.Koizumi, Mood-perception of interior colors in a gym, Proceedings of SPIE Vol.4421(2002)404-408.

[2] J.W.von Goethe, Theory of Colours, 1970, MIT press.

[3] J.Itten and F.Birren, The elements of color, 1970, John Wiley and Sons, Inc.

[4] H.Noguchi and T.Sakaguchi, Effect of illuminance and color temperature on lowering of physiological activity, Applied Human Science Vol.18(1999)117-123.

[5] K.Ishibasi, S.Ueda, and A.Yasukouchi, Effects of mental task on heart rate variability during graded head-up tilt, Applied Human Science Vol.18(1999)225-231.

[6] B.Pomeranz et al., Assessment of autonomic function in humans by heart rate spectral analysis. American Journal of Physiology Vol.248(1985)H151-H153.

[7] G.Wyszecki and W.S.Stiles, Color Science, 2nd Edition, 1982, John Willy and Sons, Inc., p410.

Cognitive aspects of color vision in natural scenes

Lucia R. Ronchi, Sergio Villani, Margherita Abbozzo

Associazione Ottica Italiana, 1 via Suor Maria Celeste, 50125 Florence, Italy

ABSTRACT

By definition, cognition is the process of knowing. Color is justifiably one of the bases of the building blocks from which perception is constructed and our memories are organized (Davidoff, 1991). At the turn of the century, the marriage of Visual Science and of Science of Cognition was a matter of fact. Accordingly, a sort of escalation was occurring, a new door was open to new explanations for every fact and/or visual effect traditionally presented in physiological and psychological terms. Operationally, the conceptual expansion was flanked by the transition from local to global, from simple to complex. In this framework, the natural scenes are called to the fore. After an abridged bibliographical review, concerning specifically color vision, some experimental data are summarized, in an experiment where the observer were instructed to "describe what they see", by using the codes of nameability

1. FOREWORD

Man made artificial environments, where color can vary in arbitrary ways, have little relation to the natural chromatic environment in which our vision evolved (Webster and Mollon, 1997). Anyhow, man reacts well in either case, apart from the fact that the natural, highly complex and textured environment is preferred at most. Various hypotheses have been proposed to explain this universally accepted fact, but the question is still open. It is as if we were behaving in two quite different states. In (natural) complex environments a sort of bottleneck (like, for instance, brightness and color constancy) is at work to speed-up and facilitate the current behavior, by avoiding overloading. In artificial environments various situations are met. As a limiting case let us quote the Disney's cartoons and strips, which layman of any age enjoyes in, even if color is reduced to a few basic categories and the surfaces are textureless.

Around the turn of the century times seemed to be ripe to study the problem of the process of complex images, and, in particular, of the natural scenes. Visual experts are conscious of the limitations of laboratory simulations and even of the advanced imaging techinques (Wolfe, 1994; Brainard, 1999; Young and Maloney, 2001). We have been trying to write a sort of book on the experiments performed by using as test objects images have the same characteristics are the natural ones, which are processed "silently", reaching through cognition the sphere of pleasure, of emotion, etc (Ronchi, 2003).

2. THE INTERLACING OF VISUAL SCIENCE WITH COGNITION: AN ESCALATION FROM SIMPLE LABORATORY SITUATIONS TO NATURAL IMAGES

Let us now try to subdivide into sections such multifaced matter, covering practically every aspect of visual functionality , concerning both practical and theorical aspects of visual process.

2.1- The quality of color reproduction in natural images

The assessment of "quality" is performed both visually and instrumentally. Let us consider first the visual assessment. Any reproduction of natural objects has a certain degree of fidelity. The deviation from perfect rendering can be assessed through a comparison between the output of the visual process and some internal reference. The quality of color reproduction, in part may be referred to a comparison of appearances, in particular a sample may be related to a memory color (Sachtler and Zaidi,1992; Zaidi, 2001). Otherwise, scaling methods may be applied. For instance, Federovskaya et al. (1997)Yendrikhovskji et al. (1999), judged perceptual image quality by the use of ten point numerical category scales of colorfulness (indicating the presence and vividness of colors in the picture, which depends on the global changes in luminance and spectral properties), and naturalness (a global perceptual attribute in determining the quality, which relies on internalized knowledge of the world, and, in agreement with Vrhel et al. (1994), is based on acceptability rather than perceptibility) Yendrikhovskji et al. also proposed a computational model by representing memory color of objects by the prototypical color of the corresponding object, based on similarity with apparent colors of object samples of every object category. Perceived similarity is described by a multivariate probability density function in an uniform color system. The main conclusion is that optimal is not synomimous with identical, and, therefore, it cannot be measured by the degree of correspondence between image and reality in physical terms. In particular, in the case of natural images, observers prefer somewhat un-natural images, more colorful and with more saturated colors.

Passing to instrumental assessment, let us recall that after a dogma relevant to machine vision and to the human visual system, the efficient exploitation of the colorimetric relationships in scenes requires a color space that is well matched to the statistical properties of scene colors. This is persuasive argument for the case of natural surfaces and illuminants, whose spectral data are subject to very strong statistical constraints.In this connection, Paltridge et al. (2001) suggested a new definition, according to which the metamerism rate is a measurement of how color categortization can fail, due to the informatopn loss when high-dimensional spectral data are down-projected one of the standard 3-D spaces.

2.2 – Contrast and contrast distribution and contrast constacy

The physical contrast of simple images is well defined and agrees with the perceived contrast, but this is not the case of complex images . In fact, a contrast defined by a single value (while the actural contrast varied across the image), does not give a full rating of the observer's empirical experience: complex images, with the same nominal contrast, often markedly differ in apparent contrast. Various new definitions have been proposed (Field, 1987; Peli, 1990; 1996; Balboa and Gryway, 2000; Bex and Makous, 2001).

The appearance of a complex image, like our natural environment, depends on a number of factors, including the spatial distribution of contrast , resulting in the global patterning of the scene. It has been shown that the frequency histograms, in natural scenes, peak at low contrasts, the average contrast being of the order of 40%. Now, the contrasts due to lighting are a minority, while the characteristic signature in real world scenes are the edges, and the occluding edges in particular, the amplitude spectra of which are of 1/f type (Elder et al., 1999; Balboa and Gryway, 2000)

Color constancy (Foster et al.1997) is defined as the ability to perceive as maintaining a constant appearance, independently of a number of experimental factors, including size and distance. For a model, let us refer to Brady and Field (1997).Briefly, the same object may appear of different colors under different illuminants, but, if not behaviorally relevant, the related changes may be disregarded, covered by the umbrella of perceptual constancy.Color constancy in natural scenes is investigated under various respects, say: discounting the illuminant, atmospheric constancy and relational constancy. Note that the algorithms based on known facts concerning the visual process valid in laboratory situations, where surfaces 3-D objects often share enough visible facets across scene and illuminants, fail in the real world, where surfaces are rough (non lambertian), in random spatial arrangements, under different illuminants (Gegenfurthner, 1998). The constancy is known to be other than perfect and complete. This fact sould not be regarded as a failure, but as an advantage, once interpreted in terms of visual multiplexing (Ronchi and Schanda, 2002). Briefly, the observer perceives the changes in appearance, (in this sense, information is preserved) but such changes may be disregarded (e.g., if not behaviorally significant) , because perceptual constancy covers them with its umbrella.

2.3 – Adaptation

Adaptation (be it light or achromatic), is a process that adjusts sensitivity according to the mean luminance and chromaticity, over some time and region of the stimulus. This process, to a large extent, reflects early retinal mechanisms, to aid vision by maintaining high contrast sensitivity over a range of absolute light levels (Webster and Mollon, 1994; 1995).Contrast adaptation (Webster anf Miyahara, 1997) adjusts sensitivity according to how the ensemble of luminances and chromaticities are distributed around the average (Webster, 1996). It has a primary cortical locus, it induces changes (that are sensitive for the feature or structure of the stimulus), in detections thresholds, as well as in the perceptual contrast, color, motion and form of suprathreshold patterns. In particular, adaptation to the spatial frequency structure in natural images may exert strong and selective influences by reducing sensitivity to low and medium spatial frequencies, biasing contrast sensitivity towards higher ones. Adaptation to natural scenes at suprathreshold contrasts adapts primarily the subset of channels at lower spatial frequencies, thus maintaining the visual system in a state of reduced sensitivity to the lower frequency range (Brady and Field, 1997) This is also the case where the observer is exposed (and thus adapted) to sequences of natural scenes. Accordingly, instead of being low-pass (as expected by minding to the classical laboratory experiments), the color Constrast Sensitivity Function becomes nearly band-pass when measured under "natural" viewing conditions (Webster, 1996)

At last, let us recall that color appearance depends on the distribution of color found in natural environments, since two forms (to light and contrast) produce independent, qualitatively different changes, in perceived color, that are specific to the distribution of color signals. In particular, changes in color appearance following contrast adaptation, can be strongly selective for any arbitrary direction in the color-luminance space (Webster and Mollon, 1997)

2.4 – Classification of natural images

In modern terms, natural images should be classifiewd starting from Uniform Space Colorimetry and reaching the keystones of perceptual organization (from segregation to representation, through segmentation). We owe to Tominaga (1992) a method based on an algorithm which yields a representation of data in the form of a set of perceptually uniform color regions

2.5 – Color in natural scenes

The first step towards the assessment of color is represented by the spectral reflectance spectra. It is known since long that the the characteristic color spectra of natural samples have smooth shapes, and may be represented as a linear combination of a few basis eigenspectra, so that the Munsell samples can be used to represent natural scenes (Vrhel et al. 1994; Parraga et al. 1998; Watchler et al. 2001). A new colorimetric color vision system, specifying the characteristics of terrains in terms of both color and spatial statistics, is due to Burton and Moorhead (1987), who showed, in particular, that the chromatic amplitude spectra of natural scenes are steeper than the achromatic ones. After Webster and Mollon (1997) the individual natural scenes in which our vision has evolved vary substantially in their mean chromaticity and luminance, in the principal color-luminance axes of their distributions and in the related range of contrast. In most natural scenes the distributions of color signals are highly restricted and strongly biased along a bluish-to-yellowish axis, intermediate to (L-M) and S- (L+M) axes. Within this gamut the color distribution for individual scenes vary widely, and significant biases in the mean chromatic constrast are found along a relatively narrow range of bluish-to-yellow green angles characteristic of scenes with lush vegetation and little sky, while a unique blue-yellow axis is more typical of arid scenes.

For a review of color appearance in natural scenes, let us refer to the paper of Howard and Burnridge (1995) where both instrumental and visual (including nameability) assessments are dealt with.

At last, let us recall the recent views in matter of color categorization, defined as a process resulting in grouping of similar terms into one class. Yendrikshowskij (2001) has studied categorization in natural scenes both in mathematical and perceptual terms. Some authors (Ishida, 2002; Okajima et al.. 2002) proposed to replace the missing 12th category (Ronchi (2000 suggested to name it "bamboo") with two non monolexemic names, green-yellow and blue-green, which seem particularly appropriate for the colors of natural scenes..

In matter of underlying physiological mechanisms, Delorme et al. (2000) showed that categorizing natural images is fast and accurate. The coarse Magnocellular information might give the access to a global shape representation of the ultra-rapid categorization of natural scenes. Such a fast process should be used as a leader to improve futher processing of color and fine details.

2.5.1 – Color and form

After Burton and Moorhead (1987) natural scenes have a complex spectral and spatial structure, and the visual system contains processes that produce spatial interactions between various kinds of responses, however, "we cannot reliably separate the attributes of color and form". Nine years later, Poisson and Wandell (1996) proposed a model where the measurements of pattern and color sensations are processed by three pattern-color separable mechanisms, combined using a vector-length decision rule.They derived the spectral and spatial tuning functions of the pattern-separable mechanisms. In 2001, Werner and Webster showed that natural images give important clues about the role of color in form perception, Apparently, we are faced with a complex problem deserving further attention

The visual system may take advantage from the constraints imposed by most natural images, which do not contain all possible spatial and chromatic variations. The domination of image content by low spatial frequencies implies that much of the information can be sampled by chromatic mechanisms, even though they have lower resolution. The attention-getting nature of color facilitates visual search, through grouping and organization of information. In natural scene image, spatial variation in illumination are ambiguous, because they can arise from lighting or changing in surface. On the other hand, the color of the illuminant remains relatively (but not completely) inaltered by shadows. Regions of common color may differ in lightness, but they are more likely to belong to a common object. Thus, being the color easily detectable, it may capture more directly the spatial distribution of objects, independently of spatial variations in lighting, even when luminance edges are camouflaged. The most typical example are the fruits among foliage. In conclusion, the purpose of color is to discriminate and identify classes of objects. Various mechanisms, at different levels across the visual pathway are called into play. In particular, to integrate color signals across space, long-range cortical interactions are necessary. Without them, we would see the forms as skeletons, based on receptor fields sensitive only to border contrast, rather than filled-in in surface.

3. STARTING THE EXPERIMENTAL SESSIONS

When undertaking our experimental sessions, going beyond the participation of the three authors, highly skilled and aware as to the purpose of the experiment, we recruited a number (ten) of students, highly motivated and with various degrees of generalized experience in a visual laboratory. We aim at assessing through codified verbal reports how the complex natural world appears to "people".We did not imagine, *a priori*, that the training period could be so long as it has actually been. In the acquaintance phase we used three different natural objcets, as is described in the following sub-sections.

3.1 – Naming the color of the flower clusters of hydrangea

First of all, a question: what is the color of this flower ? The immediate response was: blue. Next, the observer was requested to match the flower to a sample of the NCS 2nd Edition. This task was performed very easily, in spite of the complexity and non-uniformity of the test object. Apparently, the observer was making reference to his internal representation of that familiar flower. The session continued, by inviting the observer to measure the local lack of uniformity of the petals: the luminance ranged from 2 to 20 cd/sq.m, the color from whitish to dense blue. After area-weighting, the observer decided that he was not faced with a bi- or multi-colored flower, but with a "blue" color, suffering from some variability

From the educational stand point, sessions like this were useful to render the student aware of the meaning of the term multiplexing, defined as the transmission of two or more messages simultaneously, over the same channel, in a way that enables them to be separated at the receiving end, by virtue of the reconstruction ability and of other capabilities of the visual system. This implies that the output signals may mutually interact,before the formation of the internal representation.

3.2 – Naming the color of the grass

When faced with a 2 sq.m lawn, viewed from a window at the first floor of a house, at a distance of about 15 m, the observer immediately declared "the grass is green". However, under repeated observations, in a serene day, at 30 min. intervals, the observer noted that the portion of the lawn invested by direct sunlight appeared more yellow than green. On the other hand, the portion covered by the shadows (casted by the structures around the lawn), appeared simply green. Data were then gathered by plotting the relative percentages of responses "green" and "yellow" versus time. A "colorimetric" exercise was then started, by looking for a correlation of such responses with the luminance, the saturation, the colorfulness and the chromaticity coordinates of the light, at the various locations.

However, this kind of activity was interrupted and postponed, when the observers realized that the green covered by shadows and half-shadows exhibited a significant blue component. A glance to the literature reveals that it is not surprising. For instance, Jordan and Mollon (1995) interpreted the unique green as an equilibrium between the subsystems that draw inputs of opposite signs from S-cones and some combination oif L- and M- cones. Moreover, Webster and Mollon (1997), Ishida (2002), Okaijma et al. (2002) all include the blue in their categorizations of natural objects. Rather, it might appear surprising that the observers started to suspect and then to declare the presence of blue sensation after a life-long exposure to an environment rich of vegetation.

3.3 – Looking at the evergreens

The observers were faced with a set of trees, in front of a window, at a viewing distance of 15 m, in a serene day, at different times of day. The category of "green" held for laurel, ivy, cypress tree, although such trees patently differed for their intracategorical location. The observers devoted several sessions to familiarize with the complexity of such (although familiar) images.From the educational stand point, they learned what "perceptual constancy" means. In fact the categorization remained unaltered, in spite of the local differences in the appearance of the new and old leafs, of the high brightness due to the luster of some leafs, etc. In conclusion, it was clear that man discounts the effects of natural illumination, as well as that of the shadows within the 3-D configuration of the tree, which vary with the Zenithal distance of the sun. By virtue of the definition of constancy, the observer refers to an intrinsically invariant surface reflectance, in spite of the variations of illumination. The surprising fact is that the percent frequency of occurrence of the sensation of blue, not perceived before, increases day-after day, across months, under repeated observations.

4 – TO CONCLUDE, A QUESTION

By considering the reaction of our observers a question arises: the assessment of the quality of a reproduced natural image, should be referred to the local degree of fidelity or to the globally synthesized internal representation ? Probably the reply lies in the distinction between perceptibility and acceptability . However, the definition and assessment of acceptability escape from the most traditional metrological framework, because , again by invoking visual multiplexing, a "personal" input imposes, producing peculiar responses like emotions, preferences, and so on, which give the observer the opportunity of demonstrating who is who.

References

BALBOA, R.M., GRYWAY, N.M. – Vision Res. **40**, 2661, (2000)
BEX, W.L., MAKOUS, W.L. – Invest.ve Ophthal. & Vis. Sci. Suppl. **42**, 616, (2001)
BRADY, N., FIELD, D.J. – Vision Res. **23**, 3367, (1997)
BRAINARD, D.H. – J.Opt.Soc.Am. **A 16**, 307, (1999)
BURTON, G.J., MOORHEAD, I.R. – Applied Optics **26**, 157, (1987)
DAVIDOFF, J. – *Cognition through Color* - The MIT Press, Cambridge, MA, 217 pp, (1991)
DELORME, A., RICHARD, G. FABRE-THORPE M. – Vision Res. **40**, 2187, (2000)
ELDER, J.H., BENIAMINOS, D. PINTILIE, G. – Invest.ve Ophthal. & Vis. Sci. Suppl. **40**, 357, (1999)
FEDEROVSKAYA, E.A., de RIDDER. H. BLOMMAERT, F.J.J. – Color Res. Appl. **22**, 96, (1997)
FIELD, D.J. – J. Opt. Soc.Am. **A4**, 2379, (1987)
FOSTER, D.H., NASCIMENTO, S.M.C., CRAVEN. B.J., LINNELL, K,J, CORNELISSEN, F.W., BRENNER, E. Vision Res. **37**, 1341, (1997)
GEGENFURTNER, K.R. – Invest.ve Ophthal. & Vis. Sci. **39**, S156, (1998)
HOWARD, C.M., BURNIDGE J.A. – J. Soc. Info Displays **2**, 37, (1994)
ISHIDA, T. – Color Res. Appl. **27**, 252, (2002)
JORDAN, G., MOLLON, J.D. – Vision Res. **35**, 613, (1995)
OKAJIMA, K., ROBERTSON, A.R., FIELDER, G.H. – Color Res. Appl. **27**, 225, (2002)
PALTRIDGE, R.J., THOMSON, M.G.A., YATES, T., WESTLAND, S. — *Proc.9th AIC Meet., SPIE Vol. 4421, p.877, Rochester, N.Y. (2001)*
PARRAGA, C.A., BRESTAFF, G., TROSCHIANKO, T.- J.Opt.Soc.Am. **A 15**, 563, (1998)
PELI, A. – J.Opt.Soc.Am. **A 7**, 2032, (1990)
RONCHI, L.R. - *Proc. AIC Color 2000, Color & Environment, Seoul, Korea, p.202, November 2000*
RONCHI, L.R. – *The Visual Science Seen from the Viewpoint of Natural Scenes, Fondazionre G. Ronchi, Florence, Italy, Vol. 77, (2003) (in press)*
RONCHI, L.R., SCHANDA, J. - *Proc. CIE Div. And Div.2 Symposium, Vesprém, Hungary, 22-24 Aug. (2002)*
SACHTLER, W., ZAIDI, Q. – J.Opt.Soc. Am. **A 9**, 877, (1992)
TOMINAGA, S. – Color Res. Appl. **17**, 230, (1992)
YANG, M.J.., MALONEY, L.T. – Vision Res. **41**, 2581, (2001)
YENDRIKOVSKIJ, S.N. – Color Res. Appl. Suppl. **26**, 35, (2001)
YENDRIKHOVSKIJ, S.N., BLOMMAERT, F.J.I., de RIDDER, H. – Color Res. Appl. **24**, 52, (1999)
VREHL, M.J., GERSHORN , R., IWAN, L.S. – Color Res. Appl. **19**, 4, (1994)
WATCHLER, T., SEJNOWSKI, T.J., ALBRIGHT, T.D. – J.Opt.Soc. Am. **A 18**, 65, (2001)
WEBSTER, M.A. – Network: Computayion in Neural System , **7**, 587, (1996)
WEBSTER, M.A., MIYAHARA, E. – J.Opt.Soc.Am. **14**, 2355, (1997)
WEBSTER, M.A., MOLLON, J.D. – Vision Res. **34**, 1993, (1994); **37**, 3283, (1997); Nature, **373**, 694, (1995)
WERNER, J.S., WEBSTER, W.A. – *Proc. 9th AIC Meet., SPIE Vol. 4421, p10, Rochester, N.Y., (2001)*
WOLFE, J.M. – Vision Res. **34**, 1187, (1994)
ZAIDI, Q. – Colorn Res. Appl. **26**, S 192, (2001)

The Manner of Viewing in Lightness Contrast-Assimilation
—Comparison between Color Experts and Naïve Observers—

Midori TAKASHIMA
Graduate School of Literature and Social Sciences, Nihon University

1. Introduction

There have been numerous studies on lightness contrast (e.g., Beck, 1972; Gilchrist, 1994; Hurvich & Jameson, 1966). On the other hand, lightness assimilation, opposite to contrast, has not so intensively been investigated. Among others, Helson (1943) was the first to introduce this term in the context of color appearance to refer to what had been called "von Bezold's spreading effect". He and his collaborators (Helson, 1964) examined most systematically the parameters determining assimilation as well as contrast. They demonstrated that narrow lines and spaces yielded assimilation, that is, the darkening of the gray background by black lines or the lightening by white lines, and wide lines and spaces yielded contrast. Lightness assimilation was also found to be greater when the lines and background were not greatly different in lightness from each other. Helson's most important contribution seems to show that both of assimilation and contrast are presented on a single continuum of the relevant parameter.

Beck (1966) reported that contrast was not influenced by repeated judgments, whereas the amount of assimilation was reduced by repetition. Moreover, he pointed out that assimilation might reflect the effects of several different factors, suggesting that some assimilation would depend on how observers view a test pattern and another type of assimilation would not be so much influenced by the manner of viewing or repeated exposure. In this concern, Festinger, Coren, and Rivers (1970) demonstrated that the way of viewing a pattern as a whole increased assimilation and the partial viewing decreased assimilation.

It has been found that past experience or some specialized knowledge affects the assimilation effect. For example, Kanisza (1979) pointed out that not all observers saw the assimilation pattern in the same way. According to him, experts of art or people accustomed to judging colors tend to make distinction between lightness and the effect of illumination, reporting the contrast effect, and the laymen tend to constantly report the lightness assimilation. Goto, Uchiyama, Takahashi, Nakamura, and Kobari (2001) investigated lightness assimilation, showing that the observers who had a lot of knowledge about color phenomena were not greatly influenced by the instruction how to see a pattern.

In the present study, we pay attention not only to the difference of past experience or knowledge but also to the problem of whether the observer's judgment depends on "lightness" or 'brightness'. In the experiments to be reported below, two groups, art students and non-art students, participated. We assume that art students like painters tend to look at a test area as "brightness", reporting contrast, and non-art students tend to see the test area as "lightness", reporting assimilation. Furthermore, two different methods of measurement, the method of paired comparison (Experiment 1) and the matching method (Experiment 2) are used. Here, we make an assumption that these two methods may induce different manners of viewing: the method of paired comparison may facilitate assimilation, whereas the matching method may lead to the perception of contrast.

2. Method

Participants

Two groups of college students participated in the experiments: 10 art students who were majoring in design engineering; and 21 non-art students who were majoring in psychology. All had normal or corrected-to-normal vision.

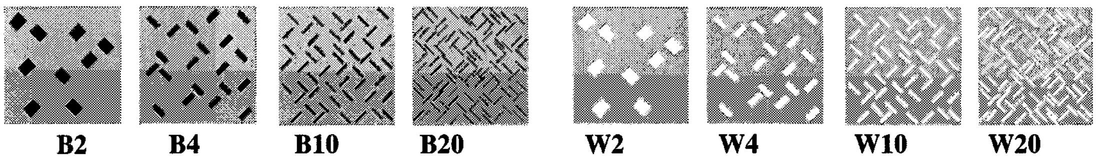

Figure 1 Examples of test patterns used in the experiments.

Stimulus Materials

As shown in Figure 1, the small rectangles looking like a patch-work on the gray background were used as a test pattern. The width of each rectangle was changed in four steps: 0.5, 1, 2.5 and 5mm. The number of the rectangles was adjusted so that the area ratio of patches to background was always 1/10. The test patterns used consisted of 4 black (N1) and 4 white (N9) patches on the gray background. One gray background (N5) in Experiment 1 and three different gray backgrounds (N4, N5 and N6) in Experiment 2 were used.

Procedure

In Experiment 1, each pair chosen from combinations of 8 patterns was randomly presented. Participants were asked to compare two test patterns and choose the lighter gray background. The number of the paired test patterns was 64 in all.

In Experiment 2, one test pattern was singly presented to each participant who was asked to judge the lightness of the gray background and choose the best match in lightness among the lightness sample varied in 11 steps (N2.5~N7.5).

3. Results

Experiment 1

We calculated psychological scales of the judged lightness of each test pattern. These scales are shown in Figures 2 and 3. For both of art students and non-art students, the test patterns with white patches were perceived to be lighter than those of black patches. As the width of white patches was decreased, lighter judgments increased.

Experiment 2

We calculated the difference in lightness between the test patterns with patches and the controlled patterns without patches. The result was shown in Figure 4 and Figure 5.

A four-way ANOVA revealed the significant main effects of the patch's width ($F(3,38)=3.61, p<.05$), of the background's lightness ($F(2,38)=5.31, p<.01$) and of the groups of participants ($F(1,38)=8.86, p<.01$). The interactions between the test pattern and the patch's color ($F(3,38)=15.51, p<.01$) and between the patch's color and the background's color ($F(2,38)=13.24, p<.01$) were also significant.

When the test patterns had white patches, as background lightness became lighter, the amount of contrast increased, but as the width of the patches decreased, assimilation increased. When the test patterns had the black patches, as the lightness of the background decreased and the width of the patches decreased, the amount of contrast increased.

4. Discussion

The task difference

In Experiment 1, participants reported that the test patterns with white patches looked lighter than those with black patches. As suggested by Festinger et al. (1970), lightness assimilation was more likely seen for the method of paired comparison.

The results of Experiments 1 and 2 were similar to each other. However it seems that the effect of the width of white patches can be seen more clearly with the method of paired comparison. On the other hand, when the patches were black the width effect seems stronger with the matching method than with paired comparison.

The difference between art and non-art students

It was clearly seen that non-art students were more likely to report assimilation than art students and that the range of illusions (from contrast to assimilation) was wider for art students than non-art students. Kanisza (1979) pointed out that the experts tended to judge lightness in the light of the effect of the

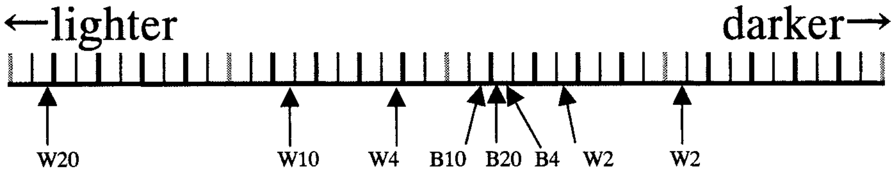

Figure 2 The scale values of lightness obtained by the method of paired comparisons for art students

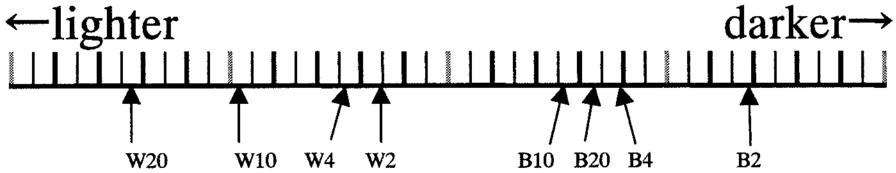

Figure 3 The scale values of lightness obtained by the method of paired comparisons for non-art students

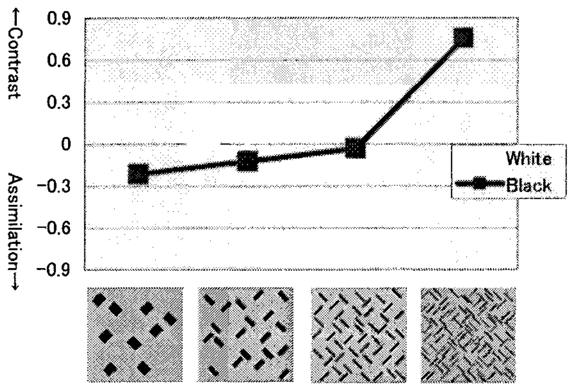

Figure 4 The results obtained by the matching method for non-art students

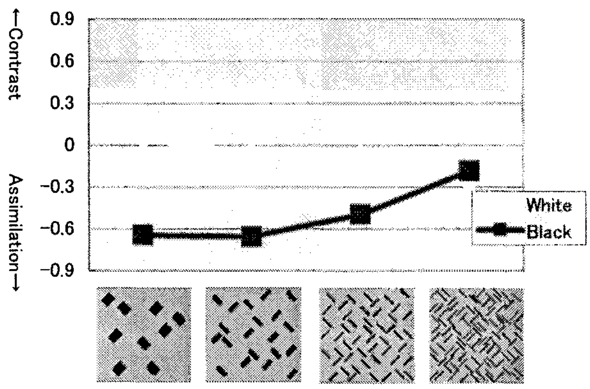

Figure 5 The results obtained by the matching method for art students

illumination, reporting contrast, whereas the laymen tended to report consistently assimilation at the verbal report. Furthermore, he demonstrated that as far as the matching method was used, there was not great difference in lightness judgments between the experts and the laymen. However, the present study showed that the non-art students tended to report more consistently assimilation than the art students in both verbal report and matching.

Goto et al. (2001) demonstrated that the art students judged lightness based on their own knowledge. Also in this study, an art student reported that he judged lightness relying on their own knowledge of lightness contrast and assimilation. Goto et al. (2001) pointed out that contrast occurred following the physiological mechanism or bottom-up processing and assimilation occurred from the cognitive mechanism or top-down processing. If that was true, the art students who had a lot of knowledge of these phenomena should have reported the assimilation because they judged the lightness from cognitive mechanism.

Beck (1966) argued that the amount of contrast was not changed even if the observer looked at the illusions figures repeatedly; but the amount of assimilation decreased. Art students should have a lot of opportunity to look at the several figures producing contrast and assimilation. Festinger et al. (1970) claimed that the observers who could pay attention to the test area tended to report the contrast. That the art students in this study tended to report contrast might be due to this attention effect. On the other hand, the non-art students who had a little or no knowledge about lightness illusions tended to report assimilation because they see the pattern as a whole.

Many non-art students tended to judge the test pattern lighter with white patches than with black ones. That is, they reported constantly assimilation based on surface lightness. Most of art students seemed to make judgments using information of lightness as well as 'brightness'.

5. Concluding Remarks

We compared differences in response to lightness assimilation and contrast phenomena between color experts and laymen. Laymen tended to response more strongly to assimilation than contrast. Experts were biased to contrast rather than assimilation. Such difference seems to be due to the manner of viewing: Experts look at the test pattern with partial, analytic viewing, whereas laymen look it as a whole. We need to examine more fully how the manner of viewing influences the kind and the amount of lightness illusion.

References

Beck, J. 1966 Contrast and assimilation in lightness judgments. *Perception and Psychophysics*, **1**, 342-344.

Beck, J. 1972 *Surface Color Perception.* Ithaca and London: Cornell University Press.

Festinger, L., Coren, S. & Rivers, G. 1970 The effect of attitudes on brightness contrast and assimilation. *American Journal of Psychology*, **83**, 189-207.

Gilchrist, A. L. 1994 *Lightness, Brightness, and Transparency.* , New Jersey: Lawrence Erlbaum Associates, Publishers Hillsdale.

Goto, T., Uchiyama, I., Takahashi, S., Nakamura, S. & Kobari, H. 2001 Effects of experience attitude on assimilation / contrast in s tripe-patterns. —observations by students majoring in arts. *Journal of the Color Science Association of Japan*, **25**, 110-111.

Helson, H. 1943 Some factor and implication of color constancy. *Journal of Optical Society of America* **33**, 555-567.

Helson, H. 1964 *Adaptation —Level Theory*. New York: Harper and Row.

Hurvich, L. M. & Jameson, D. 1966 *The Perception of Brightness and Darkness.* Boston: Allyn and Bacon, Inc.

Kanizsa, G. 1979 *Organization in vision: Essays on Gestalt perception*. New York: Prarger.

Colorimetry: Colorfastness to Light and Changes in Fluorescence of Paper and Textiles

Helen H. Epps
The University of Georgia, Athens, Georgia, USA

Abstract
Fluorescent colored materials, including textiles and paper, often have poor colorfastness to light. In many cases, as color fades due to exposure to sunlight or artificial light, the level of fluorescence also changes. As fluorescence is decreased, the visibility of the material decreases. This may be problematic, depending on the use of the item. The use of a single monochromator spectrometer, as opposed to a dual monochromator instrument, in the measurement of fluorescent materials typically leads to results which are either incomplete or erroneous. A dual monochromator instrument provides one method for accurately separating true reflected color from color that is due to luminescence. In this research, various materials which exhibited apparent fluorescence, were exposed to simulated sunlight. Spectral changes in the materials indicated that in most of the materials, both the reflected color and the level of fluorescence had changed after exposure to light. However, the extent of color change and fluorescence change varied among the materials. Some materials appeared more fluorescent after short-term light exposure, while others were less fluorescent.

INTRODUCTION

Previous research addressed the problem of color measurement of fluorescent textiles using a single monochromator spectrometer, as opposed to a dual monochromator instrument [1]. The dual monochromator instrument allows precise separation of spectral data due to luminescence (fluorescence), from spectral data associated with the actual color of the specimen (reflectance). Difficulties associated with using various color measurement methods with fluorescent materials have been studied extensively by other researchers [2- 4]. The problems are magnified when the purpose of the measurement is to monitor changes in color as the specimen is exposed to light. Using a traditional, single-monochromator colorimeter or spectrophotometer, it is not possible to distinguish between a change in reflectance and a change in luminescence. Such an instrument produces a spectrum, often referred to as a reflectance spectrum, which, in the case of fluorescent materials, is in fact a combination of both reflectance and luminescence.

The purpose of this research was to examine colorfastness to light, and changes in fluorescence of textile and paper materials as the materials were exposed to artificial sunlight in a weatherometer.

PROCEDURE

Textile and paper materials that represented a wide range of colors and different levels of apparent fluorescence were used in the study. The sample included 10 textile materials and 12 paper specimens.

A Labsphere BFC-450 bispectral fluorescence colorimeter was used to analyzed spectral radiance factors at every 10 nm of the visible region from 380 to 780 nm, based on incident light that spanned the range of 300 to 780 nm. The instrument utilizes two monochromators, namely an excitation monochromator which separates light before it reaches the specimen, and an emission monochromator which enables measurement of the light at different wavelengths as it is emitted from the specimen.

After measurement, color change was induced instrumentally using an Atlas 3500 weatherometer with controlled light, temperature, and humidity. A continuous light exposure mode that simulated exposure to direct sunlight, was followed. The duration of exposure for the study was determined in a preliminary test in which samples of three of the most highly fluorescent materials were exposed in the weatherometer, and were measured after 1, 2, 5, 10, and 12 hours of exposure. Based on this preliminary experiment, it was determined that 10 hours of weatherometer exposure produced sufficient change in overall color and in fluorescence to facilitate comparisons among samples and to evaluate the use of the BFC instrument as a tool in such lightfastness and fluorescence studies.

SUMMARY OF RESULTS

For each material, the reflectance spectrum, the luminescence spectrum, and the spectrum which represented the total of the two, were recorded. Each of the specimens became lighter during exposure, and some of the materials showed minor hue shifts. As each of the specimens became lighter after weatherometer exposure, there were changes in fluorescence. In each case, the color changes, in particular, the changes in lightness, were visible. Some of the specimens showed a visible change in fluorescence. In every case, changes in fluorescence were measurable. While it was expected that changes in the fluorescent component of the total spectrum might directly parallel changes in reflectance, such was not the case. Among all of the samples, generally, two patterns of change were noted. First, some materials became less fluorescent after the 10-hour exposure. However, some of the specimens showed an increase in the fluorescent component of the spectrum after exposure.

While the reason for an increase in apparent fluorescence was not investigated experimentally, it is possible that such an apparent increase may accompany the loss of coloration which, prior to exposure in the weatherometer, had masked the fluorescent characteristic of the material. With a longer exposure time, fluorescence would be expected to decrease. Futher study is needed in order to determine whether this occurs.

IMPLICATIONS

Careful measurement of color spectra of materials before and after exposure to light can be useful in evaluating the performance of different types of materials. Changes in fluorescence spectra cannot be accurately predicted from reflectance spectra alone. Patterns of change in both color and fluorescence vary with the material and its original hue and lightness. Although the dyes and pigments were not analyzed, the different results between the various materials indicate that changes are specific to the particular colorant.

A bispectral reflectance instrument is one method that can provide accurate measurements of both reflectance and fluorescent components and can be used to monitor changes in both components due to exposure to light.

REFERENCES

[1] Epps, H. H. Color Measurement of Fluorescent Textiles. Book of Proceedings, AIC Color 2002 SI: Color and Textiles, Maribor, Slovenia, pp. 230-234.

[2] Aspland, R. A., Maseka, K. D. and Shiwani, S. A. The Emission and Absorption Spectra of Polyester Fabrics Dyed with Fluorescent Disperse Dyes, Treated with FBA's, AATCC International Conference and Exhibition Book of Papers, NC, USA, 2001, pp. 398-402.

[3] Bemska, J. Influence of Fiber Materials on the Course of Occurrence of Fluorescence. Fibers and Textiles in Eastern Europe, April/June 2001, pp. 54-57.

[4] Gundlach, D. and Terstiege, H. Problems in Measurement of Fluorescent Materials. Color Research and Application, Vol. 19, No. 6, 1994, pp. 427-436.

Recognition of the space illumination as the main determinant of the border of the color mode change

Yuwadee Thiangthangtum*, Mitsuo Ikeda and Hiroyuki Shinoda
Faculty of Science and Engineering, Ritsumeikan University

ABSTRACT

To investigate the border of the color appearance mode is very important in lighting design. The color appearance of an object changes from the object color to the unnatural color and to the light source color when its luminance is gradually increased by local illumination. According to the concept of the recognized visual space of illumination RVSI the border of the object color mode is reached when the luminance of the object is made higher than the size of the brightness perception for a space where the object is placed. To confirm this explanation the border was determined in one case for various room illuminances while keeping the immediate surrounding luminance of a test stimulus constant, and in another case for a constant room illuminance while changing the surrounding luminance by employing different lightness. The border luminance of the test stimulus was almost proportional to the room illuminance in the former case, and it only slightly increased for higher lightness in the latter case to confirm the prediction from RVSI. But there was some effect observed coming from the immediate surrounding. The immediate surrounding field was varied in size from a small to large while keeping the room illuminance constant. The border luminance decreased for larger fields when the lightness of the surround was very low at N4. We conclude that the border is mainly determined by the room illuminance, but it is affected by the lightness of the immediate surrounding to some extent. Recognition of the space illumination as a main determinant of the border of the color mode change.

Keyword: Recognized visual space of illumination (RVSI), Surround luminance, Color appearance mode, Object color, Light source color.

1. INTRODUCTION

When one comes into a lit room he/she immediately understands how the room is illuminated. We express this situation as that he constructed a recognized visual space of illumination, RVSI for the room, which is expressed by a circle as shown in Fig.1. All the objects in the room appear normal in their color as they locate inside the RVSI as shown by O_n. If we illuminate the object O_n locally by a spot light in addition to the ceiling light, the luminance increases and its position in RVSI moves toward the edge of the circle. But as long as it remains inside the RVSI the appearance remains normal as an object in the room although its lightness increases. For a further increase of the spotlight, the position goes beyond the circle, and its appearance becomes unnatural as an object placed in the room as indicated by O_u. For a further increase, the object comes to a position such as shown by O_l and the object finally begins to shine. There exist two borders at the increase of the spotlight, the border from the natural object color to the unnatural object color, ${}_nB_u$, and the border from the object color to the light source color, ${}_oB_l$. It is an important conclusion of the RVSI theory that these borders are determined by the size of RVSI or the illumination level of the room and not by the luminance of the immediate surrounding of the object.

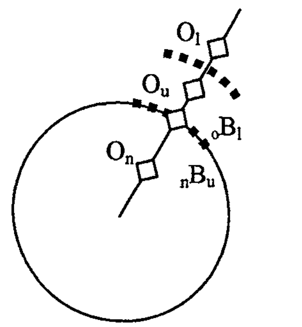

Fig.1 Scheme shows the color mode change by the concept of

To know how the border ${}_nB_u$ is determined in relation to the room illuminance is useful in designing the visual environment because an object of unnatural appearance draws people's attention. Ikeda et al.[1, 2, 3] showed that the border was proportional to the room illuminace to confirm one aspect of RVSI theory, but they did not show that the border did not depend on the luminance of the immediate surrounding. In the present paper we will show that nBu is solely determined by the room illuminance and independent to the immediate surrounding luminance.

2. EXPERIMENT 1
EFFECT OF ROOM ILLUMINATION

2.1 Apparatus

Two series, I-series and L-series, were conducted. In the I-series the border ${}_nB_u$ was determined for various illuminance but for a constant luminance of the immediate surrounding, 23.2 cd/m^2. In the L-series the border was determined for various luminance of immediate surrounding but for a fixed illuminance of a room, 100 lx. We can expect from the former experiment the border changes for different illuminance but from the latter it remains constant.

The experiment was carried in a normal room with various decorations such as artificial flowers, dolls, books, and a framed picture as shown in Fig.2. The room was illuminated by fluorescent lamps of the daylight type. An aperture of 2.2 x 2.2 cm was opened on the front wall to serve as the test stimulus T. Behind the aperture a color chart was placed and it was illuminated by other fluorescent lamps so that the luminance could be changed independently from the room illuminance by a subject. When a subject looked at the aperture from the distance 126 cm he saw the color chart of 1 x 1degree as if it was pasted on the front wall. T was surrounded by an immediate surrounding S of the size 12 x 12 cm or 5.5 x 5.5 degrees in visual angle.

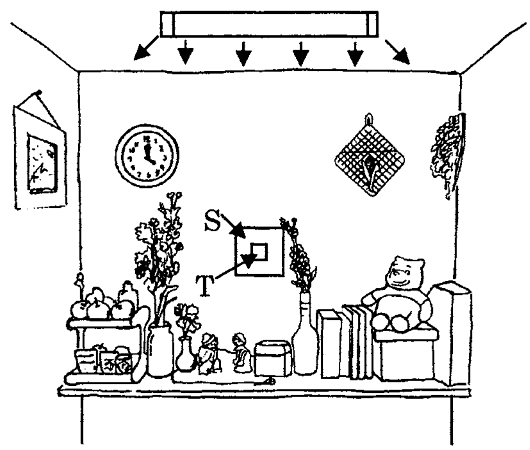

Fig.2 Subject's front view. T: test stimulus , S:immediate surrounding.

2.2 Conditions and Procedure

Five color charts were used for T, 5R4/10, 5Y7/10, 5G5/10, 10B4/10 and N5. In I -Series, four room illuminance, 100, 133, 257 and 600 lx, and the luminance of S, 23.2 cd/m^2 were employed. The lightness of N9, N8, N6 and N4 were used to achieve the constant luminance. N9 was of the white wallpaper. In L-Series, gray patches of N4, N6, N8 and the wall paper of N9 were used for S and their luminance were 4.04, 9.44, 18.4 and 23.2 cd/m^2, respectively, under the illumination of 100 lx. As the control experiment the border was measured for the room illuminance, 133 lx, 257 lx and 600 lx without using the gray patch for S but only the wallpaper.

The subject observed the appearance of the test stimulus whether it appeared natural or unnatural as an object placed in the room and set the luminance at the border by the method of adjustment. He was asked not to fixate his eyes all the time at the target but to look around the room from time to time. He used both eyes and wore a cap to eliminate the ceiling lamps from the initial visual information.

Five subjects participated in the experiment, MI (69 years old, male), RY (27, female), YT (26, female), HY (25, male) and SP (24, female).

2.3. Results of Experiment 1

Results of I-series are shown in Fig. 3a for the subject MI. Test stimuli are denoted by different signs. Along the abscissa the room illuminance is and along the ordinate the border luminance of the test stimulus, both in logarithmic unit. Each point represents the average of ten adjustments and vertical bars show the standard deviations. For all the color charts the border luminance is almost proportionally to the room illuminance in spite of a fixed luminance of the immediate surrounding to confirm the prediction made on the RVSI theory. Results of L-Series are shown in Fig.3b, where along the abscissa the luminance of the immediate surrounding is taken. The room illuminance was kept at 100 lx. The border $_nB_u$ changes little in spite of different luminance of the immediate surrounding, again confirming the prediction. Vertical positions of the test stimuli varies depending on the color. The curve N5 is much higher than the other four curves to imply that colored charts reach the border at lower luminance than white.

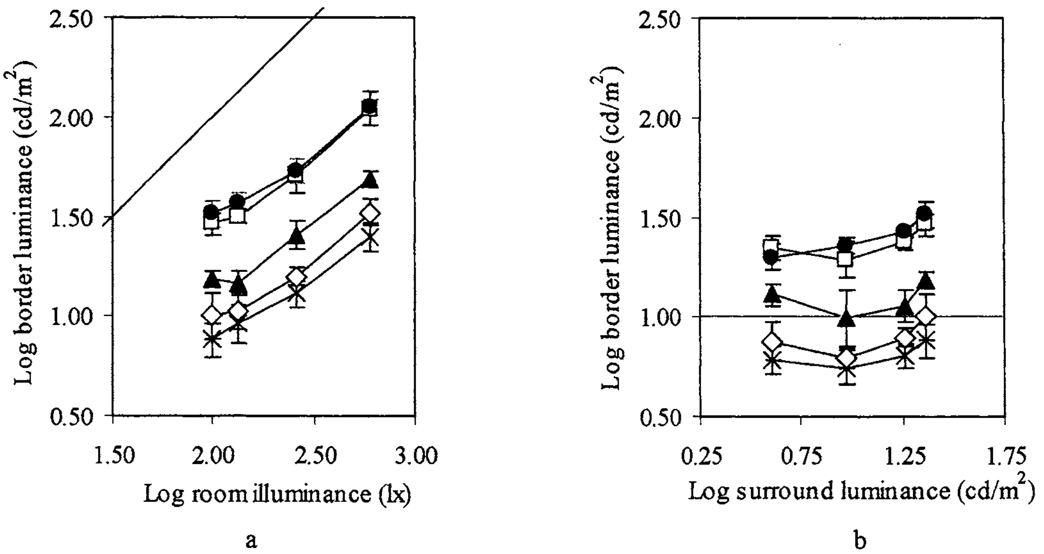

Fig.3 a, results of I-series; b, L-series. Subject, MI. Test stimuli;◇, 5R4/10;□ , 5Y7/10;▲ , 5G5/10; ×, 10B4/10; O , N5.

3. EXPERIMENT 2
SIZE EFFECT OF IMMEDIATE SURROUNDING

3.1 Apparatus

Although the prediction about the border $_nB_u$ was mostly confirmed by Experiment 1, we notice some deviation from the prediction. Slopes in Fig.3a were slightly shallower than unity and those in Fig.3b slightly elevated. There was some the effect of the immediate surrounding lightness. The low lightness of N4 might lowered the border more than the high lightness. If this is so, the lowering effect will become stronger if the size of the immediate surrounding is enlarged. In Experiment 2 we will investigate the size effect of the immediate surrounding.

The same experimental room was used as Experiment 1 with a modification for the immediate surrounding S, which was made replaceable by different size of surrounding.

3.2 Conditions and Procedure

Immediate surroundings of five different size were employed, 3 x 3, 6 x 6, 12 x 12, 18.2 x 25.7 and 36.4 cm x 51.4 cm, which corresponded to 1.4 x 1.4, 2.7 x 2.7, 5.5 x 5.5, 8.2 x 11.5 and 16.1 degrees x 22.2 degrees in visual angle, respectively. The same conditions were used as Experiment 1 as to the room illumination and the luminance of the immediate surrounding.

One new subject HA (24 years old, male) joined to the previous five subjects. The subject's task was same as Experiment 1.

3.3 Results of Experiment 2

There are much more data in Experiment 2 than Experiment 1 and we will show some typical data only. Fig.4a shows the results of I-series for the test stimulus 5Y7/10 and for the subject MI. Along the abscissa the area of the immediate surrounding is taken and along the ordinate the border luminance. Three curves represent different Munsell Value of the surrounding, but a same luminance at 23.2cd/m^2. In other words, the room illuminance was adjusted to have the same luminance. The curve with open circles is from the combination N4 and 600 lx, filled triangle N6 and 257 lx, and open squares N8 and 133 lx.

We can confirm here again that the border is mainly determined by the room illuminance. The curve from the room illuminance 600 lx is highest among three. And a new finding here is a slight decrease of the curve, as the surrounding size increases in spite of the fact that is not change in other conditions. There is the size effect of the immediate surrounding for the border.[4] The decrease is smaller for other conditions where higher lightness was employed for the surrounding and with N8 the curve is almost flat implying no size effect.

Fig.4b shows the results of L-series. Three curves represent different gray Munsell Value and luminance of the immediate surrounding, but a same illuminance at 100 lx. The curve with open circles is from the combination N4 and 4.04 cd/cm^2, filled triangles N6 and 9.44 cd/m^2, and open squares N8 and 23.2cd/m^2. All three curves slightly decrease for larger area of surrounding to show the size effect. There seems no difference among the three curves. The same room illuminace of 100 lx kept the border same.

To conclude, the border for the color appearance mode from the natural object color to the unnatural object color $_{n}B_{u}$, is determined mainly by the space illumination. There exists a slight effect for the determination from the immediate surrounding if its size is large and has low lightness, and probably if the room illuminance is high.

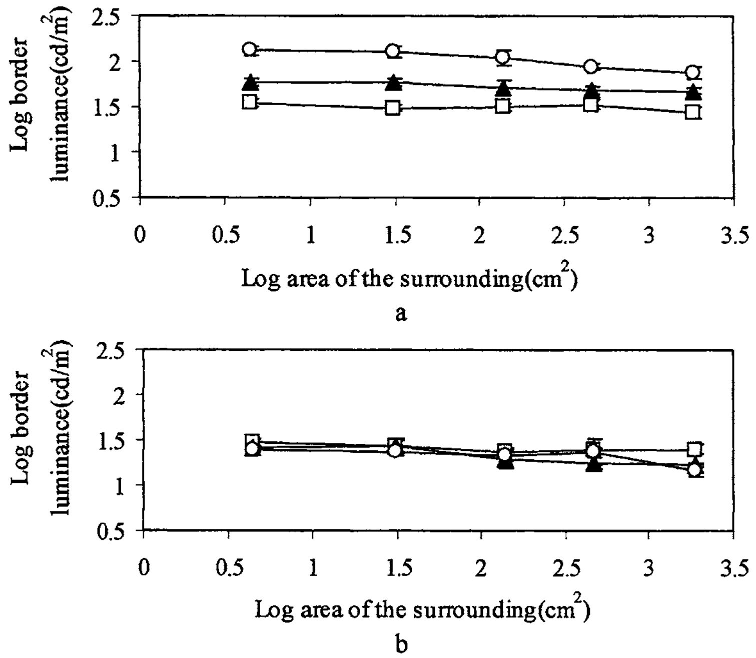

Fig.4 a, results of I-series; b, L-series. Subject, MI. Lightness of the surrounding: ○, *N4* ; ▲, *N6* ; □, *N8.*

References

1. M. Ikeda, K. Motonaga, N. Matsuzawa and T. Ishida: *J. Optics*. (Kogaku), 22(1993) 289-298 (in Japanese).

2. Y. Thiangthangtum, R. Yamauchi, P. Pungrassamee, A. Hansuebsai and M. Ikeda: *Proc. AIC*, Soul, (2000) 84-88.

3. H. Yamaguchi, H. Shinoda and M. Ikeda: *J. Illum. Eng. Inst. Jpn.* 86 (2002) 830-836 (in Japanese).

4. M. Ikeda, S. Fukumura, N. Matsuzawa and T. Ishida: *J. Optics* (Kogaku), 23(1994) 42-49. (in Japanese).

---

*Correspondence; gr024014@se.ritsumei.ac.jp; Department of Photonics, Faculty of Science and Engineering, Ritsumeikan University, Nojihigashi, Kusatsu-city 525-8577 Japan

Instrumental Measurement and Visual Estimation of Gonio-Apparent Paint Surfaces

Hirotoshi Arai and Gorow Baba
MURAKAMI Color Research Laboratory, Tokyo, JAPAN

ABSTRACT

To estimate the gonioapparent properties of metallic and pearlescent paint finishes, samples of metal-flake and pearl-mica pigmented paint surfaces were prepared. For these samples, spectral reflectance factors for various geometric conditions were measured by gonio-spectrophotometer, and from these spectral reflectance factors, colorimetric values were calculated. Furthermore, spectral reflectance factors were treated by principal component analysis, and flake orientation in the paint layer was supposed. On the other hand, these samples were visually estimated by sensory inspection, using direct viewer. Finally, quantities related gonioapparent properties were proposed.

1. INTRIDUCTION

For metallic paint finishes, many estimation methods for appearance of these surfaces were carried out in these several years. In United States, ASTM E2194 Standard Practice for Multi-Angle Color Measurement of Metal Flake Pigmented Materials was adopted, but this method is not applicable to pearlescent or pearl-mica paint finishes. In Germany, DIN 6175-2 Tolerances for automotive paints - Part 2: Goniochromatic paints was adopted in 2001, and this standard specifies tolerances of color difference by 4-directional color measurement for anisotropic automotive paints, but not specifies the estimation method of appearance of these paint finishes. In this study, using metal flake, pearl-mica and related paint samples, flake orientation in vehicle layer was estimated from spatial distributions of spectral reflectance factor of these samples, and quantities related to gonioapparent properties were supposed, considering the results of sensory inspections.

2. EXPERIMENTS

2.1 Samples

For this experiment, 12 metallic, 24 pearl-mica and 4 solid paint color samples were prepared. Name and identification of samples are shown in Table 1.

Table 1 Name and identification of metallic, pearl-mica and solid paint color samples.

upper coat		average particle size (μ m)	base coat	ID	200b	Flop
Silver Metallic	Fine	10	---	A1	20.06	10.03
	Medium Fine	16	---	B1	31.15	15.58
	Medium	17	---	C1	35.57	17.78
	Coarse	27	---	D1	39.81	19.90
Blue Metallic	Fine	10	---	A2	22.01	11.01
	Medium Fine	16	---	B2	37.90	18.95
	Medium	17	---	C2	42.45	21.23
	Coarse	27	---	D2	47.74	23.87
Red Metallic	Fine	10	---	A3	20.79	10.40
	Medium Fine	16	---	B3	33.01	16.51
	Medium	17	---	C3	40.02	20.01
	Coarse	27	---	D3	43.42	21.71
Solid Color	Blue		---	Bl	0.08	0.00
	Green		---	Gr	0.06	0.04
	Red		---	Re	-0.12	0.00
	Yellow		---	Ye	-0.12	0.10
Silver Pearl-Mica	Fine	10	White	F	3.14	2.64
			Black	Fb	6.38	7.61
	Medium	18	White	G	6.94	5.03
			Black	Gb	13.66	15.75
	Coarse	50	White	H	6.02	3.53
			Black	Hb	16.80	20.47
Interference Pearl-Mica	Gold	18	White	I	14.14	3.69
			Black	Ib	16.50	13.52
	Red	18	White	J	13.82	1.97
			Black	Jb	16.52	12.43
	Blue	18	White	K	16.38	1.35
			Black	Kb	14.04	10.37
	Green	18	White	L	9.50	2.85
			Black	Lb	13.68	11.29
Colored Pearl-Mica	Russet	18	White	M	9.44	7.09
			Black	Mb	14.20	15.62
	Gold	18	White	N	8.48	3.83
			Black	Nb	14.26	12.74
	Infinit	18	White	O	13.56	2.91
			Black	Ob	14.28	17.79
	Silver Gray	18	White	P	12.40	9.48
			Black	Pb	14.50	18.60
	MIO Pearl	13	White	Q	3.84	7.46
			Black	Qb	8.24	14.14

Color of metallic samples were silver, blue and red, and for each group, 4 kinds of aluminum flake were used. Pearl-mica samples were silver pearl-mica, interference pearl-mica and colored pearl-mica. All pearl-mica samples were treated on white and black backgrounds. On all samples, clear top coat was applied.

2.2 Gonio-spectrohpotometric measurements

For this experiment, Murakami Model GCMS-3B, Gonio-Spectrophotometric Color Measurement System was used. Geometric and spectral conditions were as follows;

a) geometric condition: incident angle: -45° (angle is shown in anormal designation)

viewing angle: from 70° to -70°, 5° interval (except near incident angle)

b) spectral condition: wavelength range: from 390nm to 730nm, 10nm interval

bandpath: ca. 10nm

For each geometric condition, spectral reflectance factor was measured.

2.3 Colorimetric calculation

From spectral reflectance factor distribution, colorimetric values (XYZ, xy, L*a*b*, L*C*h*) were calculated for CIE standard illuminant D65 and CIE 1931 colorimetric standard observer.

2.4 Statistical analysis

By gonio-spectrophotometric measurements, data set of spectral reflectance factor for various viewing angles were obtained. Fig. 1 shows spectral reflectance factor distribution of silver metallic, coarse and interference pearl-mica, red. Variance -covariance matrix of spectral reflectance factor and viewing angles, from 0° to +35°, were treated by principal component analysis. Fig. 2 shows principal component score of silver metallic, coarse and interference pearl-mica, red. Table 2 shows eigenvalue, proportion and cumulative proportion of silver metallic, coarse and interference pearl-mica, red.

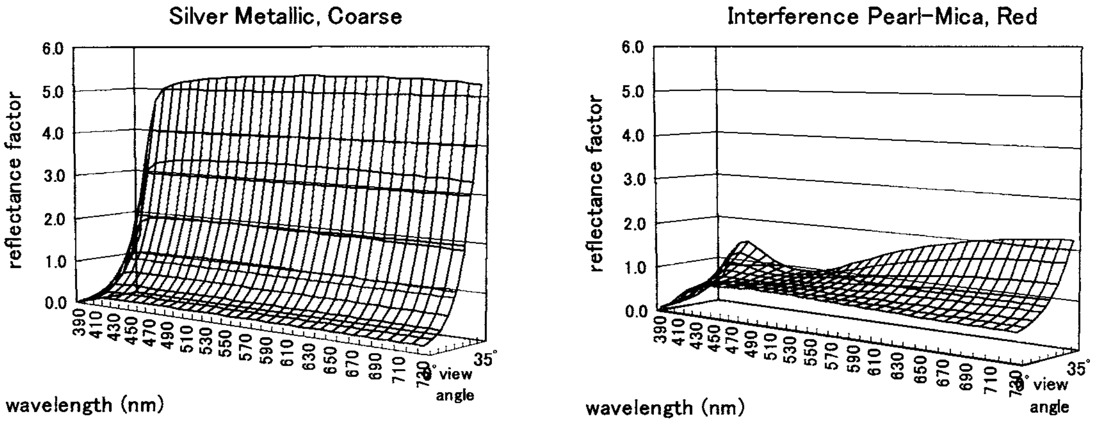

Fig. 1 Spectral reflectance factor distribution of silver metallic, coarse and interference pearl-mica, red.

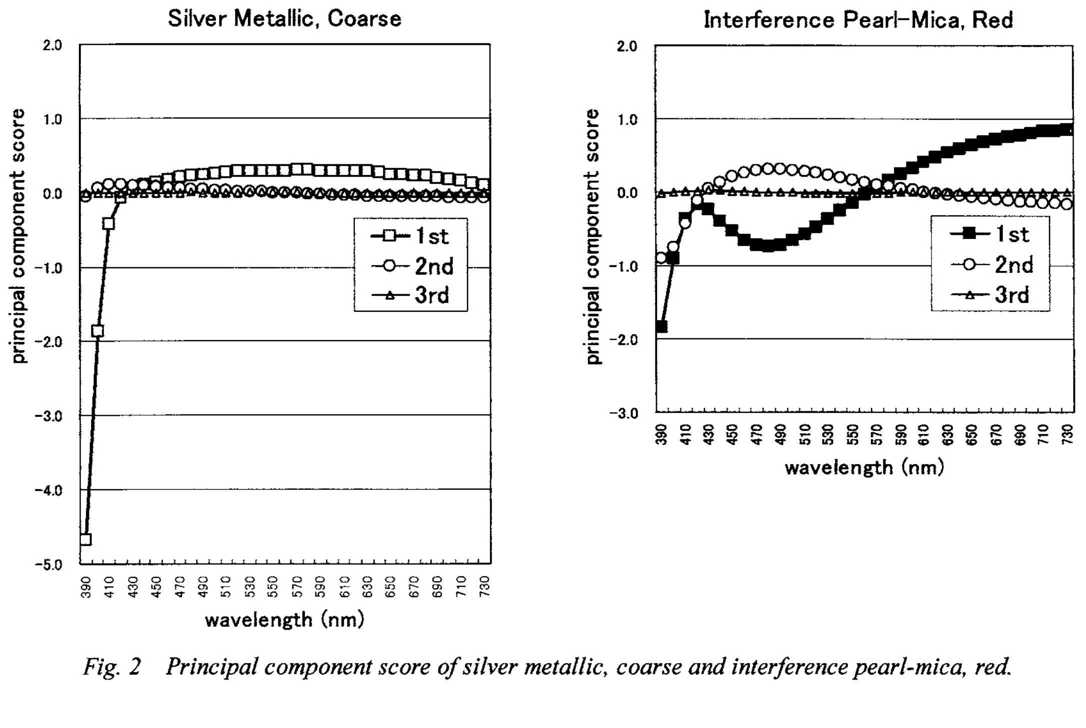

Fig. 2 Principal component score of silver metallic, coarse and interference pearl-mica, red.

Table 2 Eigenvalue, proportion and cumulative proportion of silver metallic, coarse and interference pearl-mica, red

Silver Metallic, Coarse

	Eigenvalue	Proportion	Cumlative prop.
1st	0.8013	99.6%	99.6%
2nd	0.0033	0.4%	100.0%
3rd	0.0000	0.0%	100.0%

Interference Pearl-Mica, Red

	Eigenvalue	Proportion	Cumlative prop.
1st	0.4281	85.2%	85.2%
2nd	0.0742	14.8%	100.0%
3rd	0.0001	0.0%	100.0%

In case of silver metallic, coarse, the proportion of the first component was 99.6%, and that of the second component was 0.4%. In case of interference pearl-mica, red, the proportion of the first component was 85.2%, and that of the second component was 14.8%. Then eigenvector of the first principal component was plotted against viewing angle, and simulated by exponential regression. The variations of eigenvector of the first principal component for viewing angle are shown in Fig. 3. The power of the simulated exponential function is listed in Table 1.

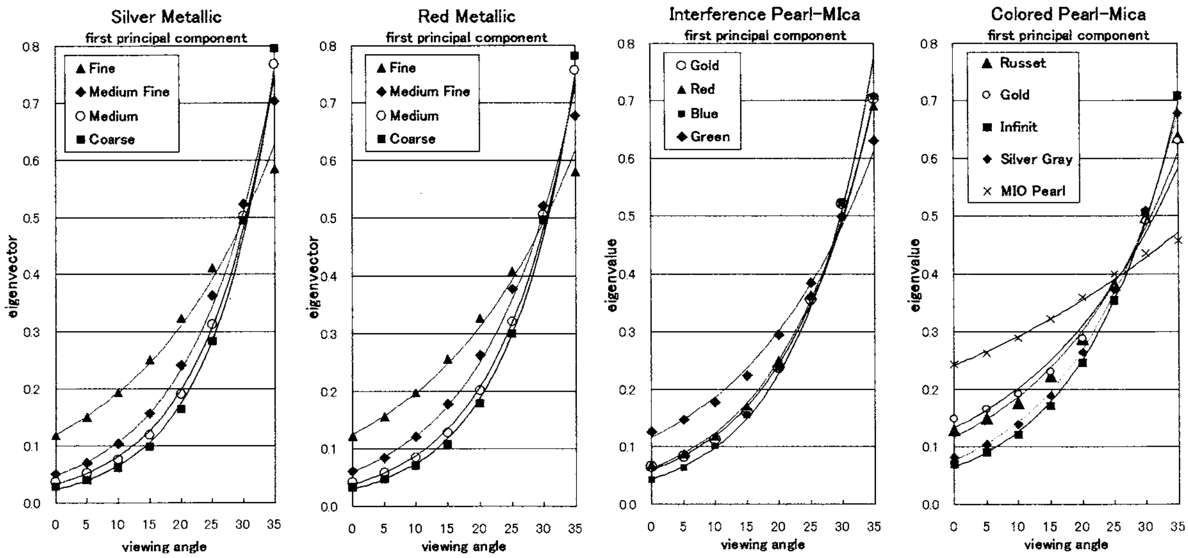

Fig. 3 Relation between the first principal component and viewing angle.

3. CONSIDERATIONS

1) In Fig. 2, in case of silver metallic, coarse, the first principal component means reflected light from aluminum flake, and the second principal component means reflected light from resin layer. In case of interference pearl-mica, red, the first principal component means reflected interference light from titanium dioxide flake, and the second principal component means reflected light from base coat. In both cases, the most of the reflected light from sample consists of two components. In metallic samples, silver, blue and red, the first principal components are not so different, because the aluminum flakes used are equal, and the second principal components are different.

2) In Fig. 3, in metallic samples, silver and red, eigenvector change of the first pricipal component with viewing angle are almost same, because the first principal component relates to reflected light from aluminum flake, and inclinations of fitting curves are in order from fine to coarse. Inclinations of eigenvector of interference pearl-mica samples are not so different from that of metallic samples.

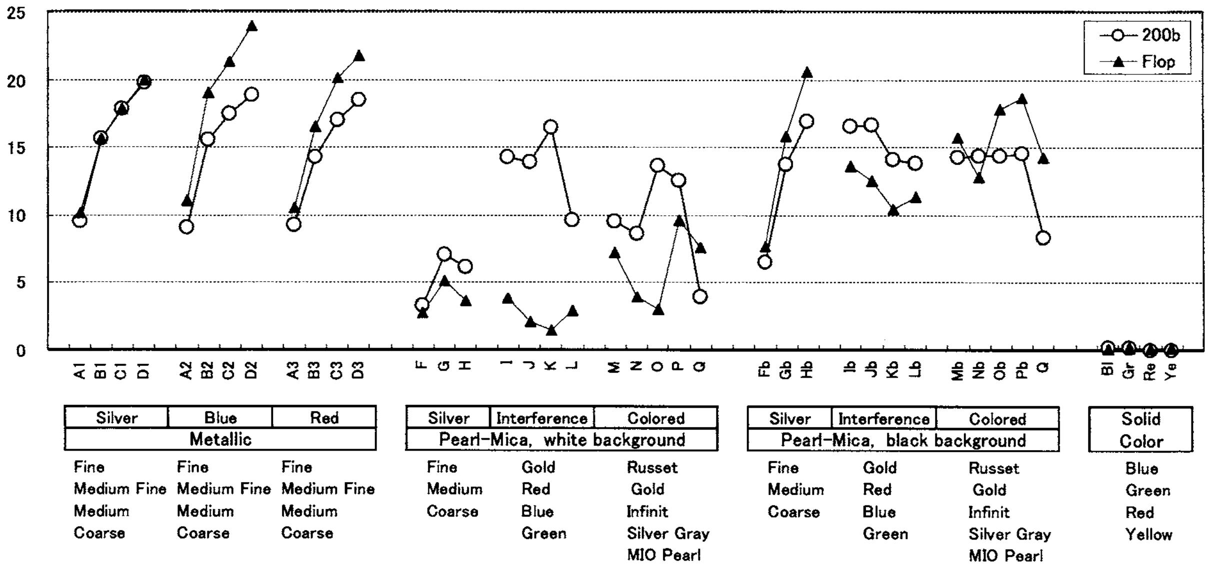

Fig. 4 Relation between power of simulated exponential function and flop value.

3) Table 1 and Fig.4 show the relation between the popwer of simulated exponential function and flop value. In this case flop values are calculated by the following equation, which was propose by D. Alman several Years ago.

$$Flop = 2.69\,(L^*_1 - L^*_3)^{1.11} / L^*_2{}^{0.86} \qquad (1)$$

Where, L^*_1, L^*_2, L^*_3: lightness at 15°, 45° and 110° (aspecular) viewing, for 45° incidence.

In Fig. 4, the power of simulated exponential function of metallic samples, silver, blue and red, are almost equal, and it means that flake orientation in metallic samples are almost same. The difference between flop value and flake orientation will be caused by the other properties than flake orientation, for example chromaticness of resin in blue and red metallic samples. Concerning to flake orientation, difference between metallic samples and pearl-mica samples is not so large, except silver pearl-mica samples.

Space Brightness of Non-Uniformly Illuminated Space Measured by Border Luminance

Hideki Yamaguchi, Hiroyuki Shinoda, and Mitsuo Ikeda
Department of Photonics, Faculty of Science and Engineering,
Ritsumeikan University

ABSTRACT

Our previous works[1), 2)] showed that perceived brightness of a room can be measured by the border luminance between natural and unnatural surface color mode. The appearance of an object of unnatural surface color mode is unnatural as an object in an illuminated room. This color appearance mode is defined as another color mode between "object color" and "light-source color". In this paper, we evaluated the brightness of a non-uniformly illuminated room by measuring the border luminance at various positions. We examined what determines and how change the border luminance in a non-uniformly illuminated room. We measured the border luminance in four differently illuminated rooms and compared the distribution of border luminance each other. Consequently, the border luminance is determined by neither the local illuminance nor the luminance of immediate surround. It is likely that the appearance of the nearest object in a 3-dimensional (3D) space not on the 2-dimensional (2D) retina is used as a clue to the space brightness. Added to this, it is found in these illuminant combinations that the border luminance has an additivity law.

KEYWORDS: space brightness, color appearance mode, non-uniform illumination, recognized visual space of illumination

1. INTRODUCTION

When we judge the color and brightness of object's surface, we, consciously or unconsciously, take into account the illumination of a space. Consequently, we can perceive the object's surface constantly although the luminance and chromaticity of object would be changed by illumination change. We call such understanding of illumination the recognized visual space of illumination, RVSI. Especially, we use a term 'brightness size' of RVSI to describe an observer's perception about intensity of illumination. When an observer recognized a room is illuminated brightly/dimly, we say the brightness size of RVSI is large/small. We define the 'border luminance' for an achromatic test patch as the brightness size of RVSI. When the luminance of the test patch is increased by an additional spotlight, the appearance of object's surface change with its luminance from natural to unnatural surface of object in the scene. This particular luminance is called border luminance.

We usually use illuminance and xy chromaticity to represent brightness and color of illumination. But these photometric values do not always fit our perception for illuminations. For example, let us suppose two differently furnished rooms with the same illuminance; one is decorated by brighter objects and the other is decorated only by darker objects. Despite of the same illuminance, we feel the former room brighter than the latter. Many researchers have studied on perceived brightness of a space, but any measurement methods have not been established yet and it is still unclear on what determines the perceived brightness. We have proposed the border luminance as a measure for the space brightness and studied on the its mechanism.

Our previous study[2)] showed that the border luminance is constant at any location in a normal room with relatively uniform illumination. There are also many situations with a non-uniform illumination in everyday lives. It is useful for lighting design to quantify the perceived brightness in a non-uniformly illuminated space. The purpose of this paper is to investigate how the border luminance changes in a non-uniformly illuminated room and what clues would be used to perceive the space brightness. In particular, we examined two possible candidates determining border luminance: horizontal illuminance and luminance distribution on walls.

2. METHODS

2.1 Equipments

An experimental room was 2.4m wide, 2.4m deep, and 2.0m high. Walls and a ceiling were made of N9.3 white wallpaper and a dark gray (N3) carpet was lined on the floor. The room was illuminated by two fluorescent lamps (daylight type, FL) equipped at the both ends of the ceiling. Each fluorescent lamp was placed 60cm away from a sidewall. Reflectors were attached on the luminaries so that the ceiling fluorescent lamps illuminated just side walls, causing very low illuminance at the center of the room. Louvers were attached/removed to make the luminance distribution uniform/non-uniform on the front wall. No objects were placed inside the room.

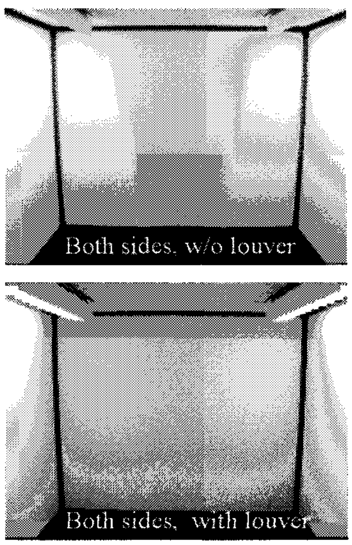

Fig.1 Observer's view.

We measured the border luminance with a test stimulus, a N5 gray patch of 6cm x 6cm that had a mat surface. A test stimulus was put on a tip of a rod at a height of 1.0 m and tilted at 45 deg. from vertical. Its surface was hardly illuminated by the ceiling light but, instead, spotlighted by a slide projector from below. We controlled the luminance of the test by the neutral density wedge filter inserted in the light path.

2.2 Conditions

We conducted the experiment under four different illumination conditions. Bilateral lighting on the both sidewalls with louver (BL) or without louver (B), unilateral lighting on the left wall with louver

(UL) or without louver (U). Observer's view in bilateral lighting conditions, B and BL, are shown in Fig.1. Notice that the luminance distribution on the front wall is uniform due to louvers. Positions of an observer and 15 measuring points are shown in Fig.2. Five positions were labeled as LL, L, C, R and RR from left to right. Three rows were labeled as lines N, M and F.

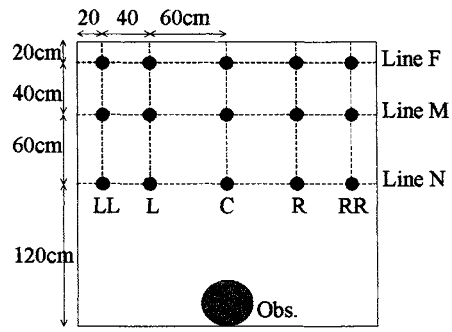

Fig.2 Top view of the room and measured position.

2.3 Procedure

The observer's task was to adjust the luminance of the test stimulus where it starts to look unnatural as an object in the room. The observers were instructed to look around the entire room rather than to gaze at the test stimulus only. Observer set the border luminance three or four times successively at each measuring position. In a single session, all positions were measured in one of the lighting conditions. Three sessions were conducted for each illumination condition to obtain 10 adjustments for each condition. Five observers, HY, HS, YH, TK, and YI participated in the experiment.

3. RESULTS AND DISCUSSIONS

The results from all observers showed the same tendency. Here a result from observer HY is shown in Fig.3 as an example. The left panels show the horizontal illuminance measured at the height of test stimulus. The right panels show the border luminance set by the observer. Top graphs are from B condition and the bottoms from BL condition. The abscissas indicate the measuring positions along the horizontal direction. Solid lines show results obtained along F, dashed lines M and dot-dashed lines N. The error bars indicate the standard deviations across 10 adjustments.

Due to the reflectors, the ceiling lights only illuminated sidewalls. The horizontal illuminance was higher near the sidewall in both conditions. At the center, the position C, the horizontal illuminance was almost the same for three rows, F, M, and N. But near the sidewall, illuminance was the lowest in F and the highest in N. In other words, the illuminance difference between the highest and the lowest was the largest

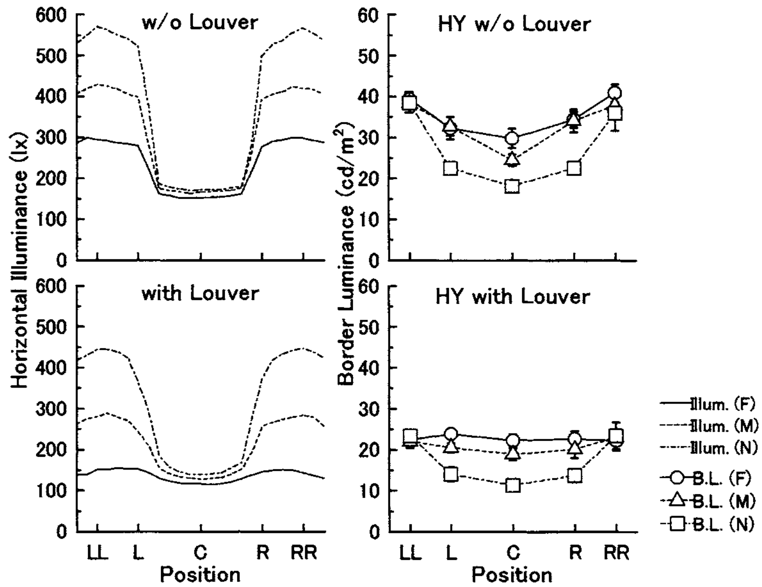

Fig.3 Results for the bilateral lighting conditions from observer HY. The left, the horizontal illuminance and the right, the border luminance.

for the line N and the smallest for F. The depth of trough in the illuminance profile is shallower at the bottom panel than the top. Especially, the illuminance profile along F is almost flat at the bottom graph.

The shapes of border luminance seem to follow those of illuminance as a whole; the border luminance was higher at the positions LL and RR than the position C in each row. The larger the depth of illuminance trough, the larger that of the border trough. Notice that the border luminances were cramped to the same level at the both ends LL and RR but that they differ at the center C. This trend is the completely opposite to that in the illuminance profiles.

Some relationship between the border luminance and the horizontal illuminance is observed. However the horizontal illuminance around the test patch is not a determinant for the brightness of a local space when there are no objects available. Interestingly, the border luminance was almost constant even along M in the lower right panel, despite that the illuminance profile was not flat as comparable to that of F in the upper left panel. This suggests that the uniform luminance distribution on the front wall would largely affect the border luminance; the position C is closer to the front wall than the sidewall and the luminance is almost uniform over the front wall as shown in Fig.1.

One might think of the luminance of the immediate surround on a retina, as a most probable factor of the border luminance. Let's focus on this point for a while. At the position C, the immediate surround for the test stimulus was the front wall and its luminance was constant for F, M, and N. This equal surround luminance cannot account for the difference in the border luminance shown in the right graphs. At the position LL or RR, the immediate surround was the sidewall on the retina but its luminance differed for F, M, and N; the highest for N and the lowest for F. Nevertheless the border luminance was cramped at the same level. Again the surround luminance fails to explain the border luminance. Neither the local illuminance nor the luminance of immediate surround can explain the border luminance. Then what could account for the border? The luminance of the nearest object in a 3-dimensional (3D) space not on the 2-dimensional (2D) retina is likely utilized for the space brightness.

In our all lighting conditions, only walls were illuminated and the illuminance was intentionally kept low at the center of the room. Since no objects were available inside the room and the carpet was almost black, only the walls seem to be clues for the perception of space brightness. The question was how the visual system could know the space brightness at the center and, in particular, how the luminance information on walls would affect to the center. Our hypothesis was that the border luminance at the center should be somehow inferred from walls. Filling in or interpolation process might function when both walls are brightly illuminated. If the hypotheses are correct, the border luminance at the center C in the bilateral condition would be higher that in the unilateral condition. The result of the

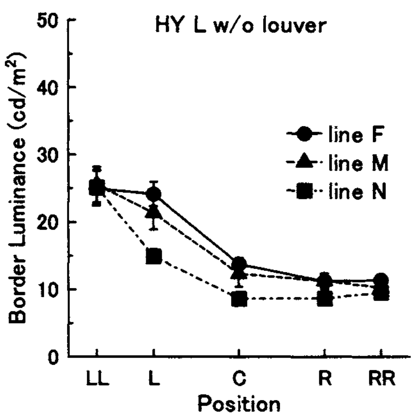

Fig.4 The border luminance in the unilateral lighting condition without louver U. The same symbols are used as in Fig. 3 except they are solid.

unilateral lighting without louver (U) is shown in Fig.4. The ordinate and the abscissa are the same as Fig.3. The same circle, triangle, and square but solid symbols are used here.

The border luminances were cramped to the same level at the both ends LL and RR and differ at the center C. These trends are the same as in the bilateral lighting condition. Since the ceiling lights of the experimental room was arranged symmetrically, we flipped the result of Fig. 4 horizontally to get the border luminances for right side wall. Then this estimated border luminance for right side lighting was added to that for left side lighting. We compared this sum with the border luminances of the bilateral condition in Fig.5. Open symbols indicate border luminances in bilateral lighting condition without louver (B), which is the replot from the right upper panel in Fig.3. Solid symbols indicate border luminances calculated from the unilateral condition. In the Fig.5, solid symbols coincide with open symbols very well. This suggests no interpolation mechanism in the border luminance, contrary to our expectation. To put it other way, the additivity law holds for the border luminance. This rule might be important and very useful for lighting design. The space brightness of a room illuminated by two or more lights could be estimated from the brightness caused by each single light. We can estimate the perceived brightness even in a complex illumination by summation of the border luminance measured in a simple illumination.

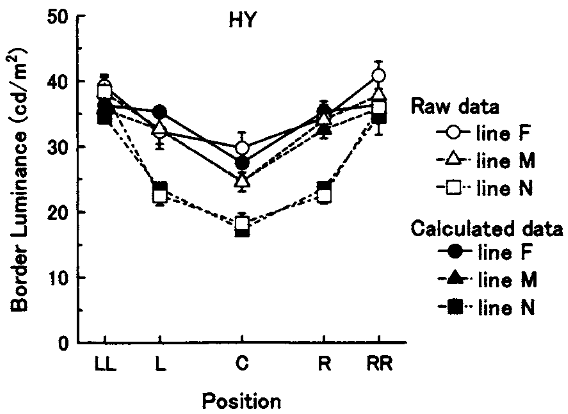

Fig.5 The border luminance for the bilateral lighting condition (B) and the estimated border by the sum of the unilateral lighting conditions (U).

4. CONCLUSION

We assessed the perceived brightness of non-uniformly illuminated room by measuring the border luminance. It was found that neither the local illuminance nor the luminance of immediate surround could explain the border luminance singly. Another important finding was that the additivity law in the border luminance holds.

1) Hideki Yamaguchi, Hiroyuki, Mitsuo Ikeda: Determinant of the size of recognized visual space of illumination in a natural environment, Proceedings of AIC meeting Seoul, pp.228-232, 2000

2) Hideki Yamaguchi, Hiroyuki Shinoda, Mitsuo Ikeda: Size of recognized visual space of illumination influenced by color scheme of interior, Proceedings of 9th congress of Int. Colour Assoc., pp.347-350, 2001

Geometrical Information Recovery from Garment Images Using Dichromatic Reflection Model

J. H. Xin, H. L. Shen
Institute of Textiles & Clothing, the Hong Kong Polytechnic University, Hong Kong

ABSTRACT

This paper deals with the recovery of the geometry of three-dimensional clothing materals from images. This geometry would be necessary and adequate for the color synthesis. As it is almost impossible to acquire the complete geometry of the surfaces of an object in an image, this study attempted to recover the implicit and relative geometry based on the dichromatic reflection model. The geometric coefficient can be calculated from either a series of reflectance or RGB signals of the imaging system. The experimental result showed that the geometry recovered is quite accurate and therefore this method is considered to be applicable for the image-based rendering with high color fidelity for garment.

Keywords: geometry recovery, dichromatic reflection model, color synthesis

1. INTRODUCTION

The color information is among the most important properties of garment, and it is also one of the serious obstacles for the textile and clothing industry moving to the virtual domain. The interaction of light with real materials is a complicated process, and the general reflection models characterize the light reflected by an object as a complex function of the geometry, the illumination, and the optical properties of the object materials. The bidirectional reflection distribution function (BRDF) [1] is always used in the modeling of the interaction in both computer graphics and computer vision. The BRDF could be either empirical determined using the physics-based models [2] or experimental measured using custom-built equipments [3]. However, it seems that neither of these two methods is applicable for the fabric materials with complex deformation.

Fortunately, for the purpose of image-based color synthesis, the complete geometry of the three-dimensional objects is not necessary. Therefore, it was desired to calculate the implicit and relative geometric information based on the dichromatic reflection model that was first proposed by Shafer [4]. Although the dichromatic reflection model has been intensively studied in the area of image segmentation [5], color constancy [6], and object rendering [7], the problem of whether the geometric information obtained was accurate enough for the color synthesis of 3-D objects has not been adequately addressed yet. In this study, the geometric information was recovered from an image and its accuracy was investigated. Based on the recovered geometry, the synthesized images were also provided in the experiment.

2. RECOVERY OF GEOMETRY FROM AN IMAGE

It is well known that for an image system, the output V_k^x at position x for the kth channel can be briefly represented as

$$V_k^x = c(x)\int L(\lambda)S_k(\lambda)R(x;\lambda)d\lambda \,. \tag{1}$$

where λ is the wavelength in the visible spectrum 400-700 nm, $c(x)$ is a constant factor related to the optical properties of the imaging device (camera), $L(\lambda)$ is the illumination, $S_k(\lambda)$ is the sensitivity function of the kth channel, and $R(x;\lambda)$ is the reflectance at position x. It is known that the reflected light can be decomposed into two components, namely surface reflection and diffuse reflection [4]. The surface reflection is dependent upon the orientation of the local surface that varies along the interface, and its wavelength composition is approximately the same as the illuminant. The body reflection is closely relative to the characteristic of the material. It is assumed in the dichromatic reflection model that the surface and body reflections can be further approximately decomposed into two independent components, i.e., spectral and geometric ones:

$$R(x;\lambda) \approx g_b(x)R_b(\lambda) + g_s(x)R_s(\lambda) \tag{2}$$

where $g_b(x)$ and $g_s(x)$ are the geometric factor of the body and the surface reflectance at position x, and $R_b(\lambda)$ and $R_s(\lambda)$ are the wavelength composition of the body and the surface reflectance respectively. As the spectral power distribution of the surface reflection is very similar to that of the incident light, equation 2 can be simplified as

$$R(x;\lambda) \approx g_b(x)R_b(\lambda) + g_s(x)R_s \tag{3}$$

Similarly, for the same material at a different position y, the reflectance is

$$R(y;\lambda) \approx g_b(y)R_b(\lambda) + g_s(y)R_s \tag{4}$$

The reflectance $R(x;\lambda)$ and $R(y;\lambda)$ can be linearly related by eliminating the term $R_b(\lambda)$ in equation 3 and 4:

$$R(y;\lambda) = aR(x;\lambda) + b + \varepsilon(\lambda) \tag{5}$$

where $\varepsilon(\lambda)$ is a random error, (a, b) is the geometric coefficient pair determined by the geometric factors $g_s(\cdot)$ and $g_b(\cdot)$. As the equation 5 is over-determined, the geometric coefficient (a, b) can be solved using the least-squares method. Combining equation 5 and equation 1 yielding

$$\begin{aligned} V_k^y &= c(y)\int L(\lambda)S_k(\lambda)\left(aR(x;\lambda)+b\right)d\lambda \\ &= c(y)\left(a\int L(\lambda)S_k(\lambda)R(x;\lambda)d\lambda + b\int L(\lambda)S_k(\lambda)d\lambda\right) \\ &= AV_k^x + BW_k \end{aligned} \tag{6}$$

where

$$A = \frac{c(y)}{c(x)}a, \quad B = c(y)b, \text{ and } W_k = \int L(\lambda)S_k(\lambda)d\lambda \tag{7}$$

Therefore, the geometric coefficient pair (A, B) can be calculated from V_k^x and V_k^y, and W_k is the camera response of a perfect white diffuser under illuminant $L(\lambda)$. As W_k is known for a given imaging system, there are three equations for a three channel camera and two unknown (A, B), the problem is also over-determined.

3. INVESTIGATION OF THE RECOVERED GEOMETRY ACCURACY

When the geometric coefficient pair (a, b) is solved, the reflectance at position y can be synthesized as

$$R^a(y;\lambda) = aR^a(x;\lambda) + b \tag{8}$$

where $R^a(x;\lambda)$ can be any target reflectance at position x. It is noted from equation 8 that the accuracy of the geometric coefficient (a, b) is very important for the color synthesis. Suppose there are N objects of the same material and shape but different colors. Then, for the ith object, the geometric coefficients (a_i, b_i) (i=1...N.) can be calculated according to equation 5 using least-squares. As (a_i, b_i) pair is related to the spectral distribution of the reflectance of the ith material, it is commonly the case that

$$(a_i, b_i) \neq (a_j, b_j) \text{ for } i \neq j \tag{9}$$

Therefore, it is necessary to study the description accuracy of the different geometric coefficient pairs.

Three polyester/cotton textile fabrics in different colors, namely blue, yellow and purple were used in the experiment. As the fabrics are deformable ones, they were wrapped onto cylinders with same radius and height to keep the same shape. They were placed on an experiment desk and the locations were kept fixed during the whole measurement and imaging procedure. A light source was tuned to provide uniform lighting on the desk. A perfect diffuser, barium sulfate coated white reference tile, was put at the same position to measure the spectral radiance of the illumination by a spectroradiometer (Photo Research model PR704). A digital camera (Canon EOS D30) was used in the imaging system. During the measurement, the distance between the spectroradiometer and the objects were kept unchanged and the measurements of different geometric positions on the object surface were achieved by tilting the spectroradiometer.

The reflectance was measured at five different but corresponding positions for the three fabrics. We took the reflectance at the first position as the reference, and calculate the geometric coefficient (a_i, b_i) at other four positions for each of the three fabrics. The distribution of the (a_i, b_i) pairs is plotted in figure 1. It is clear that for each position, the variation of the coefficient a_i is quite small. It is also found from figure 1 that a_i and b_i were always negatively correlated, i.e., when the value of a_i is high, the value of b_i becomes low, and vise versa. Due to this characteristic, the difference between the synthesized reflectances using different (a_i, b_i) pairs should be relatively small as the variation of a_i is compensated by the inverse variation of b_i to some degree.

The accuracy of the (a_i, b_i) pairs can be evaluated by the color difference between the measured and the synthesized reflectance. The color difference values were calculated between the reflectance of a position on the blue fabric and the synthesized reflectance of the corresponding positions (listed in table 1). As the (a_1, b_1) is solved directly by the reflectance data of the blue fabric, the color difference values of the first column in table 1 are accordingly the lowest among all the results. On the other hand, as the reflectance of the position five is the smallest of all, the color difference value for that position is the highest due to the high relative error in the synthesized reflectance. Overall, the color difference values listed in table 1 are quite small. These results verify the color accuracy of the prediction using the geometric coefficients developed in this study.

Error! Not a valid link.

Fig.1. The distribution of the geometric coefficient (a_i, b_i) pairs for the fabrics

Table 1. The color difference $\Delta E^*_{CMC(1:1)}$ between the synthesized and the measured reflectance using different (a_i, b_i) pairs for the three fabrics

	1st pair	2nd pair	3rd pair
Pos 1-2	0.269	0.601	0.335
Pos 1-3	0.294	1.035	0.302
Pos 1-4	0.398	1.210	0.501
Pos 1-5	0.915	2.280	1.706

As given in equation 6, the geometric coefficient (A, B) can also be calculated directly from images provided that the camera is linear. With the solved (A, B), new images with arbitrary tristimulus value can be used for color synthesis. Figure 2 shows an example, where (A, B) was calculated from the original blue image and a target color was chosen from the target image. From the comparison of the synthesized image and the target image, it was found that the geometry recovered with dichromatic reflection model is quite accurate.

4. CONCLUSIONS

In this study, the accuracy of the dichromatic reflection model in color synthesis was investigated for the textile materials. The geometry information can be calculated from either the reflectance series or the RGB values in an image. The color difference and the synthesized color image showed that the recovered of the geometry is accurate enough for the synthesis of textile fabrics in an image. Therefore, the technique presented in this study could be used in the simulation of garment with high color fidelity, and will contribute to the virtual design, manufacturing and retailing of products.

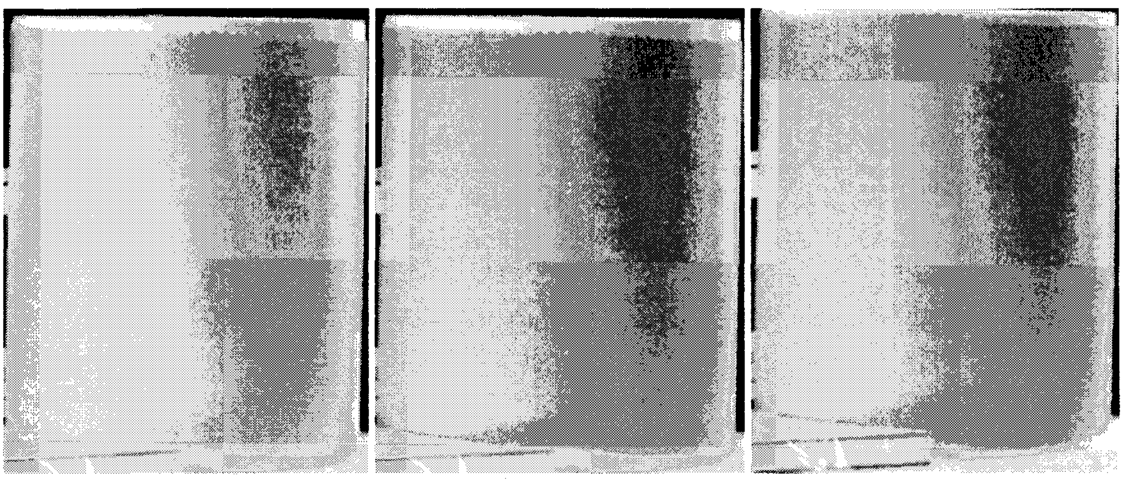

(a) (b) (c)

Fig.2. The color synthesis for fabrics under the same illumination condition. (a) Original blue fabric image; (b) Synthesized purple fabric image; (c) Target purple fabric image.

ACKNOWLEDGEMENT

We wish to thank the Hong Kong Polytechnic University for supporting the funding of this research project.

REFERENCE

[1] F. E. Nicodemus, J. C. Richmond, J. J. Hsia, I. W. Ginsberg, and T. Limperis, "Geometric considerations and nomenclature for reflectance," National Bureau of Standards, U.S. Monograph. 160, 1997

[2] J. Fi. Blinn, "Models of light refection for computer synthesized pictures", Computer Graphics, 11, 1977, pp. 192-198

[3] G. J. Ward. "Measuring and modeling anisotropic reflection", Computer Graphics, 26, 1992, pp. 265-272

[4] S. A. Shafer, "Using color to separate reflection components", Color Research and Application, 10, 1985, pp.210-218

[5] G. Healey, "Using color for geometry-insensitive segmentation", Journal of Optical Society of America A, 6, 1989, pp.920-937

[6] S. Tominaga, and B. Wandell, "Component estimation of surface spectral reflectance", Journal of the Optical Society of America A, 7(2), 1990, pp.312-317

[7] S. Tominaga, "Dichromatic reflection models for rendering object surfaces", Journal of imaging science and technology, 40(6), 1996, pp.549-555

Color Appearance Mode Change of CRT Monitor

N. Janchidfah*, P. Pungrassamee*, H. Shinoda**
* Dept of Imaging Science, Chulalongkorn University, Thailand,
** Dept of Photonics, Ritsumekan University, Japan

ABSTRACT

The border of the Recognized Visual Space of Illumination (RVSI) is the transition point of color appearance mode. This experiment was conducted to investigate the border luminance of color stimuli displayed on a CRT monitor. The task of observers was to set the luminance of color stimuli at the border between object and light source color mode. The border was found to be high for colors that have chromaticity-coordinates close to those of the illumination in the observer's room. More saturated colors had lower border luminance. The high border luminance of observer's room was found to be higher than that of low illumination. The result implies that the color displayed on the CRT monitor can change their appearance depending on the illumination condition in the room.

Keywords: The Recognized Visual Space of Illumination, CRT display, color appearance mode

1. INTRODUCTION

In many cases a CRT is viewed under ambient illumination. Thus, appearance of color on the CRT is influenced by several factors such as chromaticity and luminance of the illuminant[1]. The color appearance mode changes depend on the illumination condition under which the CRT monitor is viewed[2]. The human visual system adapts to the surrounding conditions, the perceived color mode are thus changed in relation to these conditions. In a certain luminance level of the ambient light the colors displayed on the CRT appear as the light emitted from the source (light source color mode). By gradually decreasing the CRT luminance, the brightness of the color changes and begins to appear like an object placed in the room (object color mode). This situation is expressed by the concept of the recognized visual space of illumination (RVSI)[3-5].

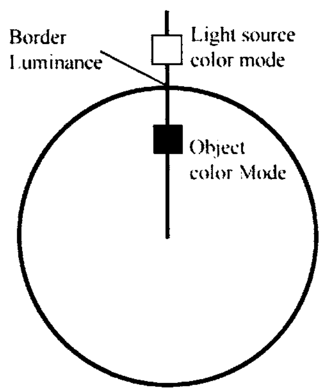

Fig. 1 Scheme of RVSI and the limit of appearance color mode

When one comes to a space he/she immediately understands how the space is illuminated. The state is expressed as that the person constructed the RVSI in his or her brain for a space. The RVSI is schematically expressed by a circle, as shown in Fig.1. The radius indicates the brightness size of illumination. The brightness size of the RVSI is small when the observer recognize the illuminance in the dimly room and the size become large when the observer recognizes it in the brighter room. The color displayed on the CRT is brighter than the room, which is expressed by a certain point outside the circle, as shown by the open square in Fig. 1. The apparent lightness of color surface appears unnaturally bright unlike the appearance of an object in the room, due the fact that it appears like an object light emitting light. When the luminance of the surface is gradually decreasing, it is getting dimmer and is beginning to appear like an object color. Finally, the appearance of the light emitted from the CRT looks like an object place in the room.

The CRT luminance at the transition of appearance mode is the border luminance of RVSI for CRT. Interestingly, the border luminance of CRT is related to the chromaticity of stimulus and the size of RVSI is proportional to the room illumination[6]. The border luminance of RVSI of the CRT monitor can be used in many applications. Any display image on CRT needs to see as the real object. This research indicated how high the luminance of the CRT display should be for the object color appearance mode. The suitable RGB code values for displaying color in object mode at that room illumination were obtained from the experiment.

This experiment measured the border luminance of 47 color stimuli displayed on the CRT in two illumination levels of ambient light and compared the border luminance obtained at two different conditions, so as to investigate the effect of chromaticity and illumination level of surrounding on the CRT color.

2. EXPERIMENT

2.1 Apparatus and Stimulus

The experimental booth divided into two rooms: the observer's room (OR) and the test room (TR), as shown in Fig. 2. The OR room was decorated as a normal living room, and was illuminated by the fluorescent lamps that controlled by a rotary switch such that their luminance could adjusted to any level. The TR was covered with a black cloth to create a complete darkness room. The size of rectangular aperture located between the OR and the TR was 2 cm. X 2 cm., subtended 1° viewing angle, and was located at 126.5 cm high from the floor which was the observer's eye level.

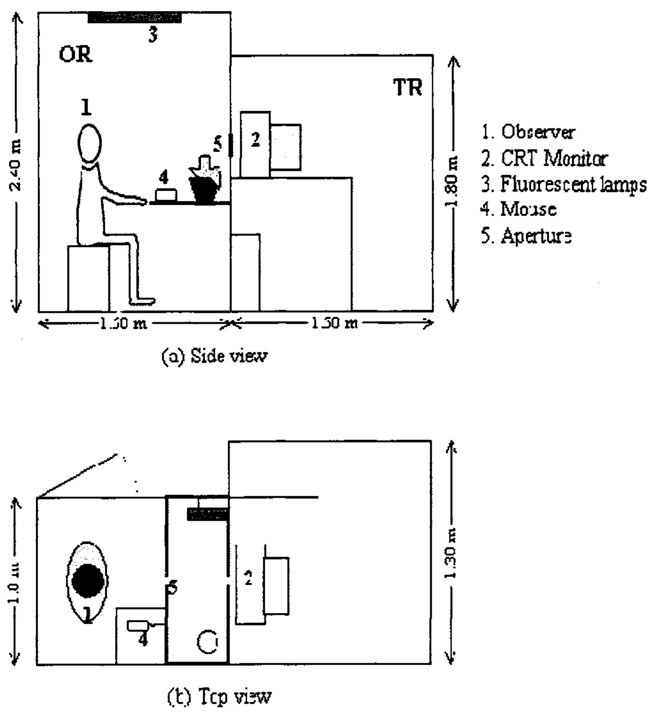

Fig.2 The Experimental Booth

The experiment was conducted using an LG-550D CRT color monitor. The CRT was set to the optimum level of brightness[7] and the GOG[8,9] model was used to characterize the monitor. The 47 test color stimuli were displayed on the monitor. The chromaticity diagram of the stimuli was shown in Fig.3. The colors were chosen to cover the monitor color gamut.

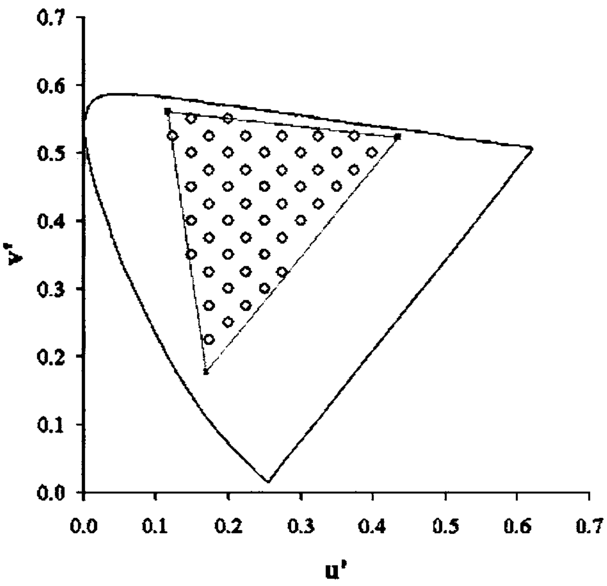

Fig.3 Color test stimulus chromaticity

2.2 Conditions, Subject and Procedure

The observer's room was illuminante with fluorescent lamps of daylight type. They having the color temperature and (u',v') Chromaticity of approximately 5000K and (0.207,0.488), respectively. Two illuminance levels were investigate in this experiment: 5 and 50 lux, respectively.

Six subjects with no deficiencies in color vision, i.e. NJ(25, male), PP(24, female), PS(25,male), WU (24, female), KJ(22,female), YT(25,female) took part in the experiment. Each subject repeated the determination for each test chart for ten times in a separated session.

The subject was in observer's room, before conducting the experiment, they were allowed to adopt to the lighting condition for minutes. They were asked to look at the color stimuli through the square aperture on the wall, then adjust the luminance of CRT (brightness of color stimulus) via a mouse or a keyboard. The task was to decrease the lightness slowly until the appearance of color reached the transition point, in which the color starts to appear like an object in the room. The observer would stop the task at this point. The data were collected.

The experiment was repeated ten times for each test stimulus in separated sessions. The data of six observers were collected and the border luminance of RVSI was obtained by calculation.

3. RESULTS AND DISCUSSION

To determine the border luminance of each stimulus on the CRT monitor, the experiment involving six subjects adjusting brightness of the CRT monitor to obtain the transition point was carried out. Each subject examined the 47 color stimuli under the 5 and 50 lux illumination conditions.

The border luminance represents the lower limit of stimulus luminance, where by the subject perceived unnatural appearance. The CRT light emission begins appearing like an object place in the room. When the luminance of stimulus was lower than the border, the appearance mode changed (from the light source color mode to the object color mode). Fig. 4 shows the results obtained from the subject NJ for 47 stimuli. The results for the OR illuminated 5 lux and 50 lux were represented by open circles and filled circle, respectively. The curves show that the borders of RVSI change individually depending on the test colors. The borders of 50 lux condition are higher than 5 lux condition in all cases. This suggests that the size of RVSI depend on illumination conditions in the room. At higher levels, the border luminance of the CRT was higher than that at the lower levels.

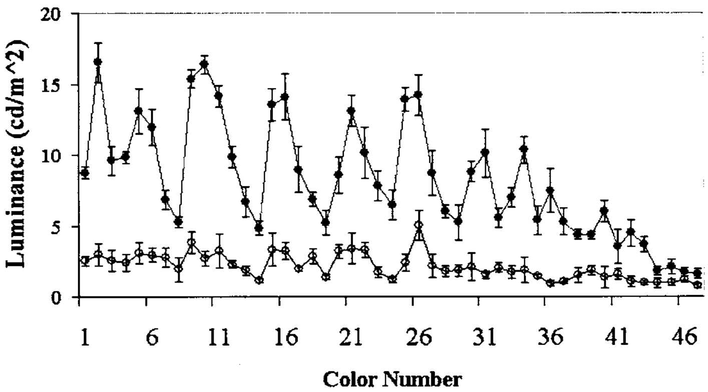

Fig. 4 The border luminance by subject NJ at 5 lux condition (open circle) and 50 lux condition (filled circle)

Each point in Fig. 4 is the average of ten determinations and the vertical lines are the standard deviations. The standard deviations of 5 lux condition was found to be smaller than those of the 50 lux condition. This is because, at 5 lux, the room was dim resulting in low colorfulness of the object in the room.

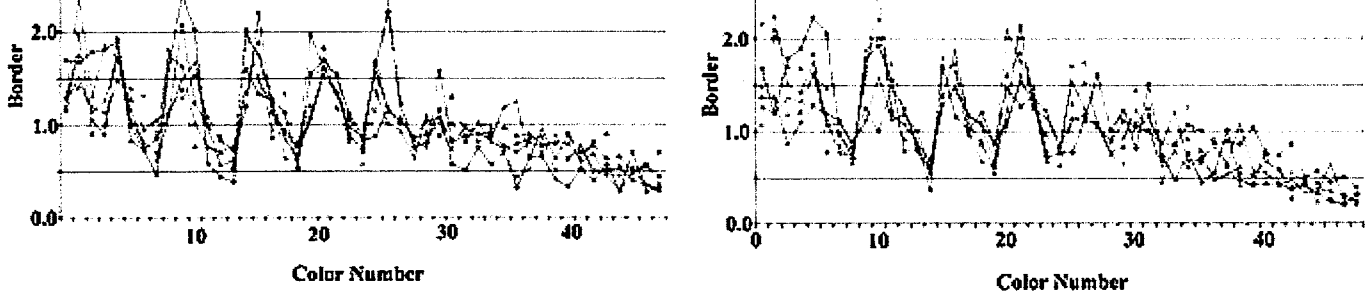

Fig. 5 the borders of RVSI of six subjects were grouped and shifted vertically by average of each subject coinciding with total average. The left chart shows the result from 5 lux room and the right from 50 lux room.

The results from all six subjects are compared in Fig. 5 by grouping them with the normalized method in vertical direction. The results showed that the shape of all curves are similar; on the other hand, the perception of the subjects was the same for most of color stimuli and slightly different for some colors. Fig. 6 shows, contour plots of average data from all subjects for two conditions. In the figures also show the chromaticity-coordinate of fluorescent lamp, that used in the observer room. The stimuli, which have the chromaticity-coordinate near the source coordinate, will have high border luminance. The border luminances were found to be low in the region of saturate color, especially pure red and pure blue. Moreover, the stimuli having low border luminances would also have small standard deviations. The result mentioned above should be refer to the CIE u'v' UCS diagram, which showed in Fig. 6

The border luminances are also plotted as a function of CIE u' chromaticity, as shown in Fig. 7. At a u' chromaticity of 0.207 (u' of the room's light source) the border luminance of test stimulus have high values.

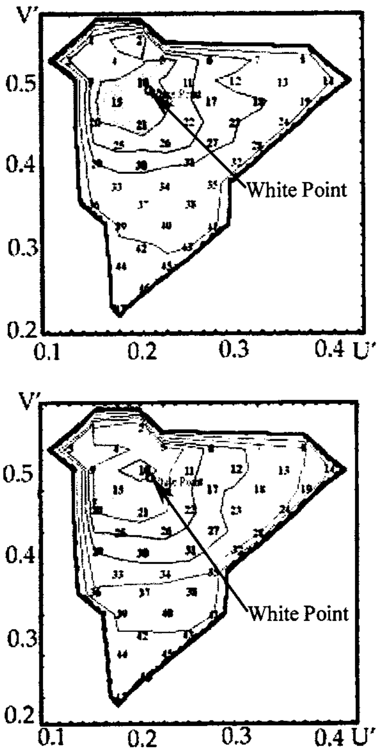

Fig. 6 Contour plots of border luminance as a function of u' and v' chromaticity : (a) 5 lux; (b) 50

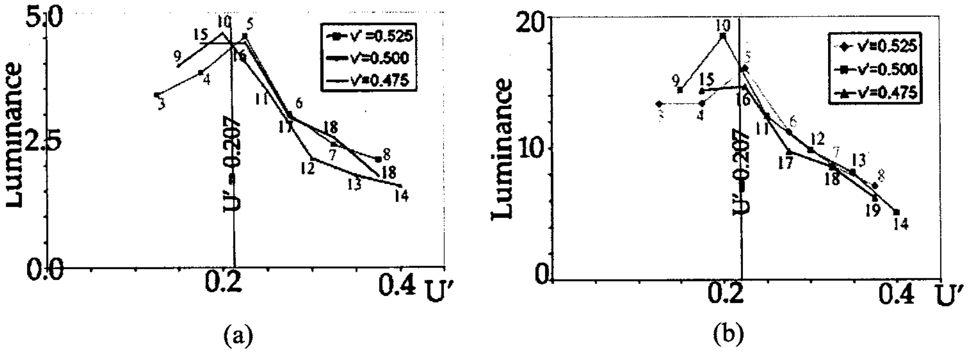

Fig. 7 Plots of border luminance as a function of u'. The numbers as shown in the chart correspond to the number of test stimulus: (a) 5 lux condition; (b) 50 lux condition.

From the border luminance data, using the inverse GOG model, the RGB code values of the border for 47 stimuli were obtained. The results are plotted in Fig. 8 showing the upper limit of the RGB values that displays the object color mode on CRT monitor. If the RGB values are less than these values the color appears in the object color mode. If the RGB values are higher than the RGB of the border, the CRT color is in the light source color mode. Note that, the upper limit of the appearance mode depended on the illumination of the observing room. For example, the limit of 50 lux was higher than that of 5 lux. The RGB border of CRT has specific values for each device, these values are for the CRT using in this experiment. Using an interpolation technique, from the RGB border of 47 test stimuli, the RGB value for every color on monitor can be found. By this method, a user can change the mode of color on the CRT monitor as desired.

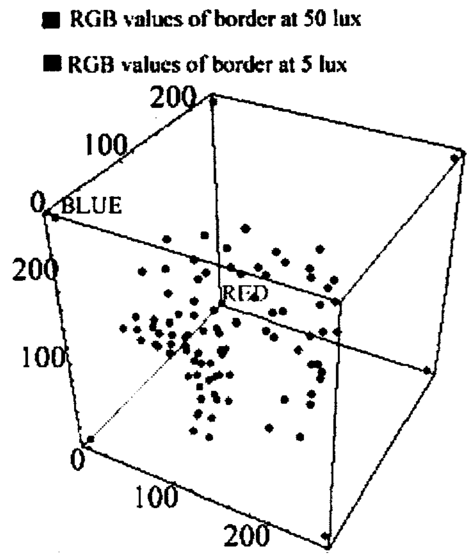

Fig.8 The border luminance of RVSI transform to the RGB code values were plotted on the space. The border was the transition point between mode of CRT display.

CONCLUSIONS

The border luminances of RVSI for colors on a CRT were obtained by determining the transition point of appearance mode from light source color mode to the object color mode. It is quite clear from the data from all subjects that the border at 50 lux observer's room illumination was higher than 5 lux condition. This can be concluded that the room illumination limited the transition point of appearance mode. The high border luminance was found in the test stimuli having the colorimetric values close to those of light source illuminated in the observer's room. More saturated color had lower border luminance. The result implies that the color displayed on the CRT can be changed their appearances depending on the illumination's condition of the room. In other words, the chrometicity of light in the room influences the color appearance of the CRT monitor. The change of the chromaticity of illumination in the observer's room may change the tendency of the border luminance on CRT display.

The results of experiment show the tendency of the border luminance for every color region corresponds to the chromaticity diagram and monitor gamut. This can help users to select the color and the luminance of CRT for displaying so that images will look like the real object, rather than self-luminance object. Also for the color reproduction from a CRT to a print, the data can establish the same color appearance mode. Users can change the mode of color appearance of the CRT by considering the RGB border luminance, i.e. increasing the RGB value more than the border value for the light source color mode and decreasing the RGB value less than the border value for the object color.

REFERENCES

1. Brainard, D. H. and Ishigawa, K. Factors Influencing the Appearance of CRT colors. *Recent Progress in Color Science* (1997): 114-118.
2. Choh, H. K., et al. Effect of Ambient Illumination on Appearance of CRT colors. *The 4th Color Imaging Conference: Color Science, System and Application* (1997): 224-226.
3. Ikeda, M., Shinoda, H. and Mizokzmi, Y. Three Dimensionality of the Recognized Visual Space of Illumination Proved by Hidden Illumination. *J. Optical Review* 5, 3 (1998): 200-205.
4. Ikeda, M., Shinoda, H. and Mizokzmi, Y. Phenomena of Apparent Lightness Interpreted by the Recognized Visual Space of Illumination. *J. Optical Review* 5, 6 (1998): 380-386.
5. Thiangthangtum, Y. *Color Mode Change of Color Charts*. Unpublished Master's Thesis, Chulalongkorn University, 2000.
6. Yamaguchi, H., Shinoda, H. and Ikeda, M. Size of Recognized Visual Space of Illumination Influenced by Color Scheme of Interior. The 9th Congress of the International Color Association (2001): 347-350.
7. Seungok, P., Hongsuk, K. and Jungki, B. Optimum Brightness Level and Simplified Characterized of CRT Color Monitor. *Col. Res. Appl.* 25, 6 (2000): 408-415.
8. Bern, R. S. Gorzynski, M. E. and Motta, R.J. CRT Colorimetry. Part I : Theory and Practice. *Col. Res. Appl.* 16, 2 (1991): 72-80.
9. Brainard, D. H., Pelli, D.G., and Robson, T. Display characterization. *The Encylopedia of Imaging Science and Technology*. J. Hornak (ed.), Wiley. (2002) 172-188.

Similarity Measurement for Images Judged by Human Subjects

S. M. Lee[1], J. H. Xin[1], S. Westland[2]

1. Institute of Textiles and Clothing, The Hong Kong Polytechnic University, Hung Hom, Kowloon, Hong Kong
2. Colour and Imaging Institute, University of Derby, Derby, United Kingdom

ABSTRACT

The wide spread use of image attracts extensive studies in image indexing and retrieval in recent years. With dynamic growth of digital communication, the retrieval of image from thousands to millions of database is becoming a difficulty. There is an urgent need for an effective image similarity algorithm for a search engine or system, which can retrieve images quickly on demand.

Image similarity measurement plays a key role in developing image retrieval system while human visual sensitivity provides the essential elements to construct such similarity algorithm. The response of human depends on a multitude of image features such as the wavelength of visual stimulus and its spatial frequency content. Existing psychophysical data with image samples of synthesized simple grating are unable to fully understand the human judgment and realize human perception of the real world. A breakthrough in image similarity research was realized by conducting a psychophysical experiment to investigate human judgment in similarity of real images of complex scenes. These psychophysical data were used to check the validity of the image similarity algorithm.

There is limited literatures focus on evaluating image similarity models in evaluating efficiency in indexing and measure similarity of complex images. This article presents a study in evaluating the similarity measurements of complex images and their feasibility in predicting human judgment in image similarity. Spectral-wise including CIELAB and Histogram Intersection whist spatiochromatic-wise S-CIELAB were evaluated and compared.

INTRODUCTION

The dramatic growth of digital color imaging industry has led to an urgent need to measure global appearance differences between two images so as to develop an effective image similarity algorithm for a search engine or system, which can retrieve images quickly on demand.

Typical approaches to image characterization and recovery have focused on spectral information but ignored spatial information. Mehtre et al. defines color image indexing and retrieval as: "Assume that there are a large number of color images in the database (Mehtre et al., 1995). Given a query image, we would like to obtain a list of images from the database which are "most" similar in color to the query image". In defining an effective color image retrieval strategy, two aspects must be considered: i) the features (index terms) representing the color information, and ii) the method measuring the similarity between the features of two images. Histogram Intersection is a critical element for indexing spectral information to develop IR. Most similarity models are based on CIE colorimetry. Spectral-wise including CIELAB and Histogram Intersection whist spatiochromatic-wise S-CIELAB (Zhang and Wandell, 1996) were evaluated and compared.

The main cue to improve the design of image similarity model and further the development of image retrieval is to take subjective judgment into account and to have a better prediction of human judgments in image similarity. In order to check their feasibility and validity in predicting human judgment in image similarity of real images of complex images, a psychophysical experiment was conducted. This article presents a study in evaluating the similarity measurements of complex images.

OVERVIEW

Color indexing (Swain, 1990) recognizes images or image components based upon histogram distributions of the color of pixels. Color histograms and histogram intersection form the backbone of Swain's method.

Traditional color difference metrics were designed for comparing color difference of homogeneous patches. A typical example, the CIELAB system (CIE 1978) is a well-known and popular international standard for measuring color differences. With complicated combinations of texture and color, digital images are generally complex scenes and they are too sophisticated to be measured by such simple pixel-by-pixel color difference metric.

The Spatial-CIELAB (S-CIELAB) system extends the CIELAB color metric to solve this problem. The S-CIELAB model applies a spatial filtering operation to the color image so as to simulate the spatial blurring by human visual system. This spatial filtering operation is separated from the CIELAB system, for the independency between color transformation and spatial structure of images and between the spatial convolution and the color of images. Therefore, this spatial processing phase can be treated as a pre-processing to the existing CIELAB system. Thus, S-CIELAB can simplify to a CIELAB color difference metric when measuring images of large uniform fields.

EVALUATIONS

A set of 180 complex images were under investigation in this paper. As S-CIELAB emphases its property in simplifying to a CIELAB color difference metric and holds promise to a smooth prediction transition from homogeneous to textures images, we used images of randomized-smooth linoleum patterns so as to test its smoothness in transition. Another reason of using these smooth patterns is to make fairer comparisons to these three models. Nine observers involved in the psychophysical experiments to make totally 1620 observations. In each observation, two images among the 180 samples were randomly selected and display in front of the observers. Observer's task was to judge the image difference by assigning a category of 1 to 5, representing extreme different to no different. Therefore, all image pairs were assigned with a category by observers. Comparisons of the performance between Histogram Intersection, CIELAB, and S-CIELAB in fitting these psychophysical results check their feasibility and validity in predicting human judgment in image similarity of real images of complex images.

The S-CIELAB show promise to the assumption that the spatial pre-processing can simulate the spatial colour sensitivity of human vision. The results prove that applying spatial processing can improve the efficiency to fit human judgment in similarity between complex images. One-way ANOVA was implemented to analyse the results. The results of F-test are tabulated in Table 1.

Table 1 Summary Table for One-way ANOVA

	F-VALUES
Histogram Intersection	167.464
CIELAB	253.843
S-CIELAB	254.419

The larger the F-value, the higher the differentiation power of the model, among the five categories judged in 1620 observations. Comparing performance of Histogram Intersection with the F-values, the S-CIELAB model performed better in predicting human judgment than CIELAB. As the images we used are spatially smooth, it is expected that this improvement would not be very significant, but satisfactory. It is ironical to note that Histogram Intersection, the most popular cue for IR, performs the worse among other models.

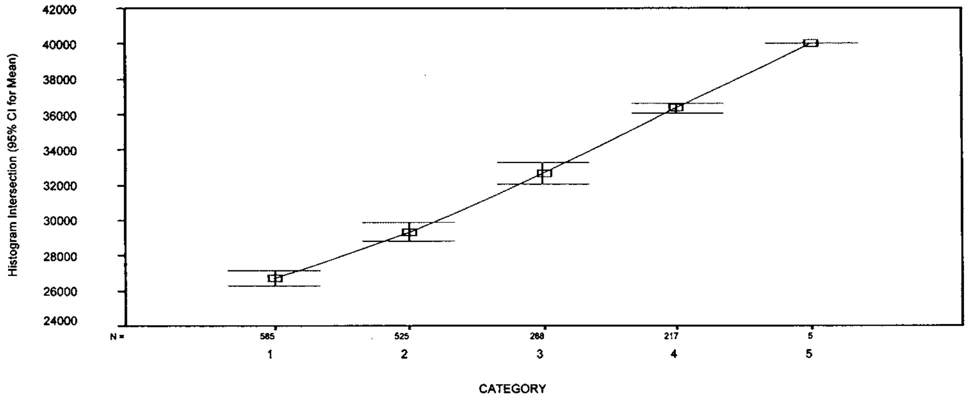

Fig. 1 Relationship between Histogram Intersection and Observer Judgments in Categories

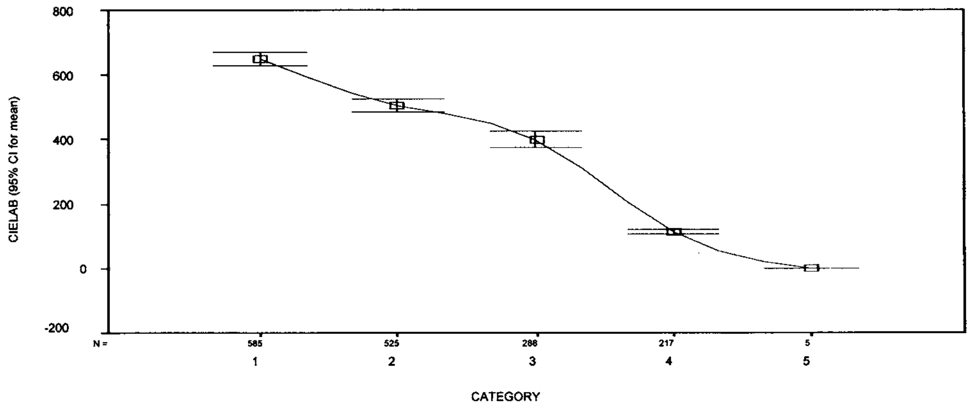

Fig. 2 Relationship between CIELAB and Observer Judgments in Categories

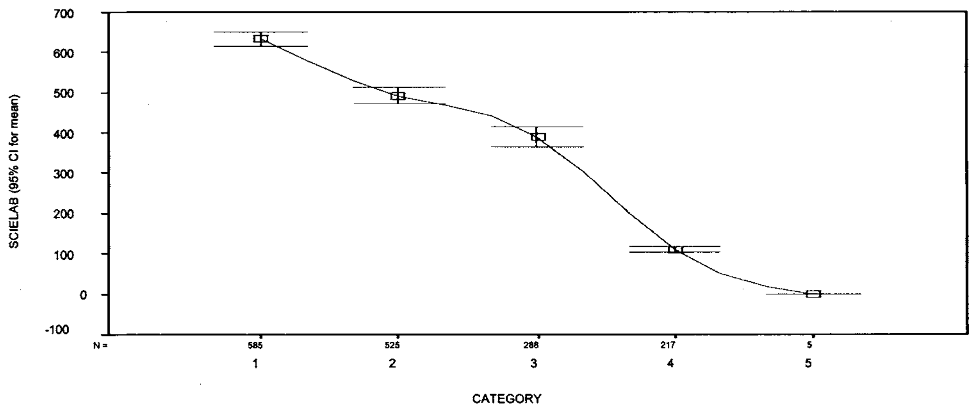

Fig. 3 Relationship between S-CIELAB and Observer Judgments in Categories

The trend-lines of the above charts illustrate that image pairs are evenly distributed in each category. Objective measurements of the differences between images (Histogram Intersection, CIELAB and S-

CIELAB) compare with the subjective judgments by observers (Category). Identical image pairs are all correctly judged by observers into Category 5.

Histogram Intersection was gradually increased, whilst CIELAB and S-CIELAB were gradually decreased with the Category, which representing the degree of similarity. The larger the values in Histogram Intersection the more similar the image pair is. Its mean differences between Category 3 and Category 4 are much less significant than that of CIELAB and S-CIELAB systems. Numerical mean differences can be found in the below table. This observation supports a psychometric phenomenon that image pairs of very similar in appearance, like images in Category 4 are easy for observers to make judgment. The narrowest range of confidence interval (CI) in Category 4 shows that it is easy for the observers to make judgment when image pairs are very similar.

Table 2 Multiple Comparisons with Tukey's HSD test

	Category (I)	Category (J)	Mean Difference (Category I and J)	Sig. (p-value)
Histogram Intersection	1	2	-2608.385641	7.23865E-14
	2	3	-3333.09625	7.16094E-14
	3	4	-3691.097974	1.03473E-13
	4	5	-3639.912442	0.523452671
CIELAB	1	2	145.8609095	7.16094E-14
	2	3	104.3278674	1.44117E-09
	3	4	286.4434318	7.16094E-14
	4	5	112.8582693	0.789731847
SCIELAB	1	2	140.3602598	7.16094E-14
	2	3	102.502203	1.00853E-09
	3	4	280.6099703	7.16094E-14
	4	5	109.2189927	0.793746024

The results of the Tukey's test showing the differences between means of each category are tabulated in Table 2. According to the above table, the p-values show that the Category 4 does not differ significantly from Category 5, implying that image pairs in Category 4 are very similar and some of them are even as similar as almost the same (Category 5). These results are consistent with the visual similarity between the image pairs.

CONCLUSIONS

The most limitation of the histogram-based approaches is due to the fact that a histogram ignores spatial information; consequently, images with quite a different appearance may be judged similar simply because they have a similar color composition. More importantly, such representations do not capture what are perceived in color images: specific correlations between colors over space produce the percepts of structures, regions, shapes which are not predictable from either treating color as an individual pixel colors or by treating each color in isolation. The histogram describes the global intensity distribution. Several images with very different spatial distributions of gray values may have similar histograms. The global nature of a histogram limits its applicability to complex scenes. It does not exploit the important fact that points from the same object are usually spatially close due to surface coherence.

With limitations of similarity measurement by spectral information, the S-CIELAB model outperforms others in predicting human judgment in image similarity proves that spatiochromatic information should be taken into account. Critical to this work is that human visual sensitivity should also be considered and the complexity of computation should be reduced. Further analysis in difference complex images can be seen in our coming paper.

ACKNOWLEDGEMENTS

I acknowledge with gratitude the Studentship for Research Postgraduate Studies, the facilities and funding of the Hong Kong Polytechnic University, which give a great support to this study.

REFERENCES

1. Swain M. J., (1990) Color indexing, *Technical Report* n. 360, University of Rochester, Rochester, New York.
2. Mehtre B. M., Kankanhalli M. S., Desai Narasimhalu A., Man G. C., (1995) Color matching for image retrieval, Pattern Recognition Letters, **16**, 325-331.
3. Zhang X, Wandell B. A., (1996) A spatial extension of CIELAB for digital color image reproduction, SID'96 Digest, 731-734

Development of Colour Appearance Models

M. R. Luo
Colour & Imaging Institute, University of Derby
Kingsway House, Kingsway
Derby DE22 3HL, United Kingdom

ABSTRACT

Colour appearance modelling has been a popular research area over the years. More recently, it is becoming even more important due to the requirement of cross-media colour reproduction in imaging industry. Before 1997, about 5 colour appearance models were developed. In 1997, CIE recommended one colour appearance model, CIECAM97s, which includes the best features from the earlier models and gives quite satisfactory predictions to the available experimental data. The model was then gone through severe trials. Some shortcomings were revealed and it was further modified. This resulted in a new model, CIECAM02, to replace CIECAM97s. This paper reviews the development of colour appearance models leading to the latest CIECAM02.

INTRODUCTION

The colour appearance of an image changes according to different viewing conditions such as media, light sources, background colours, and luminance levels. This phenomenon causes severe problems in industrial colour control. For example, colour reproduction engineers desire to faithfully reproduce the original presented on a different medium, known as cross-media reproduction. The media involved might include original scenes, transparencies, monitors, photographs or reflection prints. A dress normally seen in daylight might be photographed and appear in a catalogue, possibly under tungsten room lighting generally with a white surround, and also on a VDU screen in a dim lit room. Traditionally obtaining the same appearance requires visual judgement by experienced workers. This process is subjective and expensive. Hence, there has long been a great demand by industrialists for the ability to accurately quantify changes in colour appearance so as to minimise observer dependencies.

Although there are many colorimetric measures such as CIELAB and CIELUV which have recommended by the CIE *(Commission Internationale de l'Eclairage)*[1], these are limited to use under a set of fixed viewing conditions: the two stimuli considered should be presented using identical media and be viewed under the same daylight viewing conditions. These measures would not work on the reproduction of colour appearance across different media. The way to solve the above problem is to apply a standardised colour appearance model, which can accurately predicting the colour appearance of colours under a wide range of viewing conditions.

THE CIE 1997 COLOUR APPEARANCE MODEL –CIECAM97s

Various colour appearance models have been developed in the recent years. At the CIE Expert Symposium '96 *Color Standards for Image Technology*, held in Vienna in 1996 [2], there was great demand by the industrialists to ask the CIE to recommend a particular colour appearance model for industrial application. Four colour appearance models were considered to be most promising: Hunt [3,4], Nayatani [5], RLAB [6] and LLAB [7]. Agreement was achieved that researchers should examine the existing colour appearance models, try to combine the best features of these models into a high performance model for general use, and test its performance against available experimental data. It was also agreed that the model should be available in a comprehensive version, and in a relatively simple version for use in limited conditions. It is worthwhile to mention that CIECAM97s was developed to follow the 12 principles set by Hunt in 1996 [2]. These are:

1. To cover comprehensive functions in order for the model to be used in a variety of applications.
2. To cover a wide range of stimulus intensities by setting a maximum in the dynamic range.
3. To include the rod vision for stimuli viewed under very low scotopic levels.
4. To predict appearance against backgrounds of different luminance factors, and simplified surround conditions: average (such as prints, textiles), dim (such as broadcast television) and dark (projected images).
5. To have a linear transform from the CIE standard colorimetric observers to the spectral sensitivities of the cones, and the $V'(\lambda)$ curve should be used to approximate rod vision.
6. To include an incomplete chromatic adaptation factor between complete and no adaptation.
7. To predict a wide range of percepts: hue angle, hue composition, brightness, lightness, colourfulness, chroma and saturation. All these percepts are important in certain applications.
8. To include a forward and a reverse mode. This is particular important in colour management systems for imaging applications.
9. To be no more complicated than is necessary to meet the above requirement.
10. To have two models for dealing with all possible and limited (but most frequent) applications respectively.
11. To perform better than or equal to the existing best colour appearance models in predicting the available experimental data sets, i.e. the LUTCHI data [8-13] and chromatic adaptation data sets [14].
12. To be available for application to unrelated colours such as those seen in dark surrounds in isolation from other colours. In addition, the model should be able to predict the simultaneous colour contrast effect.

The majority of the above principles were successfully achieved. At its meeting held in Kyoto in 1997, CIE Technical Committee TC1-34 *Testing colour appearance models* agreed to adopt a simple version, which is named CIECAM97s [15,16]. The 's' stands for the 'simple'. The inclusion of the year 97 in the designation is intended to indicate the interim nature of the model, depending upon the availability of better models expected to emerge in the future. It is recommended that the model should be applied for colour image processing to achieve successful colour reproduction across different media such as prints, monitors and transparencies. It should be pointed out that the adjective 'simple' is relative. The model is simple in the sense that various features which should be included in a comprehensive model were not considered.

The structure of the CIECAM97s is given in Fig. 1. The input parameters include x, y and Y of sample under the test illuminant and a set of viewing parameters: x_w, y_w and Y_w of the reference white under the test illuminant, the luminance factor of background, the luminance of the reference white together with parameters defining the surround conditions. The model comprises five parts: a *cone response transform* to convert the colorimetric values to *RGB cone* signals via a matrix transform, a *chromatic adaptation transform* to predict the corresponding colour from the test to reference illuminant, a *dynamic response function* to predict the extent of changes of responses according to different luminance levels, *colour and achromatic signal processes* to obtain various perceptual attributes and *colour spaces* formed by the combinations of different perceptual attributes.

The perceptual attributes predicted by CIECAM97s are described below.

Brightness (Q)	*a visual sensation according to which an area appears to exhibit more or less light.*
Lightness (J)	*the brightness of an area judged relative to the brightness of a reference white*
Colourfulness (M)	*a visual sensation according to which an area appears be more or less its hue*
Chroma (C)	*the colourfulness of an area judged as a proportion of the brightness of a reference white*
Saturation (s)	*the colourfulness of an area judged in proportion to its brightness*
Hue (H or h)	*the attribute of a visual sensation according to which an area appears to be similar to one, or to proportions of two, of the perceived colours red, yellow, green and blue*

The CIECAM97s model predicts many visual phenomena. These are given below.

Chromatic adaptation	*change of colour appearance from one illuminant to the other*
Steven effect	*change of brightness contrast due to different luminance levels*
Hunt effect	*change of colourfulness due to different luminance levels*
Surround effect	*change of appearance due to different surround conditions*
Lightness contrast effect	*change of lightness due to the luminance factors of backgrounds*

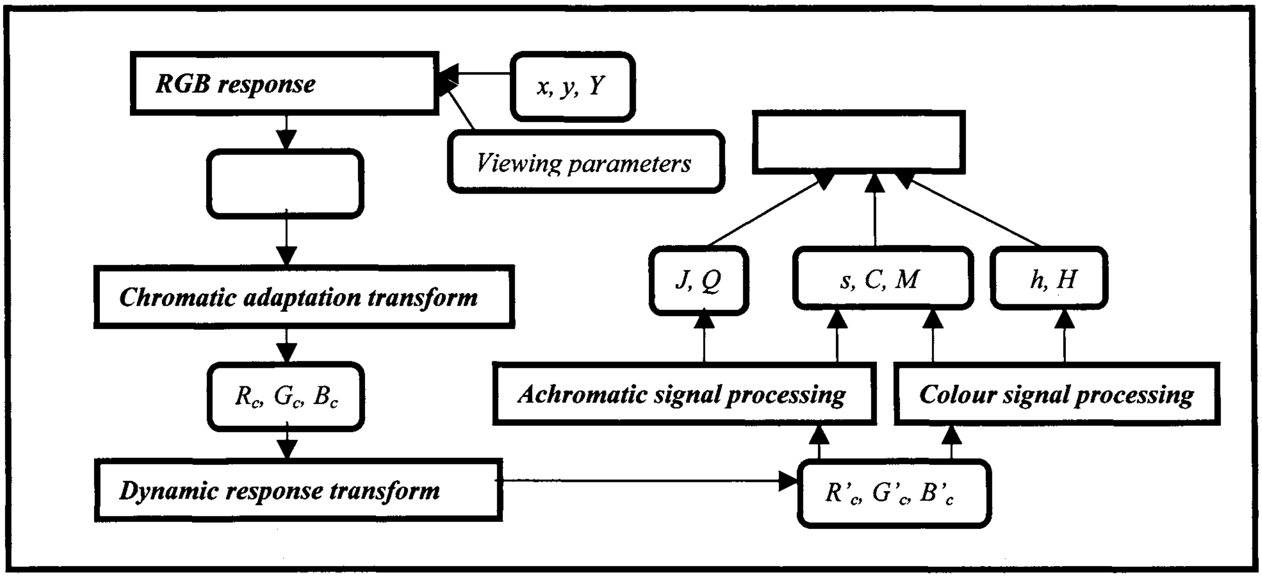

Fig. 1 The structure of CIE colour appearance models

THE CIE 2002 COLOUR APPEARANCE MODEL -CIECAM02

Since the publication of CIECAM97s [15] in 1997, the model has been extensively tested. Although it performs well in many areas dealing with digital colour imaging, some shortcomings[17-23] were found. These were reported to the CIE Technical Committee, TC8-01 *Colour Appearance Models for Colour Management Applications.* In 2002, a new colour appearance model [24], CIECAM02, was recommended. It has the same structure, perceptual attributes and visual phenomena of CIECAM97s but includes many improvements in predicting available data and some simplifications. The revisions are:

1. a revised lightness scale *(J)* giving a zero lightness when Y value is zero under all surround conditions,
2. a change of chromatic induction factor *(N_c)* from 1.05 to 0.95 for the dim surround application to ensure a smooth transition of the factor from average, dim to dark surround conditions,
3. a linear chromatic adaptation transform to remove the power factor for calculating blue response in the original transform and to predict the available data more accurately,
4. a new non-linear dynamic response function to ensure an invariant of saturation and hue for colours having a given chromaticity but changes of Y tristimulus value,
5. a new chroma scale *(C)* to ensure small values for near neutral colours,
6. a new saturation scale *(s)* to improve the prediction to the newly accumulated experimental data,
7. a relationship between c and N_c parameters was established to allow for intermediate surround conditions,
8. a simplification of the calculation of incomplete adaptation factor *(D)*,
9. a simplification of the calculation of eccentricity factor *(e)*.

The CIECAM02 has also been tested using various data sets [25]. The results from two revised scales are given here to illustrate the extent of improvements. The first is a new chroma scale, which is illustrated in Figs. 2a, 2b and 2c by plotting the Munsell Chroma data against the predictions from CIECAM97s, CIELAB and CIECAM02, respectively. In each plot the 45^o and best-fit lines are also shown. For perfect agreement, the points should be coincident with the 45^o lines. Fig. 2a clearly shows a too high prediction from CIECAM97s for colours that are close to neutral with Munsell chroma near zero. For colour reproduction it is important to reproduce near neutral colours accurately. The intercepts on the vertical axes of the best-fit lines in Fig. 2 are a measure of how well the models predict the chroma of near neutral colours; ideally the intercepts should always be zero. These intercepts are 0.6, 1.5 and 0.1 in Munsell Chorma unit for CIECAM02, CIECAM97s and CIELAB, respectively. It is thus clear that the CIECAM02 intercept is much better than that of CIECAM97s and gives the least spread of the data amongst the three models studied.

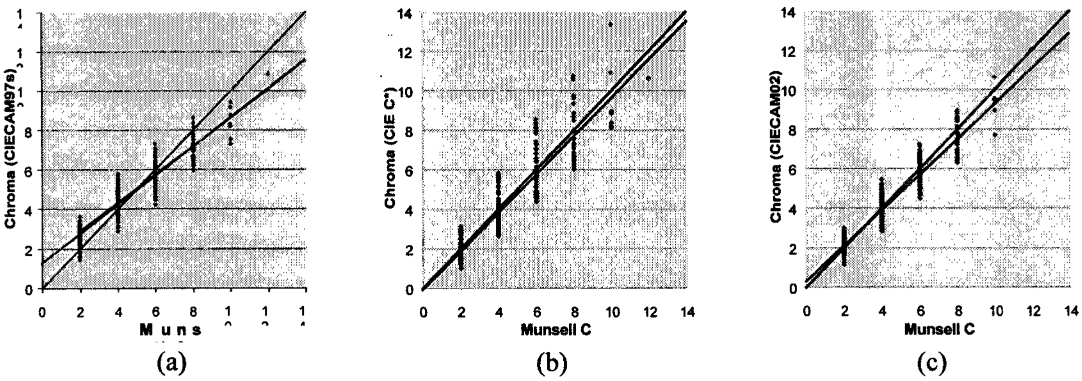

Fig. 2 The chroma predictions from (a) CIECAM97s, (b) CIELAB, and (c) CIECAM02 plotted against Munsell chroma.

Another example is to show the improvement for solving a shortcoming in the CIECAM97s saturation scale, i.e. large changes in saturation occur for colours having a given chromaticity but different Y values. This is illustrated in Figs. 3a and 3b, for values of the adapting luminance, L_a, equal to 2 and 2000 cd/m^2, respectively. (The colour used had $x = 0.3618$ and $y = 0.4483$, the reference white having $x = 0.3127$, $y = 0.3290$, and $Y = 100$.) It can be seen that the saturation scale ($s_{CIECAM97s}$) of CIECAM97s predicts very large variations for different Y values. However, there is almost no change for the saturation scale ($s_{CIECAM02}$) of CIECAM02.

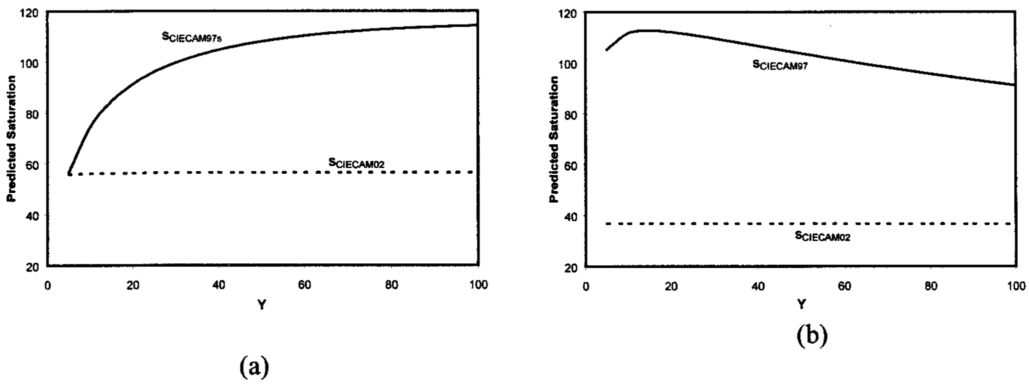

Fig. 3 The change of saturation with changes in luminance factor for a typical color as predicted by CIECAM97s ($s_{CIECAM97s}$) and CIECAM02 ($s_{CIECAM02}$) for adapting luminance at L_a of (a) 2 cd/m^2 and (b) 2000 cd/m^2.

CONCLUSIONS

Colour appearance has been a popular research area in recent years due to the need for successful colour image reproduction across different media and viewing conditions. This led to the accumulation of various colour appearance data sets and the development of colour appearance models. This paper reviews the development of colour appearance models. Particular attention was paid to the two CIE colour appearance models, CIECAM97s and CIECAM02. The latter is expected to be officially adopted by the CIE to replace the earlier CIECAM97s.

REFERENCES

1. CIE, Publ. No. 15.2, Colorimetry, 2nd Ed., Central Bureau of the CIE, Vienna, Austria (1986).
2. CIE, Proceedings of the CIE Expert Symposium '96 Colour Standards for Image Technology, CIE Publ. No. x010-1996, Central Bureau of the CIE, Vienna, Austria (1996).
3. R.W.G. Hunt, Revised colour-appearance model for related and unrelated Colours, *Color Res. Appl.* **14** 146-165 (1991).
4. R.W.G. Hunt and M. R. Luo, An improved predictor of colourfulness in a model of colour vision, *Col. Res. & Appl.*, **19** 23-26 (1994).
5. Y. Nayatany, H. Sobagaki, K. Hashimoto and T. Yano, Field trials of a nonlinear color-appearance model, *Col. Res. Appl.* **22** 240-258 (1997).
6. M. D. Fairchild, Refinement of the RLAB color space, *Color Res. Appl.* **21** 338-346 (1996).
7. M. R. Luo, M. C. Lo and W. G. Kuo, The LLAB(l:c) colour model, *Col. Res. Appl.* **21** 412-428 (1996).

8. M. R. Luo and R. W. G. Hunt. Testing colour appearance models using corresponding-colour and magnitude-estimation data sets, *Color Res. Appl.* **23**, 147-153 (1998).
9. M. R. Luo, A. A. Clarke, P. A. Rhodes, A. Schappo, S. A. R. Scrivener, and C. J. Tait, Quantifying color appearance: Part I – LUTCHI colour appearance data, *Color Res. Appl.* **16**, 166-180 (1991).
10. M.R.Luo, X.W.Gao, P.A.Rhodes, H.J.Xin, A.A.Clarke, and S.A.R.Scrivener, Quantifying colour appearance: Part III - Supplementary LUTCHI colour appearance data, *Color Res. Appl.*, **18**, 98-113 (1993).
11. M. R. Luo, X. W. Gao, P. A. Rhodes, H. J. Xin, A. A. Clarke, and S. A. R.S crivener, Quantifying colour appearance: Part IV- Transmissive Media, *Color Res. Appl.*, **18**,191-209 (1993).
12. W. G. Kuo, M. R. Luo, and H. Bez. Various chromatic-adaptation transforms tested using new colour appearance data in textile, *Color Res. Appl.* **20**, 313-327 (1995).
13. L. G. Juan and M. R. Luo. Magnitude estimation for scaling saturation. *Proc. 9th Session of the Association Internationale de la Couleur (AIC Color 2001), Rochester, USA* , (June 2001), Proceedings of SPIE vol. 4421, 575-578 (2002).
14. M. R. Luo and R. W. G. Hunt, A chromatic adaptation transform and a colour inconstancy index, *Color Res. Appl.*, **23** 154-158 (1998).
15. CIE Publication 131, The CIE 1997 Interim Colour Appearance Model (Simple Version), CIECAM97s, (1998).
16. M. R. Luo and R. W. G. Hunt, The structures of the CIE 1997 colour appearance model (CIECAM97s), *Color Res. Appl.*, **23**, 138-146 (1998).
17. N. Moroney, A comparison of CIELAB and CIECAM97s. *Proceeding of the Sixth Color Imaging Conference: Color Science, Systems, and Applications*, 17-21 (1998).
18. T. Newman and E. Pirrotta, The darker side of color appearance models and gamut mapping, *Colour Image Science 2000*, University of Derby, 215-223 (2000).
19. C. J. Li, M. R. Luo, and R.W. G. Hunt. A revision of the CIECAM97s Model, *Color Res. Appl.*, **25**, 260-266 (2000)
20. M. D. Fairchild. A revision of CIECAM97s for practical applications, *Color Res Appl.*, **26**, 418-427 (2001).
21. C. J. Li, M. R. Luo, B.Rigg and R. W. G.Hunt, CMC 2000 Chromatic Adaptation Transform, CMCCAT2000, *Color Res. Appl.*. **27**, 49-58 (2002)
22. R. W. G. Hunt, C. J. Li, G. Juan and M. R. Luo, Further refinements to CIECAM97s, *Color Res. Appl.*. **27** 164-170 (2002).
23. R. W. G. Hunt, C. J. Li, and M. R. Luo, Dynamic cone response function for models of colour appearance, *Color Res. Appl.*. **28** 82-88 (2003).
24. N. Moroney, M. D. Fairchild, R.W.G. Hunt, C Li, M. R. Luo and T. Newman, The CIECAM02 Color Appearance Model, The tenth Color Imaging Conference, IS&T and SID, Scottsdale, Arizona, 13-15 November, 23-27 (2002).
25. C. J. Li , M. R. Luo, R. W. G. Hunt, N. Maroney, M. D. Fairchild and T. Newman, Comparing Colour Appearance Models, The tenth Color Imaging Conference, IS&T and SID, Scottsdale, Arizona, 13-15 November, 28-32 (2002).

Colour Image Quality Assessment using the CIECAM97s Model

Andrew N. Chalmers & Snjezana Soltic

Department of Electrical and Electronic Engineering
Manukau Institute of Technology, Auckland, New Zealand

E-mail: chalmers@manukau.ac.nz, ssoltic@manukau.ac.nz

ABSTRACT

This paper investigates the correlation between subjectively-evaluated image quality and a proposed set of quality metrics derived from digitized image data using the colour appearance attributes of the CIECAM97s colour appearance model. A display-system model has been included since the purpose is to model the appearance of image colours reproduced on the display. The mean and standard deviation of CIECAM chroma (or alternatively CIECAM saturation) are shown to be suitable metrics.

Keywords: image colour appearance, colour display system, colour appearance model.

1. INTRODUCTION

The general objective of this work is to develop predictors for subjective colour preferences in image reproduction, in order to facilitate the automation of image colour quality enhancement. Work by De Ridder *et al* [1, 2] has concluded that the CIELUV chroma difference and chroma scatter (as measured by the standard deviation) can together serve as a measure of perceived naturalness and image quality.

The present investigation tests the prospects of developing an image colour quality metric from the various appearance attributes predicted by the CIE colour appearance model CIECAM97s.

1.1 Background

The colour images used in this study were originally created as a video sequence for the judgement of the suitability of different light sources for scene illumination in television production [3]. Each test image was made under a different test light-source, and was presented alongside a reference image by making use of a vertical split-screen effect. The reference images were taken under standard (tungsten-halogen) studio illumination. Two test objects were used in each test – a Macbeth ColorChecker® test chart, and an ink-printed portrait.

For each test image, the video camera controls were adjusted by an expert operator to yield the best possible approximation to true grey-scale rendition. In general, therefore, there was little difference in the lightnesses of the test and reference halves of each test image – but, in some cases, there were significant differences in chromatic content. The colour deviations in the test images are regarded as representative of the types of colour errors that may typically occur under uncontrolled conditions in colour photography.

The test scenes in the video sequence were judged by a panel of 25 observers for the perceptibility and acceptability of the colour deviations in the test images; and their responses (based on two grading scales) have been used to formulate a "mean subjective rating" (MSR) [3].

1.2 New Work

The video images have now been digitized, and their colour content examined by use of digital image analysis techniques. This work has utilized the CIE colour appearance model CIECAM97s [4] to simulate the viewing conditions that existed in the original experiment – permitting the computation of the colour appearance of each significant colour region. Because of the volume of data, it has been most practical to work with overall measures, such as averages and standard deviations – and this paper will show the degree of correlation of these quantities with the previously assessed MSR.

The following metrics have been proposed as potential candidates for the estimation of image colour quality:

i). Average CIECAM saturation or chroma

ii). Standard deviation in CIECAM saturation or chroma

iii). Average difference in CIECAM saturation or chroma between test and reference colour patches in the images.

The proposals under items i) and ii) are investigated for their suitability for use in automated image colour quality optimization in electronic photographic systems. It is recognized that the proposals under iii) are unlikely to be a practical proposition since their implementation would require the existence of a comparison (reference) image which would not normally be available in general picture-taking applications – but they have been included here for academic interest since the data were available.

2. MODELLING THE APPEARANCE OF DISPLAYED COLOURS

2.1 The Display System

The images in the original experiment were displayed on a television picture tube for the subjective tests that led to the formulation of the MSR. In this investigation, therefore, it is necessary to include the display system in devising a model that attempts to track the MSR.

The cathode-ray tube is an additive colour-mixing device that can be characterized by two stages: a nonlinear transformation stage, and a linear colour-mixing transformation.

2.2 Display Gamma

First there is a nonlinear transformation between the luminance reproduced on the screen and the corresponding input voltage, expressed as:

$$L = V^{\gamma} \quad (1)$$

where L represents the luminance of the screen, V is the normalized voltage, and γ (gamma) represents the nonlinearity of the system.

Monitor gamma has been well documented in relation to the design and operation of broadcast television systems, leading to the implementation of a gamma-correction stage in the television transmission signal processing chain [5]. Hunt [6] has stated that television displays have a gamma of 2.8 ± 0.3.

Modelling of the display gamma has been achieved by use of the transformation:

$$P' = P^{\gamma} \quad (2)$$

where P represents the primary colours R, G, B (respectively) which are the normalized numerical pixel values obtained from the digitized version of the image.

2.3 Display Primaries and White Point

For any pixel within the display, the perceived pixel colour will be the synthesis, in the viewer's eye, of the three primary-coloured luminances produced at that point of the screen. The model for this process is a multiple linear transformation where the set of chromaticities of the red, green and blue phosphors are transformed to device-independent CIE tristimulus values. This transformation is determined by the white point setting of the monitor, as well as the CIE chromaticity coordinates of the red, green and blue phosphors.

In the original experiment, the display white was set to CIE Illuminant C. This was chosen for ease of set-up as an Illuminant C reference source was available and, in each test and reference image, the screen reproduction of the white patch on the Macbeth ColorChecker was set to be a visual match to this reference source. The screen primaries for the monitor in question were specified as conforming to the EBU primaries, and these values [7] have been assumed in formulating the display model.

This combination of primaries and white point leads to the following transformation matrix:

$$\begin{bmatrix} X \\ Y \\ Z \end{bmatrix} = \begin{bmatrix} 0.4514 & 0.3329 & 0.1965 \\ 0.2327 & 0.6887 & 0.0786 \\ 0.0212 & 0.1263 & 1.0348 \end{bmatrix} \cdot \begin{bmatrix} R' \\ G' \\ B' \end{bmatrix} \tag{3}$$

It is planned that a future extension of this work will examine the consequences of different choices of primaries.

2.4 Modelling Colour Appearance

The intention here is to obtain a numerical description of the appearance of the colours on the display, by use of a colour appearance model. Colour appearance models (CAMs) allow the mathematical description and prediction of the appearance of colour stimuli in a variety of viewing conditions.

CIECAM97s is currently the official CIE colour appearance model. It is probably the best general-purpose technique currently available, but it is a relatively complex model. It can predict a number of appearance attributes, including: hue angle (h), chroma (C), saturation (s), colourfulness (M), lightness (J), and brightness (Q).

Input data for this model are as follows:

$[X, Y, Z]$ - the relative tristimulus values of the test stimulus in the source conditions, given by Equation (3).

$[X_W, Y_W, Z_W]$ - the relative tristimulus values of the source white in the source conditions. In this work, these are the tristimulus values of CIE Illuminant C, normalized so as to make $Y_W = 255$.

L_A - the adapting field luminance. In this work, L_A is taken as 70 cd/m^2.

Y_b - the relative luminance of the source background in the source conditions (often taken to be 20%, and this value is used here).

Plus the viewing condition parameters:
c - for the impact of the surround = 0.59 here.
N_c - a chromatic induction factor = 1.10 here.
F_{LL} - a lightness contrast factor = 1.0 here.
F - a factor for degree of adaptation = 0.9 here.

These numerical values have been selected according to the recommendations [4] for the computation of colour appearance for dim surround conditions.

2.5 Complete Model

The input to the model is the *RGB* triplet obtained from the digital image data for the colour being displayed at a specified region. These are converted to *R'G'B'* by applying equation (2), and then to *XYZ* tristimulus values by equation (3). The latter are applied as input to the CIECAM calculation process which produces the outputs C (chroma) and s (saturation) selected for further analysis.

3. TESTING THE MODEL

This Section describes the comparison of the model outputs with the previously obtained MSR values, to investigate the correlation of different metrics with the MSR.

The original video sequence contained a set of 22 test images. In each case a vertical split-screen effect was used to present the test image on the left half-screen, and the reference image on the right. Each test comprised a comparison pair of (test and reference) Macbeth ColorChecker images, immediately followed by a similar comparison pair of portrait images.

3.1 General Procedure

For the present analysis, the Macbeth ColorChecker images were digitized using the on-board frame-grabber of a Silicon Graphics Indy® workstation. The sampling of the ColorChecker colour patches on each digitized image was performed by utilizing a Windows® application package (ImageLab®) which allowed the operator

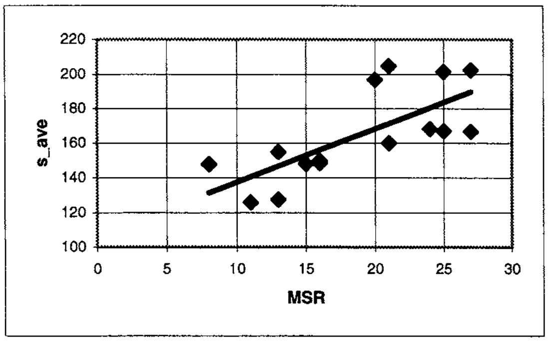

Figure 1: Correlation of mean saturation with MSR: Correlation: $R^2 = 0.52$

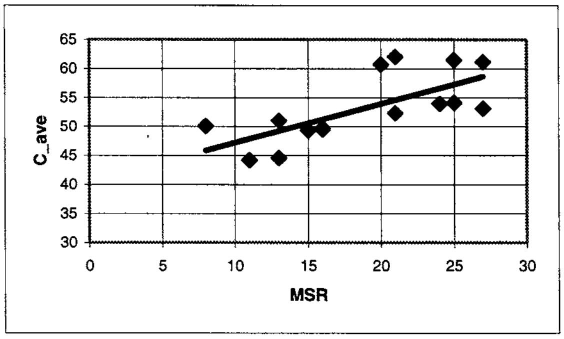

Figure 2: Correlation of mean chroma with MSR: Correlation: $R^2 = 0.50$

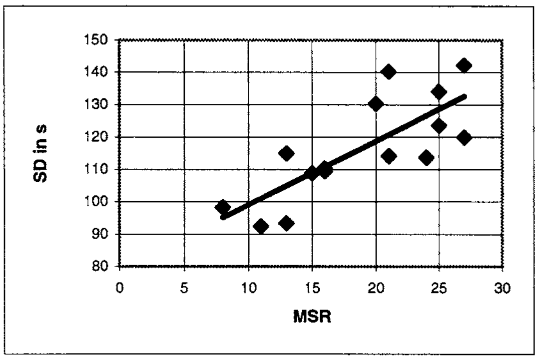

Figure 3: Correlation of standard deviation in saturation with MSR: Correlation: $R^2 = 0.60$

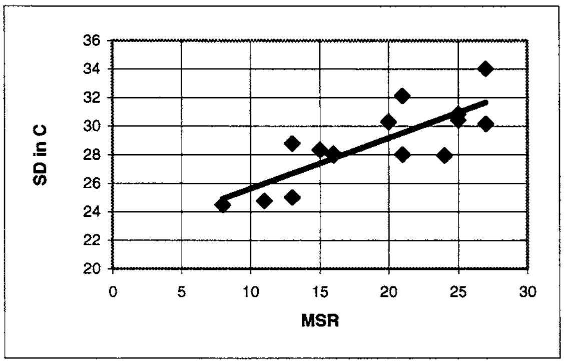

Figure 4: Correlation of standard deviation in chroma with MSR: Correlation: $R^2 = 0.65$

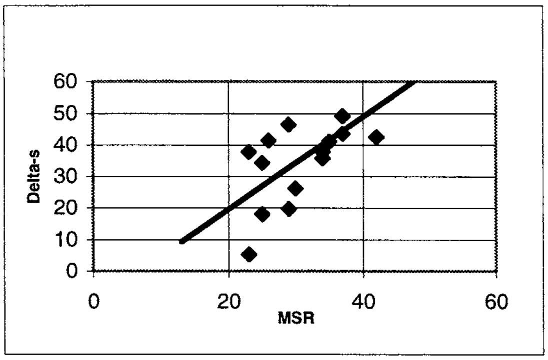

Figure 5: Correlation of mean saturation difference (test vs. reference image) with MSR: Correlation: $R^2 = 0.41$

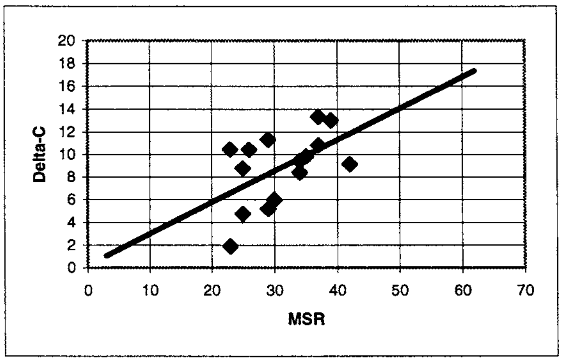

Figure 6: Correlation of mean chroma difference (test vs. reference image) with MSR: Correlation: $R^2 = 0.28$

to select a rectangle (in this case a 21×21 pixel square – *i.e.* 441 pixels – close to the centre of each colour patch) from which the *RGB* pixel values were read out to the model.

The *RGB* values of the 441 pixels for each colour patch were used to compute an arithmetic mean *RGB* triplet for the patch. These values were used in subsequent processing, first for gamma conversion, then the transformation to *XYZ* tristimulus values, and finally the calculation of CIECAM97s colour appearance attributes under the conditions of the subjective experiment. This was done for the 24 test and 24 reference samples appearing in each of the 22 ColorChecker images.

At the end of this process, it was clear that some form of data reduction and interpretation was necessary to reduce the volume of data, and the following were adopted as potential colour quality metrics:

- Average (arithmetic mean) CIECAM saturation *s* for the 24 test samples in each image: *s_ave*
- Average (arithmetic mean) CIECAM chroma *C* for the 24 test samples in each image: *C_ave*
- Standard deviation in CIECAM saturation *s* for the 24 test samples in each image: *SD in s*
- Standard deviation in CIECAM chroma *C* for the 24 test samples in each image: *SD in C*
- Average (arithmetic mean) CIECAM saturation difference between the 24 corresponding pairs of colour patches in the test and reference halves of each image: *Delta-s*
- Average (arithmetic mean) CIECAM chroma difference between the 24 corresponding pairs of colour patches in the test and reference halves of each image: *Delta-C*.

To determine the merits of these metrics as candidates for the prediction of perceived image colour quality, each of them was tested for its correlation with the previously established MSR.

3.2 Results

The results of this investigation, for a display gamma of 2.8, are shown in Figures 1 to 6. In each case, the correlation coefficient (R^2) is quoted in the caption.

Figures 1 and 2 suggest that both the mean CIECAM saturation and chroma, with their moderately significant correlation with the MSR, could be useful predictors of image colour quality – with mean saturation slightly outperforming mean chroma.

Figures 3 and 4, however, show improved levels of correlation of the standard deviations *SD in s* and *SD in C* with the MSR, and these metrics appear to be reliable predictors of image colour quality. In this instance, the chroma metric slightly outperforms the saturation metric.

It had been considered likely that the *Delta-s* and *Delta-C* metrics would give the highest correlations with the MSR on the grounds that, in arriving at their subjective evaluations of each image, the observers would have been simultaneously viewing the test and reference halves of each image, and would (presumably) have been likely to assign a rating based on their perception of the colour differences. The low correlations evidenced in Figures 5 and 6, however, suggest that more complex mechanisms were possibly at work.

4. CONCLUSIONS

The metrics *s_ave*, *SD in s*, *C_ave*, *SD in C* are all suitable for use as image colour quality metrics – with the standard deviations being superior to the arithmetic means. However, the correlations are not as strong as may be desired. It may be possible to derive a more robust predictor of image quality by combining two or more of these metrics into a single figure of merit.

5. ACKNOWLEDGEMENTS

Thanks are due to The Department of Electrical and Electronic Engineering at Manukau Institute of Technology for support of this research.

6. REFERENCES

[1] H. De Ridder, F.J.J. Blommaert & E.A. Fedorovskaya., SPIE Procs., Vol. 2411, pp. 51-61 (1995).

[2] E.A. Fedorovskaya, H. De Ridder & F.J.J. Blommaert, Color Res. & Applic., Vol. 22, pp. 96-110 (1997).

[3] A.N. Chalmers, Trans. SAIEE, Vol. 17, pp. 89-96 (1986).

[4] CIE, The CIE 1997 Interim Color Appearance model (Simple Version), CIECAM97s, CIE Technical Report, Publication No. 131-1998, CIE Central Bureau, Vienna (1998).

[5] G.H. Hutson, Colour Television Theory, McGraw-Hill, London, pp. 24, 62 (1971).

[6] R.W.G. Hunt, The Reproduction of Colour in Photography, Printing & Television, Fountain Press, UK, p. 386 (1975).

[7] H. Lang, Color displays in K. Nassau (Ed.), Color for Science, Art and Technology, Elsevier, Amsterdam, pp. 444-446 (1998).

The Accuracy of Polynomial Models for Characterising Digital Cameras

Changjun Li, Guihua Cui, and M Ronnier Luo
Colour & Imaging Institute
University of Derby, UK

ABSTRACT

Polynomial models are widely used for characterising digital cameras, because they can be applied without knowledge of the camera's sensors. This paper describes the polynomial model based on the least square (LS) method for characterising the digital camera. The change of order from the second to fifth degree polynomial was also examined in terms of their accuracy. The results showed that the fourth order polynomial gives the best predictions according to the mean and maximum colour differences for the LS method. Finally, the model was used to determine the optimum shutter speed to achieve the highest accuracy for characterising a digital camera.

Keywords: CIE colorimetry, colour difference, digital camera characterisation, shutter speed, least-square method.

INTRODUCTION

With the recent large progress in the development of digital colour cameras, they are now being applied for measuring surface colours. Some systems have already achieved satisfactory results [1,2]. They have advantages over the conventional colour measurement instruments by capturing the total appearance of the object including colour, texture, gloss and other factors. They also have much less restriction on the size and shape of the object or scene and the uniformity of the surface, since small areas of the image can be examined, and the colours for large patches can be average.

The major requirement for a colour measurement equipment is to be highly repeatable and accurate. However, when capturing the same scene or object, the output RGB signals from different cameras or from the same camera with different settings such as shutter speed, exposure are not the same. The way to overcome the problem is known as *device characterisation.* It is a method to convert a device's primaries (a camera's RGB signals) to the CIE tristimulus values. It is the mathematical structure and efficiency of this characterisation method that dictates the overall performance of a camera.

Mapping camera signal RGB to CIE tsristimulus values XYZ has been intensively studied and a number of methods such as look up table [3,4], spectral sensitivity [5], metamer constrained [6], neural network [4] and polynomial [3,4,7] have been derived.

This study is focused only on the polynomial characterisation model. Many parameters could affect the performance of the polynomial models such as the number and distribution of reference and test samples, the number of terms in the model, the measures used to determine the goodness of fit, the effect of camera settings such as shutter speed, exposure. This study aims to investigate some of these effects. A Canon camera was used in this study. 240 colours in a Gretag Macbeth Color Check Digital Chart [11] were used as the reference target. The 24 colours in a Gretag Macbeth Color Check Chart [12] were used as test colours. The polynomial model based on Least Square (LS) method was first implemented and tested. The extent to which the models' performance was affected by the order of the polynomial was then studied. Finally, the camera's shutter speed was varied to investigate the characterisation models' performance.

POLYNOMIAL MODEL BASED ON LEAST SQUARES METHOD

Equation (1) is a general expression of a polynomial characterisation model.

$$X = \sum_{0 \le j_1 + j_2 + j_3 \le n} a_{X,j_1,j_2,j_3} R^{j_1} G^{j_2} B^{j_3}$$
$$Y = \sum_{0 \le j_1 + j_2 + j_3 \le n} a_{Y,j_1,j_2,j_3} R^{j_1} G^{j_2} B^{j_3} \qquad (1)$$
$$Z = \sum_{0 \le j_1 + j_2 + j_3 \le n} a_{Z,j_1,j_2,j_3} R^{j_1} G^{j_2} B^{j_3}$$

where *R*, *G* and *B* are camera signals and *X*, *Y* and *Z* are the CIE tristimulus values; n is the order of the polynomial and j_1, j_2, j_3 are nonnegative integer indices; a_{X,j_1,j_2,j_3}, a_{Y,j_1,j_2,j_3}, a_{Z,j_1,j_2,j_3} are the model coefficients to be determined. For $n = 1$, equation (1) becomes equation (2).

$$X = a_{X,0,0,0} + a_{X,1,0,0}R + a_{X,0,1,0}G + a_{X,0,0,1}B$$
$$Y = a_{Y,0,0,0} + a_{Y,1,0,0}R + a_{Y,0,1,0}G + a_{Y,0,0,1}B \qquad (2)$$
$$Z = a_{X,0,0,0} + a_{Z,1,0,0}R + a_{Z,0,1,0}G + a_{Z,0,0,1}B$$

Equation (1) can be presented in matrix form as given in equation (3).

$$u = Ac \qquad (3)$$

where, for $n=1$,

$$u = \begin{pmatrix} X \\ Y \\ Z \end{pmatrix}, \quad A = \begin{pmatrix} a_{X,0,0,0} & a_{X,1,0,0} & a_{X,0,1,0} & a_{X,0,0,1} \\ a_{Y,0,0,0} & a_{Y,1,0,0} & a_{Y,0,1,0} & a_{Y,0,0,1} \\ a_{X,0,0,0} & a_{Z,1,0,0} & a_{Z,0,1,0} & a_{Z,0,0,1} \end{pmatrix}, \quad c = \begin{pmatrix} 1 \\ R \\ G \\ B \end{pmatrix}$$

Thus, A is a 3 by 4 matrix for $n=1$. All the sizes of the column vectors u and c together with the matrix A for n from 1, 2, 3, 4 and 5 are listed in Table 2.

N	u	$A\ (3\times N)$	c
1	3	3×4	4
2	3	3×10	10
3	3	3×20	20
4	3	3×35	35
5	3	3×56	56

Table 1: Sizes of vectors u, c and matrix A for n =1 to 5

Once the coefficients in matrix A are determined, then for any given camera *R,G,B* signals, the corresponding CIE tristimulus values *X,Y,Z* can be calculated using equations (1) For determining the coefficients in matrix *A*, a GretagMacbeth ColorChecker DC [11] was used as a reference target, which includes 12 by 20 colour patches. For each colour, the CIE tristimulus values *X,Y,Z* were measured using a spectrophotometer under CIE D65 and 1964 colorimetric observer and camera *R,G,B* signals were also obtained by imaging the colour patch using a Canon Power Shot Pro90IS camera. Therefore, for the *ith* colour patch, vector $c^{(i)}$ and $u^{(i)}$ were formed using camera signals and tristimulus values in equation (3), respectively. Ideally, a matrix *A* is chosen so that

$$u^{(i)} = Ac^{(i)}, \quad i = 1,2,\cdots,m \qquad (4)$$

where *m* is the number of colour patches.

However, *m* is normally greater than *N*, the number of columns in matrix *A*, so that it is impossible to choose a matrix *A* to satisfy equation (4).

However, matrix *A* can be obtained by minimising the square of mathematical distance: $\| u^{(i)} - Ac^{(i)} \|$ defined by equation (5).

$$\| u^{(i)} - Ac^{(i)} \| = \sqrt{(X_i - \tilde{X}_i)^2 + (Y_i - \tilde{Y}_i)^2 + (Z_i - \tilde{Z}_i)^2} \qquad (5)$$

where

$$u^{(i)} = \begin{pmatrix} X_i \\ Y_i \\ Z_i \end{pmatrix}, \text{ and } Ac^{(i)} = \begin{pmatrix} \tilde{X}_i \\ \tilde{Y}_i \\ \tilde{Z}_i \end{pmatrix} \quad (6)$$

The above can be written as equation (7) and is named the **Least-Square (LS) method.**

$$\frac{Min}{A}\{ \sum_{i=1}^{m} \| u^{(i)} - Ac^{(i)} \|^2 \} = \frac{Min}{A}\{ \sum_{i=1}^{m} (X_i - \tilde{X}_i)^2 + \sum_{i=1}^{m} (Y_i - \tilde{Y}_i)^2 + \sum_{i=1}^{m} (Z_i - \tilde{Z}_i)^2 \} \quad (7)$$

Let

$$U = (u^{(1)}, u^{(2)}, \cdots, u^{(m)}) \text{ and } C = (c^{(1)}, c^{(2)}, \cdots, c^{(m)}) \quad (8)$$

then by the well-known method for solving a least-square problem [13], the solution A of the above problem is given by:

$$A = UC^T (CC^T)^{-1}. \quad (9)$$

Thus, the LS method determines the matrix A so that $Ac^{(i)}$ is as close to $u^{(i)}$ as possible in terms of geometrical distance in *XYZ* space (see equation (5)). The final expression for A can be explicitly given in terms of matrices U and C.

POLYNOMIAL ORDER EFFECT

The polynomial order effect is examined in this section. In equation (3), the *RGB* signals of the reference chart were used to form the vectors $c^{(i)}$ and again the measured *XYZ* values from the DC target were used to form the vectors $u^{(i)}$. Many sets of coefficients in matrix A were determined by changing the order of the polynomial from 2, 3, 4 to 5 using the LS method. These were then used to calculate the average (Ave) and maximum (Max) colour-difference between the measured and predicted tristimulus values from all 240 colours in the reference target. Hong *et al* [7] found that the models' performances could be improved by the inclusion of a cross term, i.e. the products of R, G, and B. Note that for n = 2, the column N in matrix A should be 10 (see Table 1. The n=2* is used here to designate N of 11 (with the addition of the RGB term). Three colour-difference formulae were used: CIELAB [14], CMC [15] and CIEDE2000 [16]. For each sample, the colour-difference was first calculated. For the whole 240 samples, the average 'Ave' and maximum 'Max' values are given in Table 2

n	*2**	*3*	*4*	*5*
N	11	20	35	56
	Ave/Max	Ave/Max	Ave/Max	Ave/Max
CIELAB	2.5/13.0	2.0/5.5	1.2/3.2	1.0/3.6
CMC	2.1/7.0	1.9/8.5	1.1/4.4	0.9/3.8
CIEDE2000	1.8/5.6	1.6/6.2	1.0/4.0	0.8/3.8

Table 2: The performance of the polynomial with the order number of 2*, 3, 4 and 5 using the reference colours

Table 2 shows that almost all models should be acceptable for graphic arts applications with all mean values less than 2.5 ΔE^*_{ab}. However, we require a mean of below 1.5 ΔE^*_{ab} for measuring surface colours. In order to achieve this, the n needs to be *4*. The performance of the method is improved with an increase of order n as expected. The largest improvement was found between n =3 and n =4 for the LS method.

Comparing the results from three colour-difference formulae, the same conclusion is drawn. The only difference is the magnitudes of the results for the three formulae studied.

The results in Table 3 were based upon only the reference target. It is desirable to test the same models using an independent data set. Hence, a Macbeth Color Checker Chart including 4 by 6 patches was used as a test set. The Chart was again imaged using the same camera, and tristimulus values were measured using the same spectrophotometer as before. The performance of the method using the test set is given in Table 3.

n	*2**	*3*	*4*	*5*
N	*11*	*20*	*35*	*56*
	Ave/Max	Ave/Max	Ave/Max	Ave/Max
CIELAB	3.5/11	2.7/6.8	2.3/5.2	5.4/73
CMC	2.6/9.3	2.3/6.8	1.7/5.0	4.4/68
CIEDE2000	2.3/7.1	1.9/5.5	1.5/5.0	3.1/39

Table 3: The performance of the polynomial with the order number of 2*, 3, 4 and 5 using the test colours

The results showed that the performances of all models in Table 4 are worse than those in Table 3 by about 30-50%. This is a well known effect due to different data sets produced with different materials and colorants giving the problem of metamerism as explained by Hong *et al* [7]. Another clear pattern was found that the 5th polynomial models performed the best using the reference set but the worst using the test set (they even predicted less accurately than the 2nd polynomial models). This is mainly caused by the 5th polynomial model being fitted to too much noise in the reference data. Hence, we can conclude that the 4th polynomial model based upon LS method should be used to characterize the particular camera investigated.

SHUTTER SPEED EFFECT

Different camera settings such as shutter speed and exposure time, can also affect the accuracy of camera characterisation models. This section provides an example on how this can be investigated. All camera settings were fixed except shutter speed. The DC target was again used and was captured at the speed of 1/50, 1/60, 1/100, 1/125, 1/200, 1/250,1/320, 1/400, 1/500, and 1/800 seconds. Hence, different sets of camera *RGB* signals are available for each speed, but they share the same set of *XYZ* values. The 4th polynomial model based upon LS method was developed for each speed condition. The results are summarised in Table 4.

It was found that the speed does affect the accuracy of the model. The results show that a too fast or too slow shutter speed will result in large errors of prediction from the models. For a too slow speed, more light will enter the camera. This results in the *RGB* signals of some pixels to be out of the dynamic range of the digital camera and their RGB signals were clipped to 255. For a too fast speed, there is insufficient light entering the camera. Hence most of the camera signals will be low together with the inclusion of much noise. These contributed to the large prediction errors as shown in Table 4. The results clearly showed that shutter speed of 1/200 is the best setting for the camera investigated.

Speed	CIELAB	CMC	CIEDE2000
	Ave/Max	Ave/Max	Ave/Max
1/800	1.8 /12.5	1.4 /9.0	1.2 /7.3
1/500	1.4 /9.1	1.2 /5.6	1.0 /4.9
1/400	1.1 /3.5	1.0 /3.4	0.9 /3.4
1/320	1.1 /3.8	1.0 /3.3	0.8 /2.7
1/250	1.0 /3.7	0.9 /3.1	0.7 /2.5
1/200	0.9 /3.5	0.8 /2.3	0.7 /2.3
1/125	1.6 /5.8	1.2 /6.8	1.0 /2.8
1/100	2.1 /10.1	1.7 /4.7	1.4 /4.3
1/60	4.7 /51.3	3.5 /24.0	3.0 /22.9
1/50	6.5 /61.3	4.9 /40.7	4.1 /26.3

Table 4: The performance of the 4th polynomial model at different shutter speeds

CONCLUSIONS

This paper describes the polynomial models based on the least squares method for characterising a digital camera. The key factor affecting the models' performances is the order of the polynomial. The findings are summarised below:

- A higher order polynomial model will perform better than a lower one with the training data set. However, the 5th order polynomial model would perform even worse than the 2nd order polynomial model when tested using the test data set. Hence, the latter model is not recommended for characterising a digital camera.
- The models' performances are worse for the test data set than for the reference data set by about 30-50% in colour-difference units. This is caused partly by the problem of metamerism.
- The results show that the 4th order polynomial model gave the best prediction regardless which data set (training and testing) and colour difference formula was used.
- A particular shutter speed setting was found to give the most accurate prediction for the polynomial model.

All the above findings are associated with a particular camera and specific test and reference colours. For different cameras under different viewing conditions, a separate study should be carried out using the methods introduced in this paper.

REFERENCES

1. Luo MR, Cui GH, Li CJ, and Dakin J, Applying digital cameras for measuring colours, AIC Color 2002 SI, Color & Textiles, Maribor, Slovenia, August 29-31, 2002, pages: 121-127.
2. Cui GH,, Luo MR, Rhodes RA, Rigg B, and Dakin A, Grading textile fastness. Part I: Using a digital camera system, Coloration Technology, 000-000 (2003).
3. Johnson T, Methods for characterising colour scanners and digital cameras, Displays 1996;16:183-191.
4. Henry RK, Color Technology for Electronic Imaging Devices, SPIE, Washington, 1996.
5. Berns RS, Shyu MJ, Colorimetric characterisation of a desk-top drum scanner using a spectral model, J Electronic Image 1995;4: 360-372.
6. Finlayson GD and Morovic PM, Metamer constrained color correction, Journal of Imaging Science and Technology 2000;44:295-300.
7. Hong GW, Luo MR and Rhodes PA, A study of digital camera colorimetric characterisation based on polynomial modelling, Color Research & Applications 2001;26:76-84.
8. Farrell JE, Cuppitt J, Saunders D, Wandell BA, Estimating Spectral Reflectance of Digital Artwork, Proceedings of the International Symposium on Multispectral Imaging and Color Reproduction for Digital Archives, pp.58-64. Chiba, Japan, October 21-22, 1999 (Society of Multispectral Imaging of Japan.)
9. Brydges D, Deppner F, Kunzili H, Heuberger K and Hersch RD, Application of a 3 CCD color camera for colorimetric and densitometric applications, Proc. SPIE 3300, 1998.
10. Burns PD and Burns RS, Analysis of multi-spectral image capture, Proc. Fourth IST&SID Color Imaging Conference, Scottsdale, Arizona, 1996.
11. Graphic Technology and Photography - Colour characterisation of digital still cameras (DSCs) using colour targets and spectral illumination, ISO 17321, WD 4, 1999.
12. The Macbeth Color Cheker, Color redition Chart, Macbeth, division of Kollmorgen Instruments Corporation.
13. Stewart, GW, Introduction to matrix computations, Academic Press, NY, 1973.
14. CIE Colorimetry, 2nd edition CIE Publ. No. 152, Vienna: Central Bureau of the CIE, 1986.
15. Clarke FJJ, McDonald R, Rigg B, Modification to the JPC79 colour difference formula, J Soc. Dyers Colour 1984; 100: 128-132 and 281-282.
16. Luo MR, Cui GH, and Rigg B, The development of the CIE 2000 colour-difference formula: CIEDE2000, Color Res. Appl. 2001; 26: 340-350.

Calculating Image Difference: a Study Based on the Use of Gamut Mapped Images

Jiang Duan, Guowei Hong, Jan Morovic and Peili Sun*
Colour & Imaging Institute, University of Derby, UK
* Department of Graphic Communications & Technology
Shin Hsin University, Taiwan, R.O.C.

ABSTRACT

This paper describes a newly developed image difference metric based on the use of gamut mapped images. In our study, reproduced images with different levels of distortion caused by various gamut mapping algorithms were simulated on a CRT display and psychophysical experiments were carried out to obtain subjective visual assessment results. During the psychophysical experiment, it was found that observers often needed to make decisions to balance overall colour difference versus local spatial details. The proposed algorithm attempted to simulate this decision making by dividing overall image difference into two separate aspects: colour and spatial details. Colour difference is computed as an average of pixel-by-pixel difference between the low frequency components of the images while the difference of spatial details is calculated from the high frequency components of the images. The results obtained so far has shown that we can better understand how the human visual system compare images and judge the difference by calculating differences of colour and spatial details separately.

INTRODUCTION

With the current rapid development of digital colour imaging, the need for developing an algorithm that can quantitatively evaluate difference between complex images becomes increasingly desirable. For example, for cross-media colour image reproduction, rendering images on various devices inevitably introduces colour changes or shifts due to the fact that the colour gamut of each device is limited and often quite different from the others. A simple method for evaluating the difference between images is by carrying out psychophysical experiments. However, this kind of assessment is subjective, complicated, difficult and time-consuming. Further, the results may vary over time and space. Therefore, it is highly desirable to have an objective image difference metric which can be implemented to obtain instant and consistent results which should also agree with the judgments of human observers. The aim of this study is to find an effective image difference metric that is compatible with the perceived image difference.

Since the conventional colour difference formulae such as CIELAB, BDF, CIE94, CMC and CIEDE2000 have obtained significant successes in many applications, they should serve as a solid foundation for developing an image based colour difference metric. Recently based on a set of complex images displayed on a CRT monitor, Song and Luo [1] conducted an experiment to determine the perceptibility threshold and acceptability tolerance for the above mentioned colour difference formulae. After weighting factors for the lightness, chroma and hue in these formulae were re-assigned to a set of optimal values which may be image dependent, they obtained some reasonable results. Zhang and Wandell [2] developed a spatial extension to CIELAB for measuring the difference between patterned images. The spatial extension applied a spatial filter operation to colour image data in order to simulate the spatial blurring by the human visual system. Considering the operation of human visual system is certainly a step forward in quantifying colour difference between images. The accuracy of calculating S-CIELAB depends very much on the accuracy of colour transformation and three spatial filters which are estimated from human psychophysical experiments. Johnson and Fairchild [3] developed a basic framework for the image based colour difference model. They made some modifications and improvements to the S-CIELAB and obtained some satisfactory results. For example, filters with more accurate contrast sensitivity functions were used to replace the original filters proposed in S-CIELAB, and a method for enhancing image differences where the human visual system was most sensitive to was introduced. Based on some existing facts that human eyes are more tolerable for the colour difference of small areas within an image than the difference over large areas of the image, certain image analysis was carried out by Hong and Luo [4] and a new algorithm was also proposed. By assigning higher weights to difference that was perceptually important, the algorithm obtained some results showing better agreement with subjective assessments.

VISUAL ASSESSMENTS

An effective image difference metric has to be consistent with the human visual judgements. The first step of our study is to collect data from some psychophysical experiments to find out how human visual systems compare images and judge the difference. For cross media colour image reproduction, the major cause for image difference is usually due to the large difference in the reproducible colour range of each device and the use of some gamut mapping algorithms. Therefore, four gamut mapping algorithms [5], namely LLIN, CARISMA, SGCK and HP_MINDE (Hue preserving minimum ΔE clipping), were selected to produce modified images with various levels of image difference. A calibrated CRT monitor's gamut was considered as the original gamut and a printer's gamut was assumed as the reproduction gamut. In the process of preparing the originals and reproductions, clipping operations were applied to all the original images chosen to ensure that all the colours in the images were within the gamut of the monitor so that these images can be displayed appropriately. Five test images, namely "Women with glass", "Flower", "Fishing tools", "Crafts" and "French women" (shown in Figure 1), were chosen from ISO [6] and Japanese SHIPP standard [7]. These images are encoded with 8 bits per channel in CIELAB colour space, and the resolution of each image is 400 by 300 pixels. Modified by the gamut mapping algorithms, five sets of images were prepared; each set included one original image and four simulated reproductions.

Although CIELAB encoding of the images provides the convenience for the mathematical calculations of image colour difference, images encoded in CIELAB cannot be directly displayed on a CRT monitor. These 8-bit CIELAB encoded data was converted to 8-bit RGB data by a CRT characterisation profile generated by the GOG model [8]. The images were then displayed on a CRT monitor for viewing, and pair comparison was adopted to evaluate the perceived image difference. The experiment was conducted on a Barco monitor in a dark room; a software was created to control the procedure and record the results. Each image displayed was surrounded with a white border which extended about 30 pixels wide and mid-grey was chosen as the background colour. Before the experiment, observers were allowed about 3 minutes to adapt to the viewing condition of the dark room and asked to sit comfortably in front of the monitor about 18 inches away; the following instruction was given:

> *In this experiment, you will be shown an original image and two reproductions of it on the monitor at each time. You are asked to select which reproduction has smaller difference with the original. If you really could not determine which one has smaller difference, you can select "SAME" button.*

For each set of images, there were six judgements to complete the pair comparison. Fifteen observers participated in the experiment. In order to have a further understanding of the observers' decisions, five out of the fifteen observers were asked to report the most important factor that had affected their judgments? Table 1 summarises the results obtained by the psychophysical experiment carried out. Z-score values for each image was computed to represent the extent of the difference between the original image and the corresponding reproduction using a gamut mapping algorithm. In this particular case, larger z-score value represents less perceived image difference. For the additional question to the 5 observers asked, they all considered that colour and spatial details were the two most important factors influencing their judgments.

IMAGE DIFFERENCE CALCULATED USING PIXEL-BY-PIXEL AVERAGE

The most straightforward way of computing colour image difference is to apply the existing colour difference formulae to images on a pixel-by-pixel basis, and then take the average as the resulting colour difference between the two images. The difference based on pixel-by-pixel average between the originals and their corresponding reproductions for the five sets of testing images were calculated using CIELAB colour difference formula. The results obtained by pixel-by-pixel average are also shown in Table 1. As can be seen from Table 1, there were some mismatch between the computed image difference and the visual assessments. For example, for "women with glass" pixel-by-pixel average ranked HP_MINDE as the best in providing the least image difference; however, visual assessments considered SGCK as the best. In fact, for all five images used, there were some mismatches (Shown as bold numbers in Table 1) between the computed difference and the difference reported by the visual assessments. This is hardly surprising as it is well known that the conventional colour difference formulae are only applicable to measure difference between large uniform colour patches and are not designed for images.

The results from visual assessments clearly showed that HP_MINDE and SGCK algorithms introduced smaller colour difference than CARISMA and LLIN did. It can be noted from Table 1 that the pixel-by-pixel average algorithm only fails in ranking the difference between HP_MINDE and SGCK reproductions, and between CARISMA and LLIN reproductions. In all the cases the algorithm can successfully predict that the simulated reproductions using either HP_MINDE or SGCK gamut mapping algorithms have smaller difference than those produced by LLIN or CARISMA gamut mapping algorithms, which is the same conclusion reached by the subjective visual assessments. Therefore, it is fair to say that the pixel-by-pixel average algorithm is pretty successful in ranking images with large colour difference. However, when the colour difference between the images is relatively small, such as those between HP_MINDE and SGCK reproductions and between CARISMA and LLIN reproductions, the performance of pixel-by-pixel average can be rather poor. This presents an apparent rationale to further investigate and develop a more effective image difference metric which can not only predict large colour difference but also small difference between images.

COLOUR VS SPATIAL DETAILS

There is much evidence that the human vision system consists of different frequency sensitive channels [9]. Low frequency components within an image correspond mainly to areas where the change of pixel values is relative smooth while high frequency components instead correspond to areas where the change of pixel values is relative sharp. Most images usually consist mainly of large areas of low frequency components such as relatively uniform region and background, which to some extent resembles the situation where the conventional colour difference formulae would be applicable. As far as high-frequency components are concerned, they are usually edges and sharp components which usually correspond to spatial details in an image. Thus in the low-frequency sensitive channel, judging overall changes of colour difference is probably the leading factor; while in the high-frequency sensitive channel, judging the difference of spatial details is the dominant factor. Enlightened by this, our proposed algorithm attempted to separate the low frequency components and the high frequency components in the images, and the differences in corresponding components are calculated using different methods respectively. The algorithm aimed to simulate what happens in the low frequency and the high frequency sensitive channels of the human visual system. Finally some compromises between the two differences are made, and an overall colour difference which corresponds to overall visual assessment is computed.

In this study, a 5×5 lowpass spatial filter with equal weighting for each pixel was applied to both the luminance and chrominance channels to extract low-frequency components of the images. And then CIELAB colour difference formulae is used to calculate the difference between the filtered originals and the reproductions for all the images on a pixel-by-pixel basis and then an average was calculated. This value is meant to represent the overall colour difference between the originals and the reproductions. It is well known that the human visual system has a much reduced sensitivity to spatial variations in the two chrominance channels relative to the sensitivity in the luminance channel. That implies although there are three visual pathways in the human colour visual system, the sharpness of a colour image depends mainly on the sharpness of the luminance components and little on the opponent-colour components. We can exploit this phenomenon by only considering the luminance channel for computing the difference of spatial details. Thus the high-frequency components from the luminance channel for a pair of images were extracted respectively, and then the absolute difference of each pixel was computed. The overall average was taken to represent the calculated difference in terms of spatial details.

There are many methods available for detecting high-frequency components in images. In this study, the simple Sobel filter, which is often used for edge detection, was applied to obtain high-pass filtered images of originals and the simulated reproductions. The reason why a Sobel filter was adopted is due to the fact that human visual system is especially sensitive to position of edges which are correspond to high frequency information[3]. When a pair of images are compared, human visual system is also very sensitive to the difference in such aspect. Some gamut mapping algorithms, for example HP_MINDE which is mainly based on clipping, tend to lose edge information and spatial details.

RESULTS AND DISCUSSIONS

Table 1 also shows the results obtained by the newly proposed algorithm. "Colour" refers to the overall colour difference which is computed as an average of pixel-by-pixel difference between the low frequency components of the images; "spatial" refers to the difference of spatial details which is calculated from the high frequency components of the images. The pixel-by-pixel average algorithm cannot match the visual assessments obtained by psychophysical experiments for all five test images used in the experiment. However, once the overall image difference was divided into two different aspects: colour and spatial details, it provided a new perspective for understanding how image differences were judged. It became pretty clear that for the four mismatch ("Woman with glass", "Flower", "Crafts" and "French woman") out of the total five test images, although their average color differences were smaller, their differences in spatial details were larger. This clearly indicated that the observers were not only judging the colour difference but also the difference in spatial details, which had played a significant role in contributing to the overall image difference. For image "Fishing tools", both CARISMA and LLIN produced similar colour and spatial differences, which corresponded reasonably well with the visual data.

Let's take image "Crafts" as an example. The first step of the new algorithm is to calculate the average colour difference using the low-pass filtered images. The colour difference between the original and CARISMA reproduction is 14.3 and 15.0 between the original and LLIN reproduction. These values should represent the difference in colour aspect and meant that the CARISMA introduced smaller colour difference than LLIN did. The second step of the proposed algorithm is to calculate the difference in spatial details. The spatial difference between the original and CARISMA reproduction is 8.3 and 6.1 between the original and LLIN reproduction. These results meant that CARISMA produced larger spatial difference than LLIN did. The image used in the experiment shows that CARISMA reproduction contains less high frequency information in the image, especially in the right bottom part of the image. LLIN reproduction shows more details and appears sharper than CARISMA reproduction. For example, the contour of the bag at the right-bottom of LLIN reproduction is clearer than that in CARISMA reproduction. It seemed that the observers were facing a quite interesting but also difficult situation. For comparing CARISMA and LLIN reproductions, in terms of colour CARISMA is closer to the original; however, in terms of spatial details, LLIN is better. To obtain the overall image difference, a simple way forward is to take the average of the two kinds of differences. This will show that the overall image difference for LLIN reproduction is slightly better than the CARISMA reproduction, which agrees with the ranking obtained by the observers. However, with the current available data for all five images, it is not clear this is the right weighting between the two kinds of differences, and further research needs to be done in this area.

CONCLUSION

In this study, image difference calculated by the conventional pixel-by-pixel average algorithm was evaluated and found that it was quite successful in predicting images with large colour difference. A new image difference algorithm based on extracting colour and spatial difference from the low frequency and high frequency components respectively was proposed, aiming to achieve better agreement with the perceived difference particularly for images with relative small difference. For the experimental results obtained so far, our proposed algorithm demonstrated its ability to compute perceived difference in both colour and spatial aspects. However, there is no further information from the observers about which factor, that is colour difference or spatial difference, dominated their judgments and what is the appropriate weighting between the two. Further research should be conducted to discover the appropriate weighting between colour and spatial details.

REFERENCES

1. T. Song, and M.R. Luo (2000) Testing colour-difference formulae on complex images using a CRT monitor. *Proceedings of 8th IS&T/SID Color Imaging Conference*, pp.44-88.
2. X. Zhang, and B.A. Wandell (1996) A spatail extension of CIELAB for digital color image reproduction. *SID Symposium Technical Digest*, 27, pp.731-734.
3. G.M. Johnson and M.D. Fairchild (2001) Darwinism of Color Image Difference Model. *Proceedings of IS&T/SID 9th Color Imaging Conference*, pp.108-112.
4. G. Hong and M.R. Luo (2001) Perceptually based colour difference for complex images", *Proceedings of the 9th Congress of the International Colour Association*, pp.618-621.
5. L.W. MacDonald and M.R. Luo (2002) *Colour Image Science Exploiting Digital Media*, John Wiley & Sons, Inc.
6. *Graphic technology – Prepress digital data exchange – XYZ/sRGB standard colour image data (XYZ/SCID)*, ISO standard 12640-2 (2000).
7. K. Sakamoto and H. Urabe (1997) Standard high precision pictures: SHIPP. *Proceedings of 5tt IS&T/SID Color Imaging Conference*, pp. 240-244.
8. R.S. Berns (1996) Methods for characterizing CRT displays, *Displays*, 16(4), pp. 173-182.
9. G. Qiu and K.M. Lam (2002) Spectrally layered color indexing. *Image and Video Retrieval*, M.S. Lew, N. Sebe, J.P. Eakins (Eds.), pp. 100-107, Springer LNCS 2383.

Figure 1 Test images used (from left to right, top to bottom) "Flower", "Crafts", "Women with glass", "Fishing tools" and "French Woman"

Images	Differences	HP_MINDE	SGCK	CARISMA	LLIN
Woman with glass	Z-score	2.6	3.9	-0.5	-6.0
	Pixel average	**7.1**	**9.9**	14.5	16.1
	Colour	7.1	9.8	14.4	16.1
	Spatial	9.6	8.6	7.3	4.3
Flower	Z-score	3.4	3.5	-0.1	-6.8
	Pixel average	**4.7**	**8.3**	10.9	14.8
	Colour	4.7	8.2	10.7	14.7
	Spatial	5.9	5.0	6.4	4.0
Fishing tools	Z-score	3.1	2.6	-2.3	-3.4
	Pixel average	6.3	8.9	**13.6**	**13.4**
	Colour	6.3	8.9	13.6	13.4
	Spatial	9.2	8.0	5.9	5.9
Crafts	Z-score	2.8	0.6	-1.9	-1.5
	Pixel average	8.7	11.3	**14.4**	**15.1**
	Colour	8.7	11.2	14.3	15.0
	Spatial	11.3	9.9	8.3	6.1
French woman	Z-score	5.5	3.6	-4.8	-4.3
	Pixel average	1.0	4.4	**9.2**	**9.8**
	Colour	1.0	4.4	9.2	9.7
	Spatial	2.1	2.3	4.0	3.4

Table 1 Results of subjective assessments, difference by pixel-by-pixel average, difference in colour and spatial details

Texture Effect on Evaluation of Colour Difference

B. Han, G. H. Cui and M. R. Luo
Colour & Imaging Institute, University of Derby
Kingsway House, Kingsway
Derby DE22 3HL, United Kingdom

ABSTRACT

Different viewing parameters affect the perceived colour-differences. This study investigated the effect of textures and separations using textile and CRT sample pairs. Each textile pair was first assessed by a panel of observers using the grey scale method. The other experiments were conducted by reproducing the textile samples on a CRT and using the same scaling method. The experiment was divided into 7 phases according to different combinations of the parameters studied. The visual results obtained from the two experiments were compared to reveal parametric effects. The performance of some chosen colour-difference formulae were also tested using the present data.

INTRODUCTION

There are parametric effects in which the perceived colour-difference of a pair of samples can change according to different viewing parameters such as different textures, separations, background colours, luminances, the physical size of samples, the magnitude of colour differences, modes of colours (surface or self-luminous). Researches have been conducted to evaluate and quantify the parametric effects on colour-difference perception for surface colours[1-3]. Since the preparation for the desired surface colour samples is tedious and costly, Cui *et al.*[4] investigated the effect of changes in viewing parameters using CRT colours. The parameters studied in their experiment were sample size, background, frame, width and colour of separation between pairs of samples. Montag and Berns[5] studied texture effect on suprathreshold lightness tolerances also using CRT colours.

The present study was to investigate the effect of texture and different sample separations on the perceived colour-differences using physical and CRT colours. For the physical sample experiment, a set of textile sample pairs were assessed by a panel of observers against a neutral background ($L^*=50$) using the grey scale method[1-4]. The CRT experiment was based upon the reproduction of those physical pairs using the same scaling method. It was divided into 7 phases according to the viewing parameters studied: samples with and without texture and pairs having different separations. Each textured sample pair had separations of a grey, a black, a modelled and a modelled colour with texture (a model was developed to simulate the colour of separation based upon two colours in a pair, which was used for the separation with and without texture). For sample pairs without texture, each pair only included a grey, a black and a no-gap separation. The experimental conditions for each phase are summarised in Table 1.

Table 1 The experimental conditions for each phase.

Phase No.	Texture	Separations
1	Physical textile sample pairs	
2	Yes	Black hairline
3	Yes	Grey hairline
4	Yes	Modelled colour hairline
5	Yes	Modelled colour hairline with texture
6	No	Black hairline
7	No	Grey hairline
8	No	No-gap

EXPERIMENTAL

Twenty-five pairs of textile samples were chosen corresponding to five colour centers: red, pink, yellowish green, green and blue. The physical size of each sample was 3 by 3 inches. A GretagMacbeth CE7000A spectrophotometer was used for measuring these colours under D65/10^0 viewing condition. Fig. 1 shows the colour distribution of these samples in CIELAB a*b* diagram. These pairs had mainly chromatic differences including chroma, hue or mixture of both differences. The average colour-difference was about 3 ΔE^*_{ab} ranging from 2 to 5 units.

CRT Performance

A 24-bit Barco monitor was used in the experiment. The white point was set to 6500K with a luminance of 90 cd/m^2. The monitor was characterised using the GOG model[6]. A Minolta CS1000 tele-spectroradiometer was used for measuring all CRT colours. The performance of the monitor was evaluated in terms of uniformity, repeatability and accuracy. The uniformity was found to have a mean ΔE^*_{ab} about 1.2 units between the centre and the other areas of the monitor for a grey colour studied. The repeatability was found to be 0.08 ΔE^*_{ab} units for a 7 hour period for the 4 monitor colours studied. Both the uniformity and repeatability are considered to be highly satisfactory.

Each physical sample was captured by a Nikon D1X digital camera, which was calibrated against a GretagMacbeth DC chart including about 240 colours. A 3x11 polynomial model was developed to convert camera RGB to XYZ values. These values were further transformed by the GOG model into monitor RGB. The textured images were then displayed on the monitor and measured. It was found that the agreement of the colour-differences between the physical and CRT pairs was about 1.3 ΔE^*_{ab} units, which was considered to be not sufficiently accurate. An iterative method was then developed by adjusting the RGB values of each pixel in the textured image to improve the colour match. The method was quite effective by achieving a mean ΔE^*_{ab} of 0.6 with a maximum of 1.5.

Visual Assessments

The colour-difference assessment using physical samples was judged twice by 11 normal colour vision observers using the grey-scale method[1-4,8]. Each pair was assessed, with the samples side by side and touching, under a D65 simulator in a VeriVide viewing cabinet. A polynomial was developed based upon the ΔE^*_{ab} of the grey scale and grades as given in eq. (1). It was used to convert visual results from grade to visual colour difference (ΔV).

$$\Delta V_i = -0.2194G_i^3 + 2.7967G_i^2 - 13.735G_i + 26.497 \quad (1)$$

When the textile sample pairs were reproduced on the monitor, it was found that the perceived colour-differences were not sufficiently large for visual assessment. This would reduce the accuracy of vissual results. Therefore, the individual colour-difference components of each pair (ΔL^*, ΔC^* and ΔH^*) was doubled with a mean of 6.1 ΔE^*_{ab}. In total, 175 (25x7) pairs of samples for all 7 phases were generated. The colour-differences of these CRT stimuli were assessed by 10 observers. Five of them repeated their visual assessments. The experimental situation is shown in Fig. 2. All the sample pairs were arranged against a mid-grey background with L* of 50. Same grey-scale method was applied in this experiment but a different grey-scale equation was used for the CRT experiments due to the change of the colour-differences in the grey scale.

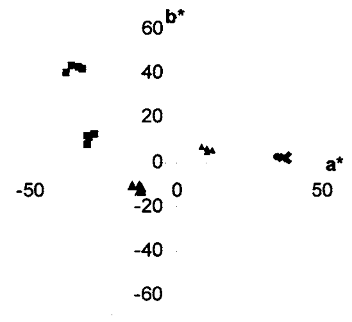

*Fig. 1 Sample distributions in a*b* diagram*

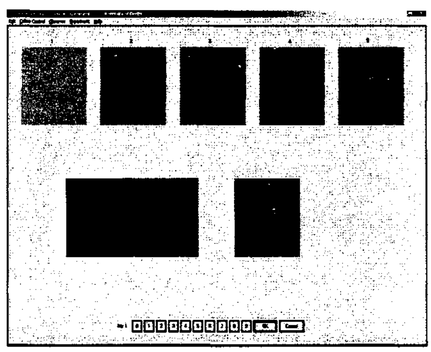

Fig 2. The arrangement of samples on CRT

RESULTS AND DISCUSSION

Observer Variations

Observer repeatability and accuracy were investigated in terms of PF/3, which was derived by Luo and Rigg[7]. For example, a PF/3 of 30 represents a 30% disagreement between the two sets of data investigated. Each observer's raw data in grades were first transformed to ΔV values using the grey-scale equations developed earlier. The PF/3 was calculated between each observer's two repeated sessions. These values for all observers in each phase was then averaged to indicate observer repeatability. For observer accuracy, the PF/3 measure was calculated between each individual observer's visual results and the mean visual results without any adjustment of their scales. It was found that the mean PF/3 value was 38 units for both accuracy and repeatability, which is considered to be typical for the colour difference assessment using the grey-scale method. The average ΔV from all observers was used to represent the mean visual results for each pair.

Evaluating Parametric Effects

Since the colour-differences for all the CRT pairs were doubled, their ΔV values thus were divided by 2 in order to directly compare with those of physical pairs (Phase 1). The parametric effects for the pairs in all phases are shown in Fig. 3. Ideally, the two sets of ΔV should lie on a 45° line. However, Fig. 3 shows that the perceived colour differences for all the CRT pairs were smaller than those of physical sample pairs. The slope between the physical phase and each CRT phase was also calculated with an average of 1.94 ranged from 1.83 to 2.23 for Phases 4 and 8 respectively. This indicates that the perceived colour differences of physical samples appear to be twice as large as than those of CRT pairs, with not much difference between different CRT phases. Cui *et al* also found little effect due to separation conditions for CRT colours. Only Phase 8 data in the present study had the same viewing condition as one of the Cui *et al* phases. Under this viewing condition, they compared their CRT data with the textile data prepared by Cheung and Rigg[8] and a paint data set prepared by RIT-DuPont[9] and found that these were 1.67 and 1.45 times larger than those of the CRT colours.

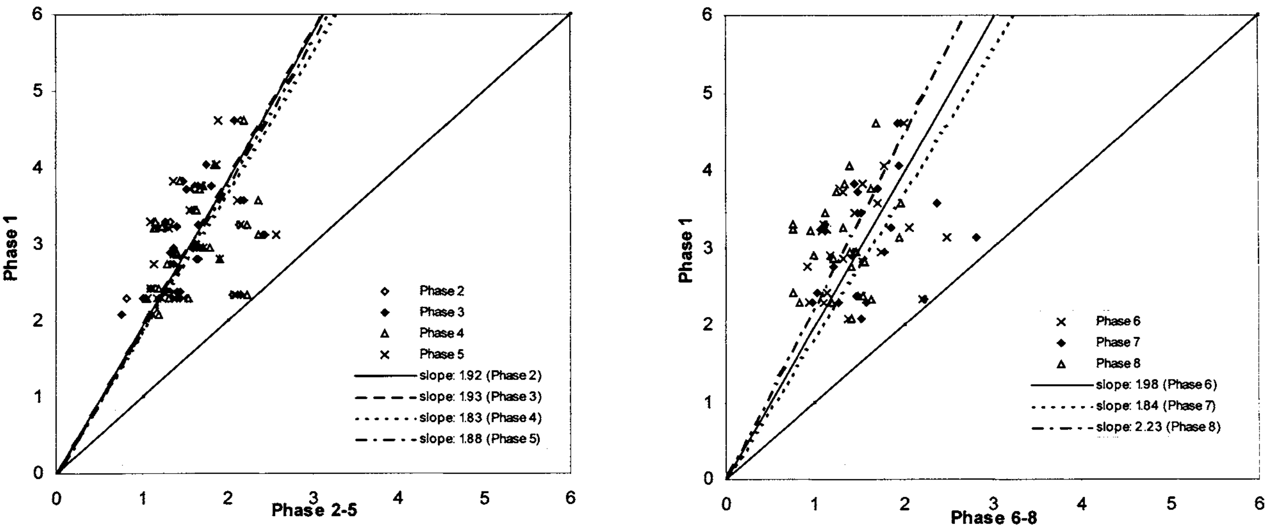

Fig.3 The ΔV values in Phase 2-8 against those in Phase 1

The agreement between the physical and CRT pairs for each phase was also examined using the PF/3 mean but each CRT phase results was adjusted by a scaling factor to have a same visual scale as that of physical samples. It was found that the PF/3 values ranged from 22% to 32%. The best and worst agreement with the physical pairs occurred for the CRT textured samples with a black or a grey separation, and no-textured samples without separation, respectively.

The PF/3 values were also used to reveal the texture effect on the perceived colour-differences. The results showed smaller PF/3 values for the textured phases (Phases 2 to 5) than those for the no textured phases (Phases 6 to 8). This indicates that the perceived colour-differences of the textured CRT pairs agreed better with those of the physical sample pairs. There was slight disagreement between textured and no-textured pairs, 14% and 17% for black and grey separations respectively (see Fig. 4). The slopes for Phase 6 vs. Phase 2 and Phase 7 vs. Phase 3 were 0.94 and

1.02, respectively. It indicates very small parametric effect due to texture. Montag and Bern[5] found that the texture had influence on lightness tolerance with average thresholds of 7.4, 6.2 and 4.0 for the full-, half- and no- texture samples respectively. In other words, the colour-difference is about twice larger for a no texture lightness pair

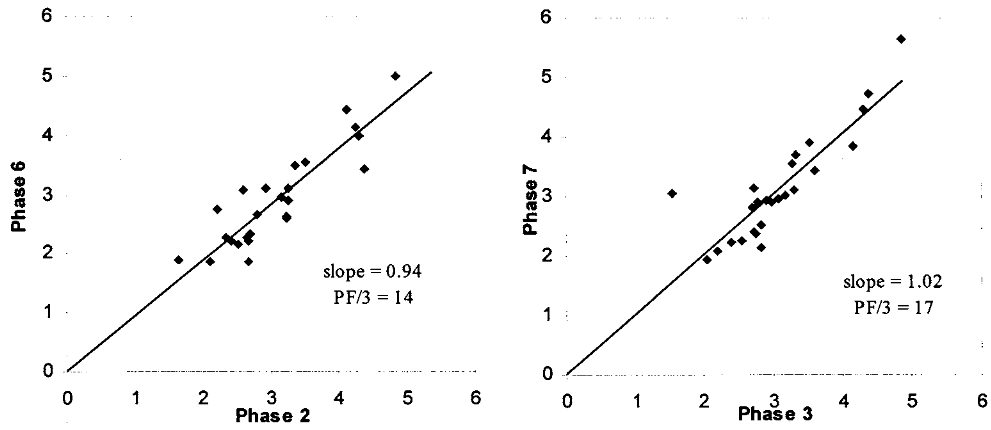

Fig. 4 The perceived colour difference between textured and non-textured sample pairs

comparing with that of a full texture pair. However, their pairs were all neural colours with variation only in lightness. Only chromatic differences were used in the present study.

Evaluating Colour Difference Formula

Five colour-difference formulae (CIELAB[10], CMC[11], CIE94[12], BFD[13], CIEDE2000[14]) were evaluated using the present data set. Each formula was tested using the visual results from each of 8 phases separately in terms of PF/3. The average PF/3 values are summarised in Table 2 according to physical sample, textured CRT sample and no textured CRT sample, respectively. It clearly shows that CIELAB colour difference formula performed the best for the physical sample and the worst for CRT no textured phases. The CMC, CIEDE2000 and BFD did not perform well for the physical samples comparing with CIELAB. For the CRT textured phases, all formulae gave the similar performance. These formulae predicted slightly more accurate for textured data than non-textured data. The mean PF/3 value of each formula in Table 2 shows little difference between different formulae.

Table 2 Performance of the colour difference formulae in terms of PF/3

Phases	CIELAB	CMC	CIE94	BFD	CIEDE2000
Physical samples	18	27	22	28	27
CRT textured phases	18	16	15	16	19
CRT no textured phases	25	19	18	19	18
Mean	20	20	18	21	21

CONCLUSIONS

The present study investigated the parametric effects using CRT colours. The results from 8 different phases were compared. It was found that different separations had little influence on the perceived colour-differences. The results from the phases with black hairline separation agree better with those of the phase using physical samples than the other phases. When there was no separation for the non-textured pairs, the perceived colour-difference could be reduced. The results also reveal a small effect on texture. The perceived colour-differences of the textured sample pairs agrees with those using physical samples better than those of the non-textured colour pairs. Since the lightness difference in those pairs was very small, there was no indication that the introduction of texture would increase the tolerance. The overall results show that the perceived colour-difference of CRT stimuli is about 50% smaller than that of the physical samples. Through the performance testing of five colour-difference formulae, it is found that there is no one colour difference formula which always outperform the others under all conditions.

REFERENCES

1. Guan SS, Luo MR. Investigation of parametric effects using small colour differences. Colour Res Appl 1999; 24:331-343.
2. Guan SS, Luo MR. Investigation of parametric effects using large colour differences. Colour Res Appl 1999; 24:356-368.
3. Xin JH, Lam CC and Luo MR. Investigation of parametric effects using medium colour difference pairs. Colour Res Appl 2001; 24:376-383.
4. Cui G, Luo MR, Rigg B and Li W. Colour-difference evaluation using CRT colours. Part II: Parametric effects. Colour Res Appl 2001; 26:403-412.
5. Montag ED, Berns RS. Lightness dependencies and the effect of texture on suprathreshold lightness tolerances. Colour Res Appl 2000; 25:241-249.
6. Berns RS. Methods for characterising CRT displays. Display 1996; 16:173-182.
7. Luo MR, and Rigg B, BFD(*l:c*) colour-difference formula, Part I—Development of the formula. J. Soc. Dyers Color 1987; 103: 86-94.
8. Cheung M, Rigg B. Colour-difference ellipsoids for five colour centers. Colour Res Appl 1986; 11:185-195.
9. Berns RS, Alman DH, Reniff L, Snyder GD, Balonon-Rosen MR. Visual determination of suprathreshold colour-difference toloerances using probit analysis. . Colour Res Appl 1991; 16:297-316.
10. CIE. Colorimetry, 2nd Ed. CIE Pub. No. 15.2 . Vienna: Central Bureau of the CIE; 1986.
11. Clarke FJJ, McDonald R, Rigg B. Modification to the JPC79 colour-difference formula. J. Soc. Dyers Color 1984; 100:128-132.
12. CIE. Technical report: industrial colour-difference evaluation. CIE Pub. No. 116. Vienna: Central Bureau of the CIE; 1995.
13. Luo MR, Rigg B. BFD(*l:c*) colour-difference formula, Part I—Development of the formula. J. Soc. Dyers Color 1987; 103:86-94.
14. Luo MR, Cui G, Rigg B.The development of the CIE 2000 colour difference formula: CIEDE2000. Color Res. Appl 2001; 26:340-350.

The Color Rendering Between a Color Proofer and a Printing Press

Mei-Chun Lo, Yui-Liang Chen, Pei-Li Sun and Ya-Hui Chiang
Department of Graphic Communications and Technology, Shih Hsin University, Taipei, Taiwan

ABSTRACT

The objective of this study is the derivation of various characterization models in 4-color process printing for achieving optimal appearance match between a color proofer and a press print. The printing characterization model included two processes. One was forward process (i.e. CMYK to CIEXYZ); the other was reverse process (i.e. CIEXYZ to CMYK).

The printing characterization models were derived from the Neugebauer type. Three models were derived here for the forward process including the broadband Yule-Nielsen modified Neugebauer, the spectral Yule-Nielsen modified Neugebauer and the cellular spectral Yule-Nielsen modified Neugebauer models. It was found the cellular spectral Y-N Neugebauer model outperformed others in the forward process. Thus it was also inverted to derive the reverse model. The Newton-Raphson iterative with multi-initial sets (MISs) approach based on the elements-category arrangement on the IT8.7/3 data set and the TLS (SVD) optimization method were found as a good combination to reduce the errors in the reverse process.

1. INTRODUCTION

Recent years have seen many alternative devices available to be chosen from different manufactures in open-systems, cross-media color reproduction environments. Consequently color management plays an important role to manage and communicate colors of the different devices in order to optimally achieve "what you see is what you get". In general, color management includes three tasks: the characterization of imaging devices, color appearance modeling and gamut mapping (MacDonald 1993).

In graphic arts industry, in order to utilize color effectively, often a proofer is employed to simulate the reproductions of a press that is used to produce high-quality printed matters for clients. In other words, both proofers and presses are the common representations of printing (output) devices for color imaging in a color reproduction system considered. The focus of this paper is, hence, the characterization of printing devices. In particular, the focus in this study is on a model, first proposed by Neugebauer (1937). Two-step process of modeling a four-color printing device was carried out. In the first step, three types of Y-N modified Neugebauer models were derived for forward process to map the CMYK data to their device independent values (i.e. CIEXYZ, CIELAB, or CIELCH), and then evaluated which one performed the best. The best one was then inverted using the GCR/UCA technique (Gray component replacement/Under-color removal). Also it was further modified to achieve a satisfactory performance. The experiments for testing both forward and reverse models are described next.

2. EXPERIMENTAL

A four-color CMYK printing device, EPSON EPL-8000 Laser Printer plus Epson RS-5000 Fiery LX RIP was used in this research. The printer first produced an IT8.7/3 test chart. The spectral reflectances were then measured using a Gretag Macbeth spectrolino (spectrophotometer) across the visible spectrum (380-730nm) at 10-nanometer intervals. Then colorimetric data including CIE XYZ, CIE LAB, and CIE LCH were calculated for CIE illuminant D_{50} and the CIE 1931 standard observers.

The overall color samples in the IT8.7/3 data set produced by the printing device were utilized to test the various characterization models in both the forward and the reverse processes. The measurements from both sixteen Neugebauer primaries and pure-tone ramps of C, M, Y, and K in the IT8.7/3, 68 samples in total, were used as the training set to estimate the dot growth functions (i.e. look-up tables (LUTs) of effectives dot areas (EDAs) to theoretical fractional dot areas (FDAs) for the C, M, Y, and K colorants by optimizing the Y-N parameter n value/values). These parameters were then used to obtain the XYZ or CMYK EDAs predictions for the CMYK digital FDAs corresponding to those patches on the IT8.7/3 test chart, in the forward or reverse process respectively.

3. THE PRINTING CHARACTERIZATION MODELS

3.1 Forward process

The first-step of characterizing the tested printing device was to derive the forward models. The forward process relates a device dependent color space, CMY/CMYK (or RGB), to a device independent color space, CIE XYZ, CIELAB, or CIE LCH. Three types of Neugebauer model were implemented in this investigation. They are the Yule-Nielsen modified, the Spectral Yule-Nielsen modified, and the Cellular spectral Yule-Nielsen modified Neugebauer models. According to the Neugebauer-type model, a given color needed to print out by a particular set of CMYK printer values is predicted by linear combinations of a small set of known colors. This set of samples is limited to sixteen primary colors, known as Neugebauer primaries, produced using the combination of C, M, Y, K colorants in amounts of 0% or 100% (i.e. solid ink) area coverage. Therefore the basic Neugebauer model in terms of broadband colorimetric specification can be expressed as:

$$X = (\sum_{i=1}^{16} a_i X_i) \qquad (1)$$

where X is the X tristimulus value of an unknown color, and X_i and a_i are the X tristimulus value and the fractional dot area (weighting factor) for the sixteen known primary colors respectively. X_i refers to the X of tristimulus values as the i-th Neugebauer primary of the known set mentioned above. The other two color stimuli, Y and Z, are given by replacing X with Y and Z respectively. Mathematically, the basic Neugebauer equations perform a linear interpolation in four-dimensional colorant (i.e. CMYK) space.

A. Broadband Yule-Nielsen modified Neugebauer model

Due to the penetration and scattering of light within the paper substrate, known as the Yule-Nielson (N-Y) effect (Yule and Nielson, 1951; Clapper and Yule, 1955), the basic Neugebauer model described above practically doesn't perform well. The N-Y effect results in a nonlinear relationship between the area coverage with colorant (i.e. effective dot area, EDA) and the corresponding XYZ tristimulus values. With the use of a power law to account for the N-Y effect, a simple modification was made to the Neugebauer model discussed previously. This modified model is so-called the broadband Yule-Nielsen modified Neugebauer model. The broadband equations (Pobboravsky and Pearson, 1972; Kita, 1989; Rolleston and Balasubramanian, 1993; Lo, 1995) for predicting X tristimulus is given by:

$$X = (\sum_{i=1}^{16} a_i X_i^{1/n})^n \qquad (2)$$

where n is often referred to as the Y-N factor (Pearson, 1980). Both the measured X_i and the weights a_i are the same as defined above. However, EDAs of C, M, Y and K in this study were computed using Yule-Nielsen equations (Pobboravsky and Pearson, 1972; Lo, 1995).

The use of the Y-N modified Neugebauer model in the characterization of the halftone printing device tested here required estimating some model-related parameters. The parameters include the XYZ values of 16 Neugebauer primaries, the CMYK dot growth (DG) functions, and the N-Y parameter (i.e. n value). The CMYK DG functions established the relationship between the digital control color values (theoretical fractional dot areas, FDAs) that drive the printer and the corresponding effective dot areas (EDAs), respectively for the C, M, Y, and K inks or colorants. The XYZ values of Neugebauer were obtained from direct measurement, while the other parameters were approximated using the SVD (Singular value decomposition) optimization method. (Press et al., 1992).

Preliminarily, a study of the application of the Y-N factor n-value in the broadband Y-N modified Neugebauer model, it was found that using two types of n-value/values, a general n-value (n_g) and a set of 4 n-values n_c, n_m, n_y, and n_k, gave better prediction performances than using only a singe n-value. The former one (i.e. n_g) was determined by optimizing both the Y-N equations and the broadband Y-N modified Neugebauer equations using the whole set of 68-samples training data; whereas the latter set of 4 n-values (n_c, n_m, n_y, and n_k) was approximated by optimizing EDAs using the Y-N equations for each of C, M, Y and K pure-tone ramps respectively. The optimized values obtained here for both n_g and (n_c, n_m, n_y, and n_k) were 2.1 and (2.0, 3.5, 1.8, 2.1) respectively. Therefore, a set of one-dimensional look-up tables (LUTs) was then generated to describe the relationships between FDAs and EDAs for each of the C, M, Y and K pure-tone ramps.

B. Spectral Yule-Nielsen Modified Neugebauer Model

It has been argued that the broadband type of Neugebauer equations is inappropriate to model a printing device (Viggiano, 1990; Yule, 1967). Therefore another Y-N modified type of the Neugebauer model dealing with the full set of visible spectral data was also derived here. This is the spectral Yule-Nielsen Modified Neugebauer Model. In this investigation, the spectral reflectances over a range of 380 nm to 730nm at 10-nm increments (i.e. 36 spectral data) were considered and are given by Equation (3).

$$R_\lambda = (\sum_{i=1}^{16} a_i R_{\lambda,i}^{1/n_\lambda})^{n_\lambda} \qquad (3)$$

where the weights a_i are the same as in Equation (1). The spectral data R_λ denote the predicted reflectances. The $R_{\lambda,i}$ are the measured spectral reflectances of the i-th Neugebauer primary of the known set mentioned previously. Merely in terms of the spectral instead of wideband approach, the spectral Y-N modified

Neugebauer model was derived in a similar fashion to implementing the Y-N modified Neugebauer model (Lino and Berns, 1998). The Yule-Nielsen n-factor n_λ varied as a function of wavelength in the format of $n_{\lambda,ink}$ or $n_{\lambda,g}$. The subscript *ink* indicates C, M, Y, or K colorant.

In a monochrome halftone process, colors are produced using only one of C, M, Y, or K inks (or colorants). Then the spectral Y-N modified Neugebauer predicted the spectral reflectances R_λ only using EDA a_{ink} and reflectance factor of both solid ink $R_{\lambda,w}$ and paper white $R_{\lambda,ink}$. The algorithm used is given by Equation (4).

$$R_\lambda = (a_{ink} R_{\lambda,ink}{}^{1/n_\lambda} + (1 - a_{ink}) R_{\lambda,w}{}^{1/n_\lambda})^{n_\lambda} \quad (4)$$

The Equation above estimated n-values (n_λ) and EDA (a_{ink}) for predicting the measured reflectances R_λ for a given color using the model described by Equation 3. Then the dot growth function (i.e. LUTs) for each of C, M, Y, and K colorants was established. The estimation of those model parameters was two-stage process. In the 1st stage, the EDAs presumedly equaled to the FDAs (i.e. theoretical dot areas); then the Y-N parameter *n* in both formats of n_λ (a general *n*-value) and $n_{\lambda,ink}$ (corresponding to each of CMYK colorants) was approximated for each wavelength using sum-of-squares reflectance error of the all 68-colors in the corresponding training sets as the minimization function (Lino and Berns, 1998). In the 2nd stage, the EDA a_{ink} was further enhanced by being optimized for every color of the corresponding ink (colorant) ramp in the training data set. Two optimization methods of the LS (least square) and the TLS (total least squares regression, i.e. SVD) (Xia et al., 1999; Berns et al., 1996) were used. Table 1 list the results tested using only the 68-colors training data set.

Table 1 The experimental results using both the LS and TLS SVD) optimization methods for deriving the spectral Yule-Nielsen modified Neugebauer model in the forward process.

		ΔE_{L*a*b*}	ΔE_{CMC}	ΔE_{BFD}	ΔE_{CIE94}	ΔE_{00}
LS	Mean	2.94	2.04	2.79	2.27	1.84
	Maximum	7.77	7.35	8.32	7.43	7.01
TLS	Mean	1.56	0.99	1.59	0.88	0.88
(SVD)	Maximum	4.21	2.99	4.96	2.51	3.02

As can be seen that the mean and maximum ΔE_{00} of TLS (SVD) approach were 0.88 and 3.02 respectively. It was superior to the LS approach where the mean and maximum ΔE_{00} were 1.84 and 7.02 respectively. Therefore the TLS optimization method further applied to derive the cellular spectral Yule-Nielsen modified Neugebauer model described later.

C. Cellular spectral Yule-Nielsen modified Neugebauer Model

With an attempt to introduce the Y-N corrections and spectral measurements into a cellular framework, the Neugebauer model was modified to interpolate within smaller subcells, rather than with the entire CMYK space. This type of Neugebauer model implemented here is known as the cellular spectral Yule-Nielsen modified Neugebauer model. The design of cellular divisions followed up the elements-category arrangement of the extended data set in IT8.7/3. Again, the similar approaches for the spectral Yule-Nielsen modified Neugebauer model above were used to derive the spectral Yule-Nielsen modified Neugebauer model.

All color samples in IT8.7/3 data set were used to test the performance of the three models. Only the spectral Yule-Nielsen modified Neugebauer model applied to the TLS (SVD) optimization approach was tested here. Table 2 lists the results. Overall, it can be seen that the cellular spectral Yule-Nielsen modified Neugebauer model outperformed to the others. Therefore, the cellular spectral Yule-Nielsen modified Neugebauer model was applied to invert the process.

Table 2 Evaluation results using the Y-N modified types of three Neugebauer models in the forward process.

		ΔE_{ab}	ΔE_{CMC}	ΔE_{BFD}	ΔE_{CIE94}	ΔE_{00}
Broadband	Mean	5.21	4.47	6.65	3.70	3.68
	Maximum	13.13	13.75	23.73	9.92	13.49
Spectral	Mean	4.71	4.42	5.96	3.60	3.44
	Maximum	10.82	13.64	17.65	8.95	10.40
Cellular	Mean	0.44	0.4	0.52	0.35	0.34
Spectral	Maximum	9.53	10.95	14.72	8.25	9.45

3.2. Reverse Process

The reverse process transforms the CIE values to device dependent CMYK signals. The GCR/UCA approach was implemented in order to derive the reverse model. Two-step approaches, including a K-value and CMY-values determinations, were carried out in the inversion of the best forward model (i.e. the cellular model).

A. K value determination

In the first process of K-value determination, the XYZ and LCH values of a given color were first entered and then the former converted into $D_{r\text{-}4c}$, $D_{g\text{-}4c}$, $D_{b\text{-}4c}$ using log-density functions. The next step was to determine a K value (i.e. EDA_k) via sequentially checking three cases recommended by Lo (1995). Case 1 used EDA_k=100 provided that all the red-, green-, and blue- colorimetric densities of the color (i.e. $D_{r\text{-}4c}$, $D_{g\text{-}4c}$ and $D_{b\text{-}4c}$) considered are larger than the corresponding channels of solid black ink (i.e. $D_{r\text{-}k\text{-}max}$, $D_{g\text{-}k\text{-}max}$ and $D_{b\text{-}k\text{-}max}$). Otherwise, Case 2 applied 0 of EDA_k when the smallest channel of $D_{r\text{-}4c}$, $D_{g\text{-}4c}$ and $D_{b\text{-}4c}$ is less than the threshold value D_{gcr}, a predetermined critical density point below which no GCR is performed. The threshold value D_{gcr}

was predetermined and had to be less than the smallest channel of (D_r, D_g and D_b) $_{3c\_max}$ (i.e. the overprint of three solid inks CMY). Finally, Case 3 adopted a GCR technique (Fisch, 1989; Juhola, 1989; Nakamura & Sayanagi, 1989) to get appropriate colorimetric densities of black ink (i.e. $D_{k\text{-}gcr}$) and then determine EDA_k via LUT_k. The parameter r_0 determined the degree (i.e. rate of gray component removed) that the GCR algorithm was applied to the color considered. A few sets of different levels of r_0 prescribed were evaluated previously to find an optimal combination of rates for gray component removed, and to ease the calculation of K-value-determination process.

B. CMY values determination

After the K value had been determined (i.e. EDA_k value determination), then the next step was to decide the CMY values. This procedure aims to predict the effective dot areas (EDAs) of CMY primary inks (i.e. EDA_c, EDA_m and EDA_y respectively). The type of Neugebauer equations is analytically noninvertible. Therefore the Newton-Raphson iterative method was employed to indirectly solve the cellular spectral Yule-Nielsen modified Neugebauer equations for CMY EDAs.

Multi-initial sets (MISs) of CMY EDAs chosen for a given color were based on the case-category for the K-value determination process. The EDAs predicted (using the best performing model found in the forward process), for all color samples in the IT8.7/3 data set, were previously grouped into three categories of data according to the case applied for the k-value determination. Then, all sets of EDAs in the same case-category were used as the MISs of EDAs for the considered color, to which this same case-category for the K-value determination was applied. Moreover, the MISs of EDAs in category of Case 2 were segmented into 10 subgroups, in terms of chroma values at 10 increments. It reduced the iterative calculation of converging for an optimal solution of CMY EDAs, needed for producing the target color using Case 2, because only one subgroup of EDAs' sets were used for the considered MISs.

Both the same procedure for the determination of both K (i.e. the determination of the level of gray component replaced, r_0) and MISs of CMY values and the iteration using the Newton-Raphson iterative method were repeated for every considered color to achieve a better approximation until ΔE_{00} value became less than a predetermined threshold.

Table 3 The evaluation results using models with different approaches derived in the reverse process.

Approaches		ΔE_{ab}	ΔE_{CMC}	ΔE_{BFD}	ΔE_{CIE94}	ΔE_{00}
Single-initial point, $(C, M, Y)_{EDA}$= (50,50,50), r_0=0.6.	Mean Maximum	16.32 111.50	13.39 65.24	21.63 145.10	11.28 64.46	11.07 65.40
Single-initial point, r_0=0.6. $(C, M, Y)_{EDA}$=(100(X/X$_w$), 100(Y/Y$_w$), 100(Z/Z$_w$)),	Mean Maximum	15.41 111.05	12.60 65.24	20.49 145.10	10.64 64.46	10.39 65.40
One initial point, r_0=0.6 $(C, M, Y)_{EDA}$=(100(X/X$_w$), 100(Y/Y$_w$) plus ω correction	Mean Maximum	15.76 128.70	12.63 65.24	21.07 147.60	10.78 64.46	10.83 67.01
MISs, r_0=0.6	Mean Maximum	3.22 29.25	2.32 11.94	3.82 32.74	1.93 10.92	1.88 11.91
MISs, r_0=0.7	Mean Maximum	3.67 33.00	2.54 13.70	4.30 36.12	2.15 12.83	2.10 13.99
MISs, r_0=0.8	Mean Maximum	4.43 36.79	3.03 16.05	5.16 43.17	2.58 14.79	2.53 16.28
MISs, r_0=(0.6,0.4)	Mean Maximum	2.74 25.61	2.07 9.42	3.28 29.98	1.72 7.42	1.66 8.38
MISs, r_0=(0.6,0.3)	Mean Maximum	2.69 21.94	2.06 7.93	3.23 25.41	1.71 6.07	1.65 6.83
MISs, r_0=(0.6,0.3,0.0)	Mean Maximum	2.56 14.08	2.00 7.85	3.09 15.25	1.66 5.77	1.60 6.03

The performance of the Newton-Raphson iterative method in one condition, r_0=0.6, was first evaluated. A step-size function ω proposed by Lino & Berns (1998) was also used to improve converging problems. It was found that there were no solutions of converging points (i.e. predicted CMY EDAs) for some test color samples when only starting with single initial set of iterative CMY EDAs. As shown in Table 3, the performance of the model was poor and a new advanced model, applying multi-initial sets (MISs) approach in the Newton-Raphson iterative method, therefore was implemented. The test results showed that an optimal solution of CMYK EDAs had been achieved for every color sample with an improvement of prediction accuracy. The results are also listed in Table 3. As can be seen, with a use of the MISs approach, the model performance significantly improved and become more pleasingly acceptable compared to those obtained by one fixed r_0 (say here 0.6) with single-initial point approach. In addition to the use of MISs approach, with a few different levels of r_0 to the K-value-determination process, the model gave much more pleasingly acceptable results compared to those obtained using only one fixed r_0. Here the approach using three different GCR' rates (r_0=0.6, r_0=0.3 and r_0=0.0) with MISs approach performed the best, with the mean and maximum ΔE_{00} of 1.60 and 6.03 respectively.

4. CONCLUSION

The characterization of the four-color printing device in this study was based on the IT8.7/3 data set. Three types of Neugebauer model were derived to characterize the printing device for forward CMYK-to-XYZ transformation. Those were: the Yule-Nielsen modified Neugebauer, the Spectral Yule-Nielsen modified Neugebauer and the Cellular Spectral Yule-Nielsen modified Neugebauer models. First of all, from a preliminary study of the application of the Y-N factor n-value in the broadband Y-N modified Neugebauer model, it was found that using two types of n-value/values, a general n-value (n_g) and a set of 4 n-values n_c, n_m, n_y, and n_k, gave better prediction performances than using only a singe n-value. When deriving the spectral Yule-Nielsen modified Neugebauer model, the TLS (SVD) method to obtain EDA values got the better results than the LS. It was accord with the results obtained by Xia et al. (1999). Two spectral Y-N modified types of Neugebauer model (including the spectral Y-N modified Neugebauer and the cellular spectral Y-N modified Neugebauer), with the use of both the Y-N corrections in the formats of both $n_{\lambda,ink}$ and $n_{\lambda,g}$ and the TLS (SVD) method, gave better prediction performances compared those obtained by the Y-N modified Neugebauer model.

Overall, in the testing of models performance in the forward process, the cellular spectral Yule-Nielsen modified Neugebauer model outperformed than others. Therefore, the cellular spectral Yule-Nielsen modified Neugebauer model was applied to the derivation of the reverse process. Further, using an advanced approach of Newton-Rapson iterative method with applying multi-initial-sets (MISs), it revealed that significant improvements had been made compared to the results obtained using single-initial-points based on Lino and Berns (1998). Moreover, if only one fixed GCR' rate was adopted, some color would produced too much black than demand. So more than one GCR' rate was tested. It was found, in addition to the use of MISs approach, with a few different levels of r_0 to the K-value-determination process, the model gave more pleasingly acceptable results compared those obtained using only one fixed r_0. Finally, the model applying the approach using three different GCR' rates of r_0=0.6, r_0=0.3 and r_0=0.0 with MISs approach outperformed the others.

The future work is using complex image to evaluate the performance of the printing characterization model derived here.

REFERENCE

1. Berns, R. S., Bose, A. and Tzeng, D.Y. (1996) "The Spectral Modeling of Large-format Ink-jet Printers", RIT Munsell Color Science Laboratory.
2. Green, P. and MacDonald, L. (2002) Color Engineering Achieving Device Independent Color, p.49-67, p.226-232.
3. Fisch, R. S. (1989). "Gary Component Replacement Research, Modeling Tone and Color Reproduction". Neugebauer Memorial Seminar on Color Reproduction, kazuo Sayanagi, Editor, SPIE Vol.1184, pp.77-92.
4. Juhola, H. (1989). "Gray Component Replacement in Newspaper Printing", SPIE Vol.1184, pp.93-100.
5. Lo, M. C. (1995). The LLab Model for Quantifying Color Appearance. PhD. Thesis, Loughborough Univ., pp. 13-27.
6. Clapper, F. R. and Yule, J. A. C. (1955), "Reproduction of Color with Halftone Images," TAGA Proc., pp. 1-14.
7. Lino, K. and Berns, R. S. (1998). "Building Color-Management Modules Using Linear Optimization I. Desktop Color System", Journal Of Imaging Science And Technology, Vol. 42, No. 1.
8. Luo, M. R. (1995) "A Review of Colour Difference Formulae." Colour Control for Surface Industries, Autumn School '95, Derby.
9. Luo, M. R. and Cui, G. and Rigg, B. (2002) "The Development of the CIE 2000 Colour Difference Formula:CIEDE2000", http://www.ifra.com/Website/ifra.nsf/html/colorqualityclub.html
10. MacDonald, L.W. (1993). "Gamut Mapping in Perceptual Colour Space", Proc. of 1th IS&T/SID Color Imaging Conference, 193-196.
11. Nakamura, C. and Sayanagi, K. (1989) "Gray Component Replacement by the Neugebauer Equations", SPIE Vol.1184, pp.50-p.63.
12. Neugebauer, H. E. J. (1937), "Die Theoretischen Grandlagen des Mehrfarthen-edruckes," Zeitschrift Wissenschaften Photography, pp. 73-89.
13. Pearson, M. (1980). "n Value for General Conditions", TAGA Proc., pp.415-425.
14. Pobboravsky, I. and Pearson, M. (1972) "Computing of Dot Areas Required to Match a Colorimetrically Specified Color using the Modified Neugerbauer Equations", TAGA Proc. pp. 65-77.
15. Press, W. H., Teukolsky, S. A., Vetterling, W. T. and Flannery, B. P. (1992) Numerical Recipes in C 2nd ed.
16. Rolleston, R. and Balasubramanian, R. (1993) "Accuracy of Various Types of Neugebauer Model", 1th IS&T/SID Color Imaging Conference, pp. 32-37.
17. Viggiano, S. J. A. (1990), "Modeling the Color of Multi-colored Halftones," TAGA Proc., pp. 44-62.
18. Xia, M., Saber, E., Sharma, G. and Tekalp, A. M. (1999) "End-to-end Color Printer Calibration by Total Least Squares Regression", IEEE Trans. Image Processing, Vol. 8, No. 5, pp. 700-716.
19. Yule, J. A. C. and Nielson, W. J. (1951), "The Penetration of Light into Paper and Its Effect on Halftone Reproduction," TAGA proc., pp. 65-76.
20. Yule, J.A.C. (1967), Principle of Color Reproduction, John Wiley & Sons, Inc, pp. 260-266 & 255-304.

Development of an Imaging Colorimeter for Skin Color Measurement and Its Clinical Application

Li Yang[1], Makio Akimoto[2] and Michio Miyakawa[3]

[1]Graduate School of Natural Science and Technology, Niigata University, 8050, Ikarashi-2, Niigata 950-2181, Japan.
[2]Institute of Science and Technology, Kanto Gakuin University, 4834, Mutsuura, Kanazawa, Yokohama 236-0032, Japan.
[3]Department of Bioscibanetics, Niigata University, 8050, Ikarashi-2, Niigata 950-2181, Japan

Examination of skin color is very important in the clinical diagnosis and cosmetic evaluation. Conventional colorimeter have proved inadequate for this purpose, since they do not provide spatial color information and because the measuring procedure randomly affects the color of the tissue. In this paper an imaging colorimeter is presented, where the non imaging optical photodetector of colorimeter is replaced with the charge-coupled device (CCD) sensor of a color video camera, enabling the independent capturing of the color information for any spatial point within its field of view. Combining imaging and colorimetry method, the acquired image is calibrated and corrected, under several ambient light conditions, providing non contact reproducible color measurements, free of the errors and the limitations present in conventional colorimeter. The technique has been used in hospital clinics for a wide variety of patients. There features highlight the potential of the imaging colorimeter as clinical and research tools for the standardization of clinical diagnosis and for the objective evaluation of treatment effectiveness.

INTRODUCTION

One of the objectives of the rehabilitation of patients with facial defects is the inconspicuous reconstruction of this defect as soon as possible after operation or trauma. Color is one of the most informative features, the visual grading of which is randomly affected by several factors, such us viewing geometry, the experience as well as the visual acuity of the observer, etc. Moreover, due to the obvious limitations in the human visual recording ability of color information, the visual monitoring of the lesion cannot be effective. Thus, visual grading and monitoring lacks of accuracy and reproducibility. Quantification of tissue lesions color features is of essential importance in clinical practice, because several tissue lesions can be identified objectively, based on measurable quantitative parameters. This is an important improvement, since *in vivo* quantitative color measurements of the lesion can provide sensitive, reproducible, and objective indexes for the correct assessment of disease severity, effectiveness of the treatment, and monitoring. For this purpose, there has been a considerable effort for the color quantification of tissue lesions. This is mainly performed by the use of colorimeter, because they have shown a highly significant correlation between visual assessment and measurements (Wilhelm et al., 1989). Colorimeter have been used in dermatology, for quantification of skin color changes (Fullerton et al., 1997; Clarys et al., 2000; Bjerring, 1995), induced by erythema and tanning (Kollias et al., 1988), by topical corticosteroid preparation (Feather et al., 1982; Queille-Roussel et al., 1991), by long term hemodialysis (Deleixhe-Mauhin et al, 1992), etc. A prerequisite for correct color measurements using these devices is the contact between the aperture of the probe and the examination area in order to eliminate the influence of the background illumination on the measured color of the area of interest. As a result, they cannot be used for color characterization of the internal organs of the human body. Moreover, this contact is the source of several errors and limitations, especially in relationship with color characterization of biological materials. Some of them are: 1) the pressure of the aperture-tissue contact causes local ischaemia and, therefore, random color alterations of the examination area; 2) illumination of turbid biological materials through a probe with a small aperture causes edge loss of light, resulting in systematic errors in color measurements; 3) color meters provide only an estimate of the average color of the area surrounded by the standard small aperture of their probe. As a result of this integration, lesions with size smaller than this aperture or with variegate colored areas cannot be characterized separately. In this paper, a imaging colorimeter with video camera is presented, which combining imaging techniques and color measurement principles, can provide non contact, two-dimensional color measurements, free of limitations and random and systematic errors which are present in conventional color meters. This system can also be adapted to any optical imaging device e.g., microscopes, endoscopes, etc. and so it can serve in standardization of clinical diagnosis, monitoring and evaluation of the effectiveness of the treatment in several medical fields using quantitative color parameters.

OPTICAL PROPERTIES OF SKIN

The skin is divided into three layers: the epidermis, the dermis, and the subcutaneous tissue. The epidermis is the outermost portion of the skin and is composed of stratified squamous epitheliums. The innermost layer of the epidermis consists of a single layer of cuboidal cells called basal cells. These cells differentiate and migrate towards the skin surface. The outer layer of the epidermis is called the stratum corneum, which is composed of flattened and dead cells. From the optical point of view, one type of regularity of the physical world has been known for a long time: the specular reflection of most surfaces appears to be white or the color of the illuminant. In general, many inhomogeneous surfaces reflect light in the following manner for see Figure 1. When light illuminates a surface, some light is reflected immediately from the interface between the surface and the air and some penetrates into the surface, is partially absorbed and partially scattered within the surface pigment material, and then is reflected back to the surface and into the air again (Scheuplein, 1964; Anderson et al., 1981; Van Gemert et al., 1989). The first component, which is reflected immediately at the interface, is usually called the specular component of the total reflected light, and the second component is called the diffuse component since the light coming out of the surface is almost random in direction. The specular component is usually more directional than the diffuse component, unless the surface is very rough. For many surfaces of inhomogeneous materials, the specular component has a spectral-energy distribution close to that of the incident light, ie., the color of the specular component is close to the illuminant color. This specular component is function of the index of refraction of the interface material. Because many types of material serving as binders or as overcoats are some sort of oil, and most oils have very constant indices of refraction for the visible wavelengths, we see specular reflection with color close to that of the incident light. The spectral-energy distribution of the diffuse component is modified by the pigments in the surface material and is what is meant by the actual color of the surface.

EXPERIMENTAL METHODS

The basic hardware components of the system are a 3-chip CCD color video camera, light source, a real-time image processing board, magneto-optics disk, and personal computer, which controls the entire system as shown Figure 2 (Akimoto et al, 1999, 2000). Both of the camera and projector are housed in a portable box, which is 120mm high, 170mm wide, and 60mm deep. The illumination is provided by a 100-V, 25-W krypton lamp, connected with color temperature conversion filter, the light of which transmitted and delivered onto the surface at an angle of 45° to the normal. The reflected light is collected by the camera at 0° to the surface normal. The housing is completely closed and has a smooth surface for easy disinfection. Electrical safety is ensured by the use of insulating materials for the housing. The base of the housing is a rectangular frame which defines the optimum distance and field of view when it is held close to the biological tissue. To avoid the significant variation in the brightness of the light source after it is turned on over 5 minutes were allowed for it to stabilize before measurements were performed. A real-time video digitizer is installed on a personal computer. The picture obtained provides a set of data which offers a spatial resolution of 768(horizontal)$\times$ 494(vertical) pixels and a color resolution of 256 levels for each band of red, green and blue (RGB), indicating that each band has an independent brightness in 256 gradations (0, darkest; 255, brightest), and that the color of each pixel is expressed by an additive mixture of the three basic colors. The auto gain regulator (a mechanism which regulates the brightness of a picture automatically) of the camera was not used. The system is calibrated for color at the color temperature of the daylight. The system is also calibrated geometrically to determine the

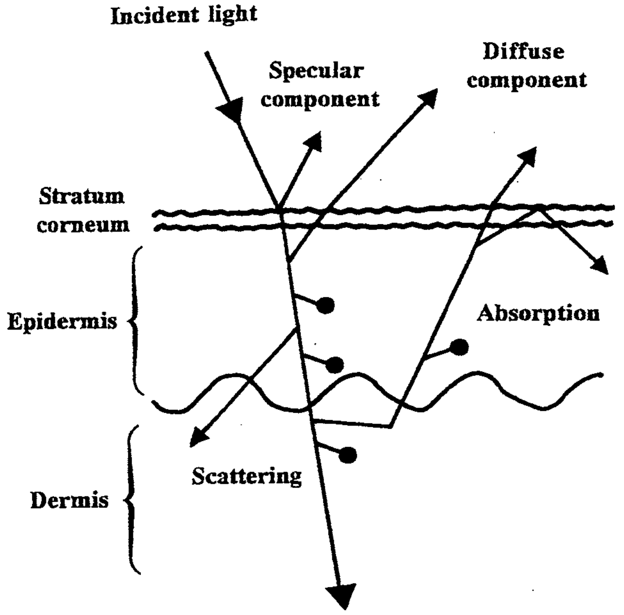

Figure 1. Schematic structure of the skin.

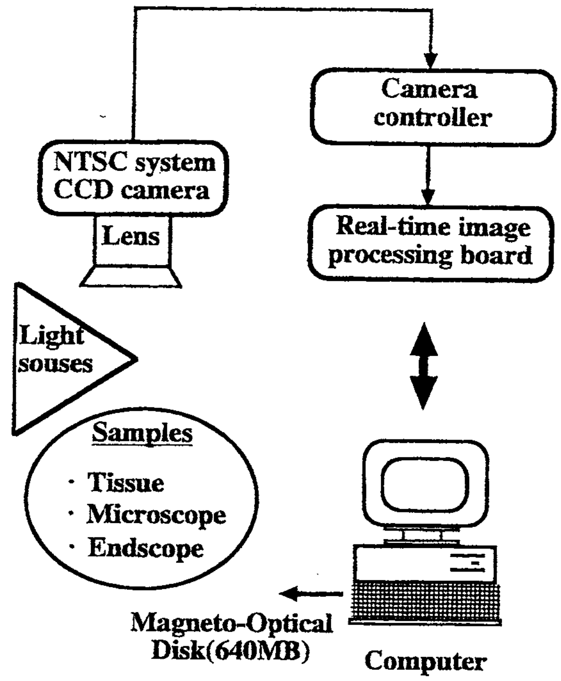

Figure 2. System utilized for the color analysis of the skin consisting of a video camera and personal computer.

relative positions of the camera and projector. The distance of the camera,s focal point from the frame at the base of the housing and the location of the focal points of the camera and projector enable all the necessary quantities, such as angles of incidence, to be derived. A thin-chip of magnesium oxide is used as a white standard and the camera color balancing controls are adjusted until all three color channels give the same output. The measuring area is equal to 55×75 mm of surface. The probe is applied on the skin surface simply by weight (1850 g). For measurements of reflected-light color, this reflected-light colorimeter offers different color systems for measurement. The L*a*b* system recommended by the CIE seems to be particularly convenient for skin color assessment. The color is expressed in a three dimensional space. The L* value (luminance) gives the relative brightness ranging from total black (L*=0) to total white (L*=100). The a* value represents the balance between red (positive values) and green (negative values). The b* value represents the balance between yellow (positive values) and blue (negative values). The color range from red to green is represented by parameter (a*) with +100 being red only and -100 green. The dimension (b*) measures the color spectrum from yellow (+) to blue (-). In the described system, the CIE-L*a*b* uniform color space is used and the derivation of the L*, a*, b*, C*, and h° color parameters from XYZ values is described. Standardization was done by video camera acquisition of 55 colors from a Munsell's color chips. Every color was also measured in CIE-L*a*b* by spectro colorimeter (CM-1000, Minolta, Osaka, Japan). In order to validate the device, we carried out acquisition of other colors, and we measured them in parallel with the Minolta colorimeter. For instrument measurement of skin color, basic studies on the eighty healthy male subjects have been chosen and divided into two groups; 40 young adults from 21 to 35 years old (average 27±4 years old) and 40 middle aged adults from 35 to 45 years old (average 40±5 years old). They were informed of the details of the experimental process and their consent was obtained prior to the measurements being made.

RESULTS AND DISCUSSION

To obtain a color representation close to that of eye vision, we expressed the RGB space in terms of a colorimetric space reference normalized by CIE-L*a*b* uniform color space. Standardization was done by video camera acquisition of 55 colors from a Munsell's color chips. Every color was also measured in CIE-L*a*b* by spectro colorimeter. For the spectrocolorimetric measurement, the field diameter was 8mm. The correlation between the two devices is shown in Figure 3. These data confirmed the spectrocolorimeter within $\pm 2\%$ of L*, a* and b*. This is good in view of the different geometry of measurement. The repeatability of the measured RGB values was estimated using a light source without background light and found to be within 1.5% of the full-scale output. The above suggests that the measurements are practically not affected from the background illumination. The aim of this study was to demonstrate that the colorimeter could measure a skin color and reproduce a rank order of the potency of the test formulations. The distribution of CIE-L*a*b* parameters for the eighty male subjects represents objectively the ventral forearm skin color phenotype of the group. The range of each color space parameter within the group provides a numerical specification of the distribution of the corresponding color attribute as it would have been visually perceived. The L* values ranged from 59.0 to 75.0 and for the histogram in Figure 4 class interval of 3 was chosen on the basis that it was over twice the mean within sample standard deviation and because it represented a difference in this color attribute that would have been just visually apparent for two colors that were otherwise similar with respect to hue angle and chroma. The apparent asymmetry of the distribution within the group was confirmed by a goodness of fit test showed that the hypothesis that the L* values were normally distributed about a mean of 68.2 could be rejected at the 95% level of confidence. This meant that there were a few individuals whose skin was much lighter than would be expected from a normally distributed range of L* values. The hue angles (h°) ranged from 54.0° to 78.0° and for the histogram in Figure 4 a class interval 5° was used because a difference of this magnitude would be visually apparent. A goodness of fit test applied to the distribution of hue angle values showed that the hypothesis that it was normal about a mean of 64.5° could not be rejected at the 95% level of confidence. A difference in hue angle was noted between some subjects as the only color attribute that distinguished them because they were otherwise similar with respect to L* and C*.

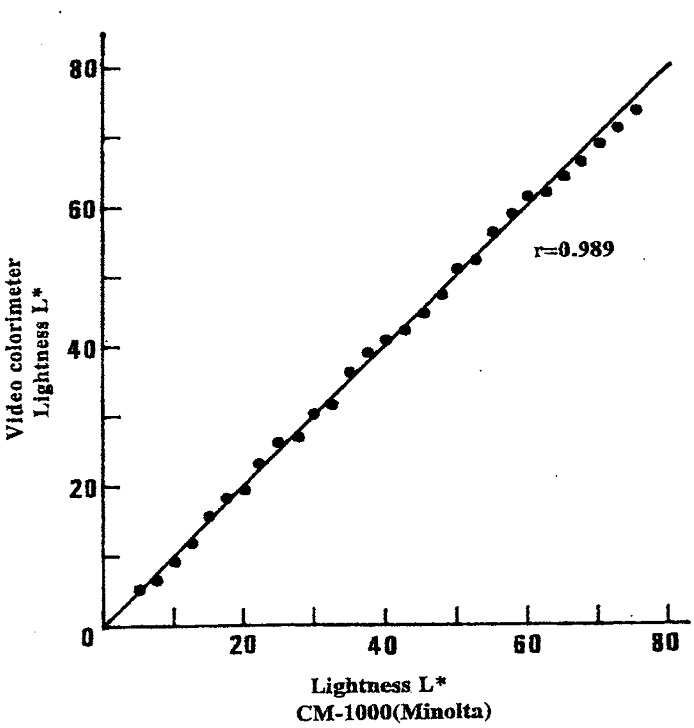

Figure 3. Correlation between the video colorimeter and the Minolta CM-1000 colorimeter for the L* colorimetric parameter.

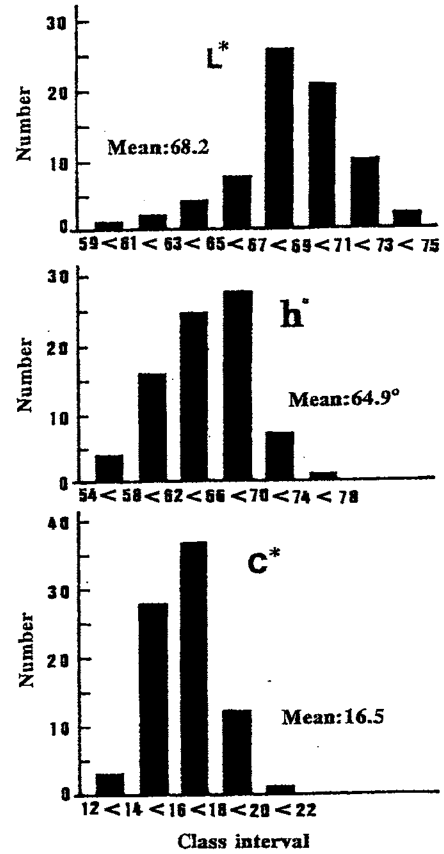

Figure 4. Distribution ventral forearm skin colors of eighty male subjects, expressed as the measured values ofCIE-L*a*b* color space, L* (top), hue angle (h°) (middle), and chroma (C*) (bottom).

4

The choroma (C*) values ranged from 12.0 to 22.0 and for the histogram in Figure 4 class interval of 3 was chosen. A goodness of fit test of the hypothesis that the values were normally distributed about a mean of 16.5 could not be rejected at the 95% level of confidence. Differences in the skin color between individuals could be identified where both the L* and h° values differed but the values for C* were similar, or where the values for both the C* and h° differed but the L* values were similar. A further possibility was identified where differences in both L* and C* were evident but the hue angles were similar. For many randomly selected pairs of individuals all three CIE-L*a*b* values were different.

CONCLUSION

Dermatologists have long tried to quantify skin color and had few results until the advent of colorimetry. With the image colorimeter, quantification of skin color has become a simple matter: skin color can be measured rapidly, non-invasively, and reproducibly. The instrument, which can be used by paramedical staff, provides data that lend themselves for comparison, irrespective of where they are collected. The instrument has enabled definition of the range of physiologic values of skin color, and has revealed marked variations between exposed and non exposed skin. Constitutional skin color characterizes an individual's phenotype better than facultative skin color and is highly indicative of vulnerability to sunlight. On the practical level, colorimetric skin color values can be used to study pigmentation capacity, to program photo chemotherapy, and to predict the risk of, and prevent, actinic cancer. Colorimetry can be used to quantify the intensity of erythema of spontaneous and experimental lesions. Algorithms used to transform RGB components in the CIE-L*a*b* colorimetric space permitted us to obtain a very good correlation with a colorimeter. This method gives visual information that is similar to the consumer's perception and enables us to quantify directly on volunteers the color of skins and their evolution with time. This kind of methodology could be adapted to other types of skin color.

References

Akimoto, M., Hata, M., Miura, Y., Numano, K., Yuge, M., Nakagawa, E.,Omi, T., Development of an Imaging Colorimeter for Noncontact Skin Color Measurement and Its Clinical Application. in Abstracts, 5th Meeting of the German-Japanese Society for Dermatology, p.54, Marburg, Germany, 1999.

Akimoto, M.,Takata, S., Hata, M., Asaeda, T., Yang, L. and Miyakawa, M., Physical Basis of Skin Color and Its Clinical Evaluation. in Proc. Progress in Electromagnetics Research Symposium, p.225, Cambridge, MA, USA, 2000.

Anderson, R.R. and Parrish, J.A., The optics of human skin. J. Invest. Dermotol., 77: 13-19, 1981.

Bjerring, P., Spectrophotometric characterization of skin pigments and skin colour. In: Serup J, Jemic CBE, eds. Handbook of non-invesive methods and the skin, Boca Raton: CRC Press, Chap. 16.1, 1995.

Clarys, P., Alewaeters, R., Lambrecht, R. and Barel, A.O., Skin color measurements: comparison between three instruments: the Chromameter, the DermaSpectrometer and the Mexameter, Skin Res. Technol., 6: 230-238, 2000.

Deleixhe-Mauhin, F., Hrezinski, J.M., Rorive, G. and Pierard, G.E., Quantification of skin color in patients undergoing maintenance hemodialysis. J. Amer. Acad. Dermatol, 27: 950-953, 1992.

Feather, J.W, Ryatt, K.S, Dawson, J.B. et al., Reflectance spectrophotometric quantification of skin colour changes induced by topical corticosteroid preparations. Br. J. Dermatol, 106: 436-444, 1982.

Fullerton, A. and Serup, J., Site, gender and age variation in normal skin colour on the back and the forearm: tristimulus colorimeter measurements, Skin Res. Technol., 3: 49-52, 1997.

Kollias, N. and Baqer, A.H., Quantitative assessment of UV-induced pigmentation and erythema. Photodermatology, 5: 53-60, 1988.

Queille-Roussel, C., Poncet, M. and Schaefer, H., Quantification of skin color changes induced by topical corticosteroid preparations using the Minolta Chroma Meter. Br.J. Dermatol, 124: 264-270, 1991.

Scheuplein, R.J., A survey of some fundamental aspects of the absorption and reflection of light by tissue, J. Soc. Cos. Chem.,15: 111-122, 1964.

Van Gemert, M.J.C, Jacques, S.L, Sterenborg, H.J.C.M. and Star, W.M., Skin optics, IEEE. Trans. Biomed. Eng., 36: 1146-1154, 1989.

Wilhelm, K.P., Surber, C. and Maibach, H.I., Quantification of sodium laurel sulfate irritant dermatitis in man: Comparison of four techniques: skin color reflectance, transepidermal water loss, laser Doppler flow measurement and visual scores. Arch Dermatol Res, 281: 293-295, 1989.

Measurement of gonio-spectral reflectance of a figured satin
--- An examination of the color recording method for Japanese KIMONO (1) ---

SUZUKI, Takuzi* and KOBAYASI, Mituo*,**
* National Museum of Japanese History
** The University of Electro-Communications

1. INTRODUCTION

KIMONO, a Japanese traditional costume, has beautiful color composition based on Japanese culture (figure 1, 2). As KIMONO is made of silk or cotton colored by natural dyes, its colors easily fade by aging or exposing to the light. It is important to record the color information to preserve our precious culture.

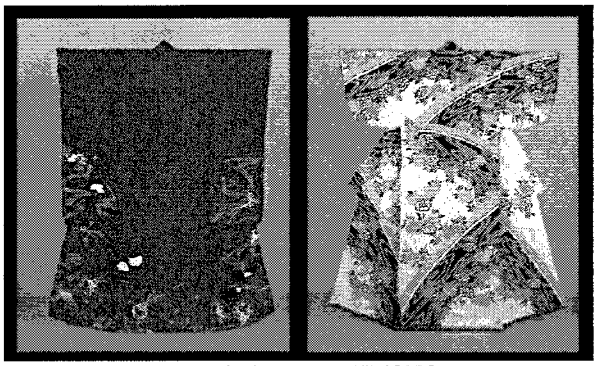

Figure 1: Japanese KIMONO

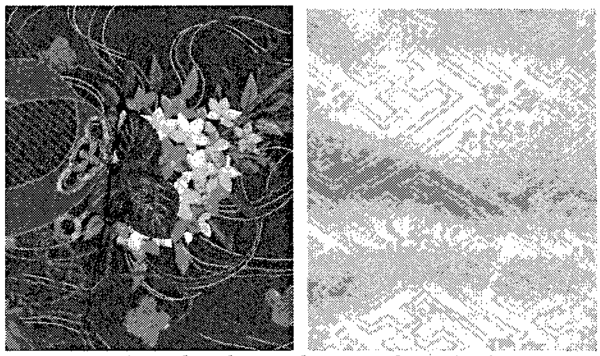

Figure 2: Embroidery and weave of KIMONO

We found two problems for recording of the color of KIMONO [1]:

1) KIMONO has too complex color composition to measure by a colorimeter;
2) Color of textile or embroidery of KIMONO changes by an illumination and by a view point.

The use of a digital still camera, suitable for capturing of color composition as an image, is an answer of the problem 1) [2].

Now we focus on the problem 2). Some kinds of embroidered silk threads glisten. Weave structures and woven patterns of fabrics are closely related to color changing. Examinations of gonio-spectral reflectance of fabrics and embroidery of KIMONO are required for understanding of color changing mechanism. But it is quite difficult to measure the whole part of a KIMONO by goniospectrophotometry. KIMONO should not be illuminated with high intensity of light for a long time for preservation.

It is one of hopeful solution to estimate color changing pattern from several images each of which has its angle and lighting. A database of gonio-spectral reflectance of several kinds of fabrics and embroideries indexed by kinds of weave structures and embroidery techniques has to be made for estimation.

This paper is a report of our first trial of measurement of gonio-spectral reflectance of fabrics of KIMONO. First, measurement of gonio-spectral reflectance of a sample is described. Second, a piece of figured satin as a sample and equipments for measurement are introduced. Finally, the results of measurement are shown.

2. MEASUREMENT OF GONIO-SPECTRAL REFLECTANCE

A light source and a measuring instrument for measurement of gonio-spectral reflectance of a sample are composed as figure 3. There are four parameters for measurement. In figure 3(a), α is an angle of an incident lay of the light source from a horizontal plane, and β is an angle of reflected light to the instrument from the horizontal plane. In figure 3(b), θ is an angle of reflected light to the instrument from a direction of the incident

* National Museum of Japanese History, 117 Jonai-cho, Sakura-shi, Chiba 285-8502, JAPAN
** The University of Electro-Communications, 1-5-1 Chofugaoka, Chofu-shi, Tokyo 182-8585, JAPAN

ray, and φ is an angle of rotation of the sample.

Measurement of 3-dimensional glossiness of cloth is introduced in a document [3]. (See figure 4.) It is difficult to give γ when the measuring instrument is fixed by a tripod for instance. We use θ instead of γ in this paper.

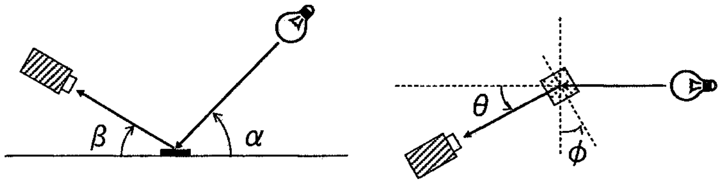

(a) side view *(b) top view*

Figure 3: Parameters of measurements of gonio-spectral reflectance

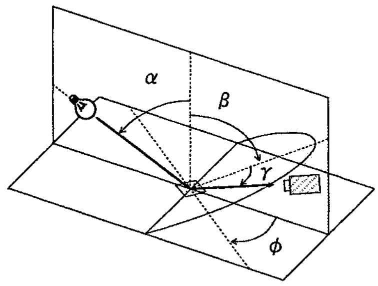

Figure 4: Measurement of 3-d glossiness (αβγ-system)[3; p.726; Fig.18-14]

3. MEASUREMENT OF A PIECE OF SATIN WEAVE FABRIC

The sample we measured is a piece of silk fabric of old KIMONO (made in early 19c.). This fabric have a *rinzu-zi* (綸子地; monochrome figured satin) weave structure. The *rinzu-zi* is one of variation of *syusu-ori* (繻子織; damask) weave [3,4]. Figure 5 shows two measurement points *a* and *b*. Point *a* looks bright and point b looks dark. Figure 6 shows enlarged images of points *a* and *b*. Angles of incident rays are different between figure 3(a) and 3(b). Light and darkness are reversed.

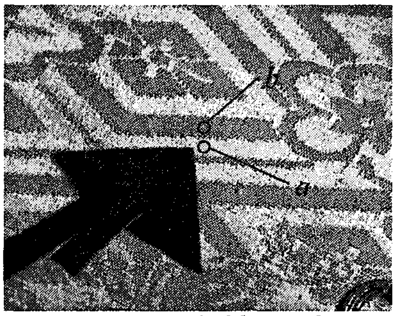

Figure 5: A sample fabric and two measurement points

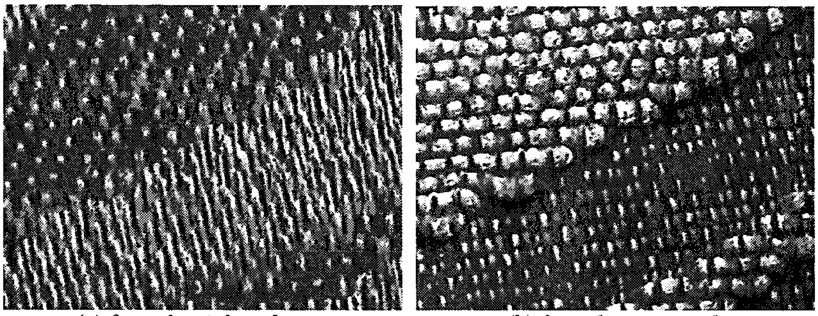

(a) from the right side *(b) from the upper side*

Figure6: Enlargement of illuminated sample

The woven pattern of the sample is a five-harness weft-faced satin figure on a five-harness warp-faced satin ground. Point *a* is warp-faced (ground), and point *b* is weft-faced (figure). Threads of a fabric glitter when incident ray cross threads. Thickness of threads is different between warps and wefts.

Figure 7 shows the setting of measurement equipments. The measuring instrument is a spectroradiometer PR-704 (Photo Research, Inc.). It is fixed on the top of the sample by a copy stand. (Hence β=90°, θ is any.) The measuring instrument will be fixed by a tripod when β is small. The light source is a xenon lamp. Light is guided by a light fiber and illuminates the sample. A turntable rotates the sample and gives φ.

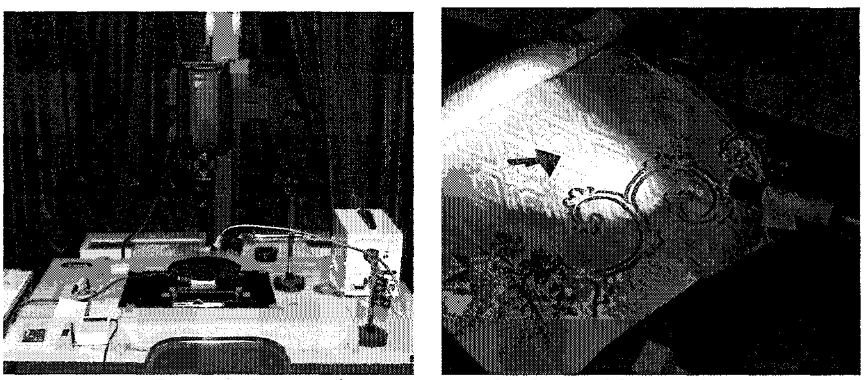

Figure 7: Setting of equipments and lighting of the sample

A spectroradiometer measures spectral radiance. To know a spectral reflectance r of the sample from a spectral radiance t, a spectral radiance t_0 of uniform reflecting diffuser (spectral reflectance is r_0) under the same illumination must be known. t and t_0 can be denoted as $t=rs$, $t_0=r_0s$, where s is spectral radiance of perfect reflecting diffuser under the illumination. Consequently $r = t/(t_0/r_0)$.

4. RESULTS

Figure 8 shows gonio-spectral reflectance of point *a*, and figure 9 shows gonio-spectral reflectance of point *b*. Where α=15°, 30°, 45°, 60°, β=90°, and φ=0°, 30°, 60°, 90°, 120°, 150°. Figure 10 shows reflectance at 550nm of points *a* and *b*. These figures give the followings:

- More sampling points of φ are required to trace increase and decrease of spectral reflectance more precisely.
- Maximum of spectral reflectance of point *a* is higher than of point *b*. Fine warps reflects light stronger than thick wefts.
- In case of α=15°, reflectance is over 100%.
- As α is smaller, spectral reflectance is changes a lot for transition of φ.
- Two peaks of change of reflectance for transition of φ are shown in figure 9(a). Small areas of wefts contribute this change.

5. CONCLUSION

Several kinds of fabrics and embroidery will be measured to establish a database of gonio-spectral reflectance. The indices of database are kinds of fiber (silk, cotton, hemp, etc.), weave structure (plane, twill, damask, etc.), dyeing, and embroidery. It is interesting task to examine possibility of estimation of color changing of KIMONO for the database. Especially we are interested in *tamamusi-ori* (玉虫織; fabric that the color of warps and wefts are different).

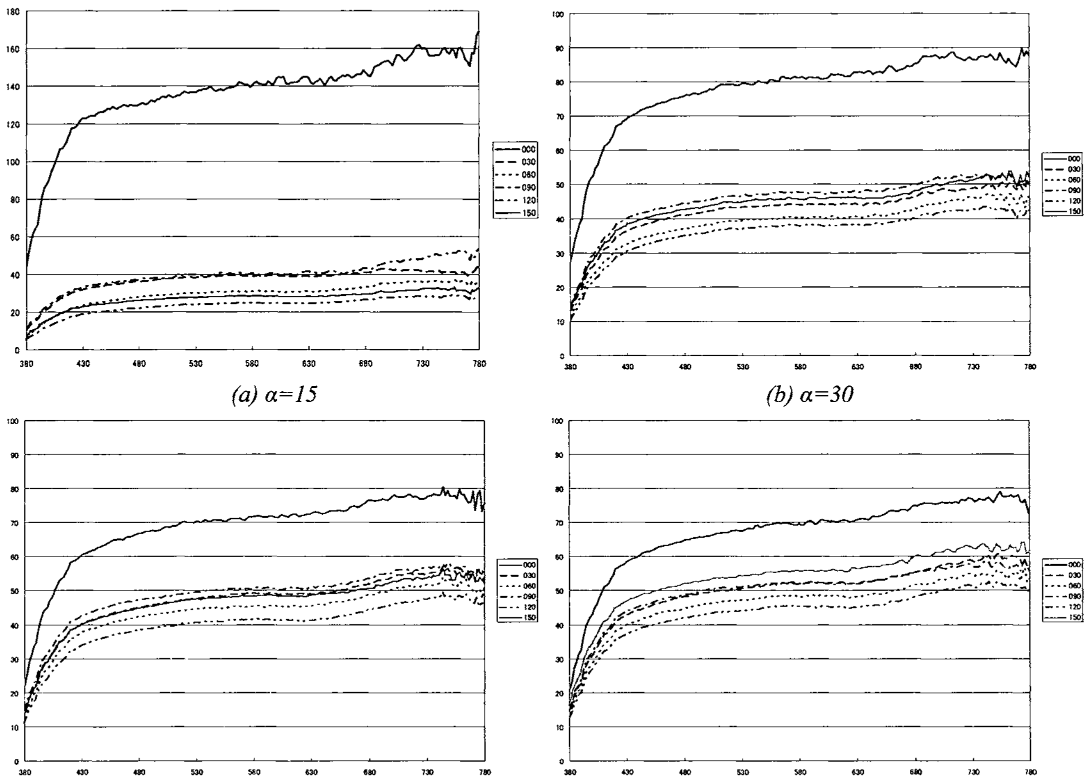

(a) α=15　(b) α=30

(c) α=45　(d) α=60

Figure 8: Gonio-spectral reflectance of point a

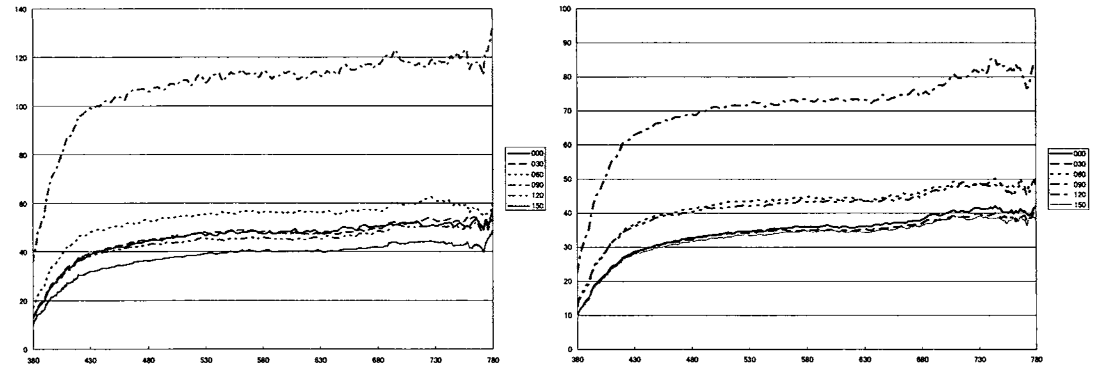

(a) α=15 (b) α=30

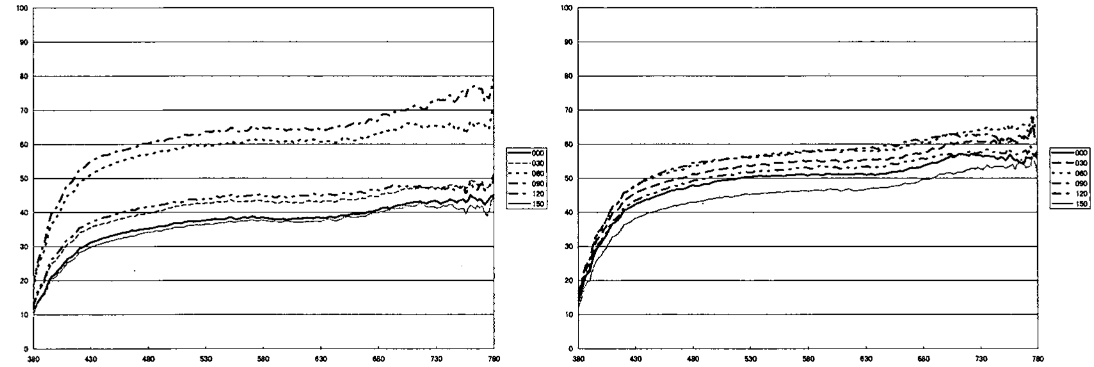

(c) α=45 (d) α=60

Figure 9: Gonio-spectral reflectance of point b

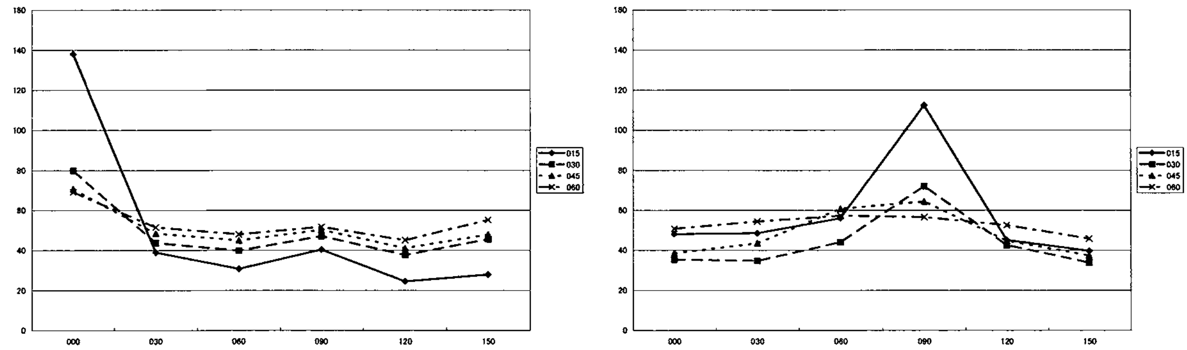

(a) point a (b) point b

Figure 10: Reflectance factor at 550nm

ACKNOWREDGEMENT

Many thanks to Mr. SAWADA, Kazuto of National Museum of Japanese History for fundamental lecture on KIMONO, selection of sample cloths, and technical suggestion as a specialist of dyeing and weaving.

REFERENCES

[1] KOBAYASI, Mituo, YAMAGUCHI, Takeshi, OGAWA, Yoshimi: An analysis of color features of Japanese traditional robes "KIMONO" in Edo-era, Proceedings of AIC 2003 Bangkok (2003-8).

[2] Takuzi SUZUKI, Mituo KOBAYASI: Accurate recording of color information of museum materials by digital still cameras --- in case of "Ukiyo-e" and "Kimono" ---, Proceedings of AIC 2002 SI, Maribor, Slovenia, pp.212-218 (2002-8).

[3] The Color Science Association of Japan (ed.): Handbook of Color Science [Second Edition], University of Tokyo Press, 1998, p.726.

[4] Sae Ogasawara: *Some to ori no kansyô kiso tisiki* (fundamentals for appreciation of dyeing and weaving), Sibundô, 1998.

[5] Amanda Mayer Stinchecum: KOSODE: 16^{th}-19^{th} Century Textiles from the Nomura Collection, Japan Society and Kodansha International, 1984.

An Evaluation of Coarse 3D Image Color Histograms for Imaging Applications

Pei-Li Sun, Zhong-Wei Zheng and Jan Morovic*

Department of Graphic Communications & Technology, Shin Hsin University, Taiwan, R.O.C.

*Colour & Imaging Institute, University of Derby, UK

ABSTRACT

Image color histograms play an important role in various imaging applications. However, for image color histograms to be more practically useful, their dimension must be reduced. In this study, five different approaches to generating coarse 3D image color histograms were examined in terms of their usability for two imaging applications: color histogram visualization and image retrieval, respectively. A psychophysical experiment in which color images were compared with their coarse image histograms (27 bins only) in CIECAM02 space was first conducted to investigate the observers' judgements on visualizing color histograms and the histograms were then used for indexing color images for information retrieval from a database. The overall results suggested that gamut segmentations with more hue categories give better performance for the above applications.

INTRODUCTION

Image color histograms have been shown to be useful tools in imaging applications such as image analysis, color visualization, content-based image retrieval and gamut mapping [1]. However, as an image's full 3D histogram contains too much information for effective color-frequency visualization and as the computational cost of using such full histograms in real-time image analysis is impractical, image color histograms that have a small number of bins and can hence be seen as coarse are needed. The number of bins in an image histogram can be reduced either by using clustering techniques or by uniformly dividing 3D color space into fewer bins. The former method results in an increasing complexity when comparing histograms of images due to the fact that the color coordinates of cluster centroids are image dependent. The latter, on the other hand, results in color space being divided in a sub-optimal way whereby individual bins end up representing features of different weights.

This paper therefore describes novel methods for dividing CIECAM02 color space [2] into 27 color regions based on hue, chroma and lightness so as to make the resulting segments suited for various imaging applications. The performances of the segmentation methods employed will then be evaluated in the following ways:

1. Performing a psychophysical experiment involving observers comparing color images with their coarse image histograms and selecting the histogram that best represents the individual images.
2. Estimating the precision of image retrieval using simple distance-based techniques with coarse (27 color region) image histograms generated using different approaches.

The results of the two evaluation methods described above will show which of the methods used to represent an image's histogram by a small number of values is most efficient for both computational and visual tasks. If such coarse image histograms are found to perform well for the imaging applications being tested, then they can be used for simple image-color-frequency visualization and also saved as tags in image files to reduce the cost of real-time image analysis.

COARSE 3D IMAGE COLOR HISTOGRAMS

In this study, image color histograms were presented on a calibrated ViewSonic 18" CRT display and viewed under dim surround conditions. The CRT display, having characteristics very close to the sRGB standard, was characterized using the GOG model [3] with a mean error of 0.88 ΔE^*_{ab} based on 27 test samples. The color gamut of the display was then divided into 27 regions based on the following five different approaches:

1. **Mode 1 (cluster):** 27 regions were formed by assigning every in-gamut color to one of 27-fixed color centroids in CIECAM02 space with minimum distance. The 27 centroids were determined by Forgy's clustering algorithm [4] where the initial cluster centroids were taken from the 27 representative colors of Mode 5 to be described later.

2. **Mode 2 (J+):** 27 regions were determined by equally separating hue angles into six segments (0, 60, 120, 180, 240 and 300 degrees); four sections for chroma (C=20 and 50 as the thresholds); three lightness sections (J=40 and 70 as the thresholds) for low- and mid-chroma regions; no lightness separation for high-chroma regions (Figure 1).

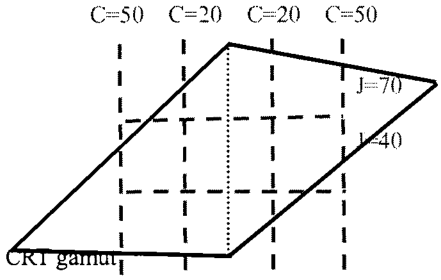

Figure 1: Mode 2 (J+)

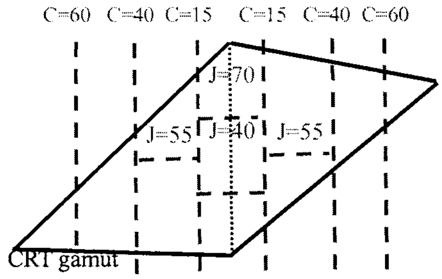

Figure 2: Mode 3 (C+)

3. **Mode 3 (C+):** Hue segmentations were identical to Mode 2, but chroma was divided into four sections (C=15, 40 and 60 as the thresholds); three lightness sections (J=40 and 70 as the thresholds) for low-chroma regions and two sections (J=55 as the threshold) for mid-chroma regions; no lightness separation for mid-high- and very-high-chroma regions (Figure 2).

4. **Mode 4 (H+):** 27 regions were obtained by equally dividing hue angles into eight segments (0, 45, 90, 135, 180, 225, 270 and 315 degrees); three sections for chroma (C=20 and 50 as the thresholds); three lightness sections (J=40 and 70 as the thresholds) for low-chroma regions and two sections (J=55 as the threshold) for mid-chroma regions; no lightness separation for high-chroma regions.

5. **Mode 5 (sRGB):** 27 regions were gained by evenly separating sRGB space into 3x3x3 sub-divisions where the thresholds for each color channel are 85 and 170 (of 255), respectively.

The five approaches designated as M1 to M5, respectively were employed to generate coarse 3D image color histograms and were tested as described in the following sections.

PSYCHOPHYSICAL EVALUATION OF HISTOGRAM VISUALIZATION

An interactive tool was developed to perform the psychophysical experiment previously mentioned. Ten natural images including four ISO/SCID standard sRGB images [6] were used to generate the five types of coarse image histograms for comparison. The test was categorized into three parts: **2D Pie Test**, **3D Bubble Test** and **2D Pie Test with Random Errors**, respectively. In the first test, images with their 5 types of pie charts were displayed successively in random order on the CRT as shown in Figure 3. The area of each piece of a pie indicates the relative pixel-frequency in a given 27-bin histogram. Observers were asked to select the chart which best represented the image's colors. The colors of the charts were displayed in two different ways: 1) color centroid of individual region was applied in **image independent mode (II)**, and 2) color centroid calculated from individual image of each region was used in **image dependent mode (ID)**. The second test was similar to the first one except that it used 3D bubbles rather than 2D pies to represent the image's color distributions (Figure 4). Note that the volume of each bubble represents the relative pixel-frequency of each histogram-bin and the position of each bubble is based on the coordinates of the image independent color centroid. The third test, using only pie charts, introduced random errors to 4 of the 5 charts (Figure 3) for each gamut separation technique. Ideally, the observers should pick up a chart with smaller histogram errors if the gamut separation is well correlated to visual perception.

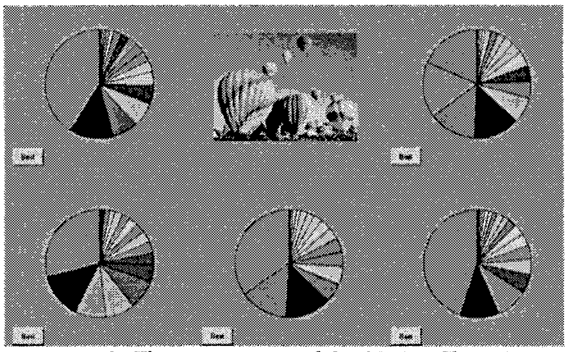

Figure 3: The interactive tool for 2D Pie Chart Test.

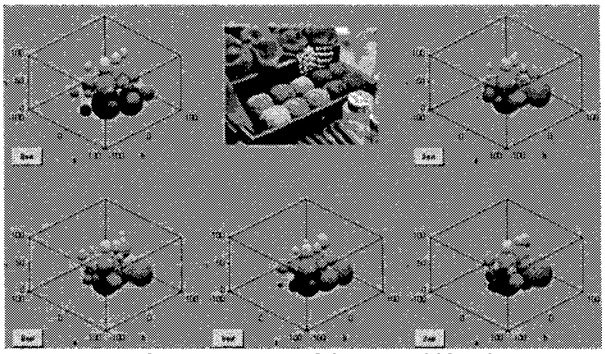

Figure 4: The interactive tool for 3D Bubble Chart Test.

Twenty color-normal observers participated in the experiment and the results are shown in Figures 5 and 6. As can be seen in Figure 5, *M1* and *M4* outperformed the other modes. This implies that coarse color histograms with well-distributed sub-spaces (*M1*) or having more categories on hue (*M4*) are preferred by the observers. Compared with the two modes, *M4*, with its regular structure, is more effective on abstracting overall color information from an image for higher-order statistics. It has also been noticed that *M5* showed serious hue errors in dark regions. Since *M5* separates colors based on sRGB space, hence it is not recommended to perform regular color segmentation on the sRGB space. Figure 6 shows the mean errors of the third test for each mode. The errors were computed using an L_2 distance metric [7] from source percentage histograms to their noise-added versions selected by the observers. *M5* (sRGB) was slightly worse than the other modes and the differences among the modes were not significant. In addition to the above results, almost all observers agreed that the image dependent mode was preferred over the image independent one for color histogram visualization.

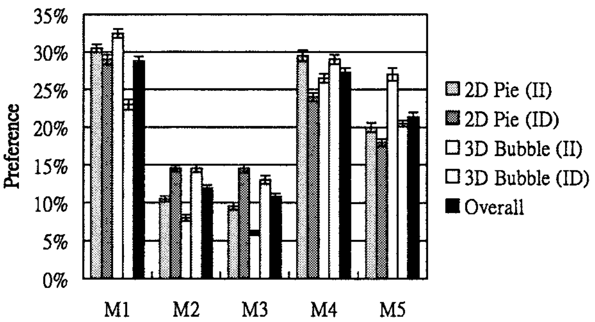

Figure 5: Preference on choosing coarse histograms.

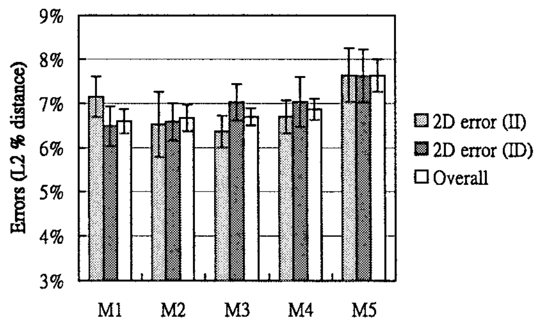

Figure 6: The results of 2D Pie Test with Random Errors.

EFFECT ON IMAGE RETRIEVAL

1,600 outdoor-scene images taken with a digital camera were used to examine the usability of the five modes for image retrieval. In the 1,600-image database, each scene had ten relative pictures shot from different viewing angles (hence having some variation in their color distributions). For image retrieval, the task was to choose any image (a query image) from the database and then to use the five types of coarse histograms generated from each image as cues for finding the ten correlated pictures from among the 1,600 images. Seven well-known similarity metrics including L_1, L_2, L_∞ distances, the Mahalanobis distance (*MD*), weighted Euclidean distance (*WED*), average color distance (*ACD*), and the Earth Mover's Distance (*EMD*) [6,7] were applied to estimate the distance between two sets of coarse histograms to indicate the correlation of a pair of images. A distance metric, L_1*dE_w, involving a weighted color difference formula was also proposed for the test. As can be seen in Equation 1, it is a combination between an L_1 distance metric and a weighted color difference formula where *H*, *Q* and *D* represent coarse histograms, query image and distance image, respectively. The color difference is calculated from the image dependent color centroids between query image and distance image for each corresponding gamut-division. The color centroids can be pre-computed and tagged to the image file for speeding up the process. The weighted coefficients (K_L,K_C,K_H) were set as (1,1,1) for "L_1*dE" and (8,8,1) for "L_1*dE_w" in this study. Note that the *EMD* metric also employs the image dependent color centroids to calculate the cross-bin deltaE distances for evaluating the similarity between two sets of coarse histograms. Since the metric involves huge iterative operations, the computation cost is much higher than all the other metrics.

$$L_1 * dE_w = \sum_{i=1}^{27}\left(\left|H_{iQ} - H_{iD}\right| \cdot \sqrt{\left(\frac{\Delta J_{i(Q-D)}}{K_L}\right)^2 + \left(\frac{\Delta C_{i(Q-D)}}{K_C}\right)^2 + \left(\frac{\Delta H_{i(Q-D)}}{K_H}\right)^2}\right) \quad \textit{Equation 1.}$$

The results of the test are partly shown in Figures 7 and 8. In the figures, three levels of a color bar indicate the rate of success for searching the ten correlated images when only taking the nearest 10, 32 and 80 images from the 1,600 samples estimated by the given metrics. The results show that the differences of gamut segmentation contribute little to their performances (Figure 7), whereas the choice of distance metrics influences the results more significantly (Figure 8). The most cost-effective metric, *ACD*, performed badly. With a trade-off between computation cost and accuracy, the L_1 metric would be a good choice. We found that the L_1*dE_w metric was superior to all the other metrics where the rate of success on weighted L_1*dE_w was about 3% higher than non-weighted L_1*dE and was virtually 1.6% higher than the time-consuming *EMD* metric. In terms of the combination between the nine metrics and the five gamut-division methods, the best and the second best were L_1*dE_w with *M3* and L_1*dE_w with *M4*, respectively. The difference of the two was only about 1.6% on the rate of success. Since the *M4* also performed well in the previous visual experiment, the *M4* which has more hue categories in gamut segmentation hence is preferable for universal applications.

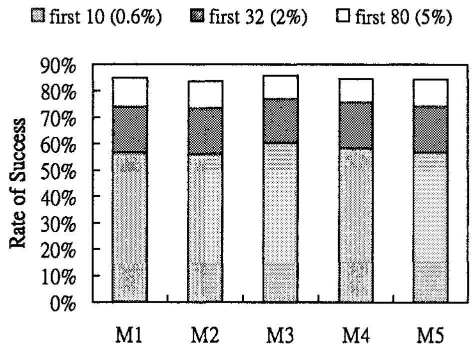

Figure 7: L_1*dE_w vs. 5 modes.

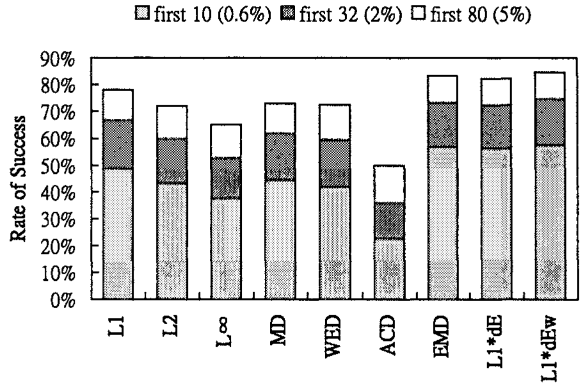

Figure 8: Overall results (5 modes) on 9 distance metrics.

CONCLUSIONS

The present study attempts to evaluate the usability of five types of coarse 3D color image histograms for two imaging applications. A psychophysical experiment in which color images were compared with their coarse image histograms in CIECAM02 color space was first performed and the results suggest that gamut segmentation with more categories for hue (*M4*) is preferable while sRGB space is not recommended for the gamut segmentation since the space is not uniform for visualization. In terms of the applications of image retrieval, the performances of the five approaches were very similar. The *M4* hence is preferable for universal applications. Finally, a metric using a weighted color difference formula are recommended for retrieving images from databases using coarse histograms. As such coarse image histograms can be saved as tags in image files to reduce the cost of real-time image analysis, the study of coarse image histograms should be extended for further applications.

REFERENCES

1. Sun P. L. and Morovic J. (2002) Three-Dimensional Histogram in Color Image Reproduction, *SPIE Proceedings*, 4663: 51-62.
2. Moroney N., Fairchild M. D., Hunt R. G. W., Li C., Luo M. R. and Newman T. (2002) CIECAM02 Color Appearance Model, *Proceedings of the 10th IS&T/SID Color Imaging Conference*, 23-27.
3. Berns R. S. (1996) Methods for Characterizing CRT Displays, *Displays*, 16: 173-182.
4. Gose E., Johnsonbaugh R. and Jost S. (1996) *Pattern Recognition and Image Analysis*, Prentice Hall, Inc., 211.
5. JIS (2000) *JIS X 9204:2000 Graphic Technology – Prepress Digital Data Exchange - XYZ/sRGB Standard Colour Image Data (XYZ/SCID).*
6. Bimbo A. D. (1999) *Visual Information Retrieval*, Morgan Kaufmann Publishers, 100-104.
7. Lew M. S. (2001) Feature Selection and Visual Learning, *Principles of Visual Information Retrieval*, M. S. Lew (e.d.), Springer, 149.

Toward mesopic color reproduction

JaeChul Shin [1], Naoki Matsuki [1], Kumiko Kikuchi [1],
Hirohisa Yaguchi [2] and Satoshi Shioiri [2]
[1]Graduate School of Science and Technology, Chiba University, Japan
[2]Department of Information and Image Sciences, Chiba University, Japan
1-33 Yayoicho, Inage-ku, Chiba 263-8522, Japan
E-mail: jcshin@graduate.chiba-u.jp

ABSTRACT

We conducted a set of experiments to investigate the color appearance by means of measuring the corresponding color of color chips under various illuminance levels, ranging from photopic to scotopic via mesopic levels. The results showed that the hue of the most color chips changed with illuminance and the manor of the hue shift depended on color, while matching points approached around neutral gray with decreasing illuminance. Chroma reduced continuously with decreasing illuminance above about 0.1 lx for reddish and yellowish color chips or above about 1 lx for greenish and bluish ones, beyond which illuminance level chroma was almost constant. The lightness of matched color decreased with decreasing illuminance, however the lightness for bluish color chips did not decrease much in general and even increased in some cases. These results provide data to build a model which can be applied to mesopic color reproductions, to predict color appearance in mesopic vision.

INTRODUCTION

Vision may be classified simply into two: photopic or cone vision and scotopic or rod vision. However, there are illuminance levels where both cones and rods are active and the vision at the levels is called as mesopic vision. Color appearance in mesopic vision differs from that in photopic vision and is not easily estimated from the knowledge of photopic and scotopic vision. In order to make color appearance model for mesopic vision, it is, therefore, necessary to consider interactions between cone and rod signals at the levels. In addition, to predict appearance of color in the evening and at night, understanding and modeling of mesopic vision are necessary.

There are a number of studies in the literature on the evaluation of color appearance in mesopic vision. These studies[2-12] have revealed existence of interaction between cones and rods related to color vision. For example, Buck et al.[8-11] have been regulating the influence of rod signals on both perceptual opponent color hue dimensions well. They suggested also directions for the color vision model to be used at low light level by summarizing of the rod influence on hue perception resulted from their psychophysical experiments.

To predict mesopic color appearance, sufficient data are needed in terms of quantitative numerical value. In this study we evaluated quantitatively the color appearance between photopic vision and mesopic vision by color matching experiments. The high accuracy data were collected and have been applied to make the model for color appearance prediction in mesopic vision. Some neural models[13-15] of color vision based on a stage theory which are now widely accepted concept have been suggested. Our model is also based on the opponent-color model known by the opponent-colors theory, which rod signal is added with all three cone types into the opponent-color model.

EXPERIMENTS

Apparatus and Stimuli

A haploscopic color matching technique was employed to match a reference color presented in right eye to the test color presented in the left eye. The illuminance of the reference fields was set constantly 1000 lx of photopic condition and the test field was designed to vary illuminance level of 1 log steps from 0.01 lx to 1000 lx by 15 fluorescent lamps simulating D65 on the height of both visual fields. The stimuli of test field were consisted of 48 color chips (JIS standard based on Munsell color system) which are shown in Figure 1. The reference stimuli were generated on a CRT display having a computer controlled VSG (visual stimulus generator by Cambridge System) with 15 bits intensity resolution for each phosphor. The stimuli sizes used in the experiments were both stimuli of 10×10 deg. square in order that rods can be intermediated on the color perceptions. A gray background covering the stimuli which was equivalent to Munsell color chip N5.

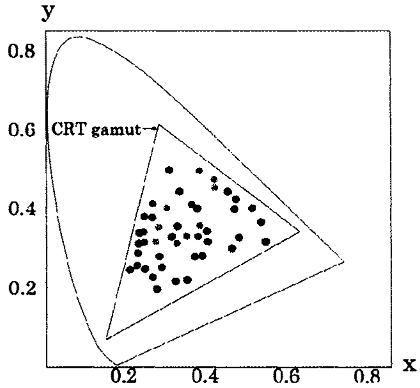

Figure 1. The chromaticities of 48 color chips on xy-chromaticity diagram

Observers

Three males and two females with normal color vision participated in the matching experiments.

Procedure

Dark adaptations were made for 15 min. in case of the illuminance levels of 1000, 100, 10 lx conditions and for 30 min. in the other cases. Immediately after a dark adaptation, observers adapted to each illuminance level for 5 min. in every conditions. Each session was started after the dark adaptation and the light adaptation. The color matching was replicated three times within a matching task for one color chip during a session. All data were obtained in terms of tristimulus values X, Y, Z.

RESULTS and DISCUSSIONS

All figures in the results show the mean of all observers for some of the test color chips. General tendencies of the results described below are robust for repeated sessions and with all observers.

Hue changes

Figure 2 show the change in color appearance of some of the test color chips in the a^*b^* plane of the CIELAB. Although the matching points approach around to the neutral gray axis with decrease in illuminance level, the way of approaching differs with different hue angles. The matching points at 0.01 lx did not compact around the neutral gray axis isotropically among chips with different hues or hue angles. The distribution appears to be somewhat bimodal (data appears to be distributed around two points). If there were no color seen at the level, the data should compact at the neutral gray. Since the results showed some variation from the simple prediction, they suggest the existence of color perception at 0.01 lx.

We summarize the details of the color changes for different color chips describing the results of selected color chips, which are Y (No. 3 or No. 4), YR (No. 6), R (No. 9)...

Y, YR color chips: After shifting toward longer wavelength at the boundary range between photopic vision and mesopic vision (10~1 lx), is the coordinates of the matching color approaches to the neutral gray axis (but the point at 0.01 lx shows the appearance is slightly reddish) in entire mesopic ranges (0.1~0.01 lx).

R, RP, P color chips: The matching point shifts toward horizontal axis (toward the longer wavelength hues) with the illuminance decrease and approaches to the point slightly reddish than the neutral gray.

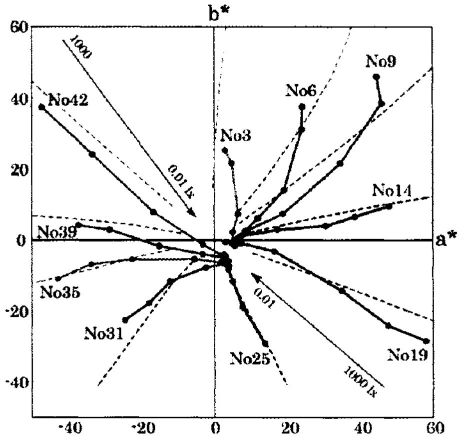

Figure 2. Change in hue appearance of each color chip at the CIELAB (Dashed lines mean the constant hue loci of Munsell color chips are equivalent to each test color chip)

PB, B color chips: The matching point of these color chips shift toward longer wavelength hues with decrease of illuminance level at the boundary range between photopic and mesopic vision and then change the direction toward shorter wavelength hues in the mesopic range. The shift toward shorter wavelength hues in the mesopic vision are consistent with a hypotheses[2-5] that rods strengthen blueness or give an influence on b/y opponent-color channel in the mesopic vision, which hypotheses is supported by many of previous studies.

BG, G, GY color chips: The point at 0.01 lx is at about (0,-5) as PB and B chips. The change of G color chips that shift to shorter wavelengths in the mesopic range suggests an inclination like that described by Buck[8-10].

Chroma changes

Figure 3 shows the chroma of the matching color as a function of illuminance level. The remarkable decrease of chroma is seen between 100 and 1 lx for reddish and yellowish color chips and between 1000 and 1 lx for greenish and bluish ones over the illuminance level. Particularly, the tendencies of decline are continuous with decrease of the illuminance level above about 0.1 lx for reddish and yellowish color chips or above about 1 lx for greenish and bluish ones. After the decline, chroma is approximately constant at a value around 5. The value at the low illuminance level depends on color chips and the value is larger for color chips with reflectance of long wavelength light than for color chips with reflectance of short wavelength light.

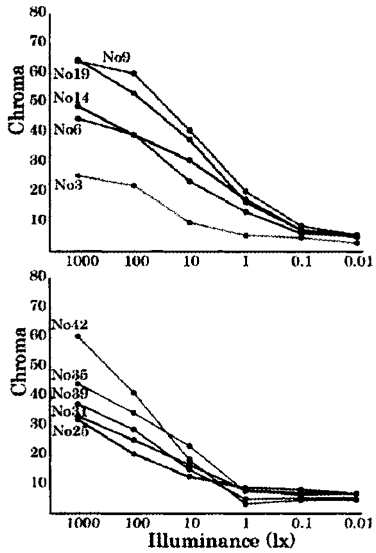

Figure 3. Chroma change of each color chip at each illuminance level

Lightness changes

Figure 4 shows the lightness changes of each color chip with the change of the illuminance level. The function of the lightness changes for different color chips can be divided into two patterns, dependently on whether the lightness increases or not in the mesopic range. The lightness for the color

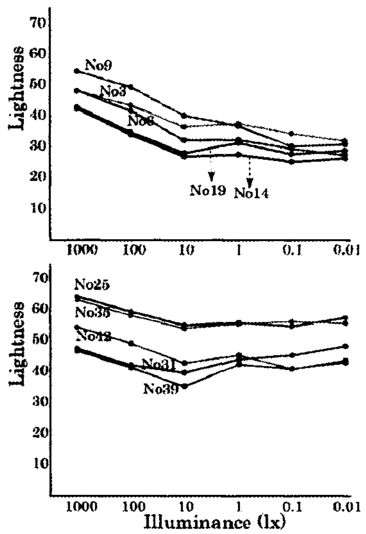

Figure 4. Lightness change of each color chip at each illuminance level

chips with reflectance of longer wavelength light monotonically decreases with decrease in illuminance level up to an illuminance level, which level depends on color chips ranging between 10 and 0.01 lx. The degree of lightness change differs according to lightness value at 1000 lx as well as hue and chroma. The lightness for the color chips with reflectance of shorter wavelength light shows a minimum value at around 10~1 lx after the decrease with luminance level and then the lightness increases with further decrease in illuminance level. The increase is prominent in P, PB color chips as expected from Purkinje shift.

We had a color matching experiment for achromatic color chips. For the achromatic stimuli we find slight shifts of the color coordinates (i.e., hue and chroma) of matched color toward the point that the matching point of the chips with long wavelength light reflectance converges. Since the shift tends to be large at the low mesopic level, it is suggested to be related to rod-cone interaction in color vision. It should be noted, however, that the shift is small and the close to the inter- and intra-observer variable of the matching data.

Modeling for Mesopic color appearance

Based on the results, a model to predict the mesopic color appearance can be constructed. To predict the mesopic color appearance, however, the rod intrusion has to be somehow taken into account the model. In addition to predicting the experimental results, the model has to have the following features.

1) The model includes gradual decrease of luminance component dependently on illuminant levels because spectral luminous efficiency changes from V (λ) to V' (λ) by rod signals intrusion.
2) The model assumes also the decrease of chromatic component with decreasing illuminance.
3) In order to explain hue shifts with illuminance, the model should be considered that the output of red/green and that of blue/yellow components changes independently with illuminance changes.

To predict the color appearance in mesopic vision, a simple model is being constructed using the experimental results. The current model is based on the conventional opponent-color models that assume the luminance channel and two opponent-color channels (red-green and blue-yellow opponent-color channel) and the rod intrusion is taken into account the model, which the dimensions of cones and rods intrusions is exchanged with weighted coefficients. The detail is shown in Eq. (1). For these equations, L, M, and S were calculated using Judd modified color matching functions that represent the cone fundamentals of Smith et al.[16].

$$\begin{aligned}
&Lum\,(E) = k(L+M)_p + (1-k)nR_p \\
&\{ (L_p/L_w)-(R_p/R_w) > 0 : k=k_1(E), \quad (L_p/L_w)-(R_p/R_w) < 0 : k=k_2(E) \} \\
&rg\,(E) = l(L-2M)_p + a(E)R_p \\
&yb\,(E) = m(L+M-S)_p + b(E)R_p
\end{aligned} \qquad (1)$$

In Eq. (1), L_p, M_p, S_p and R_p, represent each cone stimulus value and rod stimulus value of the color appearance at 1000 lx, and $(L+M)_p$, $(L-2M)_p$, and $(L+M-S)_p$, represent luminance, red-green and blue-yellow opponent-color components. Weighting coefficient, $k_1(E)$, $k_2(E)$, $m(E)$, $a(E)$ and $b(E)$ are functions of illuminance E lx and n is a quota that transformations rod stimulus value from photopic vision to scotopic vision. L_w and R_w are each stimulus value for white.

Table 1. Weighting coefficient value for the model (n=0.24)

	1000 lx	100 lx	10 lx	1 lx	0.1 lx	0.01 lx
k1	1.000	0.742	0.176	0.162	0.052	0.082
k2	1.000	0.674	0.000	0.000	0.000	0.000
l	1.000	0.745	0.408	0.189	0.051	0.023
m	1.000	0.691	0.310	0.134	0.044	0.018
a	0.000	0.003	0.001	-0.003	-0.007	-0.008
b	0.000	0.017	0.025	0.023	0.015	0.018

Table 1 showed the weighting coefficients for the model which obtained from the results.

The performance of the model was evaluated using the color differences. The color differences ΔE_{ab^*} on the CIELAB between the predicted value and the experimental value are showed in figure 5. The color differences ΔE_{ab^*} of mean are about 4~5 that the prediction of the model is unsatisfactory now. The unsatisfactory prediction might be due to the lightness of P, PB color chips. It should be improved in the future works.

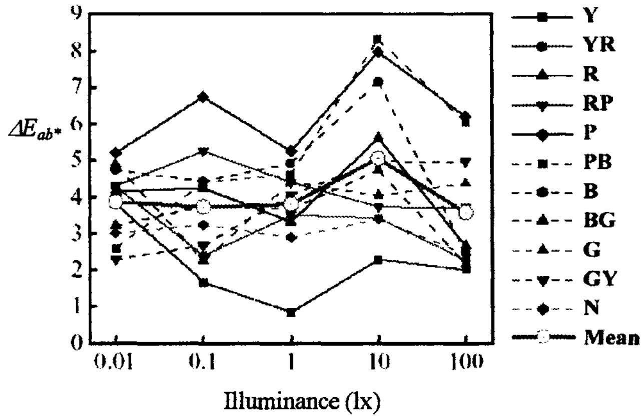

Figure 5. Color differences between predicted value and experimental value

REFERENCES

1. Hunt RWG. Light and dark adaptation and the perception of color. J Opt Soc Am 1952;42:190-199.

2. Stabell B, Stabell U. The effect of rod activity on colour matching functions. Vision Res 1975;15:1119-1123.

3. Stabell B, Stabell U. Rod and cone contribution to peripheral colour vision. Vision Res 1976;16:1099-1104.

4. Stabell B, Stabell U. Rod and cone contributions to change in hue with eccentricity. Vision Res 1979;19:1121-1125.

5. Stabell U, Stabell B. Mechanisms of chromatic rod vision in scotopic illumination. Vision Res 1994;34:1019 -1027.

6. Stabell U, Stabell B. Chromatic rod-cone interaction during dark adaptation. J Opt Soc Am 1998;15:2809-2815.

7. Buck SL. Influence of rod signals on hue perception: evidence from successive scotopic color contrast. Vision Res 1997;37:1295-1301.

8. Buck SL, Knight R, Fowler G, Hunt B. Rod influence on hue-scaling function. Vision Res 1998;38:3259-3263.

9. Buck SL, Knight RF, Bechtold J. Opponent-color models and the influence of rod signals on the loci of unique hues. Vision Res 2000;40:3333-3344.

10. Buck .L. What is the hue of rod vision? Color Res Appl Suppl 2001;26:S57.

11. Yaguchi H, Monma C, Tokunaga K, Miyake Y. Color appearance in mesopic vision. In: Color Vision Deficiencies, Tokyo, 1990. p 21-28.

12. Momma C, Honma S, Yaguchi H, Shioiri S, Haneishi H, Miyake Y. Haploscopic color matching for surface color in mesopic vision. Jpn J Opt (Kogaku) 1993;22:273-280. (in Japanese)

13. Wyszecki G., Stiles W. Color Science: concepts and methods, quantitative data and formulae. 2nd ed. New York: Wiley; 1982. 633 p

14. Boynton RM, Kaiser PK. Human Color Vision. 2nd ed. J Opt Soc Am: 1996.

15. De Valois RL, De Valois KK. A multi-stage color model. Vision Res 1993;33:1053-1065

16. Smith VC, Pokorny J. Spectral sensitivity of the foveal cone photopigments between 400 and 500 nm. Vision Res 1975;15:161-171.

The Color Constancy of Light Source Color Mode on a Mobile Phone Display

Sarin Phongbangly*, Mitsuo Ikeda, and Hiroyuki Shinoda
Major of Photonics, Department of Information Science and System Engineering, Ritsumeikan University, Japan

*Major of Photonics, Department of Information Science and System Engineering, Ritsumeikan University, 1-1-1 Noji-higashi, Kusatsu, Shiga, 525-8577, Japan
E-mail address: gr023016@se.ritsumei.ac.jp

1. ABSTRACT

Color appearance can be classified into 3 modes; object color, unnatural color, and light source color, according to the relation between its luminance and surrounding environment. The color constancy doesn't always hold on a self-luminous display, unlike on a reflecting surface. When colors on a mobile phone display, emitting light physically, are recognized as object colors, their appearance are quite unstable depending on illuminant change, for example from fluorescence to tungsten lamp. The purpose of this research is to achieve the color constancy on a mobile phone display. We expect if the luminance of colors is increased high enough to become a light source color, its color appearances should be independent of the environment. Color appearance change associating with illuminant change from 6500 K to 2856 K was measured using the elementary color naming. Eleven colors were investigated with two different color modes. If our hypothesis is correct, the colors in the light source color mode should appear the same regardless of color temperature of illumination.

Key words: Color constancy, Mode of color appearance, Object color, Light source color, RVSI

2. INTRODUCTION

According to the recognized visual space of illumination, RVSI theory[1], color appearance can be classified into 3 modes[2]; object color, unnatural color, and light source color, depending on the relation of luminance between itself and surrounding environment. In the case of object color mode, we perceive its appearance as natural as an object in the room. If we continuously increase the luminance or brightness of that object, the appearance would be perceived as unnatural color and light source color mode respectively. Unlike object color, in the case of light source color mode, the appearance seems that an object itself radiates light.

In general, an object can be physically classified into two types; reflecting and self-luminous object. The former one is a typical object that reflects illumination to the eyes; therefore its incoming light property is controlled by that illumination. In contrast, the latter one is a self emitting light object, such as a mobile phone display, which it emits light to the eyes directly independent from the illumination; in other word, its physical ray is constant. Both types of this object can appear as object color mode or light source color mode depending on the situation.

In consideration of a reflecting object in object color mode, such as a paper, we have a color constancy to perceive its color the same although it is perceived under the different types of illumination. This can be explained by the RVSI schemes in figure 1. F_x is a fundamental axis, R_x is a recognition axis, and I_x is an illumination axis. In a room that is illuminated by a white light F_x, R_x and I_x locate in the same direction (same as F_x position in the figure). When the illumination of the room is changed, for instance, from a white light to a reddish light, I_x shifts from its original place toward right as shown in figure 1 (a). A black square in the figure represents the appearance of that object; the place inside the circle border means this object tends to appears in object color mode, on the other hand, the placed beyond the circle border means it tends to appears in light source color mode. Here the black square sticks to the I_x because it is a reflecting light of the illumination directly as described. However, not only the I_x and the square but also our recognition axis, R_x, shifts toward the same direction although it is not exactly coincide with the I_x, which shown by the angle θ_1. Since this angle is very small, its appearance is not changed; therefore the color constancy holds.

Unlike reflecting object, the black square for the self-luminous object does not move and stay still on F_x regardless of the shift of I_x. In this case, the θ_2 in figure 1 (b), which represents the angle between the black square and R_x, become large in opposite direction. This causes a color shift in appearance toward green [3];

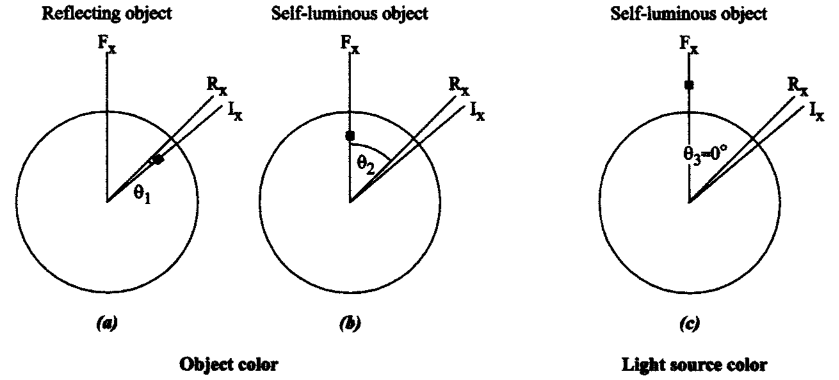

***Figure 1** The schemes of RVSI. Figure (a) and (b) show the appearance in object color mode of a reflecting object and a self-luminous object respectively. Figure (c) shows the proposed solution; the appearance of self-luminous object in the case of light source color mode. F_x is a fundamental axis, I_x is an illumination axis and R_x is a recognition axis. A black square shows a characteristic of an appearance we perceive.*

therefore, the color constancy fails. This is a normal situation of mobile phone display. When it appears as an object color mode its appearance is unstable across the different illuminations.

How can the problem of color constancy failure be solved? According to the RVSI concept, if the object appears in light source color mode, its color appearance is not determined by the R_x anymore; the appearance of light source color mode is given by the angle between that black square and F_x. For example, an emitting white light from the mobile phone display, represented by the black square on the F_x in figure 1 (c), would be placed outside the circle border when its luminance is high enough to appear as a light source color mode. Even though R_x shifts toward red, following the I_x, the appearance of this light now is stable. In this case, the θ_3 is 0 degree which results in white color appearance.

The purpose of this research is to achieve color consistence on a mobile phone display through the change of illumination. We expect if the luminance of colors is increased high enough to appear in light source color mode, those colors should be free from environment and kept consistence against the change of illuminant color.

3. EXPERIMENT

3.1 Apparatus

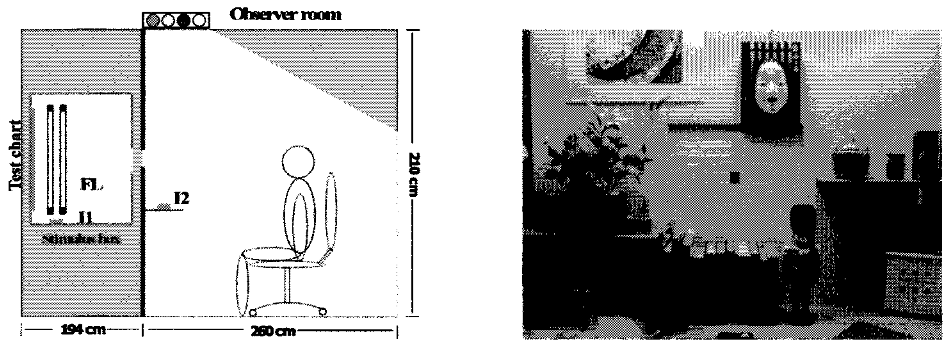

***Figure 2** a (left) A drawing of the side view of the apparatus. The apparatus composed of an observer room and a stimulus box. Four fluorescent lamps, FL, were used to illuminate the test charts. Two illuminometers were placed inside the stimulus box and the observer room, I1 and I2 respectively, to keep the conditions constant. Figure b (right) is an observer view in the real scene. Inside an observer room was decorated by various color objects, such as a mask, a toy, books, etc.*

The apparatus composed of an observer room and a test stimulus box as in figure 2 (a). The observer room was illuminated by color fluorescent lamps, which can achieve two types of illumination, A and D65. The room was decorated by various color objects, such as, books, a mask, flowers, toys, etc. figure 2 (b) shows what observer saw inside the room. A gray rectangular at the center of a figure was the aperture, which observers could see through it and perceived the test chart inside stimulus box, located behind the wall. The stimulus box was created to simulate a mobile phone display, which is self-luminous. Inside the box color charts were illuminated by four fluorescent lamps so that it was bright enough to obtain both object color and light source color modes. I1 and I2 were the illuminometers used to keep the illuminance inside the stimulus box and observer room constant respectively.

The aperture size was 3.3 x 4.1 cm^2, which is the actual size of mobile phone display. The distance between observer and aperture was not so strict because it was in consideration of the size constancy.

3.2 Conditions

Eleven Munsell test charts; 5RP 5/10, 5P 4/10, 5B 5/8, 5BG 5/8, 5G 5/10, 5GY 6/10, 5Y 6/10, 5YR 5/12, 5R 5/12, 5PB 4/10, and N8, were observed under two types of illumination; A and D65, in observer room. Those test chart's colors were kept physically constant through the experiment. The illuminations in observer room were also kept constant at 50 lx in both conditions. Two appearance modes of the test charts, object color mode and light source color mode, were presented to observers by keeping the illuminance inside the stimulus box constant at 20 lx for object color mode and 2100 lx and 4300 lx for light source color mode of illumination type A and D65 respectively. There are five observers participated in this experiment. Observers saw the test charts binocularly. All have normal color vision.

3.3 Procedure

At first, before starting the experiment, all observers were asked to find the border of eleven Munsell test patch appearances in both illuminations, A and D65, between object color mode and unnatural color mode and between unnatural color mode and light source color mode by adjusting method. Then, after that, the conditions, illuminance values in stimulus box, of appearances in object color mode and light source color mode were set by choosing the illuminances at the intersection of all observers in both conditions. Therefore at the setting conditions all observers would perceive the same appearance.

During the experiment observers were asked to do elementary color naming. Each session composed of eleven test charts, 2 types of illuminations, A and D65, and 2 modes of color appearance, object color and light source color. The session was repeated 10 times by all observers.

4. RESULTS AND DISCUSSION

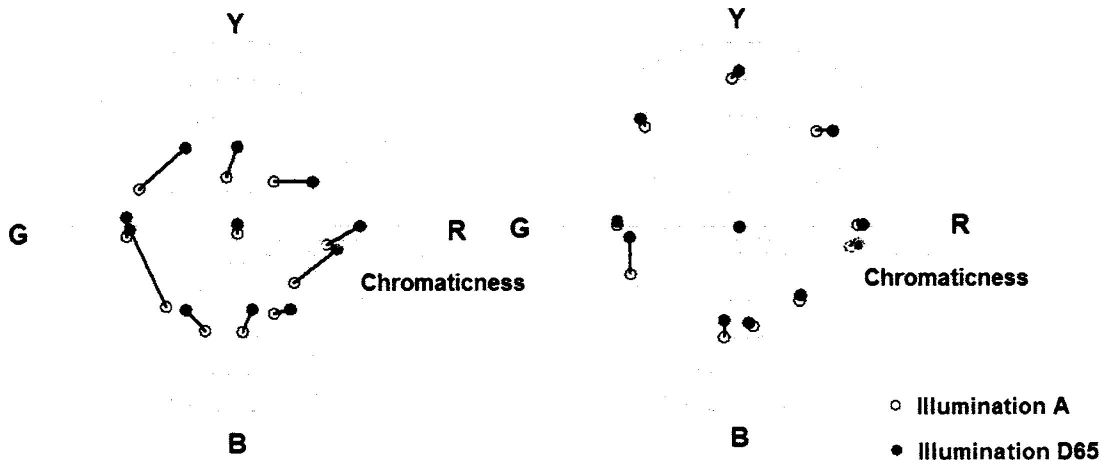

(a) Object Color Mode *(b) Light Source Color Mode*

Figure 3 *Results from observer AH. Polar graphs show percentage of chromaticness in the radius axis. Using angular axis shows hue of colors; 100% red, yellow, green, and blue correspond to counterclockwise 0, 90, 180, and 270 degree respectively. White circles are the results from illumination A and black circles are the results from illumination D65. Each dot came from a mean of 10 repeats. Figure (a) and (b) are the results of object color mode and light source color mode respectively.*

Figure 3 shows polar graphs of the results from observer AH. Radius axis represents a percentage of chromaticness and the angular axis displays hues; 100% red, yellow, green, and blue respond to the counterclockwise angle of 0, 90, 180, and 270 degree respectively. The results show large hue shifts on object color mode when the room illumination was changed from A to D65. On the other hand, the shifts are very small in the case of light source color mode or even no shift in some colors. Other four observers have the same tendency of results, figure 4.

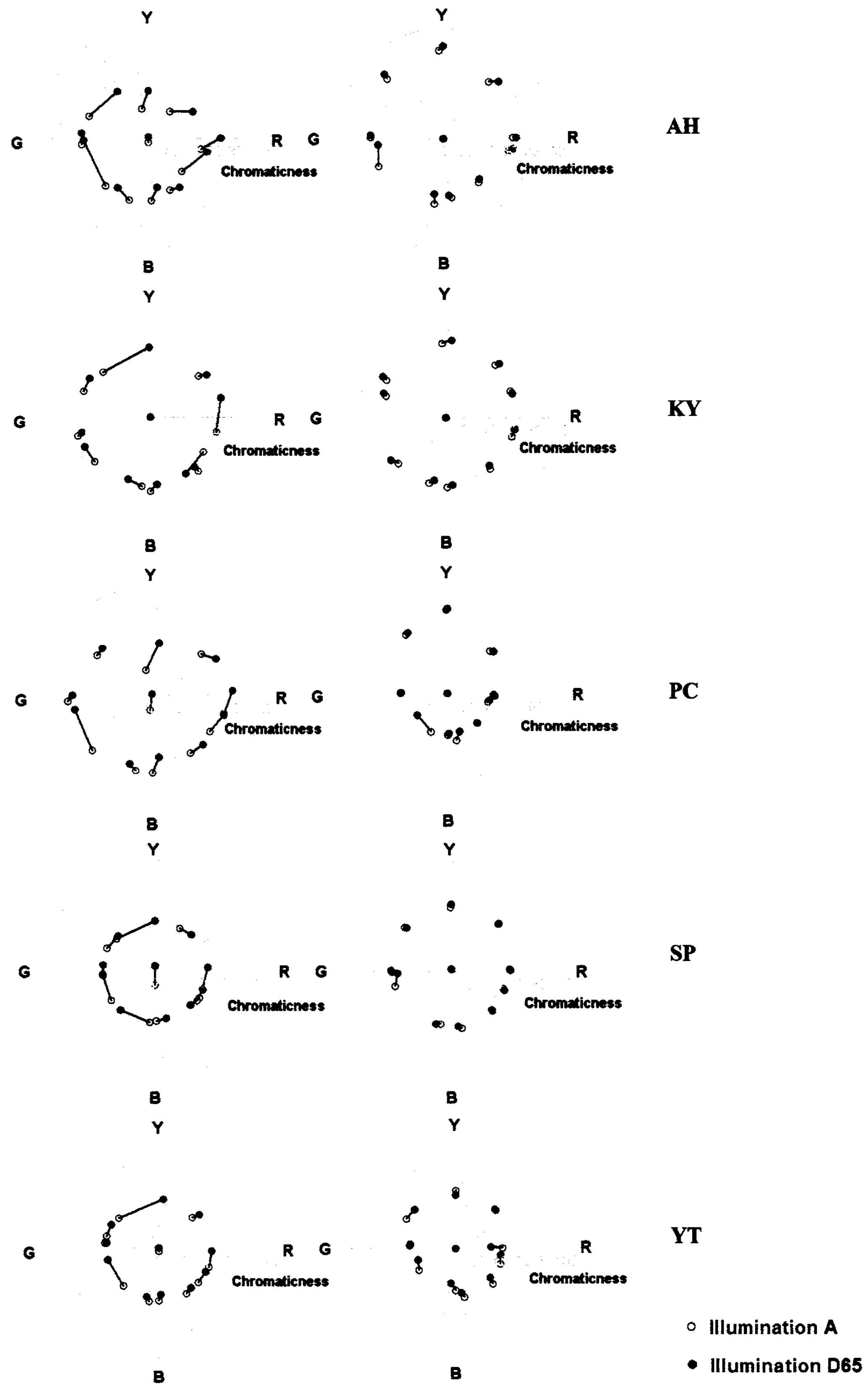

Figure 4 *Results of all observers. Angular axis of polar graph represents hues and radius axis shows percentage of chromaticness. White and black circles are the results observed from the illumination A and D65 respectively.*

The results confirm our expectation that the appearance in light source color mode is independent from the illumination of environment. Therefore in the case of self-luminous display, such as a mobile phone monitor, we can achieve color consistence across different illumination by increasing its luminance until it becomes light source color mode.

Nonetheless, the results show that observers still perceived little shifts even in light source condition. Those shifts could be easily eradicated if we continue increasing the luminance a little bit more. The condition of light source color mode in this experiment was set only a little bit beyond the border because of the restriction of equipments. Therefore it could be possible that one still can not perceive it as completely as in light source color mode, which consequently the appearance is not completely independent from the environment yet.

However, it can be concluded that the characteristic of light source color is not affected from RVSI.

5. REFERENCES

[1] M. Ikeda, H. Shinoda, and Y. Mizokami: Phenomena of Apparent Lightness Interpreted by Recognized Visual Space of Illumination. Opt. Rev. **5** (1998) pp.380-386.

[2] Y. Thiangthangtum, R.Yamauchi, P.Pungrassamee, A.Hansuebsai, and M. Ikeda: Determination of Borders of Object Color Mode at Various Environmental Illuminance. Proc. AIC, Soul (2000), pp.84-88.

[3] M. Ikeda, Y. Mizokami, S. Nakane, and H. Shinoda: Color Appearance of a Patch Explained by RVSI for the Conditions of Various Colors of Room Illumination and of Various Luminance Levels of the Patch. Opt Rev. **9** (2002) pp. 1-8.

The Effect of Perceptual Texture Features on Color Variation of Texture Image

Shao Sijie[1], J.H. Xin[1], Korris Chung Fu-Lai[2]
1. Institute of Textiles & Clothing, the Hong Kong Polytechnic University
2. Department of Computing, the Hong Kong Polytechnic University

ABSTRACT

In this paper, relationship between perceptual texture features and color attributes values variation of texture image under CIELAB color space are investigated. The algorithm is based on the subband decomposition of texture images in the color space of CIEXYZ through Gabor wavelet filters and extraction of the perceptional texture features from the Y channel of CIEXYZ color space. The directionality and coarseness perceptual texture features effect on color variation of texture image are respectively discussed in this study. The correlation analysis shows that the coarseness feature has more strength correlation on color change of texture image than directionality effect. Furthermore, the color becomes darker and less saturated along with the increase of surface coarseness of texture image.

1. INTRODUCTION

Texture information is indispensable for the realistic rendering since it adds surface details that have a directly impact on colour information in the textile samples. Currently, there are few effective methodologies to guarantee a high-fidelity of colour rendering when texture information is mapped into solid colour image.

In previous studies, texture has been extensively investigated in the areas of image processing (texture classification and segmentation), computer graphics (texture synthesis and mapping), visualization (display simulating real scenes) and cognitive psychology (understanding the human visual system). Although each of these communities focuses on different tasks, texture and color properties are often treated separately rather than collectively.

The interaction between color and the texture structure of a coloured object has been investigated by some researchers. Lee et al [1] explored visual perception of texture of textiles. They pointed out that a correlation may exist between the psychological factors and surface characteristics of textile fabrics. However, their research was limited only to gray samples and surface texture structures of different kinds of materials with different physical properties such as yarn thickness, density, twist, cover factor. Edul N. et al. [2] obtained a relationship between the gloss property and perceived color variation. However, the direct relationship between the surface geometric characteristic and the color variation was not considered in their model. In another paper [3], a roughness index was used to quantitatively descript surface topographic characteristic and evaluated the color change due to surface roughness using the CIELAB system. Texture analysis [4-6] has been widely studied and algorithms for texture analysis range from using random field models to multi-resolution filtering techniques such as Gabor filter and wavelet transform [7]. Gabor filters have been presented in several works on image processing; however, most of these works are related to texture classification and segmentation [8-10], image recognition [11].

In this study, the relationship between perceptional texture feature extracted from the subband image filtered by Gabor wavelets and the variations of color appearance of color texture image is investigated. The results may contribute to the accurate simulation of color texture image.

2. EXPERIMENTAL

Preparation of textile samples

This study was aimed at firstly building database of color texture image of various colour fabric patterns. Seventeen types of different texture fabric including to plain, twill and satin and their variations were woven. Each texture samples were dyed to three colours, i.e., red, green, and blue, using reactive dyestuffs Then, all physical samples were captured by Canon EOS-D30 digital camera in a resolution of 256 by 256 pixels that gave approximately equal visual appearances to those of the physical samples.

Camera calibration by polynomial modeling

Due to the fact that RGB response are device dependent, a transform that define a mapping between camera RGB signals and device-independent color space, such as XYZ, is necessary for high-fidelity rendering of color texture image. In this study, 24 tiles of color textile patches used as reference target were captured in a VeriVide CAC-120 viewing cabinet under a D65 simulator with grey backgrounds. The measurement geometry was 45/0. The digital camera produced RGB values for each color patch on the reference target. Each color patch's XYZ values were measured by spectrophotometer COLOR-EYE 7000A from GretagMacbeth using a large aperture. According to previous literature of calibrating digital camera [11-12], the polynomial transformation between camera RGB values and their corresponding XYZ values was used in this project. The transformation matrix with the terms of [R G B RG RB GB R^2 G^2 B^2 RGB 1] has been shown to provide satisfactory characterization accuracy. The mapping from RGB to XYZ can be represented by

$$B_{XYZ} = MA_{RGB}$$

where M is the transform matrix, B and A denote the XYZ and RGB values matrix respectively. The optimal solution of M by means of least-mean-square method is obtained

$$M = (A^T A)^{-1} A^T B \tag{1}$$

where A^T denotes the transpose of A and A^{-1} is the inverse of A. The average prediction error is 2.3 ΔE CMC(2:1) units. All following perceptual texture features were extracted from the image of Y channel under XYZ color space.

3. TEXTURE FEATURE EXTRACTION

Gabor Function and wavelets

A two dimensional Gabor function g(x, y) can be specified by the frequency of the sinusoid W and the standard deviations of the Gaussian σ_x and σ_y as:

$$g(x,y) = \left(\frac{1}{2\pi\sigma_x\sigma_y}\right)\exp\left[-\frac{1}{2}\left(\frac{x^2}{\sigma_x^2}+\frac{y^2}{\sigma_y^2}\right)+2\pi jWx\right] \tag{2}$$

Gabor function forms a complete but non-orthogonal basis set. Expanding a signal using this basis provides a localized frequency description. A class of self-similar functions, referred to as Gabor wavelets in the following discussion, is now considered. Let $g(x,y)$ be the mother Gabor wavelet, then this self-similar filter dictionary can be obtained by appropriate dilations and rotations of $g(x,y)$ through the generating function:

$$g_{mn}(x,y) = a^{-m} g(x',y'), \quad a>1, \quad m,n = Integer \tag{3}$$

$$x' = a^{-m}(x\cos\theta + y\sin\theta), \text{ and } y' = a^{-m}(-x\cos\theta + y\sin\theta),$$

where $\theta = n\pi / K$ with m and n indicating the scale and orientation, respectively. K is the total number of orientations desired. The scale factor a^{-m} in (3) is used to normalize the energy independent m.

The Fourier transform of Gabor function $g(x, y)$ can be written as:

$$G(u,v) = \frac{1}{2\pi\sigma_u\sigma_v}\exp\left\{-\frac{1}{2}[\frac{(u-W)^2}{\sigma_u^2}+\frac{(v-W)^2}{\sigma_v^2}]\right\} \quad (4)$$

where $\sigma_u = 1/2\pi\sigma_x$ and $\sigma_v = 1/2\pi\sigma_y$. In order to reduce the non-orthogonality of the Gabor wavelets, the design strategy is used to project the filters so as to ensure that the half-peak magnitude supports of the filter responses in the frequency spectrum are in contact with each other. Let U_l and U_h denote the lower and upper center frequencies of interest. The S parameter is the number of scales in the desirable multi-resolution decomposition procedure. This results in the following formulae for computing the filter parameters σ_u and σ_v:

$$a = (\frac{U_h}{U_l})^{\frac{1}{S-1}} ,$$

$$\sigma_v = \tan(\frac{\pi}{2K})[U_h - (\frac{\sigma_u^2}{U_h})2\ln 2][2\ln 2 - \frac{(2\ln 2)^2\sigma_u^2}{U_h^2}]^{-1/2} \quad (5)$$

where $W = U_h$ and $m = 0,1,\ldots,S-1$. In this work, the Gabor wavelet was projected using four scales (S=4) and twelve orientation (K=12) with the lower and upper center frequencies specified as $U_l = 0.05$ and $U_h = 0.4$ cycles/pixel, respectively.

Perceptional texture extraction

Given an image Y(x,y), its Gabor wavelet transform is defined as

$$GW_{mn}(x,y) = \iint Y(x_1,y_1)g^*_{mn}(x-x_1,y-y_1)dx_1dy_1$$

where * represent the complex conjugate. In order to obtain an analysis independent of texture intensity, the image, i.e., Y(x,y), was first normalized

$$Y(x,y) = \frac{Y(x,y)-Y_M}{\sigma_y} \quad (6)$$

where Y_M and σ_y represent the mean and standard variance of Y values of image respectively.

Directionality

Due to the spatially homogeneous pattern in the local region of experimental texture image, the mean power spectrum uP_{mn} at the different orientation on each scale is defined as

$$uP_{mn} = \frac{1}{N^2}\sum_i\sum_j |GW_{mn}(x,y)|^2 \quad (7)$$

where N is the size of texture image. In general, if it the texture has many lines or edge in a given direction θ, the power spectrum tends to give high values point between θ and $\theta+\frac{\pi}{2}$. In order to access the dominant direction angle of texture image, the parameter SP_n was defined to be the sum of power spectrum of different scales at the same orientation and the parameter r_m to be the region for which the maxima is obtained, hence

$$SP_n = \sum_m uP_{mn}\,,\ r_m = \arg\max_n SP_n \quad (8)$$

Finally, the dominant direction angle of texture image corresponding to the maximum power spectrum at which r_m is obtained is given as

$$\theta_d = (r_m - 1)/K*\pi \quad (9)$$

Figure 1 shows three examples of texture images, whose dominant directions are respectively equal to 0, $\pi/4$ and $5\pi/6$.

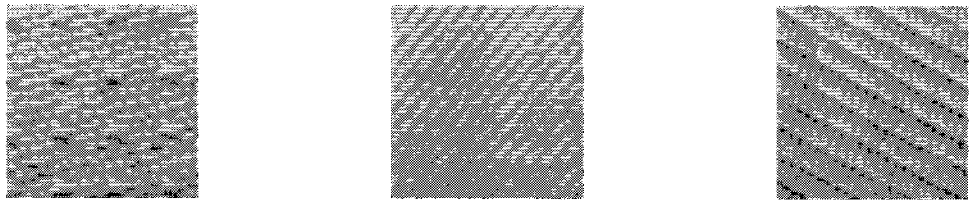

$\theta_d = 0$ $\theta_d = \pi / 4$ $\theta_d = 5\pi / 6$

Figure 1. Dominant direction of texture image

Coarseness measure

In order to access the coarseness of a texture image, the parameter RP_m corresponding to the ratio of relative power spectrum of neighboring scale at the dominant orientation of texture image is defined as

$$RP_m = \frac{uP_{d,m} / a^m}{uP_{d,m+1} / a^{m+1}} \qquad (10)$$

For the smooth texture, power spectrum distributes on the large scale and thus RP_m shows small ratio value; on the other hand, the coarse texture has a power energy distribution on the small scale and hence shows large ratio values. In this study, the coarseness measure M_c was defined by the maximum ratio of RP_m among all the scales.

$$M_c = \arg\max_m RP_m \qquad (11)$$

Figure 2 shows three examples of texture image with different coarseness measure.

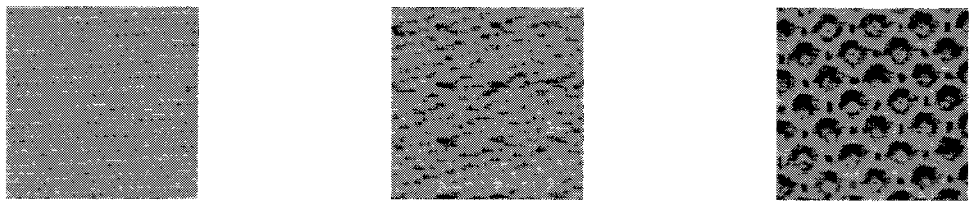

$M_c = 0.238$ $M_c = 2.98$ $M_c = 3.39$

Figure 2. Coarseness measure of texture image

4. RESULTS AND DISCUSSION

Correlation analysis between perceptional texture feature and color variation of texture image

In order to discuss above two defined texture features, i.e., directionality and coarseness, and their effect on the color variation of texture image, the correlation between texture feature and color variation was analyzed. Table I shows that correlation coefficients between directionality and lightness, chroma and hue angle variation among red, green and blue texture image are all below to 0.4, indicating that this feature has feeble effect on color variation of texture image. The negative coefficients represent negative correlation. However, the absolute correlation coefficients between coarseness and color change except hue angle are higher than 0.89, indicating that coarseness has a stronger effect on the lightness and chroma variation of texture image. However, hue values are not influenced by the coarseness effect of texture image. In the following discussion, only coarseness feature effect on color change of texture image was analyzed.

Table 1: Analysis of correlation between texture feature and color variation of texture image

	Correlation coefficients								
	L_R	C_R	h_R	L_G	C_G	h_G	L_B	C_B	h_B
directionality	0.09	0.12	-0.12	-0.29	-0.09	0.37	0.18	0.12	-0.25
coarseness	-0.89	-0.90	-0.24	-0.97	-0.91	0.28	-0.97	-0.97	0.09

Regression analysis between coarseness and color change

Single regression analysis was applied in this study; in which coarseness factor was an independent variable and lightness, and chroma variation were dependent variables. Figure 3 shows that the lightness of texture image becomes darker together with the increase of surface coarseness of texture image, which may be attributed to the specular reflection formation on the smooth texture. Furthermore, the blue texture images show larger lightness variations than green and red ones, indicating that darker texture images are more easily influenced by the coarseness effect. In addition to that, the texture image becomes less saturated with the increase of surface coarseness of texture images.

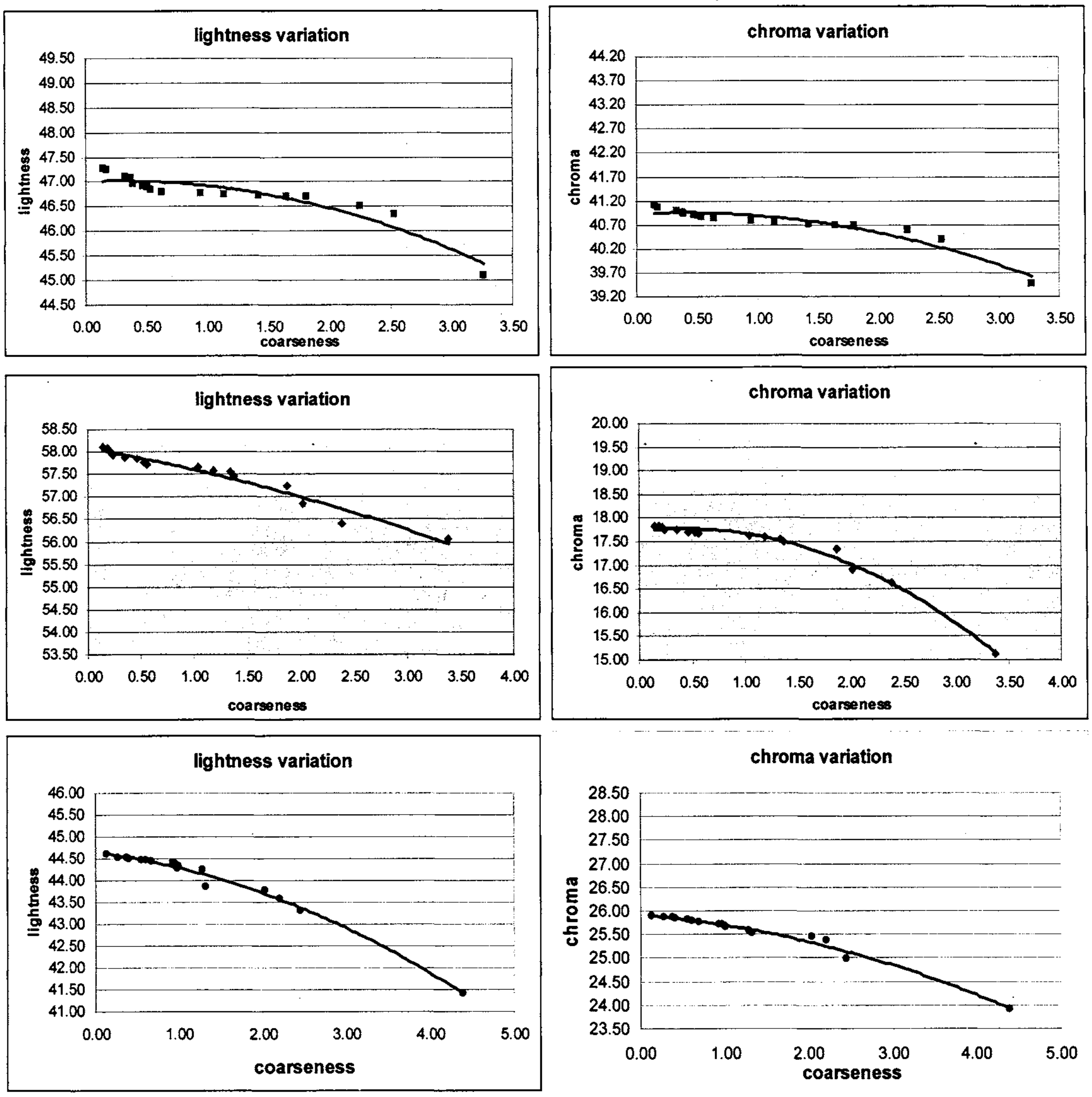

Figure 3: lightness, chroma and hue angle change along with coarseness measure (top two: red; mid two: green; and bottom two: blue texture image samples)

5. CONCLUSION

In this study, the perceptional texture features, such as directionality and coarseness, extracted from color image based on Gabor wavelet transform is applied to analyze relationship between these features and color variation. The correlation analysis between texture features and color variation shows that directionality of texture surface has weak effect on the color variation of texture image. However, the color variation is strongly related to the surface coarseness property of texture images. It has been show that texture image becomes darker and less saturated with the increase of surface coarseness property. The hue values of color texture image are not related to the coarseness and directionality properties according to the correlation analysis.

ACKNOWLEDGMENT

The authors wish to acknowledge the funding by Research Grants Council of The Hong Kong Government and the Hong Kong Polytechnic University.

REFERENCE

1 Wonjoung Lee, Masako Sato, Visual perception of texture of textiles, Color Research and Application,Vol.26, No.6, Dec. 2001, PP469 ~477

2 Lionel Simonot, Mady Elias, Color change due to surface state Modification, Color Research and Application, Vol.28, No.1, Feb. 2003, PP45 ~49

3 Edul N. Dalal and Kristen M. Natale-Hoffman, The effect of Gloss on Color, Color research and application, Vol. 24, No. 5, Oct. 1999.

4 Tamura, H., Mori, S., and Yamawaki, T., Textura features correspouding to visual perception. IEEE Transaction Systems, Man and Cybernetics, Vol.8 PP460~473, 1982

5 Rao , A. R. and Lohse, G.L. Toward a texture naming system: Identifying relevant dimensions of texture. Vision Research. 36(11):1649-1669

6 Tamura, H., Mori, S., and Yamawakim T. Textural features corresponding to visual perception. IEEE Transactions Systems, Man and Cybernetics, 8:460-473.

7 T. Chang and C.-C. J. Kuo, Texture analysis and classification with tree-structured wavelet transform. IEEE Transaction on Image Processing, vol.2, no.4, pp. 429-441, Oct. 1993.

8 Turner Mr. Texture discrimination by Gabor functions. Biological Cybernetics, 55:71-82, 1986

9 Jain AK and Farrokhnia F. Unsupervised texture segmentation using Gabor filters. Pattern Recognition, 24(12): 1167-1186, 1991

10 Dunn D, Higgins WE, and Wakeley J. Texture segmentation using 2-D gabor elementary functions. IEEE Transactions on Pattern Analysis and Machine Intelligencem 16(2): 130-149, 1994., Ill. , June. 1992

11 P.C. Hung, Colorimetric calibration in electronic imaging devices using a look-up table model and interpolation, Journal of Electronic Imaging, vol 2, pp 53-61, 1993.

12 Kobus Barnard, Brian Funt, Camera characterization for color research, Color research and application, vol 27(3), pp152-163, June, 2002

Development of a Computer Program for Identification of Weave Patterns

Pranut Potiyaraj and Benchaphon Sawangharsub
Department of Materials Science, Faculty of Science, Chulalongkorn University
Bangkok 10330 THAILAND e-mail: pranut@sc.chula.ac.th

Abstract

Weave patterns affect end-use properties of woven fabrics. Identification of weave patterns has been done traditionally by visual evaluation. This is prone to errors as depends on the skill of inspectors. This research aims to develop an algorithm and a computer program for identification of weave. The fabric images were analyzed by calculation color differences between each pixel. It was found that color different data obtained directly could not be used. Thus, the autocorrelation technique was performed on the image prior to the calculation. A diagram acquired from the calculated color differences were made available. Position of each yarn float was then obtained by detecting upper and lower peak of the curve in the diagram. Length of each float can be obtained using information about yarn size. A Visual Basic program was developed based on the above algorithm. Images of a square-inch woven fabric were obtained using an ordinary scanner with resolution of 600 dots per inch and saved in bitmap format. Users were asked to specify the scanning lines, vertically and horizontally. Weave pattern was then displayed. It was found that preciseness of the program to analyze number of yarns in each direction and the weave pattern can be identified depended on the selected scanning lines. Average scanning time for each fabric is around 15 seconds.

Introduction

Woven fabrics are constructed by interlacement of warp and weft yarns at 90 degrees to each other. At a particular intersection, the warp end can be placed either over or under the pick. Combinations of these arrangements form the fabric. The area that contains one complete weave is termed as a weave repeat. The numbers of ends and picks required in a repeat are called the warp repeat and the weft repeat, respectively. The smallest possible weave repeat contains two ends and two picks. Figure 1 shows a woven fabric which can be represented by a weave repeat in Figure 2.

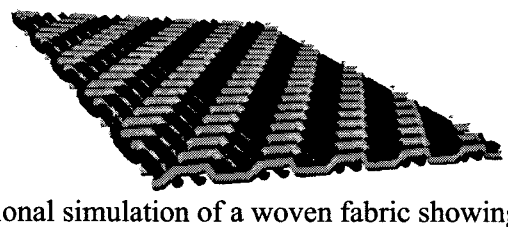

Fig.1 A three-dimensional simulation of a woven fabric showing warp-over-weft and weft-over-warp interlacing points

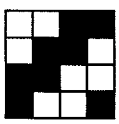

Fig.2 A weave repeat representing the fabric in Figure 1

Weave pattern greatly affect optical and mechanical properties of fabrics. Traditionally, a weave pattern can be determined by visual inspection of woven fabrics. However, visual inspection is time consuming and depends on skills of the inspector. This research thus proposes a computerized method for evaluation of weave patterns from fabrics.

Fabric evaluation using computerized systems are welled established based on image analysis technique. Generally, fabric images are captured using digital image capturing systems which are complicated. [1] Some efforts have been made so that a simple scanner can be used as a capturing tool.[2] Weave pattern evaluation is conversely little studied. [3-5]

Fabric Image Preparation

Two major types of woven fabrics were considered in this research, namely, plain and twill fabrics. They were scanned using a HP scanjet 5470c at the resolution of 600 dpi. The scanned images were kept in bitmap format. The images were converted to grayscale mode. Equalization was then performed on the images in order to make distinction between free spaces and yarn-occupied spaces. The examples were shown in Figure 3.

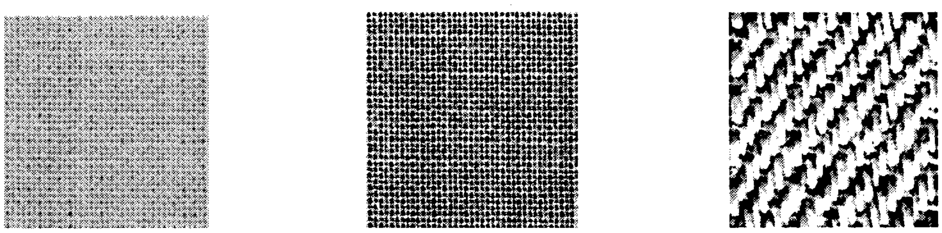

(a) (b) (c)

Figure 3 Scanned images of (a) a plain fabric (b) a plain fabric after equalization (c) a twill fabric after equalization

Image Analysis

When scanning through a selected line in a prepared fabric image, one would encounter alternate bright and dark area. A bright area is found when the yarn float is presence while a dark area is found when the yarn going down to interlace with the corresponding yarn or at the space which was not cover by warp or weft. Luminance at each pixel along a selected line in a fabric image can be calculated from RGB data according to Grassmann's law. A plot of luminance at each pixel is shown in Figure 4. It can be seen that peaks are presence in various width and height. The interpretation could be error easily.

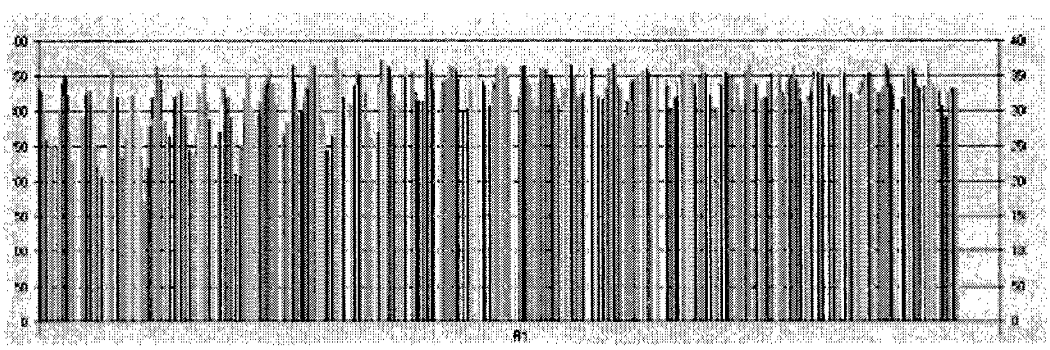

Figure 4 Luminance curve of a plain fabric

In order to make these peaks uniform, the autocorrelation method can be adopted using the following equations.

$$C_{x,0} = \sum_{i}^{M}\sum_{j}^{N} G_{i,j} G_{i-x,j} \qquad (1)$$

$$C_{0,y} = \sum_{i}^{M}\sum_{j}^{N} G_{i,j} G_{i,j-y} \qquad (2)$$

where $G_{i,j}$ luminance at coordinate (i, j)

M the maximum scanning point in the warp direction

N the maximum scanning point in the weft direction

$C_{x,0}$ autocorrelation values at points along the warp

$C_{0,y}$ autocorrelation values at points along the weft

x and y are the coordinates of pixel in the warp and weft direction , respectively.

The same data using in Figure 4 was then recalculated and consequently gave a plot with uniform peaks as shown in Figure 5.

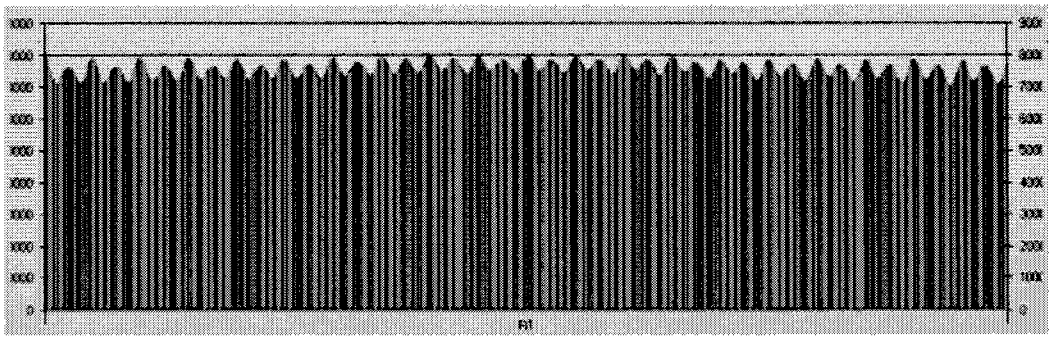

Figure 5 Autocorrelation curve of a plain fabric

Applying the same technique, twill fabrics were evaluated. The autocorrelation curve of a twill fabric can be shown as in Figure 6.

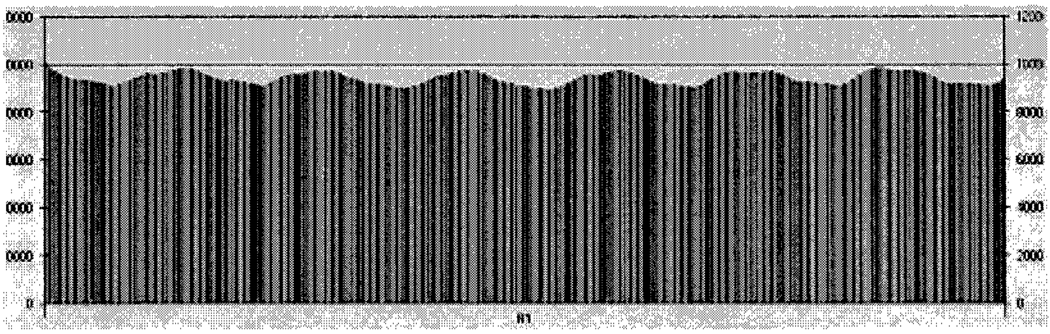

Figure 6 Autocorrelation curve for a twill fabric

Weave Identification

Width of each peak can be calculated by detecting the lowest point at each wave. This lowest point is the point where the slope of curve changes. This can be determined using the following equation.

$$C_{x,0} = \left(C_{(x+1),0} - C_{(x,0)}\right)/(x+1) - x \quad (3)$$

$$C_{0,y} = \left(C_{0,(y+1)} - C_{(0,y)}\right)/(y+1) - y \quad (4)$$

Width of each peak can be then compared. For the plain weave, width of peaks is approximately equal in warp and weft directions. Contrarily, for twill fabrics, width of peaks is markedly different in warp and weft directions. This information can be interpret so that the weave pattern is successfully identified.

Algorithm Implementation

Visual Basic 6.0 was used for developing a program based on Windows platform. The program as shown in Figure 7 can analyze fabrics images and then weave patterns are identified. Users choose a file which contains the equalized image of fabric. Then, scanning lines would be selected (shown as crossed lines in Figure 7). The program can calculate the number of yarns in each direction and also the weave pattern of the fabric.

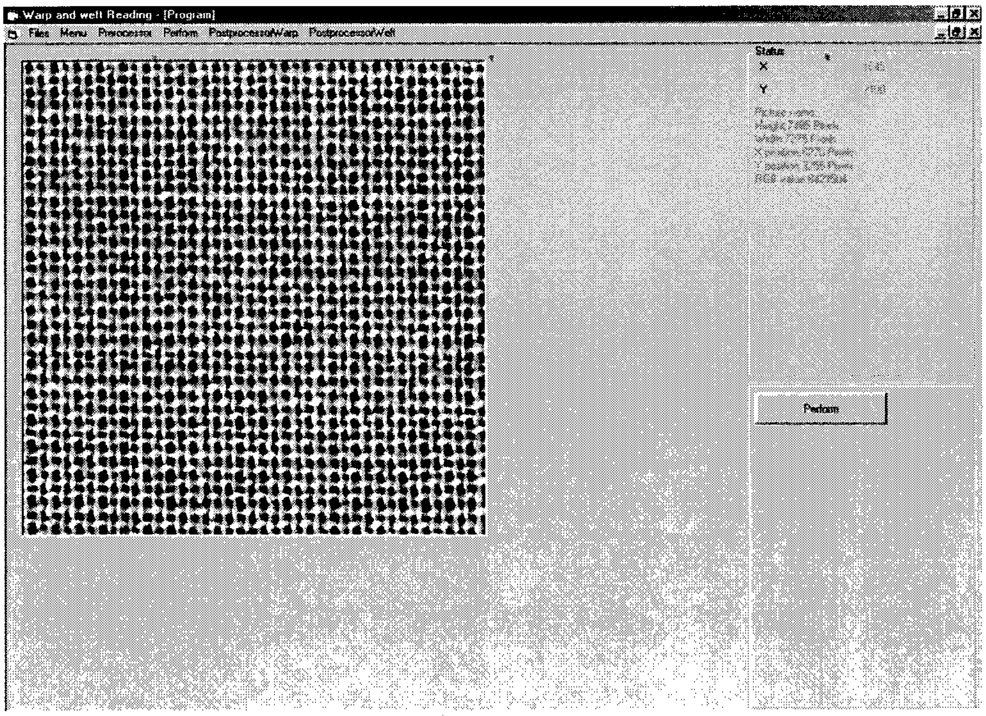

Figure 7 Weave identification program interface

The experimental results indicated that the program can identify most of plain fabrics correctly. However, in the case of twill fabrics, the correct scanning was around 70%. This is due to the fact that twill weaves are much more complicated than the plain weave. The precision of counting the number of yarns was about 90%. It was realized that the position where users choose the scanning lines is very important. It should align perfectly with a warp yarn and the corresponding weft yarn. This may be difficult to achieve since yarns in fabrics tend to offset from the straight and perpendicular lines. The scanning times were reported by the program. It was pointed out that the average time used was 15 seconds. Obviously, this is quicker comparing with visual inspection.

Conclusions

A computer program for identification of weave patterns from woven fabrics was developed. The fabrics were first scanned using an ordinary scanner. The fabric images were converted to grayscale figures and were processed using equalization method. Autocorrelation was performed at every pixel in the equalized images and autocorrelation curves were then plotted. The distances between peaks of autocorrelation curves were used to distinguish between the plain and twill weaves. The data could also be used to interpret the position of each interlacing point. Consequently, weave patterns were identified. It was found that the program can identify about 70% of fabrics correctly. Preciseness of the program to analyze weave patterns depended on the selected scanning lines. The scanning time was about 15 seconds for each fabric.

REFERENCES

1. Ohta, K., Sakaue, K., and Tamura, H., Pattern Recognition of Fabrics Surfaces Journal of the Textile Machinery Society of Japan, Proceedings, 1986, **32**(1), 7-10.
2. Sakaguchi, A., Kim, H., Matsumoto, Y., and Toriumi, K., Woven Fabric Quality Evaluation Using Image Analysis Textile Research Journal, 2000, **70**(11), 950-956..
3. Kinoshita, M., Hashimoto, Y., Akiyama, R., and Uchiyama, S., Determination of Weave Type in Woven Fabric by Digital Image Processing Journal of the Textile Machinery Society of Japan, Proceedings, 1989, **35**(2), 1-4.
4. Huang, C.C., Lui, S.C., and Yu, W.H., Woven Fabric Analysis by Image Processing Part I: Identification of Weave Patterns Textile Research Journal, 2000, **70**(6), 481-485.
5. Kang, T.J., Kim, C.H., and Oh, K.W., Automatic Recognition of Fabric Weave Patterns by Digital Image Analysis Textile Research Journal, 1999, **69**(2), 77-83.

Color Naming as Brand Identity

Hyeon-Jeong Suk*, Hans Irtel**, Yujin Kim***and Kyungjae Lee****

*International Institute for Integral Design
** University of Mannheim,
*** Korea Advanced Institute of Science and Technology
**** Purdue University

INTRODUCTION

Since the differentiation of product features among competitors became one of the major brand identity policies of marketers and designers, it became an important issue to name the product ambiguous color naming, which increases consumers' likelihood of purchase (Miler, 2002)(Molyvia, Prashant & Joan Meyers-Levy, 1998). Color Naming, as such, plays a key role in color marketing beyond indication of alternatives.
On the other hand, some researches recently have shown that color naming is reflecting semantic characteristics within surrounding context such as types of language (Hardin, C. L. & Maffi, Luisa, 1997)(Roberson, D., Davies, I. & Davidoff, J. 2000) and types of product (Suk & Kown, 2000) consumers associate with, and hence indicated possible miscommunication respectively (Jameson, 2002).
From the both arguments, it is assumed that color naming which makes the product attractive is rather abstract and unusual, which actually decreases the universality of the color perception. This contradictive hypothesis is the very sensitive matter for designers and markets, especially if the product is globally distributed and purchased.

This paper, therefore, intends to investigate the usage of product color naming designed for the specific product, to figure out those explanations in consumer context, in different cultural environment.
A color palette with 20 color was given to apply for two kinds of product, with obvious brand image such as nail lacquer from Lancôme Paris and Smart from Daimler Chrysler. The survey was conveyed with 3 groups of participants in Germany, South Korea and United States of America in German, Korean and English language.

KEYWORDS

Color naming, Brand identity, Cross-cultural, Global marketing, Product Color

1. BACKGROUND AND GOAL

Consumers are confronting a huge variety of product color in online shopping as well as traditional offline market. Color naming in terms of communication for product color information, has been one of the best ways to carry the color information, because it can represent, as such, a certain color and it can be translated into another language and is text, which may reduce a lot of POP processing: displaying products for every color on the shelves or presenting images of all kinds of color of the product on the online market(Suk, 2000).
The market nowadays is getting more competitive than ever and in order to establish and appeal the unique and positive product identity became one of the most important issues for marketers and designer, because a sum of every single image of the product results in the end the brand identity of the company. The color name of the product color is, therefore, a creativity driven marketing tool, which still arises question on the issues, how it should be then.

There, however, has been lack of research on color naming and color perception in the context of market situation, even if some researches have been discussed on cross cultural and inter cultural differences in perceiving color from the given color names (fig.1).

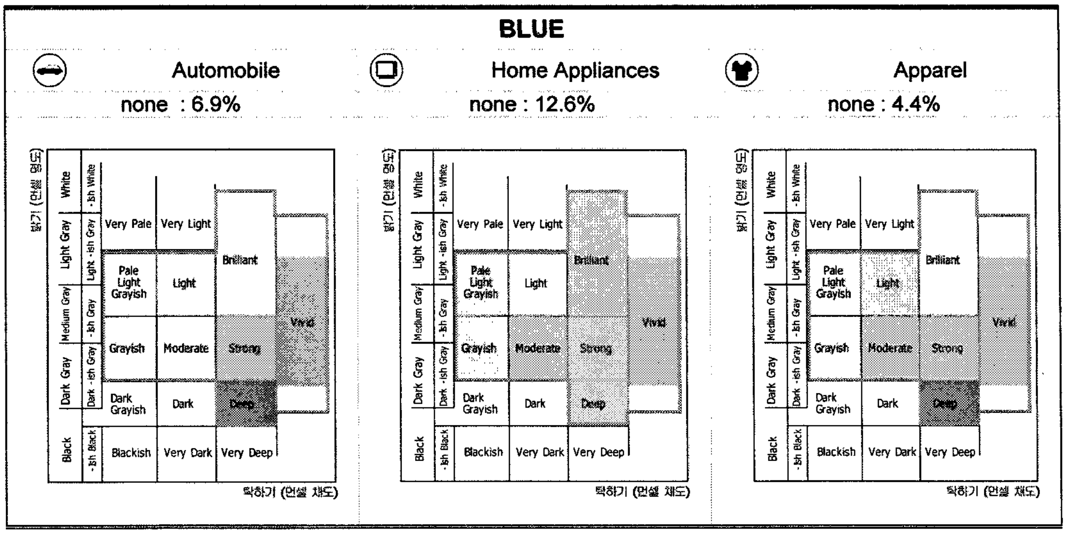

Fig 1. color perception associated from color name appears differently across product types, Suk 2000

The purpose of this paper is, therefore, to deepening the research on product color naming in the perspective of product identity and eventually brand identity by finding the consumers' preferred ways of expressing color naming for different situations. A color naming matrix was developed and used to analyse color naming.

2. DEVELOPMENT OF RESEARCH METHODOLOGY

2.1 Color naming categorization

Standard organisations have systemised color naming, such as basic color name and universal/ traditional color name. In addition to this ISCC-NBS system suggests categorization with Munsell value and Chroma system to indicate a certain tone of the color, which could be simply combined with color naming, such as 'dark red' or 'light red' (Stromer 2002). In this paper the categories of color naming are extended to symbolic one, which in general sense, is not implying any specific color, but could be used for expressing a flavour or image. As the fig.2 shows the symbolic color name was sub categorised into 3 groups, such as color related, product related and pure abstract one.
The hierarchical order(fig.2) is applied to illustrating part of the color name adding the tone part, so that a matrix to analyse color naming is set up (table 1).

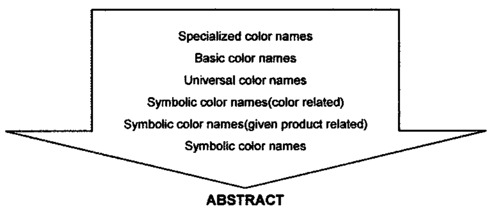

Fig.2 an order of categories of color naming

		illustrating					
		null	basic incl. Specialised term	tone	universal	symbolic - farbe	symbolic
main	specialised term	*magenta*	*reddish*	*dark*	*bloody*	*jealous*	*energetic*
	basic	*red*	*reddish red*	*dark red*	*bloody red*	*jealous red*	*energetic red*
	universal	*blood*	*reddish blood*	*dark blood*	*bloody blood*	*jealous blood*	*energetic blood*
	symbolic-farbe	*jeal*	*reddish jeal*	*dark jeal*	*bloody jeal*	*jealous jeal*	*energetic jeal*
	symbolic	*energy*	*reddish energy*	*dark energy*	*bloody energy*	*jealous energy*	*energetic energy*

Table 1. Matrix for color naming analysis and examples

3. EMPIRICAL STUDY

3.1 SURVEY PLAN

A color palette consists of 20 color chips- 8 from nail lacquers, 7 from Smart and the rest ones, fluorescent orange for example, to be able to cover wider range of color spectrum. From the pilot survey with 7 people in Germany it was discovered that the memory effect was unfortunately significant, even if the survey contains refreshing stage for changing the topic. Therefore the survey has proceeded in two processes:

Flow type A: to write down color names without product association and then color names for two types of products like nail lacquer from Lancôme Paris and Smart from Daimler Chrysler.

Flow type B: people conveyed the process skipping the stage to write them down without product association. The left vertical arrow in figure 4 is illustrating this case.

67 people- 23 Germans, 31 Koreans 10 Americans, 2 Chinese, 1 French and 1 Swedish- have participated in Germany, South Korea and USA in their own mother languages except those 2 Chinese in Germany(in English), 1 French(in German), 1 Swedish(in German), living in Germany.

No.1 RAL 1017 Saffron yellow	No.2 RAL 6036 Pearl opal green	No.3 RAL 5026 Pearl night blue	No.4 RAL 6019 Pastel green	No5 RAL 3015 Light pink
No.6 RAL 9023 Pearl dark grey	No.7 RAL 7046 Telegrey 2	No.8 RAL 4002 Red violet	No.9 RAL 3020 Traffic red	N0.10 RAL 3003 Ruby red
No.11 RAL 3007 Black red	No.12 RAL 9005 Jet black	No.13 RAL 6006 Grey olive	No.14 RAL 9010 Pure white	No.15 RAL 4012 Pearl blackberry
No.16 RAL 5017 Traffic blue	No.17 RAL 1021 Rape yellow	No.18 RAL 4006 Traffic purple	No.19 RAL 2007 Luminous bright orange	No.20 RAL 4003 Heather violet

Fig 3. Palette composition for nail lacquer: for smart, the color chips were rearranged

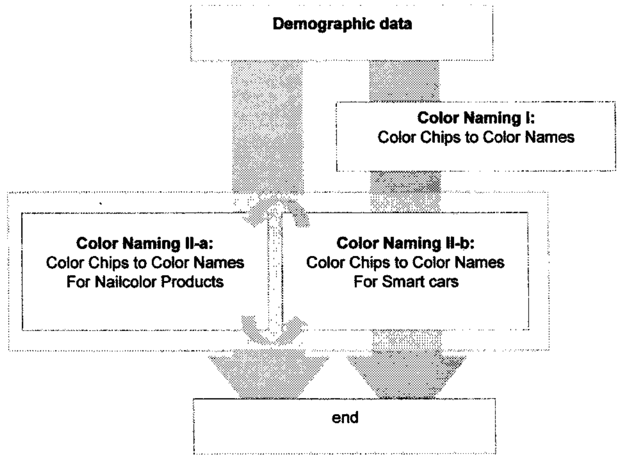

Fig 4. Survey flow

4. RESULTS

4.1 Color naming as color identification

First of all it was examined how consumers are identifying the given color without any additional association. As the palette displayed 20 color chips, which are twice then so called basic color name, in this stage it was also intended to see how the secondary 10 color are diversified by consumers. The table 2 presents the results, indicating that all three groups have concentrated on basic color naming(German 23%, Korean 36.5%, and American 22%) or basic color naming combined with tone scale(German 30%, Korean 23.8%, and American 20%). Related with high concentration on universal color naming among Korean participants, it could be a supportive explanation that more than half of the survey participants were design students, already well trained with color substance. Moreover the subtle differences between 3 cultural groups appeared already, Americans showing more individual results from the beginning.

		illustrating					
		null	basic incl. Specialised term	tone	universal	symbolic	symbolic (non-color)
main	specialised term	4.3%	0.4%	0.4%	0.0%	0.0%	0.0%
	basic	23.9%	8.6%	30.0%	8.2%	5.7%	4.3%
	universal	7.9%	0.0%	0.7%	0.0%	0.0%	0.0%
	symbolic	2.1%	0.7%	0.0%	0.0%	0.0%	0.0%
	symbolic (non-color)	0.0%	0.7%	0.0%	2.1%	0.0%	0.0%

		illustrating					
		null	basic incl. Specialised term	tone	universal	symbolic	symbolic (non-color)
main	specialised term	5.3%	0.0%	1.3%	0.0%	0.0%	0.0%
	basic	36.5%	6.3%	23.8%	1.5%	1.5%	3.3%
	universal	12.3%	0.5%	2.3%	0.0%	0.0%	0.5%
	symbolic	2.8%	0.0%	0.5%	0.0%	0.0%	0.0%
	symbolic (non-color)	1.5%	0.3%	0.0%	0.3%	0.0%	0.0%

		illustrating					
		null	basic incl. Specialised term	tone	universal	symbolic	symbolic (non-color)
main	specialised term	7.5%	0.0%	0.0%	0.0%	0.0%	0.0%
	basic	22.0%	3.0%	20.0%	[illegible]	5.5%	[illegible]
	universal	[illegible]	1.0%	2.5%	0.5%	0.5%	0.5%
	symbolic	2.0%	0.0%	0.0%	0.0%	0.0%	0.0%
	symbolic (non-color)	1.5%	1.0%	0.5%	0.0%	0.0%	0.5%

Table 2. Color naming from 14 Germans(left), 20 Koreans, and 10 Americans(right) without product association

4.2 Color naming as brand image

For the next stage, people were asked to suppose themselves as a marketing director, preparing for a new launching in their own domestic market. Table 3 below illustrates the results and it is significant that the color naming is shifted from basic color naming to universal or symbolic ones. In comparison with the previous test (table 2), it appears continuously that the Americans were using more individual expression than Germans and Koreans.

		illustrating						
		null	basic incl. Specialised term	tone	universal	symbolic - farbe	symbolic - product	symbolic
main	specialised term	1.5%	0.0%	0.0%	0.0%	0.0%	0.0%	0.4%
	basic	8.8%	2.7%	9.6%	4.6%	7.7%	2.7%	16.5%
	universal	16.2%	0.8%	2.7%	0.0%	0.4%	1.2%	2.7%
	symbolic-farbe	5.0%	3.1%	1.2%	0.0%	0.0%	0.0%	0.4%
	symbolic-product	0.8%	0.4%	0.0%	0.0%	0.0%	0.0%	0.8%
	symbolic	3.8%	1.2%	0.8%	0.8%	1.2%	0.4%	1.9%

		illustrating						
		null	basic incl Specialised term	tone	universal	symbolic	symbol (product)	symbolic (non-color)
main	specialised term	1.0%	0.0%	0.8%	0.0%	0.0%	0.0%	0.0%
	basic	13.0%	2.8%	14.3%	6.0%	6.5%	3.0%	11.5%
	universal	10.5%	1.8%	1.0%	0.3%	1.0%	0.0%	1.5%
	symbolic	4.0%	0.5%	1.0%	0.0%	0.3%	0.0%	3.3%
	symbol (product)	1.8%	0.5%	0.3%	0.0%	0.3%	0.8%	1.3%
	symbolic (non-color)	5.8%	1.3%	0.8%	0.0%	0.8%	0.5%	2.5%

		illustrating						
		null	basic incl. Specialised term	tone	universal	symbolic - farbe	symbolic - product	symbolic
main	specialised term	1.0%	0.0%	0.0%	0.0%	0.0%	0.0%	1.5%
	basic	1.5%	1.0%	2.5%	4.0%	3.5%	4.5%	15.0%
	universal	5.5%	0.0%	0.5%	0.0%	0.5%	1.0%	4.5%
	symbolic-farbe	9.5%	1.0%	0.0%	0.5%	1.0%	0.0%	2.0%
	symbolic-product	2.5%	0.0%	0.5%	0.0%	0.5%	1.0%	0.0%
	symbolic	19.0%	3.5%	0.0%	0.5%	1.5%	0.5%	10.0%

Table 3. Color naming from 23 Germans(left), 31 Koreans, and 10 Americans(right) for nail lacquer by Lancôme

The symbolic expressions related with the given products, however, were quite seldom in both product types as well as in all of three cultural groups.

4.3 Color naming in foreign languages

Even if each group had its own survey version in their mother languages and the survey directions were given also in the local language, there was an obvious tendency to use foreign languages to create product color naming. As table 4 shows exemplary case from one Korean participant, where most of the answers to color identification not associated with products were expressed in Korean, but answers to color naming for the products were either in Korean orthography sounding English words, or in English.

* : color names in Korean but written for sounding English words

1. color naming without products			3. color naming for Lancome nail lacquer			2. color naming for Smart		
nr.	original data	in English	nr.	original data	in English	nr.	original data	in English
1	개나리	golden bell	1	봄의 향기	spring fragance	1	business yellow	
2	카키	khaki	2	미혹의 숲속	infatuating forest	2	deep green	
3	남	navy blue	3	여원의 바다	calm sea	3	space blue	
4	연 록	pale green	4	코튼* 그린*	cotton green	4	sky green	
5	분홍	pink	5	핑크* 레이디*	pink lady	5	oriental skin	
6	실버*	silver	6	사이버* 메탈릭*	cyber metallic	6	metal silver	
7	회	grey	7	시티* 헌터*	city hunter	7	young grey	

Table 4. Example data from a survey participant in South Korea, showing expressions in different ways and languages

Interestingly this phenomenon were found with majority of participants, who were not necessarily bilingual or trilingual and they mostly do not use them at all in daily lives. Most of Germans and Koreans were toward English and Americans were toward French.

5. DISCUSSION AND FUTURE RESEARCH

5.1 Conclusion and Future Research

The tone denomination is generally used to specify and to differentiate between color, when they have close hue values. In expressing a certain association, however, people are generating individual terms, even if it might less clear to communicate the color information itself. The frequent usage of foreign language is in this sense, often accepted by consumers.

The cross-cultural research has been one of the main aspects of this paper in order to find out general explanation as well as to deal with local issues. Based on this paper, it is expected in the future to broaden the cultural domain of the empirical study, especially to other different language groups and in parallel it will be necessary to diagnose and to clarify the mental process for association from brand image to color information and vice versa.

ACKNOWLEDGEMENT

The survey material was supported in part by L'Oreal Art and Science Foundation in Japan.

REFERENCES

Hardin, C. L. & Maffi, Luisa (1997) Edited. *Color categories in thought and language*. New York, NY, US: Cambridge University Press

Jameson K.A. (2002 Under Review for Publication), Culture and Cognition: What is Universal about the Representation of Color Experience?, University of California

Miler, E.G.(2002). *Shades of Meaning: The Effects of Color and Flavor Names on Purchase Intentions*, Ph.D. Dissertation, The Wharton School, University of Pennsylvania, Philadelphia

Molaviya, Prashant and Joan Meyers-Levy(1998), Understanding consumers' response to incongruent product information: New research and insights, *Advances in Consumer Researches*, 25, 115

Roberson, D., Davies, I. & Davidoff, J. (2000). Color categories are not universal: Replications and new evidence from a stone-age culture. *Journal of Experimental Psychology: General*, 129, 369-398

Stromer K. (2002), *Farbsysteme*, Dumont Cologne

Suk H. J.(2000). *A Study on the Characteristics of Product Colour on the Internet*, Master dissertation, Korea Advanced Institute of Science and Technology

Suk H.J. & Kwon E.S.(2002). A Study on the Characteristics of Product Color on the Internet – with an Emphasis on the Interaction between the Expression of Product Color Information and Color Perception- *Conference Proceeding of Design 2002- Dubrovnik*, Vol.1 (pp.423-426)

Interior and Exterior Colors Used by One Home Building Company in New Houses in the Kyoto and Osaka Region

Haruyo Ohno[1] Shoko Shibano[2]
[1]Otemae University, Hyogo, Japan, [2]ELBADESIGN, Kyoto, Japan

ABSTRACT

There are some colors that are more often used in the residential environment. In color planning, it is important to gauge how these colors are evaluated and how they affect people physiologically and psychologically. Here, we report the results of a survey concerning interior and exterior colors used by one home building company.

Keywords: *Interior colors、Exterior colors、Home building company, New house*

1.INTRODUCTION

As one measure to improve the environment for local residents, local governments in Japan have recently begun taking into consideration the attractiveness of towns. They have issued ordinances on landscaping to guide the design of cityscapes, and they have become interested in promoting landscapes which harmonize with nature and which are consistent with the history of the local area. At the same time, in their brochures, major home building companies in our country explain to consumers color planning for new houses, emphasizing that it is important that exterior colors should blend in with surroundings and interior colors should make the living space comfortable for residents. Furthermore, in their exhibition houses they propose color plans which take the surrounding environment into consideration. If new houses are built with color plans based on these premises, when completed they should blend in well with their surroundings and contribute to an attractive cityscape. Also, the interiors should form comfortable living spaces.

However, currently unconventional colors are often seen in exteriors and interiors of new houses, even the ones built by major home building companies. Therefore, this makes us think that greater consideration needs to be given to promoting color plans which maintain a harmonious cityscape, blend in with the environment and contribute to comfortable interior living spaces.

Thus, we decided to research colors used for exteriors and interiors of new houses in two areas. One area is Kyoto city and its suburbs, where the public is very interested in maintaining an appropriate cityscape, as evidenced by the early introduction of ordinances on landscaping to preserve the historic appearance of the city. The other area is Osaka city and its suburbs, where recently the local government drew up basic plans concerning landscaping.

2. Comparison with past research

In the past, some data on exterior colors of commercial buildings were gathered in the course of research on landscape planning for urban areas, but there has been no work on residential buildings. In the

1960's Kan and others reported their research on interior colors. However, these studies are more than 40 years old. In 1992, Ohno et al reported the results of research on interior colors of 136 houses in Osaka and its suburbs. According to this research, warm colors (Y, YR) were used for more than 50% of ceilings, walls and floors of entrances, living rooms, dining rooms and private rooms. These results are consistent with those of Kan et al reporting the use of warm colors. It was also found that blue-red colors (PB, P, RP) were used more frequently, although these colors still accounted for less than 10% of total colors. Based on these results, and in order to form better cityscapes and interiors, it is important to obtain recent data on color plans.

3. METHOD

This research targeted homes constructed with the two-by-four method and ordered by individuals in Kyoto and Osaka, and their suburbs. The target houses were chosen from new house orders received from 1998 to 2000 by the Kyoto and Osaka branches of one company. Data were gathered on types of community, the area covered by the building itself, total floor area of the interior, the owners' household, exterior colors of the south elevation and the elevation of the main entrance (the north elevation was targeted when the entrance was located on the south), exterior areas and colors on ceilings, walls and floors of interiors. Also, data were collected on who actually chose colors of houses. For exterior colors, data were collected concerning roofs, walls, window frames, front doors and back doors. For interior colors, entrances and halls, Japanese style rooms, main bedrooms, children's rooms, and living/dining-rooms and living/dining-room/kitchens were surveyed. Table 1 shows data abstracted from studies of new houses in Kyoto and Osaka.

1) **Exterior colors**

Table 1 shows colors used for south sides of surveyed homes in Kyoto(K1～24) and Osaka(01～024). In Kyoto, black was used for a little less than 40% of roofs and R series colors accounted for 40%. In Osaka, black was used for a little more than 40% of roofs and GY, G series colors accounted for a little less than 40%. In both areas chromatic colors of low brightness/low chroma were used.In Kyoto, YR colors were used for 40% of exterior walls and Y colors were used for 20%. R, RP, P, PB, GY, G were also used. In Osaka, YR was used for 40% of exterior walls, Y was used for a little more than 40%, and R and GY colors accounted for the remainder. For walls, warm colors were widely used, and in both Kyoto and Osaka colors of high brightness and middle chroma were used a lot, accounting for 40%.

Normally, in color plans, low chroma is considered to be desirable for exteriors of houses because it blends in with the surroundings. However, middle chroma colors were commonly used for the exteriors of the new houses which we surveyed. Therefore, those houses might not blend in well with their surroundings. Most window frames were either white or black. Half of window frames surveyed were white and a little more than 40% of them were black. Achromatic color accounted for 90%.

Half of front doors were black and half were white. For back doors, almost the same colors were used as for window frames. These colors used for window frames, front doors and back doors are very different from the warm colors of the brown series, colors of conventional wooden houses in Japan.

2) **Interior colors**

Figure 1 shows frequencies of color phases used for walls of entrances and halls, living/dining- rooms, living/dining-room/kitchens, main bedrooms, children's rooms and Japanese style rooms in new houses listed in Table 1. The results are listed for the Kyoto and Osaka areas, respectively. As shown, Y colors were used for 80% of entrances in Kyoto and 50% in Osaka. YR colors accounted for 20% of entrances in Kyoto and 40% in

Osaka. For living/dining-rooms and living/dining-room/kitchens, Y accounted for a little less than 40% in both areas. YR accounted for 50% in Kyoto and 40% in Osaka. Y colors were used for 60% of main bedrooms in Kyoto and 40% in Osaka. YR colors accounted for 20% in Kyoto and 50% in Osaka, and other colors accounted for 20% in Kyoto and 10% in Osaka. YR colors were used in a little more than 50% of children's rooms in both areas. Y colors were used in 20% of children's rooms in Kyoto and a little more than 30% in Osaka. PB, GY and B were also used. For Japanese style rooms, except for the color of the tatami mats (GY), YR colors accounted for 55% in Kyoto and a little more than 30% in Osaka. Y colors accounted for 30% in Kyoto and 55% in Osaka.

For major color phases of floors in Kyoto, YR colors were used for i) 80% of entrances and halls, ii) 60% of living/dining-rooms and living/dining-rooms/kitchens, iii) 90% of main bedrooms and iv) 90% of children's rooms. In Osaka, YR colors were used a lot, accounting for 90%, 30%, a little more than 60% and 90%, respectively, of the four types of rooms listed above. Most of the remaining space employed Y colors. We also saw that a variety of color phases were used on ceilings and walls of children's rooms.

3) **Who chooses color schemes**

We surveyed who actually chooses color schemes, because it is thought that exterior colors of houses have a great impact on whether a home blends in with its surroundings (Table 1). In Kyoto, the choice of exterior colors was made by the husband 60% of the time, and in Osaka, exterior colors were chosen together by the husband and wife 60% of the time. In Kyoto, interior colors were chosen by the husband or wife alone in more than 30% of cases. In Osaka, the wife alone chose interior colors in 60% of cases, and the wife and husband chose together in 30% of cases.

Hence, we see a difference between Kyoto and Osaka in how couples handle the decision of color schemes. In Kyoto, many men participated in deciding the colors of their houses. In Osaka, about 30% of men decided the interior and exterior colors of their homes.

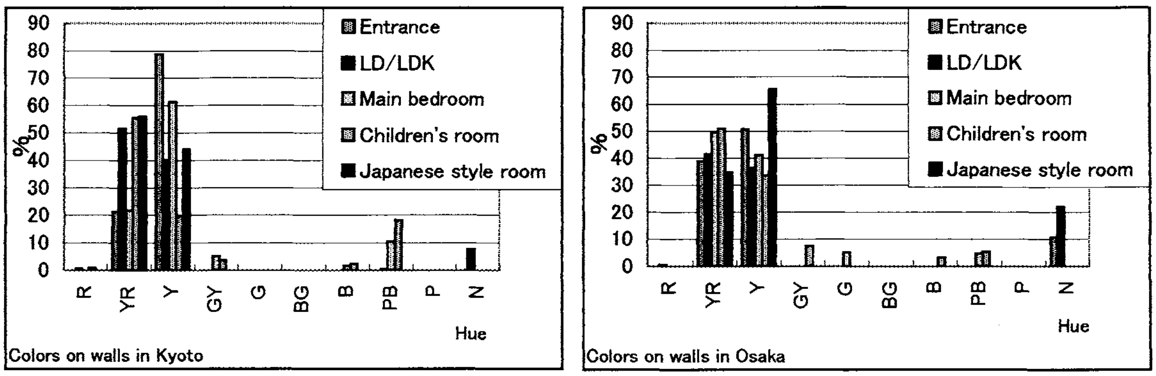

Fig. 1 Interior colors of new houses in Kyoto and Osaka :

**LD/LDK = living/dining-rooms and living/dining-room/kitchens*

Usually, designers working for housing companies talk with owners about interior and exterior colors of homes. When owners express a preference for an exterior color which does not blend in with surrounding buildings and the environment, designers suggest alternative schemes. However, in reality those suggestions are usually not accepted, and the colors originally chosen by the owners are used. For interior colors, in most cases, owners request color plans that match the attractive photos in the sales brochures. And even when designers explain to owners that these brochures are for drawing people's attention and may not provide the most comfortable living space, the likely result may be the opposite of what is hoped for by the company. The owner may actually start to think of changing companies, not color schemes, which does not solve the problem of color coordination. This suggests the need for some education of consumers concerning the role of color in the interior living environment.

Table 1. Exterior Colors of New Houses in Kyoto and Osaka

①	②	③	④	⑤	⑥	⑦	⑧	⑨	①	②	③	④	⑤	⑥	⑦	⑧	⑨
K-1	40	98.4	H	H	3500-3999	52	N2	1.2Y7.5/1.6	O-1	30	175	H+W	H	2500-2999	78	2.5G3/4	8YR6.5/3.5
K-2	40	163.9	H	W	3000-3499	77	N 1	2.5Y9/1	O-2	60	125.8	H+W	H	2500-2999	66	N2	5GY3.7/4.6
K-3	50	59.6	H	H	2000-2499	38	5GY3/1	10RP6.6/2.2	O-3	30,70	199.5	H	H	3500-3999	109	5GY3/1	5YR7/45
K-4	20	130	H	W	2500-2999	91	10R2/2	8.5YR8/3.8	O-4	60	94.9	H	W	2000-2499	91	N2	4.4Y4.5/4.6
K-5	50	132.8	H	W	2000-2499	39	10R2/2	10YR7/4	O-5	40	164.3	H+W	W	2000-2499	63	N2	4.4Y4.5/4.6
K-6	40	125.8	H	H	3000-3499	85	2.5G3/4	2.5Y9/1	O-6	40	170	H+W	W	3000-3499	50	N2	6.7R7.1/1.3
K-7	40	155.1	H	M	2500-2999	49	10B6/2	6.7R7.1/1.3	O-7	50	177	H+W	H+W	2500-2999	78	5GY3/1	10YR7/4
K-8	30	159.3	H	M	4000 以上	82	10R2/2	5YR7/4.5	O-8	30	185.2	H+W	W	3000-3499	85	10B6/2	4YR5/1
K-9	30	184.6	H	M+S	3000-3499	93	N2	5.3YR7.3/2	O-9	30	173.9	H	H	3000-3499	68	10R3/2	10R5.5/6.5
K-10	60	165.6	W	W	4000 以上	61	10R3/2	10P6.2/0.8	O-10	40	165.6	W	W	2500-2999	96	1.7GY7.2/0.7	5YR7.5/1.5
K-11	70	204.2	H	H	3500-3999	105	N2	5YR8.5/1	O-11	50	183.8	H+W	H+W	3000-3499	122	N2	2.5Y9/1
K-12	40	109.9	W	H	2500-2999	81	N2	5GY7/4	O-12	30	110.9	H+W	H+W	2500-2999	92	5GY3/1	2Y8/1
K-13	30	137.3	H	H	2000-2499	104	10R3/3	3G3/4	O-13	50	153.8	F	W	3000-3499	89	N2	8YR8.5/2
K-14	30	97.8	H	H	1500-1999	77	N2	2.2Y7.3/6.8	O-14	30	157	H+W	W	3000-3499	105	N2	8YR5.5/8
K-15	30	125.8	H	W	1500-1999	58	10R3/2	10R5.5/6.5	O-15	30	144.9	H	H	2000-2499	65	N2	8YR8.5/2
K-16	30	102.6	H	H+W	1500-1999	70	10B2/2	9.1PB2.3/8	O-16	40	99	H+W	W	3000-3499	102	5GY3/1	2.5Y8.5/1
K-17	30	105.9	H+W	H+W	2000-2499	47	10R2/2	5YR7/4.5	O-17	40	135.5	H+W	H+W	2000-2499	68	5GY3/1	2.5Y8/4
K-18	30	131.2	U	U	1500-1999	66	N2	10R5.5/6.5	O-18	50	126.6	W	W	2000-2499	146	N2	2.5Y6/1.5
K-19	30	142.8	U	U	1500-1999	68	5GY3/1	10P6.2/0.8	O-19	40	239.5	H	H+W	4000 以上	60	10R3/2	7.5YR5/6
K-20	30	119.2	U	U	1500-1999	56	10R2/2	2.5Y8.5/1	O-20	30	119.2	H+W	H+W	2000-2499	49	10R2/2	5Y9/3.5
K-21	30	124.2	U	U	1500-1999	51	N2	10YR7/1	O-21	40	113	H	H+W	2500-2999	63	N2	5YR7/4.5
K-22	50	152.4	W	W	1500-1999	56	10R2/2	5YR8.5/1	O-22	30	161.8	H+W	W	2500-2999	88	5GY3/1	2.5Y8/4
K-23	40	132.5	H+W	H	2000-2499	36	N2	5YR8.5/1	O-23	40	151.1	H+W	H+W	3000-3499	76	N2	2.5Y8.5/1
K-24	50	139.9	H+W	H	2500-2999	80	10R2/2	5YR7/2	O-24	40	125.9	W	W	4000 以上	79	5GY3/1	10YR7/4

①Number ②Age Group of Owner ③Total Floor Area (㎡) ⑥Building Costs 0000 yen ⑦Area of South Wall ⑧Roof ⑨Wall ④Who Decides Exteriors: Husband=H, Husband and Wife=H+W, Wife=W, Mother and Sister=M+S, Unknown=U
⑤Who Decides Interiors: Husband=H, Husband and Wife=H+W, Wife=W, Mother and Sister=M+S, Unknown=U

4. Conclusions

For roofs, low brightness/low chroma of black and R colors were used.

On exterior walls, high brightness/middle chroma Y and YR - warm colors - were often used. However, R, RP and PB accounted for 20% of exterior walls, and GY and G were also used.

For interior colors, Y and YR were used a lot in entrances and halls, living room/kitchens, main bedrooms and children's rooms. PB, GY, N, R and other colors were also used.

Who decides exterior colors? In Kyoto, husbands do in many cases. In Osaka, the husband and wife chose together.

Who decides interior colors? In Kyoto, only the husband, only the wife or the two together account for approximately equal percentages. In Osaka wives decided in more than half of all cases.

Within the scope of our research, how couples are involved in choosing colors varies from area to area.

Acknowledgment

The author expresses her gratitude to the students at Otemae Junior College and Otemae University for their cooperation in this research.

References

1) Iijima Shoji: Toshi Keikan Kankyo to Kankyo Hozen/Keisei Seisaku, Okayama Shouka Daigaku Gakujyutu Kenkyugyousyo 2001.3 (Shouji Iijima: Cityscape Environment and Measures of Landscape Conservation/Formation, Academic Research Book of Okayama College of Commerce, March 2001)

2) Kyoto no Machi no Iro Sinpojium Sougou Houkokusyo:Kyoto no Machi no Iro Sinpojium Sosiki Iinkai, 1992.3 (Comprehensive Report on Symposium of Town Color in Kyoto: Committee of Symposium of Town Color in Kyoto, Feb. 1992)

3) Yawaragi Osaka/Machi no Iro:Osakasi Sikisai Keikan Keikaku Gaidobukku 1996.3 (Calm Osaka/Color of Town: Guidebook of Color Landscape Project of Osaka City, June 1996)

4) Inagaki Takuzo: Toshi no Shikisai Bunseki ni Kansuru Ichikousatu, Nihon Kenchiku Gakkai Gakujyutu, Kouen Kougaisyu/Kankyo Kougaku (1987) 429—430 (Takuzo Inagaki: A Study of Analysis of City Color, Architecture Society of Japan, Summary of Lectures/Environmental Engineering (1987) 429—430)

5) Inui Masao: Kenchiku no Hyojyun Shikisai Seijyo nikanshite, Nihon Kenchiku Gakkai Ronbun Houkokusyu Gougai (1965) 404 (Masao Inui: About Standard Color Properties of Architecture, Special Edition of Paper Reports by Architecture Society of Japan, (1965) 404

6) Inui Masao, Watanabe Keiko: Naisouzai Shikisai no Jissei Bunseki narabini Hyojyunka ni kansuru Kenkyu, Kenchiku Kenkyu Houkoku Dai 50 gou (1967) 1 ~26 (Masao Inui, Keiko Watanabe: Research on Analysis and Standardization of Interior Material Colors, Architecture Research Report No.50 (1967) 1 ~26

7) Ohono Haruyo, Inoue Youko: Interia no Iro to Zairyo-Jyutaku no Baai- Nihon Kenchiku Gakkai Kinki Shibu Kenkyu Houkokusyu, (1994) 85~88 (Haruyo Ohno, Youko Inoue: Interior Color and Material-the case of houses- Study Reports of Kinki Branch of Architecture Society of Japan, (1994) 85~88

Prof. Dr., Haruyo Ohno, Faculty of Socio-cultural studies, Otemae University ,2-2-2, Inano, Itami, Hyogo, Japan 664-0861, E-mail:ohnoh@otemae.ac.jp

Designer, Shyoko Shibano, ELBADESIGN ,17-72,Terayama, Hirono, Uji, Kyoto, Japan 611-0031

Research on appearance rate of "Trendy colors" and "Regularly-used colors"

Chieko UDAGAWA
Mejiro Design College

It is said that the fashion colors in clothes originates in Inter-color. However, at the present, no one has analyzed what constitutes "trendy colors" or the fashion industry's "regularly-used colors" for a particular season. I had an opportunity to obtain the fashion photo collection of photojournalist Kazuo Ooishi. The fashion photo collection contains about 80,000 pictures of the Paris and Milan clothing collections from 1981 to and including 1999. From all 80,000 photographs, I am using only those from the Paris fashion collections of 1998 and 1999. Using these photographs, with the aide of computer technology, I will analyze the appearance rate of "trendy colors" and "regularly-used colors" and try to theorize it.

1. Introduction

For clothes, general consumers in Japan often use the words "regularly-used color" or "trendy color." However, in trend information by magazines and other media to encourage people to consume on clothes, they often use such ambiguous expressions as "such and such colors are standing out" or "there are signs of some colors that will be trendy." Japan Fashion Color Association (JAFCA) defines "regularly-used colors" to be stably popular, i.e., colors that the consuming public will buy at any time. Some ambiguity, however, exists between "stability" and the appearance rate at collections. In order to clear the ambiguity and explain the trendiness of certain colors, I have chosen to analyze the frequency of colors used in a Paris collection during a two year period.

2. Method

2-1. Objects of Analysis

Among the photographs to be analyzed, about a 1,000 of them were selected from each of the following four fashion seasons of the Paris collections, of 1998 spring/summer ("S/S"), 1998 autumn/winter ("A/W"), 1999 S/S, and 1999 A/W. I have chosen to analyze the works of top-ranked designers, as judged by fashion buyers and the fashion media.

2-2. Contents of Analysis

About four thousand photographs were placed in the computer software. They were then classified into three blocks, described below, noting the designer, fashion year, and season depicted in each photograph. A reference software is made to classify each basic color, dominant color, assort color, and accent color. On items with many colors, classification is made according to the rate of color area of the four types of colors stated above. The 3 blocks are as follows:

Outer tops: jackets, coats, and cardigans to wear over other clothes.
Inner tops: blouses, sweaters, one-pieces to wear directly on underwear to cover the upper half of the body.
Bottoms: pants, skirts to cover the lower half of the body.

The photographs to be used for the classification might have different lights and backgrounds, as used by a particular designer. Moreover there might be shadows of clothes caused by the movements of the models. So, the clothing depicted in the pictures are classified through human sight without color temperature adjustment. The number of colors to be classified is 15 in total: 11 fundamental colors (white, black, red, green, yellow, blue, brown, purple, pink, orange, gray) by B. Berlin and P. Kay, and indigo, beige, olive, the regularly-used colors in Japan and metal-color used for fasteners and buttons. I also had 75 students studying colors at Mejiro Design College classify 199 colors from PCCS (color system developed in Japan specifically used for educational purpose) Harmonic Color Card as background research. However, the results of this background research are not included in this paper's discussion.

3. Result

Table 1 shows the number of appearances of basic color, dominant color, assort color, and accent color in each year, seasons and the items of clothing contained in the software described above.

Tabie 1

1998 S/S	Outer tops				Inner tops				Bottoms			
	basic	dominant	assort	accent	basic	dominant	assort	accent	basic	dominant	assort	accent
Red	10	6	4	5	50	15	7	10	25	8	4	7
Orange	14	5	5	3	28	12	17	11	22	8	0	7
Yellow	12	4	4	3	24	20	10	9	19	10	6	3
Green	8	6	3	2	8	18	2	8	6	6	2	4
Blue	32	4	3	2	53	20	7	16	53	19	7	13
Purple	12	6	1	3	34	11	2	3	12	13	13	4
Pink	23	1	2	6	42	9	13	5	31	3	7	1
Brown	34	12	4	9	59	14	6	18	57	14	3	8
Beige	28	11	3	3	69	27	8	8	42	13	2	3
Indigo	5	1	1	0	24	6	0	3	12	2	0	1
Olive	2	0	1	0	5	0	0	0	4	0	0	0
White	65	26	4	21	201	43	18	37	110	20	12	19
Grey	67	10	4	11	118	42	5	10	92	23	7	7
Brack	119	6	3	12	282	29	9	29	211	60	4	8
Metal	4	3	0	19	17	2	1	24	7	2	0	8
Total	435	101	42	99	1004	268	105	191	703	201	67	93

1998 A/W	Outer tops				Inner tops				Bottoms			
	basic	dominant	assort	accent	basic	dominant	assort	accent	basic	dominant	assort	accent
Red	38	12	5	10	56	14	5	20	31	8	1	3
Orange	10	11	2	3	11	5	1	2	8	3	2	4
Yellow	13	10	10	8	21	9	5	7	10	4	3	2
Green	0	3	2	4	1	0	3	4	1	1	2	2
Blue	31	11	7	13	43	21	11	12	37	9	7	5
Purple	15	2	5	4	14	14	1	1	12	1	1	3
Pink	22	7	5	2	25	12	7	7	16	11	4	1
Brown	56	14	16	12	47	12	10	8	46	7	3	0
Beige	43	6	1	4	27	7	9	4	27	7	2	4
Indigo	22	2	0	3	25	2	2	2	24	3	0	0
Olive	1	1	0	0	2	0	0	0	0	1	0	0
White	68	38	10	18	137	44	19	37	62	25	7	18
Grey	271	55	8	22	286	61	16	17	337	44	7	8
Brack	195	31	17	65	298	40	17	35	231	23	6	8
Metal	17	11	0	74	17	27	4	43	21	10	3	14
Total	802	214	88	242	1010	268	110	199	863	157	48	72

1999 S/S	Outer tops				Inner tops				Bottoms			
	basic	dominant	assort	accent	basic	dominant	assort	accent	basic	dominant	assort	accent
Red	11	1	2	13	24	5	12	21	16	3	3	13
Orange	6	0	0	1	4	1	4	20	12	12	0	1
Yellow	7	0	8	1	1	0	10	6	7	3	6	4
Green	0	1	2	0	0	1	3	6	3	1	0	3
Blue	46	4	5	8	8	12	12	11	66	5	3	5
Purple	6	0	0	3	25	1	6	3	7	0	4	1
Pink	4	1	3	6	21	3	8	8	12	0	4	3
Brown	16	3	5	4	20	5	6	6	19	5	3	2
Beige	29	1	2	1	50	1	1	1	52	0	2	1
Indigo	14	1	1	0	17	3	3	0	12	0	1	0
Olive	4	0	0	0	1	0	0	0	6	0	0	0
White	120	3	14	14	314	13	6	36	207	6	9	6
Grey	53	1	3	1	78	7	7	4	70	4	20	6
Brack	112	6	3	19	172	26	8	23	169	9	4	5
Metal	0	0	2	17	2	0	3	11	3	0	1	4
Total	428	22	50	88	737	78	89	156	661	48	60	54

1999 A/W	Outer tops				Inner tops				Bottoms			
	basic	dominant	assort	accent	basic	dominant	assort	accent	basic	dominant	assort	accent
Red	36	11	5	15	56	21	6	25	32	7	3	18
Orange	5	4	0	2	20	7	3	6	8	3	2	7
Yellow	14	4	7	3	26	8	7	13	16	6	10	7
Green	3	1	1	0	5	5	3	5	6	2	1	2
Blue	16	10	2	18	32	20	8	13	29	14	9	13
Purple	11	3	1	1	16	3	3	7	14	5	3	1
Pink	12	6	2	7	21	10	7	10	20	8	5	10
Brown	89	23	4	9	71	15	2	7	80	3	7	6
Beige	13	9	8	8	40	7	10	21	34	5	4	12
Indigo	13	0	0	1	13	1	0	1	20	0	0	0
Olive	2	0	0	1	2	1	1	0	0	0	1	0
White	93	21	5	28	212	21	4	47	164	13	3	33
Grey	120	14	3	23	122	61	5	15	141	8	1	7
Brack	186	18	9	33	344	29	5	49	293	23	4	23
Metal	8	0	0	28	12	9	2	15	10	4	1	3
Total	623	124	47	177	992	218	66	234	867	101	54	142

The stably popular colors, meaning "regularly-used colors," according to the data from JAFCA and the colors predicted to be popular and actually popular in the season researched, are as follows:

Regularly-used colors: stably popular colors at any time. In Japan, those colors are white, black, indigo, brown including beige, and gray.

Predicted and actually popular colors in certain seasons:

1998 S/S: pink and purple in pastel tones, and black
1998 A/W: gray, and, in early spring, off-white is somewhat popular
1999 S/S: white, trend of returning colors starts
1999 A/W: brown, beige, and khaki

3-1. Appearance rate of colors of the four color types

The appearance rate of colors of the four color types (basic color, dominant color, assort color, and accent color) was calculated as the rate against the total number of appearances on each color type, after adding the total number of each color according to basic color, dominant color, assort color, and accent color in the 3 blocks of clothing item classification. It is shown on Table 2.

Table 2

1998 S/S	basic	dominant	assort	accent	total
Red	3.97	5.09	7.01	5.99	4.59
Orange	2.99	4.39	10.28	5.72	4.01
Yellow	2.57	5.96	9.95	4.09	3.77
Green	1.03	5.26	3.27	3.81	2.22
Blue	6.44	7.54	7.94	6.81	6.77
Purple	2.24	5.26	7.48	2.72	3.16
Pink	4.48	2.28	10.28	3.27	4.34
Brown	7	7.02	6.07	6.81	6.92
Beige	6.49	8.95	6.07	3.81	6.59
Indigo	1.91	1.58	0.47	1.09	1.67
Olive	0.51	0	0.47	0	0.36
White	17.55	15.61	15.89	20.98	17.49
Grey	12.93	13.16	7.48	7.63	12.03
Brack	28.57	16.67	7.48	13.35	23.44
Metal	1.31	1.23	0.47	13.9	2.64

1999 S/S	basic	dominant	assort	accent	total
Red	3.32	5.96	8.54	15.77	5.02
Orange	1.43	8.61	2.01	7.38	2.47
Yellow	0.98	1.99	12.06	3.69	2.14
Green	0.2	1.99	2.51	3.02	0.81
Blue	7.8	13.91	10.05	8.05	7.48
Purple	2.47	0.66	5.03	2.35	2.27
Pink	2.41	2.65	7.54	5.7	2.95
Brown	3.58	8.61	7.04	4.03	3.8
Beige	8.52	1.32	2.51	1.01	5.7
Indigo	2.8	2.65	2.51	0	2.1
Olive	0.72	0	0	0	0.44
White	41.68	14.57	14.57	18.79	30.26
Grey	13.07	7.95	15.08	3.69	10.28
Brack	29.45	27.15	7.54	15.77	22.49
Metal	0.2	1.99	3.02	10.74	1.78

1998 A/W	basic	dominant	assort	accent	total
Red	4.67	5.32	4.47	6.46	4.99
Orange	1.08	2.97	2.03	1.37	1.47
Yellow	1.64	3.6	7.32	3.33	2.51
Green	0.07	0.63	2.85	1.96	0.57
Blue	4.15	6.42	10.16	6.07	5.08
Purple	1.53	2.66	2.85	1.57	1.79
Pink	2.36	4.69	4.07	1.96	2.92
Brown	5.57	5.16	11.79	3.91	5.67
Beige	3.63	3.13	4.88	2.35	3.46
Indigo	2.65	1.1	0.81	0.98	2.09
Olive	0.11	0.31	0	0	0.12
White	9.98	16.74	14.63	14.29	11.86
Grey	33.42	25.04	12.6	9.2	27.81
Brack	27.07	14.71	16.26	21.15	23.73
Metal	2.06	7.51	2.85	25.64	5.92

1999 A/W	basic	dominant	assort	accent	total
Red	5	8.8	8.64	10.49	6.46
Orange	1.33	3.16	3.09	2.71	1.84
Yellow	2.26	4.06	14.81	4.16	3.32
Green	0.56	1.81	3.09	1.27	0.93
Blue	3.1	9.93	11.73	7.96	5.05
Purple	1.65	2.48	4.32	1.63	1.87
Pink	2.14	5.42	8.64	4.88	3.24
Brown	9.67	9.26	5.56	3.98	8.57
Beige	3.51	4.74	13.58	7.41	4.7
Indigo	1.85	0.23	0	0.36	1.35
Olive	0.16	0.23	0.62	0.18	0.19
White	18.9	12.42	7.41	19.53	17.69
Grey	15.43	18.74	5.56	8.14	14.29
Brack	33.24	15.8	11.11	18.99	27.97
Metal	1.21	2.93	1.85	8.32	2.53

3-2. Appearance rate of the same color of each type

The appearance rate of the same color of each type was calculated as the rate against the total number of appearances on each color, after adding the total number of each color, basic color, dominant color, assort color, and accent color in the 3 blocks of the clothing item classification. It is shown in Table 3.

Tabte 3

1998 S/S	basic	dominant	assort	accent
Red	56.29	19.21	9.93	14.57
Orange	48.48	18.94	16.67	15.91
Yellow	44.35	27.42	16.13	12.1
Green	30.14	41.1	9.59	19.18
Blue	61.19	19.28	7.62	11.21
Purple	46.15	28.85	15.38	9.62
Pink	67.13	9.09	15.38	8.39
Brown	65.79	17.54	5.7	10.96
Beige	64.06	23.5	5.99	6.45
Indigo	74.55	16.36	1.82	7.27
Olive	91.67	0	8.33	0
White	65.28	15.45	5.9	13.37
Grey	69.95	18.94	4.04	7.07
Brack	79.27	12.31	2.07	6.35
Metal	32.18	8.05	1.15	58.62

1999 S/S	basic	dominant	assort	accent
Red	41.13	7.26	13.71	37.9
Orange	36.07	21.13	6.56	36.07
Yellow	28.3	5.66	45.28	20.75
Green	15	15	25	45
Blue	64.86	11.35	10.81	12.97
Purple	67.86	1.79	17.86	12.5
Pink	50.68	5.48	20.55	23.29
Brown	58.51	13.83	14.89	12.77
Beige	92.91	1.42	3.55	2.13
Indigo	82.69	7.69	9.62	0
Olive	100	0	0	0
White	85.7	2.94	3.88	7.49
Grey	79.13	4.72	11.81	4.33
Brack	81.47	7.37	2.7	8.45
Metal	6.82	6.82	13.64	72.73

1998 A/W	basic	dominant	assort	accent
Red	61.58	16.75	5.42	16.26
Orange	48.33	31.67	8.33	11.67
Yellow	43.14	22.55	17.65	16.67
Green	8.69	17.39	30.43	43.78
Blue	53.62	19.81	12.08	14.49
Purple	56.16	23.29	9.59	10.96
Pink	52.94	25.21	13.45	8.4
Brown	64.5	14.28	12.55	8.66
Beige	68.79	14.18	8.51	8.51
Indigo	83.53	8.24	1.18	5.88
Olive	60	40	0	0
White	55.28	22.15	7.45	15.11
Grey	78.99	14.13	2.74	4.15
Brack	74.95	9.73	4.14	11.18
Metal	22.82	19.92	2.9	54.35

1999 A/W	basic	dominant	assort	accent
Red	52.77	16.6	5.96	24.68
Orange	49.25	20.9	7.46	22.39
Yellow	46.28	14.88	19.83	19.01
Green	41.18	23.53	14.71	20.59
Blue	41.85	23.91	10.33	23.91
Purple	60.29	16.18	10.29	13.24
Pink	44.91	20.34	11.86	22.88
Brown	76.92	13.14	2.88	7.51
Beige	50.88	12.28	12.87	23.98
Indigo	93.88	2.04	0	4.08
Olive	57.14	14.29	14.29	14.29
White	72.83	8.54	1.86	16.77
Grey	73.65	15.96	1.73	8.65
Brack	81.1	6.88	1.77	10.31
Metal	32.61	14.13	3.26	50

4.Examination

4-1. Appearance rate of colors of the four color types

Comparing Table 2 with "regularly-used color" and "trendy color" of each season, not much change is to be seen in the appearance rate of each type. However, the following result was acquired as the appearance rate of color itself, regardless of the type.

1) Among "regularly-used colors," achromatic color, **brown** including beige, boasts more than a 10% of appearance rate in all seasons.
2) In each season, the appearance rate of the color called "trendy color" is more or less 1.5 times more than the average year in the case of chromatic color, and more than twice in the case of achromatic color.

The result above shows that "regularly-used colors" in clothes are popular. In fact, a review of the tables reveals that certain colors have a frequency in appearance of higher than 10%. Interestingly, the color of indigo appeared in less than 10% of the photographs of the Paris collection discussed herein. Indigo, however, enjoys much greater popularity among Japanese consumers of clothing. Colors can be deemed "trendy" when there is a marked increase in the use of the color over the previous year. In the case of chromatic colors, a rate of appearance of over 1.5 times than that of the previous years qualifies for being considered "trendy." Achromatic colors, as "regularly-used color" needs double the rate of appearance or, at the very least, more than the usual rate in order to be considered "trendy." In the 1998 S/S collection, the color black enjoyed an appearance rate of nearly double that of achromatic colors.

4-2. Appearance rate of the same color of each type

Comparing Table 3 with "trendy colors" in each of the four fashion seasons under discussion, white and chromatic colors -- except beige -- show remarkable increase in large areas of basic color and dominant color. Gray and black, used in 70% of basic color, however, do not show any change in the appearance rate of each type of color (basic color, etc.).The result above shows that "trendy color" in clothes, with a few exceptions, can be predicted according to the change of the appearance rate of a collection's colors.

5. Conclusion

The analysis of fashion photographs shows that "regularly-used color" in clothes has more than a 10% appearance rate in every season and provides a stable popularity. This research also shows that colors will stand out when the appearance rate reaches 1.5 times in the case of chromatic color and twice in the case of achromatic color in comparatively large rates of appearance every fashion season. The reference software made for this research has provided for the classification of total silhouette, length of the clothes, and textile on each item of clothing, and the colors used. Therefore, some future examination and research on the relation between silhouette and color, image of color with silhouette, and between textile and color will be done.

The relation between stone color and streetscape color on various blocks in a city
-A case study at Ghent in Flanders, Belgium-

Shoji IIJIMA, Professor , Dr.(Eng.)
Okayama Shoka University

Takuzo INAGAKI, Professor , Dr.(Eng.)
Daido Institute of Technology

Keywords : Stone color , Townscape color , Color investigation

ABSTRACT

It is said that colors of streetscape are affected by building materials. Especially, in cities where stone materials are predominant, streetscape colors are expected to be determined by the nature of stones. In Ghent, it is known that houses made of stones and bricks have been well-ordered since the Middle Ages at Graslei, which is well-known for the Guild Houses. On the whole, the color of the streetscape may be harmonious with slight varieties.

In this study, stones of each building on 3 blocks (Graslei .Korenlei, Krannlei and Veldstaat) and symbolic buildings in Ghent (Fig.1) are classified and their colors are measured by Munsell color chart .

As a result, 2 types of stones which are slate (5PB5/4), medium-coarse sandstone (2.5Y8/2) are identified. It is also found that the composition of stones of buildings is explanatory of the old streetscape color. Furthermore, the significant similarities between old streetscape colors (Graslei, Krannlei) and modern streetscape colors (Veldstaat) are observed. Therefore, this study shows the systematic view of streetscape colors at the city, where stones are widely used.

1. INTRODUCTION

There have been a number of publication on streetscape colors. However, few have referred to stones that constitute streetscape colors. But, year by year the importance of colors of streetscape are recognized for color planning. So, it is important to focus on stone colors in order to understand urban color environments.

It is said that the color of the city is in connection with the types of stones which make up the urban fabric of the city. Especially, at cities where stone materials are predominant, streetscape colors are expected to be determined by the nature of stones. Particular stone types may appear frequently throughout the old European cities. So, street colors are affected by building materials.

In Ghent, houses made of stones and bricks have been well-ordered since the Middle Ages on Graslei, which is well-known for the Guild Houses. In this city the colors of the streetscape are harmonious with slight varieties.

In this study, stones of each building on 3 blocks (Graslei, Kraannlei and Veldstaat) and symbolic

Fig. 1 Location of investigation blocks in Ghent

Table 1 Color of symbolic buildings in Ghent

Name of building	stone type	stone name	color
Belfort	A Type	Slate	5PB5/4-5PB8/1
Lankenhalle	B type	Sand stone	5Y9/1-5Y8/3
St.baafskathedraal	B type	Sand stone	5Y9/1-5Y3/1

Table 2 Color of Graslei and Korenlei

Site	Building No.	Base color	Material	Acccent color	Material
(south)	No.1	2.5YR4/8	Brick	2.5YR/4/1	Sand stone(B) **
	No.2	N9.5	Painting	2.5Y9/4	Painting
	No.3	2.5YR4/6	Brick	5B6/2	Slate (A)*
	No.4	10YR9/2	Brick		
	No.5	N9	Painting		
	No.6	N9.5	Painting		
Korenlei	No.7	5Y9/1	Painting	N9.5	Painting
	No.8	2.5Y8/2	Sand stone(B)		
	No.9	10R5/8	Brick		
	No.10	10R4/8	Brick	2.5Y6/4	Sand stone(B)
	No.11	10R8/4	Painting	2.5R9/1	Painting
	No.12	10R5/8	Brick		
(north)	No.13	2.5R9/1	Painting		
(north)	No.14	5YR4/4	Brick		
	No.15	10R4/3	Brick		
	No.16	10R4/3	Brick		
	No.17	10R5/8	Brick		
Graslei	No.18	10YR8/3	Sand stone(B)	7.5PB5/1	Slate (A)
	No.19	2.5Y9/2	Sand stone(B)		
	No.20	5PB5/1	Slate (A)		
	No.21	10R5/12	Brick	2.5Y9/2	Sand stone(B)
	No.22	10R5/12	Brick	10YR8/2	Sand stone(B)
	No.23	7.5YR7/6	Sand stone(B)		
(south)	No.24	5Y9/1	Sand stone(B)		

* : A type (likeness in color to Belfort)

** : Btype (likeness in color to St.baafskathedraal)

Table 3 Color of Kraannlei

Building No.	Base color	Material
No.1(south)	7.5B9/2	Painting
No.2	2.5YR6/12	Painting
No.3	10R5/10	Brick
No.4	10R6/10	Brick
No.5	5YR4/1	Sand stone(B)*
No.6	5Y8/2	Sand stone(B)
No.7	10R5/10	Brick
No.8	N9.5	Painting
No.9	10R4/10	Brick
No.10	7.5R7/8	Painting
No.11	10R5/8	Brick
No.12	7.5YR7/10	Painting
No.13	7.5R8/6	Painting
No.14	2.5Y9/4	Painting
No.15	10YR7/8	Painting
No.16	2.5G5/4	Painting
No.17	10R6/10	Painting
No.18	2.5Y9/1	Painting
No.19	2.5Y9/2	Painting
No.20	N9.5	Painting
No.21	N9.5	Painting
No.22	N9	Painting
No.23	2.5Y7/4	Sand stone(B)
No.24	2.5Y3/2	Brick(coated)
No.25	2.5B9/1	Painting
No.26	2.5Y8/2	Sand stone(B)
No27 (north)	10R5/10	Brick

* : Btype (likeness in color to St.baafskathedraal)

buildings in Ghent , Flanders, Belgium are classified and their colors are measured by Munsell color chart .

The aim of this study is to extract attributes of colors in Ghent , to show the systematic view of streetscape colors in the city where stones are widely used, and to present the basic data for color planning .

2. INVESTIGATION

Color investigations were carried out on 3 blocks (Graslei, Krannlei and Veldstaat) and symbolic buildings in Ghent (Fig.1).

In each block , wall colors are measured according to the Munsell book of color based on JIS Z 8721. The measured data consists of Munsell hue, Munsell value and Munsell chroma. Hue refers to the quality of a color that distinguishes red, blue, green and etcetera. Value is the lightness of a color. Chroma is the purity or intensity of a color. In order to measure base color of wall in practice, those wall colors observed in the largest area were regarded as representative.

3. RESULTS

3.1 Color of symbolic building

Table 1 shows the wall color attributes of symbolic buildings. Belfort consists of slate (A type) and it looks bluish grey (5PB5/4-5PB8/1). Lankenhalle is made of sand stones (B type), and appears yellow grey (5Y9/1-5Y8/3). St.baafskathedraal consists of sand stones (B type) and looks dark grey and yellow grey (5Y9/1-5Y31). As to St.baafskathedraal , there are dark grey part (5Y3/1, 20%) on it due to weathering and coating.

They, people there can command the symbolic buildings , therefor it seems that the stone materials used in the symbolic buildings are familiar to them. And, it is arguable that stone colors of symbolic buildings may be regarded as symbolic color in Ghent.

3.2 Color of Graslei and Korenlei

Table 2 shows attributes of colors at Graslei and Korenlei. As to base color, bricks and sandstones (B) are predominant, so R, YR and Y hues are predominant. As to accent color , YR ,Y(Sand stone(B)) and B , PB (Slate(A)) are remarkable.

3.3 Color of Kraannlei

Table 3 shows attributes of colors at Kraannlei . About base color , painting is predominant. However, R, YR and Y hues are predominant like Graslei and Korenlei. Moreover, bricks and sandstones (B) are perceived somehow remarkably.

3.4 Color of Veldstaat

On Veldstaat, most of buildings are commercial facilities .

Table 4 shows color attributes on Veldstaat. On the upper floor, painting is predominant. However , YR and R hues are predominant.

4 . DISCUSSION

Table 5 shows the utilization of stones of each block. On Graslei and Korenlei, sandstones (B) and bricks without painting are noticed. On Kraannlei , sandstones (B) , bricks and painted wall are widely observed. On Veldstaat, painting is predominant. It is also pointed out that the different utilization of stones and various presence of painting among blocks are identified .

However, table 6 shows the similarity of colors among blocks irrespective of different utilization of

Table 4 Color of Veldstaat

Site	Building No.	Ground floor		Upper floor	
		Base color	Material	Base color	Material
(north)	No.1	10R4/10	Brick	10R4/10	Brick
	No.2	5Y9/2	Painting	5Y7/1	Painting
	No.3	2.5Y8/1	Coarse sand stone	2.5Y8/4	Sand stone(B)*
	No.4	N9	Coarse sand stone	7.5Y7/6	Fine red sand stone
	No.5	5Y9/2	Painting	N9.5	Painting
	No.6	2.5R4/10	Painting	2.5R4/10	Painting
East saide	No.7	N9	Painting	2.5Y9/1	Painting
	No.8	2.5Y9/1	Painting	2.5Y9/1	Painting
	No.9	5Y9/2	Painting	7.5YR5/12	Brick
	No.10	N9.5	Painting	7.5YR9/2	Painting
	No.11	7.5G8/1	Greenish fine sand stone	5Y8/2	Painting
	No.12	10YR9/3	Painting	10YR9/3	Painting
(south)	No.13	2.5Y9/2	Painting	2.5Y9/2	Painting
(north)	No.14	N2	Crystalline lime stone	2.5Y9/2	New ceramic material
	No.15	N7	Painting	2.5Y9/2	New ceramic material
	No.16	N9	Painting	2.5YR9/1	Painting
	No.17	N9	Painting	2.5Y9/2	Painting
	No.18	2.5PB3/1	Crystalline lime stone	2.5Y5/2	Painting
	No.19	2.5PB2/1	Crystalline lime stone	2.5Y9/2	Painting
West side	No.20	2.5Y9/3	Painting	2.5Y9/3	Painting
	No.21	2.5Y9/3	Painting	2.5Y9/3	Painting
	No.22	2.5Y8/3	Painting	2.5Y9/1	Painting
	No.23	7.5Y9/1	Painting	7.5Y9/1	Painting
	No.24	5Y9/2	Painting	5Y9/1	Painting
	No.25	5Y9/1	Painting	5Y9/2	Painting
	No.26	10Y9/2	Painting	10Y9/2	Painting
	No.27	5Y9/1	Painting	5Y9/1	Painting
	No.28	5PB3/6	Painting	5PB3/6	Painting
(south)	No.29	10YR9/1	Crystalline lime stone	7.5R9/2	Painting

* : Btype (likeness in color to St.baafskathedraal)

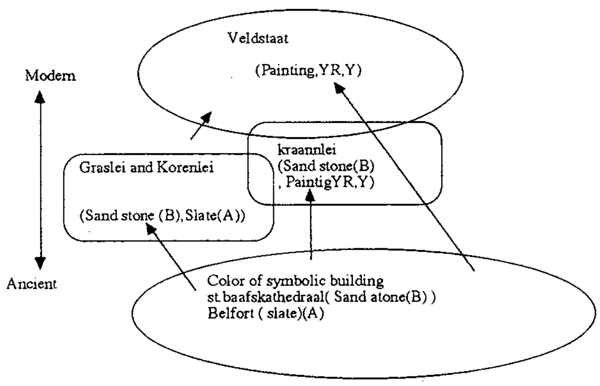

Fig.2 Color system of in Ghent

Table 5 Stone Attributes of each block

block	No.of building	Rate of Sand stone (B)	Rate of slate (A)	Rate of Brick*	Rate of with painting
Graslei and Korenlei	24	21%	5%	50%	25%
Krannlei	27	15%	0%	26%	60%
Veldstaat (upper floor)	29	3%	0%	7%	79%

* : Rate of brick without painting

Table 6 Base color Attributes of each block

block	No.of building	Rate of R,YR Y hue	Rate of except for R,YR,Y	Rate of achromatic
Graslei and Korenlei	24	83%	4%	13%
Krannlei	27	74%	11%	15%
Veldstaat (upper floor)	29	93%	4%	3.50%

stones and various presence of painting. It is suggested that they, people there utilize a limited range of painting color (R,YR ,Y hue) , and that, as the result , the color of the streetscape may be harmonious with slight varieties on the whole (Fig.2).

And, it may be arguable that social consciousness and cultural tradition about color environment may influence actual colors in the streetscape in Ghent. Therefor, painting color should be investigate from the standpoints of the environmental psychology and community system.

From now on, utilization of stone and painting will be concretely considered in connection with regional color attributes.

5. CONCLUSION

(1) Color attributes in Ghent are identified through investigation about the utilization of stones on symbolic buildings and 3 blocks (Graslei, Krannlei and Veldstaat)

(2) They people there utilize limited painting color (R,YR ,Y hue) , and in Ghent, on the whole, the color of the streetscape is harmonious with slight varieties.

REFERENCES

1) Masao INUI : "Kenchiku-no shikisai-sekkei (color Design of Buildings) ", Kajima Institute publishing Co.ltd., Tokyo, 1976, (in Japanese).

2) Shoji IIJIMA, "A comparative study on the relation between the color traits in a city landscape and its mesoclimate with reference to several cities from the Pacific area to the Sea of Japan area in south-west Japan", Proceedings of Pan Pacific Symposium on Building and Urban Environmental Conditioning in Asia, pp.243-251, 1995

3) Shoji IIJIMA, "The Local color traits in connection with snowy climate in the Tohoku area", Summary Papers of Third International Conference on Snow Engineering, pp. 255-256, 1996

4) Inui,M.;"The role of colour in urban environment." GOODSCENE 05, Published by TOKYO ELECTRIC POWER CO ., INC,1991 , pp.6-15, (in Japanese).

5) Iijima,Shoji,1994. "A Structural Approach to Urban Landscape" , Journal of Okayama Shoka University Vol.30 No.1 pp.121-141. (In Japanese)

6)Iijima, Shoji,1995a. "Study on Relationship between Local Color Attributes of Streetscape and Climatic Elements" ,Papers on City Planning, No.30, PP. 271-276.

7)Imui,Masao,1982. "Cross-Cultural Differences in Perception of the Visual Environment " Proceedings 7th Session of the International Association for People-Environment Studies.

8) Shoji IIJIMA," Comparative Study on inter-city Attributes of Facility Color around Several Districts in local Cities", Research of Regional Facility No.15, 1997(A)

9) Shoji IIJIMA, " CROSS-CULTURAL COLOR DIFFERENCES OF COMMERCIAL FACILITY BETWEEN GREAT BRITAIN AND JAPAN", Proceeding of AIC,1997(B)

Color Composition Features of Magazine Advertisements

Kiwamu MAKI

Assoc. Prof.

Dept. of Human Environmental Sciences

Faculty of Human Life Sciences

Jissen Women's University

1. INTRODUCTION

Advertisements are appealing messages designed by advertisers to persuade consumers into making various purchases. This study analyzes the color composition of commodity colors and background colors used in actual advertisement inserts in currently published magazines. Subsequently the roles that color plays in advertising expression is discussed, especially from the viewpoint of color harmony.

2. METHOD

More than 500 advertisement inserts were collected from magazines published in Japan and the U.S.; this included nine fashion magazines, five informational magazines, and three cooking magazines. The advertisement samples were classified according to category type as shown in Table 1.

Three attributes of color (Munsell hue, value and, chroma) were measured using a colorimeter with a focus on

Table 1. The advertisements used in analysis

	Category	contents	Japan	U.S.	total
A	Cosmetics	Skin care, foundation, lipstick, perfume	78	14	92
B	Pharmaceuticals and Bath Products	Medicine or pills, cleansers, medicines for external application, eye lotion, shampoo, bath goods	62	16	78
C	Fashion Brands	Fashion wear, sports wear/sports shoes, underwear, shoes, bags	49	26	75
D	Accessories	Accessories, wristwatches	28	8	36
E	Food	Noodles, pasta, seasoning, candy, desserts, water, alcohol	63	13	76
F	Electric Appliances	Cellular phones, computers, cameras, TVs, vacuum cleaners	34	13	47
G	Automobiles	Automobiles	24	7	31
H	Credit Cards	Credit cards	6	2	8
I	Amusement and Entertainment	Travel, books and publications, horse racing	54	2	56
J	Livingware and Goods	Kitchen ware/goods, pet goods	11	2	13
K	Tobacco	Cigarettes	7	10	17
L	Corporate Advertisements		21	6	27
			437	119	556

Figure1. Samples which are used to analize the color composition

two sections of the advertisements; commodity area and background area. In cases where the commodity or background area consisted of two or more colors, multiple sections were measured (the color of the section the widest area was referred to as Color 1, and the second widest as Color 2, and so on). If a color wasn't uniform over an entire area, for example, in the case of a photo or gradation, two or three points which were determined to represent the area by three measurers were measured.

3. RESULTS

3-1. ANALYSIS OF INTERRELATIONS AMONG BACKGROUND COLORS

The frequency of occurrence of hue in Background Color 1 compared to Background Color 2 is shown in Table 2. Table 2 indicates that the most frequent pattern is a combination of chromatic color and achromatic color, which accounts for almost 50% of the whole (163/304). Almost all of the Munsell values for the background achromatic colors were 8.5 or 9.0 (201/211). Thus, this result is interpreted to mean that the most frequent background color combination is white and chromatic colors. Moreover, this tendency becomes even clearer when we take into account that a Munsell value of 9.0 was recorded for the 38 chromatic colors in Background Color 1.

The second most frequent pattern is shown as a line from the upper left to the lower right (surrounded by a broken line) in Table 2, which indicates a similar hue color combination. This pattern accounts for close to one third of the total (87/304). Such kind of pattern is frequently seen in the areas of Cosmetics, Accessories, Food, Electric Appliances and Automobiles when data listed by category type is analyzed.

Finally, we looked at the usage rate difference among hue colors. White is used most frequently, and Y to PB colors are used second most frequently, followed by R to YR colors. P to RP colors are rarely used. In particular, BG to PB hue colors are used frequently for advertisements involving clothes, pharmaceuticals, and amusement/entertainment.

Table 2. Hue analysis of background colors.

		Background Color 2 (Hue)											sub		
		R	YR	Y	GY	G	BG	B	PB	P	RP	N	total	blank	total
Background Color 1 (Hue)	R	3	1	2		1						6	13	8	21
	YR	1			1			2	1			5	10	3	13
	Y		2	4	1	2	4		1			8	22	14	36
	GY	2	1	1	1	4	1		1			10	21	15	36
	G	1	1	1	5	4	5	2	1	1		11	32	19	51
	BG		2	1	1	4	5	7	3	1	1	13	38	22	60
	B			3	1		4	10	3	1		7	29	19	48
	PB	1		2		3	5	7	9	2		20	49	17	66
	P									1	1		2	2	4
	RP			1	1			1			2	1	6	1	7
	N	4	5	10	5	6	10	15	15		4	8	82	129	211
	blank													3	3
total		12	12	25	16	24	34	44	34	6	8	89	304	252	556

3-2. ANALYSIS OF INTERRELATIONS AMONG BACKGROUND COLORS AND COMMODITY COLORS

Table 3 shows the frequency of occurrence of hue in Commodity Color 1 compared to Commodity Background Color 1. Commodity background color, e.g. the color next to the commodity photo, is often similar to Background Color 1, but is not necessarily always the same.

The number of the commodity color in each hue doesn't show much difference, except for P and RP colors where it is less, and achromatic color (white) where it is larger than the others. Meanwhile, commodity background color differs according to usage. White represents a third of the total (169/464), and BG to PB colors account for another third (146/464).

However, no interrelation was found among commodity color and commodity background color. The line from the upper left to the lower right is not clear in Table 3, and there are one or more samples in almost all of the cells from R to PB.

Although commodity color deviation is observed when the data of each commodity category type is analyzed (for example, white is frequently used as a commodity background color for Cosmetics, the commodity color used for Pharmaceuticals is typically white, and Fashion Brands use various colors), the interrelation among commodity color and its background color is not clear. The fact that white is often used as a background color for Pharmaceuticals is only one example of a clear relation.

Table 3. Hue analysis of commodity color and background color of it

		Commodity Background Color 1 (Hue)												
		R	YR	Y	GY	G	BG	B	PB	P	RP	N	blank	total
Commodity Color 1 (Hue)	R	4	2	3	3	1	6	6	6		1	17		49
	YR	1	2	1	3	5	2	1	2			14		31
	Y	1	4	4	7	2	3	4	5	1		12		43
	GY		2	4	3	2	3	2				9		25
	G	3	2	1	2	5	3	1	5			10		32
	BG		1	9		4	11	2	3			14		44
	B	2	2	2		2	4	5	8			20	1	46
	PB	1	2	2	4	1	2	6	6	2		18		44
	P					1	1		1			1		4
	RP		1	2	1	2		1	1	2	2	4		16
	N	2	8	5	9	9	19	13	14	1	1	49	1	131
	blank											1	90	91
total		14	26	33	32	34	54	41	51	6	4	169	92	556

4. DISCUSSION

Rating experiments of various color-simulated scenes such as streetscapes, interiors and table coordination which the author and colleagues have conducted before show a prevailing similarity, especially in terms of the hue-related similarities regarding color harmony. In the analysis described above, such kind of color composition was observed for similar hue background colors. However, this varies widely for commodity color and background color matching, not only for the described hue analysis but also for analysis of value and chroma which was not mentioned.

Analysis of value and chroma reveals that there are no samples where the R to GY commodity background colors have a value less than five when the commodity color has a chroma of more than seven.

When the value of commodity color is higher than seven and the chroma is less than four, there are few samples where the chroma of commodity background color is less than four and the value is between three to six .

Considering these results and the fact that white and bluish colors are used frequently, background color is determined to clearly attract attention and to create a strong impression, and color matching among commodity and background colors should not be important for advertisers and designers.

5. CONCLUSION

1. The most frequently used background color is white, which is the base color used in magazines.

2. The combination of white and chromatic colors is the most frequent pattern of background color matching.

3. Chromatic color combination, the second most frequent pattern, shows many cases where similar hue colors are used. Such kind of pattern is frequent in the areas of Cosmetics, Accessories, Food, Electric Appliances and Automobiles.

4. There is a small interrelation among commodity color and background color.

ACKNOWLEDGEMENT

The author wishes to extend tremendous appreciation for the support provided by Kaori Takenouchi, Emi Uehara and Keiko Takahashi who conducted color measurement for the samples.

REFERENCES

1) K. Maki, S. Iijima : An Examination of the Validity of Judd's Four Principles of Color Harmony in Streetscape Evaluation, Proceedings of the 8th Congress of the International Colour Association (Kyoto), pp.687-690, 1997.

2) Kiwamu Maki : Impression Comparison Among Four Color-simulated Scenes, Journal of the Color Science Association of Japan, volume26, No.4, pp.224-235, 2002 (in Japanese).

An AIC International Color Research Survey for Divers Disciplines

Christina M. Burton, MFA, ASID, IESNA, ISCC, IDEC

Interior Architecture, University of Wisconsin-Stevens Point, U.S.A.

INTRODUCTION AND REVIEW OF THE LITERATURE

The world is impacted by the use of color in products in our homes, work, and play spaces. Many decisions are made everyday about the selection of these colors by divers disciplines, such as interior designers, architects, artists, educators, chemists, psychologists, and others. What information and research is available to professionals that make color decisions? A review of the literature reveals that the information about color relates to color trends and forecasting, anecdotal information, and color studies that may or may not be based on scientific research. "Color can play a role in healing…most of the research data on color is out-of-date" (Marberry 1995).

Some documentation about color research needs was established in the U.S.A. in 1983. A successful method for a lighting research agenda continued the use of roundtables with Illumination Roundtable III. Professionals from a variety of disciplines met to identify user needs during the decade and establish a basic and applied research agenda for lighting. Valuable guidance from this agenda set research goals for subsequent decades of research. These research goals included several color and light issues across disciplines (EPRI 1984). Though roundtables offer an excellent format for this type of collaboration, expense would prohibit the use of this method on a large scale for international color collaboration.

At the Seventh AIC Congress, in Budapest, Hungary the results of a color survey were presented "A Challenge for a Potential Global Color Research Agenda in 2000". In this survey the respondents stated that the existing color research was not applicable (30.6%), not appropriate (16.7%), and not available (13.9%) (Burton 1993). The need for documentation of international color research needs for divers disciplines became apparent.

OBJECTIVES AND METHODOLOGY

A variety of methodologies to document international color research needs were considered. After a thorough investigation of these methods, the most practical and appropriate choice was an international web survey for data collection. The advantages of a web-based survey outweigh the disadvantages. Advantages include low administrative costs and the fact that it is self-administered. The web-based survey is a time efficient method for data collection, analysis and reporting, and provides for ease of delivery and follow-up. The response rates are better than other methods. The researcher controls the question order and response. The disadvantages are few and include access to WWW, out-of-date email addresses, privacy issues, control of the respondent, and security and data integrity.

A 'Blue Ribbon Panel' of selected professionals involved with color contributed to the refinement of the survey instrument. Objectives of the survey document data related to how professionals use color, the time involved making color decisions, where they obtain color information/research, problems and strengths of the information/research, areas of color that need research, and possible funding sources for future research.

The sample for the survey is taken from the membership lists of the Association Internationale de la Couleur (AIC, International Colour Association). The AIC is the main color organization comprised of various national color bodies with the objectives of encouraging all aspects of color research, of disseminating the knowledge gained from research, and of promoting its application to solutions of problems in the field of science, art, design and industry on an international basis. This sample crosses cultural and geographic boundaries and represents divers populations. The web site for the AIC is www.AIC-Color.org or www.AIC-Colour.org.

The Member Nations of the AIC include the following countries:

> Argentina, Australia, Austria, People's Republic of Bulgaria, People's Republic of China, France, Great Britain, Hungary, India, Italy, Japan, Republic of Korea, Netherlands, Norway, Poland, Republic of Singapore, Slovenia, Republic of South Africa, Spain, Sweden, Switzerland, and the United States of America.

The Observer Nations of the AIC include:

> Canada, Denmark, Greece, Republic of Ireland, Republic of Panama, and the Slovak Republic.

Initial contact with the representative of each country was made by letter, email, or fax requesting updated email membership lists. If a country did not have a color organization, then that contact person was encouraged to email the survey to other color professionals to represent the needs of their country. If privacy concerns existed, then the same procedure was implemented. Each contact person was asked to document the number of emails sent out for statistical purposes. A follow-up email was sent to all thanking them for their participation in the survey and requesting a response if none had been sent.

SELECTED AREAS OF COLOR RESEARCH STUDY

Finding a cohesive way to survey and study the broad range of issues related to color research presented an interesting challenge. In an overview of how these areas could best be categorized, one source provided the best general grouping. The source was from Professor Antal Nemcsics, President of the Hungarian National Colour Committee for AIC's COLOUR 93 mailer/circular and stated six (6) topic areas: 1) fundamentals, 2) colorimetry, 3) color systems, 4) human factors, 5) application, and 6) education.

After consultation with the 'Blue Ribbon' panel, there were some changes and reordering of the areas with subsequent refinement. The finalized areas of color research are divided into in six (6) categories and survey participants prioritize their needs for research ranking high priority to low priority.

1) Human factors: color preference, color association, biological effects of color, color psychology, theories of color harmony, color and function, and color and illumination.

2) Applications: industrial applications, color reproductions, color formations, high definition TV and monitor, color identity of prints, color design in interiors, graphics, product design, architecture, and landscaping, color in fine arts, and computerized color design.

3) Communications: signaling, signing, stimulation, color order systems, color collections, and printed electronic color.

4) Education: teaching color at ages 0-12, ages 13-18, and high school levels, university and post graduate training and color teaching aids.

5) Color perception: color vision, color appearance, color adaptation, color contrast, color constancy,
color memory.

6) Color measurement: colorimetry, color standardization, color difference, metamerism, fluorescence, instrumentation, and color systems.

CONCLUSION

Professionals make many decisions about the colors for products that are used in spaces and colors that impact homes, work, and play spaces. In *Color Consulting: A Survey of International Color Design,* Harold Linton states that within the setting of rapidly expanding communication and planning technologies in design and art, the twenty-first century holds a growing promise for great diversity of interdisciplinary involvement among many fields of color experience.

The documentation of the first international color research survey provides valuable information about color decisions and establishes future research needs across the divers professions. The results document the similarities and differences between the professions and different countries. The international color research study has implications for global, national, and local populations for research and education.

SELECTED REFERENCES

Beamon, K. (2001). Rainbow Effect. *Hospitality Design.* August, p. 40-43.

Burton, C. (1993). A Challenge for a Potential Global Research Agenda in 2000. *The 7th Congress of the AIC, Colour '93,* p. 115-116.

Electric Power Research Institute (1984). *Illumination Roundtable III – Lighting Research and Education for the Eighties.* EM-3627. Research Project 2285-5.

Fehrman, K. and Fehrman, C. (2000). *Color: The Secret Influence.* New Jersey: Prentice Hall.

Feisner, E.A. (2001). *Color Studies.* New York: Fairchild Publications Inc.

Inter-Society Color Council Newsletters. New York, New York.

Kilmer, R. and Kilmer, W.O. (1992). *Designing Interiors.* Australia: Thomson Learning Inc.

Linton, H. (1991). *Color Consulting: A Survey of International Color Design.* New York: Van Nostrand Reinhold.

Long, R. (2001). Healing by Design. *Health Facilities Management.* November, p. 20-22.

Malkin, J. (2001). A Tour of the Healing Environment. *Healthcare/Design.* November, p. 12-19. Marberry, S. and Zagon, L. (1995) *The Power of Color: Creating Healthy Interior Spaces.* New York: John Wiley & Sons Inc.

An Analysis of Color Features of Japanese Traditional Robes "Kimono" in Edo-era

KOBAYASI Mituo,*,** YAMAGUCHI Takeshi,* and OGAWA Yoshimi*
*The University of Electro-Communications
**National Museum of Japanese History

Keywords : "kimono', color combination, digital camera, neural network

1. INTRODUCTION

"Kimono" is a Japanese traditional robe with a wide sleeves and a sash. Kimono especially in Edo-era (1603 -1835) is valuable as a work of art.

National Museum of Japanese History preserves a famous collection of kimono in Edo-era called "Nomura Collection[1]", which consists of more than 200 pieces of kimono worn by the noble women. The collected kimono are created by the excellent techniques of the period, weaving, dyeing and embroidery. Each kimono consists of textiles decorated with artistic design and refined colors(Figure 1).

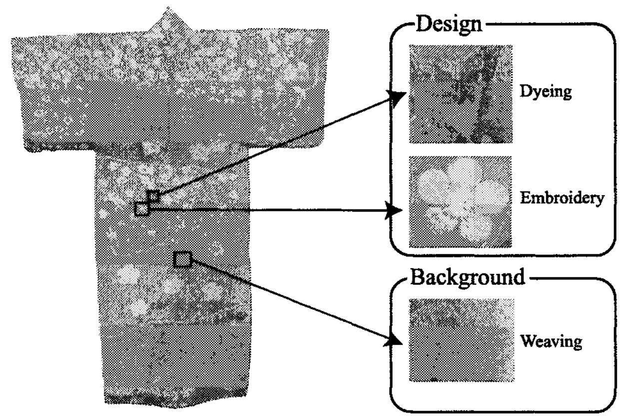

Figure 1. composition of a kimono

Since these kimono are made of silk and colored by natural dyes and preserved for more than 300 years, cloths are getting to be damaged and colors are fading. Digital archiving will be one of the methods for preserving the data of historical materials like kimono.

We have made a project to measure the colors of kimono in the Nomura Collection in an attempt to propose methods for preserving digital color values of kimono and for analyzing the color features of kimono.

Some pieces of kimono in the collection are measured by three methods:

1) perceptual observation using Munsell color chart,
2) physical measurement by a colorimeter, and
3) estimation of color values from an image obtained by a digital camera.

Problems or issues for color measurement of kimono based on our experience as well as analysis of color features of kimono based on the data obtained by the methods 1) and 2) have been reported.[2]

Methods 1) and 2) are rather time-consuming and have a possibility of staining cloths, while method 3) does not have such shortcomings besides having the advantage of obtaining color information of many points at once. However, in the present time , we can not find an easy procedure to obtain machine independent color values from an output image of a merchandized digital camera.

In this paper a simple estimating method of color values from digital camera images is proposed, and then the obtained data are compared with the data obtained by the method 2) to clarify color features of kimono in NCS color space.

This study is one of the experiments to search appropriate methods for recording color infomation of historical materials and to utilize the recorded data for cultural studies.

* The University of Electro-Communications, 1-5-1 Chofugaoka, Chofu-shi, Tokyo 182-8585, JAPAN.
** National Museum of Japanese History, 117 Jonai-cho, Sakura-shi, Chiba 285-8502, JAPAN.

2. EXPERIMENT OF COLOR MEASUREMENT

2.1. Practice of color measurement

Some kimono materials were carried into a special room for inspection of historical garments. We put a piece of kimono on a special large hanger. The illumination was the mixture of a natural light from the north-side window, fluorescent lights from the ceiling of the room, and a pair of xenon-lamps approximating the D65 illuminant.

Several points of target on a kimono were measured using a colorimeter "Minolta CM-2600d" in order to compare with the method 3). Figure 2 is a scene of measurement using a colorimeter. When we place a colorimeter on a cloth we must put a small board behind the cloth to fix the position of measurement. Here a matte black board was used because the reflection from the board must be prevented.

As for the estimation of color values from an image, a commonly used digital camera "Olympus C3040ZOOM" was used. When we take a picture, a few parameters for the white-balance and for the exposure are fixed.

2.2. Estimation of color values from the output of a digital camera

As the output RGB values generated by a digital camera are machine-dependent, transformation from the RGB values to universal color values (e.g. XYZ tristimulus values) is necessary(Figure3). Our procedure of estimating a color value is described below:

i) Take a picture of a kimono and a gray scale of which the spectral reflectance is known. The gray scale is used as a reference.

ii) Get a RGB value of the reference and a RGB value of the target from a digital camera image.

iii) Transform a RGB value to a tristimulus value as a light color.

iv) Calculate a tristimulus value as an object color from the light color of the reference and the light color of the target.

If a tristimulus value under a given illuminant is required, Von Kries transformation will be applied.

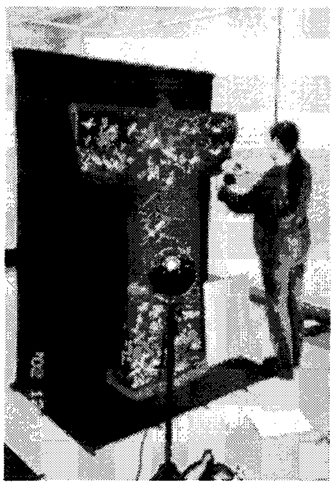

Figure 2. scene of color measurement using a colorimeter

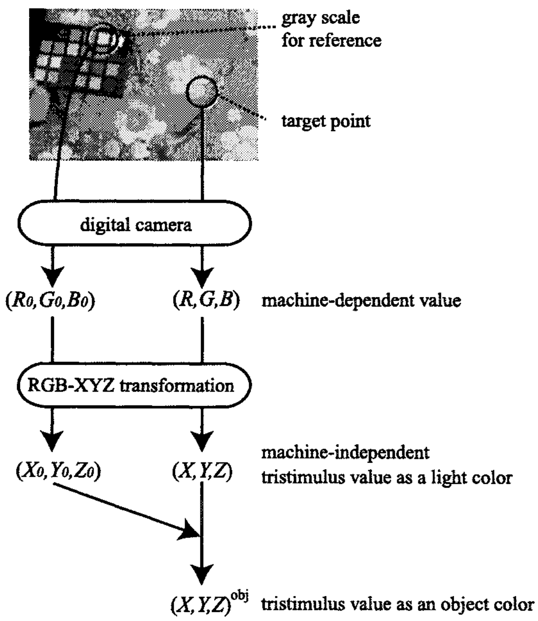

Figure 3. estimation of a color value from the outoput of a digital camera

2.3. RGB-XYZ transformation by neural net

In our recent study, the transformation was realized by a piecewise cubic polynomial.[3] However, this transformation was rather complex. In this study a single artificial neural network was adopted for the RGB-XYZ transformation. A neural network is suitable for such a nonlinear transformation, if we have no intrinsic mathematical model for the transformation. Our transformation is constructed by a feed-forward neural network, which has one input layer with 3 neurons, one output layer with 3 neurons, and two hidden layers with 6 neurons (Figure 4). Training of neural network was performed by the method of back-propagation. Ninety six RGB-XYZ pairs were used for training.

As for the accuracy of the constructed network, the average of differences ΔX,ΔY, and ΔZ between the actual value and the estimated value were 0.5~0.7 for the given training data. These numbers are converted roughly to 4.7 in terms of ΔE^* in CIELAB. It turns out that the neural network is applicable to the estimation of color values.

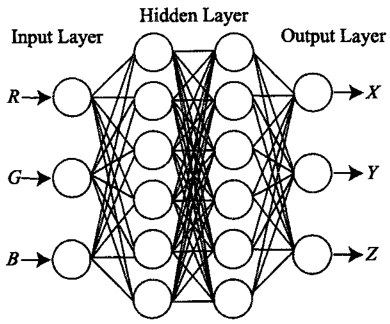

Figure 4. structure of neural network

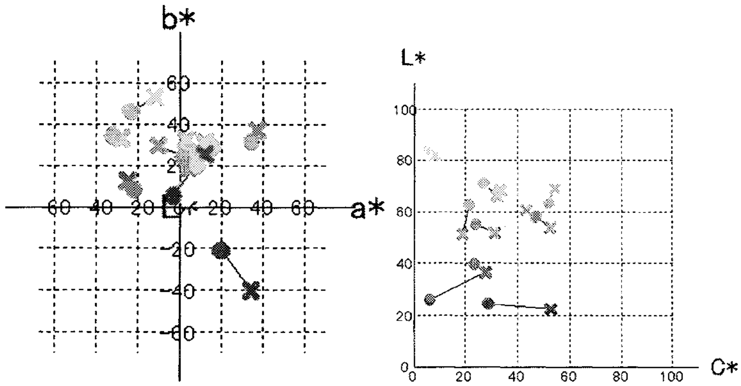

(b)a^*b^* graph

(b)L^*C^* graph

Figure 5. color difference of color pairs measured by the method 3(●) and by the method 2(×)

2.4. Comparison between digital camera and colorimeter

Eleven points representing major colors of a kimono were measured by the methods 2) and 3). Color differences of eleven pairs of the color values were calculated and plotted in CIELAB color space (Figure 5).

Figure 5 tells that most pairs except two pairs resemble each other. Two pairs with low lightness have large color differences especially in chroma ($\Delta C^* > 20$) in either case. The average of the color differeces ΔE^*, ΔL^*, ΔC^*, ΔH^* are 11.0, 4.2, 7.4, and 5.7, respectively.

These differences, probably dependent on the accuracy of RGB-XYZ transformation, are a little larger than the existing result.[2] It is expected that these differences will be diminished by increasing the number of training data and revision of the structure of the network.

3. ANALYSIS OF COLOR FEATURES

In this section, color features of kimono are analyzed in NCS color space based on the color values obtained by method 2) and by method 3). In the following,

(DC) indicates the data obtained by a digital camera,
which consists of 142 color values for 17 pieces of kimono, and
(CM) indicates the data obtained by a colorimeter,
which consists of 108 color values for 16 pieces of kimono.

3.1. Color distribution

In this paper a point in the NCS color triangle is named "tone" instead of "nuance". Figure 6 shows color distributions of (DC) and (CM) in the color circle and in the color triangle.

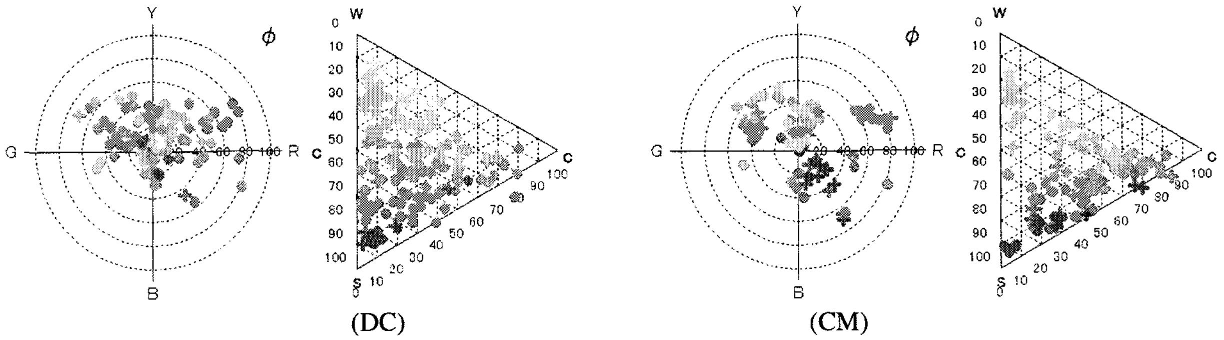

Figure 6. color distribution of all colors of kimono in NCS

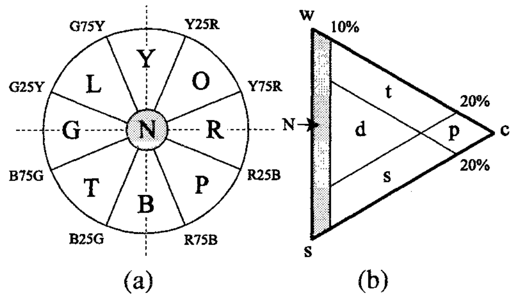

Figure 7. division of color circle and color triangle

Table 1. classfication into chromatic and achromatic colors

	(DC)	(CM)	total
chromatic color	104 (73%)	87 (81%)	191 (76%)
achromatic color	38 (27%)	21 (19%)	59 (24%)
total	142	108	250

Table 2. frequency of colors of all kimono

(hue frequency)

hue	(DC)	(CM)	total
Y	27 (26%)	21 (24%)	48 (25%)
O	23 (22%)	17 (20%)	40 (21%)
R	14 (14%)	7 (8.1%)	21 (11%)
P	3 (2.9%)	13 (15%)	16 (8.4%)
B	8 (7.7%)	7 (8.1%)	15 (7.9%)
T	1 (1.0%)	0 (0%)	1 (0.52%)
G	6 (5.8%)	7 (8.1%)	13 (6.8%)
L	22 (21%)	15 (17%)	37 (19%)
total	104	87	191

(tone frequency)

tone	(DC)	(CM)	total
p	3 (2.9%)	6 (6.9%)	9 (4.7%)
t	13 (13%)	1 (1.2%)	14 (7.4%)
s	37 (34%)	55 (63%)	92 (48%)
d	51 (49%)	25 (29%)	76 (40%)
total	104	87	191

For quantitative analysis, the color circle is divided into 9 regions as indicated in Figure 7(a), and the color triangle is divided into 5 regions as indicated in Figure 7(b). The color values of (DC) and (CM) were first classfied into two categories, chromatic and achromatic colors(Table 1). Then chromatic colors were classfied into 8×4 categories identified by a pair of hue name and tone name. Summerizing the results two tables are obtained; one is classification by hue and the other is classification by tone(Table 2).

It can be observed from Table 2 that Y(yellow), O(orange) and L(leaf) are the hues frequently used. T (turquoise) is very few. We noticed gold was used abundantly as decoration of the kimono. Gold is classified into Y. This could be the reason why the frequency of Y is high. With regard to the classification of tone, frequencies of s (shade) and d (dull) are high. It is said that people in Edo-era preferred(or obliged to use) warm colors with shade and dull tones.

3.2. Color feature of each kimono

Colors and color combinations used in each kimono are analyzed according to the classification indicated in Figure 7. In this analysis the achromatic colors are excluded because white is used in all kimono and black including Fe has been faded. The result of the analysis for (DC) and (CM) is shown in Table 3. "ref#" is a reference number in the catalogue[1] , "pattern of hue" indicates a set of major hues, or a combination of hues used in a kimono, and "pattern of tone" indicates the major tones, or a combination of tones used in a kimono. (ref# 273 and 278 are included in both (DC) and (CM). The total number of kimono, therefore, is 31 pieces.) It can be observed that Y(yellow) is used for most of the kimono (87% = 27 pieces / 31 pieces) and O(orange) or L(leaf) is used for many kimono (81% = 25 pieces / 31 pieces). YOL is the pattern of hue most frequently used (52% = 16 pieces / 31 pieces). In terms of tone, all the colors include either s (shade) or d (dull). The pattern "sd" , a combination of s(shade) and d(dull), is used in 27 pieces (87%) of kimono.

To summarize, the color features of the 31 pieces of kimono obtained by the results of section 3.1 and 3.2 show that Y(yellow), O(orange) and L(leaf) are the main hues used, and the tones of the colors are mostly s(shade) or d(dull).

Table 3. combination pattern of each kimono

(DC)

ref#	pattern of hue	pattern of tone
19	YOL	sd
28	YL	sd
42	YORL	tsd
44	L	s
88	YOR	tsd
89	YOBG	tsd
99	YRPBL	sd
110	YL	s
132	YOL	tsd
136	OBL	tsd
167	RB	sd
168	YB	d
206	YRL	sd
244	YOBGL	sd
247	YORTL	tsd
273	YOPGL	psd
278	YRPG	ptsd

(CM)

ref#	pattern of hue	pattern of tone
039	YOGL	sd
047	YRBG	psd
092	YOPBL	sd
126	YR	ps
134	YORBGL	psd
152	YORBL	sd
158	YOBGL	sd
161	OB	sd
180	YOPL	psd
214	YP	sd
224	YOPL	sd
242	YOPL	sd
243	YOPL	sd
273	YOPGL	tsd
274	YORPGL	psd
278	YRPG	psd

4. CONCLUSION

Colors of some kimono in Edo-period were measured by a digital camera and by a colorimeter. A simple estimating method of color values from the output of a digital camera using a neural network was proposed. Obtained data were analyzed in NCS color space, which revealed some color features of the kimono.

Automatic extraction of colors from a digital camera image and improvement in accuracy of RGB-XYZ transformation are some of the future problems.

ACKNOWLEDGEMENT

Many thanks to Mr.SAWADA Kazuto (National Museum of Japanese History) and Ms.TAKAHASHI Minori (The University of Electro-Communications) for helpful advices in advancing the study, and to Mr.SUZUKI Takuzi (National Musium of Japanese History) for cooperative works on experiment.

REFERENCES

1. National museum of Japanese history:Edo a la Mode - Aesthetic Lineages Seen in Kosode Kimono Motifs -, NHK Promotions, (in Japanese) 1999.
2. KOBAYASI Mituo, OGAWA Yoshimi: An Analysis of Color Features of "Kimono" in Edo-era, Color Forum Japan 2002 Proceedings, pp.47-50, (in Japanese)2002.
3. SUZUKI Takuzi, KOBAYASHI Mituo: Accrate Recording of Color Information of Museum Materials by Digital Still Cameras –In Case of "Ukiyo-e" and "Kimono"–, Proceedings of AIC Color 2001 SI, Color & Textiles, pp.212-218, Maribor, Slovenia, 2002.

Making Exterior Color line of Residential Area through Sensibility Evaluation Method

Jin - Sook Lee , Mi – Jin Lee

1. INTRODUCTION

Residential area is the most basic apace which consists of a city and is most intimate with the human living. In city scenery, since the scenery of residential area influences a lot on determining the image or characteristics, the exterior color of residential area is so important component that makes the image of entire city scenery. With the lack of perception on exterior color of residents and developers, however, the planning of exterior color is carried out without a systematic plan method or a special guide. And, it can be a main factor which deteriorates whole quality of city scenery. Therefore, the set-up of a guide that can arrange exterior color of those residential area is required badly.

This paper is to analyse color characteristics according to the image of exterior color of residential area, to make properly quantitative evaluation structure, and to suggest the colors match regarding image for the plan of exterior color of residential area.

The contents of this paper are as follows: 1) in terms of how residents evaluate exterior color of residential area with what kind of view point via Repertory Grid Developmental method, we extracted evaluation structure model which arranged systematically reaction on environment of residents exterior color, and selected the vocabulary of image to use in evaluation experiment. 2) we produced the evaluation object and conducted the experiment by computer simulation, and then analysed and extracted color characteristics according to the image of exterior color of residential area. 3) we suggested the colors match of exterior color of residential area based on the extracted color characteristics.

2. COLOR EVALUATION STRUCTURE EXTRCTION & COLOR IMAGE SELECTION

2.1 Experiment outline of color evaluation structure extraction

In order to extract evaluation structure of exterior color of residential area, the research method was Repertory Grid Developmental method or the way of an interview-investigation of with inductive questions. This way consists of making element, extraction of evaluation items, and laddering. The element was made by street scenery of residential area using computer simulation. Picture 1 shows the example of element. Testees consisted of 20 university students and graduate students who major in architecture as an expert group acknowledged that they have the ability of perception and judgement on color. Table 1 shows the composition of the testees

Figure 1. The example of element

Table 1. Testees

Sex	Female : 9, Male: 11
Position	Graduate Students : 14 Senior Students : 6
Age	23 ~ 30
Total	20

2.2 Analysis

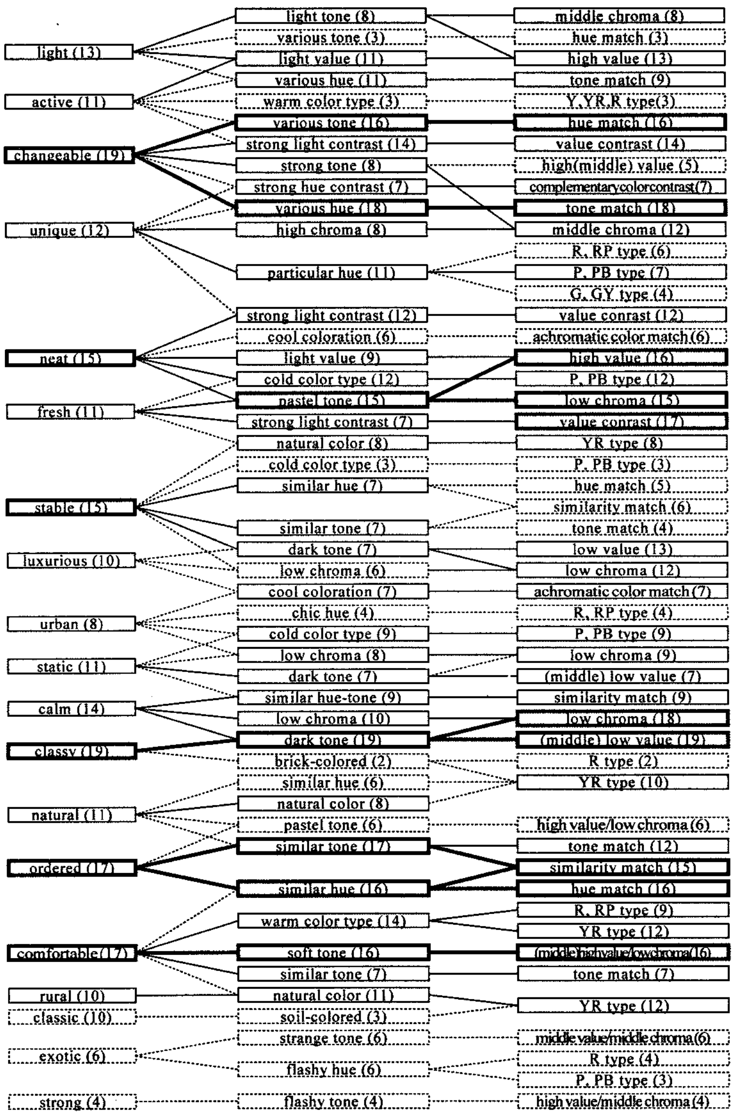

: less than 6 14 : an 15

Figure 2. Color evaluation structure model

After analysing all the evaluation items which the testees expressed, although some expressions seemed odd a bit, we worked on putting those expression into similar contents. Through this process, all the 162 evaluation items were integrated into 75 items. For the integrated evaluation items, we collected the number of testees about a causal sequence on the step of laddering, and than made a degree network map that indicates a causal sequence of evaluation items. Figure shows the relation with a network map after selecting more than degree 3 in this network. In a network map, the item on the left side is the lowest evaluation by ladder-up, and the item on the right side is the lowest evaluation by ladder-down. Also, the whole layout is done by a hand with the basic idea to make the line cross that indicates a causal sequence small as much as possible. As the result of those analysises, total 19 adjects as evaluation items were selected out, and they can be divided into 5 parts. 「light」 and 「active」 color are influenced a lot by YR,Y and R type of high value/middle chroma. 「stable」, 「luxurious」, and 「classy」 color are influenced by PR and R type of middle·low value/low chroma Also, 「neat」, 「fresh」 and 「citied」 color are influenced by P and PC type as a cold color of high value/low chroma, 「static」 and 「calm」 color by a cold color of middle·low value/low chroma, and 「natural」, 「comfortable」 and 「rural」 color by YR type of high value/low chroma.

2.3 Color image selection

Color image selected things of more than degree 7 at the network map of figure 2. As a result of that, the selected color image is as same as Table 2.

Table 2. Evaluation Vocabulary

light, active, changeable, unique, neat, fresh, stable, luxurious, urban, static, calm, classy, natural, ordered, comfortable, rural

3. EVALUATION EXPERIMENT FOR COLOR CHARACTERISTIC ANALYSIS

ACCORDING TO IMAGE

3.1 Outline of evaluation experiment

3.1.1 Evaluation variable & evaluation object

Evaluation variable is classified with a match type, and each match type is a hue, value, and chroma. On this paper, the match type was divided into similarity match, hue match, tone match, and achromatic color match.

Evaluation object was produced via computer simulation based on the coloration match of neighborhood buildings. Evaluation object produced total 171 items after selecting them variously in order to measure color effect more clearly and not to lean down to a certain thing according to a hue, value and chroma. The example of evaluation object is indicated in figure 3.

3.1.2 Experiment method & testees

The experiment was kept up an entering side intensity of illumination as same as when color was produced according to color prototype sensitive to light, and conducted at Muchang Lab. The evaluation object used 16 color images(Table 2) extracted from evaluation structure. Psychological reactions of testees were measured with the method of 7 value steps. 25 graduate students who major in architecture as an expert group acknowledged that they have the ability of perception and judgement on architecture color and also has the number of evaluation items on environment a lot for safe evaluation were picked out as testees. The structure is as same as Table 3.

Figure 3. The example of experimental object

Table 3. Testees

Sex	Female : 13, Male: 12
Position	Graduate Students : 18 Senior Students : 7
Age	23 ~ 30
Total	25

3.2 Experiment result & analysis

3.2.1 Analysis method

Data was dealt with SPSS/PC+or Statistics package, 16 color images were dealt with score 1~7 after dividing them according to vocabulary. Also, Multiple regression analysis was carried out, based on the color image, in order to analyse quantitatively visual effect by experiment factors and color characteristics according to evaluation factors.

3.2.2 Color characteristic according to image

We analysed color characteristics according to evaluation factors like Table 4 as each match type after conducting Multiple regression analysis based on 16 images in order to analyse quantitatively a visual effect by experiment factors selected above 2.3.

For example, according to each category quantity, 「natural」 and 「comfortable」 image were indicated on high value/low chroma of YR and R type in similarity match, on low chroma of PB, YR, and RP type in color match, and on high value/low chroma of the contrast match with combination of PB-YR-B-BG and GY-PB-Y-YR in tone match. In an achromatic match, the combination of a cold color and an achromatic color of middle value or the combination of only an achromatic colors was indicated as the most comfortable and the most natural colors.

Harmony	Categories		Sample	light	active	Change-able	unique	neat	fresh	stable	luxurious	urban	static	calm	classy	natural	ordered	Comfort-able	rural
Simil a-rity	Hue	R	10	0.305	0.502	0.159	-0.057	0.375	0.360	0.305	0.402	0.157	-0.049	0.150	0.236	0.416	0.239	0.487	0.313
		YR	12	0.253	0.366	0.279	-0.120	0.244	0.390	0.219	0.391	0.198	0.073	0.191	0.212	0.452	0.154	0.376	0.506
		Y	8	0.103	0.191	-0.006	0.022	0.010	0.109	0.098	0.130	0.109	-0.007	0.088	0.166	0.116	0.073	0.188	0.344
		GY	12	0.176	-0.005	0.006	0.238	-0.135	0.029	-0.429	-0.479	-0.391	-0.437	-0.596	-0.478	-0.352	-0.318	-0.354	-0.083
		G	5	0.295	0.201	0.074	-0.139	0.115	0.303	-0.106	-0.136	0.057	-0.076	-0.185	-0.423	-0.034	0.012	-0.188	0.042
		BG	6	-0.017	-0.192	0.109	0.105	-0.268	-0.318	-0.322	-0.469	-0.498	-0.193	-0.336	-0.281	-0.395	-0.335	-0.330	-0.193
		B	12	-0.377	-0.422	-0.284	-0.059	-0.285	-0.388	-0.192	-0.359	-0.115	-0.117	-0.023	-0.055	-0.335	-0.111	-0.294	-0.389
		PB	12	-0.480	-0.465	-0.228	-0.225	-0.022	-0.258	0.318	0.195	0.425	0.443	0.580	0.369	0.072	0.209	0.063	-0.233
		P	5	0.100	-0.032	0.187	0.295	0.124	-0.068	0.003	0.260	0.273	-0.035	0.039	-0.079	0.016	-0.028	-0.086	-0.246
		RP	4	-0.152	0.014	-0.196	0.241	-0.260	-0.254	-0.096	0.039	-0.191	-0.023	-0.221	-0.018	-0.168	-0.019	-0.128	-0.328
	Value	High	31	1.190	0.984	0.335	0.061	0.942	1.155	0.008	0.008	0.540	-0.514	-0.188	-0.598	0.364	0.217	0.277	0.108
		Middle	32	-0.409	-0.341	-0.018	-0.037	-0.378	-0.438	0.120	0.120	-0.164	0.237	0.180	0.262	-0.033	-0.052	0.044	0.078
		Low	23	-1.035	-0.852	-0.427	-0.030	-0.744	-0.948	-0.177	-0.177	-0.500	0.363	0.003	0.441	-0.445	-0.221	-0.433	-0.253
	Chroma	Middle	42	0.009	0.046	-0.166	0.379	-0.287	-0.188	-0.505	-0.485	-0.349	-0.300	-0.527	-0.423	-0.520	-0.302	-0.527	-0.304
		Low	44	-0.009	-0.044	0.159	-0.361	0.274	0.180	0.482	0.463	0.333	0.287	0.503	0.404	0.496	0.289	0.503	0.290
Hue	Hue	R	2	-0.410	-0.070	0.116	-0.222	-0.064	0.026	0.194	0.226	-0.124	0.164	0.170	0.134	0.150	0.030	0.126	0.352
		YR	2	0.050	0.030	0.236	0.418	0.036	-0.214	-0.026	0.126	-0.244	0.124	0.050	0.474	0.070	-0.070	0.226	0.212
		Y	2	0.130	0.070	0.156	-0.102	-0.304	-0.214	-0.306	-0.374	-0.304	-0.296	-0.430	-0.306	-0.290	-0.590	-0.194	-0.008
		GY	2	0.270	0.210	0.036	0.158	-0.224	0.046	-0.426	-0.394	-0.264	-0.276	-0.470	-0.386	-0.370	-0.350	-0.454	-0.088
		G	2	0.190	0.238	-0.144	-0.162	0.296	0.406	0.194	0.006	0.076	0.104	0.190	-0.206	0.110	0.250	0.186	0.412
		BG	2	-0.290	-0.490	-0.324	-0.222	-0.204	-0114	0.034	-0.314	-0.204	0.024	0.110	-0.266	-0.130	0.130	-0.334	-0.168
		B	2	-0.050	-0.190	-0.264	-0.062	0.016	-0.034	-0.066	-0.114	0.196	0.124	0.050	-0.246	-0.150	0.090	-0.054	-0.228
		PB	2	0.070	0.110	-0.024	-0.482	0.536	0.246	0.614	0.866	0.916	0.484	0.750	0.694	0.870	0.630	0.606	0.112
		P	2	-0.110	-0.110	0.136	0.418	-0.144	-0.314	-0.446	-0.234	-0.184	-0.276	-0.510	-0.126	-0.470	-0.310	-0.254	-0.628
		RP	2	0.150	0.210	0.076	0.258	0.056	0.166	0.234	0.206	0.136	-0.176	0.090	0.234	0.210	0.190	0.146	0.032
	Chroma	Middle	10	-0.070	-0.218	0.036	0.414	-0.460	-0.390	-0.678	-0.718	-0.536	-0.312	-0.706	-0.538	-0.730	-0.586	-0.726	-0.404
		Low	10	0.070	0.218	-0.036	-0.414	0.460	0.390	0.678	0.718	0.536	0.312	0.706	0.538	0.730	0.586	0.726	0.404
Tone	Hue	PB,YR,B,BG	6	-0.143	-0.079	0.037	-0.149	0.049	0.153	0.215	0.199	0.200	0.157	0.243	0.281	0.164	0.174	0.208	0.180
		P,Y,PB,B	6	-0.076	-0.046	0.031	-0.135	-0.071	-0.060	-0.052	0.059	-0.047	0.024	0.05	0.021	0.084	-0.046	-0.065	0.053
		GY,PB,Y,YR	6	0.033	0.078	-0.051	-0.093	0.075	0.045	0.088	0.098	0.081	0.172	0.155	0.108	0.156	0.087	0.361	0.026
		BG,RP,G,GY	5	-0.118	0.058	0.206	0.196	-0.124	-0.019	-0.102	-0.089	-0.079	-0.130	-0.063	-0.076	-0.126	-0.120	-0.173	0.003
		GY,BG	6	0.244	0.148	-0.174	0.085	0.089	0.100	0.008	-0.021	-0.007	-0.029	-0.024	-0.079	-0.003	0.054	0.002	-0.040
		B,G,PB	6	0.071	-0.172	0.051	0.131	-0.051	-0.234	-0.085	-0.174	-0.080	-0.129	-0.024	-0.139	-0.163	-0.092	-0.165	-0.094
		R,P,YR	6	-0.063	0.028	-0.103	-0.149	0.103	0.060	0.082	0.066	0.026	-0.023	0.070	-0.039	0.024	0.028	-0.012	-0.114
		YR,RP,Y	6	0.031	-0.006	0.037	0.145	-0.091	-0.047	-0.172	-0.154	-0.107	-0.063	-0.217	-0.092	-0.156	-0.106	-0.185	-0.014
	Value	High	15	1.330	1.221	0.018	-0.118	1.155	1.421	0.306	0.511	0.754	-0.204	0.113	-0.327	0.655	0.691	0.515	0.347
		Middle	16	-0.308	-0.226	0.142	0.054	-0.358	-0.451	-0.075	-0.176	-0.230	-0.012	-0.004	0.057	-0.206	-0.293	-0.159	-0.077
		Low	16	-0.938	-0.879	-0.159	0.057	-0.725	-0.881	-0.212	-0.303	-0477	0.203	-0.102	0.249	-0.408	-0.355	-0.324	-0.249
	Chroma	Middle	23	-0.010	-0.060	0.312	0.374	-0.337	-0.243	-0.487	-0.430	-0.306	-0.364	-0.523	-0.340	-0.475	-0.487	-0.491	-0.280
		Low	24	0.010	0.057	-0.299	-0.358	0.323	0.233	0.467	0.412	0.293	0.349	0.502	0.326	0.455	0.467	0.470	0.269
Achro-matic color	Hue	Warm	7	0.124	0.188	0.011	0.080	0.011	0.086	-0.073	0.004	-0.041	-0.088	-0.137	-0.095	0.016	0.046	0.015	0.036
		Neutral	3	-0.082	-0.042	0.343	-0.004	-0.193	-0.091	-0.087	-0.276	-0.162	-0.233	-0.133	-0.209	-0.193	-0.296	-0.138	0.022
		Cool	6	-0.116	-0.136	-0.267	-0.091	0.093	-0.044	0.053	0.071	0.071	0.173	0.140	0.098	0.060	0.071	0.016	-0.013
		Achromatic	2	0.035	-0.188	0.250	-0.001	-0.029	-0.030	0.227	0.187	0.172	0.139	0.259	0.351	0.056	0.068	0.109	-0.095
	Value	High	6	0.101	0.043	0.021	0.113	0.036	0.083	-0.040	-0.009	0.015	-0.001	0.024	-0.093	-0.022	0.034	-0.081	-0.060
		Middle	12	-0.051	-0.021	-0.011	-0.057	-0.018	-0.041	0.020	0.004	-0.007	0.001	-0.012	0.046	0.011	-0.017	0.040	0.030

[shaded box] : The highest value in the score of the category

Table 4. The effect table by image types

According to each category quantity, 「urban」 and 「ordered」 image were shown on high value/low chroma of PB, R, P type in similarity, on low chroma of PB in color match, and on high value/low chroma of the contrast match with the combination of PB-YR-B-BG in tone match. In an achromatic color match, only the combination of achromatic colors of high value or the combination of a cold color and a cold color and an achromatic color showed ordered and urban image so well.

4. MAKING COLORATION PALN ACCORDING TO COLOR CHARACTERISTICS OF EACH IMAGE

Through experiment result above, we made coloration palette, and coloration plan was made on the basis of street scenery with 5 buildings. As an example, 「natural」 and 「comfortable」 image and 「light」 and 「active」 image are as follows:

7.5YR 9/2	10YR 9/2	10YR 9/1	5YR 9/1	2.5YR 9/2
7.5R 9/2	10R 9/2	5R 9/2	5R 9/1	7.5R 9/2
5PB 3/1	5PB 9/2	5PB 6/1	5PB 9/1	5PB 6/2
5YR 3/1	5YR 9/2	5YR 6/1	5YR 9/1	5YR 6/2
5PB 9/1	5YR 9/1	5B 9/1	5YR 9/1	5BG 9/1
5GY 9/1	5PB 9/1	5Y 9/1	5PB 9/1	5YR 9/1
N7	5PB 9/1	N7	5B 9/2	N7.5

The coloration plan of 「natural」 and 「comfortable」 image is proper on similarity match as a warm color type of high value/low chroma, on color match as low chroma of YR and PB types, on tone match as high value/low chroma of PB-YR-B-BG type and GY-PB-Y-YR type, and an achromatic color match as the combination of a cold color type and an archromatic color of middle value.

5YR 7/4	2.5YR 8/6	5YR 7/6	7.5YR 8/4	5YR 7/4
2.5R 8/6	5R 8/4	5R 7/4	5R 7/6	5R 7/4
2.5G 7/4	5G 8/6	5G 7/6	7.5G 8/4	5G 7/4
5GY 3/1	5GY 9/2	5GY 6/1	5GY 9/1	5GY 6/2
5RP 9/2	5RP 6/1	5RP 3/1	5RP 6/2	5RP 9/1
5G 9/1	5Y 9/1	5BG 9/1	5Y 9/1	5G 9/1
N9.5	5YR 9/1	N9	5Y 9/2	N9.5

The coloration plan of 「light」 and 「active」 image is appropriate to similarity match as a warm color type of high value/middle chroma, to color match as low chroma of GY and RP type, to tone match as high value/middle chroma of G-Y-BG type, and to an achromatic color match as the combination of a warm color type of high value and an achromatic color.

5. CONCLUSION

At first, in this paper we extracted evaluation structure model of exterior color of residential area via Repertory Grid Developmental method, and from this basis selected color image. Also, we extracted color characteristics according to each image after conducting and analysing evaluation experiment through computer simulation, and then made coloration plan.

This paper focused only on color as factor. However, form is an important environmental composition factor as much as color. Therefore, color and form must be considered together, in the planning of exterior of residential estates, which will be future research agenda.

Jin - Sook Lee, Mi – Jin Lee
Dept. Architecture, College of Engineering, ChungNam National University
Kungdong220, YOUSUNGKU, TAEJON 305-764, KOREA
Phone : +82-42-821-7733
Fax : +82-42-823-9467
E-mail : js_lee@cnu.ac.kr

How to teach colour and encourage colour communication

Berit Bergström

Scandinavian Colour Institute AB

ABSTRACT

The purposes of this paper are:
- to show how colour research is related to colour education and can become an important source of stimulation
- to show how colour education is a good way of spreading (disseminating) the results of colour research
- to show the importance of colour education for professionals working in different areas where colour plays an essential part

Keywords: colour education, colour studies, colour research, colour communication

1. INTRODUCTION

Colour research, colour education and colour usage are three interacting factors in colour communication, all dependent on each other. Without the one or the other, we cannot achieve a satisfactory result. Colour education is a good way of disseminating the results of colour research so that they can be made available to the users. It is important that the knowledge, which exists, about e.g. the importance of colour for man and the environment reaches the architect so that he or she can take this into consideration in the colouring of a house. I shall show how an understanding of colour as a visual phenomenon can simplify colour communication for professional users of colour. Amongst other things, I shall show how we work in the field of colour education. Special pedagogic techniques have been developed thanks to a close cooperation with colour research.

2. COLOUR RESEARCH AND COLOUR EDUCATION STIMULATE EACH OTHER

Colour research is related to colour education and can become an important source of stimulation. In the 1940's and 1950's, in Sweden, Dr. Tryggve Johansson, with his broad knowledge of colour as a visual phenomenon, laid the foundations for a Swedish tradition of colour education. The courses were then held in collaboration with the Swedish Society of Crafts and Design and the course which was received with the greatest enthusiasm was "the Colour School", a colour workshop with an emphasis on teachers, researchers, architects, designers, technicians, artists, - all dealing in colour questions.

After Tryggve Johansson, his assistants continued the course but its direction changed more towards the practical application of the colour system within furnishing and design. At the end of the 1960's, Prof. Anders Hård took over the responsibility for the Colour School. His colour research became an important source of stimulation, and the Colour School proved in turn to be an important source of inspiration for colour research. During the years when Anders Hård led the Colour School, a pedagogic system and study material were developed which still largely survive in today's course activities. In the early 1980's, the Scandinavian Colour Institute took over responsibility for the summer course "the Colour School".

These summer workshops became a breeding ground for Swedish colour research and many methods and colour tests were developed which are still used in colour education. One study, Hård & Hård (1991), that was carried out during this time was about the way in which colour changes with distance. A number of untrained observers studied how the colour of leafy trees changed from the inherent colour of the leaf with increasing viewing distance up to a distance of 20 km.

Colour education is an important and necessary source of stimulation for colour research, to inspire students to continue studying colour theories and the effects of colours. If we had no colour education, there would be no new generation of colour researchers.

3. COLOUR EDUCATION – A GOOD WAY OF SPREADING THE RESULTS OF COLOUR RESEARCH

Colour education is a good way of spreading the results of colour research to a wide range of professionals working with colour. Teachers of colour education have a natural function in spreading research results, awakening an interest in colour research, and also receiving a feedback response relating to methods etc. Basic professional training must be regarded as one of the main gateways for the communication of the latest findings in colour research. The initial interest in colour research can be most easily developed in this way.

Colour research and environmental design
In a study carried out by Janssens (1995) about colour research and environmental design, the aims were:

- to investigate the current level of knowledge regarding the results of colour research
- to reveal the existing myths and beliefs about colour
- to document the use of colours in everyday design work.

These aspects were assessed by practising colour designers through interviewing a large number of design experts.

A questionnaire was developed where some of the questions were: Preferred source of colour research information, Attitudes towards colour research, What is known about colour research? How do the research results reach the practitioners? How is this knowledge used in the practical work?

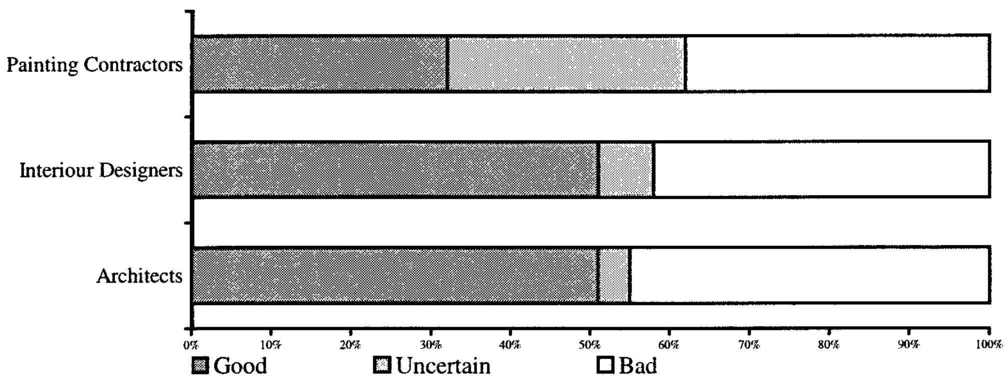

Fig. 1 The designers' knowledge of colour research Janssens, 1995 (A summary of the answers of the questionnaire)

It was established that the interviewed practitioners had a relatively limited knowledge of the results of colour research. One problem revealed by the study was the definition of the concept of colour research. Another problem was the translation of the researcher's language into reality. It is extremely important to translate the researcher's reports into a popular scientific version, which the designer can easily absorb. This will also increase the understanding of and the need for colour research, and make it easier to show the users the practical use of colour research. Here, colour education enters as an important factor in spreading the research results to facilitate colour communication among the practitioners.

4. THE IMPORTANCE OF COLOUR EDUCATION

The workshops within the Colour Institute have continued since the 1950's but their direction has moved towards the practical application of colour as a visual phenomenon within furnishing and design, and this has now led to a wide range of colour courses for professionals in the colour field. The course program covers the whole field of colour from courses in colour science, colouring, decorative painting techniques and colour materials adapted for the building industry to courses in colour measurement, colour control, colour and design, and colour in print for industry and the graphic arts sector.

The summer course has continued, and it gathers people from the whole world such as architects, designers, professors, teachers, people from painting companies and paint manufacturers, and also those who work with colour in industrial companies, administrators, and advertising agencies. They all work with colour as a visual phenomenon, but their different experiences and different cultural backgrounds give the course its special and appreciated character. The course lasts for six days, and this gives the participants the opportunity to work very intensively with colour and seems to inspire them to work even harder towards greater knowledge and a deeper understanding of colour.

The architect and the designer need to learn the results of colour research into colour meaning and how colour affects us, so that they can make the right colour choices.

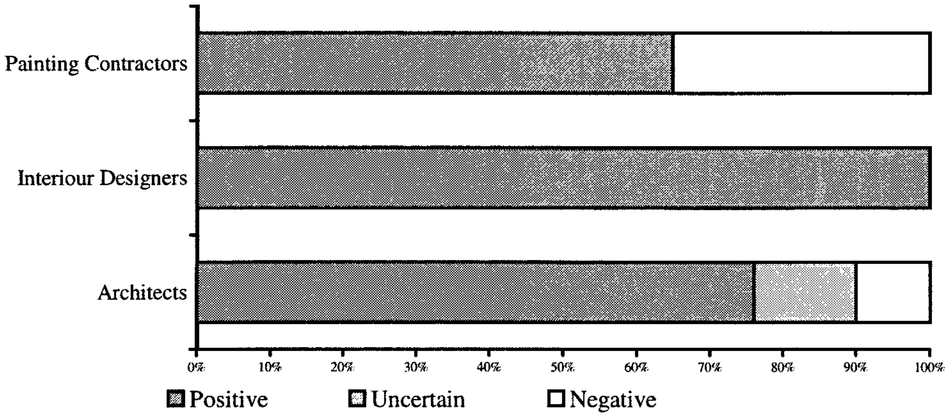

Fig. 2 The interviewed designers' attitudes towards colour research about colour appearance Janssens, 1995

Architects and designers also need methods and a colour language to decide and combine choices of colour and for identifying and analysing existing colours, for illustrating ideas and presenting colour proposals. Technicians need to learn about colour measurement and how the colour is mixed and, in order to communicate with the designer, they need a system based on the way people see colours. This will give the researcher an opportunity to see the application and use in colour design of the results of his/her work, and it makes it possible for the designer to work more consciously with colours.

Some example of practical research results
In the study by Janssens (1995), it is suggested that, in order to improve the rendering and gathering of knowledge on colour research results, handbooks should be compiled, illustrating practical research results with realistic examples. Here are some practical examples where the results of colour research have been translated into practical tools and handbooks within the fields of colouring and design. This simplifies and encourages colour communication. It also gives architects and designers the opportunity to benefit research and development for practical use in their daily work with colour.

- An anthology by Hård, Küller, Sivik, Svedmyr, Tonnquist (1995) has been written about the researchers' work and the development of the NCS system. This anthology has been presented in a popular version by Bergström (1996).

- What colour is the red house? This thesis on the perceived colour of painted facades by Fridell Anter (2000) has resulted in a book with a lot of practical examples Färgen på huset (The colour of the house) Fridell Anter, Svedmyr (2003). This is intended for architects and others choosing façade colours. If you choose a colour from a set of colour samples, you will face difficulties which previous research has not addressed. This work aims to aid such colour design by exploring different models and methods.

- Colour scales of traditional pigments for external painting Fridell Anter, Svedmyr (1996). This is a presentation of traditional pigments and the NCS colours that can be obtained with them. NCS tradition contents two colour blocks illustrating the colour areas of these traditional pigments. These are also colours that have been used in traditional European architecture.

- Nature's colour palette, Fridell Anter (1996). This is an investigation of the inherent colours of vegetation, stones and ground. These results are also presented in a practical handbook for architects Utvändig färgsättning (External Colouring) Enberg, Fridell Anter (1997).

5. HOW CAN WE PROCEED?

How can we proceed forward? Is there any forum within which we can further develop the cooperation between research, education and practical usage? How can we spread our different models for colour education out into the world?

The AIC Study Group on Colour Education
The Study Group on Colour Education within AIC (Association Internationale de la Couleur) provides opportunities for the spreading of new results within colour teaching. The Study group is an international network of scientists, teachers within the field of colour (colour theory, colour design, colour psychology etc.) and other professionals such as designers and architects with a specific interest in colour education. Its aims include the exchange of knowledge and experience among its members and the stimulation of colour teaching and research.

How can we develop the future and be a part of this Study Group on Colour Education? It can become a unique network in colour education if we can get more members from even more countries. So, I extend to all of you working with colour education a very warm welcome. Just send me an e-mail at swedish.colour.center@ncscolour.com and I will send you more information. I also hope that the activities among the AIC members will increase and that we shall be able to develop an even better network for the exchange of experience. We really have good opportunities to do that.

It should really not be at all difficult to spread knowledge about a subject that seems to involve and interest most people. Everybody seems to have an opinion about colour as soon as the subject comes up on the agenda. The question is only how to make everybody understand that colour is in the first place a visual experience. Only then can we avoid misunderstandings and only then we can teach how to describe colour in order to facilitate colour communication and make the best use of research results.

REFERENCES

Bergström, B., Att välja färg, BFR T7:96, (An outline of Swedish colour research regarding colour and colour design), Swedish Council for Building Research, Stockholm 1996.
Enberg K., Fridell Anter, K., Utvändig färgsättning (External Colouring), Swedish Council for Building Research, Stockholm 1997.
Fridell Anter, K., Nature's colour palette. Inherent colours of vegetation, stones and ground, Scandinavian Colour Institute AB, Stockholm 1966.
Fridell Anter, K. Svedmyr, Å., Colour scales of traditional pigments for external painting, Scandinavian Colour Institute AB, Stockholm 1966.
Fridell Anter, K., What colour is the red house? Perceived colour of painted facades, Royal Institute of Technology, Stockholm, 2000.
Fridell Anter, K., Svedmyr, Å., Färgen på huset (The colour on the house), Formas, Stockholm, 2003.
Hård, A., Hård, T., NCS a method for determining perceived colours of objects in environment, observed under various external conditions, AIC'91, Sydney, 1991.
Janssens, J., Färgforskning och miljögestaltning. (Colour research and environmental design), Miljöpsykologiska Monografier nr 11, Sektionen för Arkitektur, LTH, Lund 1995.

AUTHORS ADDRESS
Berit Bergström
Scandinavian Colour Institute AB
Box 49022, SE-100 28 Stockholm, SWEDEN
Phone: + 46 8 617 47 00
Fax: + 46 8 617 47 47
E-mail: berit.bergstrom@ncscolour.com

Application of Geometrical System for Harmonious Color Selection

Vojko Pogacar, Vera Golob
University of Maribor, Faculty of Mechanical Engineering, Slovenia

INTRODUCTION

Selection of harmonious color combinations is nearly always influenced by the individual's subjective taste. There is a variety of different color selection systems worldwide (5,8,13,14,16,18), according to personal, seasonal or fashional selections and many more.

Colors are in fact a kind of linguistic elements of visual language (3,7,10). Therefore, it is necessary to define it's use to more predictable logic and useful system. Legislature of color grammar is in three-dimensional system, therefore is difficult to understand and visualize the whole complexity of 3D color system.

It is somehow normal that color-cut of the color solid was usually presented as a triangle in two-dimensional space, what was easier to understand and use in the past (5,13,14). Nowdays, computers are more and more important in dealing with colors (13,14,15,22). They are a helpfull tool for color observations and now, by computers it is much easier to manipulate with colors in their 3D space. Guttenbergs invention of printing was a background for the developement of communication legislature, the grammar of spoken and written language. Therefore, computers become a proper ground for the development of visual linguistic systems, where colors are among important elements of the visual communication system (3,4,7,10).

Between terms *harmonious colors* and *harmonious colors selection* are differences, as each harmonious entity is defined as correlation among special color shades. That is in analogy with music, where specific harmony of sound is defined by various musical accords (2,4,7). The basic idea of this paper is to present the improvement of a color selecting system to the level that a nonprofessional individual, involved with colors could use our selecting tools more efficiently in order to get more appropriate and harmonious selection of color-shades.

METHODS

Most classical principles of harmonious color selections are based on triangular monochromatic color-cut (Figure 1) (6) with their catalogue system (Figure 2 and Figure 3), where we can observe the color span among one chromatic color and white and black (13,14).

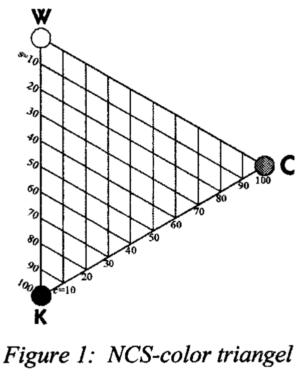

Figure 1: NCS-color triangel

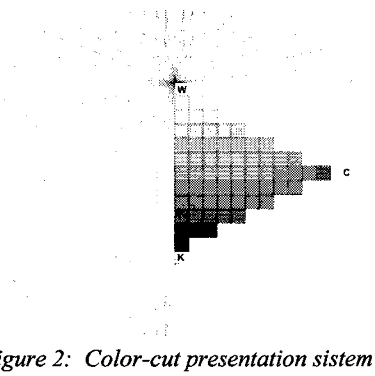

Figure 2: Color-cut presentation sistem

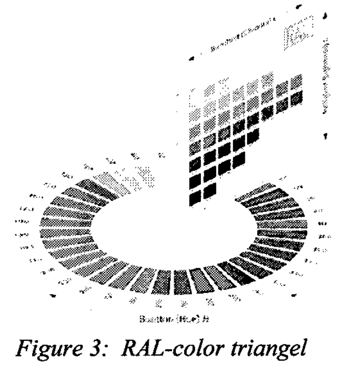

Figure 3: RAL-color triangel

Each color-tone is defined most precisely by it's most contrast complement color (1,12). The position of this complement shade of color in the color solid is reflected across the central point on the black-and-white axis (Figure 4). Contrast colors are most complementary and form an equilibrated color entity, named color harmony.

In accordance with these observations we accomplished a monochromatic color scale by it's antagonistic one (1,12). A pair of two antagonistic harmonious colors is achieved by projection through different levels of achromatic scale axis of the color solid. Such a relation is based on two-dimensional correlation.

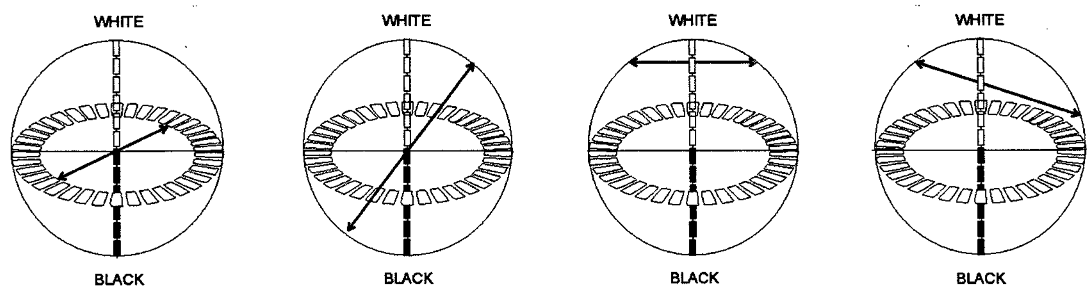

Figure 4: Basic complementary principles

Besides direct contrast-combinations of complementary shades of colors (Figure 4), we have also indirect complementary substitute-combinations (Figure 5) (1,12,15,21,20) of two, three, four, five or even more shades of color-combination entities, but such relations become more complex and most often three dimensional positioned in color space (11,22).

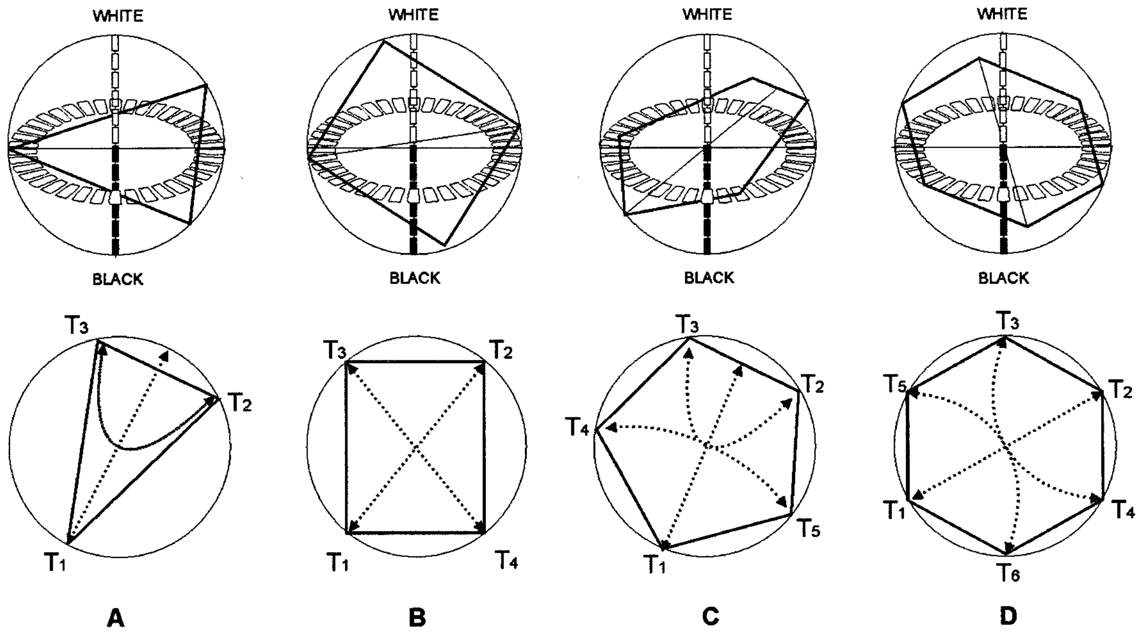

Figure 5: Complementary substitutions of two-A, three-B, four-C and five-D

Numerous substitutes (20,21), evidently decrease contrasts among color-tones, what leads to the appearence of more simultaneous effect, that invokes just the contrary tendences to the color contrast occurence. In this case a certain phenomenon occures, by which two close shades of a color push each other a bit from their places towards the closest neighbour. It means that in this relation the main significance of a certain color shade is changed a bit (22). Two color-tones gain dual visual effect. For example, when color Orange (O) is close to Orange-Yellow (OY) tone, it pushes OY towards Yellow (Y) and the same OY pushes O towards deaper Red (R) (Figure 6).

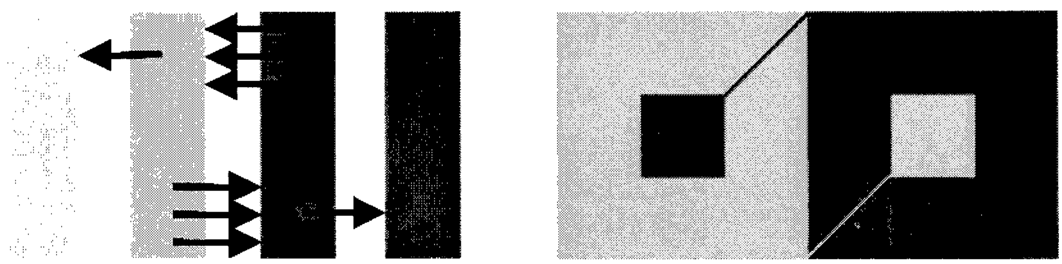

Figure 6: Sequence of simultaneus suppresion efekt

As a consequence, more substitutes are invoked and instability of neighbour shades of color is increased. This simultaneous suppresion effect should be taken into account, if we want to achieve exact color combination. We have to do certain corrections to achieve common visual harmonious result (1,5,17).

My basic idea is to unite antagonistic triangles and form them into *bipolar color-cut rhombi*© (Figure 7). Their symetry across the acromatic axis is always optimaly correlated to the selected colors in any system (Figure 8 and Figure 9). This solution could be a logic evolutive principle for monochromatic triangle system (13,14). Colors rely on dualism, and only one color does not exist for itself (1,5,12,17). Each color shade is accomplished and is in harmony with it's antagonistic one. Direct opposition best define substantial features of a certain color shade.

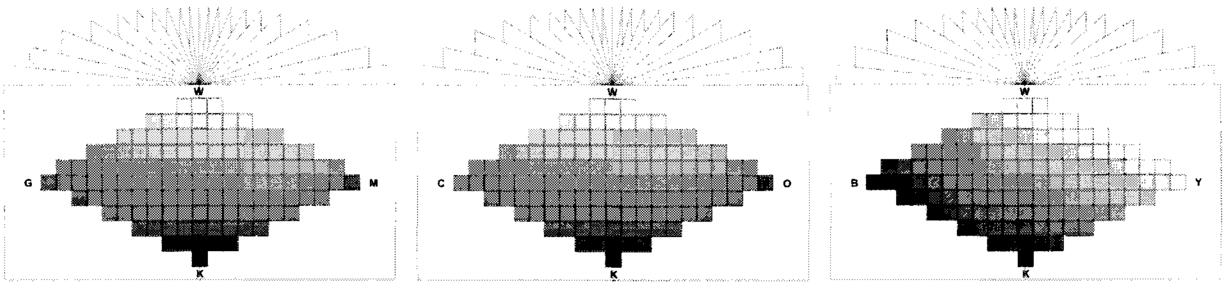

Figure 7: three basic bipolar rhombi

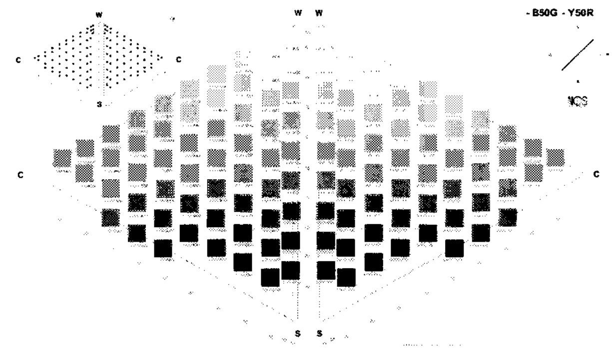

Figure 8: example of bipolar rhombus for NCS system

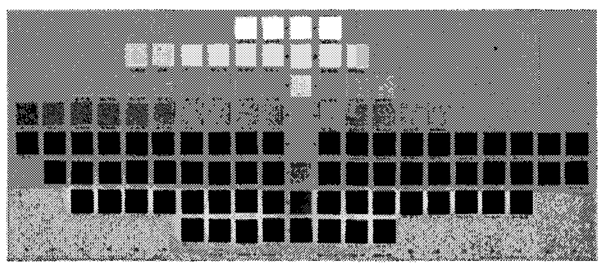

Figure 9: example of bipolar rhombus for RAL system

For more selective and refined color selection, we developed special *cascade color system*©, based on the *bipolar color-cut rhombi* (2,3,6,11).Color solid is stratified in horizontal segments and devided in nine grey levels of sections among black and white. These sections are devided then in equatorial cascades, intermedial cascades and polar cascades (Figure 10).

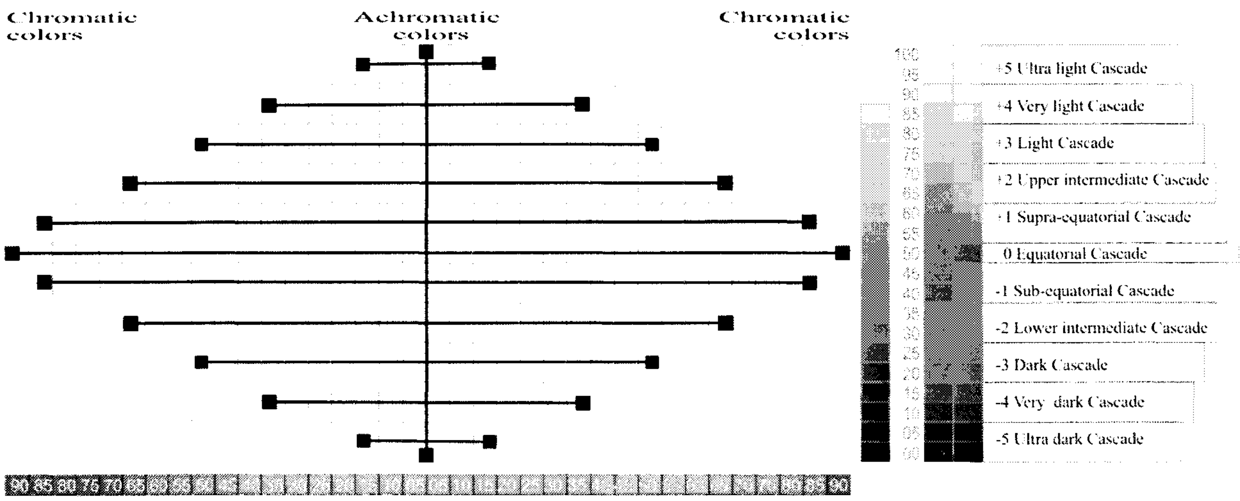

Figure 10: cascade color system based on the bipolar color-cut rhombus

Observations within our model show that five positive cascades rely on the dominant equatorial cascade and five negative lay under. The number of cascades may be simply increased in accordance with the vertical grey scale segmentation of color body.

It's notable that each step upwards equator increases lightness-values of cascades to the pure white. In opposition, downwards from equator in each next cascade lightness is declined to final black.

We may practice selections on the level of each cascade separately: totaly horizontal or slightly diagonal. We may have selections among different cascades, depending on concept of selection. Selection planes may lay ortogonal or under any angle in colour space. Equilibrium centre of the selective plane is always placed somewhere on the acromatic axis in color solid or space (2,4,5,11,20,21,22).

Out of wide range of potentials, depending on the number of colors in color wheal in equatorial level, I present only few examples of the basic bipolar color-cut rhombi in Figure 11.

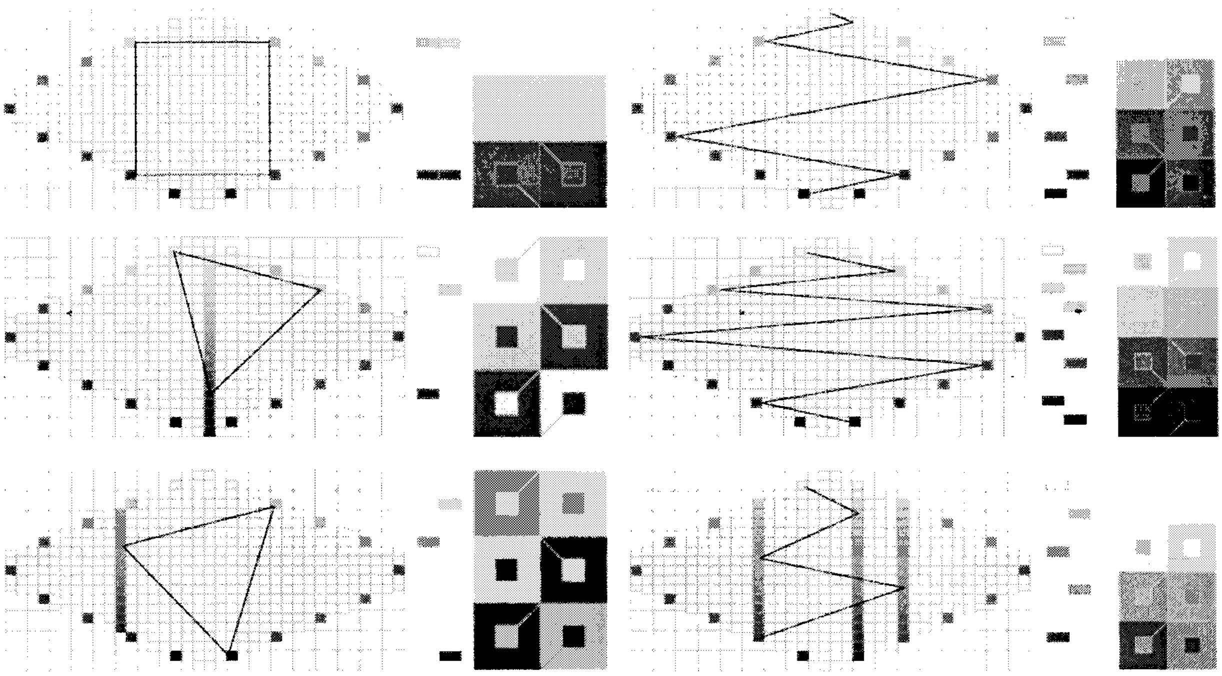

Figure 11: Some examples of Geometrical system for harmonious colors selection

CONCLUSIONS

There are numbers of color-selection potentials. It is impossible to define them all, but the bipolar geometrical system for harmonious color selection is logic one and a useful tool as well. To analyse interesting harmonious color combinations, found already in nature, and to make color selections, our system is useful, more systematic, logic and transparent. Presented principle creates conditions for heterogenious, but optimal color combinations.

It could become a useful tool in many branches of industry, where selections of colors are of vital importance, as in the field of design, advertising, printing, textile industry, etc. and can be applied to almost all existing color models and systems as CIE-LAB, NCS, RAL, Pantone etc.

According to the specific deformation of each color system, we can predict, that the results of harmonious selections will be different in spite of the equal staring points. Within the same system color combinations will always be optimally coordinated in harmony.

REFERENCES

1. Itten J: Kunst der Farbe. Ravensburg: Otto Maier, 1987
2. Pogacar V: Color cyclomatics. Ljubljana: Likovne besede, 1994;29-34:92-97,124.
3. Pogacar V: Colours as linguistic elements of the visual communication system. V: Golob V, Jeler S, Stjepanovic Z (ur.). Color & textiles, Book of Abstracts. Maribor: Slovenian Colorist Association, Faculty of Mechanical Engineering, Textile Department, 2002:27.

4. Pogacar V: Color cyclomatics. V: Jeler S (ur.). IV. International conference. Color and colorymetric. Book of proceedings. Maribor: Univerza v Mariboru - Tehniska fakulteta, Slovenski center za barvo in Drustvo koloristov Slovenije, 1994:10.
5. Küppers H: Harmonielehre der Farben. Theoretische Grundlagen der Farbengestaltung. 1st Edition. Kőln: Du Mont Buchverlag, 1989:12-242.
6. Jeler S: Barvni sistemi. V: Jeler S (ur.), Kumar M (ur.). Interdisciplinarnost barve. Maribor: Drustvo koloristov Slovenije, 2001:165-195.
7. Berlin B, Kay P: Basic Color Terms: Their Universality and Evolution, 2nd ed. Berkley: CSLI Publications, 1999:1-174.
8. Allen G: The Color-Sense. London: Tubner and Company, 1879.
9. Kuzmic M, Pogacar V, Golob V: Colorimetrical evaluation of colors in four-season typology. V: Golob V, Jeler S, Stjepanovic Z (ur.). Color & textiles, Book of Abstracts. Maribor: Slovenian Colorist Association, Faculty of Mechanical Engineering, Textile Department, 2002:16.
10. Jakobson R, Halle M: Fundamentals of Language. The Hague: Mouton, 1956
11. Golob V, Golob D: Teorija barvne metrike. V: Jeler S (ur.), Kumar M (ur.). Interdisciplinarnost barve. Maribor: Društvo koloristov Slovenije, 2001:201-230.
12. Itten J: Der Farbstern. Ravensburg: Otto Maier, 1985
13. http://www.ral.de/farben/
14. http://www.ncscolour.com/
15. Homann P: Digitales Colormanagement. Heidelberg: Springer Verlag, 2000
16. Benad M: Farbgestaltung. Stutgart-München: Deutsche Verlag, 2001
17. Küppers H: Das Grundgesetz der Farbenlehre. Köln: Dumont, 1978
18. Trstenjak A: Človek in barve. Ljubljana: Univerzum, 1978
19. Butina M: Mala likovna teorija. Ljubljana: Debora, 2000:103-114.
20. www.cs.iupui.edu-~pellison-colorlab
21. Marx E: Die Farb kontraste. Ravensburg: Otto Maier Verlag, 1973
22. http://www.adobe.com/support/techguides/color/colortheory/

Desaturation of the perceived illumination in the ambegujas display

Da Pos O.*, Bergström S.S.°, Cernuschi C.*

*University of Padua, Italy - °University of Umea, Sweden

ABSTRACT

Ambegujas is an interesting reversible figure in which at least four different spatial configuration can be perceived in different times. At each spatial organization colours undergo striking perceptual modifications passing from surface to light and to transparent mode. Colours in the light mode appear not to belong to the surface of the perceived object, but as cast light which progressively desaturate during observation. The desaturation has been measured by matching the colours seen in the light mode with test colours in the surface mode. Corrugated Mondrian were used because surface colours and coloured illumination could be perceived as stable characteristics of different planes of the figure. In two experiments the distance of the matched surface colours from the neutral point in a L*a*b* space was consistently and significantly shorter than the distance of the correspondent colours seen in the light mode. The difference can be considered as a measure of the desaturation which colours of the same colorimetric characteristics show when passing from a surface to a light mode of appearance. The colour changes observed in these phenomena are considered inside a new approach of colour constancy.

INTRODUCTION

Ambegujas consists of a vertical rectangle divided into six parts of the same size, three in the top and three in the bottom section (Fig. 1): in the top row the colour sequence is light, dark, and light orange; the colour sequence in the correspondent bottom row is light, dark, and light blue. Ambegujas is a reversible figure which can appear organised in at least four different 3D configurations. Changes in perceived surface colour and illumination are peculiar aspects of the display and occur with the different perceived structures.

One striking feature of the perceived illumination is its 'tendency' to appear chromatically neutral, that is strongly desaturated. We examined the two folds compatible with two specific cases of surface colour and illumination combination: when the vertical folding is perceived like a folded screen, two surface colours (orange and blue) are seen under two levels of neutral illumination, high in the front sides, and low/shadowed in the middle slanting side; in the other case of horizontal folding, both in the upper and in the lower side of the resulting trihedron two almost neutral greys (light, dark, light) are perceived on each side, one side appearing lighted by warm and the other by cold illumination.

The desaturation perceived in the coloured illumination has been measured in a series of experiments by using a 3D stable configuration (corrugated Mondrian) to avoid figure reversals. In this configuration, a special colour organization produces two similar but logically distinguishable effects: the perception of a transparent film or of a coloured illumination. Both percepts derive from chromatic (similarity) and figural (grouping) factors connecting areas of the same hue. When chromatic illumination is the unifying factor the illumination colours appear desaturated as compared with the surface colours perceived when the same colour stimuli are arranged in a different spatial configuration (vertical folding). This effect in which colour is seen as belonging to the illumination and not to the surface of the object is quite frequently experienced, and was the central study interest of our research.

a) 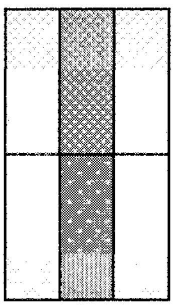 b) 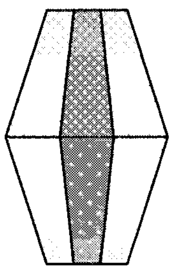 c) 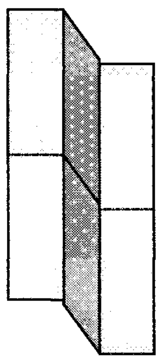

Fig. 1 Schematic representation of the original Ambegujas (a), and two frequent perceptive alternatives (b = horizontal folding, and c = vertical folding).

EXPERIMENT 1

The aim of this experiment was to quantify the desaturation undergone by colours which appear as cast light, as respect to the higher saturation of colours having the same chromaticity and luminance but perceived in the surface mode. In the Ambegujas display the difference between the two modes of colour appearance is perceptible whenever the spatial organization appears to change from the vertical to the horizontal direction of bending.

The subject has little control on which of the two possibilities is given in a particular moment; moreover the reversibility of the two configurations has no regular timing, with the consequence that it is impossible to be sure that any colour evaluation is provided when the stimulus is perceived in the wanted spatial organization. Therefore we used the corrugated Mondrian (Fig. 2) to stabilize the two different percept. In this figure the spatial configuration can exhibit little changes, basically its structure can be seen as either convex or concave: in both cases however the perceived illumination over the different sections of the figure does not change as consequence of the spatial variation (only the direction of the light is different). Colours in the front surfaces always appear differently illuminated in comparison with colours lying in the oblique planes, but we could avoid chromatic changes in the perceived illumination by intermixing chromatic and achromatic colours, with the result that no chromatic common component could be extracted from the different areas belonging to a particular plane. The illumination therefore could be perceived as different only from the point of view of its intensity, and did not interfere with the chromatic characteristics of the surface colours. The idea of this research is to measure the desaturation of the colours perceived in the light mode by matching them with colours perceived in the surface mode.

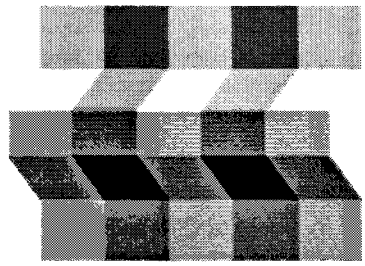

Fig. 2 - Corrugated Mondrian

Material and method.

Stimuli were presented in a 17" calibrated monitor (Post & Calhoun, 1989) in a completely dark room and consisted of a central corrugated Mondrian horizontally oriented as in Fig. 3, surrounded by 12 other corrugated Mondrians vertically oriented as in Fig. 4.The colours of the original Ambegujas, once the blue and once the orange pair, were reproduced in the dotted areas of the central comparison display (**m** was the light and **n** was the dark colour).

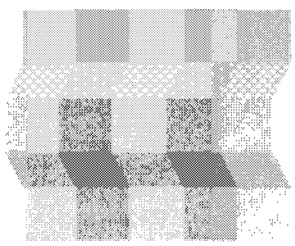

Fig. 3 – The series of m and n colours give a strong impression of light cast on grey surfaces.

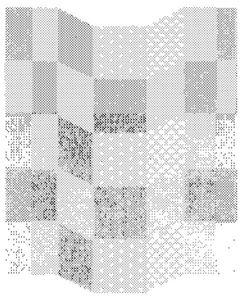

Fig. 4. – m' and n' give here a clear impression of surface colours.

colour	*L**	*a**	*b**
light orange	58	65	70
dark orange	43	60	41
light blue	58	0	50
dark blue	43	0	50

Tab. 1 – Specification of the colours reproducing the original Ambegujas shades in the comparison stimulus (horizontal corrugated Mondrian).

The other areas were respectively light and dark greys (L* = 62 and L* = 55). In a preliminary experiment two subjects found the closest match between the original Ambegujas colour m (Fig. 3) appearing in the light mode) and m' (appearing in the surface mode, Fig. 4); in the same way a match was also found between n and n'. Twelve pairs of colours, random variations of the original m' and n', were then specified so to fill a spherical region in the L*a*b* space having m' and n' in its centre. Four sets of test stimuli were prepared, one for each colour of the original Ambegujas (dark blue, light blue, dark orange, light orange). In each set only the light colour m' (or the dark colour n') was varying in the 12 vertical displays simultaneously presented, while the other colour of the pair was kept constant (n' or m' respectively). 28 subjects, whose normal colour vision was verified, volunteered in the experiment. They sat at a distance of 1 m from the screen and had to choose the vertical Mondrian in which the test colour (either m' or n') was the closest match of the corresponding comparison colour in the horizontal Mondrian. Half subjects performed the task with the series of m n colours in the upward oblique plane of the horizontal Mondrian, while for the other half group the Mondrian was rotated of 180° deg. The other 12 vertical Mondrians remained always in the same orientation, although randomly placed around the centre horizontal Mondrian.

Results.

As only colour saturation was the focus of this research, results are presented and discussed in relation to the a* and b* colour dimensions (Tab. 2). Variations in the L* dimension were irrelevant, and no significant difference was found between the comparison and the test lightness.

Orange - 28 subjects

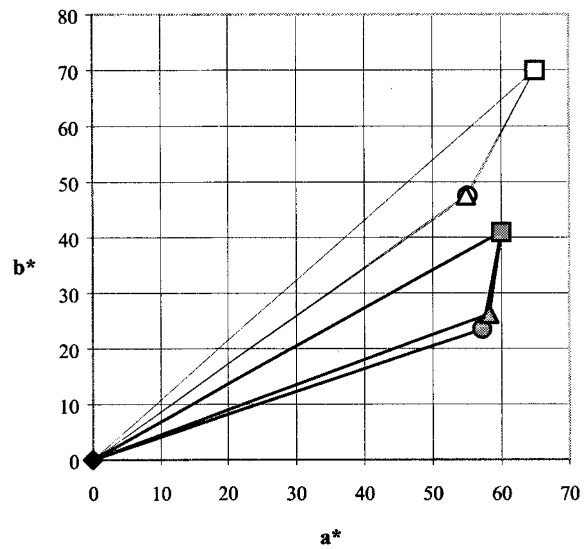

Fig. 5. Position of the colours (in the surface mode) matching the orange comparison shades in an isoluminant a*b* plane. Squares = comparison orange (in the light mode); diamond = achromatic point; circle = downward position of the comparison colours in the horizontal corrugated Mondrian; triangle = upward position; open symbols = light colours; filled symbols = dark colours.

comp. colours		direction	a*	b*
blue	dark	up	6.21	-37.93
		down	3.71	-38
	light	up	2.71	-43.64
		down	3	-43.93
orange	dark	up	57.21	23.43
		down	58.21	26.21
	light	up	55.14	47.43
		down	54.86	47.57

Table 2. a* and b* specification of the matching colours in the test displays.

Blue - 28 ss

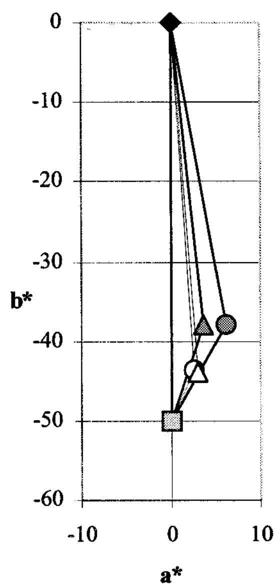

Fig. 6. The same as in fig. 5 for the blue colour.

The average distance of the test colours from the achromatic point is always significantly different and much shorter than the distance of the corresponding colours erceived in the comparison display (light mode), hence showing a strong desaturation. For the dark orange, the distance of the surface colour from the neutral point is Δ_{ab} = 62.83 vs Δ_{ab} = 72.67 ($p < 0.0000$) of the original in the light mode, and for the light orange Δ_{ab} = 72.67 vs Δ_{ab} = 95.52 ($p < 0.0000$); for the dark blue colours the average distance of the matching colours from the neutral is Δ_{ab} = 38.31 vs Δ_{ab} = 50 ($p < 0.0000$), and for the dark blue Δ_{ab} = 43.88 vs Δ_{ab} = 50 ($p < 0.0001$). Dark blue and light orange are desaturated by about the 23%, while light blue and dark orange by about the 13%.

Discussion.

The desaturation of the colours which appear in the light mode when the Ambegujas is perceived horizontally folded, has been measured through a match with surface colours in corrugated Mondrians. The degree of saturation is relevant and seems to depend on the hue and the lightness of the comparison colours, but not on their upward or downward orientation.

EXPERIMENT 2

The task of choosing a match within 12 alternatives at the same time seemed rather difficult for the subjects. For this reason a second experiment was run in which only six test colours were present at a time. Moreover, as test colours were not significantly different in lightness from the comparison colours, in the second experiment the test colours could differ only for two close lightness levels.

Material and method.

The same corrugated Mondrian as in experiment 1 were used and displayed in the same way in a CRT monitor. Instead of 12 only 6 vertical test Mondrians were surrounding the comparison one in the centre of the screen. The colours were chosen to better represent that part of the colour space where the choice of the subjects was concentrated in the previous experiment. Lightness was limited to 2 close levels, and a* and b* were regularly varied to represent six colours located at the vertices of an hexagon in a L*a*b* colour plane around the matching colour chosen in the previous experiment (in the second lightness plane the hexagon was rotated of 30° degrees). 12 subjects with normal colour vision took part to the experiment. In a first trial they had to chose the colour in the test Mondrians resembling most closely to the correspondent colour in the comparison Mondrian; the same procedure was replicated with the six different test Mondrians. Lastly subjects had to chose among their two previous results which test colour was most closely matching the comparison one.

Results.

Table 3 show the a* and b* values of the test colours chosen by the subjects to match the correspondent comparison colours. Results are illustrated in Fig. 6 and Fig. 7, and appear very similar to those of the previous experiment.

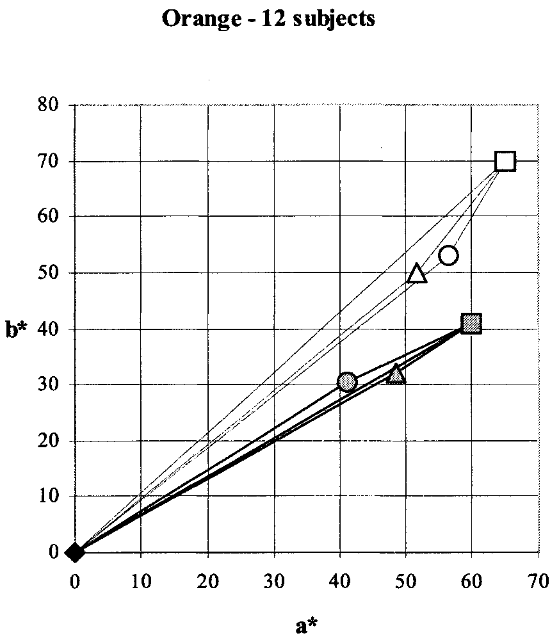

Fig. 6. Position of the colours (in the surface mode) matching the orange comparison shades in an isoluminant a*b* plane. Squares = comparison orange (in the light mode); diamond = achromatic point; circle = downward position of the comparison colours in the horizontal corrugated Mondrian; triangle = upward position; open symbols = light colours; filled symbols = dark colours.

comp. colours		direction	a*	b*
blue	dark	up	-5.83	-39.5
		down	2.71	-43.64
	light	up	-6.67	-41
		down	-2.5	-42.5
orange	dark	up	41.17	30.5
		down	48.67	32
	light	up	56.67	53
		down	51.67	50

Table 3. a* and b* specification of the matching colours in the test displays.

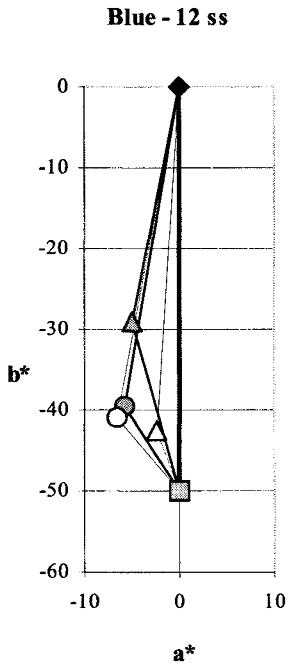

Fig. 7. The same as in fig. 6 for the blue colour.

As in the previous experiment the chosen colours appear much less saturated than the comparison ones. For the dark orange, the distance of the surface colour from the neutral point is $\Delta_{ab} = 54.74$ vs $\Delta_{ab} = 72.67$ ($p < 0.0000$) of the original in the light mode, and for the light orange $\Delta_{ab} = 74.75$ vs $\Delta_{ab} = 95.52$ ($p < 0.0000$); for the dark blue colours the average distance of the matching colours from the neutral is $\Delta_{ab} = 38.68$ vs $\Delta_{ab} = 50$ ($p < 0.0000$), and for the dark blue $\Delta_{ab} = 42.06$ vs $\Delta_{ab} = 50$ ($p < 0.0001$).On the average the saturation decreases by about 23%.

Discussion.

As in the previous experiment, the desaturation of the colours which appear in the light mode when the Ambegujas is perceived horizontally pleated, has been here measured through a match with surface colours in corrugated

Mondrians. The degree of desaturation is again relevant but more uniform than in the previous experiment as regard the different hues and lightness.

CONCLUSIONS

When in an ambiguous figure the perception of a surface colour changes into the perception of a coloured illumination a strong colour desaturation also occurring which reverses when surface colours are again perceived. The phenomenon was described by Jakobsson and colleagues (19) in the Ambegujas display and has been shown not to consist in an adaptation process. Results from 2 experiments show that the degree of desaturation is quite high, more than 20% in the L*a*b* colour space. Data collected from other similar experiments show that the effect is robust and consistent: fig. 8 and 9 present the results of 64 subjects, included those of the experiments previously described, and confirm the high desaturation undergone by colours when perceived in the light mode (on the average more than 18% for all colours in all conditions).

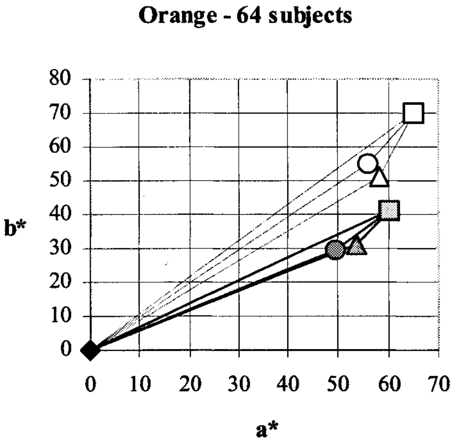

Fig. 8. Position of the colours (in the surface mode) matching the orange comparison shades in an isoluminant a*b* plane. Squares = comparison orange (in the light mode); diamond = achromatic point; circle = downward position of the comparison colours in the horizontal corrugated Mondrian; triangle = upward position; open symbols = light colours; filled symbols = dark colours.

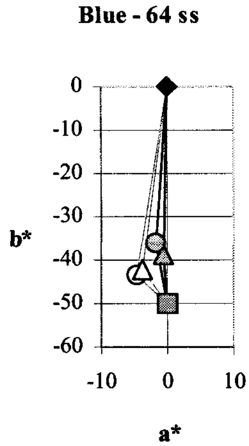

Fig. 9. The same as in fig. 8 as regard to the blue colourr

The distance of the matched dark blue colours from the achromatic point is Δ_{ab} = 37.52 and of the light blue of Δ_{ab} = 43.01, vs Δ_{ab} = 50 of the comparison blues; the distance of the matched dark orange colours from the achromatic point is Δ_{ab} = 59.76 vs Δ_{ab} = 72.67 and of the light orange of Δ_{ab} = 77.85 vs Δ_{ab} = 95.52 of the comparison oranges. All the differences are statistically higly significant ($p < 0.0000$).

The analysis of the Ambegujas phenomenon performed in this research seems to support the need of a new theory about colour constancy. Whenever possible our visual system extracts from the colour stimulation a common component which is perceived as the illumination falling on the surfaces, and what remains goes to form the surface colours. The process takes place separately in different frames hierarchically organized, as it happens for the lightness perception (Gilchrist et al. 1999). In the vertical folding the front planes show a common level of illumination falling equally over the orange and the blue areas, while in the oblique plane the illumination is still uniform over the two regions but at a lower level than in the front plane. In the horizontal folding of the Ambegujas the illumination over the upper plane derives from two orange areas: it takes the common orange hue and appears as a warm illumination; similarly in the lower plane the illumination takes the bluish common component, and appear cold. Two consequences derive from this process: first, the chromatic component which goes to characterize the illumination leaves the surfaces almost achromatic (as we actually perceive them), and second, the illumination tend to be perceived as achromatic, or at least as much desaturated as possible, which is confirmed by the present research. It would be therefore important to check whether these two aspects of the separation between surface colours and illumination can be generalized to all situations in which colour constancy is assumed to work.

REFERENCES

Bergström, S. S. (1982). *Illumination, color, and three-dimensional form.* In J. Beck (Ed.), Organization and representation in perception. Hillsdale, NJ: Erlbaum.

Gilchrist, AL., Kossifydis, C., Bonato, F., Agostini, T., Cataliotti, J., Li, X., Spehar, B., Annan, V., Economou, E. *An anchoring theory of lightness perception.* Psychol. Rev. 1999, **106**, 795-834.

Jakobsson T., Bergström, S. S., Gustafsson K.A., Fedorovskaya E., *Ambiguities in colour constancy and shape from shading.* Perception, 1997; Vol 26(4): 531-541

Post D. , Calhoun C.S. *An evaluation of methods for producing desired colors on CRT monitors.* Color Research and Application. 1989, 14: 172-186

Relation between the Light Fastness and UV-rays Blocking Property of Disperse Dyes on the Polyester Fabrics

Tomoko Mima[1], Masako Sato[2],

Tadashi Takatsuka[3], Yoshihiro Yobiko[3], Hideo Asazawa[3]

[1] Seian University of Art and Design, [2] Osaka City University,

[3] Technology Research Institute of Osaka Prefecture, Japan

ABSTRACT

As the shorter wavelength of UVC and UVB than UVA-rays recently arrive into the atmosphere, the human bodies might be in danger. If the dye on the textile could absorb not only the visible light but also the UV-rays, the colored clothes might be able to block the harmful UV-rays by decreasing transmittance and then protect the human bodies.

But, the UV-rays saving high energy might also destroy the structure of dye molecular. The light fastness property of dyed fabric is also an important character from a viewpoint of aesthetic sense of textile.

The purpose of this study is to investigate the relation between the light fastness of disperse dyes on the polyester fabric and its blocking property against UV-rays. The light fastness property of polyester taffeta fabrics dyed with different types of disperse dyes (red, yellow and blue) was tested by irradiation of xenon lamp. The results were as follow.

Color fading of dyed fabrics depended on the structure of dyes. Yellow dyes were examined high grade of color fading and high blocking efficiency against UV-rays. If the dye having low light fastness could dye the fabric with dark shade, the fabric might have high blocking efficiency after irradiation.

Keywords: blocking property against UV-rays, disperse dye, polyester fabric, color fastness to light

1. INTRODUCTION

If the dye could strongly absorb not only the visible rays but also UV-rays, it might be expected as a superior blocking material against the harmful UV-rays. On the other hand, color fastness to light of dyed fabrics is expected as aesthetic sense.

In the previous studies, the authors have reported the mechanism of UV-rays blocking by colored polyester and cotton fabrics dyed with disperse and direct dyes respectively (1, 2, 3, 4). Polyester fabric, even on the non-dyed fabric, would be a superior blocking material showing more than 90% blocking efficiency against UVB-rays.

The other, cotton fabric dyed with direct dye was examined to have much higher UV-blocking efficiency in the region of UVA than the efficiency of polyester fabric dyed with disperse dye. Disperse dyes of red and blue were inferior to direct dyes of each red and blue. The yellow colored fabrics dyed with disperse and direct dyes were examined higher than red and blue colored fabrics.

In this study the relation between UV-rays blocking property of dyed fabric and its color fastness to light was investigated.

The polyester taffeta fabrics respectively dyed with eight kinds of disperse dyes and categorized into three color names as red, yellow and blue and they were tested on photo –fading by irradiation of xenon arc lamp.

2. EXPERIMENTAL PROCEDURE

2.1. Fabric and dye materials

Polyester taffeta fabric woven with 81d yarn was used for the substrate of dyeing. Table1 shows the dye name and the number of C.I., and its molar weight of disperse dyes used. The fabrics and the dyes used in this study were the same as used in the previous study (4). The dyes were purity known reagent grade by Aldrich Chemical Company. Test pieces of fabric were dyed into fore levels of lightness using different concentration of dying baths. Table 2 shows the dying conditions of them. The dyed fabrics resulted in different depths of colors from pale to dark shade.

Table 1. Characteristics of disperse dye

Dye name	(C.I.No)	M.W
Red1	(C.I.11110)	314
Red13	(C.I.11115)	349
Yellow3	(C.I.11855)	269
Yellow7	(C.I.26090)	316
Yellow9	(C.I.10375)	274
Blue1	(C.I.64500)	268
Blue3	(C.I.61505)	296
Blue14	(C.I.61500)	266
Orange1	(C.I.11080)	318
Orange3	(C.I.11005)	242
Orange11	(C.I.60700)	237

Table 2. Dyeing condition(Disperse dye)

Conc of dye ($\times 10^{-4}$mol/l)	Dyeing auxiliaries	
	Sodium laurylate(0.05sol)	Acetic asid(1%sol)
(1) 0.2	15cc/60cc	0.3cc/60cc
(2) 0.5	15cc/60cc	0.3cc/60cc
(3) 2.0	15cc/60cc	0.3cc/60cc
(4) 4.0	15cc/60cc	0.3cc/60cc
Bath ratio	1: 30	
Temperature	135℃	
Time	60min	

2.2. Examination of fastness property of dyed fabric

The fastness property of dyed fabric was examined as function of irradiation time (five, ten and twenty hours) by xenon arc lamp using Super Xenon Weather Meter-SC-750-WA (SUGA Weathering Technology Co. Japan).

Pieces of Blue Scale (JIS Light Fastness Standards) were used for the indicator of light blocking by dyed fabric. That is to say, the dyed fabric was attached on the piece of Blue Scale and fixed to the window of device for irradiation (see Fig.1). After irradiation the dyed fabrics were measured on the luminous reflectance and examined fastness property of grade by visually comparing to the Blue Scale swatch.

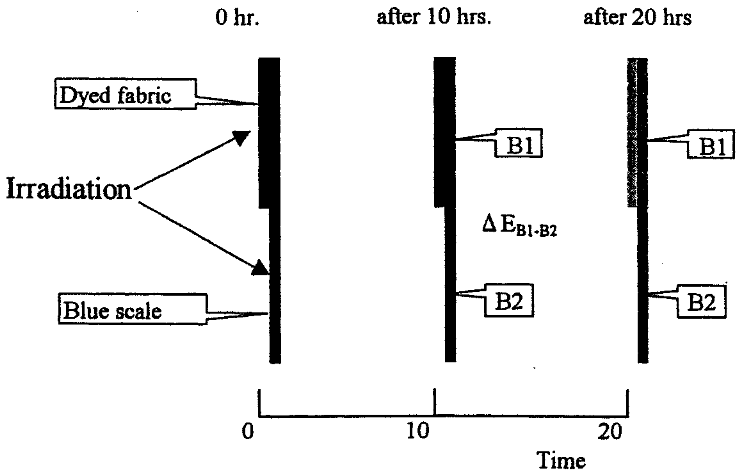

Fig.1 The dyed fabric and blue scale fixed on the window of the irradiation.

2.3. Evaluation of UV blocking property of dyed fabric.

UV blocking property was examined using two methods. The one is measuring the spectral transmittance of dyed fabrics before and after irradiation using UV-VIS SPECTRO PHOTO METER (UV-3000, SHIMADZU, Japan) and the other is examination of the color difference between B1-B2 (showed in Fig.1). The later $\Delta E_{B1\text{-}B2}$ shows the blocking property of dyed fabric indirectly. The transmittance of fabric was also examined at the region from 200 to 800 nm.

3. RESULTS AND DISCUSSION

3.1 Effects of irradiation time on the color fastness property of dyed fabrics.

Table 3 shows the color fastness to light of dyed fabrics as examples of Disperse Red1, Blue3 and Yellow3. The numbers in bracket in the dying condition columns show the dye concentration of dying bath, namely (2) 0.5×10^{4} mol/l, (3) 2.0×10^{4} mol/l, (4) 4.0×10^{4} mol/l. Color fastness to light was shown in the square bracket by Grade of Light Fastness Standard.

The difference of the color fastness between 10 and 20 hours of each dye, Red1, Blue3 and Yellow3, were not recognized from the Grade Number of Blue Scale. The fabrics dyed with Red1 and Blue3 were examined lower color fastness to light as compared to the fabrics dyed with Yellow3. The fabrics dyed with Yellow3 showed the highest color fastness to light in all of the dyes used in this experiment. It was investigated in general that yellow dyes might be excellent and Red and Blues dyes might be worth against the color fading.

Table3. Color fastness to light of dyed fabrics

Sample \ Dye condition / Time		(2) 0.5×10^{-4}mol/l	(3) 2.0×10^{-4}mol/l	(4) 4.0×10^{-4}mol/l
Disperse Red1	Original piece	[3]		
	10hr	[3]	[3]	[3]
	20hr	[3]	[3]	[3]
Disperse Yellow3	Original piece			
	10hr	[5]	[5]	[6]
	20hr	[5]	[5]	[6]
Disperse Blue3	Original piece			
	10hr	[3]	[3]	[3]
	20hr	[3]	[3]	[3]

The number in square bracket indicates the fastness property to light after irradiation.

3.2 Effects of irradiation time on the transmittance of dyed fabrics

Fig2 shows the effects of irradiation times on the transmittance of the dyed fabric as examples of Yellow3.

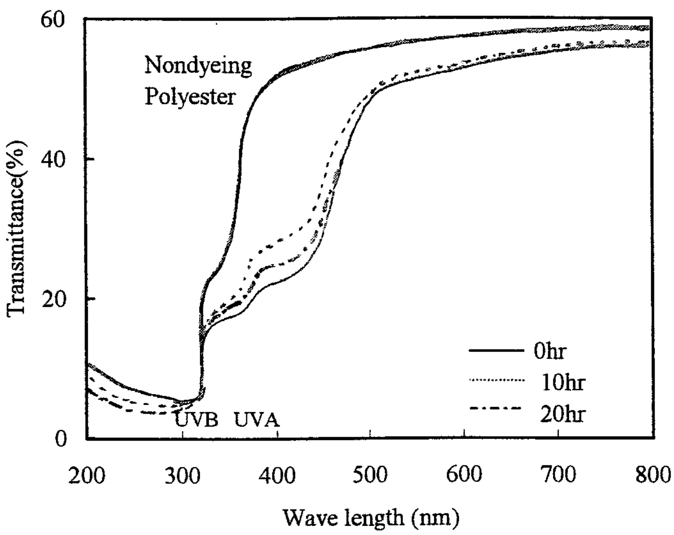

Fig. 2 Spectral transmittance curve of dyed fabrics (Disperse Yellow3)

The number 3 in round bracket shows the dye concentration of dying bath. The transmittance curves of dyed fabric with Yellow3 incleased as irradiation hours. Effects of irradiation time on transmittance curves of other dyes were examined similar to Yellow3.

3.3 The relation between color fastness and blocking property of dyed fabric.

Table 4 shows luminous reflectance, blocking property of fabrics before and after irradiation and $\Delta E_{B1\text{-}B2}$ after irradiation.

The number in bracket shows the dye concentration of dyeing bath. Generally the difference of the luminous reflectance (Y%) of dyed fabrics before and after irradiation indicates the property of color fastness to light. The differences of Y% before and after irradiation with three Yellow dyes were little, and the difference of Red1 was large. It is expected that Yellow3 is the most excellent of all and Red1 and Blue3 are inferior to color fastness.

Though $\Delta E_{B1\text{-}B2}$ is shows by blocking property of dyed fabrics after irradiation indirectly, the blocking (%) calculated from transmittance might directly show the blocking efficiency . If the dye having low light fastness could dye the fabric with dark shade, the fabric might have high blocking efficiency after irradiation.

Table 4. Luminous reflectance and blocking property of dark shade dyed fabrics after irradiation

Properties / Samples	Before irradiation(0hr)		After irradiation(20hr)			
	Samples		Samples		Blue Scale (Standard 3)	
	Y(%)	Blocking(%)	Y(%)	Blocking(%)	Y(%)	$\Delta E_{B1\text{-}B2}$
Nondyed Polyester fabric	72.3	73.6	71.7	73.5	8.5	9.6
Blue scale (4)	7.7				10.0	
Disperse Red1 (4)	17.0	90.0	22.7	89.6	7.8	15.6
Disperse Red13 (4)	8.7	89.8	11.4	88.8	7.8	15.6
Disperse Yellow3 (4)	54.4	96.7	54.2	96.0	7.8	16.2
Disperse Yellow7 (4)	36.0	97.0	37.7	96.5	7.6	17.2
Disperse Yellow9 (4)	39.7	95.5	40.8	95.3	7.6	17.0
Disperse Blue1 (4)	15.9	85.9	18.8	84.3	8.0	14.2
Disperse Blue3 (4)	8.1	91.0	9.5	90.0	7.6	18.2
Disperse Blue14 (4)	12.0	88.5	12.1	87.7	7.7	16.6

Y(%) indicates luminous refrectance

Blocking(%) indicates blocking efficiency against UVT(280~400nm)

Blue Scale (Standard 3) meens light fastness standard (Standard 3)

Y(%) and $\Delta E_{B1\text{-}B2}$ indicate value of Blue Scale (Standard 3)

4. CONCULUSION

This article was investigated to the blocking property of dyed fabric for the purpose of protecting human bodies. Effect of dye structure, absorption property of UVA-ray, UVB-ray, and visible rays of dyes, color fastness property of dyed fabrics, blocking property of dyed fabrics were discussed. Yellow dyes were examined high grade of color fading and high blocking efficiency against UV-rays. If the dye having low light fastness could dye the fabric with dark shade, the fabric might have high blocking efficiency after irradiation.

. REFERENCES

1)T. Mima and M. Sato, Ultraviolet rays Shielding by Dyed Fabrics, The Proceeding of AIC 2000, Seoul, p.p. 260-263, 2000

2) T. Mima and M. Sato, Studies on Ultraviolet Rays Shielding Properties of Dyed Fabrics, Part1: Cotton Fabrics Dyed with Direct Dyes, Jpn. Res. Assn. Text. End-Uses, Vol. No3, pp. 36-46 , 2000

3)T. Mima and M. Sato, Relation between Blocking Property against UV-rays by Dyed Fabrics and Its Color Fastness to Light, The Proceeding of AIC 2001, Rochester, p.p. 260-263, 2001

4) T. Mima and M. Sato, Blocking Property against UV-rays: Effect of Fabric and Dye Materials, The Proceeding of AIC 2002, Slovenia , p.p. 296-301, 2002

Overt and Covert Effects of Color Lighting during Simple Task

Shin'ya TAKAHASHI (Nagoya University)

Under the color lighting, red, green, blue, or yellow, 120 subjects did the Kraepelin-type addition task, and their task performance and psychological process were analyzed. As a result, the color of lighting had the most distinct effect on the impression ratings of color lighting itself; the red lighting made a cheerful impression, the blue lighting made a refined impression, and the green lighting and the yellow lighting made a calm impression. As for the task performance, it was found that the subjects in yellow condition performed the task at a steadier pace than those in red condition. But the color of lighting did not influenced a productivity or an accuracy of the task. Also, there was no clear effect of the color of lighting on the subjects' fatigue or time estimation. The difficulty of dealing with the effect of environmental colors was discussed.

INTRODUCTION

The effect of environmental colors upon task performance or work efficiency is of a practical as well as theoretical interest. In various places, some specific colors are used with the aim of improving performance. For example, recently, the color of a track that was traditionally reddish brown became changed to blue in some sports grounds in Japan because of the expectation that blue enhances athletes' concentration and helps them make good records. However, it seems that such application of color goes too far ahead of a scientific knowledge, so the importance of a theoretical study of color psychology is more and more increasing.

There have been many studies about emotional effects of colors. For example, Omori *et al.* (2002) analyzed psychological and physiological effects of color stimuli and found that a large stimulus of pure red or purple-blue and a small stimulus of pure yellow-red or bright blue made observers felt rested and comfortable. This is, so to speak, the effect of *color as a visual object* (objective color). On the other hand, the effect of *color as one of environmental factors* (environmental color) has not been studied enough so far. Specifically there are few reports of an experimental study which evaluated the effect of environmental color on the task performance. Considering practical problems, however, the effect of environmental color is more important than that of objective color, since it is rather unusual to see colors without doing any other works. Consequently, in this study, I varied the color of lighting during simple task and examined the effects it would produce on the task performance and performer's mental state.

METHODS

Subjects

120 undergraduates (59 males and 61 females) participated as subjects. They were divided into four groups, and each group was assigned to one of four color lighting conditions; red, green, blue, and yellow.

Instruments

Color beam bulbs (National BF110V80W-R, -G, -B, -Y) were used to illuminate an experimental room. In each color lighting condition, five color beam bulbs were turned on. Illuminance at the top of a table on which subjects performed the task was set at 440 lux in all color lighting conditions and in white lighting control condition.

Task

Kraepelin-type addition task was used. Subjects added adjoining two numbers as fast and accurately as possible. Changing the line every 40 seconds, the task was continued for 440 seconds (11 lines). Subjects were not informed about such time setting in advance.

Procedure

All subjects repeated the task twice, first under the white lighting (control condition), second under the color lighting (red, green, blue, or yellow; experimental condition). Between the tasks, subjects rested for few minutes with their eyes closed. After finishing the second task, they were asked to answer the questionnaire. Total time of an experiment was approximately 30 minutes.

Questionnaire

The questionnaire was composed of three parts. Part 1 asked subject to estimate the time he/she spent on the second task under color lighting, and also to judge the relative length of the second task compared with the first task under white lighting. Part 2 asked about subject's physical fatigue, mental fatigue, and sleepiness on 4-point scales. Part 3 was a series of SD (semantic differential) scales asking about the impression of color lighting. It included 30 pairs of antonymic adjectives, for example, "heavy-light," "old-new," "soft-hard," "cold-warm," "weak-strong," etc.

RESULTS

In this study, the effects which manifested upon performance measures of the task were regarded as *overt effects*, whereas the effects upon psychological measures included in the questionnaire were regarded as *covert effects*. The basic assumption of this classification is that an apparent performance of the task would be influenced indirectly by the color lighting, being mediated by some psychological process such as subjective estimation of time lapse, physical or mental fatigue, and impression of the color lighting itself.

Overt Effects

Four indices of the task performance were analyzed; (1) an averaged amount of addition work per unit time (40 seconds), (2) a standard deviation of the amounts of addition work per unit time, (3) an averaged difference between amounts of addition work in sequential two lines, and (4) total number of error answers in the task. In order to offset individual differences and clarify the effects of color lighting, the data obtained in the color lighting condition were transformed into relative values compared with the data obtained in the white lighting condition in each subject.[1)]

Table 1 shows the results of these indices (actual data and relative values) in each condition. A one-way analysis of variance (ANOVA) revealed a significant main effect of color condition on the relative values of averaged difference (F=2.85, df=3,116, p<.05). Post-hoc comparison by Tukey HSD clarified that the relative

---

1) An averaged amount, a standard deviation, and an averaged difference were transformed into the ratio between two values. A total error was transformed into the difference between two values. So, for example, a relative value "1.2" of an averaged amount means 20% increase, and a relative value "-3" of a total error means decrease of three errors.

Table 1 Results of task performance in each color condition
(actual data in a first row and relative values in a second row of each index)

	Red		Green		Blue		Yellow	
	White	Color	White	Color	White	Color	White	Color
Averaged amount	39.26	42.15	40.96	44.17	40.75	43.42	38.50	41.06
	1.074		1.078		1.067		1.069	
Standard deviation	3.36	3.97	3.45	3.62	3.52	4.15	3.44	3.57
	1.302		1.104		1.322		1.106	
Averaged difference	3.16	3.99	3.22	3.50	3.55	3.91	3.35	3.25
	1.467		1.205		1.240		1.037	
Total error	1.93	1.60	3.27	2.30	2.63	2.57	1.50	1.57
	-0.33		-0.97		-0.06		0.07	

value in red condition (1.467) was significantly higher than that in yellow condition (1.037). As for other indices, the effect of color condition was not significant.

Covert Effects

(1) Time Estimation

Table 2 shows the results about time estimation. As for the estimated time of the second task, no significant difference was found among color conditions, though the estimated time in yellow condition is considerably shorter than the estimated times in other conditions. It is obviously due to the large SDs on these data (presented in parentheses). In fact, some subjects estimated a real lapse of 440 seconds at 60 seconds (1 minute), and others estimated it at 900 seconds (15 minutes). Then I classified the data in three categories; ~180 seconds (3 minutes), 181 seconds ~ 599 seconds, and 600 seconds (10 minutes) ~. As shown in Table 3, such classification clarified that the frequency of both extremes is greater in green and blue conditions than in red and yellow conditions. This difference was found to be significant (χ^2=14.45, *df*=6, *p*<.05).

On the other hand, the color of lighting did not influence the judgement of relative length of the task under color lighting compared with the task under white lighting (see Table 2).

Table 2 Results of time estimation in each color condition

		Red	Green	Blue	Yellow
Estimated Time (second) *SD in parentheses		361.5 (156.5)	342.2 (185.1)	350.6 (225.9)	307.5 (160.6)
Comparison with White Lighting Condition (Number of Subjects)	Shorter	8	8	9	11
	Same	14	15	14	11
	Longer	8	7	7	8

Table 3 Number of subjects included in each of three categories of estimated time in each color condition

	R	G	B	Y
~180s	3	10	9	4
181s~599s	23	12	14	23
600s~	4	8	7	3

(2) Fatigue and Sleepiness

Subject's physical fatigue, mental fatigue, and sleepiness, were measured on 4-point scales; from "0" (none) to "3" (very). It was shown by the one-way ANOVA that the color of lighting did not produce significant effect on these measures. Mean of all data for physical fatigue, mental fatigue, and sleepiness was 1.77, 1.23, and 1.38, respectively.

(3) Impression of Color Lighting

A factor analysis was performed, using a principal component analysis for factor extraction and a varimax rotation, on the impression ratings of color lighting. Judging from a decrement of the Eigenvalues, I obtained three factors which explained 53.8% of a total variance. The first factor was labelled as *Calmness* since the items such as "temperate," "relieved," and "relaxed" had high factor loadings. The second factor was labelled as *Refinedness* since the items such as "sharp," "clear," and "vivid" had high factor loadings. The third factor was labelled as *Cheerfulness* since the items such as "lively," "vigorous," and "happy" had high factor loadings.

Figures 1(a) ~ 1(c) show the results of these factors in each color condition. There was a significant main effect of color condition in every factors (Calmness, F=10.52, df=3,116, p<.01; Refinedness, F=27.26, df=3,116, p<.01; Cheerfulness, F=12.61, df=3,116, p<.01). Post-hoc comparison by Tukey HSD clarified that Calmness was significantly lower in red condition than in other three conditions, Refinedness was higher in blue condition than in other three conditions and also higher in green condition than in yellow condition, and Cheerfulness was higher in red condition than in other three conditions (p<.05).

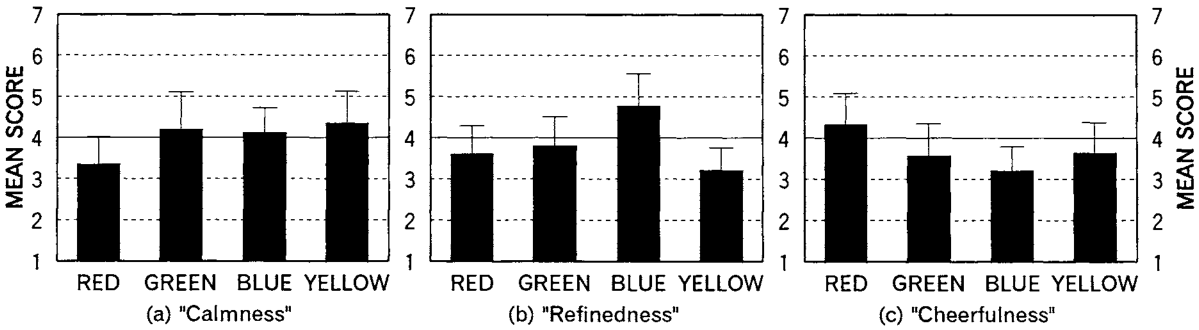

Figure 1 Mean scores of each of the three factors in each color condition

DISCUSSION

In this study, the effects of the color of lighting upon task performance (*overt effects*) were evaluated in three aspects; a productivity, a stability, and an accuracy. As a result, the color of lighting had significant effect only on a stability of the work, namely, the index of an averaged difference. More concretely, subjects in yellow condition performed the task at a steadier pace than those in red condition. To consider this together with the results of impression ratings (see Figure 1), it is supposed that the red lighting with cheerful (but less calm) impression attracted more attention of subjects, so they could not concentrate on the task. Contrastingly, subjects might be able to devote themselves to their work under the yellow lighting with calm and tender impression. However it must be noticed that indices other than the averaged difference were not influenced by the color of lighting. Especially, a productivity of the work (the averaged amount), which is the most important index in a sense, was not influenced at all (see Table 1). Consequently, it may be more valid to conclude that the subjects in all color conditions finally achieved the task with the same productivity and the same accuracy regardless of the nature of an impression each color lighting gives.

As for *covert effects* of color lighting, on the other hand, some effects were found to be significant. The most clearest was the impression ratings of color lighting partly mentioned above. To summarize the results shown in Figure 1, the red lighting made a cheerful impression, the blue lighting made a refined impression, and the green lighting and the yellow lighting made a calm impression. These results are not necessarily in conformity with the consensus on what is called color affection, but such disagreement is probably due to the distinction between objects to be examined; the color of lighting in this study, and usually colored paper in the color affection studies. For example, yellow is generally said to be "gay" and "dynamic," but in this study yellow lighting made rather "calm" and "tender" impression probably because its perceived strength of color was weaker than other color lightings. Nevertheless, the impression of red, green, and blue lightings roughly agreed with the previous findings of color affection studies.

Another effect, though less evident, was found in the time estimation measure. As shown in Table 3, there were more subjects who answered either extremely short time (less than 3 minutes) or extremely long time (more than 10 minutes) in green and blue conditions than in red and yellow conditions. However, it is not easy to give a reasonable explanation of this result. It may be the genuine effect of green and blue which are said to be "commonly favored colors," or may be an accidental artifact caused by the assignment of subjects. In any case, further study with more subjects is necessary to solve this problem and also to judge the credibility of a remarkable underestimation in yellow condition.

CONCLUSION

Four colors of lighting, red, green, blue, and yellow, made the characteristic impressions on subjects, but they only had limited and unclear effects on the task performance or psychological process of subjects. It may be the case, as Davidoff (1991) argued, that the environmental colors have their effects only upon the response bias of subjects. Another possibility to be considered is that the effect of environmental colors may not be universal; i.e., it depend largely on the other environmental and subjective factors such as a kind of work, a color preference, etc. This view would pose a serious problem to a theoretical consideration of the color effect as well as the practical use of colors. If, for example, some positive effect was produced by the individually prefered color no matter what it is, then should we call it the effect of color? The author's opinion is that it is no longer the effect of color, but is the effect of good feelings created by the favorite color. And such effect would be brought about in the same way by other environmental factors such as a favorite music, a favorite fragrance, etc. In this case, it is no longer the peculiar effect of color.

The effect of the environmental colors is indeed an attractive topic to researchers and designers. But it is necessary to accumulate an accurate knowledge both in the laboratory and in the field in order to obtain the desired effect. Too much amplified discussion and application should be refrained.

REFERENCES

Davidoff, J. 1991 *Cognition through color.* Cambridge, MA: The MIT Press.

Omori, M., Hashimoto, R., & Kato, Y. 2002 Relation between psychological and physiological responces on color stimulus. *Journal of the Color Science Association of Japan*, **26**, 50-63. [In Japanese with English abstract]

Proportional dye concentration errors and repeatability of dyeing polyacrylic with basic dyes

Boris Sluban, Mihaela Pozderec and Olivera Šauperl
University of Maribor, Slovenia
E-mail: boris.sluban@uni-mb.si

Abstract

The colorant concentration errors are subdivided to random (weighing) errors and proportional (strength) errors. In the present research the impact of proportional concentration errors was examined in laboratory experiments with several different recipes for a neutral medium lightness target colour. The first aim was to check experimentally the hypothesis about the lack of correlation between the sensitivity of the recipe colour to random (weighing) errors and the sensitivity of the recipe colour to proportional (strength) errors. The second aim was to assess the amount of scattering of the recipe colour with respect to each of both mentioned types of concentration errors for various recipes for a middle-lightness grey target.

INTRODUCTION

Colorant concentration errors are one of several types of inevitable small random errors in coloration process, which affect the accuracy and repeatability of dyeing. According to Alman's computer simulations[1] the impact of random weighing errors is the biggest at low concentrations, the impact of strength errors is the biggest at middle-range concentrations and both types of errors are less important at high concentrations. In the previous research the relative importance of random concentration errors was studied for the case of dyeing polyacrylic with basic dyes. In cases of the recipes for light less saturated target colours a weak, but still statistically significant correlation between the predicted sensitivity[2] of the recipe colour to random weighing errors and the observed repeatability of the recipe colour was found[3].

In the first part of present research[4] some measures for sensitivity of the recipe colour to strength errors were studied. The neutral grey target colour with lightness $L^*=50$ was chosen as recipes for such target are expected to contain some dyes in middle-range concentrations where the influence of the proportional concentration errors is the biggest. For this particular grey target eight different three-dye recipes were treated. For each recipe considered the initial dye concentrations in a recipe were perturbed according to a chosen pattern in order to simulate the effect of strength error in amount of one and two standard deviation from the declared strength, respectively. Then the corresponding colour changes were predicted. The standard deviation of these predicted colour positions in CMC(2:1) metrics was used as a measure for the sensitivity of the recipe colour to strength errors. Another measure for sensitivity to strength errors could be the maximal predicted colour difference resulting from the mentioned perturbation pattern. It was found that eight different recipes for the considered medium lightness grey target exhibited very different sensitivities to strength errors – the sensitivity of the most sensitive recipe was more than 7-times bigger than the sensitivity of the least sensitive one. Although the recipe, least sensitive to weighing errors, was also least sensitive to strength errors, no regular linear correlation between the predicted sensitivities to random (weighing) errors and the predicted sensitivities to proportional (strength) errors was observed.

In the second part of the research it was tried to experimentally check the above mentioned predicted relations among the sensitivities of various recipes to strength errors and, at the same time, to assess and mutually compare the contributions of random and proportional errors for the mentioned eight recipes for middle-lighness grey target. For this sake, the measured colour changes and scattering of colour in groups of dyed samples corresponding to different recipes (and related perturbation patterns) were analysed and compared with the predicted colour changes and the predicted scattering.

SIMULATING THE EFFECT OF STRENGTH ERROR

In match prediction calculations and in laboratory dyeing of polyacrylic the following basic dyes and their optical data were used:

Maxilon Gelb 5GL 300%	(in tables: Y)	Maxilon Rot 2GL-N 200%	(in tables: J)
Maxilon Goldgelb GL 200%	(in tables: G)	Maxilon Blau GRL 300%	(in tables: B)
Maxilon Rot GRL 180%	(in tables: R)	Maxilon Marinenblau FRL 200%	(in tables: M)
Maxilon Rot MRL 200%	(in tables: K)	Maxilon Schwarz	(in tables: C).

The producer assures the strength of all batches of any particular basic dye to be within ±5% of the declared value. Under assumption that the strength deviations of batches are distributed normally, it follows that the above 5% strength deviation represent about three standard deviations of the normal distribution mentioned. Consequently, standard strength error of each particular dye was assessed to (1/3)x5% ≈ 1,7%.

In each three-dye recipe (c_1, c_2, c_3) considered the perturbations Δc_1, Δc_2, Δc_3 of initial dye concentrations c_1, c_2, c_3 corresponding to a 1,7% strength error were determined:

$$\Delta c_1 = 0{,}017\, c_1, \qquad \Delta c_2 = 0{,}017\, c_2, \qquad \Delta c_3 = 0{,}017\, c_3 .$$

The dye concentrations c_1, c_2, c_3 in the recipe were simultaneously changed according to the following pattern (see Oulton and Chen[5]) to get 27 different combinations of perturbations Δc_i, i=1,2,3:

	c_1	c_2	c_3		c_1	c_2	c_3		c_1	c_2	c_3		c_1	c_2	c_3		c_1	c_2	c_3
1.	+	0	0	7.	+	+	0	13.	−	+	+	19.	0	+	−	25.	+	+	+
2.	0	+	0	8.	+	0	+	14.	+	−	+	20.	0	−	+	26.	−	−	−
3.	0	0	+	9.	0	+	+	15.	+	+	−	21.	+	0	−	27.	0	0	0
4.	−	0	0	10.	−	−	0	16.	+	−	−	22.	−	0	+				
5.	0	−	0	11.	−	0	−	17.	−	+	−	23.	+	−	0				
6.	0	0	−	12.	0	−	−	18.	−	−	+	24.	−	+	0				

The sign + signifies a positive change Δc_i, sign − signifies a negative change ($-\Delta c_i$) and 0 means, that the concentration of the i-th dye is not changed. The above perturbation pattern simulates the combined effect of strength errors of individual dyes in the amount of one standard deviation. The 27 colour changes and corresponding CMC(2:1) colour differences $\Delta E_{\mathrm{k,\,predicted}}$ resulting from this pattern were predicted. The root mean square colour difference:

$$\sigma_{\mathrm{j}} = \sigma_{\mathrm{j,\,predicted}} = \sqrt{\frac{1}{26}\sum_{\mathrm{k}=1}^{27} \Delta E^2_{\mathrm{k,predicted}}}$$

represents the standard deviation of predicted colour positions resulting from the above perturbation pattern for individual dye concentrations in j-th recipe (j=1,2,...8). The value σ_{j} is a measure of the sensitivity of the j-th recipe to the standard strength error (which is in our case 1,7%). Further, the numbers $\sigma_1, \sigma_2, \ldots, \sigma_8$ will be used to mutually compare the sensitivities of the eight recipes to the strength errors.

After the described prediction had been made, physical samples were produced in laboratory dyeing. For each of eight recipes (three-dye combinations) for target Grey 50, eight repeated dyeings according to original non-perturbed recipe were carried out first. In this way, the amount of the experimental noise (which included also the effect of random concentration error) was assessed. Then 27 samples were dyed with the same three-dye combination according to 27 perturbations (of the original recipe) in the above presented manner for 1,7% strength error. The colour of the obtained samples was measured and the standard deviation $\sigma_{\mathrm{j,\,experimental}}$ of these colour positions was calculated in the usual way:

$$\sigma_{\mathrm{j,\,experimental}} = \sqrt{\frac{1}{26}\sum_{\mathrm{k}=1}^{27} \Delta E^2_{\mathrm{k,experimental}}}$$

where $\Delta E_{\mathrm{k,\,experimental}}$ is the colour difference between the colour of actual sample and the centroid (average) of colour positions of 27 samples corresponding to the particular dye combination. The experimentally obtained standard deviations $\sigma_{1,\text{experimental}}$, $\sigma_{2,\text{experimental}}$, ..., $\sigma_{8,\text{experimental}}$ of colour were compared mutually as well as to the predicted standard deviations $\sigma_{1,\text{predicted}}$, $\sigma_{2,\text{predicted}}$, ..., $\sigma_{8,\text{predicted}}$.

In the same way, 27 samples per each of the eight mentioned three-dye combination were produced according to the perturbation scheme for 3,4% strength error (3,4% = two standard strength errors). Again the scattering of colour positions of samples was evaluated by the standard deviation of colour positions of 27 samples.

Note also, that the maximum of the 27 colour deviations ($\Delta E_{k,\text{predicted}}$)$_j$ resulted from the perturbation pattern of a particular j-th recipe for the maximal permissible 5% strength error represents the worst-case error of recipe colour originating solely from strength errors of the basic dyes treated.

RESULTS AND DISCUSSION

In Table I the data related to eight recipes matching the neutral grey target with lightness L^*=50 are presented. The recipes – dye combination is indicated by a short three-letter designation – are displayed in the order of their increasing sensitivities s_1, s_2,..., s_8 to random (weighing) error[2]. According to each of these eight recipes eight repeated dyeings were carried out in order to assess the experimental noise – the scattering of recipe colour due to errors, different from the strength error (e.g. random weighing error, etc.). The standard deviations of that scatter are presented in the fourth row of Table I. With the exception of the biggest value 0,34 unit all remaining values range from 0,23 to 0,28 CMC(2:1) unit. Therefore, in the case of these eight recipes for middle-lightness grey target the differences in predicted sensitivities s_j to random weighing errors had no impact on repeatability of the recipe colour.

In the fifth row of the table the predicted standard deviations $\sigma_{j,\text{predicted}}$ are displayed, each of them represents a measure for sensitivity of the recipe colour to 1,7% strength errors. Big differences among particular values $\sigma_{1,\text{predicted}}$, $\sigma_{2,\text{predicted}}$, ..., $\sigma_{8,\text{predicted}}$ can be seen. The standard deviation $\sigma_{1,\text{predicted}}$=0,12 unit for the Recipe 1 is exceptionally low. The two biggest standard deviations $\sigma_{7,\text{predicted}}$=0,89 and $\sigma_{5,\text{predicted}}$=0,80 correspond to recipes 7 and 5, respectively. The remaining five recipes produce the standard deviations $\sigma_{j,\text{predicted}}$ between 0,46 and 0,56 unit. Therefore, the Recipe 1 is the least sensitive to strength errors, the recipes 7 and 5 are the most sensitive to strength errors, the remaining five recipes are almost equally sensitive to strength errors.

Regarding the main question of this research we see that the regular increasing of the predicted values s_1, s_2,..., s_8 is not followed by a systematic increase or decrease in predicted values $\sigma_{1,\text{predicted}}$, $\sigma_{2,\text{predicted}}$, ..., $\sigma_{8,\text{predicted}}$. Recipe 1 is least sensitive to both random (weighing) and proportional (strength) errors and the two most sensitive recipes to strength errors are among more sensitive ones to random weighing errors. But at the other hand, Recipe 8, which is the most sensitive to weighing errors, is slightly less sensitive to strength errors than Recipe 2, which is second least sensitive to weighing errors. We conclude that there is no clear linear correlation between the predicted sensitivities s_j to random (weighing) errors and the predicted sensitivities $\sigma_{j,\text{predicted}}$ to proportional (strength) errors.

In the sixth row of Table I the experimentally produced standard deviations $\sigma_{1,\text{experimental}}$, $\sigma_{2,\text{experimental}}$, ..., $\sigma_{8,\text{experimental}}$ of colour in 27-member groups of samples produced according to perturbation schemes for 1,7% strength error are presented. Due to experimental noise, the experimentally obtained standard deviations $\sigma_{j,\text{experimental}}$ slightly differ from the predicted standard deviations $\sigma_{j,\text{predicted}}$, but they are roughly consistent with the predicted standard deviations in the following sense: again Recipe 1 produced the lowest experimental standard deviation $\sigma_{1,\text{experimental}}$=0,36, and again no experimental standard deviation of colour for 1,7% strength error perturbation scheme was bigger than the experimental standard deviations $\sigma_{7,\text{experimental}}$=0,66 and $\sigma_{5,\text{experimental}}$=0,71 related to recipes 5 and 7, respectively. Keeping in mind that the standard deviation of colour of repeated dyeings (see the fourth row in Table I) was between 0,23 and 0,34 CMC(2:1) unit, we can see that for Recipe 1 the scattering of colour due to 1,7% strength error, assessed by the number $\sigma_{1,\text{predicted}}$=0,12 represents a minor part of the total experimental scattering evaluated by $\sigma_{1,\text{experimental}}$=0,36. On the other hand, in cases of recipes 7 and 5, the scattering due to 1,7 % strength error (assessed by $\sigma_{7,\text{predicted}}$=0,89 and $\sigma_{5,\text{predicted}}$=0,80) is responsible for the major part of the experimental scatterings (evaluated by $\sigma_{7,\text{experimental}}$=0,66 and $\sigma_{5,\text{experimental}}=0{,}71$) produced by perturbations of recipes 7 and 5, respectively. This feature will be even more evident and expressive in the case of perturbation scheme for 3,4% strength error.

The maximal deviations $\max\{(\Delta E_k)_j; 1 \le k \le 27\}$ resulting from the perturbation patterns (for 1,7% strength error) of particular recipes are presented in the seventh row of Table I. They vary in the same way as the predicted sensitivities $\sigma_{j,\text{predicted}}$ do, individual $(\max \Delta E_k)_j$ can be up to 70% bigger than the corresponding value $\sigma_{j,\text{predicted}}$. The lowest of them is $(\max \Delta E_k)_1=0{,}15$ unit, the biggest two are $(\max\ \Delta E_k)_7=1{,}32$ and $(\max \Delta E_k)_5=1{,}16$. The remaining five $(\max \Delta E_k)_j$ are similar to each other, they lie between 0,79 and 0,91 unit.

The properties of normal distribution imply that the 95% of all batches of basic dyes should be within average ± 2 standard deviations of the related normal distribution, that is, within $100\% \pm 3{,}4\%$ of the declared strength. The predicted sensitivities to 3,4 % strength error for the eight considered recipes are presented in the eighth row of Table I. They are doubled values $2\sigma_{j,\text{predicted}}$ of the values $\sigma_{j,\text{predicted}}$ from the fifth row of the table. The corresponding experimental standard deviations $\sigma_{j,\text{experimental}}$, which resulted from the perturbation scheme for 3,4% strength error, are presented in the ninth row of Table I. With the exception of cases of recipes 1, 3 and 8, they are roughly doubled values of the corresponding experimental standard deviations for 1,7% strength error, presented in the sixth row of the table. It is important to see that in the case of Recipe 1 the predicted contribution of 3,4% strength error (evaluated as $\sigma_{1,\text{predicted for } 3.4\%}=0{,}23$) is at the same level as the estimate 0,23 CMC(2:1) unit for experimental noise. For all remaining recipes, the experimental standard deviations $\sigma_{j,\text{experimental}, 3.4\%}$ range between 0,84 and 1,34 unit of colour difference and are thus three or more times bigger than the estimated experimental noise with the standard deviations ranging from 0,23 to 0,34 unit. Therefore, in the case of 3,4% strength errors, both predicted and experimental scattering of colour (resulting from a perturbation pattern) indicate, that with the exception of Recipe 1 the contribution of strength errors represents the vast majority of the total scattering of colour. Thus it would be of interest to note this obvious advantage of Recipe 1 in advance.

The maximal deviations $(\max \Delta E_k)_j$ resulted from the perturbation patterns for 3,4% strength error are presented in the last row of the table. They are doubled values from the seventh row, corresponding to 1,7% strength error.

Table I. *The predicted and experimental sensitivities to 1,7% and 3,4% strength error in regard to the predicted sensitivities to random weighing errors of eight recipes for neutral grey target with lightness L*=50. Standard deviations of colour are expressed in CMC(2:1) units of colour difference.*

1	Recipe number j	1	2	3	4	5	6	7	8
2	Dye combination	BCJ	BGJ	YBJ	GMJ	YRB	RGM	YBK	GKM
3	Predicted sensitivity s_j (to random concentration errors)	**238**	**309**	**330**	**372**	**506**	**589**	**657**	**747**
	Standard deviation of repeated dyeings	0,23	0,25	0,28	0,27	0,34	0,23	0,23	0,26
5	Predicted standard deviation $\sigma_{j,\text{predicted}}$ (predicted sensitivity to 1,7% strength errors)	**0,12**	**0,52**	**0,53**	**0,46**	**0,80**	**0,56**	**0,89**	**0,50**
6	Experimental std. deviation $\sigma_{j,\text{experimental}}$ (for 1,7% strength error)	**0,36**	**0,48**	**0,66**	**0,48**	**0,71**	**0,48**	**0,66**	**0,64**
7	Predict. $(\max \Delta E_k)_j$ for 1,7% strength error	0,15	0,90	0,87	0,79	1,16	0,91	1,32	0,81
8	$2\sigma_{j,\text{pred.}}$ (sensitivity to 3,4% strength error)	**0,23**	**1,04**	**1,06**	**0,92**	**1,60**	**1,12**	**1,78**	**1,00**
9	Experimental std. deviation $\sigma_{j,\text{experimental}}$ (for 3,4% strength error)	**0,48**	**0,95**	**0,90**	**0,84**	**1,34**	**0,97**	**1,21**	**0,95**
10	Predict. $(\max \Delta E_k)_j$ for 3,4% strength error	0,29	1,80	1,74	1,59	2,32	1,82	2,62	1,62

Values from rows 3, 4, 5, 6, 8, 9 of Table I, which describe the relation between recipe colour sensitivity to strength and to weighing error, are presented graphically in Fig. 1.

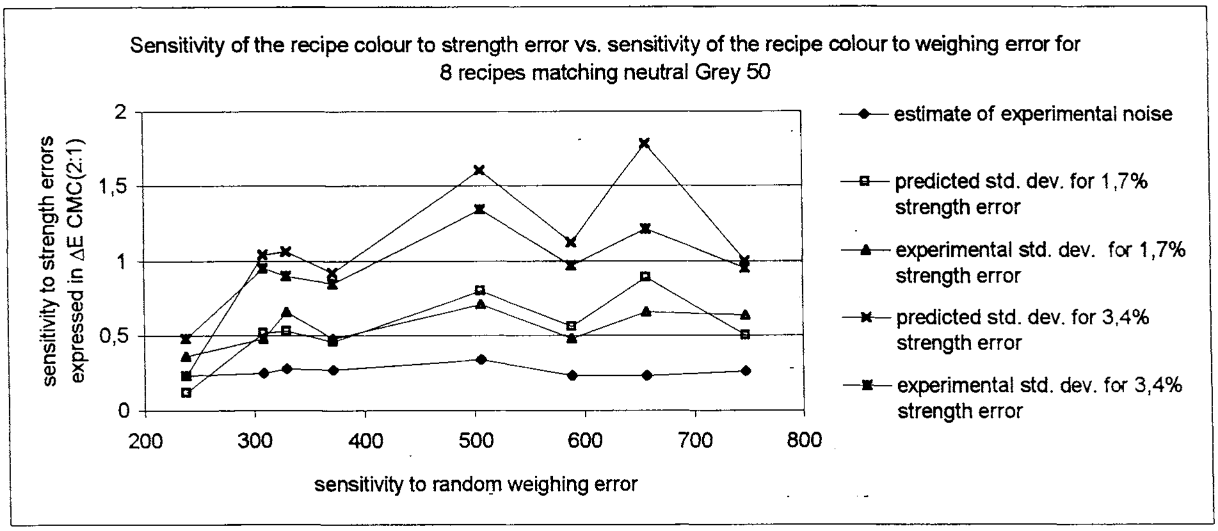

Fig. 1. Predicted and experimental sensitivities of the recipe colour to 1,7 and 3,4% strength errors (i.e. standard deviations of colour resulting from perturbation schemes for 1,7 and 3,4 % strength errors) in regard to the sensitivity of the recipe colour to weighing errors for 8 recipes matching neutral grey with lightness L=50.*

SUMMARY

The recipes for mid-lightness neutral grey target exhibited a large variation in predicted sensitivities of their colour to strength errors – the sensitivity of the most sensitive recipe was more than 7-times bigger than the sensitivity of the least sensitive one. The worst-case colour error originating solely from 3,4% strength error for the least sensitive recipe is only 0,29 CMC(2:1) unit, but for the most sensitive recipe it reaches the value of 2,62 CMC(2:1) unit. Although the recipe, least sensitive to weighing errors, was also least sensitive to strength errors, no clear linear correlation between the predicted sensitivities s_j to random (weighing) errors and the predicted sensitivities $\sigma_{j,\text{predicted}}$ to proportional (strength) errors was observed.

For all eight three-dye combinations treated laboratory dyeings were carried out according to the same perturbation schemes as used in predictions. The scattering of colour in obtained groups of samples was, generally, in accordance with the predicted standard deviations resulting from perturbation schemes for particular recipes. Experimental results confirmed the above observation about the lack of correlation between sensitivities of the recipe colour to weighing and strength errors.

It was possible to find the recipe where the standard strength error (1,7% in the case considered) produced the scattering of colour, which was smaller than the estimated experimental noise. For the remaining recipes, the impact of 1,7% strength error was equal to or bigger than the estimated experimental noise. At 3,4% level of strength error for the best recipe, the contribution of strength error and experimental noise were nearly the same, in cases of remaining recipes the contribution of strength error to total scattering of colour was essentially (up to four times) bigger than the experimental noise.

CONCLUSIONS

In the case of recipes for mid-lightness grey target, experimental results confirmed the prediction about the lack of correlation between sensitivities of the recipe colour to weighing and strength errors. The contribution of standard strength error (1,7% for basic dyes on acrylic) to total colour error was usually at least equal to or even bigger than the contribution of all other experimental errors. The recipe with the smallest predicted sensitivity to strength errors performed clearly best at both 1,7% and 3,4% level of strength error, for this particular recipe the contribution of 1,7% strength error was even lower than the experimental noise.

References

1. D. H. Alman, *Color Res. Appl.*, **11** (1986), 153-159.
2. B. Sluban and J. H. Nobbs, *Color Res. Appl.*, **20** (1995), 226-234.
3. B. Sluban and O. Šauperl, 19th IFATCC Congress, Paris (2002) (CD-ROM)
4. B. Sluban and O. Šauperl, 3rd AUTEX Conference, Gdansk (2003), to appear
5. D. P. Oulton and P. Chen, J.S.D.C., **111** (1995) 237-244

Color Terms and the Concept of Color of the Thais in the Sukhothai Period and at the Present Time

Supamas Engchuan
Department of English, Faculty of Liberal Arts
Thammasat University, Thailand
E-mail: fujianman@hotmail.com

Introduction

"Color" is a phenomenon which every human being in every ethnic group, in every language, encounters and senses by his visualization. The study of color appeals to scholars in various disciplines namely; scientists, psychologists, neurologists, ethnologists, as well as linguists. Researchers on different aspects of color then have been carried out by those aforementioned scholars.

According to the beliefs put forth by the ethnolinguists, "color terms" are good examples of linguistic items from which the speakers' worldviews are reflected. People living together in one place, sharing the same culture, speaking the same language, perceive the same color categories as encoded in their language. In contrast, people, living in different places, possessing different cultures, speaking different languages, differently categorize the color in the world around them. What is implied here is that the color words unveil how the people view the world around them and how they categorize their experience.

Previous studies of color terms

The earliest ethnolinguistic study of color is marked by the study of Hanunoo color categories carried out by Harold D. Conklin (1955). The study aimed at categorizing colors from the point of view of the native speaker of a language.

The study revealed that four basic color terms exist in Hanunoo. They are:

1. (Ma) bi:ru = dark color referring to black, violet, indigo, blue, dark green, dark grey, etc.
2. (Ma) lagti? = bright color referring to white and many light colors.
3. (Ma) rara? = reddish color referring to maroon, red orange and yellow.
4. (Ma) latuy = greenish color referring to light green, yellow and light hrown.

(The translation of each color term is taken from Prasithrathsint (1995))

Brightness and freshness are two dimensions of contrast used in distinguishing the above four colors.

Besides Conklin's work, the most significant work which may be regarded as the prototypical research on color and as the catalyst of the following researches is the work of Berlin and Kay (Berlin and Kay 1969) They published their work in the hook entitled "Basic Color Terms : Their Universality and Evolution."

This book presents the findings of unrelated language families. Around 329 color chips from the Munsell Color Company glued on stiff cardboard were used plus the researchers' interview with the native speakers of those languages.

From the findings of Berlin and Kay's study, the following scale of color evolution, which they call an implicational scale is derived:

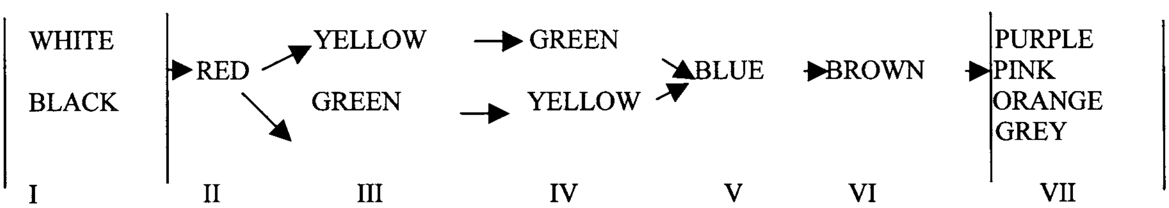

Figure 1 Implicational Scale of Color Evolution (adapted from Berlin and Kay 1969)

In 1975, based on his later study, Kay (Kay 1975) himself adjusted the theory by proposing GRUE (GREEN/Blue) category on the scale proposed in 1969. The category called Grue might emerge before or after YELLOW as the following adjusted scale shows:

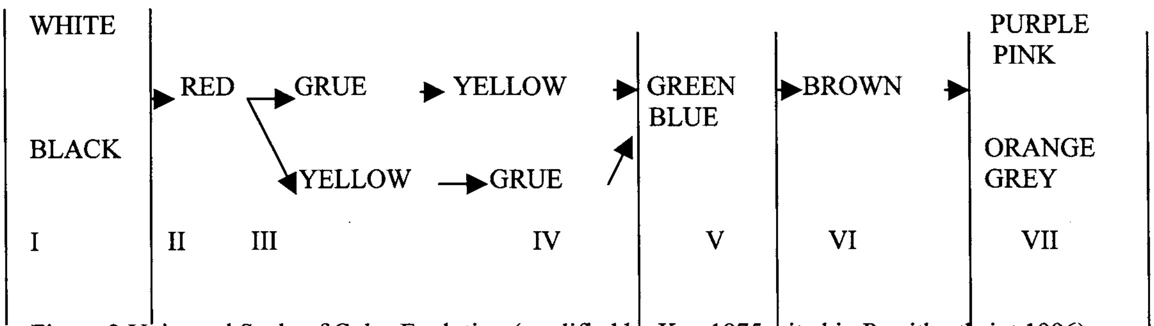

Figure 2 Universal Scale of Color Evolution (modified by Kay 1975, cited in Prasithrathsint 1996).

Kay and McDaniel (Kay and McDaniel 1978),later in 1978, introduced the use of fuzzy set theory into the study of basic color categories. They showed that the meanings of color display substantial linguistic universals and that these semantic universals are based on pan-human neuro-physiological processes in the perception of color. They also suggest that these human processes are the basic of the universal patterns in the meanings of basic color terms.

Purpose and Hypothesis

The main purpose of this study is to analyze the basic color terms, the boundaries and foci of the basic color categories, the change in color categorization and concept, as well as the non-basic color terms in the Sukhothai period and at the present time.

In carrying out this research, I hypothesized that:

1. The number of the basic color terms as well as basic color categories in Sukhothai Thai is less than that of those at the present time.
2. The meanings of the basic color terms in Sukhothai Thai are much more overlapped than those of the basic color terms at the present time.
3. The color boundary of the basic color terms in Sukhothai Thai is broader than that of the basic color terms at the present time.
4. The color conceptualization and the color perception of the present day Thai are not different.

Procedures

The procedures used in this study are divided into 2 processes:

1) Data gathering and 2) Data analysis.

<u>1) Data gathering</u>

The data used in this study are from 3 sources : those in Sukhothai Thai are from all available literatures left while those at the present time are from sampling literatures as well as those from the present day Thai informants.

<u>2) Data analysis</u>

In analyzing the data from both periods, the researcher separated those data into two groups: the basic color terms and the non-basic color terms.

For the basic color terms, they were analysed in order to find out their linguistic structures, their metaphorical objects, their evolution as well as their boundaries.

<u>Basic color terms in Sukhothai Period and in the present-day Thai</u>

<u>Color Evolution</u>

The analysis shows that those five basic color terms evolution in Sukhothai Thai, WHITE, BLACK, RED YELLOW and GREEN may color as WHITE, BLACK in stage I, RED in stage II, YELLOW in stage III, and GREEN in stage IV respectively as the figure 3 shown below:

WHITE BLACK	→	RED	→	YELLOW	→	GREEN
I		II		III		IV

Figure 3. Five basic color terms evolution in Sukhothai

while those twelve basic color terms in the present-day Thai may occur as WHITE, BLACK in stage I, RED in stage II, YELLOW in stage III, GREEN in stage IV, BLUE (ฟ้า /น้ำเงิน) in stage V, BROWN in stage VI, and PURPLE, PINK, ORANGE and GRAY in stage VII respectively as the figure 4 shown below:

WHITE BLACK	→	RED	→	YELLOW	→	GREEN	→	BLUE	→	BROWN	→	PURPLE PINK ORANGE GRAY
I		II		III		IV		V		VI		VII

Figure 4. Twelve basic colour terms in the present day

Speaking about the color evolution, it might be that those basic color terms in Sukhothai and in the present day Thai occur in the same stages as Berlin and Kay proposed.

Color Boundaries and Foci of Basic color Categories

The analyses of the boundaries and the foci of the basic color categories in Sukhothai period and in the present day Thai, by the support of the scientific equipments, show that, in Sukhothai period, as shown in a figure 5, the boundary of each basic color category is different. The boundary of GREEN is the largest while that of WHITE is the narrowest. It is very interesting to note that the boundary of GREEN, which should be in the GREEN area, is in PURPLE area. This may be assumed that the boundary of GREEN might cover the areas of GREEN, BLUE, and PURPLE. About the foci, it is shown that the foci of each basic color category is in its color boundary except that of GREEN which is in PURPLE boundary.

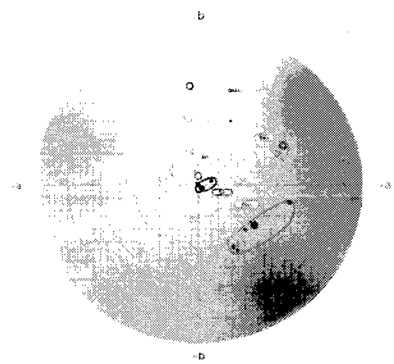

Figure 5. The boundaries of basic color categories in Sukhothai

At the Present time, as shown in the figure 6: it shows that most basic color categories have boundaries in their own color areas while those of some are overlapped. For their foci, all of them have their foci in their own color boundaries.

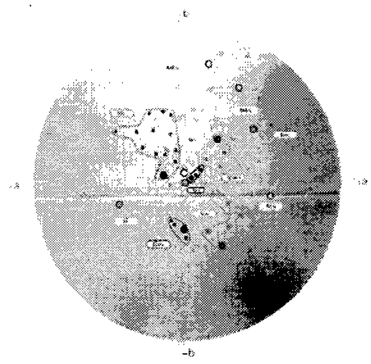

Figure 6. The boundaries of basic color categories in the present day

In addition to the boundaries and foci of the basic color categories in the present day Thai derived from the metaphorical expressions above, their boundaries and foci are also elicited from the present Thai informants as shown in Figure 7:

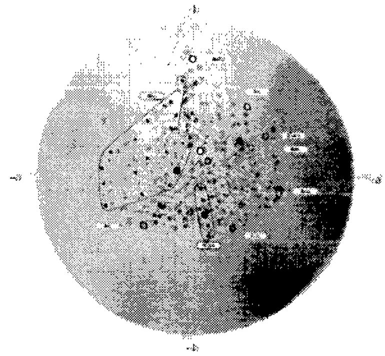

Figure 7. The boundaries of basic color categories in the present day, derived from the metaphorical expressions

This kind of study shows that the boundaries of twelve basic color categories are intensely overlapped. This supports the fussy set theory of Paul Kay and Chad McDaniel (Kay and MC Daniel, 1978 in Prasithrathsint 1995) that color has no boundary. The foci of all basic color categories exist within their own color boundaries.

When compared with those color boundaries and foci of the color categories derived from the metaphorical expressions, it can be seen that there exists a similarity. The color boundaries and foci of basic color categories of both studies are in their own color areas. This confirms that those derived from the metaphorical expressions and those elicited from the informants in Sukhothai period might not be different.

Besides, when comparing the color boundaries and foci of the basic color categories derived from the metaphorical expressions in Sukhothai period and at the present time, it can be seen that the color boundaries are in their own color areas and the color foci exist in their own color boundaries in both periods. The difference is that the boundary of GREEN in Sukhothai period covers GREEN, BLUE, and PURPLE color areas while that of GREEN in the present day Thai is in its own area.

Conclusion

The analysis of the color terms in Sukhothai period and at the present time unveils that number of basic color terms representing color categories in Sukhothai and in the present day Thai is different. There are five in Sukhothai period while there are twelve in the present day Thai. This shows that color conceptualization of Thais is changed from Sukhothai period to the present time. The meanings of the color terms are also different in both periods.

The boundaries and foci of the basic color terms derived from the metaphorical expression and elicited from the informants in both periods are not different. It then can be assumed that if we had elicited the color terms from the Thai people in Sukhothai period , the color boundaries and foci of those color categories should not have been different from those derived from the metaphorical expressions in such period.

It is very interesting to note that GREEN, a basic color category in Sukhothat period, covers GREEN, BLUE, and PURPLE color areas.

Last but not least, this study shows the significances that the color conceptualization of the Thais has been changed and that the linguistic study can be integrated with the scientific study. That means thing found in culture which is specific can be described by scientific principle which is universal.

REFERENCES

Berlin, Brent and Paul Kay. 1969. Basic Color Terms : Their Universality and Evolution. Berkeley : University of California Press.

Conklin, Harold D. 1955. Hanunoo color categories. Southwestern Journal of Anthropology II (399-44). Also in Hymes, Dell (ed.). 1964. Language in Culture and Society. New Yong : Harper and Row.

Kay, Paul. 1975. Synchronic Variability and diachronic change in basic color terms. Language in Society. 4, 257 – 27.

Kay, Paul and Chad K. McDaniel. 1978. The linguistic significance of the meanings of basic color terms. Language. 54.3 (610 – 646).

Research on Assessing Change in Color of the Road Sign by Colorimetric Evaluation

Ikuko Okamoto [1], Masashi Kobayashi [2] and Wonjong Lee [2]
[1] Osaka Kyoiku University, Osaka, Japan
[2] Osaka-Shoin University, Osaka, Japan

Abstract

There are 13,000,000 road signs in Japan in March, 2000, and they keep increasing now, too. At present, the item about the maintenance of the sign and its control is founded in Japanese Road Traffic Act. But, the control system of the road sign by assessing change in color of the sign isn't established.

As the environment factors concerned with the deterioration of the road sign can be indicated ultraviolet rays, temperature, water, air pollution material, and so on. The influence of the ultraviolet rays is shifted by the direction where a road sign is installed. Therefore, even if it is the signs installed at the same time, it can be thought that the exchange-and repair time of the installed signs is different as the case may be. It is more desirable that the road signs are renewed based on colorimetric evaluation than it's based on the years after they are installed.

We proposed the method of the decision and the standard on assessing change in color of the road sign.

Keywords: *road sign, change in color, color difference, evaluation*

INTRODUCTION

Recently, as for Japan, the number of dead persons of the traffic accident shows a tendency of decreasing. The phenomenon causes such cases as the improvement of the vehicles design technology, the progress of the medical technology and the improvement of the traffic environment of the road. JCASM*[1] has shown a change until 1998 since 1966 about the amount of investment toward the maintenance of the sign and the number of dead persons of the traffic accident [1]. According to the increase of number of the signs the number of dead persons of the traffic accident decreases after 1975 to 60% ± 10% in comparison with 16,765 dead persons at the time of the peak in 1970. The road sign contributes to the traffic safety. The Road Traffic Act has done the additions of the road sign and those revisions abundantly until now. But, there is little description about the color as visual communication in this law. We often see the conditions with road signs which an exchange and repair necessary left.

At present, visual comparison of the color of paints and colorimetry (measurement) are prescribed in the Japanese Industrial Standard JIS K 5600-4-3 (1999) "Testing methods for paints-Part 4: Visual characteristics of film". JPMA*[2] reported a method for specification of color differences for discoloration of coatings in 1994[2]. That report in consideration of the big color difference area proposes equation of color differences (CIELCH) which shows high correlation with the visual evaluation in comparison with CIELAB color difference of the Japanese Industrial Standard.

By using CIELCH we examine some methods in place of the decision method of road signs through the administrator's subjectivity. We paid attention to the red as safety color being used for the sign which means prohibition in road traffic function.

*[1]: *Japan Contractors Association of Traffic Signs and Lane Makings*
*[2]: *Japan Paint Manufacturers Association*

EXPERIMENTS

Colorimeter (CHROMA METER CS-100A, MINOLTA CO., LTD) was used for the purpose of measuring colors. Measurement value was analyzed by the colorimeter control software (V-SCAN CHROMA, NAMOTO Trading Co., LTD). The strength of the ultraviolet rays was measured by using UV radiometer (UM-10, UM-360, MINOLTA CO., LTD) in Sakai City. And, spectral sensitivity of radiation detector was 310nm～400nm. The measurement of Irradiance was done in the fine days to in January, 2002 from August, 2001. We measured irradiance in every one hour to 15:00 from 11:00, and got a mean.
We analyzed color difference by using the standard color and the colorimetric data of the road signs by equation of color differences which were recommended by the JPMA report "Research on the methods for evaluating discoloration of coatings" [2]. Fig.1 shows the attribute of red being used as a standard color of the road sign.

Table 1: *Specification of standard color*

	Munsell HVC	*Y*	*x*	*y*	*L**	*a**	*b**	*C**
Red	7.5R 4/13.5	46.60	0.56	0.33	73.93	81.21	51.82	96.33

We measured the color based on JIS Z 8722 (2000) "Methods of color measurement - Reflecting and transmitting objects ". Furthermore, L*a*b* was calculated by JIS Z 8729 (1994) "Color specification - CIE LAB and CIELUV color spaces". Then, Equations of color differences of CIELCH as the reference were shown. Metric chroma (C^*_1, C^*_2) of the sample 1 and the sample 2 was calculated by using the following Equation *(1)*. ΔL^*, ΔC^*, ΔH^* was calculated by using the following Equation *(2)*, *(3)* and *(4)*.

$$C^*_1 = (a^{*2}_1 + b^{*2}_1)^{1/2} \quad (1)$$
$$\Delta L^* = L^*_1 - L^*_2 \quad (2)$$
$$\Delta C^* = C^*_1 - C^*_2 \quad (3)$$
$$\Delta H^* = S[2(C^*_1 C^*_2 - a^*_1 a^*_2 - b^*_1 b^*_2)]^{1/2} \quad (4)$$

Where $a^*_1 b^*_2 > a^*_2 b^*_1$, $S = -1$. And in the other cases $S = +1$.
ΔE^*_{CH} of color difference was calculated by using the following Equation *(5)*.

$$\Delta E^*_{CH} = [(\Delta L^*)^2 + (\Delta C^*/S_C)^2 - (\Delta H^*/S_H)^2]^{1/2} \quad (5)$$

Where $S_C = 1 + 0.045\, C^*_1$, $S_H = 1 + 0.015\, C^*_1$.

RESULTS AND DISCUSSION

1. Change in color of the road signs

Road signs are important for the smooth traffic and the safety. But, they are in the open air, and deteriorate by ultraviolet rays, heat (temperature), the water, the environment factor such as air pollution material, and so on. Therefore, the control of the sign becomes necessary to maintain the function of that visual communication. Change in color of the road sign varies with the direction where they are installed. Figure 1 shows various signs and that chromaticity and ΔE^*_{CH}. The values of ΔE^*_{CH} of the signs which were established within a year are small like *(c) (g)*. The *Y* values of these signs are low in comparison with the others, and ΔL^* values are small. By the way *(b) (f)* and *(d) (e)* are double-faced type. Furthermore, *(b) (d)* face to the south and *(e) (f)* face to the north. The values of ΔE^*_{CH} of the signs facing to the south are big, and their progress of the deterioration is fast.

Y	1.03E+03
x	0.53
y	0.35
ΔE^*_{CH}	164.6

South-facing (a)

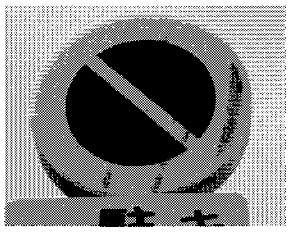

Y	1.32E+04
x	0.36
y	0.36
ΔE^*_{CH}	501.2

South-facing (b)

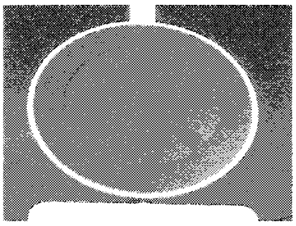

Y	0.32E+03
x	0.44
y	0.32
ΔE^*_{CH}	81.1

South-facing (c)

Y	7.41E+03
x	0.35
y	0.35
ΔE^*_{CH}	397.6

South-facing (d)

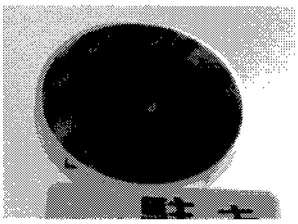

Y	1.96E+03
x	0.43
y	0.32
ΔE^*_{CH}	223.6

North-facing (e)

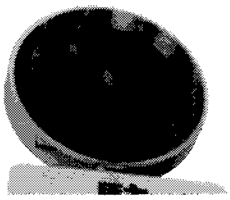

Y	0.54E+03
x	0.42
y	0.30
ΔE^*_{CH}	114.9

North-facing (f)

Y	0.27E+03
x	0.43
y	0.32
ΔE^*_{CH}	71.7

North-facing (g)

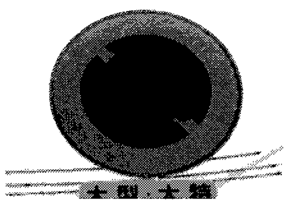

Y	8.63E+03
x	0.38
y	0.37
ΔE^*_{CH}	423.9

West-facing (h)

***Figure1:** Relationship between the direction which the road sign board faces, and change in color*

We measured the strength of the ultraviolet rays which cause discoloration of coatings. Figure2 shows irradiance of the ultraviolet rays in each direction of north and south. The noticeable difference of the value of irradiance is recognized by the direction. Then, values facing to the south have been rising during autumn from summer. As for this measurement period, the irradiance facing to the south shows about 17-20 times in comparison with it facing to the north. Therefore we can say, the environment that road signs are installed, especially the direction influences the exchange time of the signs and repair time. In other words, we should not manage a sign by the years after the establishment and the visual observation, but we think that it should be checked independently by the chromaticity information and those conditions that it was installed.

2. Evaluation of change in color of the road sign

How to indicate a difference in color of the non-luminous object colors by the Japanese Industrial Standard is the same as two kinds of methods (CIELAB, CIELUV) prescribed with CIE. But, as for those color difference formulas, the problem of the conformity is pointed out by the difference in color. And, the conformity of color difference formulas are different from case by case if the cause of change in color depends on the change in hue, or the change in lightness, or the change in chromaticness, and so on. Figure3 shows correlation with Y and ΔE^*_{CH}. Change in color of the road signs appears as the rise in the Y value and the decline of the x value. The change in chromaticity occurs in the road signs that chalking progresses, too (see *(b)*, *(d)* in Figure1). We think that the simple evaluation of the road signs become possible by Y of the colorimetry data. By the way, it was used the color chip of *7.5R 4/13.5* in this research. Therefore, the difference in Y value of the standard color and the test colors grow big, and the value of ΔE^*_{CH} are grow up consequently, too. The examination when it is based on the road sign's own initial color is a coming subject.

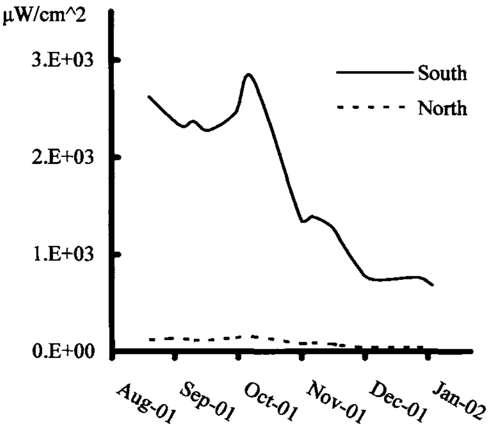

Figure2: *The amount of ultraviolet rays in the northern and the southern direction*

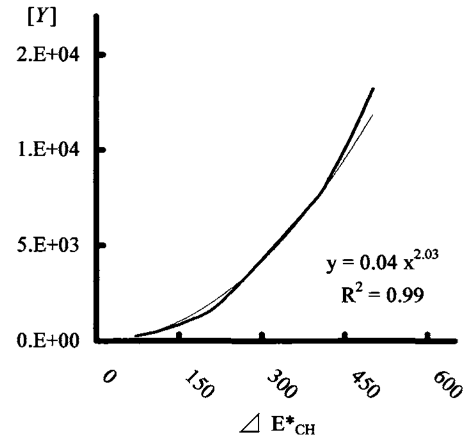

Figure3: *Correlation of Y with* ΔE^*_{CH}

CONCLUSIONS

We examined the assessment of the change in color of the road sign by colorimetric evaluation. Change in color of the road sign varies in the direction where they are installed. The values of ΔE^*_{CH} of the signs facing to the south are big, and their progress of the deterioration is fast. We should not manage a sign by the years after the establishment and the visual observation, but we think that it should be checked independently by the chromaticity information and those conditions that were installed. Correlation is recognized as Y and ΔE^*_{CH}. Change in color of the road signs appears as the rise in the Y value and the decline of the x value. Therefore, the examination when it is based on the road sign's own initial color is a coming subject.

ACKNOWLEDGEMENT

The authors gratefully acknowledge the invaluable assistance of Mr. Daisuke Yamamoto.

REFERENCE

[1] http://www.zenhyokyo.or.jp/gate.html

[2] Japan Paint Manufacturers Association, *Research on the methods for evaluating discoloration of coatings, Report* (1994)

Prof. Dr. Ikuko OKAMOTO, Osaka Kyoiku University, Faculty of Education, Department of Arts and Sciences, 4-691-1 Asahigaoka, Kashiwara, Osaka 582-8582, Japan. Phone, +81-729-78-3602, E-mail: okamoto@cc.osaka-kyoiku.ac.jp

Associate Prof. Dr. Masashi KOBAYASHI, Osaka-Shoin University, Faculty of Arts and Science, Department of Clothing, 4-2-26 Hishiya Nishi, Higashi-Osaka, Osaka 577-8550, Japan. Phone, +81-6-6723-8227, Fax: +81-6-6723-8227, E-mail: kobayashi.masashi@osaka-shoin.ac.jp

Dr. Wonjong LEE (Research worker), Osaka-Shoin University, Faculty of Arts and Science, Department of Clothing, 4-2-26 Hishiya Nishi, Higashi-Osaka, Osaka 577-8550, Japan. Phone, +81-6-6723-8227, Fax: +81-6-6723-8227, E-mail: wlee@livedoor.com

Proposal for standardization of object-color

Hiroaki SOBAGAKI
Joshibi University of Art and Design

1. Introduction

Munsell color atlas is widely used as a standard for object-color. Colorimetric values (x, y, Y) of Munsell Color Order system are specified by CIE standard illuminant C and CIE 1931 standard colorimetric observer. Japanese Industrial Standard, JIS Z8721 (Colour specification – Specification according to their three attributes) also utilizes Munsell Color Order system as standard for object-color.

In color related industries, CIE standard illuminant D65 simulators are used rather than CIE standard illuminant C. With this tendency, colorimetric values (x, y, Y) of Munsell Color Order system under CIE standard illuminant D65 has been requested from color industries.

The author would like to propose of colorimetric values (x, y, Y) of Munsell Color Order system with respect to CIE standard illuminant D65 and CIE 1964 supplementary standard colorimetric observer.

2. Method

All the measured spectral reflectance distributions on the JIS Z8721 Standard Color Atlas [1] were kindly supplied from the Japan Color Research Institute.

2.1 Sample

(1) Number of sample : 1,569.
(2) Range of wavelength : 400nm – 700nm.
(3) Wavelength interval : 10nm.
(4) Munsell Hues (40) : 2.5R, 5R, 7.5R, 10R, 2.5YR, 5YR,..., 7.5RP, 10RP.
(5) Munsell Value (8) : 2, 3, 4, 5, 6, 7, 8, 9.
(6) Munsell Chroma(8) : 2, 3, 4, 6, 8, 10, 12, 14.

2.2 Analysis

The principal component analysis was applied to all the measured spectral reflectance distributions. The analysis was made for each of five color groups R, Y, G, B and P by the Munsell principal hues. Figure 1 shows the color group and the range of Munsell hues. The color group R includes all the colors with Munsell hue notation from 2.5RP, through 5R, to 7.5YR.

Average and three eigen vectors were extracted from each of the five color groups. Table 1 shows the cumulative contribution factors on the first three components. They are always above 99.5% and quite high.

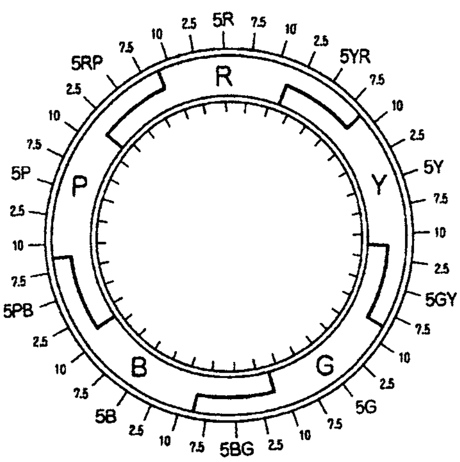

Fig.1 Color group and its range of Munsell hue.

Table 1 Contribution of the extracted component for each color group.

Color group	Contribution of each component(%) R1	R2	R3	Cumlative contribution(%)
R	85.3	12.2	2.0	99.5
Y	87.6	9.3	2.9	99.8
G	91.8	5.5	2.3	99.6
B	94.3	3.8	1.7	99.8
P	90.9	6.9	1.7	99.5

3. Results

Figure 2 shows the average and three eigen vectors of color group R. By use of an average and three eigen vectors, detailed calculation method of the spectral reflectance distributions with specified Munsell notation and tristimulus values refer to the reference [2]. Figure 3 shows comparison between measured and estimated spectral reflectance distributions. Real line corresponds to measured and real line with • symbol corresponds to estimated spectral reflectance distributions. (a): 5Y 5/6, (b): 5P 5/8.

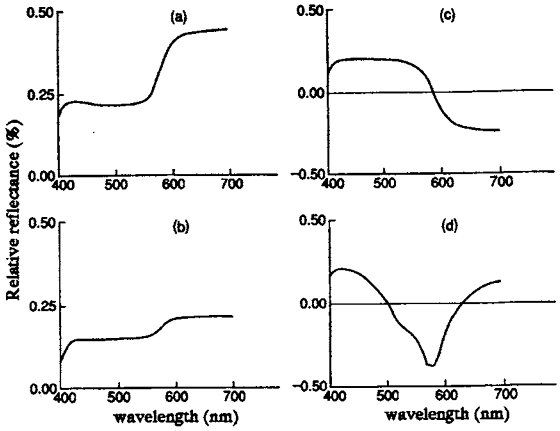

Fig.2 Average and three eigen vectors of color group R.
(a) Average, (b) First, (c) Second, and (d) Third eigen vector.

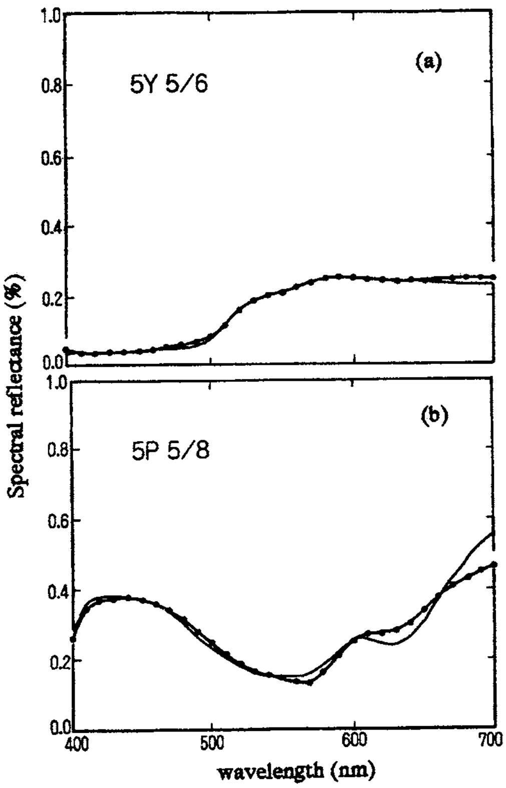

Fig.3 Comparison between measured (real line) and estimated (● symbol) spectral reflectance distributions.

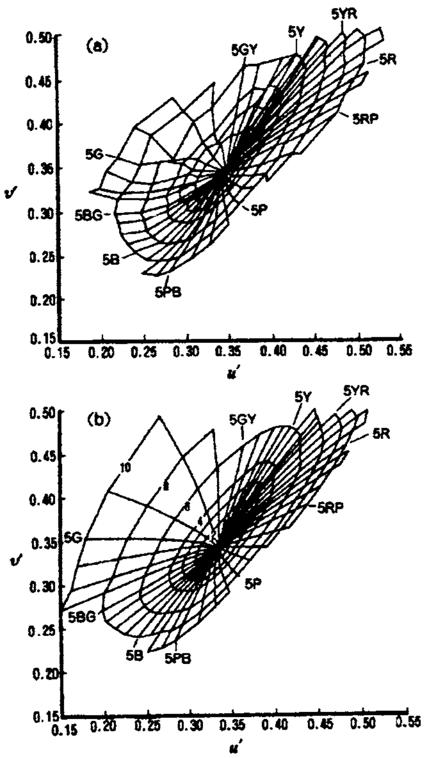

Fig.4 Equi-hue and chroma locus with Munsell value 5/
Upper figure corresponds to the measured spectral reflectance distribution and lower figure corresponds to the estimated ones.

Figure 4 shows equi-hue and equi-chroma locus with Munsell value 5/. These figures obtained with respect to Thornton's theoretical spectral power distribution, spectral reflectance distributions of Munsell colors and CIE 1931 standard colorimetric observer. The upper figure was computed by the measured spectral reflectance distribution of Munsell colors. The lower figure was computed by the estimated spectral reflectance distributions of this method. The above results suggest that the average and three eigen vectors are made in the estimated of spectral reflectance distribution of Munsell colors

4. Discussion

In the actual color gamut, the spectral reflectance distribution $\rho(\lambda)$ of Munsell colors could be estimated by use of the average and three eigen vectors. So, the author tried to estimate the spectral reflectance distribution (abbreviated as SRD from here) of Munsell colors in the whole of color gamut of the Munsell Color Space. However, the estimated SRDs did not satisfy an object-color condition $(0 \leq \rho(\lambda) \leq 1)$ in the highly saturated Munsell colors. Therefore, the author devised a calculation algorithm to estimate the SRD of highly saturated Munsell colors. The basic idea of the calculation algorithm uses the SRD of highly saturated color (a), that of the semi-optimal color (b), and that of achromatic color (c). Figure 5 shows schematically the basic idea of the algorithm. SRDs of highly saturated color could be estimated due to linear combination of the above three kinds of SRDs. Refer to reference [3] for the detailed calculation procedure. By using the above estimated SRDs, the tristimulus values of all Munsell colors were computed by use of CIE standard illuminant D65 and CIE 1964 supplementary standard colorimetric observer.

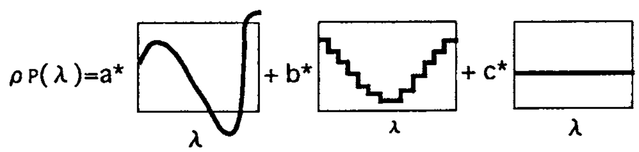

Fig.5 Basic idea of calculation algorithm by linear combination of three kinds of spectral reflectance distributions.

Figure 6 shows equi-hue and equi-chroma locus under CIE standard illuminant D65 with Munsell value 5/.

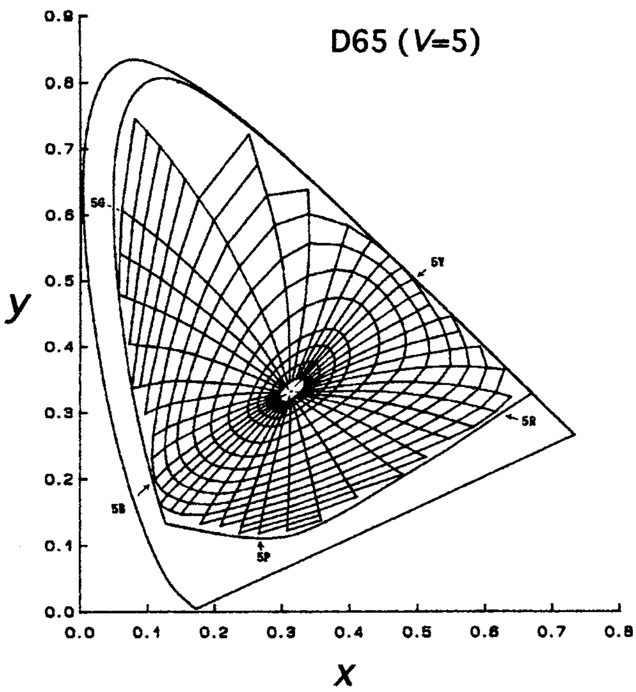

Fig.6 Equi-hue and chroma locus under CIE standard illuminant D65 with Munsell value 5/.

5. Conclusions

1) The author proposed a method for deriving the SRDs for highly saturated colors.
2) The SRDs of all the colors in Munsell Color Order system were estimated by use of the proposed method.
3) We defined the chromaticity coordinates of the colors in the Japanese Industrial Standard JIS Z8721 under CIE standard illuminant D65.

Reference

[1] "Standard Color Atlas (Glossary)" of Japanese Industrial Standard JIS Z8721 (1977).

[2] H. Sobagaki, K. Takahama, and Y. Nayatani: Estimation of spectral reflectance functions for Munsell renotations, AIC COLOR89, Vol.II, pp156-158(1989).

[3] H. Sobagaki and K. Takahama: Estimation of spectral reflectance distributions of highly saturated colors in Munsell Color Order system, J. Light & Vis. Env., Vol.82, No.11, pp902-916(1998).

Making Evaluation Prediction Model of Interior Finishing Materials by CG

Jin - Sook Lee, Eun – Mi Jin, You – Mi Park

1. INTRODUCTION

This paper is to figure out evaluation charateristics according to kinds and colors of finishing materials of image types for interior area planning, to make prediction model for its application, and based on that, to increase up pleasantness of interior area using proper finishing materials on planning interior area.

The concrete processes are as follows: On 1st step, as the classification step of finishing materials used mainly in interior, we selected finishing materials used mainly in interior based on a previous research, conducted color survey with real samples of selected finishing materials, and understood the color range used now according to finishing materials. On 2nd step, as the step of evaluation experiment, we carried out evaluation experiment using CG(Computer Graphics) based on selected finishing materials and researched color. On 3rd step, we figured out evaluation characteristics that evaluation factors or kinds and hue, value, and chroma of finishing materials influenced on image in interior area based on the result of evaluation experiment. On 4th step, we finally made prediction model on the kinds and colors for application on planning interior area.

2. SELECTION & COLOR RESEARCH OF INTERIOR FINISHING MATERIALS

We found that woods, stones, tiles, paintings, bricks, and wallpapers are mainly used in interior area after researching and analysing a previous research on the present condition analysis of finishing materials. Since in terms of double paintings, the suffice quality could be quite different according to the method of construction and paintings, paintings, which named as sprayings in the method of construction, were divided into two things by changing the suffice roughness. Therefore, on this research, woods, stones, tiles, paintings, sprayings, bricks, and wallpapers including 6 finishing materials and sprayings or one of the methods of construction of paintings were selected as interior finishing materials.

Color research checked optical color survy and Chroma Meter, MINOLTA, CR-200 by Munsell Color System with now producing and circulating real samples of finishing materials.

3. EVALUATION EXPERIMENT

This paper produced and conducted an evaluation object by CG with the wall-side which visual effect is so big in the space of less than a certain size among the ceiling, wall, floor as 1st element of space construction since in the research that matched a color and suggested interior mood, the color of wall finishing materials was more important than the color of floor or ceiling finishing materials.

3.1 Evaluation factors

In general, this research took the kinds and colors of finishing materials as evaluation factors because interior finishing materials were expressed by the quality or color of a material itself. Also, color was divided into hue, value, chroma, and the kind of finishing materials, the color of finishing materials, value, and chroma were selected as evaluation factors. Finishing materials were woods, stones, tiles, paintings, sprayings, bricks, and wallpapers used mainly in interior area. Color was selected based on the colors of Table 1 researched in 2.2, and the color was selected after being classified R(Red),YR(Yellow Red), Y(Yellow), GY(Green Yellow), G(Green), BG(Blue Green), B(Blue), PB(Purple Blue), P(Purple), RP(Red Purple), and N(Neutral) as color, high value (7~10), middle value(4~6), and low value(0~3) as value, and high chroma(more than 8), middle chroma(4~7), low chroma(0~3) based on Munsell Color System.

3.2 Evaluation object

Evaluation object produced total 180 things as a way to change finishing materials and color on the wall-side of interior perspective area(Scale1/20) of 4,800 X 6000 X 2700 using CG. The example of evaluation object is as follows.

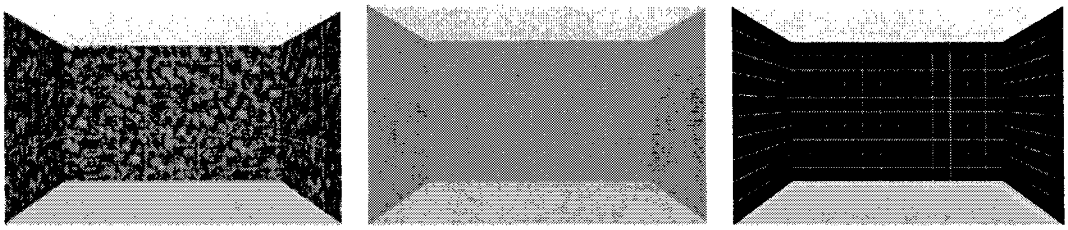

Stone 10B 4/1 Tile 7.5PB 2/4 Painting 7.5B 6/10

figure 1. The example of experimental object

3.3 Evaluation Vocabulary

Evaluation vocabulary was selected as the vocabulary that could express the image of finishing materials and colors among adjects that expressed the image of interior area based on the result of a previous research on interior color and material quality. That is as same as Table 1.

Table 1. Evaluation Vocabulary

Open	Bright	Light	Active	Indivisual	Coarse	Fine	Clear	Exuberant	Strong
Calm	Natural	Rough	Classy	Elegant	Soft	Cool	Warm	Smooth	

3.4 Testees

Testees consisted of 30 graduate students and junior or senior students of Architecture department who were acknowledged to have an ability of perception or judgement on architecture area, finishing materials, and color for safe evaluation. The composition of the testees is as same as Table 2.

Table 2. Testees

Sex	Male : 15, Female : 15
Position	Graduate Students : 13, Senior Student : 17
Total	30

3.5 Evaluation method

This experiment was made with a wall-side which influenced image of interior area, and the ceiling and floor of evaluation object was fixed to N8 and N6 which affected visual sight a little. Also, the CRT monitor and the observant distance were 35 ㎝ in consideration of human sight 30°, and evaluation vocabularies extracted from 3.3 were used as evaluation items. Evaluation method was 7 value steps in order to check the psychological reaction of the testees.

4. ANALYSIS FOR PREDICTION MODEL MAKING

4.1 Analysis method

Data was dealt with statistics package or SPSS/PC+. The method divided into 7 steps, gave score 1~7 to them, and we checked credibility of data after calculating average standard deviation dispersion of each item. Also, we carried out factor analysis, and extracted representative image in order to make sure psychological structure in finishing materials evaluation of interior area, and then we made prediction model through Multiple regression analysis by HAYASI I program.

4.2 Representative image type extraction

In interior area, we accomplished factors analysis in order to analyse psychological structure clearly on image evaluation according to the kind of finishing materials and the change of color, and as the result of that, 19 adjectives were classified to total 5 axises.

When we look into concretely, we named the 1st factor consisted of evaluation items of 「Open」, 「Bright」, 「Light」, 「Active」, 「Clear」 as 『Capability』 axis, the 2nd factor consisted of evaluation items of 「Exuberant」, 「Strong」, 「Individual」, 「Calm」, 「Natural」 as 『Activity』 axis, the 3rd factor consisted of evaluation item of 「Smooth」, 「Coarse」, 「Rough」, 「Soft」 as 『Materials quality』 axis, the 4th factor consisted of evaluation item of 「Elegant」, 「Classy」 as 『Evaluation』, and the 5th factor consisted of evaluation item of 「Warm」, 「Cool」 as 『Warmness』 axis.

In following analysis, we intend to select the representative adject which has +factor load quality and - factor load quality in extracted 5 axises or 『Capability』, 『Activity』, 『Materials quality』, 『Evaluation』, 『Warmness』 and to analyse image.

『Capability』 evaluation axis was classified as [Open · Bright] image, 『Activity』 evaluation axis as [Gorgeous · Strong] image with +factor load quality and [Quiet · Natural] image with - factor load quality, 『Materials quality』 evaluation axis as [Smooth · Elaborate] with +factor load quality and [Coarse · Rough] image with - factor load quality. 『Evaluation』 evaluation axis was classified as [Elegant · Courteous] image, and 『Warmness』 evaluation axis as [Warm] image with +factor load quality and [Cool] image with - factor load quality.

8 image types were extracted from 5 axises as representative type, and this paper on analysis from now is willing to describe extracted image types.

4.3 Influence analysis according to evaluation factors

By Multiple regression analysis, we analysed the influence by evaluation factors through multiple · partial correlation coefficient and factor range, and the result is as same as Table 3.

When we looked into influence chart of factors with factors range and correlation coefficient in order to find out evaluation factors relative a lot to interior area image, [Open · Bright] image was influenced most by value, [Gorgeous · Strong] and [Calm · Natural] images by the kind of finishing materials and chroma, [Smooth · Fine], [Coarse · Rough], and [Elegant · Classy] images by the kind of finishing materials, and [Warm] & [Cool] images by hue.

Table 3.The influence by evaluation factors

Evaluation Vocabulary	Multiple correlation coefficient	Partial correlation coefficient(range)			
		Finishing materials	Hue	Value	Chroma
Open · Bright	0.8919	0.582(0.951)	0.297(0.411)	**0.820(1.386)**	0.171(0.224)
Exuberant · Strong	0.8155	**0.660(1.579)**	0.276(0.533)	0.465(0.845	**0.643(1.751)**
Calm · Natural	0.7983	**0.624(1.060)**	0.323(0.383)	0.3919(0.431	**0.532(1.140)**
Smooth · Fine	0.9484	**0.948(2.320)**	0.248(0.301)	0.274(0.168)	0.077(0.104)
Coarse · Rough	0.9661	**0.965(2.517)**	0.325(0.303)	0.232(0.232	0.192(0.192)
Elegant · Classy	0.8530	**0.703(1.083)**	0.473(0.537)	**0.641(0.871**	0.454(0.915)
Cool	0.8567	0.315(0.476)	**0.827(1.774)**	0.318(0.309)	0.300(0.508)
Warm	0.8496	0.270(0.425)	**0.810(1.895)**	0.482(0.604	0.312(0.529)

ıe highest value in the score of the Partial correlation coefficient : ıy 0.1from highest value

4.4 Influence analysis according to each category

Table 4 shows the influence chart according to a representative image type based on the result from Multiple regression analysis. By selecting finishing materials, hue, value, and chroma which the figures are highest with reference to following category quantity, we can increase up each image-producing effect on planning interior area.

For example, [Open · Bright] image among adjectives of 『Capability』 evaluation axis was highest when the kind of finishing materials was wallpapers. And, Y and B types for the color, high value for value, and middle chroma for chroma were high as well. So, If you choose wallpapers for finishing materials, and high value· middle chroma of Y and B types for interior area, you can produce [Open · Bright] image area so well.

Table 4. The Influence analysis according to each category

	categorie	Open · Bright	Exuberant · Strong	Calm · Natural	Smooth · Fine	Coarse · Rough	Elegant · Classy	Cool	Warm
Finishing materials	Tile	0.189	-0.054	-0.134	**0.962**	-0.995	-0.488	0.063	-0.033
	Painting	-0.046	0.000	-0.342	0.849	-1.065	-0.404	-0.011	-0.093
	Spraying	-0.002	-0.120	0.092	-1.357	**1.452**	-0.028	-0.100	0.111
	Brick	-0.193	-0.789	0.330	-0.444	0.164	0.043	-0.117	0.046
	Stone	-0.348	**0.790**	-0.303	0.234	0.094	**0.595**	**0.243**	-0.169
	Wood	0.250	-0.710	**0.717**	0.320	-0.405	0.319	-0.233	**0.256**
	Wallpaper	**0.603**	-0.075	0.384	-0.373	0.287	-0.188	-0.080	0.116
Hue	R	0.001	0.159	0.026	-0.051	0.026	0.118	-0.565	**0.647**
	YR	-0.042	-0.183	**0.204**	0.038	-0.058	**0.251**	-0.446	0.375
	Y	**0.203**	0.044	-0.043	-0.013	-0.101	-0.087	-0.458	0.459
	GY	-0.066	-0.131	-0.151	-0.030	0.061	-0.236	0.285	-0.264
	G	-0.148	0.021	-0.178	0.080	-0.071	-0.285	0.612	-0.694
	BG	-0.209	-0.154	0.000	-0.106	0.071	-0.039	0.903	-0.857
	B	0.157	0.091	-0.114	**0.107**	0.090	-0.213	**1.209**	-1.248
	PB	0.099	0.227	-0.177	0.014	-0.030	-0.287	1.009	-0.838
	P	-0.065	0.113	-0.050	-0.194	0.163	-0.109	0.308	-0.059
	RP	-0.128	**0.269**	-0.155	-0.138	**0.202**	0.112	-0.395	0.361
	N	-0.172	-0.264	-0.054	0.060	0.007	-0.186	0.341	-0.601
Value	Low	-0.850	**0.640**	-0.270	-0.092	**0.143**	**0.585**	**0.164**	-0.357
	Middle	-0.442	0.018	-0.125	-0.076	0.072	0.172	0.150	-0.220
	High	**0.536**	-0.204	**0.161**	**0.076**	-0.089	-0.285	-0.145	**0.247**
Chroma	Low	-0.030	**-0.244**	**0.127**	-0.008	-0.017	**0.096**	**0.074**	-0.081
	Middle	**0.128**	0.735	-0.351	**0.038**	0.039	-0.257	-0.226	0.252
	High	-0.096	1.506	-1.012	-0.066	**0.176**	-0.819	-0.434	**0.447**

ie highest value in the score of the category

5. PEDICTION MODEL MAKING ACCORDING TO AN IMAGE TYPE FOR INTERIOR PLAN

Based on the analysis result, this paper presented prediction model for an interior finishing materials plan after making a network map according to image, and the example is figure 2.

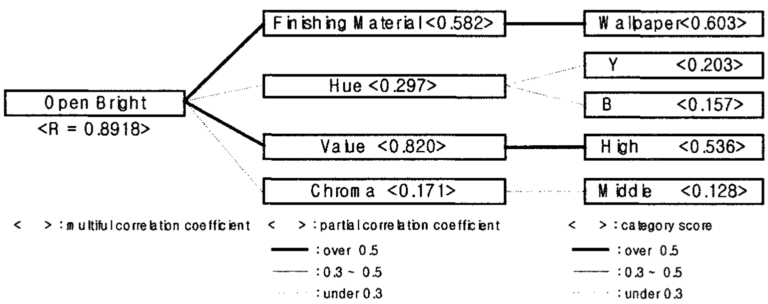

figure 2. The prediction model for an interior finishing materials plan

6. CONCLUSION

This paper made prediction model that could apply them into real area planning after figuring out the kinds and colors of finishing materials according to image types. The prediction model understood a psychological structure, and extracted representative image through factor analysis based on the result of evaluation experiment. And after conducting Multiple regression analysis with representative image, we made evaluation prediction model of interior finishing materials with influential evaluation factors and causes based on that.

The summary of the result of this paper are as follows:

1. [Open · Bright] image was influenced most by value. So, If you want to produce such mood, you`d better increase up value, use wallpapers that has low material quality as finishing materials, and choose Y or B type as hue and middle chroma.

2. In the pursuit of [Exuberant · Strong] image, It is effective for you to consider the kinds of finishing materials and the chroma. If you use stones as finishing materials, RP or PB type as hue, low value, and high chroma, you can make interior area of [Exuberant · Strong] image.

3. You should consider the kind of finishing materials at first for [Calm · Natural] image. You can increase up the effect by using woods as finishing materials, YR or R type as hue, high value, and low chroma.

4. It is proper to choose it after considering the kind of finishing materials for [Smooth · Fine] image. The use of tiles or paintings can be effective. And, to keep up B type as hue, high value, and middle chroma is favorable for [Smooth · Fine] image production.

5. [Coarse · Rough] image was influenced a lot by finishing materials. So, the use of sprayings as finishing materials is effective, which has influence of materials quality most. To use RP or P type, low value, and high chroma is proper for [Coarse · Rough] image.

6. The choice of stones as finishing materials for [Elegant · Classy] image is most effective, and the effect can be increasable by YR type as hue and by low value and chroma.

7. [Warm] image is influenced most by hue. So, to choose warm colors of R, YR, and Y type is desirable, and the choice of woods as finishing materials and high value and chroma is helpful for producing the image.

8. The choice of finishing materials of cold color types of B, PB, and BG type is most proper for[Cool] image, and the kind is stones. The effect producing interior mood of cold image can be heightened by the use of low value and chroma.

Jin - Sook Lee, Mi – Jin Lee
Dept. Architecture, College of Engineering, ChungNam National University
Kungdong220, YOUSUNGKU, TAEJON 305-764, KOREA
Phone : +82-42-821-7733
Fax : +82-42-823-9467
E-mail : js_lee@cnu.ac.kr

A New Sapphire Grading System Set Up by The Gem And Jewelry Institute of Thailand (GIT) for the Gemstone Industry

Prof. Sakda Siripant* and the working committee**
The Gem and Jewelry Institute of Thailand

1. Introduction

In normal practice, gem traders appraise gemstones through the quality evaluation of four main factors-color, clarity (or transparency), cut and brilliance. This subjective evaluation depends on experience of traders.

Accurate color description and color matching in faceted transparent sapphire with a color chip is a difficult, subjective and debatable process. This is because these sapphires are three-dimensional objects, characterized by dichroism, reflection and refraction, inclusions and fluorescence that influence their color appearance. Accurate color evaluation (description) in gemstones also depends on the observer's visual spectral responsivity, the lighting conditions during color evaluation and surrounding colors.

An important visual color communication system that has been accepted and used by various industries including the gemstones is the Munsell System for color notation. Many people thought it would be extremely difficult to match the vibrant color of a transparent gemstone to the opaque, glossy color chips in the Munsell Color Book.

However after practice, it was proven to researchers that it could be done quite easily and with excellent results.

In order to strengthen the subjective evaluation of the gemstones more efficiently, we also used objective or instrument derived data grouped under the heading quality and natural value.

2. Methods used for sapphire grading and results

In general there are three factors governing the assessment of a sapphire, namely: beauty, quality and natural value (natural or synthetic origin) as shown in Figure 1.

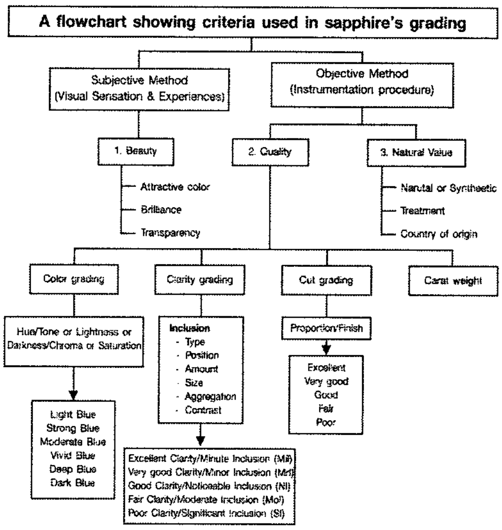

Figure 1 A flowchart showing criteria used in sapphire's grading

2.1 Subjective method

2.1.1 Beauty: This is the most important easily seen aspect of a gemstone and a strong factor in determining its value. Beauty is a subjective word. It is, in fact, a collective term combining the attractive color, brilliance and transparency when assessing a sapphire or, for that matter any gemstone.

a) The attractive color of a sapphire usually depends on personal and cultural tastes. The key to its attractive color is not merely the gemstones simple two-dimensional color, but the balance of light and dark tones in a mosaic-like pattern that gives the gem a wonderful three-dimensional color appearance. This is the effect of reflection and refraction caused by good and proper faceting. The purer blue of the sapphire, the greater the price the gemstone can command.

b) The brilliance of a sapphire is caused by light refracted and reflected from a properly faceted gem. As the brilliance increases sapphire become more valuable. (Figure 2)

c) Transparency and the lack of inclusions and blemishes combined with its brilliance are what make a sapphire so beautiful and valuable. (Figure 3)

Figure 2 Light refracted and reflected from a faceted gem

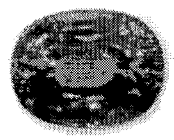

Figure 3 Inclusions and blemishes

2.1.2 Results: Three criteria, attractive color, brilliance and transparency were used by the GIT's researchers to select three sets of standard sapphires weighing from 0.75 to 1 carats from three different geographic regions. Include were one set of Thai, Sri Lanka and Madagascar sapphires. Five stones in each set have the same hue but different chroma levels ranging from dark to light. (Figure 4)

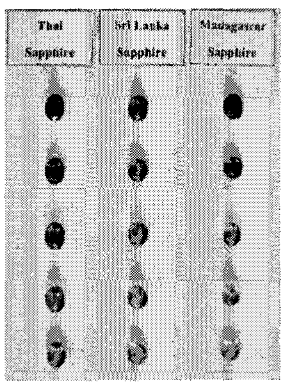

Figure 4 Three sets of Thai, Sri Lanka and Madagascar sapphires

Three standard sapphire sets were used to conduct the color preference survey. The participants in this study were buyers and gemmologists from various countries who attended the 31st Gem and Jewelry Fair in Bangkok during the 26th February – 2nd March 2002. The participants were divided into 6 groups and numbered by geographic origins - Thais 67, American 25, European 49, Asia 59, Africa 11 and Australia 8. The results of the Color Preference Survey are shown in Figure 5 – Figure 8.

While researching the color preferences of Sapphires from various regions it was found that the **Thais** prefer Sapphires of Thai origin more than other types from a samples test of 67 people.
Thai Sapphire (56.7%) Sri Lanka Sapphire (55.2%)
Madagascar Sapphire (50.7%)

Figure 5 Thai color preference

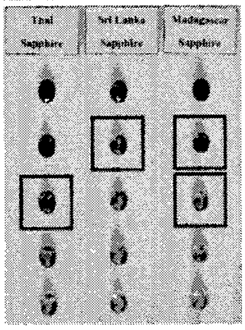

Americans prefer Sri Lankan Sapphires (52.0%) from a sample test of 25 persons.
Thai Sapphire (22.0%) Sri Lanka Sapphire (52.0%)
Madagascar Sapphire (44.0%)

Figure 6 Americans color preference

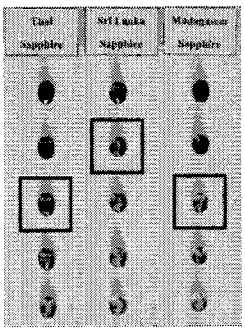

Europeans prefer Sri Lankan Sapphires and Madagascar Sapphires (55.1%) from a sample test of 49 persons.
Thai Sapphire (40.8%) Sri Lanka Sapphire (55.1%)
Madagascar Sapphire (55.1%)

Figure 7 Europeans color preference

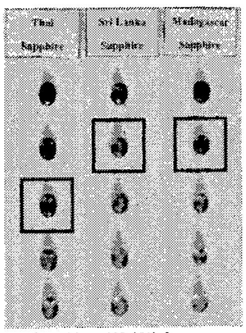

Asians prefer Thai Sapphires (42.4%) from a sample test of 59 persons.
Thai Sapphire (42.4%) Sri Lanka Sapphire (40.7%)
Madagascar Sapphire (39.0%)

Figure 8 Asians color preference

2.2 Objective method

In order to evaluate three of the important factors contributing to the subjective beauty of a sapphire more precisely we used quantitative methods grouped under the heading "Quality" and "Natural Value".

2.2.1 Quality: The quality of a sapphire is based on 4 independent criteria: color, clarity, cut grading and carat weight.

2.2.1.1 Color Grading

The color of a sapphire determines at least 50% of its final market value. The color grading of sapphires is very difficult and more subjective than grading diamonds because we must consider three separate components that are both independent and interrelated, namely hue, tone (lightness or darkness) and chroma or saturation (color intensity). The GIT method has been designed to provide a meaningful grading system that is easily understood and used.

Hue describes the dominant and additional colors in a gemstone that are visible to the naked eye. In our example, a purplish blue (PB) sapphire has blue as the dominant color and purple as the secondary color.

Value is the lightness or darkness of a color sensation.

Chroma or Saturation is best described as the strength or intensity of the hue sensation. The GIT Color Grading System is primarily based on the Munsell Color Chart. (Figure 9)

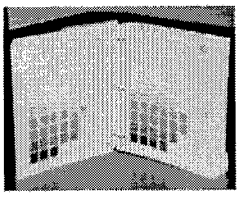

Figure 9 Munsell Color Charts

Figure 10 Color matching between a sapphire and Munsell color chip

Each sapphire was matched to the appropriate Munsell color chip and viewed under a standard 5,000 Kelvin light source. (Figure 10) Then, each stone in the standard sets was assigned a Munsell color code and name. The color codes were converted to color names in the ISCC-NBS of the ASTM color chart. (Figure 11 – Figure 13) Additionally the Munsell color code can be converted into the color coordinates of the L*u*v* and L*a*b* systems. (Figure 14) Please refer to the research *A Gems Color Communication System* conducted by Prof. Sakda Siripant in 1999.***

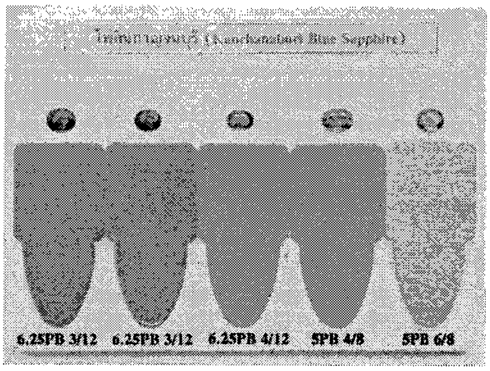

Figure 11 Thai sapphires with color codes

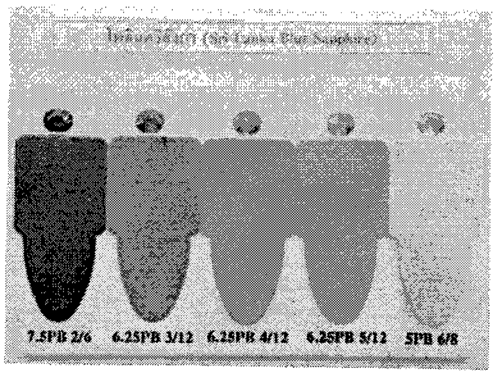

Figure 12 Sri Lanka sapphires with color codes

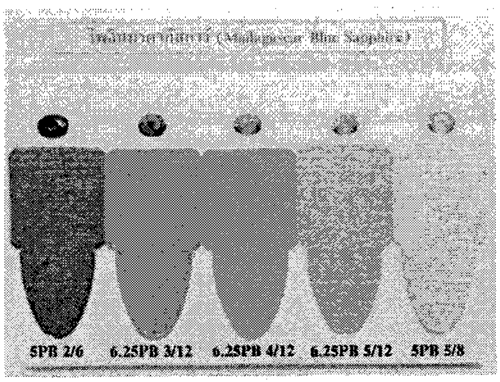

Figure 13 Madagascar sapphires with color codes

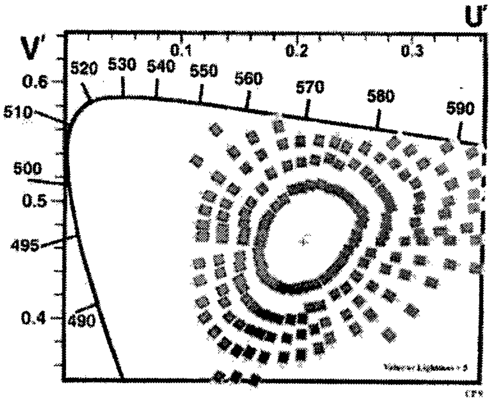

Figure 14 CIE 1976 uniformity chromaticity scale U' V' diagram

2.2.1.2 Clarity Grading

Clarity is the second most important factor when evaluating sapphires. The clarity of the stone is worth between 20 and 30% in the grading system. The clarity of a sapphire is first determined with naked eyes and then under 10x magnification. Next, a point system that takes into account the following factors as shown in Table 1 is used. The point system and naked eyes assessment is used to assign the final clarity grade as shown in Table 2.

Table 1 The point system for clarity grading of sapphires

Point	Type of Inclusion	Position	Number	Related Size	Aggregation	Contrast
4	Severe	Table	Numerous	Large	Dense all over	Very High
3	High	Crown	Moderate	Medium	Locally dense	High
2	Moderate	Girdle	Few	Small	Disperse	Moderate
1	Low	Pavilion	Very Few	Very Small	Isolate	Low
Rate						

Remark: Type of inclusion is determined by negative effect on appearance and durability

Table 2 The final clarity grade

Clarity Grading of Sapphire		
Excellent	Minute Inclusion (MI)	Very difficult to see with naked eyes
Very Good	Minor Inclusion (MrI)	Difficult to see with naked eyes
Good	Noticeable Inclusion (NI)	Just able to see with naked eyes
Fair	Moderate Inclusion (MoI 1-2)	Easy to see with naked eyes
Poor	Significant Inclusion (SI 1-2)	Very easy to see with naked eyes

2.2.1.3 Cut Grading

Cutting is the third important factor when evaluating sapphires. The cut component is worth 10% to 20% of the value in a grading system. Criteria for cut grading are the proportion (Figure 15) and finish of a sapphire.

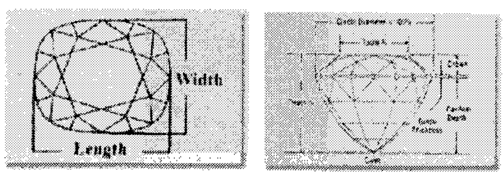

Figure 15 The proportion of a sapphire

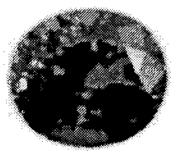

Figure 16 Face-up proportion

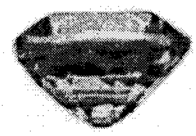

Figure 17 Profile proportion

A. Proportion: There are three criteria used to assess proportion

1) Face-up Proportion: When viewed in the face-up position, the opposite parts of the faceted stone should be exactly the same size and well shaped. The overall effect should be appealing to our eyes. (Figure 16)

2) Profile Proportion: When viewed from the side of the table, the culet should be exactly centered, the girdle not wavy and the pavilion bulge should be even. Depth percentage (the height of a sapphire measured from table to culet, divided by the width and multiplied by 100) should normally be between 60 and 70%. The crown height-pavilion depth ratio should vary between 1:2 to 1:4. (Figure 17)

3) Brilliance: The light returned from a gemstone to the eye is known as brilliance. As the brilliance increases sapphire become more valuable. When light leakage occurs, it is known as windowing. When dark areas are visible, it is known as extinction.

B. Finish: There are two criteria used to assess finish

1) Polish: consider the surface characteristics

2) Distorted facet: consider shape, position and arrangement of facets. Then the point system and naked eyes assessment is used to assign the final cut grading as shown in Table 3.

Table 3 Cut grading system of a sapphire

		Cutting Grade		
Excellent	Very Good	Good	Fair	Poor

2.2.1.4 Weight (in carats) will determine the price of the stone. A large-sized sapphire will have a higher price per carat than that of a smaller-sized sapphire of the same quality.

2.2.2 Natural Value:

The authenticity of these standard sapphire sets was identified by using an Energy Dispersive X-ray Fluorescence Spectrophotometer (EDXRF), UV-VIS-NIR and FTIR Spectrophotometers. All sapphires in these standard sapphire sets are natural. They have been heat-treated. Countries of origins of the first, second and third sets are Sri Lanka, Kanchanaburi (Thailand) and Madagascar respectively.

3. Conclusion

Three sets of standard sapphires weighing from 0.75 to 1 carats were obtained by careful selection based on three criteria, attractive color, brilliance and transparency. The quality and authenticity of the standard blue sapphire were also determined by the instrumentation procedure described above. These standard sets were used to conduct the color preference survey. It was found that Thai people prefer the moderate blue of Thai sapphire the most, the vivid blue of Sri Lanka sapphire the second and the strong blue of Madagascar the third. American people prefer the vivid blue of Sri Lanka sapphire the most, the moderate blue of Thai sapphire and the vivid blue of Madagascar the second. European people prefer the vivid blue of Madagascar sapphire and strong blue of Sri Lanka the most, the moderate blue of Thai sapphire the second. Asian people prefer the moderate blue of Thai sapphire and strong blue of Sri Lanka the most, the vivid blue of Madagascar sapphire the second.

In normal practice, GIT uses these three standard sets (Sri Lanka sapphire set, Kanchanaburi sapphires set and Madagascar sapphire set) and their color codes and names as master standard sapphires to conduct subjective color matching and grading with customer's blue sapphires.

The visual Munsell color description was correlated with instrumental measurement of a color by using spectrophotometer. The results of the new sapphire grading system is accurate enough to satisfy a scientist and usable enough to satisfy manufacturers and traders. The new sapphire grading system was described in the GIT Identification Report used to promote the sale of sapphires in the Sapphire Year 2003.

We hope that The Ruby and Sapphire Year 2003 will be a year of Serenity, Wealth and Achievement.

---

* Director of the Gem and Jewelry Institute of Thailand

** GIT Academicians

1. Prof. Sakda Siripant
2. Dr. Phongchan Chanthayos
3. Mr. Sakrapee Saejoo
4. Ms. Siraprapa Kaewmanee
5. Mr. Sutas Singbamroong
6. Mr. Thanong Leelawatanasuk
7. Assoc.Prof.Dr. Visut Pisutha-Arnond
8. Dr. Pornsawat Wathanakul
9. Ms. Wilawan Atichat

*** Sakda Siripant, "Color communication system for gems", *Journal of Gems and Gemmology*, Gemmological Institute of America, Vol. 35, No. 3, 1999. pp. 162-163 (This research project was sponsored by the Thailand Research Fund.)

Paints as 'Magnets' to Guide the Mixing Process

Paul Green-Armytage, Curtin University of Technology, Western Australia

INTRODUCTION

According to Roy Osborne, 'The first essential of practical colour study is to develop the skill to obtain any colour quickly and accurately.' (Osborne 1990, p 16). Michael Wilcox, however, claims that 'Even after many years of experience most artists find difficulty mixing colours.' (Wilcox 1987, p 3). If artists have difficulty obtaining the colours they want from 'mixing colours' it could be that the difficulty stems from the phrase itself. To produce the colours for the paintings we see and admire in art galleries artists do not 'mix colours' they mix paints. In this paper an approach to producing desired colours from paint mixtures is described which depends on making a clear distinction between paints as substances and the colours we experience when we look at those substances.

THE NCS AS A 'MAP'

The *Natural ColourSystem* (NCS) (Hard & Sivik 1981) provides a model of colours as visual experiences. The colours we see in the world around us have their places in the NCS model according as how they appear more or less yellowish, reddish, bluish, greenish, whitish and blackish. A given paint, used unmixed and straight from the tube, has a characteristic appearance that can be located in the NCS model. The dimensions of that appearance, in NCS terms, are *hue* – relative yellowness, redness, blueness and greenness, and *nuance* – relative whiteness, blackness and chromaticness. On the scale of chromaticness pure grey is 0 and the most vivid colour imaginable is 100, vivid orange being more chromatic than dull brown. A colour's hue and chromaticness can be plotted on the circular plan view of the NCS model. Colours of the same hue are on the same radial line (fig 1). Colours of the same chromaticness are on the same ring (fig 2). This plan view of the NCS can be used as a map on which the route to the desired colour can be plotted.

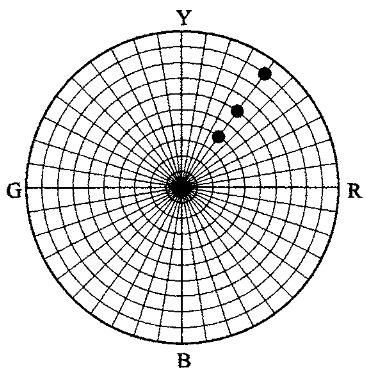

Fig 1 Colours of the same hue are located on the same radial line on the NCS Map.

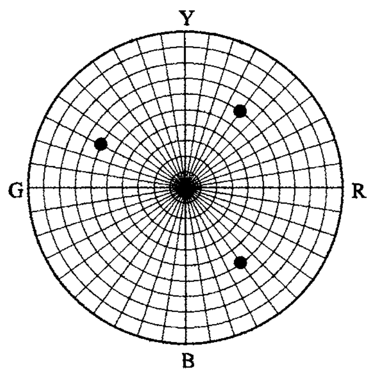

Fig 2 Colours of the same chromaticness are located on the same ring on the NCS Map.

MIXTURE LINES AND COLOUR GAMUT

If two paints are to be mixed the appearance of each paint can be marked as a point on the NCS Map. The appearance of the mixtures in varying proportions of those two paints can be plotted as a 'mixture line' connecting the two points. Such mixture lines are usually curved. The reasons for the lines being curved are complex; it is enough for artists to be aware that mixture lines are likely to be curved when plotted on this NCS Map and to know what steps to take to guide a paint mixture to the desired appearance.

To increase the range of colour appearances that can be produced from mixing paints, more than two paints are required. The paints chosen will depend on the range of colours you want to produce. A minimum set of paints to produce a useful range of colour appearances is the equivalent of the set of inks used for reproducing coloured photographs. If opaque paints such as designers' gouache are to be used a 'white' paint will be needed as well as the equivalent of the printers' Cyan, Magenta, Yellow, and Black (CMYK). Five paints such as *Rowney* Process Cyan, Process Magenta, Process Yellow, Permanent White and Jet Black can be marked on the NCS Map (fig 3). The mixture lines connecting Process Cyan to Process Magenta, Process Magenta to Process Yellow and Process Yellow to Process Cyan mark the limits of the colour gamut achievable with these paints. To achieve more chromatic colours beyond these mixture lines additional paints will be needed. An extended gamut achieved by including Ultramarine, Brilliant Red and Brilliant Green is illustrated in fig 4.

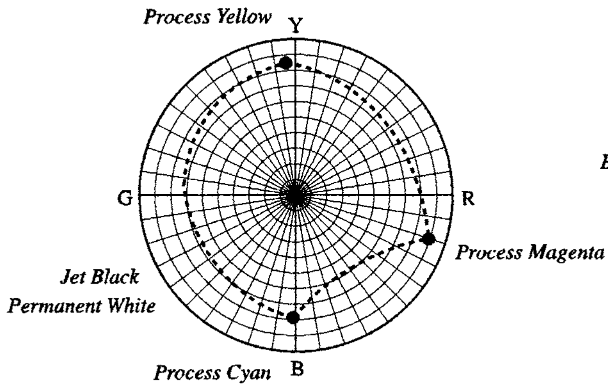

Fig 3 Five paints from the Rowney range of Designers' Gouache paints located on the NCS Map according to their appearances. The mixture lines connecting Process Cyan, Process Magenta and Process Yellow define the limits of the colour gamut achievable with this set of paints.
Note: Permanent White and Jet Black are located in the centre of the circle.

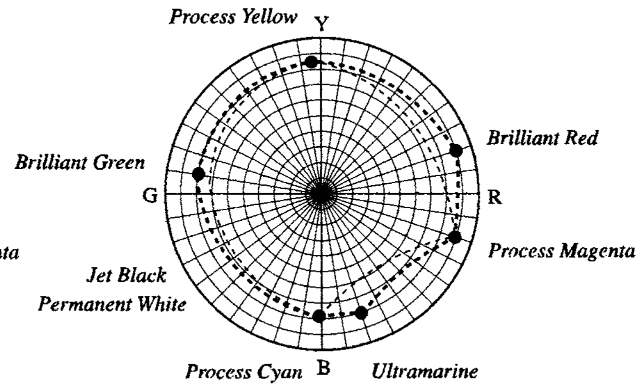

Fig 4 Introduction of additional paints can increase the achievable colour gamut.

PAINTS AS 'MAGNETS'

Just as you can mark the positions of your paints on the NCS Map, so can you mark the position of the colour you want to produce. To achieve that colour appearance you can think of your paints as 'magnets' which can be used to guide the mixture towards the target. Start by squeezing out onto your palette some of the paint that is nearest in appearance to the desired colour. As you mix in another paint you will move the appearance of the mixed paint in the direction of that other paint as though that paint were a magnet. You can use paints such as Process Cyan, Process Magenta and Process Yellow to guide the mixture to the desired hue and chromaticness and adjust the whiteness and blackness by using Permanent White and Jet Black as additional magnets. Depending on the paints you are using and the colour appearance you want to achieve there can be more than one combination of paint magnets that can be used to reach the target (figs 5 and 6).

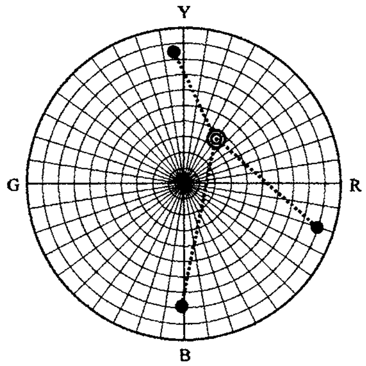

Fig 5 A dull Brown can be produced with a mixture of three paints: Process Yellow, Process Magenta and Process Cyan. A small quantity of Process Cyan has the effect of reducing the chromaticness and darkening the appearance of the colour that results from a mixture of Process Yellow and Process Magenta alone.

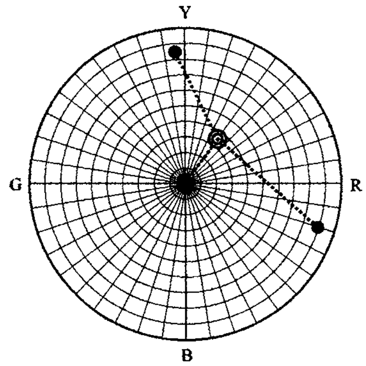

Fig 6 A very similar dull Brown can be produced With a mixture of Process Yellow, Process Magenta, Permanent White and Jet Black. The Permanent White and Jet Black can produce the same changes in appearance that was produced by including Process Cyan in the mixture illustrated in fig 5.

CONCLUSION

It is comparatively easy to produce a desired colour by using the NCS Map and by thinking of your paints as magnets that can be used to guide the appearance of the mixture to your target. The appearances of your paints and the appearance you want to achieve can be marked on the NCS Map. The extent of the colour gamut achievable with a given set of paints is defined by the mixture lines which connect the paints. If the colour you want is beyond that gamut you may be able to reach it by using additional paints. Depending on the relationship between the locations of your paint magnets and the target colour alternative mixing recipes can be identified.

REFERENCES

Hard, A. & Sivik, L. 1981, 'NCS - Natural Color System: A Swedish Standard for Color Notation', *Color Research and Application*, vol. 6, no. 3.

Osborne, R. 1990, 'Teaching Colour', *The Artist*, April, pp. 14-16.

Wilcox, M. 1987, *Blue and Yellow don't make Green*, Artways, Perth, Western Australia.

Representational Relation of *Bora* (Bluish-purple) and *Jaju*(Reddish-purple) in Korean Color Naming[+]

Young-Sun Kim*, Hyensou Pak, Min-mo Koo, Myung-Sun Yeo, Kyung-Kee Oh, Mahn-Young Lee**

* Behavioral Science Research Center, Korea University, 1, 5-Ka, Anam-dong, Sungbuk-ku, Seoul, 136-701 Korea

** Dept. of Psychology, Korea University, 1, 5-Ka, Anam-dong, Sungbuk-ku, Seoul, 136-701 Korea

This study was supported by grant from the Korea Research Foundation (KRF-2002-074-HS-1504)

1. Introduction

The Munsell Color System that is widely used in Korea and international color society is constructed in the basis of five color axes including Red, Yellow, Green, Blue, and Purple. And, color naming system of ISCC-NBS and national standard of many countries have their roots in the Munsell System and provide the practical naming systems that is consisted of various combinations of color-names and modifiers to every fields.

Purple is a basic color-name that appears in the seventh stage in the evolutionary theory of Berlin & Kay (1969) for color terms. After the landmark of theory, there are abundant evidences from anthropological, psychological, and linguistic researches that purple has a definite status as a basic color in many regions and cultures (Kay & McDaniel, 1978; MacLaury, 1992; Archibald, 1989, Johansson & Hofland, 1989; Boynton & Olson, 1987; Uchikawa & Boynton, 1987). But, there are some cases that purple's status as a basic color-name is relatively weak or unstable according to language. Russian is a typical case of such language. Russian doesn't have a equivalent color-name for purple, and even *fioletovij* suggested as a promising candidate for purple is a recent color-name that appeared in eighteenth century (Corbett & Morgan, 1988; Moss, 1989a, 1989b).

Similarly, it is uncertain what color-name is proper to purple and what color-name people use for the color space that English native speaker refer to as purple. Most of people know purple as *Jaju* and violet as *Bora* in Korea, and they use them naturally in daily life. However, KSA 0010, the national standard of Korea, used *Bora* for purple, and some of experts on color and design area interpret and use it in the same way. Therefore, there is a disagreement in using color-name for purple in Korea.

The psychological studies for color perception and representation of Korean in terms of percentile rating and color naming found that *Bora* was closer to basic color and superior to *Jaju* in presentational region and frequency (Lee, 1983; Kim, 1998; Kim, Pak, & Lee, 2001). According to an recent anthropological research of the variation and the development of color classification in Korea, *Bora* was easily considered as a basic color for purple in younger generation and *Jaju* was gradually recognized as a subcategory of Bora (Kim, 2000). This study attempts to obtain a necessary experimental evidence for examining to which level of systematic color-name system we classify *Bora* and *Jaju*. Three experimental conditions were introduced for the purpose. We observed the spatial presentation of *Jaju* under Munsell color system in the first condition, those of *Bora* in the second condition, and those of both simultaneously in third condition.

2. Method

2.1 Subjects

Twenty-eight students of Korea University who were taking 'Understanding of Psychology' class participated in the experiment. They were normal in color vision

.

2.2 Materials

Four hundred and forty eight stimulus color chips were selected from *The Munsell Book of Color* (Glossy). They range from 5PB to 5R including all of brightness and chromaticity values. Each of them was mounted on a gray card (N7) of 130cm × 100cm and observed under the illumination condition of daylight (Examolite, D65).

2.3 Procedure

Before entering into experiment, subjects were adapted by illumination and received instruction at the same time. The required task of subjects was to select the most proper color-name for the each color chip among a given example. Then, they had to write down the number of the color-name to a matching blank

Val	Chr	5PB	7.5 PB	10P B	2.5 P	5P	7.5 P	10P	2.5 RP	5RP	7.5 RP	10R P	2.5 R	5R
8	2	0	7	0	0	0	0	0	0	0	0	0	0	0
	4	0	0	7	14	31	8	7	0	0	0	0	0	0
	6	0					6	7	0	0	0	0	0	0
	8													
	10													
	12													
	14													
	16													
7	2	0	0	0	0	0	0	0	0	0	0	0	0	0
	4	0	0	7	25	36	21	25	6	0	0	0	0	0
	6	0	0	21	44	67	21	7	0	8	0	0	0	0
	8	0	7	17	57	50	6	25	0	0	0	0	0	8
	10								7	0				0
	12													
	14													
	16													
6	2	0	0	0	0	0	0	0	0	6	0	0	0	0
	4	0	0	7	17	50	14	33	13	7	8	0	0	0
	6	0	0	19	44	43	50	14	17	21	0	0	0	0
	8	0	7	19	42	50	50	33	25	0	0	0	0	0
	10	0	0	21			43	21	7	0	0	0	0	0
	12								7	7	0	7	0	0
	14													
	16													
5	2	0	0	0	0	0	0	0	0	0	6	6	0	0
	4	0	8	14	31	36	50	29	50	6	0	7	0	0
	6	0	0	25	64	79	71	56	31	29	13	0	0	0
	8	0	0	14	44	75	75	64	33	21	21	8	0	0
	10	0	0	33	79	79	71	69	29	25	7	0	6	0
	12	0						43	19	36	8	7	0	0
	14										7	6	7	7
	16													
4	2	0	0	0	0	13	7	0	7	0	0	0	0	0
	4	0	0	0	29	64	93	81	86	8	7	8	0	0
	6	0	0	29	29	58	92	93	79	86	38	7	6	0
	8	0	0	14	43	94	83	100	92	83	50	25	0	0
	10	0	0	25	50	75	94	100	93	100	86	33	6	0
	12	0	0	7	63	71	92	100	88	63	86	25	7	0
	14											19	0	0
	16													
3	2	0	0	0	7	7	8	17	29	6	0	0	0	0
	4	0	0	6	38	42	64	88	94	57	29	7	0	0
	6	0	0	0	57	79	79	100	92	92	56	29	8	0
	8	0	0	8	42	50	100	100	100	83	92	38	8	7
	10	0	0	14	50	100	100	100	100	79	93	57	7	0
	12		0											
	14													
	16													
2	2	0	0	0	0	0	8	17	0	7	7	0	0	0
	4	0	0	0	31	44	63	71	75	50	36	19	0	7
	6	0	0	0	21	81	64	79	93	88	71	67	29	14
	8	0	7	0	36	57			93	93	83	64	43	19
	10		7	0	71									
	12													
	14													
	16													

Figure 1. Representation of *Jaju* in Munsell space

Val	Chr	5PB	7.5 PB	10P B	2.5 P	5P	7.5 P	10P	2.5 RP	5RP	7.5 RP	10R P	2.5 R	5R
8	2	0	0	0	0	0	0	0	0	0	0	0	0	0
	4	0	0	29	36	63	42	21	7	0	0	0	0	6
	6	0					31	14	0	0	0	0	0	0
	8													
	10													
	12													
	14													
	16													
7	2	0	0	0	0	0	8	0	7	0	0	0	0	0
	4	0	0	43	83	86	57	33	0	0	0	0	0	0
	6	8	0	71	94	100	36	7	13	0	0	0	0	0
	8	0	7	67	100	93	44	8	7	0	0	0	0	0
	10								0	0				0
	12													
	14													
	16													
6	2	0	0	0	0	0	7	13	7	0	0	0	0	0
	4	0	0	21	92	92	71	58	31	0	0	6	0	7
	6	0	7	75	100	100	71	36	33	0	0	0	8	6
	8	0	0	81	92	100	83	25	8	0	0	0	7	0
	10	0	0	71			88	14	0	0	0	0	0	0
	12								0	0	0	0	0	0
	14													
	16													
5	2	0	0	0	0	0	7	0	8	0	0	6	0	0
	4	0	0	29	69	86	94	79	50	13	0	0	0	0
	6	0	7	75	100	93	100	75	31	29	0	0	0	0
	8	0	0	64	100	94	100	86	25	7	0	0	0	0
	10	0	6	83	100	100	93	81	7	0	0	0	0	0
	12	0						57	31	0	0	0	0	0
	14										0	0	0	0
	16													
4	2	0	0	0	0	13	7	7	0	0	0	0	0	0
	4	0	0	50	79	100	100	88	71	50	0	0	0	0
	6	0	0	50	100	100	100	93	93	50	13	0	0	0
	8	0	7	64	100	100	100	100	92	50	21	0	0	0
	10	0	0	83	100	100	100	100	71	36	7	0	0	0
	12	0	0	64	100	100	100	100	63	19	14	0	0	0
	14											0	0	0
	16													
3	2	0	0	0	7	21	33	50	7	13	0	0	0	0
	4	0	0	25	81	100	86	94	88	50	7	0	0	0
	6	0	0	29	100	100	100	100	92	75	25	0	8	0
	8	0	0	50	100	100	93	100	93	58	50	0	0	0
	10	0	0	64	100	100	100	100	92	57	14	0	0	0
	12		0											
	14													
	16													
2	2	0	0	6	8	21	17	33	14	7	0	0	0	0
	4	0	0	21	56	81	88	93	94	57	29	6	6	0
	6	0	0	21	64	100	100	100	86	69	50	33	0	0
	8	0	0	42	71	93			86	79	67	50	14	0
	10		0	21	93									
	12													
	14													
	16													

Figure 2. Representation of *Bora* in Munsell space

cell of response sheet. Nine color-names including *Jaju* but excluding *Bora* were provided as examples in the first condition, but another 9 color-names including *Bora* but excluding *Jaju* were given to subjects in the second condition. In the last condition, both of them were included to example in the response sheet.

3. Results

The frequency of selected color-names in each experimental condition was analyzed. Figure 1, 2, and 3 show the percentile rates of naming frequency in each condition. *Jaju* and *Bora* were widely used and overlapped across broad color representational space that corresponds to purple in first and second condition. But, when two color-names were included into the example, the picture of color representational space became different from the previous ones. That is, *Bora* was used more broadly and frequently as compared with *Jaju* that shrunken toward red area. Moreover, the foci of two color categories also showed different aspects each other. In contrast to the focus of *Bora* nearly didn't change, the focus of *Jaju* was weaken and moved toward red. A kind of dynamics between two color-names seems to operate in the situation. Certainly, *Bora* is more dominant than *Jaju* in purple of color representation of Korean.

Val	Chr	5PB	7.5PB	10PB	2.5P	5P	7.5P	10P	2.5RP	5RP	7.5RP	10RP	2.5R	5R	5PB	7.5PB	10PB	2.5P	5P	7.5P	10P	2.5RP	5RP	7.5RP	10RP	2.5R	5R
8	2	0	0	0	0	0	0	0	0	0	0	0	0	0	0	0	0	0	0	0	0	0	0	0	0	0	0
	4	0	0	21	57	69	50	0	0	0	0	0	0	0	0	0	0	0	0	0	7	7	0	0	0	0	0
	6	0					25	7	0	0	0	0	0	0	0					0	0	0	0	0	0	0	0
	8																										
	10																										
	12																										
	14																										
	16																										
7	2	0	0	0	0	0	0	0	0	0	0		0	0	0	0	0	0	0	0	0	0	0	0	0	0	0
	4	0	6	29	92	86	43	33	0	7	0	0	0	0	0	0	0	0	0	0	8	0	0	7	0	0	0
	6	0	7	64	100	92	71	21	13	0	0	0	0	0	0	0	0	0	0	0	0	0	0	0	0	0	0
	8	0	7	58	93	86	38	0	7	0	0	0	0	0	0	0	0	0	7	6	0	0	0	0	0	0	0
	10								0	0				0								0	0				0
	12																										
	14																										
	16																										
6	2	0	0	0	0	0	7	0	0	0	0	0	0	0	0	0		0	0	0	0	0	0	0	0	0	0
	4	0	0	43	75	86	79	58	19	0	0	6	0	0	0	0	0	0	0	0	0	6	7	0	0	0	0
	6	0	7	69	100	100	86	57	8	0	0	0	0	0	0	0	0	0	0	0	7	17	7	0	0	0	0
	8	0	7	88	100	100	33	25	0	0	0	0	0	0	0	0	0	0	0	17	8	0	6	0	0	7	0
	10	0	0	64			79	7	7	0	0	0	0	0	0	0	0			0	14	0	0	0	0	0	0
	12								0	0	0	0	0	0								0	7	0	0	0	0
	14																										
	16																										
5	2	0	0	0	0	0	14	0	0	0	0	0	0	0	0	0	0	0	0	0	0	0	0	0	0	0	0
	4	0	0	29	63	86	88	79	58	6	0	0	0	0	0	0	0	0	0	0	7	8	19	0	0	0	0
	6	0	0	67	100	100	93	75	25	7	0	0	0	0	0	0	0	0	0	0	6	50	7	0	0	0	0
	8	0	6	79	100	100	88	43	8	0	0	0	0	0	0	0	0	0	0	13	21	33	14	7	8	0	0
	10	0	0	67	93	100	79	63	0	0	0	0	0	0	0	0	0	0	0	14	13	21	17	0	19	6	0
	12	0						36	6	0	0	0	0	0	0						21	38	21	17	7	13	0
	14										0	0	0	0										0	19	7	7
	16																										
4	2	0	0	0	0	13	14	0	0	0	0	0	0	0	0	0	0	0	0	0	7	7	0	0	0	0	0
	4	0	0	50	86	79	86	81	71	8	0	0	0	0	0	0	0	0	0	7	13	21	17	14	0	0	0
	6	0	0	64	100	100	83	93	43	0	0	0	0	0	0	0	7	0	0	17	7	43	79	38	0	0	0
	8	0	0	86	100	100	67	71	17	0	0	0	0	0	0	0	0	0	0	33	21	75	92	43	17	0	8
	10	0	0	75	100	100	94	88	36	0	0	0	0	0	0	0	0	0	0	6	13	43	79	57	25	19	0
	12	0	0	50	100	100	83	64	25	0	0	0	0	0	0	0	0	0	0	17	36	69	81	79	25	0	0
	14											0	0	0											25	7	0
	16																										
3	2	0	0	0	14	36	33	17	7	0	0	0	0	0	0	0	0	0	0	0	0	0	0	0	0	0	0
	4	0	0	38	88	92	93	75	38	7	0	0	0	0	0	0	0	0	8	7	19	38	36	14	7	0	0
	6	6	0	43	93	100	100	67	50	8	0	0	0	0	0	0	0	7	0	0	33	50	92	44	43	0	0
	8	0	0	58	92	92	86	64	29	8	0	0	0	0	0	0	0	8	8	14	36	71	92	83	44	25	0
	10	0	0	71	92	86	79	75	25	0	0	0	0	0	0	0	0	0	14	21	25	75	93	93	79	7	0
	12		0													0											
	14																										
	16																										
2	2	0	0	0	0	7	8	8	7	0	7	0	0	0	0	0	0	0	0	0	0	0	0	0	0	0	0
	4	0	0	7	56	81	81	79	50	29	7	0	0	0	8	0	0	0	6	6	14	31	29	29	6	6	0
	6	0	0	21	86	94	93	86	64	38	36	8	0	0	0	0	0	7	6	7	7	36	50	50	58	50	14
	8	0	0	17	93	100			43	43	17	0	0	0	0	0	8	0	0			57	50	67	86	50	13
	10		0	36	93											0	7	7									
	12																										
	14																										
	16																										

Figure 3. Representations of *Bora* and *Jaju* in Munsell space

4. Discussion

From the result of this study, it is possible to infer that *Bora* is psychologically more salient and stable than *Jaju* in corresponding purple area in Korean, although each of them can be used interchangeably to some extent. Therefore, if *Bora* and *Jaju* have basicness as a color-name, we can locate *Bora* to first level and *Jaju* to second level of systematic color naming system.

On the other hand, it is necessary to call 'Bluish purple' for *Bora* and 'Reddish purple' for *Jaju* instead of 'Violet' and 'Purple', because they could be included to same category, purple, altogether and people show a general tendency to name the near area to blue as *Bora* and the near area to red as *Jaju*. In addition, if *Bora* and *Jaju* are used for violet and purple continuously as this situation, they can cause the misunderstanding and confusion to the people's mind in using color-names.

In this context, following studies are required to confirm the possibility that purple has divided or evolved to new categories, *Bora* 'bluish purple' and *Jaju* 'reddish purple' in Korean as two blue colors of Russian did.

References

1) Archibald, J. (1989). A lexical model of color space. In Corrigan, Eckman, & Noonan (Eds.), *Current Issues In Linguistic Theory ser. 4: Linguistic Categorization* (pp. 31-53).

2) Berlin, B., & Kay, P. (1969). *Basic color terms: their universality and evolution*. Berkeley and Los Angeles: University of California.

3) Boynton, R. M. & Olson, C. X. (1987). Locating basic colors in the OSA space. *Color Research and Application, 12, 2,* 94-105.

4) Corbett, G., & Morgan, G. (1988). Color terms in Russian: reflections of typological constraints in a single language. *Journal of Linguistics, 24,* 31-64.

5) Johansson, S., & Hofland, K. (1989). *Frequency Analysis of English Vocabulary and Grammar Based on the LOB Corpus. Vol. 1: Tag Frequencies and Word Frequencies*. Oxford: Clarendon.

6) Kay, P., & McDaniel, C. K. (1978). The linguistic significance of the meanings of basic color terms. *Language, 54(3),* 610-646.

7) KCIS (1991). Korean Industrial Standard Colour Name (KS A 0011).

8) Kim, S. H. (2000). A study on the variation and the development of color classification in Korea. *Journal of Korean Society of Color Studies, 14(3),* 206-212.

9) Kim, Y. S. (1998). *Korean basic color-names and their representations in color space*. Doctoral dissertation. Korea University, Seoul. Korea.

10) Kim, Y. S., Pak, H. S., & Lee, Y. H. (2001). A study of Munsell color space for Korean color names (□). *Journal of Korean Society of Color Studies, 15(1),* 29-36.

11) Lee, M. Y. (1983). *A study of elemental hues with color-naming techniques*. Doctoral dissertation. Korea University, Seoul. Korea.

12) MacLaury, R. E. (1992). From brightness to hue. *Current Anthropology, 33*, 137-186.

13) Moroney, N. (2003). Unconstrained web-based color naming experiment. In R. Eschbach & G. G. Marcu (Eds.), *Color Imaging: Device-Independent Color, Color Hardcopy, and Graphic Art VIII.*

14) Moss, A. E. (1989). Does Russian have a basic term for purple? *Linguistics, 27,* 145-155.

15) NBS. (1976). *Color: Universal language and dictionary of names*. USA: NBS.

16) Uchikawa, H., & Boynton, R. M. (1987). Categorical color perception of Japanese observers: comparisons with that of Americans. *Vision Research, 27(10),* 1825-1833.

The perceptual properties of the unique color on the hue-inclusiveness rating task

Kyung-Kee Oh*, Oh-Sang Kwon*, Iin-Ji Kim**, Young-Sun Kim*, Mahn-Young Lee**

* Behavioral Science Research Center, Korea University, 1, 5-Ka, Anam-dong, Sungbuk-ku, Seoul, 136-701 Korea
** Dept. of Psychology, Korea University, 1, 5-Ka, Anam-dong, Sungbuk-ku, Seoul, 136-701 Korea
This study was supported by grant from the Korea Research Foundation (KRF-2002-074-HS-1504)

1. Introduction

The anthropological studies including Berlin and Kay(1969)'s theory of basic color terms concerning the color naming have focused the evolutionary process the primary color name system.. The results of these studies have suggested a critical significance to apprehend the categorical structure of color perception.

By Berlin and Kay(1969)'s theory, color languages have acquired up to a total number of eleven basic color terms, that is, black, red, green, yellow, blue, orange, purple, brown, pink, & gray. Above all, red, green, blue, yellow of these are the primary basic color terms, having a perceptual distinctiveness, were regarded as the frame of the evolutional process of color names (Hardin & Maffi, 1997; Maund, 1995; MacLaury, 1997). Above four unique colors(red, green, blue, & yellow) have been considered to take charge a important role of the evolutional process about the color names.

Unique color(hue) is perceptually unmixed of other colors, cannot be further described by the use of the hue names other than its own(also referred to as unitary color), and containing no other chromatic component. The four unique colors are thought to be basic component out of which binary hues are composed. According to opponent-process theory, an appearance of a unique color is produced when one of the two chromatic opponent channel is in balance and the other is either positive or negative.

The each of unique colors shows no perceptual similarity to any of the others. Thus a color stimulus perceived to be unique red is judged to be neither yellow nor blue. Similarly, unique yellow is neither red nor green; unique green is neither yellow nor blue; unique blue is neither green nor red.

Based upon this definition of unique color, this study attempted to search for the exact unique colors on the Munsell color space(1st experiment) and to verify the differences of perceptual properties between unique colors and nonunique colors on performing the hue-inclusiveness rating task(2nd experiment). If the unique color has intrinsically the unique and pure property, firstly we can infer that the unique color would show the higher hue-inclusiveness rating tendency compared to ununique color which can be mixed of unique color. Secondly, the participants' variation of rating response at the unique color-the ununique color would be lower and stable than the unique color-the unique color.

2. Method

2.1 Participants

Seventy-four undergraduates of Korea University who were taking 'Introduction to Psychology' course' participated in the first experiment, thirty-five in the second experiment and they had normal color vision..

2.2 Materials

Above all, the candidates for unique colors were decided from the principle described at the previous studies (Lee, 1983; Kim, 1998; Kim, Pak, & Lee, 2001). Four unique colors selected in the first experiment and the sixteen unique colors adjacent to unique colors selected from *The Munsell Book of Color*(Glossy) were used as experimental stimuli, controlling the level of brightness and saturation. Each of them was mounted on a gray card (N7) of 130cm × 100cm and presented to participant under the illumination condition of daylight (Examolite, D65).

2.3 Experimental Design

Three factors (kind of hue, the type of pair, the hue distance between the unique color and the nonunique color) were manipulated as within subject factor.

2.4 Procedure

Before entering into experiment, participants were adapted by illumination and received the instructions about the experimental procedures at the same time. In the first experiment, participants were required to select the most pure(unique) color chip among given four classes of color chips. Then, they had to write down the number of the 25 color-chips at the blank of response sheet. In the second experiment, participants were presented with pairs of color chips in the order of the unique color(standard color)-the nonunique color (comparative color), or the reverse order. Then, they were asked to rate the percentage of hue-degree which the standard color was included in the comparative color. Each pair of color chips was repeatedly rated with four-separated sessions. The order of presentation both of the pairs and of unique colors were counterbalanced.

Table 1. the frequency of unique color : Red, Green, Blue, and Yellow

Count

Hue	Brightness		saturation 6 order 1	saturation 8 order 1	saturation 10 order 1	saturation 12 order 1	saturation 14 order 1	saturation 16 order 1
B	2.0	5PB		9(6.1)[a]				
	3.0	10B			8(5.4)			
		2.5PB			57(38.5)			
		5PB			50(33.8)			
	4.0	10B			5(3.4)			
		2.5PB			4(2.7)			
		5PB				8(5.4)		
	5.0	10B				5(3.4)		
		2.5PB				1(0.7)		
		7.5B			1(0.7)			
G	2.0	10G	2(1.4)					
		5G	4(2.7)					
		7.5G	2(1.4)					
	3.0	10G		3(2.0)				
		2.5G			35(23.6)			
		5G		24(16.2)				
		7.5G		28(18.9)				
	4.0	10G			3(2.0)			
		2.5G			17(11.5)			
		5G			17(11.5)			
		7.5G			12(8.1)			
	5.0	2.5G				1(0.7)		
R	2.0	7.5R		4(2.7)				
	3.0	10R			5(3.4)			
		5R			6(4.1)			
		7.5R				89(60.1)		
	4.0	7.5R						43(29.1)
Y	7.0	10YR					2(1.4)	
		2.5Y				5(3.4)		
		5Y				4(2.7)		
		7.5Y				1(0.7)		
	8.0	10Y				1(0.7)		
		10YR					2(1.4)	
		2.5Y						28(18.9)
		5Y					26(17.6)	
		7.5Y				8(5.4)		
	8.5	10Y				1(0.7)		
		2.5Y				7(4.7)		
		5Y					57(38.5)	
		7.5Y				6(4.1)		

a. % within each unique color

3. Results

Table 1 showed the frequency of color chips selected as the each of four unique colors obtained from the first experiment. Based upon response frequency, four unique colors were selected as follows: red – 7.5R 3/12, green- 2.5G 3/10, blue- 2.5PB 3/10, and yellow- 5Y 8.5/14.

Table 2 showed the mean rating scores and the mean variation of rating response by unique colors, the type of pair, & the distance between unique color and nonunique color. As results of 3-way anova based upon these three factors, each showed the statistically significant main effects(F(3,106)=6.99, *MSe=445.6, p=.009*; F(1, 35)=34.48, *MSe=773.38, p=.009*; F(F(1,35)= 99. 84, *MSe=405.07, p=.001)*. Generally, the pair of unique color (UC)-nonunique color(NC) was consistently rated more highly than the pair of the nonunique color-unique color. The pair of UC-NC also showed less fluctuation of rating response between 4-sessions than the pair of NC-UC. These phenomena seemed to support the definition of the unique color that had not to be perceived as a mixture of nonunique colors.

Table 2. The mean proportion of hue-inclusiveness and the mean variation between 4 rating scores(n=37)

Hue		type of pairs: U.C.-N.C.[a] proportion	U.C.-N.C.[a] variation of 4-rating scores	N.C.-U.C. proportion	N.C.-U.C. variation of 4-rating scores
B	mean	57.15	12.81	37.49	10.80
	Std. Dev.	17.27	8.84	23.97	8.33
G	mean	56.56	9.56	50.74	11.85
	Std. Dev.	23.43	6.94	26.69	9.30
R	mean	51.68	8.19	44.31	11.91
	Std. Dev.	21.58	7.40	23.35	8.63
Y	mean	67.81	9.34	46.23	10.64
	Std. Dev.	18.73	6.73	24.84	7.65
tot	mean	58.30	9.98	44.69	11.30
	Std. Dev.	21.13	7.68	25.07	8.47

a. U.C.:Unique Color ; N.C.: Nonunique Color

4. Discussion

This study aimed for searching the exact identity of unique colors on the Munsell color space and the perceptual attributes of them superior to the nonunique colors affecting the color perception.. From the result of this study, it is possible to infer that the unique color is perceptually more salient and stable than nonunique colors in rating the hue-inclusiveness between colors.

However, it would be premature to conclude from this result that the unique color is crucial for perceiving colors. The possibility of confusing 'uniquness' of color and 'typicality' of color in case of the focal color is open to further discussion.

Therefore, in order to apprehend the exact nature of unique colors, it would required the various, elaborate experimental task on the future research, for example, the similarity-rating task between unique color and nonunique color, and the color-classification task.

References

1. Berlin, B., & Kay, P.(1969). Basic color terms: their universality and evolution. Berkeley and Los Angeles: University of California.
2. Hardin, C.L. & Maffi, L.(1997). Color categories in thought and language. Cambridge University Press.
3. Kim, Y. S., Pak, H. S., & Lee, Y. H. (2001). A study of Munsell color space for Korean color names. *Journal of Korean Society of Color Studies, 15(1),* 29-36.
4. Kim, Y. S. (1998). *Korean basic color-names and their representations in color space.* Doctoral dissertation. Korea University, Seoul. Korea
5. Kwon, O. S. (2001). A study on the order of basic -color-term appearance by psychological distances between focal colors. Master's dissertation. Korea University, Seoul. Korea.
6. Lee, M. Y. (1983). *A study of elemental hues with color-naming techniques.* Doctoral dissertation. Korea University, Seoul. Korea.
7. MacLaury, R.E.(1997). Color and Cognition in Mesoamerica constructing categories as vantages, Autin : Univ. of Texa Press.
8. Maund, J.B.(1995). Colors : Their nature and representation, Cambridge University Press

Bibliographical database on color:
Information and statistics that can be extracted from it

José Luis Caivano
National Council for Research, and Buenos Aires University, Argentina

Since 2001, a project has been carried out to compile a bibliographical database on color that includes books, old manuscripts, doctoral dissertations and any other single publication (excluding articles in journals). In the AIC Congress 2001, in Rochester, a first stage of this work was presented (Caivano 2002); now, the project is more developed, and I would like to go further and show some other aspects.

The bibliographical database is basically arranged in chronological order, taking into account the date of the first edition of a book in its original language. For texts produced before the invention of printing, the date of writing is considered, and the same is valid for posthumous editions. Following this criteria, an entry is made for every first edition or production of a book (falling within the life span of the author), and all posterior editions and translations are included in the same entry. The fields for each entry are:

1) Author [date of birth and death]	6) Publisher
2) Year of publication	7) Subject
3) Title	8) Decimal classification
4) Language	9) Posterior editions in the original language
5) City of publication and country	10) Translations and posterior editions in other languages

The basic criteria used to organize some of these fields have been described in Caivano (2002).

The bibliography is available on the Internet, at www.fadu.uba.ar/sicyt/color/bib.htm. At present it can be accessed in two versions: in Word document format, and in searchable database format. In this last version, the user has the possibility of making searches by any of the fields numbered from 1 to 8 in the list above, and also to get the complete bibliography arranged either chronologically or alphabetically, by first author. Every bibliographical entry has been classified by subject, which is described in words and numbers, according to the Universal Decimal Classification.

At the moment of writing this paper (June 2003), the database has 2,721 entries for first editions in the original language, and 3,564 entries if we also consider posterior editions and translations. It covers a period of 2,363 years, since 360 before Christ to 2003. At present, we assume that we have recorded almost all books on color published (in original editions) in the main Western countries. The languages in which the coverage is fairly complete are six: English, French, German, Italian, Portuguese, and Spanish. The database also includes books written in other 17 languages, with a total of 23 different languages. As for the countries in which first editions were published, the database includes 52 different ones.

We have been using several kinds of sources to obtain the data: direct contact with the books in libraries and bookstores in various countries (Argentina, Australia, Bolivia, Brazil, England, France, Italy, USA), other bibliographies or compilations of color sources, references in books and journals to which we had direct access, book reviews and announcements in journals and newsletters, the Internet, and information sent by the own authors. Of the 2,721 primary sources listed to date, we had direct access to around 400; the data of the remaining ones have been taken mainly from references in books and articles.

How do we realize that the database is fairly complete, at least for the mentioned languages? Basically, because when we look at the references in books or articles that come to our hands, we usually obtain no new entries, and the data we already have appear repeated again and again. This situation enables us to perform some statistical analysis on the compiled data, with a good degree of accuracy.

In putting the accent on the original dates of publication or production of books, and the consequent chronological arrangement, this bibliographical database allows situating the sources in their historical context, and thus, the emergence of ideas, theories and techniques can be compared on a contemporary basis. The user of the database will find also the translations and posterior editions of a book (which for ancient books are often the sources he can access to), but he may relate them to the original source. By this way, the use of systems of bibliographical references that make a distinction between accessed source and original source is allowed. In any piece of research, the accessed source must appear due to an elementary scientific honesty, in relation to the document that the researcher had in his hands, while the original source serves to put a quotation, idea, or reference in its historical context.

But in addition to the bibliographical information itself, which is the main purpose of the database, some of the interesting information that can be extracted from it is:

- The ranking of the most prolific authors of books on color (see Table 1).
- The ranking of the most used languages in first editions or manuscripts (see Table 2).
- The fluctuation of the most used languages along the centuries (see Table 3).
- The ranking of publishers of first editions (see Table 4).
- The ranking of cities and countries where first editions were published (see Tables 5 and 6).
- The comparative evolution of productivity of books on color (see Table 7).

Additionally, while this is not developed or shown here for reasons of space, the following information could be extracted:

- The ranking of the most prolific editors or compilers of books on color.
- The ranking of the most visited subjects.
- The fluctuation of subjects along the centuries, and the appearance of new subjects.

Table 1 shows the ranking of the most prolific authors of books on color. Of course, this is not an absolute measure, because we are not considering the length of the books (nor the fact that there are authors that have published just one or two books, but hundreds of articles in journals, which are not recorded here). Also, the table does not include co-authors. Thus, it should be taken with these limitations in mind.

Table 2 shows the ranking of languages, and Table 3 depicts how the main languages were changing along the centuries in being at the top: from Greek and Latin (during the Ancient times and the Middle Age) to Italian and Latin (in the Renaissance), the appearance of French in the 17th century, then English and French dominating the 18th and 19th centuries, while German began to raise, then English and German in the first half of the 20th century, and finally only English dominating over other languages in the second half of the 20th century.

In Table 4 we can see the ranking of publishers, where we also include the institutions where doctoral dissertations have been produced, and some scientific institutions that also publish books (such as the CIE, the Scandinavian Color Institute, etc.). Again, the quantity or number of publications does not mean total volume of production, because, for instance, the relatively short documents usually published by the Scandinavian Color Institute or the CIE (except for the proceedings of congresses) are not comparable (in terms of volume or quantity of pages) with the longer books usually published by commercial publishers.

Table 6 shows the number of books produced by country. This is mainly valid for Western countries were the six mentioned languages are spoken (English, French, German, Italian, Portuguese, Spanish). In addition to old Greek and Latin, the coverage in Swedish, Slovenian, and Hungarian is fairly good. But we did not have still full access to sources or libraries in some countries from East Europe, Asia, and Africa.

In Table 7 we can appreciate the evolution of productivity of books on color during the 20th century, year by year. Some references are included on important dates both in the world history and in relation to color science (such as the foundations of the CIE and the AIC). It is interesting to note the years in which the production declined, those in which raised again, and some years which may be seen as departing points, such as 1922, after which the production never went under 10 books per year (except for 1943, in the middle of World War II), the years preceding and following the two wars (for instance, the sequence going from 1946 to 1949), and the year 1974, which seems to stand out clearly. As for the years approaching 2000, which show a little decay, this may not be the real situation, but may be due to some lack of information, which is normal when one approaches the present. The reason is that one of the main sources we use to obtain the data are the bibliographical references in books, proceedings, and journals, and normally, from the moment of its publication, it takes some time for a book to be included as references in other sources.

Summing up, the aim of this paper has been to present the most updated version of the bibliographical database on color, and to show some tables and conclusions derived from simple statistical analysis.

ACKNOWLEDGEMENTS

The researchers joining the author are R. Amuchástegui, G. Cutuli, M. Echegaray, J. Garavaglia, M. López, M. Musso, M. Net, A. Pappier, P. Valle, and especially P. Becerra. Thanks are due also to J. Becerra, J. Agostinelli, M. Ardanaz, J. De Franceschi, M. Juncal, M. Pujol, and C. Manganiello, for collaboration, and to many authors who provided data. The work is supported by the University of Buenos Aires.

REFERENCE

Caivano, J. 2002. "Interactive bibliographical database on color", in *AIC 2001, Proceedings of the 9th Congress* (Bellingham, WA: International Society for Optical Engineering, Proceedings SPIE vol. 4421), 967-970.

Table 1. Most prolific authors of books on color (only the first author is taken into account).

	authors (or first authors)	**number of books**
1	Faber BIRREN	31
2	Heinrich FRIELING	16
3	Friedrich W. OSTWALD	15
4	Lars SIVIK	11
5	Michel E. CHEVREUL	10
6	Harald KÜPPERS	9
7	Antal NEMCSICS	8
8	Louis CHESKIN	7
	Anders HÅRD	7
	Arthur POPE	7
	Nikolai V. SEROV	7
9	Giovanni BRINO	6
	Karin FRIDELL ANTER	6
	Matthew LUCKIESH	6
	Max LÜSCHER	6
	Lia LUZZATTO	6
	Aemilius MÜLLER	6
10	Hugo F. MAGNUS	5
	William D. WRIGHT	5
11	William ABNEY	4
	Arthur Bruce ALLEN	4
	Milton BRADLEY	4
	Jack Howard COOTE	4
	Eric P. DANGER	4
	Leatrice EISEMAN	4
	Ralph M. EVANS	4
	George FIELD	4
	Theo GIMBEL	4
	Alfred HICKETHIER	4
	John HUTCHINGS	4
	Deane B. JUDD	4
	Shigenobu KOBAYASHI	4
	Arthur Pillans LAURIE	4
	Harold LINTON	4
	Roberto D. LOZANO	4
	Albert H. MUNSELL	4
	Michel PASTOUREAU	4
	E. B. RABKIN	4
	Manfred RICHTER	4

Table 2. Number of first editions published or manuscripts produced in the main languages registered in the database.

	languages	**number of books**	**per cent**
1	English	1,540	56.6
2	German	397	14.6
3	French	286	10.5
4	Italian	133	4.9
5	Spanish	112	4.1
6	Russian	48	1.8
7	Latin	38	1.4
8	Dutch	33	1.2
9	Swedish	31	1.1
10	Japanese	21	0.8
11	Portuguese	14	0.5
	other languages	68	2.5
	total	**2,721**	**100**

Table 3. Fluctuation of languages along the years.

	years	**languages**	**number of books**
Until 1500	360 BC - 999 AC	**Greek**	8
		Latin	2
	1000-1499	**Latin**	9
		Italian	4
From 1500 to 1900 (spans of 100 years)	1500-1599	**Italian**	9
		Latin	6
		German	1
	1600-1699	**Latin**	15
		French	10
		English	2
		Italian	1
		Swedish	1
	1700-1799	**English**	18
		French	15
		Italian	9
		German	7
		Latin	4
		Portuguese	3
	1800-1899	**English**	106
		French	71
		German	45
		Italian	11
		Latin	3
		Hungarian	1
		Portuguese	1
		Spanish	1
		Swedish	1
From 1900 to 2000 (spans of 50 years)	1900-1949	**English**	396
		German	126
		French	47
		Russian	19
		Italian	17
		Spanish	11
		Dutch	5
		Swedish	3
	1950-1999	**English**	973
		German	216
		French	141
		Spanish	94
		Italian	79
		Russian	28
		Dutch	27
		Swedish	25
		Japanese	17
		Portuguese	9
		Hungarian	7
		Slovenian	5
		Danish	4
		Polish	4
		Czech	2
		Norwegian	2
		Chinese	1
		Finish	1
		Greek	1
		Korean	1
		Rumanian	1
		Turkish	1

Table 4. Top 22 publishers or institutions where more number of first editions were published (or PhD thesis were produced).

	publishers	number of books
1	John Wiley & Sons	45
2	Van Nostrand	44
3	Commission Int. de l'Eclairage	41
4	Springer	24
5	McGraw-Hill	22
6	Muster-Schmidt	20
7	Academic Press	16
	Scandinavian Color Institute	16
8	Cambridge University Press	15
9	SPIE	14
10	Chapman & Hall	13
	MacMillan	13
	Unesma	13
11	Watson-Guptill	12
12	Adam Hilger	11
	DuMont	11
	Oxford University Press	11
	Pitman	11
	Prentice-Hall	11
13	Dunod	10
	Hoepli	10
	Rockport Publishers	10

Table 5. Top 25 cities where more number of first editions where published or manuscripts produced.

	cities	number of books
1	New York, USA	373
2	London, England	346
3	Paris, France	237
4	Berlin, Germany	67
5	Leipzig, Germany	55
6	Chicago, USA	42
7	Stockholm, Sweden	40
	Washington DC, USA	40
8	Munich, Germany	39
9	Milan, Italy	37
10	Vienna, Austria	33
11	Tokyo, Japan	32
12	Stuttgart, Germany	30
13	Buenos Aires, Argentina	27
	Boston, USA	27
14	Cambridge, Mass., USA	26
15	Göttingen, Germany	22
	Philadelphia, USA	22
16	Barcelona, Spain	19
	Madrid, Spain	19
17	Amsterdam, The Netherlands	18
	Ann Arbor, Michigan, USA	18
18	Venice, Italy	17
	Florence, Italy	17
19	Basel, Switzerland	16

Table 6. Number of first editions published or manuscripts produced by country, according to the information in the bibliographical database.

	countries	number of books	per cent
1	USA	841	30.91
2	England	450	16.54
3	Germany	349	12.83
4	France	266	9.78
5	Italy	145	5.33
6	Sweden	60	2.20
7	The Netherlands	59	2.17
8	Spain	58	2.13
9	Switzerland	54	1.98
10	Russia	50	1.83
11	Japan	43	1.58
12	Austria	40	1.47
13	Argentina	32	1.17
14	Belgium	17	0.62
15	Canada	14	0.51
16	Brazil	12	0.44
	Hungary	12	0.44
17	Slovenia	11	0.40
18	Denmark	8	0.29
	Mexico	8	0.29
19	Greece	7	0.26
	Norway	7	0.26
	Venezuela	7	0.26
20	Finland	6	0.22
	Poland	6	0.22
	Scotland	6	0.22
21	Czech Republic	5	0.18
	Korea	5	0.18
22	China	4	0.15
23	Australia	3	0.11
	Chile	3	0.11
	India	3	0.11
24	Bulgaria	2	0.07
	Egypt	2	0.07
	Latvia	2	0.07
	Portugal	2	0.07
	Turkey	2	0.07
	Uruguay	2	0.07
25	Bolivia	1	0.04
	Colombia	1	0.04
	Ecuador	1	0.04
	Estonia	1	0.04
	Israel	1	0.04
	Lebanon	1	0.04
	Malta	1	0.04
	Monaco	1	0.04
	New Zealand	1	0.04
	Peru	1	0.04
	Puerto Rico	1	0.04
	Rumania	1	0.04
	Slovakia	1	0.04
	South Africa	1	0.04
	Ukrania	1	0.04
	unknown	103	3.79
	total	**2,721**	**100**

Table 7. Fluctuation of the number of books, year by year, from 1900 to 2000.

year	number of books	
1900	11	
1901	6	
1902	6	
1903	6	
1904	7	
1905	8	
1906	9	
1907	9	
1908	8	
1909	5	
1910	6	
1911	6	
1912	13	
1913	9	CIE found.
1914	5	World War I
1915	11	World War I
1916	13	World War I
1917	5	World War I
1918	13	World War I
1919	8	
1920	8	
1921	9	
1922	13	
1923	17	
1924	17	
1925	11	
1926	13	
1927	14	
1928	18	
1929	17	
1930	20	
1931	11	
1932	15	
1933	14	
1934	15	
1935	15	
1936	11	
1937	16	
1938	22	
1939	14	World War II
1940	15	World War II
1941	15	World War II
1942	15	World War II
1943	9	World War II
1944	13	World War II
1945	10	World War II
1946	16	
1947	17	
1948	24	
1949	38	
1950	25	

year	number of books	
1950	25	
1951	31	
1952	28	
1953	23	
1954	30	
1955	26	
1956	30	
1957	23	
1958	15	
1959	22	
1960	21	
1961	23	
1962	27	
1963	29	
1964	29	
1965	22	
1966	35	
1967	40	AIC found.
1968	31	
1969	36	
1970	42	
1971	41	
1972	37	
1973	34	
1974	58	
1975	38	
1976	39	
1977	25	
1978	28	
1979	27	
1980	26	
1981	26	
1982	27	
1983	30	
1984	36	
1985	26	
1986	34	
1987	42	
1988	29	
1989	46	
1990	44	
1991	33	
1992	29	
1993	43	
1994	44	
1995	49	
1996	45	
1997	48	
1998	41	
1999	43	
2000	39	

José Luis Caivano
SICyT-FADU-UBA
Ciudad Universitaria Pab. 3 piso 4
C1428BFA Buenos Aires, Argentina
jcaivano@fadu.uba.ar

ARTIFICIAL ENVIRONMENT, CYBER SPACE AND NEW COLOURS PROJECTS

Lia Luzzatto and Renata Pompas (Istituto Europeo di Design, Italia)
http://www.color-and-colors.it

INTRODUCTION

Some years ago we did some research about the colours of clothing, starting from Roman times and arriving at the XX century (1997). This research led us to understand the ideological, commercial, social and material causes which – from the past to the present - have characterised collective taste with specific ranges of colour, through particular historical periods. While we were doing this study we came across the phenomenon of digital colours[1].

In fact in the mid Nineties some particular social groups, such as artists or sub-cultural spontaneous movements, were fascinated by the shining quality of digital colors. So they adopted fluorescent nuances for their artificial symbolic aspects, alluding to technological immaterial worlds, to the boundless net, without place nor time, into which the Cyber Community had been developing.

We wrote in our book that the Cyberpunks and the Techno groups had introduced some violent fluorescent and acid shades into hair, make-up and fabrics, showing their rebellion against nature and naturalness.

Corrosive and bitter colors functional to the light of mega-concerts, found their greatest place in synthetic fabrics, plastics and artificial leathers. In fact these colors are very suitable for the artificial flashing lights of discos ad nightclubs, and for the pounding, repetitive beat of Techno Music.

This subject fascinated us and so we have been continuing to work on it. In fact digital colors have invaded our community both in work and leisure, in public and private spaces, becoming an indispensable presence of the constructed environment.

So we thought that we would present some of our reflections to the esteemed members of AIC during this 2003 Bangkok Meeting, and we like to call these shades "cyber colors", quoting the famous expression of William Gibson (1986)[2].

Looking for any products and images alluding to digital colors – in textiles, fashion, design, furnishing and advertising – we have been helped by the students of post-university courses in Advertising who, with a good preparation in visual communication, have been navigating the Net for a long time, comparing the use of colors among disparate Web sites.

We certainly don't think that digital colors empty material colors of all their meaning, but we would like to highlight their presence in the chromatic landscape, and their ability and power to create new taxonomies of meaning.

NATURE VERSUS CULTURE

The cultural view of colour allows us to formulate cognitive categories. The linguistic and mental framework of this view is the result of considerable experience and it is continually being updated as it acquires elements of innovation.

On this subject, the hypotheses advanced by Brent Berlin and Paul Kay (1969) and by Giorgio Raimondo Cardona (1985) are well known. According to Berlin and Kay the cognitive and nominal view of colour is organized according to a cultural progression of an evolutionary kind[3], while Cardona maintains that different visual habits, dictated by context, develop different sensitivities and thus different taxonomies[4].

The perception of colours is therefore a dynamic ability, subject to moments of strong evolution and change.

We believe that the daily introduction of cyber colours into the cognitive process stimulates the redefinition of the taxonomies of colour and meaning, and that this process, which has already begun, is leading to results that have yet to be analysed systematically.

Conceptually the starting point of the reflection that we are putting forward today can be traced back to the time when humanity began to observe, discover, study and manufacture colouring substances with a view to intervening on reality and changing it.

The change from a state of nature to a state of culture is also highlighted by the coloured covering given to man's constructs, as a sign and symbol of his power and his capacity to differentiate.

The last of these great moments prior to the era of computers was that of the industrial mass production of chemical colours and their spread on a massive scale: a revolution of perception which was at first a surprise but which then accustomed the eye and the mind to a new and unusual range of colours with a fixed quality and an inexhaustible reproducibility.

If in the mid nineteenth century the textile market was invaded by Perkin's "mauve", obtained by transforming the waste products of mineral tar[5], in 1935 it was the Italian dressmaker Elsa Schiapparelli, much beloved by artists, who with the paint colourist Jean Clément first produced a vivid cyclamen shade, known as shocking pink.

Later it was the French artist Yves Klein who together with the chemist Edouard Adam in 1956 perfected an extremely saturated, brilliant ultramarine blue the chemical formula of which was patented with the name of YKB, Yves Klein Blue, in 1960.[6]

Since then the study of colorants, dyes and paints has continued to forge ahead and a wide variety of shades have come on to the market, some glossy, some translucent and some transparent; some with particular kinds of luminescence or shines. Phosphorescent, fluorescent colours, ranges sensitive to light and others sensitive to heat. Colours with a metallic appearance give the effect of gold, bronze and silver; shades with changing iridescent tones and opalescent shades that give off dual reflections; colours with a mirror-like effect that communicate a sense of variability.

FROM MATTER TO LIGHT

The process which took colour from matter to immateriality took place with the reproduction of colour through its fragmentation into pixels.

Digital screens, which exercise a mathematical control over the emission of colour, move the axis of vision from unity to division, from substance to light.

While chemical colouring covered the constructed environment with a superficial layer that was both stable and homogeneous, making the appearance of buildings, walls, rooms, furnishings, objects and materials uniform; digital colours have the opposite effect, causing an adjustment towards a chromatic view based on immateriality.

Digital colour creates a luminous coloured flow, which is both fluctuant and perturbable and which leads through screens into a parallel world of colour, superimposed upon the real world. A fluctuating impalpable colour, freed of the presence of an objective support, which changes the order of sensorial perception.

For the first time in the history of mankind we can see images constructed merely from the colours of light, without reference to substance.

Colour thus becomes subject, form, movement and action.

Already thirty-five years ago Stanley Kubrick, in "*2001: A Space Odyssey*", portrayed crossing into the fourth dimension as a dreamlike trip in a kaleidoscopic whirlwind of colours which were themselves the subject of the experience. Today the contrast between substance and appearance and between materiality and immateriality has been superseded by digital colours, a phantasmal presence of simulated subjectivity.

From now on "Switching on colours" is not merely a metaphor, but a gesture that takes our eyes into the illusory depth of screens illuminated from behind which have unlimited potential for changing external appearances. While these screens construct a new reality, they at the same time de-structure visual sensation, uncoupling it from the other senses: touch, taste and smell.

In nature the formation and the knowledge of colour pass through matter and activate all of the five senses which become fixed in the image transmitted through sight. In the evocative or imaginary world of screens, digital colour is perceived only through the sense of sight and so has to recover from previous memories its link with its multi-sensory identity, which is now abstract rather than physical.

We believe that the colours of electronic images need to be adapted to the new chromatic information available, need to be detached from their natural reference and that since they produce a different new effect of reality they are actually act on their context, modifying it.

The universe of light colours and that of pigment colours confront each other and if at the beginning screen colours were attempting to imitate the colours of nature, today pigment chemistry is attempting to imitate the colours found on screens.

The language of colour influenced by the digital experience has become part of a broader project: from fashion to design, from advertising to graphics, from cartoons to the cinema.

So where metal was the image and the symbol of technological society, now cyber colour has become the image and the symbol of digital society.

TOWARDS THE CREATION OF NEW SYMBOLS

In our opinion the colours of screens have generated and could still generate new codes of meaning.

Let us consider green for example: a natural, ecological, reassuring, protective and everlasting colour, which takes on a more sinister and worrying note in the nightly bombardment broadcast by television; or the green that we can see on ufology websites where it hints at the existence of aliens.

Let us consider the different communicative effect of shocking pink, so frivolous and sensual, which in cyberspace takes on a new technological meaning, one that is artificial and strictly digital, indicating the virtual quality of what is seen.

And let us consider red, which we frequently find used around the edges of web pages, such as for example in frames and the borders of images. A red which alone assumes responsibility for showing the way round the page and indicating the directions to be followed from one page to the next, calling them up directly from the unconscious of the observer.

Lastly we reach blue, the colour of spirituality and affection, which has become the symbol of cyber space just as before it was the symbol of celestial space. In the virtual depths of the Internet, blue, which is one of the most widespread colours, represents the universe to be explored by surfing the Net and provides the confidence and the authority necessary to avoid succumbing to the fear of getting lost in hyperspace.

A reassuring role but one that is contradicted by the alarming blue screen with the code numbers of the error, announcing the tragic death of an OS system and of Microsoft Windows.

To conclude, we would also like to reflect on the power of the web, which offers itself as the navigable cyber space of the global village. In this space colours and functions tend to unify languages and symbols.

The flow of the web eliminates boundaries and creates cross-contamination between cultures, produces stylistic eclecticism, weakens the awareness of being part of history, transforms time into a perpetual present and reduces the intensity of other deeper levels of communication.

A kind of communication that shortens the life of feeling and sentiment. Thus the intensity of digital colours is not matched by an intensity of emotion.

Lastly, we would like to close our paper with an [i]image taken from the film THE MATRIX, the symbolic icon of which – represented by the uninterrupted flow of the strings of numbers of the system that will regulate the cyber universe - is a pulsating greenish luminescence of numbers.

REFERENCES

[1] Luzzatto Lia, Pompas Renata. I colori del vestire. Variazioni – Ritorni – persistenze, 1987 (The clothing colors. Changes- Memories – Persistence)

[2] Gibson William, Burning Chrome. 1986

[3] Berlin Brent, Kay Paul. Basic Color Term. Their universality and their evolution. 1969

[4] Cardona Raimondo, La foresta di piume. Manuale di etnoscienza. 1985

[5] Garfield Simon. Mauve. 2002

[6] Weitemeier Hannah. Yves Klein 1928 – 1962. International Klein Blue.1995

i

Experience of Light, Colour and Space in Reality compared to Virtual Reality

Monica Billger, School of Architecture,
Chalmers University of Technology, Sweden

INTRODUCTION

One limit of the computational modelling of architecture is that digital models do not show the same colour phenomena as real rooms. The fast technical development provides us with better and better computer graphics and faster rendering techniques, however the reliability and usability is delimited by lack of knowledge about how humans perceive spatial colour phenomena. The difficulty to visualize and comprehend the way chosen colours will appear in a planned building is a well-known problem in the design process. Factors as illumination, colour combinations and textures affect the appearance of coloured surfaces in rooms. The problem of informing about colour phenomena in rooms is obvious. 3D-viualisations and VR-simulations ought to have potential to correctly present planned environments and solve this colour communication problem. The crucial problem is how reliable these simulations are today.

This paper discusses questions concerning the potential for Virtual Reality to become a usable design tool for the planning of light and colour in buildings. It presents preliminary results from comparisons between a real room (a full scale model) and a virtual environment viewed on desktop PC (3D-studio/Lightscape) and in an Immersive/CAVE based system (dVise), here referred to as the 3D-cube. We have studied the appearance of light and colours, as well as the observers' total impression of the room.

The comparison points out unsatisfying differences in shadowing and colour appearance. The great colour variations on equally painted surfaces, which were perceived in the real room, did not show in the digital models. In the digital models, the shadows were greyish and thin, as they were placed on a separate layer on top of the coloured surfaces. We also faced problems to simulate the colours of the areas painted in very light nuances; even the illuminated areas became too greyish. Some of the differences had to do with arbitrariness of setting up parameters for material properties in the light calculation software.

BACKGROUND

There is no absolute definition of the term Virtual Reality but here is meant a computer-generated 3D world that allows the user to feel present and interact with the world in real time. Traditional design tools, such as plans, perspectives and sections, have difficulties to represent the three-dimensional world correctly [1]. Laymen have usually problems to understand them [2, p.52], which hinder participation in the design process. VR may reduce errors due to abstract representation [1] and it enables presence [3] in another world than the real, which can be of great advantage during a planning process. Immersive VR may also give a more account sense of relative straight-line distance compared to desktop [4]. 2001 Nilson [5] stated that there are two focuses of VR-studies in the field of Architecture; one is on functional and ergonomical studies from a user perspective, and the other on visualization of Architecture regarding aspects as spaciousness. Very little is published concerning *colour appearance* in real rooms compared to virtual rooms. However, colour is considered as one aspect among other in the discussion on experience of space in scale models, full-scale models and virtual reality. Martens et. al points out the importance of colour and material regarding the perception of three-dimensional objects [6]. One pilot study reports that colour and texture seems to have an impact on size [7].

It is extremely difficult to predict the way the colour of a small sample will appear, when applied in full scale in a building, since the light in the room affects the visual appearance heavily. One can say that surfaces in a room works as filters for the striking light [8]. This depends on physical properties of the light and the room surfaces, such as flux and angle of the striking light and the texture and colour of the surface. Human perception depends also on the state of adaptation and the complex way our brain treats the information of spectral composition that reaches our eyes [9]. We interpret the whole situation, not each local point. For the 10 last years, several research projects on Colour appearance in Architecture have been carried out in Sweden. Much effort has been put on methodological questions. To identify the colour we perceive in rooms or on buildings is problematic. One aspect is that no instrument can measure what one sees; a reliable method that involves human observers is required. Our need to study real environments to obtain results that we consider meaningful and useful, requires us to consider the complexity of the context as an essential feature of the studied situation. To tackle this complexity, methods and concepts were developed as shown in [10,11,12].

Due to the complexity of the interaction between light and objects, the central conceptual and practical problem of computer graphics is the problem of lighting scenes [13, p. 73-74]. In most computer graphics today the goal is not to make correct simulations of reality, but visualizations that look good [13,14]. The light calculation programme software Lightscape (plug-in to 3Dmax) uses radiosity to calculate how much light that strikes back from a surface. How much the colour of the surface should change the colour of the "bouncing" light is defined in the colour bleeding scale. This is done arbitrary, because there are no recommendations built upon knowledge on how coloured surfaces reflect upon each other.

PROBLEMS AND AIMS

The main goal is to contribute to a deeper understanding of the perception of colours and display differences and similarities between the experience of real and VR-simulated room. The outcome of the project can provide us with tools that enable us to create reliable virtual rooms to pedagogically display various colour phenomena and to communicate colour appearance during the design process.

The main problem dealt with in this paper is whether light- and colour phenomena appear in the same way in digital models as in real rooms. The phenomena focused on are: contrast effects, reflections from one surface upon the other, shadow colours and perceived colour of light. There are several steps to be aware of when transforming a Lightscape model into a 3D-cube model. Information is lost during the process. The light and colour quality is worse in the 3D-cube than on the desktop, however for the participants' sense of involvement and presence there may be advantages of being immersed by the room. A previous pilot study showed that the poor light situation in this immersive space laboratory makes it meaningless to compare the exact colour appearance of each surface to the original room [15]. Thus, the colour and light phenomena were closer examined in reality and desktop. I will briefly deal with the ways the different spaces were experienced and consider what meaning it has to the understanding of the room when the quality in colour and light differs. It is important to stress that it is not the participants' evaluation of this particular experimental room that is of interest; it is the correspondence between the evaluations made in the different situations.

EXPERIMENTAL DESIGN

The virtual room studies were carried out in an immersive space laboratory (3D-cube) and on desktop PC. The IPT type system was a 3x3x3 meter TAN 3D Cube with stereo projection on five walls (no ceiling). The application was run on a Silicon Graphics Onyx2 Infinity Reality with 8 MIPS R10000 processors, 2GB RAM and 3 graphic pipes. The participant wore Crystal Eyes shutter glasses with a Polhemus tracking device and used the dVise 3-D mouse for navigation. Note that the 3D-cube gave a stereoscopic effect, which the desktop did not provide. *The real room studies* were carried out in a specially designed 25 m2 experimental room. Three different light situations were used: tungsten and fluorescent 2700K and 3000K. Data was collected via video recording the participants, interviews and questionnaires. Six techniques are used for evaluating light, colour and space: free descriptions of the room as a whole, semantic differential scaling with open scales complemented by the participants motivation behind the scaling: visual evaluation of light [16]; semantic descriptions of the colours using everyday language and the NCS (Natural Colour System)-terminology, magnitude estimation [17] and colour matching with a Colour Reference Box [10]. The four first techniques were used with all participants and the last two techniques with fewer well-trained observers. Totally 56 observers were involved; between 10 and 30 participated in each situation. The preliminary results presented in this paper are based on 10 desktop studies, 22 real room studies and 26 cave studies. It only includes studies of one light situation: fluorescent 3000K.

As pointed out earlier, there was no use to focus on a comparison between each coloured surface in reality and in the cave; we were interested in the relation between the surfaces. The colour design of the room is complex (see Fig.1). It was designed in order to get clear examples of how simultaneous contrast and reflections cause different appearances of two yellow hues in two nuances. In this paper, I focus on the sides of the upper cube of the two standing in top of each other, and the areas painted in the lightest nuance.

The desktop model was studied in a dark room. The digital model was built in 3D Studio Viz. The light calculations were made in Lightscape. The producer of the light fixtures used in the real room has created digital models to use in the software Lightscape, and we placed these fixtures in the model and made all the set-ups for calculating the light after their recommendations. We used the digital software NCS palette to define the colours of the different surfaces. To use this model in the immersive space laboratory, we translated it into division mock-up, dVise 6.0. To compensate for poor colour quality and low light level, the colourfulness of the surfaces was increased by approximately 25 %.

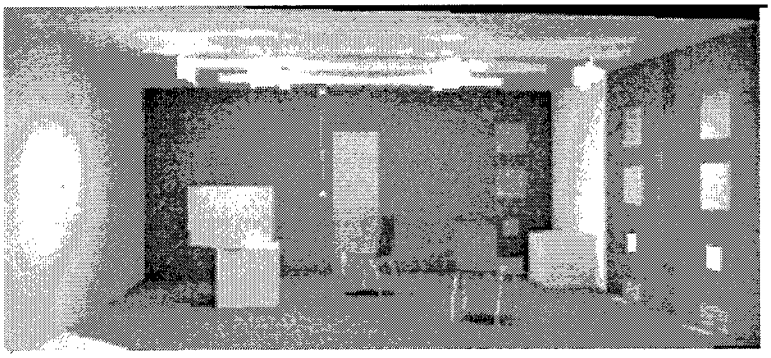

View towards the door.

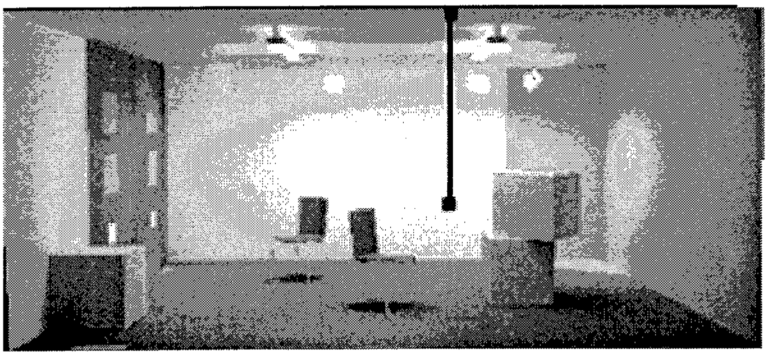

View from the door.

Figure 1. *The digital room model seen from two opposite perspectives. In order to get clear examples of simultaneous contrast, smaller squares were painted on different backgrounds and large areas of different colours met on the same wall. To get distinct examples of reflections one corner had the same green-yellow paint on the floor and the two adjacent wall, and the sides cubes standing on the floor faced differently painted walls.*

The six paints used in the room were NCS:
S 5005-Y (grey floor)
S 2050-Y75R (red)
S 2050-G10Y (green)
S1030-G90Y (greenish yellow)
S 1030-Y10R (reddish yellow)
S0510-G90Y (light green-yellow)
S0510-Y10R (light red-yellow)

RESULTS

Space

Everyone could recognize the room from one situation to the other, however they expressed that the experiences were very different. Especially between the cave and reality. For example, the experience of the real room and the 3D-cube simulation differed in aspects as warmth, harmony, heaviness and distinctiveness. The desktop room was found to be very distinct; the indistinctiveness of the cave room gave more room for interpretations. It was difficult to tell the difference between corner, colour or shadow. The 13 participants, who had not seen the real room in advance, described the cave room in a more varied way. It was not obvious that it was a rectangular box-shaped room. Some interpreted lighter coloured areas as openings. One said that it was made of concrete; many expressed that there were no clues to materials at all.

Light

The perceived light situation in the desktop model corresponded well to the real room in all aspects except for the colour of the shadows.

Light level: In the real room, the participants agreed on a light level between 6 and 8 on a 10-graded scale. The desktop model was perceived as somewhat lighter, between 7 and 9. In the cave, the level was estimated between 3-6. The question was more difficult in this situation, *e.g.* some participants described it as they could interpret the model as a simulation of a light room, although it was dark in the cave.

Light distribution and shadows: In desktop the shadows were found to be natural in that sense that they seemed to be in the right place, however they were too achromatic. They were described as greyish and thin, as they were placed on a separate layer on top of the coloured surfaces. In the 3D-cube model, the participants did not accept the light distribution. The light did not seem to come from the light fixtures and the shadows were unnatural and misplaced. It was very annoying to realize that one has to "light up" the pre-rendered digital model with the software's own light!

Perceived colour of light: Most participants found the light in the room to be cold or neutral in all situations. In desktop and reality it had basically no colour; some participants found it yellowish in reality. However, in the cave it was grey, and more participants found the perceived colour of light to be warm than in the other situations. Different meanings were expressed whether it had a tinge towards violet, red, blue or yellow.

Colour

In reality, the differently painted surfaces had strong effect on each other by reflections. This caused great colour variations on equally painted surfaces that did not show in the virtual rooms. The sides of the upper cube phased differently painted walls. It was painted in NCS 1030-Y10R. In reality the different sides had so different colours that many participants thought I had painted them differently (see fig. 2).

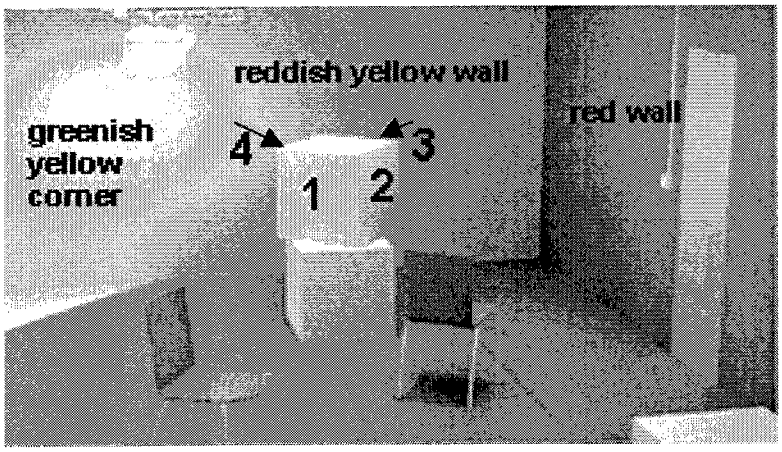

Figure 2. The cubes on the floor differed distinctly from the background wall painted with the same paint, the overall impression of them was yellower than the wall. However, many participants questioned that they were painted equally. Side 1 had a yellow hue. Side 2 was redder. Side 3, facing the reddish yellow wall, was more colourful, and side 4, towards the green-yellow corner, was more greenish (lemon yellow).

There is no recommendation for setting the colour bleeding scale based on science; there is praxis among skilled professionals based on experience. 100% colour bleeding is the default value according to Lightscape's help-file that recommends this value when making a light analysis. This is said to give physically accurate results during radiosity processing. However, 100% degree of colour bleeding did not result in greater colour variations, instead the colour blending between the surfaces resulted in a room, where the grey and yellow (light and strong nuances) surfaces were all reddish beige.

The skilled professional, who modelled the light fixtures in the digital model suggested 4-15% colour bleeding for the matt surfaces in the room. This showed to be a far too low degree, and we are at the moment elaborating with this scale. Preliminary results from having tested to manipulate a few surfaces in the model, tell us that at least 40% colour bleeding is needed; and that different levels is needed for different colours.

We had great problems to simulate the areas in the lightest nuances (area 5- 8 on fig.3). These areas, painted with NCS 0510-G90Y or NCS 0510-Y10R, became too greyish in the digital models. In reality, the white fluorescent (3000K) illumination made the long light wall (6) almost white, the short wall (5) was light beige. The small squares were white with a tint of pink (7) and green (8). This was not seen at all in the digital rooms. In fact, even a white wall became grey in the Lightscape rendering process.

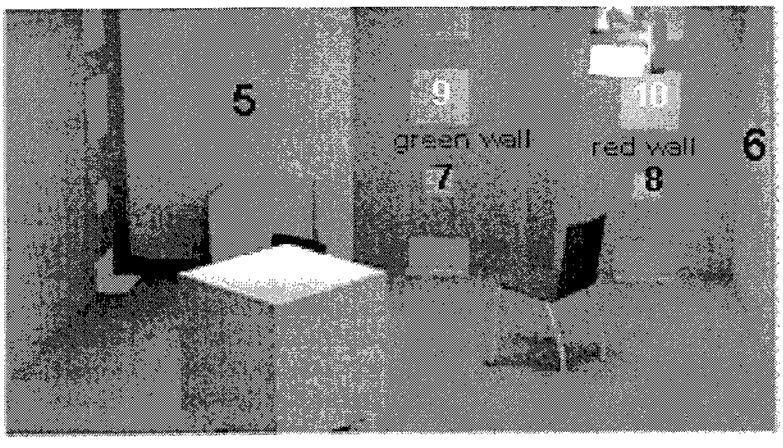

***Figure 3.** The areas in the lightest nuance were difficult to simulate. They appeared too greyish in the digital models. The small squares (7 and 8)that were strikingly whitish in reality, were hardly noticed in the digital models. The light areas were painted in:*
5 and 7: NCS S0510-G90Y
6 and 8: NCS S0510-Y10R
The larger squares were painted in the stronger nuance of the yellow hues. On the red and green background area 9 (1030-G90Y) and 10(1030-Y10R) appeared almost equal in hue.

CONCLUSIONS

The work with translating visual phenomena to virtual simulations needs to be further explored. We need to know how to correctly set the parameters for the physical properties in computer software such as Lightscape in order to achieve correct simulations; not only create pictures that look good. To make this possible, we need to define the magnitude of perceived colour reflections, in order to translate this knowledge into rules of thumb for setting the colour bleeding scale.

ACKNOWLEDGEMENTS

My greatest thanks to my assistants Beata Stahre and Ylva Konradsson, who have carried out a great deal of the interviews. Many thanks to Kristian Renström, Fagerhult, who made the modeling in Lightscape and taught me to manipulate with the software, and to Kasper Lennqvist and Björn Gross, who made the 3D –studio model Thanks to Johan Kihlström, CKK, who helped me converting the Lightscape models and get them into the Cave. This work was made possible by grants from the Swedish Research Council and the Swedish research council for environment, agricultural sciences and spatial planning.

REFERENCES

1. **Dorta, Tomas and Lanlande, Philippe,** The impact of Virtual Reality on the Design process, In: Seebohm T. *Ed*: Proceedings of ACADIA 98, pp.138-163 (October 1998, Quebec City, Canada)
2. **Hornyánsky Dahlbom, Elisabeth,** Att forma sitt rum: Fullskalemodellering i participatoriska designprocesser, *Diss.*, LTH, Inst.för Byggnadsfunktionslära, Lund;1998
3. **Riva Guiseppe**, From Technology to Communication: Psycho-social Issues in Developing Virtual Environments. Journal of Visual Languages and computing; 10;p.87-97;1999
4. **Waller, David**, *Factors Affecting The Perception of Interobject Distances in Virtual Environments,* Presence: Teleoperators and Virtual Environments, vol 8;no 6;657-670;1999
5. **Nilsson, Alexander,** VR-forskning i Sverige, Dagsläge och framtida riktlinjer, Report for KFB (Kommunikationsforskningsberedningen), In press: CTH; Göteborg; 2000.
6. **Martens B.,Uhl, M.,Tschuppik, W-M. and Voigt. A.,** *Synagogue Neudergasse: A virtual recontruction in Vienna,* In: Construction of digital space, Proceedings of 4th SIGRADI, Rio di Janeiro, 2000
7. **Hornyansky Elisabeth and Rydberg Mitchell, Birgitta,**
8. **Billger Monica,** Colour Combinations Effects in Experimental Rooms. *Colour research and application, no 4;p. 230-242;1999*
9. **Zeki Semir,** A vision of the brain, Blackwell Scientific, Oxford, 1993
10. **Billger Monica,** *COLOUR IN ENCLOSED SPACE: Observation of Colour Phenomena and Development of Methods for Identification of Colour Appearance in Rooms.* CTH: Doctorate thesis, Ny serie nr 518;1999.
11. **Fridell Anter, Karin,** What colour is the red house?, KTH: Doctorate thesis, Trita-ARK-Akademisk avhandling 2000:4
12. **Hårleman, Maud,** Färg i norr och södervettande rum: kulörtonförskjutning genom varierande ljusförhållanden, KTH, Trita-ARK-Forskningspublikation 2000:4
13. **Slater, Mel and Steed, Anthony and Crysanthou, Yiorgos,** Computer graphics and virtual environment: From realism to realtime; University College London, Pearson Education Limited; 2002
14. **Wishar Peter,** Digital Space: Designing virtual Environments, McGraw-Hill, New York, 1998
15. **Billger Monica and d'Elia Stefano,** Colour appearance in virtual reality: a comparison between a full-scale room and a virtual reality simulation. In: *AIC Color 2001, Proceedings of the Ninth Congress of the International Colour Association, Rochester NY, USA*; 2001;
16. **Liljefors, Anders och Ejhed, Jan,** Bättre belysning: om metoder för belysningsplanering. Stockholm: Statens råd för Byggnadsforskning: Solna: Svensk Byggtjänst; 1990.
17. **Hård, Anders, Sivik Lars, and Tonnquist Gunnar,.** NCS, natural Color System - from concept to Research and Applications, part I, Col. Res. Appl. 21(3); pp.180-205;1996

A Study on Evaluation of the Interior Atmospheres and the Choice of Behavior with Effects of Lighting, Color and Gloss

Takuzo INAGAKI (Professor, Department of Architecture, Faculty of Engineering, Daido Institute of Technology)
Shoji IIJIMA (Professor, Department of Environmental and Tourism Science, Faculty of Commerce, Okayama Shoka University)

INTRODUCTION

By many foresighted researches, psychological effects of lighting and color individually were clarified, and this knowledge has been applied for interior design. Therefore the effects of gloss, one of the important visual information elements, have not been clarified because they are difficult to quantify.

This study aims to clarify not only the main effects of lighting, color and gloss but also interactions of them by use of design of experiment- table of orthogonal arrays L_{16}.

EXPERIMENT

1.Design of experiment

In this study, nine factors were adopted; lighting, three attributes of color and gloss of wall and these of floor. These nine factors were arranged as shown Table 1. By use of this design of experiment, main effects of these nine factors and four interactions were to be examined.

2.Device of experiment

The scale-model was made on a scale of 1:10. This scale-model was lit by fluorescent lamps or incandescent lamps. Two ceilings were made for each illuminant, and these colors were fixed at N9. Three surfaces of wall and floor boards were changeable. Two chairs and a table were arranged for imparting reality, and these colors were also fixed at N9. Subjects could look around the interior space through the oval-shaped aperture.

3.Procedure of experiment

Questionnaire was composed of two questions; one was attempted to evaluate atmospheres of the interior space by SD method, the other was attempted to evaluate suitability of 14 behaviors in this space.

As shown Table 1, 16 stimuli which were combined by nine factors, were presented for subjects. These 16 stimuli were presented by random order. Subjects were 20 architecture majors(10 male, 10 female).

Table 1 The layout of experiment by design of experiment-orthogonal table L_{16}

Factor / Stimulus	Lighting	Hue of Wall	Lighting × H.of W.	Hue of Floor	Lighting × H.of F.	H.of W. × H.of F.	Value of Wall	Chroma of Wall	Gloss of Wall	Value of Floor	Chroma of Wall	e (error)	e (error)	Lighting × G.of F.	Gloss of Floor
①	**Fluo.**	10YR	(1)	10YR	(1)	(1)	8	5	G	6	5	(1)	(1)	(1)	G
②	**Fluo.**	10YR	(1)	10YR	(1)	(1)	8	2	M	4	2	(2)	(2)	(2)	M
③	**Fluo.**	10YR	(1)	10B	(2)	(2)	6	5	G	6	5	(2)	(2)	(2)	M
④	**Fluo.**	10YR	(1)	10B	(2)	(2)	6	2	M	4	2	(1)	(1)	(1)	G
⑤	**Fluo.**	10B	(2)	10YR	(1)	(2)	6	5	G	4	2	(1)	(1)	(2)	M
⑥	**Fluo.**	10B	(2)	10YR	(1)	(2)	6	2	M	6	5	(2)	(2)	(1)	G
⑦	**Fluo.**	10B	(2)	10B	(2)	(1)	8	5	G	4	2	(2)	(2)	(1)	G
⑧	**Fluo.**	10B	(2)	10B	(2)	(1)	8	2	M	6	5	(1)	(1)	(2)	M
⑨	**Incan.**	10YR	(2)	10YR	(2)	(2)	6	5	M	6	2	(1)	(2)	(1)	M
⑩	**Incan.**	10YR	(2)	10YR	(2)	(2)	6	2	G	4	5	(2)	(1)	(2)	G
⑪	**Incan.**	10YR	(2)	10B	(1)	(1)	8	5	M	6	2	(2)	(1)	(2)	G
⑫	**Incan.**	10YR	(2)	10B	(1)	(1)	8	2	G	4	5	(1)	(2)	(1)	M
⑬	**Incan.**	10B	(1)	10YR	(2)	(1)	8	5	M	4	5	(1)	(2)	(2)	G
⑭	**Incan.**	10B	(1)	10YR	(2)	(1)	8	2	G	6	2	(2)	(1)	(1)	M
⑮	**Incan.**	10B	(1)	10B	(1)	(2)	6	5	M	4	5	(2)	(1)	(1)	M
⑯	**Incan.**	10B	(1)	10B	(1)	(2)	6	2	G	6	2	(1)	(2)	(2)	G

Fluo. :Fluorescent Lamp, **Incan.**:Incandescent Lamp, **G:**Glossy Finish, **M:**Mat Finish, H:Hue
W:Wall, F:Floor, G:Gloss, ×:Interaction between two factors
and so forth

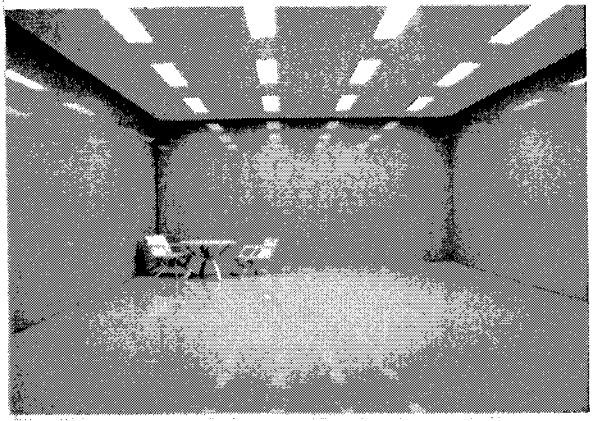

① Fluo., W:10YR8/5(G), F:10YR6/5(G)

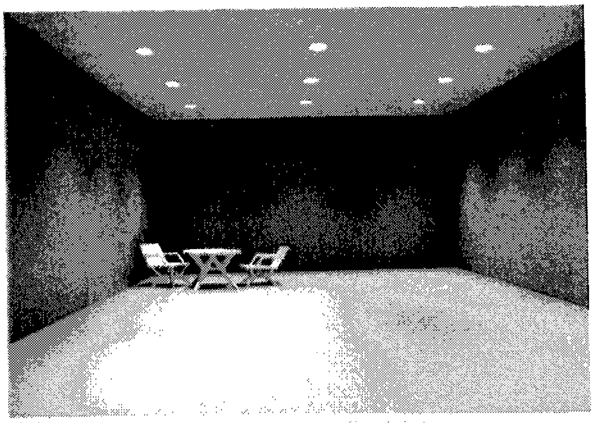

⑨ Incan., W:10YR6/5(M), F:10YR6/2(M)

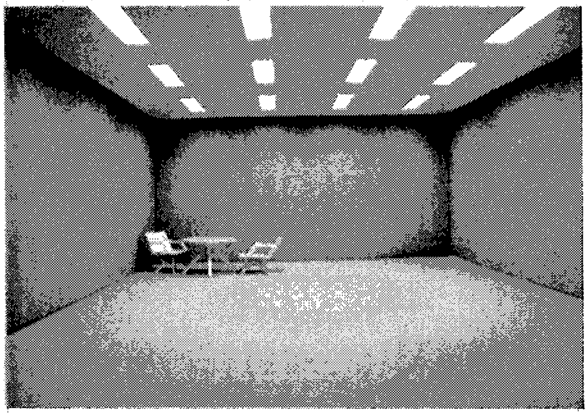

② Fluo., W:10YR8/2(M), F:10YR4/2(M)

⑩ Incan., W:10YR6/2(G), F:10YR4/5(G)

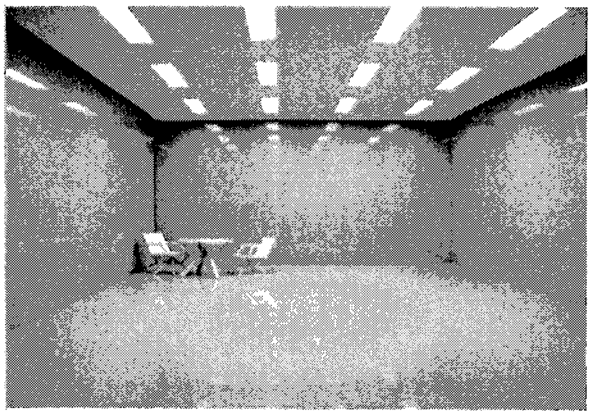

⑦ Fluo., W:10B8/5(G), F:10B4/2(G)

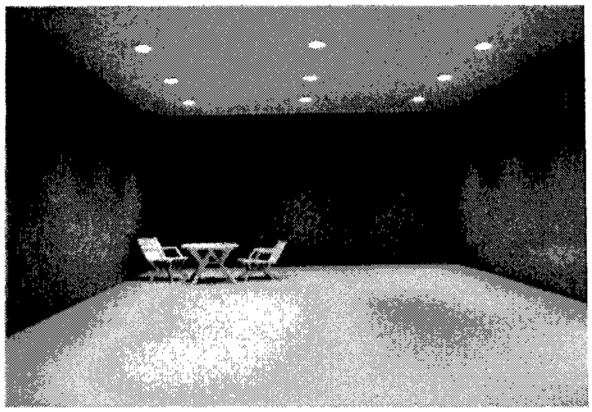

⑮ Incan., W:10B6/5(M), F:10B4/5(M)

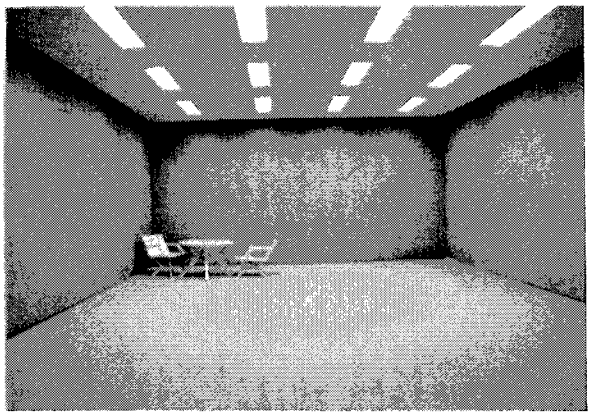

⑧ Fluo., W:10B8/2(M), F:10B6/5(M)

⑯ Incan., W:10B6/2(G), F:10B6/2(G)

Photo 1 Samples of stimuli No. of ○ corresponds with No. of stimulus in Table 1

Table 2 Factor analysis in evaluation on atmospheres

Adjective \ Factor	Factor I Comfort	Factor II Gorgeousness	Factor III Routine
luxury	**0.9007**	0.3298	− 0.2586
favorite	**0.8896**	0.3983	0.1115
calm	**0.8739**	0.0323	0.4193
convenient	**0.8554**	0.3810	0.2546
soft	**0.8521**	0.1757	0.4296
feminine	**0.7698**	0.2538	**0.5255**
warm	**0.7694**	− 0.0530	**0.5201**
bright	− 0.0687	**0.9337**	0.2975
loud	0.2874	**0.8880**	− 0.0625
spacious	0.2788	**0.8408**	0.0443
neat	**0.5380**	**0.8011**	0.0071
advanced	0.0249	**0.7609**	**− 0.5994**
busy	0.3031	**0.6333**	0.4447
usual	0.3306	0.1430	**0.8980**
common	0.1925	0.0254	**0.8158**
proportion(%)	38.0	30.1	21.2
cumulative proportion(%)	38.0	68.1	89.3

Bold face: factor loading is more than 0.5

Table 3 Analysis of variance(each factor) in evaluation on atmospheres

Factor		Factor I Comfort	Factor II Gorgeousness	Factor III Routine
Lighting		* * Incan.	* Flou.	
Wall	Hue			* * YR
	Value		* 8	* 8
	Chroma			
	Gloss			
Floor	Hue			* * YR
	Value		* 6	
	Chroma			* 2
	Gloss			
Lighting×Hue of W.				
Lighting×Hue of F.				
Lighting×Gloss of F.				
Hue of Wall ×Hue of Floor		* YR × YR (B × YR)		

* :level of significance=5%, * * :level of significance=1%

Table 4 Analysis of variance(each adjective) in evaluation on atmospheres

	Adjective \ Factor	Lighting	Wall Hue	Wall Value	Wall Chroma	Wall Gloss	Floor Hue	Floor Value	Floor Chroma	Floor Gloss	Lighting × Hue of W.	Lighting × Hue of F.	Lighting × Gloss of F.	W.Hue × Hue of F.
I	luxury										I. × YR			B × B
	favorite													
	calm	Incan.												
	convenient													YR × YR
	soft	**Incan.**	YR	8				6						
	feminine	Incan.	YR	8			YR	6						
	warm	**Incan.**	**YR**	**8**			**YR**	**6**						
II	bright	**Fluo.**		**8**				6						
	loud		B	**8**				**6**			F. × B	I. × YR		
	spacious													
	neat													
	advanced		**B**				B							
	busy			8				**6**						
III	usual		**YR**	8			**YR**	6						
	common		YR						2				F. × M	

Bold face: level of significance=1%
and so forth

RESULTS

Obtained data were examined, as a result a significant difference based on sex was not noticed.

1.Evaluation of atmospheres

Obtained data were processed by factor analysis, then three dimensions were extracted; Comfort, Gorgeousness and Routine.

The use of incandescent lamps and the accordance of hue make the interior atmospheres comfortable. And the use of fluorescent lamps and bright finished wall and floor make the impression gorgeous. Moreover colors which are popular and used in high frequency − warm hue, high value and low chroma − make the interior space routine (Table 3).

As shown in Table 4, furthermore, the detailed examines on the individual adjectives were carried out.

The use of incandescent lamps, colors of high value and low chroma make the interior atmosphere soft, feminine and warm. The combination of cool hue makes the space luxury, but that of warm hue makes the space convenient.

About adjective 'loud', two interactions concerning light were confirmed.

The use of warm hue on wall and floor makes the atmosphere usual. About adjective 'common', the only one interaction concerning gloss was confirmed.

Above mentioned, the informations concerning the effects on the individual adjectives were obtained.

Table 5 Factor analysis in choice of behavior

Behavior \ Factor	Factor Ⅰ Relaxation	Factor Ⅱ Intelligence	Factor Ⅲ Motivation	Factor Ⅳ Entertainment
have a meal	**0.9302**	− 0.0430	− 0.2537	− 0.0486
have a party	**0.9234**	− 0.0826	0.2130	− 0.1967
spend a time with friend	**0.8688**	− 0.0273	− 0.0344	0.3379
spend a time with lover	**0.8271**	0.1695	− 0.3216	0.1019
lie on the floor	**0.8067**	0.2112	− 0.1555	0.1299
listen to the music	**0.6533**	0.3670	− 0.2268	**− 0.5323**
read books	− 0.0006	**0.8810**	− 0.0676	0.2317
think about something	− 0.2315	**0.8605**	− 0.2284	− 0.1674
run away	**− 0.5594**	**− 0.7149**	− 0.1096	0.0622
want to do nothing	**− 0.6393**	**− 0.6987**	− 0.1366	0.1640
paint	0.2526	0.3488	**0.8350**	− 0.0361
exercise	− 0.3591	− 0.2165	**0.7268**	0.0202
drink	0.3342	0.3696	**− 0.6966**	− 0.0312
watch television	0.1374	0.0515	− 0.0271	**0.9606**
proportion(%)	38.1	21.7	14.9	10.8
cumulative proportion(%)	38.1	59.8	74.7	85.5

Table 6 Analysis of variance(each factor) in choice of behavior

Factor		Factor Ⅰ Relaxation	Factor Ⅱ Intelligence	Factor Ⅲ Motivation	Factor Ⅳ Entertainment
Lighting		* Incan.		* * Fluo.	
Wall	Hue		* YR	* B	
	Value			* 8	
	Chroma		* 2		
	Gloss		* * M		* M
Floor	Hue				
	Value				* 6
	Chroma				
	Gloss				
Lighting × Hue of W.					
Lighting ×Hue of F.					* F. ×YR (I. ×YR)
Lighting ×G. of F.			* I. ×M (F. ×M)		
Hue of W. ×Hue of F.			* B× B (B × YR)		

2. Choice of behavior

By factor analysis, four dimensions were extracted; they were named Relaxation, Intelligence, Motivation and Entertainment.

The light color and low illuminance of incandescent lamps give people relaxation.

The warm color, low chroma and mat finish inspired subjects with intelligence. Two interactions also inspired intelligence.

The cool hue and high illuminance of fluorescent lamps, cool hue and high value of wall give subjects motivation to do something ambitious.

Glossy finished wall and medium value of floor entertained men.

Moreover the effects of surroundings on each behavior were examined.

The use of incandescent lamps were suitable for relaxing behavior; to spend a time with close men.

The four behaviors connecting with factor 2. were influenced by many interactions. So it is necessary to take account of these interactions for creating intellectual space.

For exercising it is effective to use fluorescent lamps and cool hue of wall. On the contrary, for drinking it is effective to use incandescent lamps and warm hue of wall.

Lastly for watching television it is suitable to provide mat-finished wall and medium value of wall for preventing glare.

CONCLUSION

By introduction of design of experiment, many main effects and some interactions of lighting, color and gloss were approved.

And the validity of design of experiment for such a research was approved.

Table 7 Analysis of variance(each behavior) in choice of behavior

	Behavior \ Factor	Lighting	Wall Hue	Wall Value	Wall Chroma	Wall Gloss	Floor Hue	Floor Value	Floor Chroma	Floor Gloss	Lighting × Hue of W.	Lighting × Hue of F.	Lighting × Gloss of F.	W.Hue × Hue of F.
Ⅰ	have a meal	**Incan.**	YR				YR							
	have a party													
	spend a time with friend	Incan.						**6**			**I. × YR**			
	spend a time with lover	**Incan.**												
	lie on the floor													
	listen to the music	Incan.												
Ⅱ	read books	**Incan.**	**YR**	**8**		**M**							**I. × M**	YR × YR
	think about something	Incan.			2	**M**	B		**2**			F. × B	I. × M	
	run away		B		**5**						F. × B	I. × YR		B × YR
	want to do nothing													B × YR
Ⅲ	paint													
	exercise	**Fluo.**	**B**								F. × B			
	drink	**Incan.**	**YR**								I. × YR			**YR×YR**
Ⅳ	watch television					**M**		**6**			I. × YR	F. × YR		

A Color Image in a Shopping Street; The Case of "Tanuki-Koji" in Sapporo

SAKAHARA Koya
Department of Architecture, Hokkaido Institute of Technology

1 Introduction

In this report, we have the purpose to get the fundamental data on a color planning at a shopping street by using a color image of passers-by. In September 2001 and 2002, we carried the research of an image at a shopping street into practice. The research zone is the third and forth blocks in "Tanuki Koji" which is one of the oldest shopping streets in Sapporo. The report has items to choose the favorite colors and the image colors of the street. We will consider these items.

The research method is an interview to the passers-by. On a favorite color and an image color, we showed them a color chart with 93 colors and we asked to choose 3 colors. We made this color chart by P.C.C.S. The two research periods are one week each. The valid data of them is 4394. 1345 were done by male and 3049 were by female. The other items of this research are the sex, the age, the purpose and the address (the nearest station on the public transportation system) of the responders. "Tanuki-Koji" is one of the main streets located in the central part of Sapporo. It has been developing together with a history of Sapporo since 1871. It has a 890-meter arcade and the 180 stores. It is a route type store town.

Fig.1 is an age structure of responders according to the sex. The number of female responders is more than the one of male. Focusing on the age, we can't see a big difference between the tow. We made a count of the passers-by at the same time with this research. In 2001, the male passers-by were 88,847 people, the female passers-by were 92,742 and the total passers-by were 181,638. In 2002, the male passers-by were 91,119 people, the female passers-by were 79,953 and the total passers-by were 170,953. We judged their sex on visual check.

On considering an error by visual check, we can't find out a large difference between men and women. The number of the female respondents of the questionnaires were overwhelmingly many. The number of the male respondents is below half of it's female one. In the age structure, the young respondents of 10s and 20s are overwhelmingly many. They occupy around 70 percents in all. The passers-by of man and woman were almost the same number. In this reason, we can say that the male don't cooperate with a questionnaire. We must consider this point to examine the result.

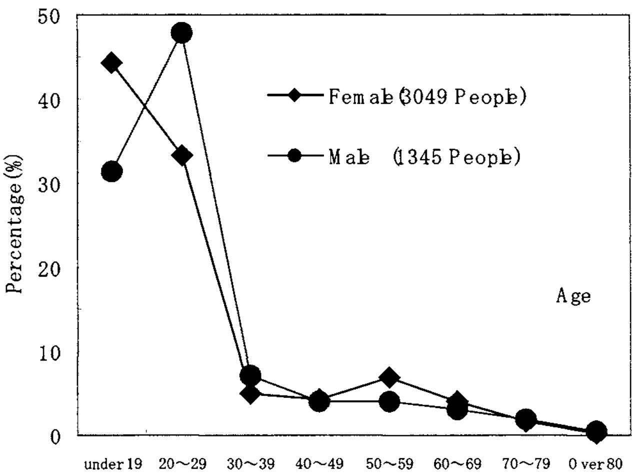

Fig.1 An age structure of responders

2 A favorite color and an image color at the shopping street

In Fig.2, we show the 10 favorite colors from the top in all. From on high, the first figure is the rate of respondents on a favorite color according to the sex. The second is the rate of respondents on a favorite color by age in the case of female. The third is the rate of respondents on a favorite color by age in the case of male.

The colors that have a big difference between men and women are Vivid Blue, Purplish Pink and Black. In a research on a favorite color in Japan, White usually comes first a high rate of respondents. But in this research, White weren't chosen as their most favorite color.. Vivid Tone got a majority. It is necessary to make a study on these results.

In the Case of female, young people tend to be fond of Purplish Pink, Vivid Yellow, Vivid Reddish Orange, Bright Greenish Blue, Pale Green and Bright Blue. In the case of male, young pepole chose Vivid Blue, Black, White and Bright Blue as their favorite. According to these, we can say that the female like the warm colors and the male prefer cool colors and achromatic colors.

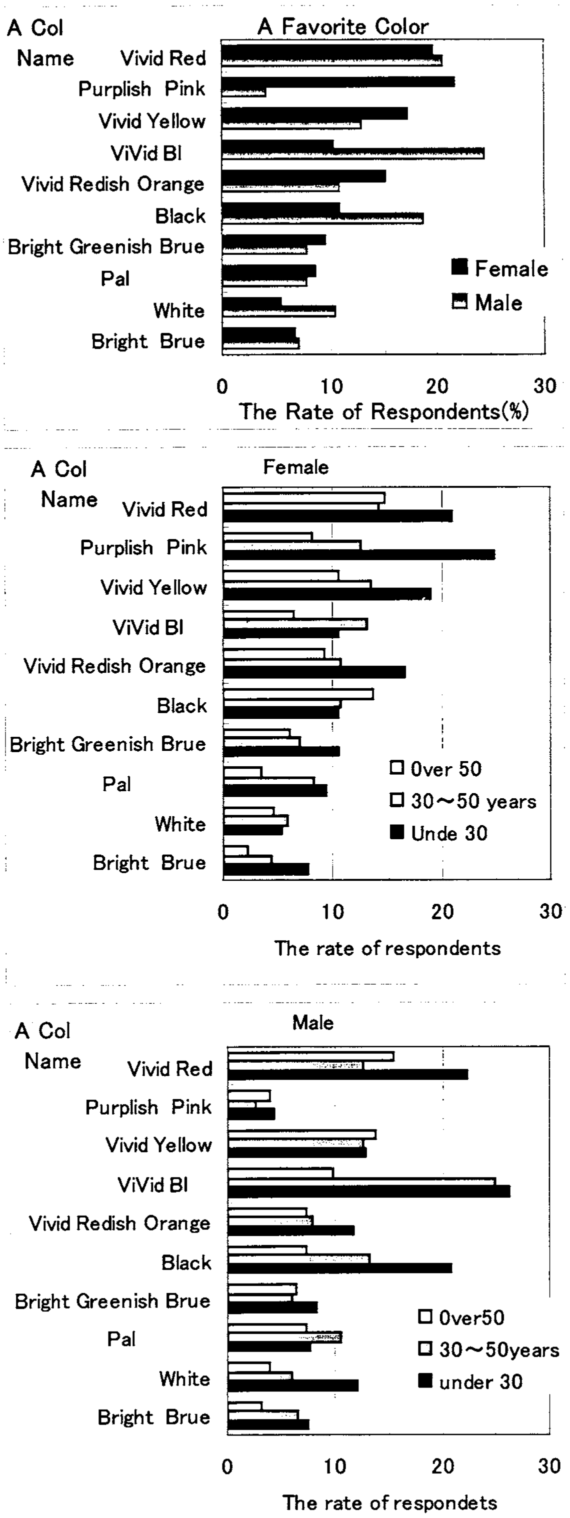

Fig.2 The 10 favorite colors by sex and age from the trop

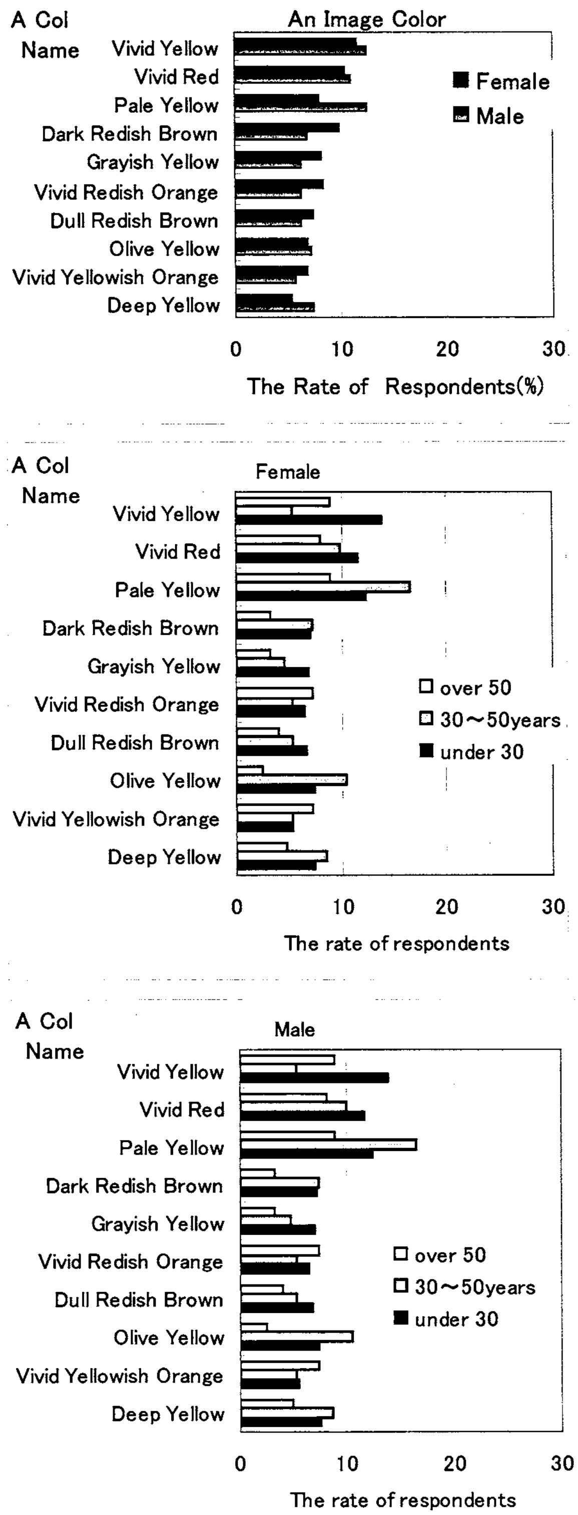

Fig.3 The 10 image colors by sex and age from the top

In Fig.3, we show 10 image colors from the top. The configuration of a figure is similar to Fig. 2. A difference between men and women isn't so large as the Fig.2. I done say, the rate of Pale Yellow chosen by male was 30% higher than the one of female. A difference between each color is trivial. We can't say any big difference between ages, but Pale Yellow is chosen by 30～50 brackets is more than others.

4 The favorite colors and the image colors by tone

In Fig4, we show the rate of respondents on the favorite colors by sex and tone. Tone having the largest difference between men and women is Light Tone. And then, next one is Achromatic Color. In comparison to the case of the top 10 colors, the difference between men and women gets a smaller. The most favorite tone is Vivid Tone.

In Fig.5, we show the case that they choose the color that belongs under the same tone as the image color of this shopping street. It is a same line as Fig. 4. We can't see the large difference between men and women. In the case of Grayish Tone , the chance to be chosen the same color tone is comparatively high. Similarly, in the case of a favorite color, Vivid tone comes the first in this time.

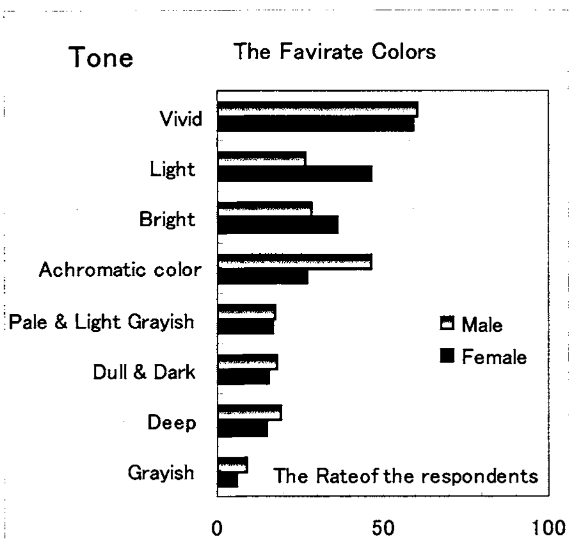

Fig.4 The rate of respondents on a favorite color by tone

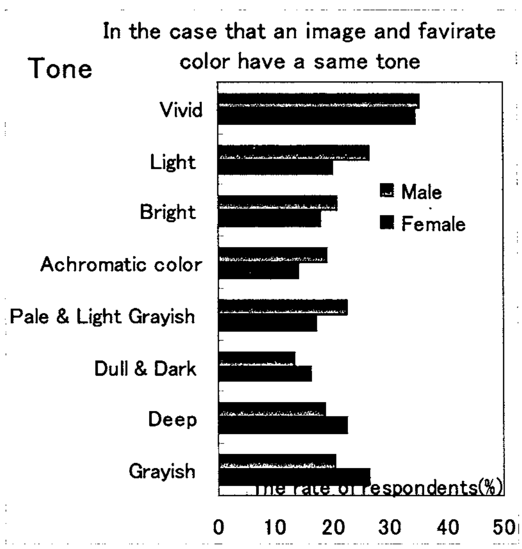

Fig. 5 The rate of respondents by tone in the Case that an image and a favorite color have a same tone

5 In the case of Vivid Tone as a favorite color

In the case of Vivid tone as a favorite color, we consider the color to choose as an image color of "Tanuki-Koji" and the physical property. The reason to take up Vivid Tone is that Vivid tone is highly chosen as a favorite color. As an image color, we take up achromatic colors and Bright Tone here. In the case that R^2 is over 0.5, we show the regression line in the figure. We consider the relation between the rate of respondents in the image colors and these lightness or the chroma.

Fig. 6 shows that they choose an achromatic color as an image color. The right is a female. The left is a male. We show the relation between the rate of respondents and the lightness by dividing the colors into the case that the lightness is over 60 and less than 60. According to comparison of men and women, the female is almost a straight line. But we can't see the large difference, in terms of trend. The relation between the two is shown by similar under convex curve of second degree in both men and women. In the case of the lightness over 60, as the lightness increases, the rate of respondents on an image color increases. In the case of the lightness less than 60, as the lightness increases, the rate of respondents on an image color decreases. We can say that the achromatic colors have a different choice trend of an image color between over 60 and less than 60.

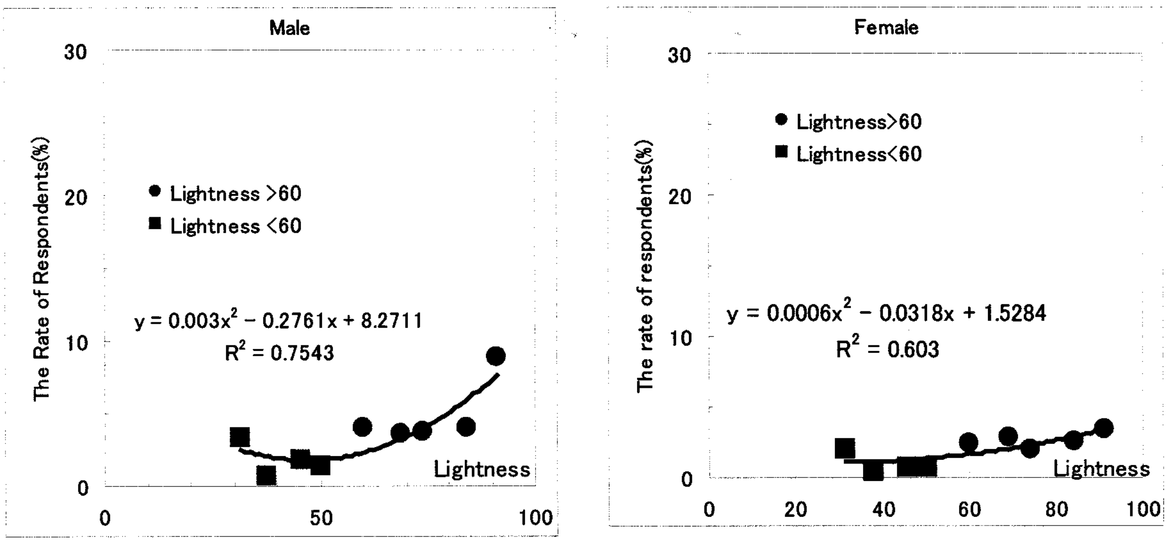

Fig.6 In the case that an image color is achromatic colors;
The relation between Lightness and the rate of respondents

In Fig.7・8, we show the case that they choose Bright Tone as an image color. Fig.7 is the relation between the rate of respondents and the lightness. The Fig.8 is the relation between the rate of respondents and the chroma. ●(black circle) in figure is a warm color, ■(black square) is a cool color.

Focusing on Fig.7, the cool colors were less chosen and the warm colors were chosen higher. The relation between the two is approximated well by an under convex curve of second degree. The R^2 is over 0.7. It is on a high level value.

In the case of female, as a warm color of a high lightness, it shows a high rate of respondents. In the case of male, there is a similar trend. The R^2 is smaller than the female. There isn't so large difference as the case of Achromatic Color (The Fig.6). We think the smaller trend between men and women.

Paying attention on Fig.8, there is a clear difference between cool colors and warm colors. Namely, as

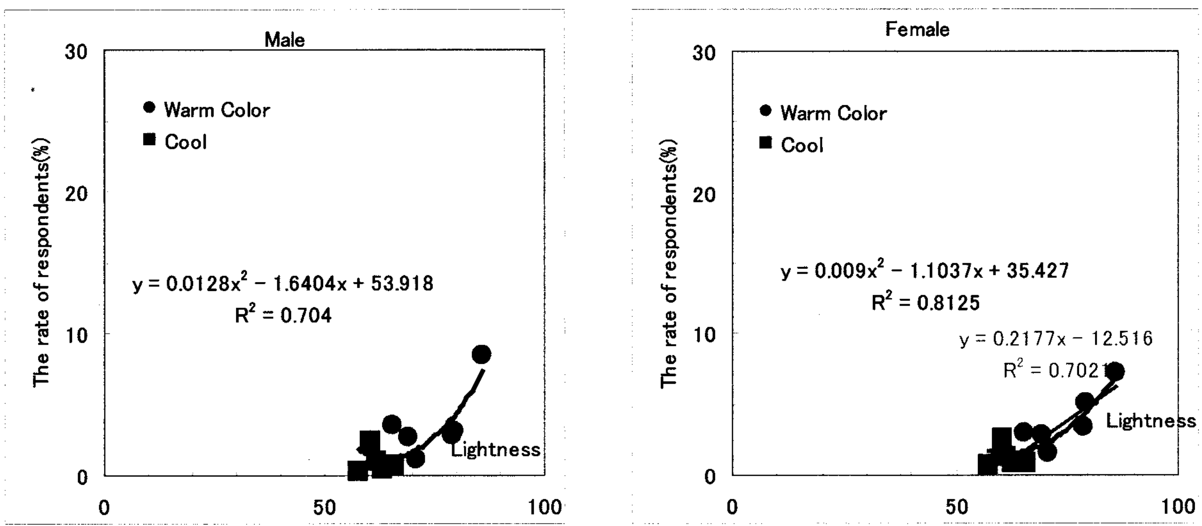

Fig.7 In the case that an image color is Bright Tone;
The relation between Lightness and the rate of respondents

the warm colors of the high chroma, it shows the high rate of respondents. As the cool colors of the high chroma, it shows the low rate of respondents. The two show the inverse trend. As the whole, the relation between the two is approximated by an under convex curve of second degree. We can hardly see the difference between men and women. The R^2 are over 0.7. These are the fairly good approximate expressions.

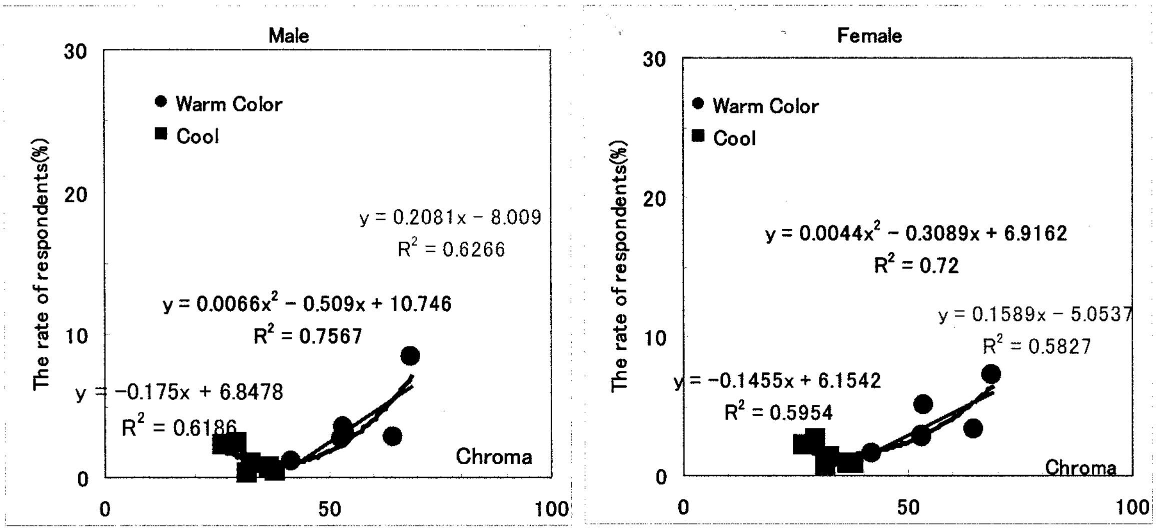

Fig.8 In the case that an image color is Bright Tone; The relation between Chroma and the rate of respondents

5 Conclusions

The following are conclusions of this report by itemizations.

1. In the past, the favorite colors had the trend that White held on the top ranks in Japan. But in this research, vivid red in the Vivid Tone came to the first. We have the different result from the past research. On these factors, we think that the regional characteristics in Hokkaido and the change of period might affect. We would like to make an analysis in many fields.
2. A favorite color has a big difference depending on a sex and an age. But an image color has a little difference.
3. In the case of Vivid tone as the favorite colors , we show the following relation between the rate of respondents and the lightness or the chroma. In the case of achromatic color, we show the different trend when the lightness is over 60 and less than 60. The two is approximated by an under convex curve of second degree as a whole. In the case of Bright Tone, we show the other trend between the warm colors and the cool colors. The two is approximated by an under convex curve of second degree as a whole. In the case of the another tones, we get the similar trends. But these R^2 and numerical formulas are different.

REFERENCES

1. A. OATA and E. KAWARA, “Shikisai to Haishoku”, Graphic Co. Publishing Ltd. 1976
2 SAKAHARE Koya, “A Color Choice for a Good Housing Environment; A Research on a repainting color over a Wall or Roof”, Proceedings of 2000 AIC Meeting Seoul Color & Environment, AIC Color 2000, P7-P11 ,2000.11

AUTHOR'S ADDRESS

SAKAHARA Koya
Dept. of Architecture, Hokkaido Institute of Technology
7-15-4-1 Maeda, Teine-ku, Sapporo, 006-8585, Japan
Phone: +81-01-6818-2243 Fax: +81-01-681-3622 E-mail sakahara@hit.ac.jp

The rhetoric of black, white and red:
Reasonability and aesthetics to persuade with color

José Luis Caivano and Mabel A. López
National Council for Research, and Buenos Aires University, Argentina

BLACK, WHITE, AND RED IN CULTURE

Why black, white, and red? Our proposal is to analyze how the use of color can be a privileged element to argue in a visual image. The values and connotations ascribed to color in the context of a visual statement work as "proofs" in reasoning of the persuasive type. In this way, the use of rhetorical figures is not an end in itself, but the visible correlate of the argumentation that works as a hidden, implicit structure of persuasion. We have chosen black, white, and red because of their high frequency in appearing, the great number of uses, and the abundance of socio-cultural interpretations —which even may be apparently paradoxical or contradictory. All these senses are latent, and coexist. Colors are reinterpreted in correspondence with the contexts of use in the texts themselves (co-text), and with the effective social contexts, which frame them in a real situation (historical space and time).

Phylogenetic argument: Before the instauration of language, the primitive man regarded red and black as colors that disturbed his rest. Since life began to develop in the forest, man became predominantly visual; food and sex were linked to light. The black night and its red prelude, sunset, announced the proximity of danger. Lacking night vision, man was exposed to predators (stronger, with better sense of smell, and more acute hearing) when the forest turned into a black depth. The red glints of fire fascinated him in those long and worrying nights in which a real and tangible danger was around. We could imagine that ancestral feeling by remembering the fear that darkness produced us when we were children.

Red and black were associated with the dangers that threatened the survival of the species. The black of night and the red of blood are alerting, warning colors. On the contrary, the white and light blue of day, the browns and greens of soil and foliage are reassuring colors.

Man built shelters, enlightened the darkness, and dominated the natural and animal world; however, his brain has not forgotten. Today, to discriminate the color of danger is not a relevant information to save the life of the species; however, there are still tracks in the archaic memory of the brain that make us react against those stimuli (López Pasquali 1998).

Feeling, thinking, naming: Berlin and Kay (1969) have investigated the basic color terms in various languages across the world. They distinguish eleven basic color terms that appear in the most different cultures: white, black, red, green, yellow, blue, brown, purple, pink, orange, and gray. At the same time, they have elaborated a theory, according to which the evolution of the color names goes through seven stages. The first one (the cultures that only have two color terms) corresponds to "white" and "black". Immediately, in the next stage, the third category to emerge is "red". It includes all red, orange, brown, pink, purple, and violet colors.

It is evident that to communicate this perceptual chromatic sensation was decisive in the primitive communities, hence, red appears next to the achromatic colors, whose distinction was equivalent to the value (light-dark). With the third category, not only a color name appears but also a new cognitive dimension: the category of chromatic color. This third term, "red", was equivalent to say "color".[1]

Ritual and religious persuasion and intimidation: The color triad of black, white, and red, pointed out by anthropologists as basic colors, appears frequently in different forms of body decoration in "primitive" cultures (Hutchings 1989). They are also the most often used colors in British and Irish folklore. They serve to distinguish the central characters or actors of a ceremony or activity. In traditional tales, the black-white opposition is used to represent the antithesis between good and evil. Red symbolizes the blood of Christ, or is used to frighten (Hutchings 1993).

1. In Spanish, "rojo" (red) is synonym of "colorado": having color, colored.

In Japan, red, white, and yellow are colors of good luck, which does not happen in the Western culture. In the cultures surveyed by Hutchings (1997), achromatic colors are associated with mourning rites (death). The use of the black-white-red triad is frequent in diverse rituals to symbolize the passage from a status to another: birth, wedding, baptisms, funerals.

In the East, red means authority, power, wealth, good luck, political ideologies; it is used to purge evil. Behind these ideas, there is a religious and philosophical background that is shared by the Oriental world (Kwon 2002).

In the West, a wristlet of coral has been used since ancient times as amulet to protect children from illness. This belief still remains in South America: a red stripe around the wrist of babies, or hidden inside their clothes, is thought to reject the negative influences (evil, envy, illness) that they attract because of their fragility and beauty.

In the Christian iconography, black and red symbolize the evil (hell, devil). However, red also acquire positive values. It represents charity, because it is the blood shed by Christ to save the world. In the images of the Virgin, the blue color of her robe means virginity, and the red color, the virtue of charity.

The power of alchemy was manifested by means of color, especially by red, white, and black. Figure 1 is the diagram by Reusner (a manuscript from c.1550) that shows the last but one phase of transmutation of basic metals into gold. We can see the White Queen, a prelude of the arrival of the Red King. The half-circle at the bottom shows the alchemic progression from black to red, passing through white. Because of this influence, Baby Jesus has been represented holding a red rose.

This chromatic triad had a place of privilege in heraldic. Norms were established with non-rigorous and even contradictory arguments. For instance, at the end of the 14th century, an English writer on heraldic, Johannes de Bado Aureo (John of the Golden Bucket), considered that red was equidistant to black and white —though he did not explain why—, and was the most appropriate color for princes and knights, because it symbolized courage. During the 19th century, a more psychological interpretation of the symbology of color was developed. The "synoptic table" by Humbert de Superville, published in 1827, characterized red as violent and expansive; white as being the state of equilibrium, calm, and clarity; and, on the other side, black as meaning convergence, concentration, and solemnity (Gage 1993: chapter 5).

BLACK, WHITE, AND RED IN THE URBAN ENVIRONMENT: PERSUASION IN MASS COMMUNICATION

Living in big urban conglomerates has lead to a modification of the material conditions of human existence. The helplessness in front of the danger, that was a characteristic of the species, the fear of night and of the own blood, that could be taken by the wild animals, have undergone some metamorphoses, but have not totally disappeared. Chromatic stimuli —mediated by culture— reproduce some of those primary feelings. Why? What for? One could ask: what is man looking for by evoking the bitter ancestral fears? Those who propose persuasive messages in the frame of mass culture, use this three-color combination in a rhetoric way, with the aim of convince, dissuade, or seduce the public.

In the new communicative and virtual environments in which man evolves, the use of color tends to produce an impact on the senses previously to any reflection on the message. This is a great advantage when competition and the ephemeral condition of communications are a constant. The rhetoric persuasion (in this case, by means of color) only is useful when there is more than one voice, precisely, in the communities where dissent is possible and the multiplicity of opinions can develop. For this reason, the birth of rhetoric happened in a democratic context (the ancient Greece), as a method to make an argument prevail.

The ancient *Rhetoric* (Aristotle 350 B.C.) is the first work that exposes a method, a technique to persuade and obtain adhesion on the part of the public. This rhetoric way was to be pursued in five steps: *inventio, dispositio, elocutio, memoria* and *actio*. In order to argue for something or against something, or about the utility or inconvenience of a certain thing, it was necessary to find what to say (the appropriate arguments), and how to say those ideas. The aspect of rhetoric concerned with the figures of speech used to persuade (how to say) is called *elocutio*. For a long time the analysis of *tropes* (figures) was extended and generalized to explain the aesthetic (creative) uses of language, its poetic function. The deviations that appear in creative texts with regard to the ordinary use of the code correspond to a plentiful repertoire of rhetorical figures that the studies on poetics were coining along the centuries.

Of the five parts in which rhetoric is organized, only two will be developed in this paper: *inventio* and *elocutio* —considered to be of central interest for visual persuasion. The person who enounces a visual discourse is giving a first step in *inventio*, looking for the chromatic arguments, i.e., proposing a pseudo-logical reasoning in which color takes part in the premises and conveys a conclusion. In a later phase, in *elocutio* —how to say—, those uses of color hold a correspondence with the employment of *tropes*, or rhetorical figures generated by a particular, intentional, or transgressive use of color. Rhetorical figures portray a conceptual or formal deviation produced in a statement with the aim of bringing the receptor to a meaning that is beyond the literal meaning.

The statements generated by the rhetoric machine —beyond the real effect on the public, whose impact is difficult to measure— intend to make the receptor reason. The persuasive message employs a logic that —differently from the scientific logic— is not based on truths, but on credible arguments, values, and presumptions accepted by the receptor. The field of the rhetoric technique is not the scientific knowledge, it is the *doxa*,[2] the current opinion, what is reasonable without mediating a demonstration of universal validity. Precisely, the *doxa* is a body of debatable knowledge, closer to "common sense" than to truth or falsity in the logical sense.

The rhetorical use of black, white, and red is based upon shared premises that connect a social group. This "ideology" comes from beliefs about human perception, metonymic associations (blood, fire, night), as well as metaphoric ones, related to cultural memory (mourning, war, purity, evil, hell, political emblems, nationalities, etc.). Some of the most frequent beliefs in the Western culture are: "Red excites vision, is alerting"; "Blood (red) is synonym of danger"; "Red is vital, passional"; "Red is joy"; "White is clean, aseptic"; "White is purity"; "White is neutrality"; "Black is sinister"; "Black is disturbing, mysterious"; "Black produces depression". The paradoxical nature of these asseverations, that acquire positive values (life, euphoria) or negative values (death, dysphoria) according to the context, is explicit.

How to convince

Once the most effective arguments have been selected to produce a greater credibility on the receptor we intend to convince, it is necessary to decide what kind of reasoning are we going to employ to persuade. The argumentative logic may adopt an *inductive* form (giving examples and models to be imitated), a *deductive* form (exposing a reasoning), or an *abductive* form (showing a feature that belongs to a case).

Induction is based on the example (*exemplum*), persuading by means of the identification of the public with the referent proposed as a model. It is the most immediate or primary form of persuasion, the one requiring less reflection on the part of the public. A particular case with certain characteristics (to be imitated or rejected) is presented, to conclude with the personal identification of the receptor with the proposed figure. It is an argument that works on the analogy. A particular kind of example is the *imago*, a well-known and socially representative image, able to embody the values that are intended to promote. In this case, the success of the argument will depend entirely on the credibility of the character.

When there is no primary identification, but a more sophisticated and mediated form of reaching the comprehension of the appellative message, it is sure that *deduction* is at work. To understand this form or argumentation, it is necessary to start with the *syllogism*, the best-known form of deductive reasoning used as a method for scientific knowledge. Beyond the scientific realm, the use of deduction as a persuasive method appears in multiple fields, such as the argumentation in journalism, advertising, politics, pedagogy, justice, the parliamentary debate, the military harangue, the religious preaching, or simply the arguments to convince someone in daily life. This reasoning, called *enthymeme*, is based upon a logical form of syllogism, but is different in the aim pursued: it does not intend to validate the truth of certain statements, instead, it intends to persuade on the basis of the proposed arguments. The premises that nurture the enthymemes are statements that appear as irrefutable, even if they are only presumably true. Something that seems evident may change with time. Presumptions are beliefs that in some circumstances would admit the contrary case (they are not absolute truths), but they are not "lies". Persuading would be an impossible task if a fertile field propitious to accept the arguments would not exist.

The *abductive* inference is posterior to the Aristotelian logic; it is an inferential model that, in a strict sense, lacks the value of truth (Peirce 1860-1908: vol. 2, par. 270). However, it is of great utility in the production of new hypothesis in the context of discovery. The persuasion that appeals to an abductive reasoning proposes an inferential leap between a feature that is shown in a particular case and a general rule, which is underlying and is recognized by the interpreter. The conclusion is about a case in which the possession of a feature implies the belongingness to that universe, class, or phenomenon. Intuition shortens the way toward comprehension, though its veracity is fragile, because the reasoning allows formulating a general conclusion from a particular situation.

---

2. *Doxa*, in Greek, means opinion, way of seeing, idea, belief. It is oposed to the true knowledge that the Greeks called *episteme* (intelligence, knowledge, wisdom, science). This distinction is basic to understand why Plato was distrutful about oratory. While science has the aim of reaching knowledge, the rethoric persuasion, the core of oratory, only looks for the adhesion of the public (many times, demagogically flattering it).

Black, white, and red in signals, propaganda, and advertising

With the aim of showing how the arguments about the black-white-red triad are embodied, we propose a typification of the presumptions about these colors trough a repertoire of examples. In all cases, the aim is that the receptor performs an action (to make or stop making something, to think or buy something). Persuasion is embodied in genres of discourse that regulate the characteristics, circulation, and functions of messages in the "designed" modern urban communication. We distinguish three modes in the use of these colors, which correspond to three persuasive genres: signaling, propaganda, and advertising. Each one will take only some of the exposed senses, and will activate a portion of the connotations ascribed to these colors.

1) Visual impact: alerting signals: Red and black on a white background assure an excellent legibility and, at the same time, a great visual impact, perceptual arguments for using this combination when a fast and efficient reading is intended. Already at the beginnings of printing, it was realized that the use of white paper, black printed letters, and red dye for highlights was very convenient, because this combination blends criteria of excellent legibility and elegance.

The genre we have chosen is signaling, which alerts the receptor by exciting vision, and persuades about the appropriate, licit, inappropriate, or illicit behaviors in the urban context. Beyond persuading, signals intend to show a quasi-universal message. To be useful, they need to portray a high degree of information that is clear and unanimous for the major part of the public.

In Figure 2 we can see urban signals from different cultures. In the logical aspect (*inventio*), they adopt the inductive way. They schematically show examples of behaviors or situations with which the addressee can identify. At the level of *elocutio*, the dominant rhetorical figure is stylization. The black color in the figure suppresses features, and outlines (on a white background) only the relevant aspects needed to recognize the object.

2) Debatable truths of propaganda messages: Red (blood) and black (night, death), with a touch of white (neutral, reassuring), are ideal to convey messages for the common good (non-commercial ones), for instance, prevention of situations with risk of death: accidents, tobacco addiction, contamination, violence, anti-war messages. The genre of propaganda promotes messages of social interest, without an explicit commercial aim. This modality has two sides: a political and a social orientation.

Figure 3 is an anti-war poster from a communist organization in Great Britain, which circulated in 1920. The argumentation appeals to an inductive logic (*exemplum*). The represented scenes (black figures on red background) correspond to World War I; the contrasting typography, "Never again", makes the inscription to stand out. The argument reminds the death and the horror of combat in the battlefield, in order to dissuade the society of a possible relapse (it was unsuccessful, we know). The used resource is the synecdoche (a part for the whole), because a partial situation is shown to represent the whole, war. Colors work in a metonymic way, showing the cause to signify the effect. The darkened figures represent death. The red of fire in the battle is the blood shed by the combatants. The white typography represents neutrality, the construction of a clear and reassuring future, antithetically opposed to the dark recent past.

In the example of Figure 4, which belongs to a campaign for prevention of traffic accidents in Miami, the argumentation does not exhibit a factual example, but resorts to an abductive logic. It is necessary to make a chain of reasoning to explain the blood on the windscreen of the car. This kind of reasoning starts with a particular case (feature) —the red blood on the windscreen—, and then evokes a general rule in the memory of the reader —"imprudence may cause accidents with serious injury (blood)". The conclusion, also a particular case, is what the message wants to show: "traffic accidents are highly dangerous because they imply risk of death". The rhetorical figure used is metonymy; there is an existential contiguity between blood and the color red (the appearance of red implies the presence of blood). At another level, the substitution of the effect (blood) for the cause (accident) is also a metonymy.

Beyond the metonymic associations analyzed, in political propaganda colors are used with a symbolic value, with a reading that is proposed from an ideological frame. The Russian poster in Figure 5 presents a red background, darkened toward the bottom. The typography that makes reference to the socialist resistance in Chile 1977 and the text "¡Venceremos!" (We shall win!) are red, and they are in contrast to the dark fascist symbols (the swastika) that "decorate" the wire fence of the concentration camps where the political prisoners were confined. The interpretation of this poster requires a greater contextual knowledge and the reading of a deductive series, a more complex kind of reasoning than bare exemplification. The argumentation takes the form of an enthymeme, and comprises a temporal dynamics. It starts from a general premise: "Fascism=black is death (the present)". The minor premise predicates upon a particular case (Chile): "Today, Chile is dominated by fascism=black". The conclusion is also a particular case: "Chile is dominated by death". The other enthymeme relates to the future and the explicit promise: "We shall win!". The major, general, premise is: “Socialism=red is freedom (future)”; “Chile can embrace the socialist=red ideology”. The conclusion is: “Chile can be freed from dictatorship”. The dominant rhetorical figure is the metaphor, because the colors themselves substitute the ideologies. The chromatic opposition (antithesis) reinforces the antagonism.

The following quotation describes the use of red as synonym of communism in the official discourse of the United States, with negative connotations that come from associating red with danger.

> The Somoza dynasty, which the marines had settled in the throne, lasted for half a century, until 1979 in which it was swept by the popular anger. Then, president Ronald Reagan rode a horse and went on to save his country, menaced by the Sandinist revolution. Nicaragua, poor among the poorest, had, in total, five elevators and a mechanical staircase that did not work. But Reagan denounced that Nicaragua was a danger; and while he was speaking, the TV showed a map of the United States that began to tinge in red from South to North, to illustrate the imminent invasion. Does president Bush copy his discourses that disseminate panic? Does Bush say Iraq where Reagan said Nicaragua? (Galeano 2003, our translation)

It is clear than in the two last examples, the interpretation of the chromatic symbol (red=socialism, or red=communism) gets a positive or negative connotation depending on who is proposing the message and who is he intending to persuade. This situation is not an error; it is simply a manifestation of the coexistence of opposite social values. The messages based upon some of these values will be credible for the sector of the public that previously adheres to that ideological corpus.

A notable mutation has been produced in the graphic messages against the recent invasion on Iraq. These messages show a curious inversion: red=war=blood symbolizes the invading allied army, while black represents oil (Iraq).

3) Chromatic sublimation: the advertising symbol: Red (liveliness, sexual passion) associated to black (night, sophistication, mystery) and white are colors used to persuade potential consumers about values or qualities ascribed to a product. The advertising genre communicates values of brands and consumption products with the intention of persuading the receptors, defined as the “target”, about the advantages of their acquisition.

According to marketing studies, red is considered “declassifier”, i.e., a color that does not contain markers of class, and for this reason is appropriate for brands of products for massive consumption (think about the successful Coca-Cola red). However, in association with black produces an “elegant” combination. Red is also said to produce a loss of sense of time, and for this reason is the preferred color (with black and white accessories) for casinos, bars, discos, and entertainment places. It is also noteworthy its use to emphasize tasteful and appetizing features in gastronomy (in packaging, advertising, brands, and architecture).

The advertisement of *Paloma Picasso* perfume (Figure 6) exorcises the phantoms about using the black-white-red triad, and exalts their positive resonance. It persuades with an inductive argumentation, the *imago* in itself (brand and image are equivalent). It starts from a particular case: Paloma Picasso dressed in red, with very red lips that make a contrast with the white skin. Black hair, eyes and gloves frame the pale face. This image is endorsed with the values of seduction, passion, aestheticism, and Spanishness, which could be emulated by any woman that consumes the advertised perfume. If there is identification with the proposed *imago* (physical type of woman, and values that embodies), the same will happen with the colors and the product; the message will succeed with that sector of consumers (target). The rhetorical figure predominating is chromatic alliteration, or repetition, which accentuates the mentioned connotative features. The whole image works in a metaphorical way; the face substitutes the scent bottle, with which shares morphological and chromatic similarities.

PARADOXES IN THE CHROMATIC ARGUMENTATION?

Good and evil, life and death, danger or liveliness, happiness or depression, clarity or enigma, seduction or poison, sex or death. In the analyzed examples, the context, the persuasive genre in question, the recognition of the addresser and the addressee of the message, allowed for the clarification of these potential ambiguities. This could make us suppose that the use of this chromatic triad is not a guarantee for a unanimous meaning, but that there exist codified meanings in relation with the contexts.

However, a hypothesis could be formulated that the most primary connotations (red=blood=alert, black=night=death), even when they can be reverted changing from a negative to a positive value, always remain as a substrate. The use of these colors in images of the devil or the vampire Dracula is not very distant from the cheerful clowns, the good Santa Claus, and the holy priests. It is not an arbitrary use of color, it is the appropriation of the negative attributes of the antagonists in order to absorb, neutralize, and exorcise them. Although these figures are known to be benefactors, they keep certain ambivalence. Not in vain their presence frighten children.

Figure 1. Black, white, and red in the symbology of alchemy. The White Rose, manuscript (Reusner c.1550, reproduced from Gage 1993, chapter 8).

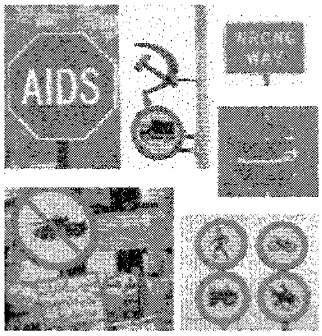

Figure 2. Alert on the road. Black, white, and red in the signals of the urban environment.

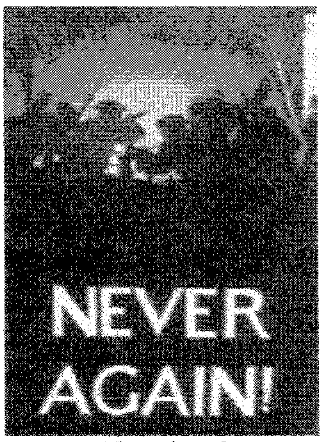

Figure 3. The color of war. "Never again", anti-war poster, Great Britain, 1920.

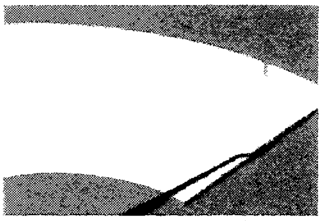

Figure 4. The color of blood. Campaign for the prevention of traffic accidents, Miami, USA, 2000.

Figure 5. Color as ideological sign. Poster by E. Kazdan, in favor of Chilean freedom from dictatorship, 1977.

Figure 6. Seduction by color in advertising. Paloma Picasso *perfume, 1998.*

REFERENCES

Aristotle. 350 B.C. *Rhetoric*, English version on the Internet, http://classics.mit.edu/Aristotle/rhetoric.html.

Berlin, B., and P. Kay. 1969. *Basic color terms* (Berkeley, CA: University of California Press).

Gage, J. 1993. *Color and culture* (Boston: Little, Brown, and Co.).

Galeano, E. 2003. Article published in *Pagina 12* (Buenos Aires), march 2003.

Hutchings, J. 1989. "Colour in folklore, superstition, tradition, and legend", in *AIC Color 89, Proceedings of the 6th Congress* (Buenos Aires: Grupo Argentino del Color), vol. II, 54.

——. 1993. "International survey on colour in folklore, belief and tradition –a progress report", in *AIC Color 93, Proceedings of the 7th Congress* (Budapest: Hungarian National Color Committee), vol. C, 153-157.

——. 1997. "Japan and Britain –A comparative colour folklore", in *AIC Color 97, Proceedings of the 8th Congress* (Kyoto: The Color Science Association of Japan), vol. II, 775-778.

Kwon, Y. 2002. "The signs and symbols of red color in East Asian countries", in *AIC Color 2002, Proceedings of the Interim Meeting* (Maribor, Slovenia: Slovenian Colorists Association), 291-295.

López Pasquali, L. 1998. *Fascinación y origen de las preferencias* (Buenos Aires: Editorial Peñafield).

Peirce, Ch. 1860-1908. *The collected papers* (Cambridge, MA: Harvard University Press, 1931-1935).

José Luis Caivano - Mabel A. López
SICyT-FADU-UBA, Ciudad Universitaria Pab. 3 piso 4
C1428BFA Buenos Aires, Argentina
jcaivano@fadu.uba.ar - ychodos@fadu.uba.ar

Effects of Light Sources and Colors of Interior Elements on Atmosphere in the Living Room

Masako Miyamoto

The University of Shiga Prefecture

1. Introduction

According to our [1)−4)] studies, the relationship between light sources and colors much affects room-atmosphere. This report is a study on visual effects of the relationship between light source, wall color, floor color, and chair color in a living room. In former studies, a lot of those kinds of studies were researched by using scale model or projecting slides or recently computer graphics. But the feeling of a presence in the model or the projection is different from that in a real room, and the scale model or the projection and the real room have different rates on evaluation of a room. Therefore, an actual model was used for the experiments.

2. Methods

2.1 Laboratory equipments

There is a waiting room and a model in the laboratory. Fig.1 shows the actual size model of a living room that is 12.67 m^2 (3.56 × 3.56 m) in area and 2.37 m in ceiling height. There are two armchairs, a sofa and a table made of glass and silver metal in the model. The color of the ceiling is 5Y9/1. The color of the curtains (acrylic 100%) is 2.5Y8/2. During experiments the curtains were always closed. Black curtains in the laboratory were closed to shut out daylight.

Luminaires for incandescent lamps or fluorescent lamps were mounted on the ceiling.

The illuminance in the waiting room was 50 lx. The light sources were white fluorescent lamps.

2.2 Analytic elements

Table 1 shows the analytic elements.

It is difficult to have an experiment for all combination of these items. Therefore three experiments were had.

2.3 Experimental methods

2.3.1 SD scales

Semantic differential technique was used to rate the room. After subjects waited for five minutes and more, they sat on the sofa in the model, and rated an atmosphere in the room immediately. A 7-point scale form was used for rating it. There were 24 scales in the form. The adjectives were originally printed in Japanese, and equivalents in English are shown in Table 2.

2.3.2 Subjects

On each condition of every experiment subjects were almost 25 students in the Nara Women's University who have good knowledge of dwelling.

Table 1 Experimental condition

Items	Categories		Exp. 1	Exp. 2	Exp. 3
Light sources	Incandescent lamp (IL,2850K)		O	O	O
	Three band incandescent-colored fluorescent lamp (EX-L,3000K)				O
	White fluorescent lamps (W,4200K)		O	O	O
	Three band natural white fluorescent lamp (EX-N,5000K)		O	O	O
Illuminances (lux)	200		O	O	O
	400		O	O	
Colors of wall	Hue	YR or R	O	O	O
		B or BG	O	O	O
	Value	6	O		
		8	O	O	O
	Chroma	2	O	O	O
		4	O		
Colors of floor	Hue	YR or R		O	
		B		O	
		N	O	O	O
	Value	3		O	
		5	O	O	O
	Chroma	3		O	
		6		O	
Colors of chairs	Hue	YR or R	O	O	O
		PB			O
	Value	2	O	O	O
		7			O
	Chroma	2	O	O	O
		7			O

2.3 Experimental methods

2.3.1 SD scales

Semantic differential technique was used to rate the room. After subjects waited for five minutes and more, they sat on the sofa in the model, and rated an atmosphere in the room immediately. A 7-point scale form was used for rating it. There were 24 scales in the form. The adjectives were originally printed in Japanese, and equivalents in English are shown in Table 2.

2.3.2 Subjects

On each condition of every experiment subjects were almost 25 students in the Nara Women's University who have good knowledge of dwelling.

3. Results and discussion

3.1 Factors concerned with an atmosphere in the living room

Four factors were firstly extracted by component factor analysis. And they were rotated by the varimax method. Each factor has an eigenvalue of over 1.0. The cumulative variance for four factors is high score, 92.7%. The result of the factor analysis is shown in Table 2.

Table 2 Principal-component factor analysis

Factor	Adjective scales	Factor loadings				Communality	Factor component
		I	II	III	IV		
I	Bright - Dark	**0.956**	0.127	0.093	0.104	0.968	Activity
	Open - Closed	**0.964**	0.14	-0.067	0.102	0.964	
	Active - Passive	**0.953**	-0.072	0.213	0.104	0.97	
	Vivid - Dull	**0.943**	0.031	0.245	-0.131	0.968	
	Cheerful - Cheerless	**0.935**	0.102	0.256	0.167	0.978	
	Clear - Hazy	**0.871**	0.124	-0.29	-0.218	0.906	
	Light - Heavy	**0.84**	0.045	-0.469	0.183	0.962	
	Restfull - Restless	**0.832**	0.469	-0.027	-0.154	0.937	
	Gay - Sober	**0.796**	-0.082	0.531	0.169	0.952	
	Distinct - Vague	**0.721**	0.065	0.397	-0.481	0.913	
	Lively - Lonely	**0.717**	0.077	0.633	0.222	0.97	
	Wide - Narrow	**0.672**	0.334	-0.511	0.218	0.871	
II	Natural - Artificial	-0.088	**0.941**	-0.14	0.127	0.929	Evaluation
	Pleasant - Unpleasant	0.171	**0.936**	0.207	0.098	0.959	
	Elegant - Vulgar	-0.199	**0.915**	-0.004	-0.068	0.881	
	Friendly - Unfriendly	0.29	**0.905**	0.12	0.177	0.948	
	Familiar - Strange	0.228	**0.787**	0.266	0.422	0.921	
	Relaxed - Tense	-0.137	**0.659**	-0.016	0.627	0.847	
III	Simple - Complex	0.093	0.22	**-0.938**	-0.069	0.942	Gorgeousness
	Gorgeous - Plain	0.232	0.298	**0.891**	0.103	0.948	
	Emotive - Emotionless	0.337	0.469	**0.723**	0.234	0.91	
	Warm - Cool	-0.059	0.313	**0.711**	0.541	0.899	
IV	Soft - Hard	0.196	0.257	0.164	**0.891**	0.926	Softness
	Feminine - Masculine	0.125	0.083	0.191	**0.845**	0.773	
	Eigenvalue	10.28	6.051	3.866	2.043		
	Variance(%) Each factor	42.8	25.2	16.1	8.5		
	Variance(%) Cumulative	42.8	68	84.2	92.7		

3.2 The effects of elements to each factor

The effects of each object to an atmosphere in the living room were taken by the relationship between the first factor scores and the second factor scores. The distribution of factor scores of objects with incandescent lamps is like that of objects with three band incandescent-colored fluorescent lamps. A lot of objects have high scores on evaluation. And objects that have high scores on evaluation have low scores on activity. Conversely, objects that have low scores on evaluation have high scores on activity. There is a converse correlation between evaluation and activity. As compared with them, objects with white fluorescent lamps or three band natural white fluorescent lamps generally have low scores on evaluation.

Objects with high value and high chroma of the chairs have high scores on activity and low scores on evaluation. The lower color temperature of light sources is, the higher evaluation of the space becomes.

3.3 Effects of each element and each category to an atmosphere in the living room

Category weights, multiple correlation coefficients and partial correlation coefficients were extracted by analysis based on the theory of quantification I.

The visual effects of each element or each category can be predicted from them. The horizontal illuminance of the center on the table and, value and chroma of chairs have effects on the SD scales that relate to activity. The multiple correlation coefficients of the SD scales that relate to evaluation are about 0.7 and lower points. It suggests that the evaluation in the room can't be taken according to only the kinds of light sources and colors in the room. However, the kinds of light sources have effects on the evaluation in the room. And the kinds of light sources and colors of chairs have effects on the SD scales that relate to factor 3 and factor 4.

3.4 The effect of each category

The category weight shows the quantity of the effect of each category. The category weights of light sources on softness and gorgeousness relate to the color temperatures. The lower the color temperature is, the more softness and gorgeousness increase. The tendency on an effect of each category to evaluation is similar to that to softness and gorgeousness. But when the category weights of an incandescent lamp and three band incandescent-colored fluorescent lamp are compared, it is found that three band incandescent-colored fluorescent lamps make higher evaluation than incandescent lamps in a room.

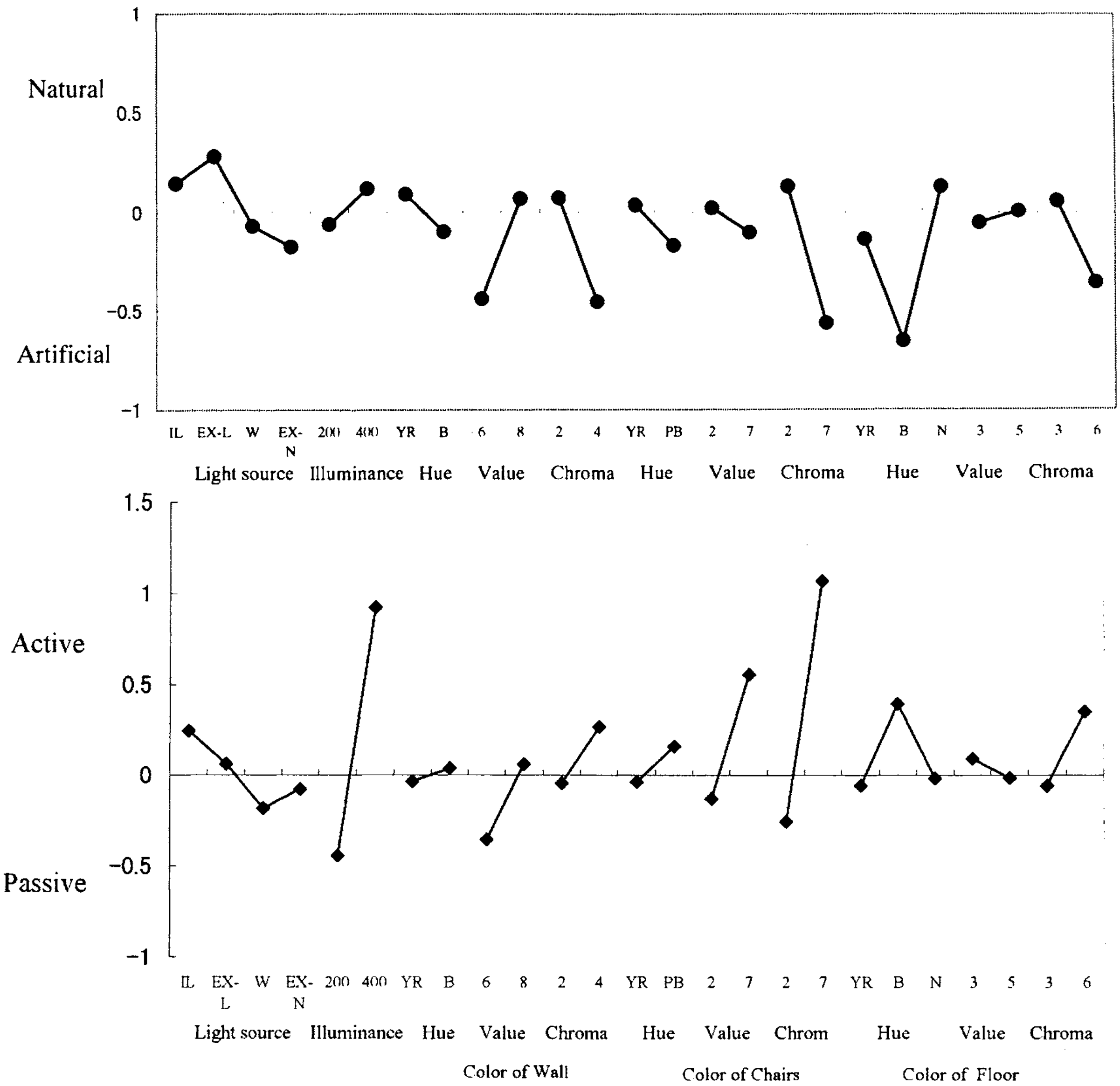

Fig.1 Category weights

4. Conclusion

The result from this study indicates that illuminance has an effect more than colors on activity in the room.

The color temperatures of light sources have effects on evaluation, gorgeousness and softness in the room very much. In the case of light source with a low color temperature the value increases. The three band incandescent-colored fluorescent lamp has similar high psychological effect to the incandescent lamp.

Color of chairs has big effects on all main factors, activity, evaluation, gorgeousness and softness in the room. Therefore, color of chairs plays an important part in making a good atmosphere in the room.

Thus, the effects of the light source and interior color for making the image of a room appropriate for the purpose were caught quantitatively.

Acknowledgement

The author would like to acknowledge the continuing guidance of honorary Professor Takuko Yanase of the Nara Women's University.

References

1) Masako Kojima: Effects, which the Light Source and the Elements around it Produce on the Atmosphere in the Living Room, Research Journal of Living Science, 34-1, pp.69-77 (1987)

2) Masako Miyamoto: Effects, which the Light Source and the Color of Carpet Produce on the Atmosphere in the Living Room, Research Journal of Living Science, 36-1, pp.35-42 (1989)

3) Masako Miyamoto and Takuko Yanase: The Effects of Light Sources and Colors of Chairs on the Atmosphere in the Living Room, J. Illum. Engng. Jpn., 77-6, pp.68-73 (1995)

4) Masako Miyamoto and Takuko Yanase: The Effects of Light Sources and on the Atmosphere in the Living Room, Sum. of Tech. Papers of Annual Meet. Architec. Inst. Jpn., pp1129-1130 (1993)

Evaluation of psychological images associated with colors as an aid for architectural color decision

Taiichiro ISHIDA and Junya SAKAI
Department of Architecture and Environmental Design, Kyoto University,
Yoshida-Honmachi, Sakyo-ku, Kyoto, 606-8501, JAPAN

ABSTRACT

Colors in architecture have strong influence on our impression of the space. In this study we examined relations between psychological images associated with colors and those with colored architectural interiors. We carried out the experiment in which subjects evaluated psychological images of individual colors and colored interiors created by computer graphics using two psychological scales: 'active-calm', 'orderly-chaotic'. It was found that color attributes such as lightness and hue are obviously linked to psychological images of the color samples. The psychological images of the colored interiors were quite different from those of the individual color samples, however, the evaluation for the colored interiors showed similar tendency regardless the type of the interiors. The results of this study have implications for considering a model to describe psychological images associated with colors in practical architectural spaces.

1. INTRODUCTION

Colors in an architectural space strongly affect our visual impressions of the space. It is necessary to use colors properly so that they match an intended image of an architectural space. There is much knowledge about psychological images associated with each of individual colors. However, no color in our living environment exists alone; we see colors applied to some objects such as buildings, clothes, and industrial products. Thus, we must consider psychological images of colors applied to the objects. Our primary question is how psychological images of individual colors change when they are applied to architectural space.

Each architectural space has unique characteristics, such as *private*, *public*, *active*, *calm*. Here we refer these characteristics of an architectural space as their context. The context of the architectural space may interact with psychological image of colors applied to that space. In other words, colors may change the contexts of the space. Several studies[1-4)] have conducted on psychological image of colors applied to practical objects. In this study we examined the relation between psychological images of individual colors and those of colored interior architectures by using systematically selected colors. This will provide useful knowledge to create an aid for determining architectural colors based on their practical psychological images.

2. EXPERIMENTAL METHODS

In the experiment, subjects evaluated psychological images of individual colors and pictures of the architectural interiors created by computer graphics. We selected 58 colors from the CIELAB color space as shown in Figure 1. In evaluating individual colors (color sample), each of these colors was presented on a CRT monitor one at time with the size of 6.8 x 9.0 deg of visual angle. The background was set to N7.5 gray.

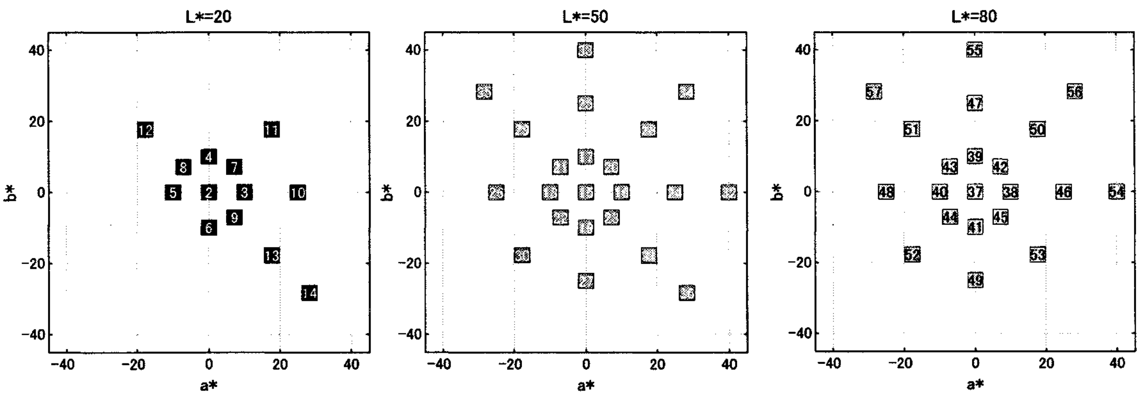

Figure 1: The color samples plotted on CIELAB space.

In addition, we made 4 types of the interior using computer graphics as shown in Figure 2. Then, each of 58 colors selected from the CIELAB space was applied to the walls of each of the four interior 3D models. Color rendering and lighting effects were computed using the software *lightscape ver 3.1.1*. Therefore, we created 232 images (=58 colors x 4 interior) in total. In evaluating the interiors, each picture was presented on the CRT monitor with the size of 33.5 x 44.7 deg of visual angle.

To evaluate psychological images of the color samples and the interiors, we employed three psychological axes. The first one is the activity axis described as some compounded feeling such as 'exciting-calm', 'active-quiet'. The second is the order axis described as some compounded feeling such as 'orderly-chaotic', 'tense-relaxed'. The third is the preference axis described as 'good-bad' or 'comfort-discomfort'. The first two axes may indicate psychological characteristics of the colors and the interiors. The third axis may indicate some integrated judgement of their values or preference. Subjects made judgements for the three axes with -10 to 10 subjective scale.

Figure 2: Pictures of the interior created by computer graphics. Meeting room, private room, living room and shop.

One of the authors and six students from the author's laboratory at Department of Architecture participated in the experiment as the subjects. A single experimental session tested either of the color samples or one of the interior colors. Subjects made subjective evaluation of the 58 color samples or colored interiors randomly presented in a given session. A subject carried out 10 sessions in total comprising 2 evaluations for each color sample and colored interior.

3. RESULTS AND DISCUSSION

Figure 3 shows typical results of the evaluation of the color samples. The evaluated score of the 'Activity' is plotted against that of the 'Order' for each color. For example, the results of the subject SH, the evaluation of the 'Activity' and 'Order' are negatively correlated in this plot. The lightness values of the color samples seem to be the primary factor in determining the psychological images of the colors. That is, higher lightness seems to induce the image of 'active' and 'chaotic' and lower lightness induce the image of 'calm' and 'orderly'. The results of the subject TI, however, do not show a simple correlation between the two evaluation scales. In this case about a dozen color samples, which had lower lightness values and hues from red to green, were judged as 'calm' and 'chaotic'. In general, the results of individual subjects were located somewhere between those two typical examples. Thus, there were apparently large individual differences among the subjects, however, the results seem to be described using some common variables. As an attempt, a liner multiple regression was applied to the result of each subject using lightness, chroma and hue as independent variables. The analysis revealed that the data of the individual subjects were fairly well fitted by a linear combination of the variables: the regression coefficient r = 0.66 to 0.90 for the 'activity' evaluation and r = 0.53 to 0.83 for the 'order' evaluation, implying that individual differences in psychological images of colors may be explained by the differences in parameters for some common variables.

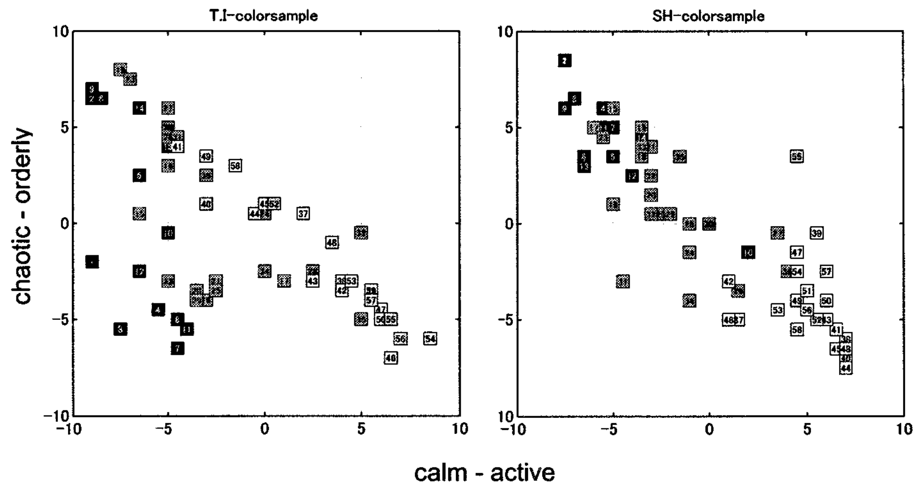

Figure 3: Typical examples of the evaluation for the color samples. (subject TI and SH)

Now consider our main question in this study. Figure 4 shows the relations between psychological images of the color samples and those of the interiors. The average of the subject's evaluations are plotted for each of the four interiors. The horizontal axis indicates the evaluation of the 'activity' and the vertical axis the 'order'. Small circles indicate the evaluation of the color sample and the end of arrow from each circle indicates the evaluation of the interior colored by the same color as the sample. The square denotes the evaluation for the line drawing of the interior, which is considered as the context of the interior without colors. As shown in this figure, the psychological images of the colored interiors greatly shift from those of the color samples. That is, psychological images of the colored interiors were quite different from those of the individual colors.

The evaluation for the colored interiors, however, showed similar tendency regardless the type of the interiors. That is, the same color gave similar psychological images to each of the four interiors, indicating that colors applied to an architectural space might have common influences on psychological images of the space.

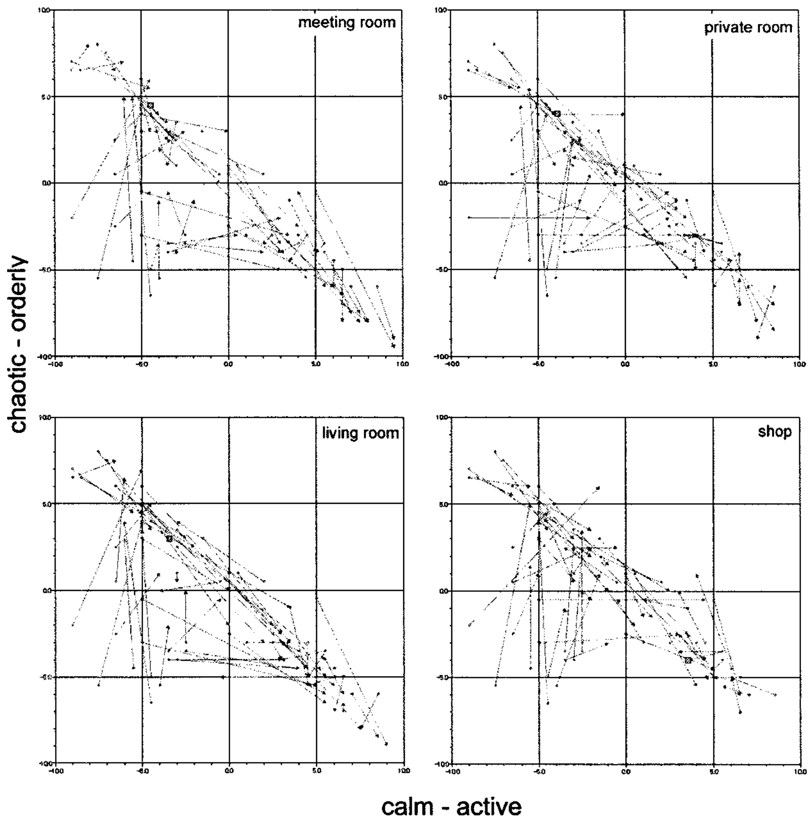

Figure 4: Relations between psychological images of the color samples and those of the interior architectures.

Figure 5 shows an example of the results of the 'preference' evaluation. The data are taken from the subject TO's results and plotted for the four interiors. The horizontal axis indicates the 'activity' evaluation, the vertical axis the 'order' evaluation. The triangle markers indicate the evaluation for the line-drawing interiors. In addition, the results of 'preference' evaluation are indicated by lightness steps of the plot markers. The 'preference' evaluations for the private room took higher values when the psychological images of the colored interiors located near to the line-drawing interior. This may indicate that the subject gave higher preference values when the image of the colored interior was matched with the context of the interior. However, for the meeting room and living room, no definite relations between the position of the line drawing and images of the interiors were found. Moreover 'preference' of the shop took relatively higher values for a wide range of psychological images regardless the position of the line drawing. The evaluation of the 'preference' seems to depend on characteristics of the interiors.

In conclusion, the judgements on the psychological image of the color samples had large individual difference among the subjects, however, they seem to be described using some common variables. The psychological images of the colored interiors were quite different from those of the individual color samples. The evaluation for the colored interiors, however, showed similar tendency regardless the type of the interiors, indicating that a color applied to architectural spaces give common influences on psychological images of the space. The evaluation of the 'preference' seems to depend on characteristics of the interiors. The results of this study have implications for considering a model to describe psychological images associated with colors in practical architectural spaces.

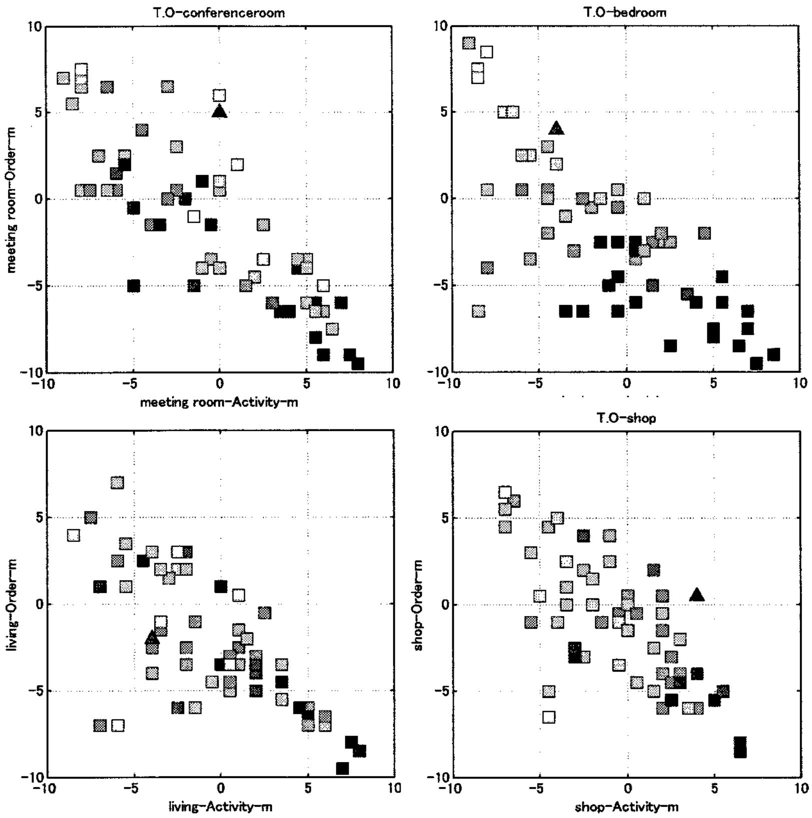

Figure 5: Relations between psychological images of the color samples and their 'preference' judgement.

REFERENCE

1) Shen, YC; Chen, YS; Hsu, WH: Quantitative evaluation of color harmony via linguistic-based image scale for interior design, COLOR Research Application, Vol.21, pp.353-374 (1996)
2) Taft, C: Color meaning and context comparisons of semantic ratings of colors on samples and objects, COLOR Research Application Vol.22, pp.40-50 (1997)
3) Nakayama K; Sato M; Sawada T: Building color selection system using neural network systems, J. Archit. Plann. Environ. Eng. No.510, pp.9-15 (1998) (*in Japanese*)
4) Yamaguchi H et al.: Sportwear design assisted tool based on human color emotion, Proc. of AIC COLOR 2000, pp.164-165 (2000)

Colors of signs at large-scale railway stations in Japan

Sari YAMAMOTO, Kazuhiro KOGA and Kiyoshi NISHIKAWA

1. INTRODUCTION

Signs are indispensable at some large-scale railway stations in the metropolitan area in Japan because several lines interchange at these stations. However, confusion can be observed due to signs being placed near other signs, facilities and advertisings. Due to many lines interchanging in a big station in the metropolitan area, colors are used to distinguish lines as shown in Fig 2.

We searched for sign problems in large-scale stations through comparative investigation between stations and other similar facilities. In addition, a questionnaire survey to station users and staff and a psychology experiment were conducted. In this research, all things to induce and to offer information guiding in the platform were defined as a sign.

Fig. 1 Sign example in station

Fig. 2 Lines and colors at T station

2. RESEARCH METHOD

This research was a joint study conducted by the Frontier Service Development Laboratory, East Japan Railway Company and the Institute of Art and Design, University of Tsukuba. The methodology of this research is shown in Fig. 3. Since this research is ongoing, the proposal has not been made yet. This research reports on the study of color through a questionnaire survey, a field survey and an experiment. This project treats typography, the layout design, and the sign system, and other factors that is displayed on signs besides color.

Space survey → Questionnaire survey → Field survey → Experiment → Proposal

Fig. 3 Flow of research

3. QUESTIONNAIRE SURVEY

The sign uses colors to display various factors such as lines, exits and entrances. It was asked whether there was a color that correctly knew these colors, and did not see it easily in the questionnaire survey. The questionnaire forms were distributed to 500 users for each T Station and U Station. The collection rate was 40%. The question and the answer concerning color are shown below:

Q: *Did you know a specific color of each line was used?*

A: *Yes* 73% *No* 20% *Don't understand* 4%

Q: *Which color or character is assumed to be the main clue when you search for platform?*

A: *Color* 15% *Character* 64% *Cannot say either* 17%

Q: *Please answer if you know what color is used to guide the entrance.*

A: *Know* 12% *Don't know* 85% *Non-responding* 3%

The correct answer is green – the color of the company. The ratio of people who answered "Green" is 79% of the person who answered "*Know*", and, in other words, a total of 9%.

Q: *Please answer if you know what color is used to guide the exit.*

A: *Know* 16% *Don't know* 81% *Non-responding* 3%

The correct answer is yellow. The ratio of people who answered "yellow" is 63% of the person who answered "*Know*", and, in other words, a total of 10%.

Q: *Please think for the entire signs at the station and tell the combination of colors and colors that cannot be easily seen in the color used.*

A: A lot of people gave yellow. The ratio was 10%. It is thought that yellow is not easily seen because the background is often white.

The combination of colors not easily seen was "Yellow and orange", "Orange and red", "Blue and light blue" and "Blue and green". It is necessary to use even such an approximation color because there are many line numbers. Is there a limit of identification by colors?

4. FIELD SURVEY

The field survey was done by taking photographs and measuring colors. First of all, colors used for lines were examined. Fig. 4 shows the distribution of line colors that the company is deciding.

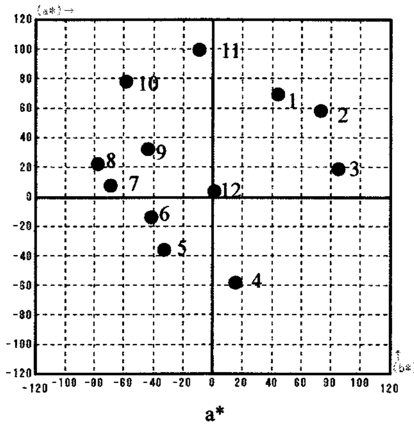

Line name in Initial

1. TK Line, UT Line, TS Line
2. CH Line (Rapid), O･I Line, MS Line
3. KY Line
4. CH Line (Limited Express), JB Line, YS･SB Line
5. KH Line, NG Line
6. SG Line
7. SI･KG Line
8. JB Line (Rapid･Local), NR Line
9. TH･JE･NG Line
10. YM Line, YH line
11. NB Line, TR Line, CH･SB Line (Local)
12. HC Line

Source: *Sign Manual*

Fig. 4 Color of each line

All these colors being used at the same time at one station hardly happens. However, because a lot of lines interchange at a large station, the approximation color might be shown. It is an example of showing the color that looks like in Fig. 5. Fig. 6 shows the distribution of these colors.

In addition, it has been found that three kinds of background colors are used for sign boards; white ground, black ground and color ground. The white grounds are used for sign boards for the inducements from the entrance to the passage and the concourse. The black grounds are used for the sign boards that show the platform number and exist along the passage. The color background is used for the entire sign board - this color is the line color. This sign board is the top and bottom of the stairs up or down to the platform as shown in Fig. 7. The line colors are being designed in a square shape on the boards of the white ground and black ground. Since the color contrasts are seen respectively with these three boards, can users see the color under these different conditions as a color of the same line?

Fig. 5 Example of sign at U Station

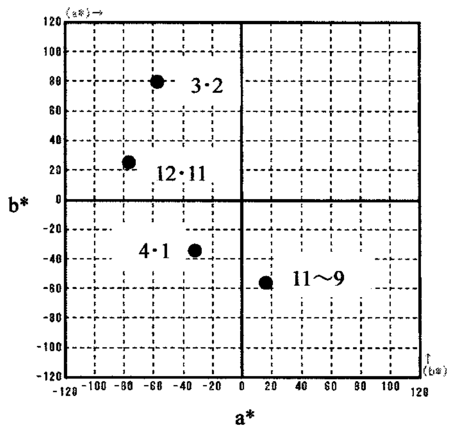

Fig. 6 Color distribution chart of Fig. 5

White ground	Black ground
Color ground	Color ground

Fig. 7 Signs of white ground, black ground and color ground

5. EXPERIMENT

Outline of experiment

The color contrast was hypothesized to be a major problem for signs from the field survey. Then, it is clarified whether the problem of color contrast misleads the user's color recognition through the psychology experiment.

The experimental apparatus is shown in Fig. 8. Stimulus is shown on CRT display as shown in Fig. 9. The subject sees the first screen for 800ms. The second screen appears after the interval of 500ms. Six colors are lined in a row on the second screen. The subject tries to look for the same color in this screen as the color shown in the first screen, and when the color is found, he pushes the key to the color number which he believes is the same. This trial is repeated 720 times. Subjects are 10 university students. In the first screen, there is a square color in a white or black background or the whole screens are colored. The second screen has a white or black background. The chromatic for the first screen are six colors. The colors used for the second screen are eight colors including the color used for the first screen. Table 1 and Fig. 10 show the colors used for the experiment. These colors are used in signs at the station.

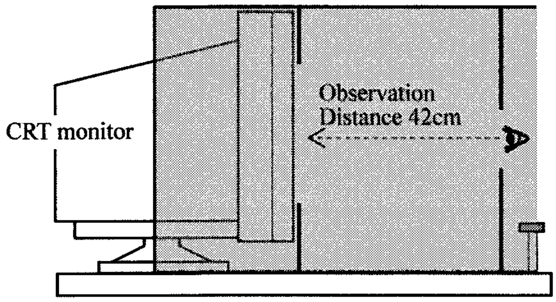

Fig. 8 Experiment apparatus

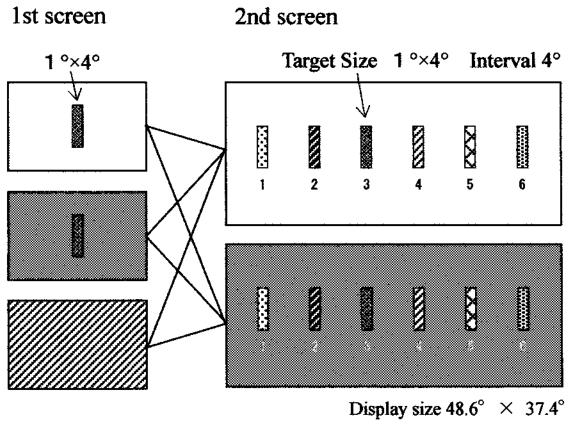

Fig. 9 Experiment stimulus

Table 1 Color used to experiment

No.	L*, a*, b* in display	Assumption line color [No. in Fig.4]
R1	67.7, 30.0, 70.5	TK Line, UT Line, TS Line [1]
R2	59.4, 54.4, 66.5	CH Line, O･I Line, MS Line [2]
R3	43.3, 57.6, 40.0	KY Line [3]
G1	69.4, -53.0, 63.6	YM Line, YH line [10]
G2	68.7, -51.5, 6.00	JO Line (express･local), NR Line [8]
G3	49.0, -45.7, 33.3	Exit [-]
B1	68.1, -20.5, -41.5	KH Line, NE Line [5]
B2	49.0, 13.8, -67.0	CH Line (express), JO Line, YS Line [4]

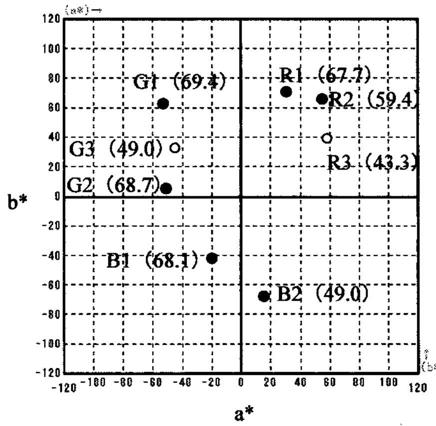

Fig. 10 Color distribution used to experiment
- ● *target colors shown in 1st screen and 2nd screen*
- ○ *blockage colors shown in 2nd screen*
- ( ) *L**

Result of experiment

An average and standard deviation of error rates for each color are shown in Fig. 11. The error rate for the color of R2 was the highest, and a significant difference was seen compared with other colors. Subjects were answering "R2" color, "R1" and "R3".$\triangle E^*$ between R1 and R2 is 26.13 and $\triangle E^*$ between R2 and R3 is 31.17. Besides this, the error rate for G2 is higher than the error rate for G1. $\triangle E^*$ between G1 and G2 is 57.50 and $\triangle E^*$ between G2 and G3 is 34.28. R2's and G2's high error rate are referred in detail.

Fig. 12 shows the error rate at each combination of the background colors. The error rate has risen when the background color changed. However, the tendency to which the error rate rose was not the same for R2 and G2 in either a white or a black background.

We examined the influence of the number of similar colors in the screen on the error rate as Fig.13. S shows that there is a similar color, and T shows that there is a target color. The error rate increase when a similar color is shown though there is little difference. In addition, the error rate rises when two similar colors are shown.

Finally, it was examined that the similar color position gave the error rate. The error rate changes depending on distance of target color and similar colors as shown in Fig. 14. It is understood that the error rate rises most when the target color is away most from two similar colors either from this figure. From such a result, identification by the color is guessed to be difficult when the similar colors are used for one sign board and there is a distance between those colors.

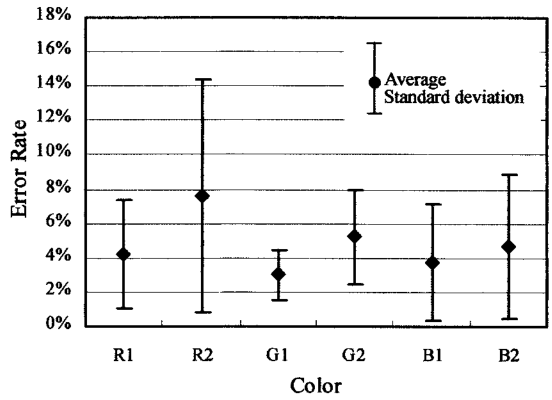

Fig. 11 Error rate according to colors

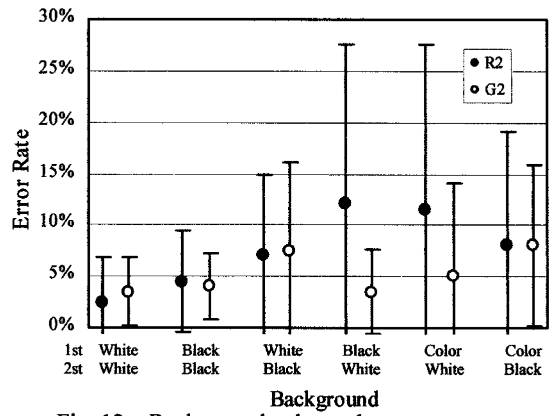

Fig. 12 Background color and error rate

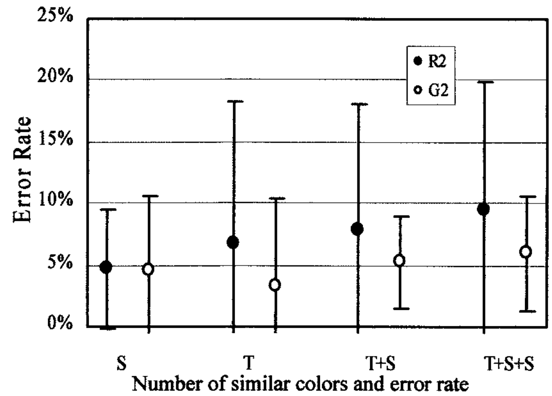

Fig. 13 Number of similar colors and error rate

S: Similar color T: Target color

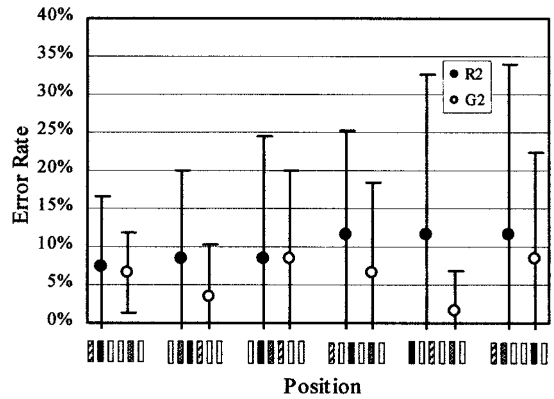

Fig. 14 Position between similar colors and error rate

Target color *Similar colors*

6. CONCLUSION

We examined factors that signs cause confusion at large-scale railway stations in Japan. It was hypothesized that the use of colors to distinguish lines was one of the factors. We showed the problem of the use of colors through a questionnaire, a field survey, and an experiment.

The following were found from the surveys and experiment:

a) There are similar colors in line colors. These similar colors might be lined in a row on the sign board.

b) The color of the background on the sign board changed occasionally. When the color of the background changed, the similar color was occasionally mistake for other similar colors at the experiment.

c) The distance between the similar colors amplified the mistake.

The experiment will be improved so that it is used for future proposal since only there was a difference of error rate in the experiment.

Acknowledgement

The authors thank Dr. S. INOUE of University of Tsukuba for help with the experiment.

Author's Affiliation

Sari YAMAMOTO

Institute of Art and Design, University of Tsukuba

Kazuhiro KOGA

East Japan Railway Company

Kiyoshi NISHIKAWA

Institute of Art and Design, University of Tsukuba

APPEARANCE IN THE TIME DIMENSION OF COLOR AND THE ENVIRONMENT Chrono-Chrome: Time-Related Color

Silvia Rizzo, Liceo Artistico N. Barabino, Genoa, Italy

Abstract

I refer to a method I have devised for color recognition on ancient 16th century frescoes that have 'faded away' with time. These frescoes ornate the facades of palaces in Genoa.
The original multitude of chromatic possibilities has been lost just like the profiles of painted figures and architectural forms that were containing them.
This color recognition method has proved effective in developing sensitivity to color as well as in designing projects to recover the drawings of these frescoes that cannot be perceived by us any more.
In other words: traces of color that are visible in areas with chromatic differences are intensified and, by deduction, fixed as graphic points. Through the repetition of this color-sign, the original drawing will appear again; a color-design pattern.
This procedure has yielded good results. I believe it is also useful to understand an environmental situation as well as its mutations and changes that are testified by appearance.

Key words: *Fresco*, Chrono-Chrome, Genoa

While continuing mycreative-investigative research work in the field of environmental color design, I have decided to present the following studies. They have been motivated and made more topical by my recent reflections which expand conventional survey and reconstruction works on *fresco* colors in urban spaces, and in historic palaces in particular (in this case in the city of Genoa), which are by now linked to the History of Art.
Following a search for new 'laws' of sensitive perceptions, and for 'rules of unlikelihood', the visible color was found to be linked to a 'chrono-chrome' (time-color) dimension: since it is not linked to 'sure' values, we are allowed to involve also the emotional sphere, which is connected with individual subjective perceptions.
In order to carry out this research on time-related color, I have employed diagrams and constructions, as if they were signs prompted by contemporary technology.
As will be illustrated in detail here below, by saturating the intensity of perceived colors and stressing contrasts, the original fresco drawing is brought back to the surface, which is both a form of expression and a history document.

Several years of investigations prompted by my specific interest in fresco painted facades and in the changes of colors worn out by aging and weathering agents have drawn my attention to a still unexplored feature, namely to the possibility to reconstruct the background drawing of these frescoes, even when their visual reading is no longer possible.
The specimens presented show, in sequence, the chrome-graphic process. Although apparently quite simple, it actually facilitates the reading of in fresco painted compositions, and at the same time makes it easier to reconstruct the basic decoration structure, namely the drawing. With the help of a photo survey, this process is carried out by first dividing the

fresco in sections and selecting small areas where different colors meet. On these meeting or separation points of said color matches, a short graphic sign is made. This small 'chrome-graphic set' is then added up to others; all together they form a pattern through which the original composition is progressively unveiled. Actually, different color hues, just like the pieces in a puzzle, will give visual life to the image. The quality of shapes is thus highlighted, and their original meaning will thus become intelligible.
The colors employed are selected from a range of colors extracted and cleared of aging and weathering agents. Hence, they will not be different from the likely background our eyes would make us select out of the current visual conditions of these decorations.
Depending on color differences, the assumed background is then progressively selected, by also considering the color differences under the likely light and shadow impact on the shapes or figures.
More complex chrome/graphic systems may be developed out of these investigations, thus providing a wider range of colors and signs.
Here, I am just outlining the procedure in very general terms, which allows us to define the original drawing as the end-product of the research work. Indeed, it is quite easy to follow the various sketched lines and obtain the basic drawing of the fresco decorations under examination.
Among the end results of this operation, the value of the drawing is further stressed, as an essential construction base, not only for restoration purposes, but also as an important element in the study of decorations. Decorations rather than painting, as was often mistakenly believed. This is actually a widely debated topic, which could be raised again when dealing with restoration works of in fresco painted facades. These in fresco paintings serve as a decoration, but they are also to be considered as the outcome of composition work on wall architecture.

References

1. Jonathan M. Woodham, Twentieth Century Design, Publ. Oxford University Press, Oxford, New York, 1997
2. Silvia Rizzo, Colour Signals in the City, 1st Price for Didactics, in Documentation, Catalogue, 3rd International Colour Design Prize, 1986/87, Publ. Farb Design, International E.V., Stuttgard, 1987
3. G. Brino, Colori di Liguria, Sagep Ed., Genova, 1991
4. Shigenobu Kobayashi, Color Image Scale, Nippon Color and Design Research Institute, publ. Kodansha, Ltd. 1991, Tokio, Inc
5. Tom Porter, The Architect's Eye, Visualisation and Depiction of Space in Aarchitecture, E&FN Spon, London, 1997

Author's address

Silvia Rizzo, Professor
Liceo Artistico Barabino, Genova
Via Mogadiscio 2A/7
16141 Genova, Italy
phone: +0039-010-8362185
fax: +0039-010-5305169
e-mail: gsonnewa@tin.it

Captions: *Some examples of the research work presented:*
Three Female Figures, Palazzo Imperiale, Piazza Campetto, Genoa
Allegory of Strength, Palazzo Pallavicino, Piazza Fontane Marose, Genoa



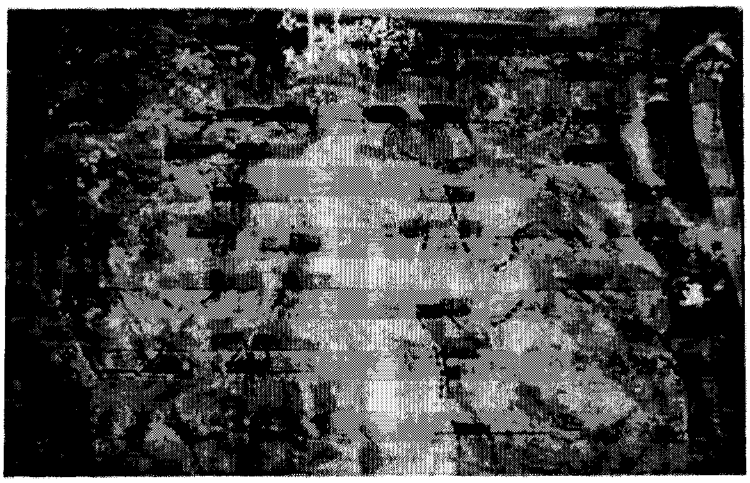


Numerical Expression of Colour Emotion and Its Application

Tetsuya Sato, John Xin*, Jim Nobbs**, Aran Hansuebsai***
Kyoto Institute of Technology, * Hong Kong Polytechnic University,
** University of Leeds, *** Chulalongkorn University

1. Introduction

Colour induces various human emotions. The emotions are expressed through words such as *deep* and *warm*. In order to analyse the emotions expressed through words, visual assessment tests against colour emotions expressed by twelve kinds of word pairs were carried out in Japan, Thailand, Hong Kong and UK. The numerical expression of each colour emotion has been tried as a equation with an ellipsoid-shape resembling that of a colour difference equation. The application of the empirical colour emotion equations derived from sensory database (database of sensory assessments) was also tried. This paper was briefly summarised about our previous studies, and showed some examples of our trials [1-7].

2. Numerical expression of colour emotion for instrumental assessment

The empirical colour emotion equations have been derived in our previous researches. These equations predict the magnitude of human emotion induced from a colour. The initial work on the numerical expression of the colour emotions included 12 sensory word pairs is in shown Table 1.

The colour emotion equation was expressed with an ellipsoid-shape equation. The shape is similar to that of colour difference equation. A colour difference value such as CIELAB ΔE^*ab is defined as a distance between colorimetric coordinates of two colours. A colour difference value is going larger with the growth of colour difference. Colour emotion values computed by the equations are going larger with the growth of colour emotions as well. A visual scale for assessing a colour emotion in the CIELAB colour space is given as Equation 1. As an example, Equation 2 is 'Soft-Hard' equation derived by Japanese assessments. As a^*_0 and b^*_0 in the Japanese assessments were zero, C^* was used in the Equation 2.

$$CE = [\{k_L(L^*-L^*_O)\}^2+\{k_A(a^*-a^*_O)\}^2+\{k_B(b^*-b^*_O)\}^2]^{1/2}+k_M \quad (1)$$

Where,

CE	:	Prediction value of a colour emotion
L^*	:	CIELAB metric lightness
a^*, b^*	:	CIELAB a^* and b^*
L^*_O, a^*_O, b^*_O	:	CIELAB L^*, a^* and b^*, when the colour emotion is minimum
k_L, k_A, k_B	:	Constants of the contribution of CIELAB L^*, a^* and b^*
k_M	:	Constant for scaling

$$SH_{JP} = [(3.2L^*)^2+\{2.4(1-\Delta h_{290}/360)C^*\}^2]^{1/2}-180 \quad (2)$$

Where,

C^*	:	CIELAB metric chroma
Δh_{290}	:	CIELAB metric hue-angle difference from h=290, $0\leqq\Delta h_{290}\leqq180$

Table 1 Sensory word pairs used for visual assessments [4,6,7]

Symbol	Japanese	English	Thai	Chinese (Cantonese)
DP	Koi - Awai	Deep - Pale	Khem - Jang	Sem - Tsin
DYP	Doutekina - Seitekina	Dynamic - Passive	Kloenwai - Sangobning	Dung - Zing
DV	Hakkirishita - Bonyarishita	Distinct - Vague	Dodden - Seed	Tsing sik - Mou wu
GP	Hadena - Jimina	Gaudy - Plain	Choodchad - Reab	Zuk Jim - Pok sou
HL	Omoi - Karui	Heavy - Light	Nuck - Bow	Zung - Hing
LD	Akarui - Kurai	Light - Dark	Sawang - Mued	Gwong - Em
SH	Yawarakai - Katai	Soft - Hard	Numnual - Kangkradang	Jau jyn - Gin ngang
SS	Medatsu - Medatanai	Striking - Subdued	Chadjan - Kamukkamoe	Dyt muk - Jau wo
SW	Tsuyoi - Yowai	Strong - Weak	Khemkang - Oanaer	Koeng - Joek
TT	Sunda - Nigotta	Transparent - Turbid	Prongsai - Tueb	Tung tau - Wen zuk
VD	Azayakana - Kusunda	Vivid - Dull	Sodsai - Mon	Sin ming - Em tam
WC	Atatakai - Tsumetai	Warm - Cool	Ron - Yen	Nyn - Lang

3. Cross-culture comparison on colour emotion

There are some differences in our colour emotions. Especially, the differences between colour emotions in two countries with different culture make our communication difficult. Therefore, it is important to know the details of the differences through cross-cultural comparison.

Table 2 shows the correlation coefficients between the 'Warm-Cool' visual assessments of the four countries. The correlation coefficients between the assessments were around 0.8. This means that 'Warm-Cool' assessments in the four countries are approximately similar. But, the relationship between the four visual assessment sets does not have so high correlation and there are some differences between them.

Table 2 The correlation coefficient between 'Warm-Cool' assessments of four countries

	Japan	UK	Thailand	Hong Kong
Japan	----	0.761	0.823	0.869
UK	0.761	----	0.818	0.712
Thailand	0.823	0.818	----	0.851
Hong Kong	0.869	0.712	0.851	----

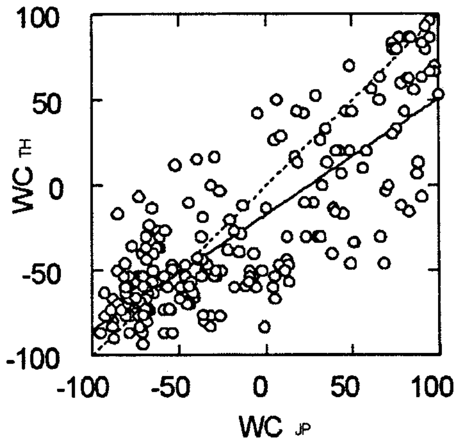

Figure 1 The comparison between 'Warm-Cool' assessments obtained in Japan and Thailand

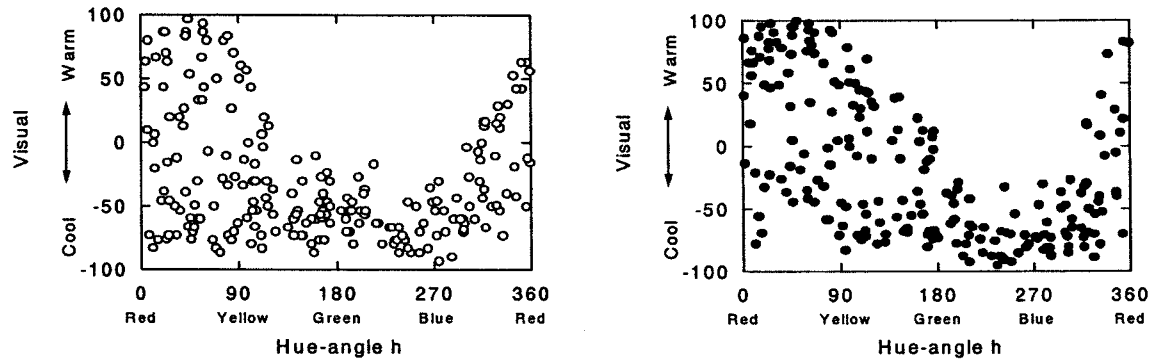

Figure 2 The comparison between 'Warm-Cool' assessments obtained in Thailand and Japan, ○:Thailand ●: Japan

Figure 1 shows the relationships between Japanese and Thai visual assessments obtained through the same experiments. The slope of a regression line on the figure was less than 45 degree. This means that Thai assessment for 'Warm-Cool' is a little cooler than Japanese assessment and there are not so many warm colours in Thailand.

Figure 2 shows the influence of hue in the 'Warm-Cool' assessment. In the both of Japanese and Thai assessments, the warmest colour was vivid orange and the coolest colour was blue green. The colour areas, where Japanese and Thai assessments are different, are orange, yellowish green and purple hue areas. Remarkably, light and dull orange colours were cool colour in Thai assessments, and all tone colours of yellowish green were also cool. But, in Japanese assessments, most of orange colours were warm, and yellowish green colours were approximately moderate.

4. Translation of colour emotion between two languages

It is difficult to communicate feelings between two languages, especially the magnitudes of the feelings. In general, a word is not corresponding to just one word in other languages.

How can we communicate the magnitude of colour emotion between two languages?

We would like to suggest a translation through colour emotion equations. For example, a translation between 'Dynamic-Passive' colour emotions expressed in Japanese and English can be done instrumentally as the following equations.

$$DyP_{JP} = [\{0.6(L^*-50)\}^2+\{4.6(1-\Delta h_{290}/360)C^*\}^2]^{1/2}-115 \quad (3)$$

$$DyP_{UK} = [\{3.5(L^*-75)\}^2+\{7.6(1-\Delta h_{290}/360)C^*\}^2]^{1/2}-195 \quad (4)$$

Equation 5 can be used for quantitative translation from the colour emotion described as 'Dynamic-Passive' in English to that described in Japanese. Equation 6 can be used for translating from the colour emotion described as 'Dynamic-Passive' in Japanese to that described in English as well as Equation 5. Through the equations, we can know the magnitude of colour emotions in foreign country.

From DyP_{UK} to DyP_{JP}:

$$DyP_{JP} = [\{0.6(L^*-50)\}^2+\{(4.6/7.6)[(DyP_{UK}+195)^2-\{3.5(L^*-75)\}^2]^{1/2}\}^2]^{1/2}-115 \quad (5)$$

From DyP_{JP} to DyP_{UK}:

$$DyP_{UK} = [\{3.5(L^*-75)\}^2+\{(7.6/4.6)[(DyP_{JP}+115)^2-\{0.6(L^*-50)\}^2]^{1/2}\}^2]^{1/2}-195 \quad (6)$$

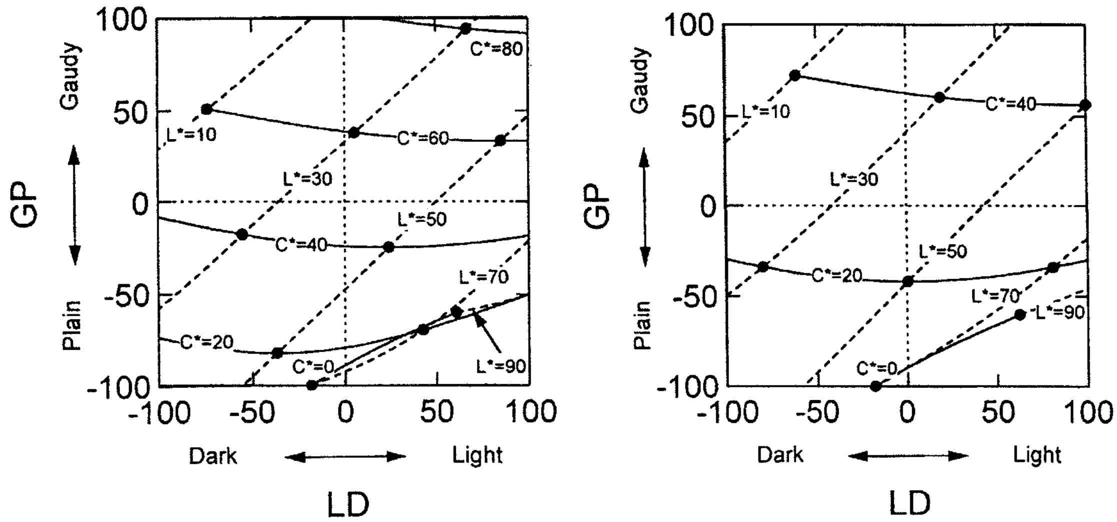

h=90, Yellow hue plane *h=270, Blue hue plane*

Figure 3 CIELAB colour system projected on the 'Light-Dark' and 'Gaudy-Plain' plane: Yellow and blue hue planes [3]

5. Development of a new colour description and communication of colour emotion

Traditional colour systems are based on three attributes such as hue, lightness and chroma. But our sensations are various. Therefore, we can develop another colour system based on the sensations as shown in Figure 3. Figure 3 shows a colour emotion description system by 'Light-Dark' and 'Gaudy-Plain', which are projected yellow and blue hue planes.

Currently, the keyword of the application of colour technology is *colour communication*. The colour communication is including colour reproduction colours and colour management. Especially, it is the most important to communicate colour images accurately. While the current application of colour communications are in the domain of colour reproduction accuracy and colour management, it is suggested in this study the communication of colour emotions induced by colours, in addition to the communication of colours. With sensory database and colour emotion equations, we envisage the development of some useful tools for *Information Technology*. Colour emotion scales obtained can be transformed to CIELCh, CIELAB, XYZ, and RGB values through a reverse operation as shown in Figure 4, which can be output as colours by display devices [5-7]. This colour output can be used by applications such as product design and development, which can then be further extended to applications on Internet. In addition, colour emotion system can be displayed on a computer monitor. Figure 5 shows an example of the interface model of the application to colour design assisted tool.

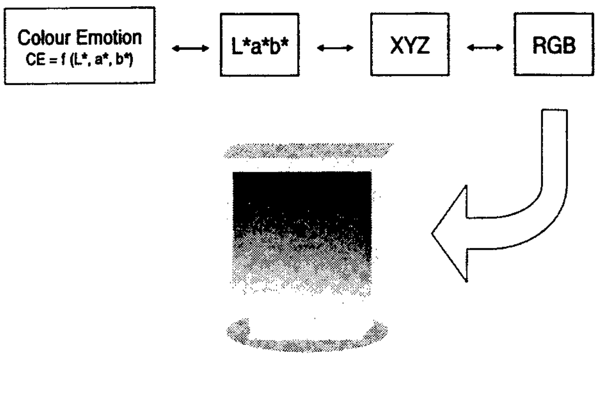

Figure 4 Process for the projection of a colour emotional diagram on a computer display [5]

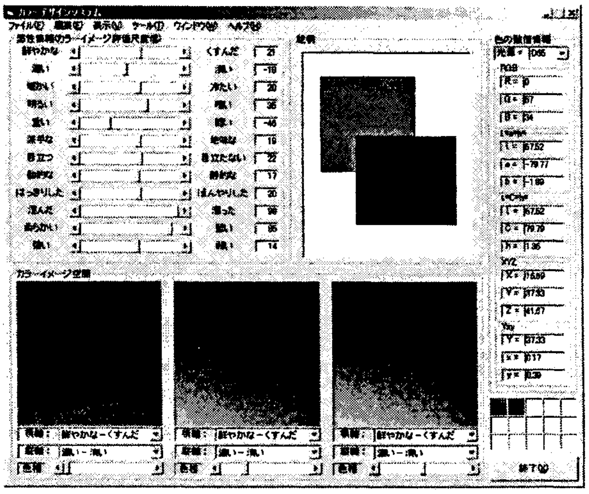

Figure 5 An example of the interface model of the application to colour design assisted tool [5]

6. Summary

Comparing the sensory assessments obtained in the four countries, we found some similarities and discrepancies among the results. For example, this study on 'Warm-Cool' colour emotion and our recent studies showed that some colour emotions were not identical. In addition, the comparison and conversion can be quantitatively done through the use of colour emotion equations. The understanding of differences in colour emotions and the use of this knowledge in the development of new products will be very important.

As further studies, the discrepancy and similarity among the assessment databases will be analysed in details. The analysis will be useful to make way for estimates of the cultural influence of each country. But the sensory database obtained in this study is not enough to discuss about the details of the influence from culture. Because just only one data set in a country was discussed in this study, and observers' age was around twenty years old. Therefore, many sensory data should be collected carefully, and the data should be analysed more quantitatively with objective viewpoints.

References

1. T.Nakamura, T.Sato, K.Teraji, and T.Fukuda, Arrangement of Color Image Words into the Non-Luminous Object Color Space (*in Japanese*), Journal of the Color Science Association of Japan, **18**, p.10-18, 1994
2. T.Nakamura, H.Hoshino, T.Sato, and K.Kajiwara, Numerical Evaluation of Colour Image Words on Colorimetry, Proceedings of the AIC'97, Kyoto Japan, p.699-702, 1997
3. T.Sato, K.Kajiwara, T.Nakamura, and H.Hoshino, Quantitative Evaluation and Categorising of Human Emotion Induced by Colour, Advances in Colour Science and Technology, **3**, p.53-59, 2000
4. T.Sato, K.Kajiwara, J.H.Xin, A.Hansuebsai, J.Nobbs, Methodology for Deriving Visual Scale Based on Colour Emotion, Proceeding of Colour and Visual Scales 2000, Egham U.K., 4 pages, not paginated, 2000
5. T.Sato, K.Morimoto, K.Kajiwara, and T.Kurokawa, Development of Sportswear Design Assisted System Based on Numerical Expression of Colour Emotion (*in Japanese*), Descente Sports Science, **21**, p.27-42, 2000
6. T.Sato, K.Kajiwara, H.Hoshino, T.Nakamura, J.H.Xin, A.Hansuebsai, and J.Nobbs, Application of Numerical Expression of Colour Emotion, Proceedings of the AIC Midterm Meeting, Seoul Korea, p.130-132, 2000
7. T.Sato, K.Kajiwara, A.Hansuebsai, J.H.Xin, J.Nobbs, Numerical Expression of Colour Emotion and Its Application, Proceedings of the AIC'01, Rochester USA, p.409-412, 2001

COLOUR AND EMOTION

Leonhard Oberascher and Michael Gallmetzer
Psychology of Architecture and Design, Austria

Abstract
After clarifying the concept of emotion, we turn to the interrelation between colour and emotion: Do people show emotion-specific colour associations or attributions? What emotional reactions can evoke colours? To answer these questions, we had subjects (1) assign colour concepts to concrete illustrations of the (presumably universal) mimic expressions of the 7 basic emotions happiness, surprise, anger, fear, disgust, sadness and contempt, (2) assign concrete colour patterns to the 7 emotional concepts, (3) represent in colour the 7 emotional concepts. Here we found conspicuous concordances. We also refer to earlier investigations into emotional valences of colours, including our own studies of colour associations. These showed clear concordances, which in turn largely correspond with the colour-coding of emotions. In conclusion we discuss the question whether and how far such results can be utilised in psychodiagnosis.

1 EMOTION – DEFINITION AND BIOLOGICAL ASPECTS

1.1 Suggested definition

Following Zimbardo (1), emotion may be defined very generally as a complex pattern of organismic changes as a reaction to stimuli (situations) perceived by an individual as being of personal significance. These include physiological and cognitive processes, feelings (subjective/internal) and behaviour (objective/external).
For further clarification, we distinguish "emotion" from related affective constructs such as "mood", "temperament", "affective style" or "emotional traits/character" (cf. 2). In agreement with Ekman & Davidson (2), we use the expressions of affective states or affects as umbrella concepts for these various affective constructs. Amongst these, "feeling", as already mentioned, refers to the subjective/internal aspect (personal "inner" perception) of emotion; emotional self-experience or self-perception, "mood", on the other hand, is distinct from "emotion" in several respects: 1. moods are not contingent psychological/physiological facts, but *a priori* categories, so to speak, of psychological/physiological activity, a vital and indispensable basic condition, the affective colouring of all our statements about life: we are always in some mood or other; 2. emotions influence our actions, whereas moods influence cognitive matters (e.g. happy/sad memories) and functional characteristics (flexibility, associative ability, creativity, speed...); 3. moods show no specific correlates in the autonomic nervous system; 4. the effect of triggers on the individual are longer and cumulative, not sudden and short-term. "Affective style" is generally used as a qualitative construct ("traits") to describe inter-individual distinctions. Therefore affective styles are (intra-)individual, largely consistent tendencies to react in emotionally relevant situations, such as hostility, euphoria, shyness or melancholy. "Temperament", on the other hand, denotes – as one aspect of affective style – a person's early (childish) affective patterns of reaction, which are consi dered to be largely innate (genetically, prenatally and perinatally determined).
Relevant here – and widely familiar – is the distinction made by the Ancient Greeks between four emotional tem peraments or humours, each determined by a dominant body fluid: sanguine/blood, melancholic/black bile, choleric/yellow bile and phlegmatic/phlegm (cf. 3, 4).

1.2 (Evolutionary) biological aspects of emotions

Darwin (1872) sees emotions as phylogenetically developed specific adaptations of the organism to typical recurrent situations (danger, death of close relatives, birth, success...); they are universal and intraspecifically inherited. On the basis of Darwin's evolutionary theory of emotions, and as an extension of it, Ekman (cf. 1) developed his "neurocultural" theory of emotion (and expression); "neurocultural" refers to the interactionism of predisposition/brain with environment/culture. The seven basic emotions – pleasure, surprise, anger, disgust, fear, sadness and contempt – appear universally (interculturally) in physiological and psychological aspects as well as in mimic expression; however, cultural conditions have a determining (standardising) influence upon which emotion (according to the hereditary repertoire) is expressed, and when. How far this universality of emotion postulated by Ekman applies also to the relationship between emotion and colour, is a central question for the investigations to be expounded below, which attempt an approach to this comprehensive topic and which, we hope, will result in the implementation of further studies.

2 EMOTION AND COLOUR – PERSPECTIVES AND EMPIRICAL APPROACH

After this brief look at the thematic complexity of our emotional world, let us now turn to our second, no less varied, thematic focus: colour. Ekman's universalistic "neurocultural" approach seems to form a suitable bridge to an account of the connection between colour and Ekman's seven universal emotions, under two different perspectives: 1. Are there regularities to be observed in assigning colours to emotions – that is, are emotions colour-coded? 2. Do different colours show characteristic emotional valences – that is, do colours have specific emotional connotations?

2.1 Colour-coding emotions

For the purpose of an (introductory) empirical discussion of the question whether people specifically colour-code emotions, we have carried out three different investigations:

1. Participants assign colour concepts to illustrations of the facial expressions of seven (basic) emotions.
2. Participants classify concrete colour patterns with the given seven (basic) emotional concepts.
3. Participants represent the seven (basic) emotional concepts in their own colour compositions.

2.1.1 Assigning colour concepts to illustrations of mimic emotional expression

We showed 13 persons (b/w) illustrations (cf. 1) of facial expressions of the seven basic emotions in the order: *pleasure, surprise, anger, disgust, fear, sadness, contempt*, and asked them to assign to these illustrations (1) up to three emotional concepts and (2) up to three colour concepts (single colours, not combinations, as in 2.1.2 and 2.1.3), and (3) to explain/account for their attributions.

Since the assigned colour concepts are merely linguistic codings, in analysing and evaluating them we have to restrict ourselves to a direct report of these concepts, so that the question remains open, of what "inner idea" of the participant, what nuance, corresponds in fact to the given colour. Nevertheless, the relative frequencies of the attributions may provide interesting initial indications of possible psychological correspondences between emotions and colours.

Despite the indifferent quality of the illustrations of facial expressions (A4 b/w photocopies), the participants usually interpreted the emotions correctly; only the expressions of surprise, sadness and contempt show deviations of between 15% and 23% – though here, too, there was some 80% agreement.

In the attribution of colour, the following colours dominate:

pleasure: (warm, cheerful, radiant, bright variants of) yellow, orange (total 69%); surprise: (conspicuous, neon) yellow, white, whitish-blue and green (total 81%); anger: (strong, fiery, blood-) red (55%) and black (10%); disgust: (bilious/dirty variants of) green and brown (total 50%); fear: (in contrast to pleasure, here more "alarming", loud, threatening, rather than warm, cheerful variants of) yellow, red (total 32%) and black (13%); sadness: grey, black and deep purple (total (53%); contempt: (bright, cold, strong, "royal" variants of) blue (48%), (cool, bright variants of) green (10%), brown and black (total 20%).

2.1.2 Assignment of concrete colour patterns to given emotional concepts

In a further experiment, we asked 43 persons (1) to classify a maximum of three colours or colour combinations each with the given seven emotional *concepts*, according to their estimation of the aptness of these colours to characterise the concepts (we preselected 16 *concrete* NCS colour patterns from which they could choose: 1. S 0570-Y yellow, 2. S0580-Y50R orange, 3. S 0580-Y90R red, 4. S 2060-R40B purple, 5. S 2565-R80B blue, 6. S 2555-B30G turquoise, 7. S 2565-G green, 8. S 0575-G40Y yellowish-green, 9. S 0500-N white, 10. S 3500-N grey, 11. S 9500-N black, 12. S 2020-Y30R beige, 13. S 6030-Y70R brown, 14. S 0520-Y90R pink, 15. S 0520-G10Y light green,16. S 0530-B light blue), and (2) to explain/account for their classification of colour patterns.

In contrast to 2.1.1, the classification of concrete colour patterns enables a more direct and objective articulation by those questioned, since there is no room for linguistic ambiguity.

For the seven emotional concepts, the 43 participants made a total of 455 colour pattern classifications (single and combined). The highest total number (single or combined, cited at optional points) of classification of a colour pattern is 33, and of citing in first place 28, in both cases for S 0570-Y yellow.

There follows an account of the principal results, first in text form (the first numeral in "()" before "/" denotes the number of classifications of the colour pattern in question in first place, singly or combined, the second numeral after "/" the total number), and subsequently – in the interests of clarity – as a histogram (the first, grey bar denotes the number of classifications in first place, the second, black bar the total number): pleasure (total 103 classifications): S 0570-Y yellow (28/33), S 0580-Y50R orange (12/28; chosen 12 times in second place!), S 0580-Y90R red (6/10), S 2565-R80B blue (5/9); combination S 0570-Y yellow + S 0580-Y50R orange (4); surprise (total 61 classifications): S 2060-R40B purple (10/10), S 0575-G40Y yellowish-green (8/12), S 2555-B30G turquoise (5/8), S 2565-G green (4/5); anger (total 58 classifications): S 0580-Y90R red (25/27), S 9500-N black (8/10), S 6030-Y70R brown (3/4); disgust (total 65 classifications): S 6030-Y70R brown (16/17), 2020-Y30R beige (13/15), S 0520-Y90R pink (9/10), S 0575-G40Y yellowish-green (6/8), S 0520-G10Y light green (6/7); fear (total 54 classifications): S 9500-N black (19/21), S 2060-R40B purple (5/5), S 0500-N white (3/4), S 3500-N grey (3/4); sadness (total 65 classifications): S 9500-N black (20/24), S 3500-N grey (12/19), S 0530-B light blue (3/4); contempt (total 54 classifications): S 2060-R40B purple (7/7), S 6030-Y70R brown (6/6), 2020-Y30R beige (5/7), S 0530-B light blue (4/5).

Apart from these 43 persons, we also questioned six black-skinned people from Western Africa. For pleasure, this group showed a tendency towards green/blue rather than yellow, for anger particularly to black, twice in combination with red, and for fear to red. For sadness they showed no difference from our other results.

International comparisons can yield information about the influence of ecological and geographical or socio-cultural factors in the colour-coding of emotions. Might the preference for green/blue over yellow as colours of pleasure in Western Africa be because in a region with an abundance of light and sun, colours representing other resources afford more pleasure and assist expression?

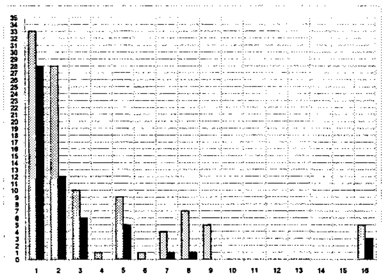

HAPPINESS

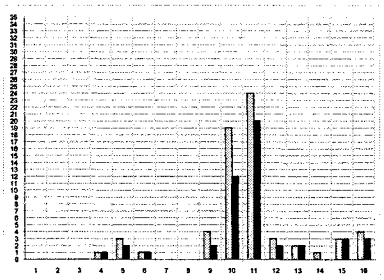

SADNESS

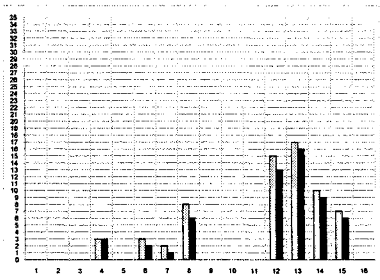

DISGUST

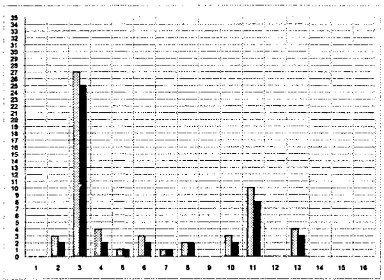

ANGER

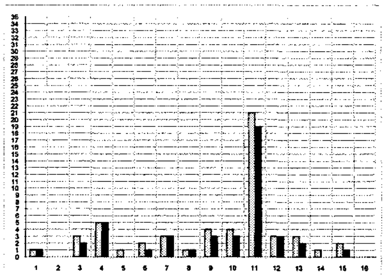

FEAR

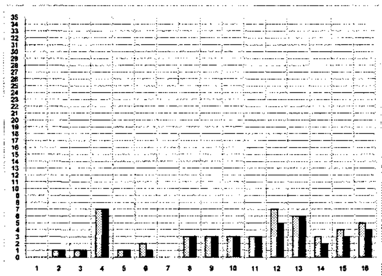

CONTEMPT

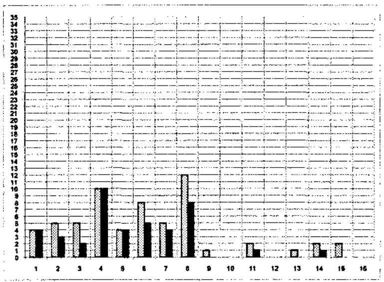

SURPRISE

The arrangement of the seven emotion-specific colour histograms shows clearly: for pleasure, anger and surprise, the (first 8) strong, bright colours predominate, and amongst these, shades of yellow and red for pleasure and anger; for sadness and fear the achromatic colours, especially black, and for disgust and contempt rather the (second 8) dull, muted colours, especially beige and brown. These different colour (character) profiles suggest a division of emotions into active, positive, open, extraverted (pleasure, anger, and probably also surprise), and passive, negative, introverted (sadness, fear). Disgust and contempt may be somewhere in the middle, linking aspects of both poles: aversion, dissociation, distance, withdrawal, often articulated very clearly, even demonstratively or

2.1.3 Colour representation of the given emotional concepts

For the third variant of our emotional colour-coding experiment, we asked 16 design students to represent in colour Ekman's seven basic emotional concepts, by creating compositions in freely chosen colours in any size up to A4. The range extended from simple geometric mono- or dichromatic right up to polychromatic, geometrically complex, abstract pictures of not dissimilar colour schemes.

In contrast to the two previously described experiments, the colour-coding method used here afforded a greater scope for expression, through its independence from language (concrete colours) and its openness. However, here the determinants and dimensions of the colour-coding are not restricted to the colours or colour combinations as in 2.1.2, but compositional characteristics such as simplicity/complexity, quiescence/movement (direction), or dynamic relationships between the colours must be taken into consideration in analysis and interpretation.

For the evaluation, we proceeded as follows:

1. We scanned all the colour compositions into the computer and standardised their sizes. 2. We arranged the 16 pictures for each emotion in a 4 x 4 square on an A4 page and processed them further using Adobe-Photoshop. For each picture, we collated closely-related shades of colour into a group, replacing them with a representative colour, for up to the four most frequently occurring colour tendencies. This gives a chromatically modified, abstracted image of the original 16-part colour compositions, a concentrated colour characterisation of each of the seven emotions. Although this step towards abstraction entails a loss of information, it reveals the predominant colour tendencies of each picture; in imitation of "psychogram", we would suggest the term "chromogram" to describe this. The most unified and characteristic chromograms emerged for pleasure, sadness, anger and fear. Here we give the predominant typical colours for each emotion-chromogram, the numerals in () signifying the number of colour compositions sharing the colour in question, in relation to all 16 colour compositions: pleasure: yellow (16/16), orange (6/16), red (5/16); surprise: yellow (10/16), blue (8/16),

yellowish-green (7/16), light turquoise (7/16), white (5/16); anger: red (16/16), black (11/16); disgust: yellowish olive-green (11/16), brown (10/16), yellowish-green (7/16), pink/purple (4/16); fear: red (10/16), black (8/16), grey (7/16), purple (5/16); sadness: black (15/16), grey (11/16); contempt: grey (7/16), blue (7/16), purple (7/16).

A notable detail: the dominating colours found by this group of young, trend-conscious design students to articulate disgust – namely, muted, "dirty", "bilious" shades of green, yellow and brown – are at present considered in furniture and interior design as trendy colours with a positive connotation! This shows once more how far socio-cultural conditions can be superimposed upon our supposedly direct (colour) judgement, founded upon evolution, and how much our feeling and perception are influenced by social trends (cf. 5a, b, c).

2.2 The emotional valence of colours

What emotional qualities are ascribed to colours? By the "emotional quality" of a colour, we understand its emotional influence on the observer. Using this, we will attempt to determine phenomenologically, through subjective experience, the emotional valence (profile, epitome of the emotional qualities) of colours.

Comprehensive and well-founded studies, such as that by Lars Sivik (6 a, b) on colour connotations already point in the direction of our question, but in the semantic differentials on which they are based, they contain no direct emotional concepts (as in Ekman) and only a few terms relevant to emotion: "welcoming/hostile", "cheerful/serious", "pleasant/unpleasant" and "beautiful/ugly".

In our own studies (cf. 7), we used the obvious method of free conceptual association, again in the variants of given colour concepts and patterns. Given below are the principal results of our investigation on colour association with a total of 51 persons. Slightly differing associations for concepts or patterns of the "intermediate colours" such as brown, purple, pink or orange may be due to the fact that these colours as concepts lead to different subjective representations (cf. 7).

The following emotionally relevant associations demonstrate two kinds: direct emotional concepts such as "plea sure" or "welcoming", and concepts obviously closely related thematically, or decisive for the emotion in question, such as "laugh", "pleasant":

- black: sadness, despair; fear (and probably determinant: dark, sombre), impotence, oppressive, cold
- red: anger; pleasure; fear
- yellow: pleasure, cheerful, open
- white: pleasure, welcoming, open; sadness(and probably determinant: cold, rigid)
- grey: loneliness, depression, dismal, indifferent
- green: probably determinant for disgust: poisonous, bile
- orange: pleasure, cheerful
- purple: sadness, loneliness, depression; probably determinant for contempt: arrogant, power, unfeeling
- brown: probably determinant for disgust: excrement, rottenness, dirt; oppressive, sluggish
- pink: probably determinant for disgust: kitsch, piglet, stomach-ache
- black-red: probably determinant for fear on the one hand and anger on the other: devil (Krampus), hell, danger

2.3 Results and discussion

Let us look first at an important aspect, a difference between our own studies (described under 2.1.2, 2.1.3 and 2.2) and studies on association by other authors (8, 9). In our studies on colour-coding as well as in those on colour association, there was a choice not only of single colours, but also of colour combinations. Attached to these, however, seems to be an individual, more comprehensive and differentiated "semantic form", which cannot be explained completely by the constituent single colours. A striking example is the red-black association "Krampus"; in Austria, South Tyrol and Bavaria, this traditional folk figure of a demon, probably heathen in origin, accompanies St. Nicholas on the night before the 6th of December in ritual midwinter processions with masks and costumes. Over 80% of the participants in our studies cited this association in first place, whereas Hackl-Grümm (8) reports that from about 650 persons "devil" was mentioned only 17 times ("Krampus" 3 times) for black, and only twice "Krampus" and 8 times the related concept of "hell" for red. Colour combinations seem better suited to characterise emotions, as our chromograms (2.1.3) show.

Basically, however, considerable agreement is shown between our three studies on specific emotional colour-coding, both in relation to each other and in comparison with Heller's (9) study, as well as between our study and those of others on colour associations (e.g. 8), irrespective of their differences in concept and method (framing of questions: from emotion to colour or vice versa; medium for colour-coding: single-colour concept, choice of concrete colour patterns or combinations, or free expression of form and colour) – particularly for the emotions of pleasure, anger, disgust, fear and sadness.

With this reservation, with reference to our own results and those of other studies essentially in agreement (particularly for the colours black, yellow, red and brown), we would suggest the following colour-emotion classifications, valid also inversely, as emotion-colour-codings: black = sadness; yellow = pleasure; red = anger; brown = disgust. Colour combinations, however – also because of their semiotic function, as in the "Krampus" example – tend to comply with the complexity of the emotions, their nuances and shades, and their interrelations: thus pleasure corresponds especially with the yellow-orange combination, with its overtones of light and warmth, and fear with black-red, which – apart from the specific associations such as Krampus,

volcano, fire... – evokes elements of eerie, unfathomable darkness and imminent danger, of oppressive menace, of being cornered, of the nervous tension immediately preceding a more or less useful counter-activity such as running away.
Our chromogram study in particular shows clearly that colour *per se* as a method of coding cannot do justice to the complexity of the emotions. Some of the free colour-compositions, especially for fear, show – in addition to the choice and combination of colour – striking graphic elements such as jagged, uneven lines.
On the other hand, of course, all colours (even single colours) evoke emotional reactions. These are to a great extent, however, individual and dependent upon context. Nevertheless, we postulate the following tendential emotional effects of colours: A room decorated in tones of yellow and orange, for instance, will tend rather to evoke pleasure for the majority of people in our culture than a black-and-grey room. Black and grey generally have an oppressive effect. The combination of black and red tends to have a menacing effect. Pink tends to evoke aversion and rejection, but in its ambivalence – not only in the USA – it also appears as a favourite colour, especially for women, according to Heller (9), even taking fourth place, with 8%, after blue, red and green.

3 THE PSYCHODIAGNOSTIC RELEVANCE OF COLOURS

In chapter 2, we attempted a conceptual and empirical approach to the interrelation between emotions and colours. The connections that emerge from this open up numerous possibilities, even demands for further and more intensive research. They also raise the question of how far concrete results of "emotion-colour research" can be of use. For this purpose, we shall discuss the utilisation for psychodiagnosis of the results of research into colour psychology. Do systemic relationships exist between specific personal characteristics such as affective states, and particular colours or colour combinations? Does an individual's choice of colour – on the basis of such relationships – enable conclusions to be drawn about aspects (including affective aspects) of his/her personality?
In their recently published book "L'enigma del colore" (The mystery of colour), Senini and Inga Sigurtà (10) devote a chapter to these questions. They emphasise the intrinsic quality of colours as "things of the soul" (p. 49), and in addition as a means of expression of our needs, because "we instinctively prefer [...] those colours which [...] best represent the variability of temperament, since the use or application of colour [...] expresses one's own psychological situation" (p. 53). Many researches and studies on colour choice and preference carried out with a view to psychodiagnosis and psychology of personality (cf. Rorschach, 1921; Pfister, 1946; Jung, 1948; Lüscher, 1945, 1949; Koch, 1953) now bear out the assumption of a link between psychological characteristics and the preference for particular colours. There is nevertheless still a lack of empirically founded theories on the diagnostic significance of preferential judgements. However, the colour-choice processes based on this – according to Halder-Sinn (11) – offer "a whole array of advantages in their application and evaluation (objectivity, freedom of language, restricted transparency, etc.), so that their further development seems useful".

References

(1) Zimbardo, P.-G. und Gerrig, R.-J.: Psychologie. Berlin: Springer-Verlag, 1999.
(2) Ekman, P. and Davidson R.-J. (Ed.): The nature of emotion. New York: Oxford University Press, 1994.
(3) Zimbardo, P.-G. and Floyd, L.-R.: Psychology and life. 1977.
(4) Hagn, H.: Farbe als Symbol. (Dissertation) Salzburg: Naturwissenschaftliche Fakultät der Universität Salzburg, 1984.
(5a) Oberascher, L.: Individual Colour Preferences - What do they Really Tell about a Person? In: Colour Report, Colour and Psychology, F 50. An Anthology edited by Lars Sivik. Göteborg: 1997, 106-108.
(5b) Oberascher, L.: The role of color in the 21st century. Color culture between homogenization and diversification. In: AIC-COLOR 97, Proceedings of the 8th Congress of the International Colour Association. Kyoto, Japan: Color Science Association of Japan, 1997, 83-89.
(5c) Oberascher, L.: Farbtrends - Farbwandel zwischen kollektiven und gruppenspezifischen Farbvorlieben. In: Inprint, Interprint Rotationsdruck GmbH & CO KG, Arnsberg, 1997, 9, 4-7. (also published in English, Italian, Russian)
(6a) Sivik, L.: Color meaning and perceptual color dimensions: A study of color samples. Göteborgs Psychological Reports., 4, No.1, 1974.
(6b) Sivik, L.: Color meaning and perceptual color dimensions: A study of exterior colors. Göteborgs Psychological Reports., 4, No.11, 1974.
(7) Oberascher, L.: Black - Meaning and Connotation in Europe and Africa. To be published in: AIC-COLOR 01 Rochester, Proceedings of the 9th Congress of the International Colour Association. Rochester, NY, USA: Spie-The International Society for Optical Engineering, 2001.
(8) Hackl-Grümm, S.: Farbstudie 1986. Wien: Psychotechnisches Institut Wien, 1986.
(9) Heller, E.: Wie Farben wirken. Reinbeck/Hamburg: Rowohlt, 1989.
(10) Senini, G. and Inga Sigurtà, E.-F.: L'enigma del colore. Bologna, Italy: Pitagora Editrice, 2002.
(11) Halder-Sinn, P.: Psychodiagnostische Wahlverfahren. In: Groffmann, K.-J. und Michael, L. (Ed.): Persö nlichkeitsdiagnostik. Enzyklopädie der Psychologie, Band 3. Göttingen: Verlag für Psychologie, Hogrefe, 1982, 529-563.

SENSORY WORDS FOR DESCRIBING AUTOMOTIVE EXTERIOR COLORS IN JAPAN, HONG KONG, CHINA AND THAILAND

Izumi Satake[1), 6)], Aran Hansuebsai[2)], John H Xin[3)], Tu Tianming[4)], Tetsuya Sato[5)], Kenji Ando [1)], Koichi Kuwano[1)], Kanji Kajiwara[6)]
[1)]Nippon Paint Co., Ltd., Tokyo, Japan, [2)]Chulalongkorn University, Bangkok, Thailand, [3)]The Hong Kong Polytechnic University, Hong Kong, China, [4)] Dong Hua University, Shanghai, China, [5)] Kyoto Institute of Technology, Kyoto, Japan, [6)] Otsuma Women's University, Tokyo, Japan

ABSTRACT

To elucidate sensory words for describing automotive exterior colors in East Asia, the words chosen by about 300 observers were analyzed. The experiments were conducted at Kyoto Institute of Technology, Nippon Paint Co., Hong Kong Polytechnic University, Dong Hua University and Chulalongkorn University by using a set of questionnaire and 12 colors of painted panels. Prior to this experiment, we selected 31 words and 12 colors from 104b Color Chart produced by Japan Color Enterprise Co., Ltd., based on the results of like-dislike tests of 101 people in Hong Kong and Japan. These results were compiled from the subjects of from 19 years old to 67 years old. Distinctively, the emotional assessments that we conducted revealed that while "bright" and "light" are chosen in Japan as the sensory words of the impression induced by Light Green, "young" and "fresh" are selected in Hong Kong.

We will discuss further characteristics of sensory words for the colors of automotive exterior in each country in detail in this paper.

1. INTRODUCTION

Over the past years, a considerable numbers of studies have been made on color preference and color cognition among different geographical areas. However, little is known about how people assess automotive exterior colors in East Asia. It is often the case that surveys by the auto manufactures, marketing companies, pigment companies have focused on more marketing standpoint. Namely, the data to show how many units of specific automotive exterior colors are sold in the East Asian market are often discussed.

Since an automobile is a global industrial product developed on a mass global scale, the global concern with color assessment on automotive exterior of different geographical areas has been growing recently.

This paper is comparative study of how people assess certain colors developed for automotive exterior touching on similarity and difference among in the East Asian countries. On the way of this process, it will be found that there are some local characteristic colors in each geographical area.

2. METHODS

The survey was conducted on 284 subjects using a questionnaire form. The subjects were the students of HPU(The Hong Kong Polytechnic University); 21.8±1.30 years old (mean±SD, n=50) including 29 males; 21.5±1.09 years old and 21 females; 22.3±1.45 years old, and those of KIT(Kyoto Institute Technology); 21.5±1.63 years old (n=75) including 54 males; 21.5±1.72 years old and 21 females; 21.5±1.44 years old, and the researchers of NP(Nippon Paint Co., Ltd.); 41.7±10.5 years old (n=93) including 68 males; 41.4±10.4 years old and 25 females; 42.6±10.8 years old, and those of CU (Chulalongkorn University);20.9±2.57 years old (n=66) including 43 males;20.8±2.85 years old and 23 females; 21.0±1.97 years old.

Color emotional assessments were performed by a set of questionnaire and painted panels (30.5x 38 cm) with

12 colors specified by the prior experiment. In the prior experiment, the subjects chose one car shape that they were most interested from 15 models, then classified 104 color samples into 3 groups- suitable, unsuitable and not corresponded – for the selected shape. Those 12 colors which differed noticeably and subtly in two subject groups of NP and KIT were determined [1] . All of them were solid colors developed without any sparkling agents. Using multi-angle spectro-photo meter (X-Rite, MA68II), the value of CIELAB of 12 Colors was measured as shown in Table 1.

Photo 1 showed the example of the painted panels on the gray colored boards which were hanged at 1.5m height and placed under sunlight to simulate how an automotive exterior color look in daylight. The order of the 12 color panels was determined by the same table of random numbers. The survey at 4 locations was conducted exactly under the same condition.

The observers were assigned to choose the most suitable sensory words from the list shown in Table 2. The experiments were conducted from the 31st of October, 2001 to the 27th of December, 2002.

Table 1 Measured Value of CIELAB of 12 Colors evaluated in the emotional assessment

Name	L*	a*	b*	c*
LIGHT GREEN	80.99	-35.38	19.74	40.52
VIVID RED	43.59	59.12	32.59	67.51
BLACK	12.46	-0.38	-2.2	2.24
BRIGHT REDDISH ORAN	60.68	39.86	34.74	52.88
YELLOWISH BROWN	49.77	25.53	42.21	49.34
WHITE	93.55	-0.53	1.23	1.34
DULL GREENISH BLUE	40.96	-15.63	-15.09	21.72
DEEP BLUE GREEN	32.29	-35.1	-4.33	35.37
VIVID PURPLE	33.11	26.99	-24.59	36.51
VIVID BLUE	39.6	-3.88	-43.96	44.13
LIGHT YELLOW	84.41	1.57	46.85	46.87
VIVID VIOLET	37.1	18.58	-42.87	46.72

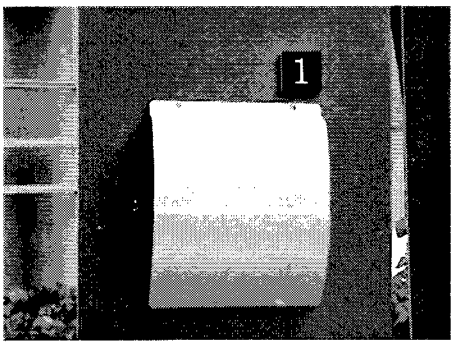

An example of the painted panels. The panel was curved to replicate an automotive door panel to simulate reflection at the highlight and shade by irradiated sunlight.

Table2 Sensory Words for the assessment

beautiful	pretty	sharp
dirty	up-to date	sport
feminine	cheerful	sporty
gaudy	colorful	vivid
interest	dull	bright
slow	young	cool
dark	fast	luxury
shiny	calm	old
heavy	fresh	trendy
light	plain	out-of-date

3. RESULTS AND DISCUSSION

The results were classified into three types according to the relation between the sensory words and colors at each location.

In the first place, we focused attention on the colors chosen for certain sensory words as most or second most suitable at more than three locations. It seems reasonable to suppose that those colors were chosen for certain sensory words in common at each location. As shown in the Figure 1, they were Black for *fast, settled, dark, heavy* and *luxury*, Yellowish Brown for *dirty, old, slow* and *dull*, Red for *fast* and *sharp*, Bright Reddish Orange for *out -of -date*, White for *bright* and Light Green for *lovely*.

In the second place, by categorizing in the similar way, it was found that some words were assessed differently at all locations. This phenomenon was especially prominent in the word *feminine* as shown in Figure 2. In this case, Vivid purple was chosen at HPU, Bright Reddish Orange at NPC, Light Yellow at CU and Light Green at KIT. The other examples were *colorful and up-to-date*. In the case with *Colorful*, Light Yellow was chosen at HPU, Vivid Violet at NPC, Red at CU and Light Green at KIT. Meanwhile, in the case with *Up-to-date*, Vivid purple was chosen at HPU, Vivid Violet at NPC, Red at CU and Vivid Blue at KIT.

Hereby, the non-physical property such as L＊a＊as in CIE LAB was applicable method for classifying the geographical characteristics.

In the meantime, the result mentioned above was different from the result of the extensive research on color cognition of the world's youth in that one of the most suitable colors for the word *Woman* was Pink [2]. It is for reason that our emotional assessment was conditioned to automotive exterior colors.

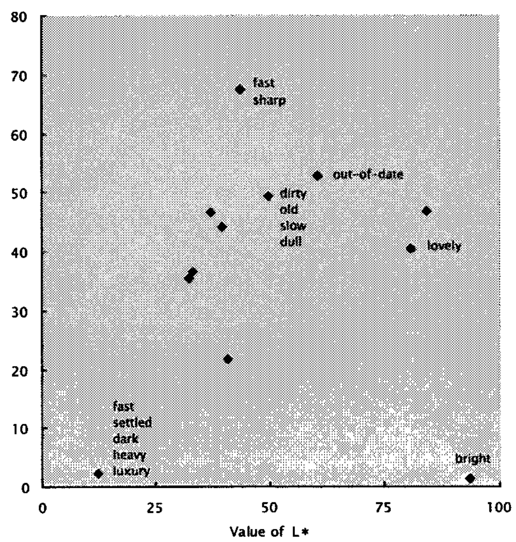

Figure 1 Case examples of the colors matched up with sensory words at more than 3 locations

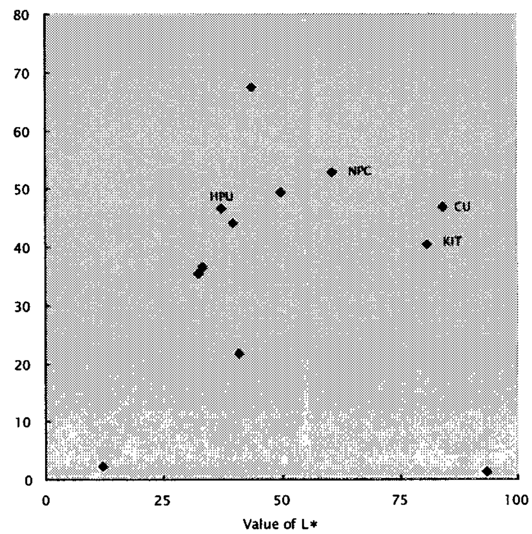

Figure 2 Case examples of the colors assessed differently at 4 locations (Example for feminine)

Furthermore, there were some colors assessed at a certain location linked with more sensory words than any other locations. Examples in this case were Black and Vivid purple. Comparing three locations, such as KIT, HPU and CU which had the similar age difference and educational back ground, Black at CU shown in Figure 3 was referred as the color linked with many more emotional words than KIT, HPU. Similarly, Vivid Purple at HPU as indicated in Figure 4 also linked with many more emotional words than KIT and CU. These results may possibly indicate that those colors are defined as a certain local characteristic color at each location and that this emotional assessment was conditioned to automotive exterior colors. The result that an identical color was chosen for many sensory words at certain location indicates that people have strong feeling about the certain colors and the phenomenon in the specific area. Hereby, it is reasonable to suppose that those colors can be defined as geographically characteristic colors.

Thus, from what has been discussed above, it is concluded that there were some characteristic sensory words which were peculiar to automotive exterior colors, and that there were some local characteristic colors for automotive exterior colors in a certain geographical area.

	CU	KIT	HPU
fast	○	○	○
beautiful	○	—	—
cool	—	○	○
settled	○	○	○
light&fast	○	—	—
sharp	○	○	—
dark	○	○	○
plain	○	—	—
trendy	○	—	○
dark	○	○	○
heavy	○	○	○
up-to-date	○	—	—
shiny	○	—	—
luxury	○	○	○

Figure 3 Distinctive case which was peculiar to CU. Black evaluated for many sensory words.

	HPU	KIT	CU
beautiful	○	—	—
sharp	○	—	—
trendy	○	—	—
vivid	○	—	—
colorful	○	—	○
up-to-date	○	—	—
shiny	—	○	—
interesting	—	—	○
luxury	○	—	—
gaudy	○	○	○
sporty	—	—	○
feminine	○	—	—

Figure 4 Distinctive case which was peculiar to HPU. Vivid Purple evaluated for many sensory words.

3. ACKNOWLEDGEMENTS

Thanks are due to Ms. Noriko Usumoto and Mr. Korn Panyavut for their assistance in collecting the material.

4. REFERENCES

[1] Satake, I.,et al., "Color Preference Study on Automotive Exterior in Hong Kong and Japan", Proceedings of the AIC Color, SI Color & Textile, Maribor Slovenia, p.377-383 (2002)

[2] Chijiiwa, Hideaki, ed. *Encyclopedia on Color Cognition of the World Youth's.* Tokyo: Kawade Shobo Shinsha , (1999)

Factors affecting Colour Harmony for Two-colour Combinations

Li-Chen Ou and M. Ronnier Luo
Colour & Imaging Institute, University of Derby
Kingsway House, Kingsway
Derby, DE22 3HL, United Kingdom

ABSTRACT

Colour harmony has long been of interest to researchers in various fields. It has been found that making a systematic investigation on colour harmony is always difficult to do. One of the main reasons is that colour harmony can be influenced by many different factors. To study this problem, we carried out a psychophysical experiment with 54 colour samples selected systematically from the CIELAB colour space. These colour samples were selected on the basis of Berlin and Kay's 11 universal colour names—black, white, grey, red, orange, yellow, green, blue, purple, pink, and brown. A total of 1431 colour pairs generated from the colour samples were assessed in the experiment, conducted on a calibrated CRT display in a dark room. The colour pairs were shown one by one on the display as two colour squares placed next to each other, with a medium-grey background. The experiment adopted a 10-point scale of forced-choice harmonious-disharmonious judgement. Seventeen subjects, including 11 males and 6 females, each with normal colour vision, took part in the experiment. Experimental results suggest three factors that affect colour harmony: hue effect, lightness sum, and chromatic difference. Quantification was made for these factors in terms of colour-appearance attributes.
Keywords: colour harmony, colour psychology.

INTRODUCTION

Colour harmony has long been an interesting topic in research fields, yet investigators still don't fully understand how it works for all kinds of colour combinations, and they find it difficult to systematically study colour harmony. One of the main reasons is that colour harmony can be influenced by many different factors. For instance, Judd and Wyszecki [1] identified a number of variables that could influence colour harmony: the absolute and relative size of areas covered by colours, the shape of elements of the design, and the meaning or interpretation of the design. However, these are not the *factors* that produce colour harmonies, but the *conditions of viewing layout* that may change the degree of colour harmony.

Early studies have revealed another kind of colour-harmony factors—colour-harmony principles. The investigators include Goethe, Chevreul, Oswald, Munsell, Itten—the list is endless. To generalise the traditional principles of colour harmony, Burchett [2] carried out a study with the method of content analysis and he found six attributes: association, order, configuration, area, interaction, and similarity. More recently, Burchett [3] reorganised these attributes into eight: order, tone, configuration, area, interaction, association, similarity, and attitude. However, all these traditional colour-harmony principles can only be applied to a limited number of colour combinations. This is simply because the early studies investigated colour harmony without a systematic method for sampling colours by taking advantage of a uniform colour space, such as the CIELAB colour space.

A better way of studying colour harmony might be following a specific viewing-layout condition and sampling colours in a systematic way. The present study focuses on two-colour combinations with the shape of square as the viewing layout. The colour samples were systematically selected to cover the entire range of hue, lightness, and chroma in the CIELAB colour space. A psychophysical experiment was conducted on a CRT display at a dark room. The experimental results clarify the connections between colour harmony and the three colour appearance attributes—hue, lightness, and chroma. From these findings, several colour-appearance-based colour-harmony factors were revealed.

METHODS

A psychophysical experiment was carried out to investigate some of the factors that affect colour harmony. In the experiment, 1431 colour pairs, generated by combinations of 54 colour samples, were assessed for colour harmony. The 54 colour samples were systematically selected from the CIELAB colour space with seven hues, three lightness levels, and two chroma levels, as shown in Fig 1. (a) and (b). The seven hues comprised red (25°), orange (60°), yellow (90°), green (150°), bluish green (205°), blue (270°), and purple (330°). The three lightness levels included 80.0, 57.5 and 35.0 in CIELAB L^*, and the two chroma levels included 25.0 and 12.5 in CIELAB C^* for each of the Lightness levels. Thus each of the seven hues gave seven different tones determined by the lightness and chroma. These included vivid, pale, dull, dark, light-greyish, greyish, and dark-greyish. For achromatic colours five lightness levels were used, including 100.0 (white), 80.0 (light grey), 57.5 (medium grey), 35.0 (dark grey), and 0 (black).

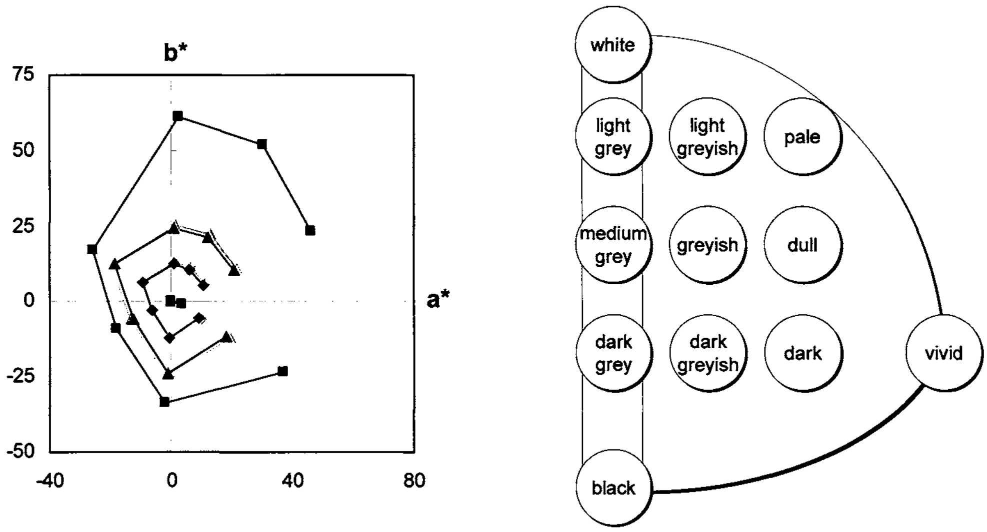

(a) *(b)*

Fig 1. The colour samples in (a) the a-b* chromaticity diagram and (b) the equal-hue (L*-C*) plane diagram.*

Seventeen observers, including 11 males and 6 females, took part in the experiment. All of them were Chinese students at the University of Derby. The experiment was conducted on a CRT display at a dark room. The observers were sitting in front of the CRT monitor with viewing distance of 17.7 inch, and were presented with a colour pair side by side in the middle of the monitor against a grey background. The colour pairs were displayed one by one in random order. The observers were asked to assess how harmonious each colour pair appeared to them by means of the categorical judgement, on the ten categories for two sides: 'extremely harmonious', 'very much harmonious', 'moderately harmonious', 'slightly harmonious', and 'just perceptibly harmonious' on the harmonious side, which were labelled the numbers from 5 to 1; on the disharmonious side were 'extremely disharmonious', 'very much disharmonious', 'moderately disharmonious', 'slightly disharmonious', and 'just perceptibly disharmonious', labelled from -5 to -1. Note that the number of zero was not among these categories. Thus the observers were forced to choose either the harmonious side or disharmonious side. The whole experiment took a period of two months to finish. Each observer attended 7 sessions, each taking about 15 min.

RESULTS AND DISCUSSION

Experimental results were transformed into colour-harmony scores by calculating the mean category value for each colour pair. From these scores several colour-harmony factors were found, as summarised below.

Hue

The experimental results indicate that the colours with the same hue tended to harmonise and therefore had a high colour-harmony score. This is called the equal-hue effect, which was found to be much more significant than other 'equal-quality' effects, such as 'equal-lightness', 'equal-chroma', and 'equal-tone', which corresponds to one of the twelve adjectives given in Fig 1 (b).

In addition, when a colour pair contained bluish colours in it, the colour pair tended to have a high colour-harmony score. This factor was labelled the *hue effect.* Note that this factor does not necessarily imply any connection between yellowish colours and low colour-harmony scores. Instead, a low colour-harmony score often occurred when a colour pair contained reddish colours. Fig 2 (a) shows the hue effect on the average colour-harmony scores. The result for each hue corresponds to one hue paired with all other hues.

The hue effect (H') was modelled in terms of the hue angle of a component colour in a pair, as given in Eq (1). Note that the coefficients in the equation have been optimised to fit the experimental results.

$$H' = -0.23 - 0.35\sin(h_{ab} + 0.83) - 0.18\sin(2h_{ab} + 1.55) \qquad (1)$$

where h_{ab} : the CIELAB hue angle of a component colour.

Lightness

Lighter colours were found more likely to harmonise than darker colours. This was called the effect of *lightness sum* (L_{sum}). It was modelled by adding together the lightness values of component colours, as given below:

$$L_{sum} = L^*_{ab,1} + L^*_{ab,2} \qquad (2)$$

where $L^*_{ab,1}$ and $L^*_{ab,2}$ are the CIELAB lightness values of colour samples 1 and 2 in a pair.

As shown in Fig 2. (b), the larger the lightness sum, the higher the colour-harmony score tended to be given. Note that the effect of lightness sum is still significant when the other factors are not kept constant. This effect implies that people tend to feel pleasant when seeing lighter colour combinations.

In addition, the lightness difference between component colours was also found having some influences on colour harmony. A low colour-harmony score often occurred when the lightness difference was too small. This also occurred when the lightness difference was too large. A high colour-harmony score was obtained only if a colour pair had a moderate size of lightness difference, provided that the other colour-harmony factors were kept constant.

Chroma

The colours with similar chroma tended to harmonise than those with dissimilar chroma. This effect was exceptionally significant when the component colours had similar hues. This effect was called the *chromatic difference* (ΔC), which combines the effects of hue difference and chroma difference, as given in Eq. (3). Note that the coefficients in the equation have been optimised to fit the experimental results.

$$\Delta C = [\Delta H^{*2}_{ab} + (\Delta C^*_{ab}/1.46)^2]^{\frac{1}{2}} \qquad (3)$$

where ΔH^*_{ab} : the CIELAB hue difference between the component colours, and

ΔC^*_{ab} : the CIELAB chroma difference between the component colours.

The experimental results show that the smaller the chromatic difference, the higher the colour-harmony score would be given, as indicated in Fig 2 (c). This effect can be made by applying both 'equal-hue' and 'equal-chroma' principles at the same time.

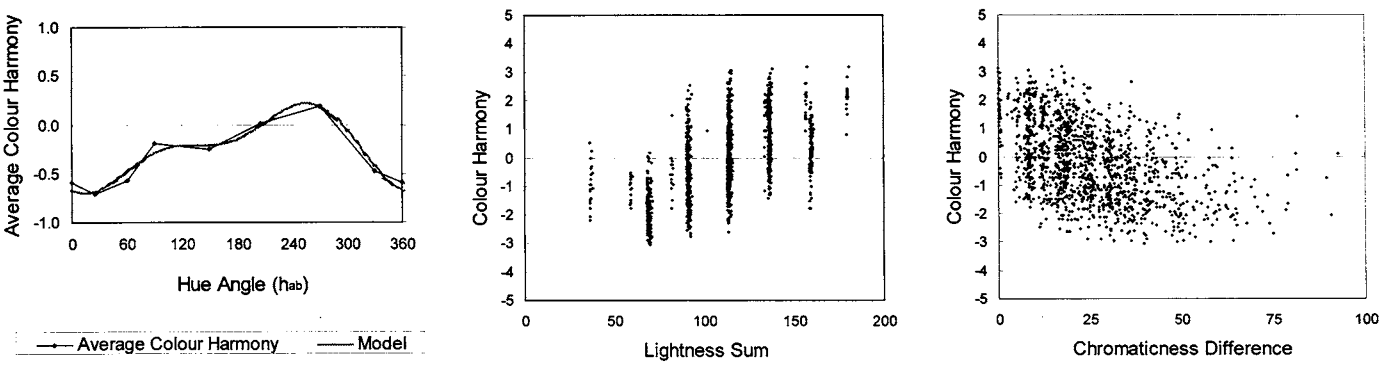

(a) *(b)* *(c)*

Fig 2. Three factors that affect colour harmony: (a) hue effect, (b) lightness sum, and (c) chromatic difference. The broken lines represent the best fitted lines to each factor.

SUMMARY

This study investigates the factors that affect colour harmony for two-colour combinations. A psychophysical experiment on a CRT display was carried out, in which 1431 colour pairs were assessed by 17 observers. The 1431 colour pairs were generated by 54 colour samples that consisted of 7 hues, 3 lightness levels, and 2 chroma levels.

Three colour-harmony factors were found, as given below:

(1) Hue effect. The colour pairs that contained bluish colours tended to have high colour-harmony scores. A low colour-harmony score often occurred on the colour pair that consisted of reddish colours. In addition, colours with neighbouring hues tended to harmonise.

(2) Lightness sum. The colours with high lightness values tended to harmonise rather than those with low lightness values.

(3) Chromatic difference. The colours with both similar chroma and similar hue tended to harmonise.

Note that the findings were obtained from a well-controlled experiment that was conducted on a CRT display at a dark room. In addition, the colour shape was fixed to square, and the background colour was kept to be medium grey throughout the experiment. Therefore, the findings may not necessarily be applicable to the conditions deviated much from those used in the current experiment. All the limitations in this study will be taken into consideration when planning the future work.

REFERENCES

1. Judd DB, Wyszecki G. Color in Business, Science and Industry. 3rd Ed. New York: John Wiley & Sons; 1975.
2. Burchett KE. Color harmony attribute. Color Research and Application 1991; 16: 275-278.
3. Burchett KE. Color harmony. Color Research and Application 2002; 27: 28-31

A Study on the Image of Colour—Shape Combinations

Wen-Yuan Lee and M. Ronnier Luo
Colour & Imaging Institute, University of Derby
Kingsway House, Kingsway
Derby, DE22 3HL, United Kingdom

ABSTRACT

This paper describes a study on the mental image affected by colour and shape. A psychophysical experiment was carried out to assess 36 samples in terms of 20 image scales by a panel of 17 subjects. All samples had three shapes (square, circle, and triangle) and 12 colours. The principal component technique was used to categorise these scales into different components. It was found that many scales were categorised in the first component and are almost the same for all three shapes. The scales in each of the 3 components based upon square samples agreed exactly with the previous study. This implies the data are highly repeatable. The results also show that the preferred colours are highly associated with clean, round, modern and cool images. The subjects prefer light green and blue circle colours with a high contrast with background.

Keywords: Image, Colorimetric values, CIELAB, Colour—Shape Combinations.

INTRODUCTION

It is intuitive for viewers to identify emotional feelings evoked by a colour. These emotional feelings are called colour emotions or colour meanings. This research is associated with *image* that is an emotional feeling or impression evoked by an object and is occurred in our mind like the mental analogue. It depends on cognitive function and occupies in between perception and intelligence [1]. Image can be conceptualised in different way: as a phenomenal experience, as an internal representation, as a stimulus attribute, and as a cognitive strategy [2]. Oxford dictionary describes image as *a mental representation of something (esp. a visible object), not by direct perception, but by memory or imagination, a mental picture or impression, an idea, or conception.* Objects include many appearance attributes such as colour, shape, texture, and gloss. However, earlier research [3-6] only focused on the impact of colour upon image and ignored the effect of shape and the other attributes. In fact, it is usually in the design world to consider colour and shape concurrently. This paper describes an experiment carried out to investigate the effect of image scales due to colour and shape.

EXPERIMENTAL

A psychophysical experiment was carried out to investigate the images affected by colour—shape combination. Three types of shape were used: square, circle, and triangle. The height of each sample was 10 cm, and was painted by 12 colours including the 11 basic colour terms (black, white, grey, red, green, yellow, blue, brown, pink, orange, and purple) proposed by Berlin and Kay [7] together with a cyan colour to give a good coverage of hue. Each colour was prepared to match to the colour coordinates of the basic colour according to the Lin *et al's study* [8]. These colours were measured by a GretagMacbeth CE-7000A spectrophotometer with the conditions of large aperture, and the inclusion of UV and specular component. Their CIELAB values are listed in Table 1 under D65 and CIE 1964 standard colorimetric observer. The colour difference, denoted as ΔE_B, was also calculated between the sample and the grey background to indicate the colour contrast. The CIELAB values in Table 1 were the average of 3 shapes for a particular colour. Each sample was assessed against a grey background with L* of 59 under a D65 simulator by a panel of 17 normal colour vision subjects (9 males and 8 females with an average age of 28 years old). They are the staff or students at the University of Derby. Each subject was asked to estimate a colour using a 7-category image scale (Table 2 showing an example of Active-Passive scale). All samples were assessed following a random order. Twenty mental image scales selected according to the studies of Osgood *et al* [9] and Ou *et al* [5]. In total, 12240 estimations were made, i.e. 20 scales x 3 shapes x 12 colours x 17 subjects.

For each sample in an image scale, the weighted mean was calculated from all subjects' estimates to represent the panel results for further analysis. For example, 2, 4, 8 and 3 subjects gave Categories 3, 4, 5 and 6 respectively (see Table 2). The weighted mean for this sample will be 4.7. There were 720 colour—shape combinations in total.

Table 1. The CIELAB values for the twelve colour samples and background

	L^*	a^*	b^*	C^*	h (°)	ΔE_B
Background	59.5	0.2	-1.9	1.9	276.0	0.0
White (W)	98.7	-0.3	1.3	1.4	105.0	39.3
Black (Bk)	29.9	-0.1	-0.6	0.6	254.9	29.6
Grey (Gy)	78.3	0.2	-1.0	1.0	278.7	18.9
Red (R)	47.8	50.2	31.0	59.0	31.7	60.9
Green (G)	56.1	-43.8	22.9	49.4	152.4	50.6
Yellow (Y)	84.1	8.9	85.1	85.6	84.0	90.8
Blue (Bl)	51.7	-4.8	-35.2	35.5	262.2	34.6
Brown (Br)	48.7	20.7	27.5	34.5	53.0	37.4
Pink (Pk)	75.2	31.8	7.7	32.8	13.6	36.6
Orange (O)	63.3	41.7	55.2	69.2	53.0	70.7
Purple (P)	47.7	30.0	-22.5	37.5	323.1	38.1
Cyan (C)	60.8	-39.2	-8.6	40.1	192.4	40.0

Table 2. A 7-category scale

	Very closely	Quite closely	Slightly	neutral	Slightly	Quite closely	Very closely	
Active	1	2	3	4	5	6	7	Passive

Table 3. Twenty pairs of mental image scales

No.		No.	
1	Active—Passive	11	Angular—Rounded
2	Heavy—Light	12	Hard—Soft
3	New—Old	13	Clean—Dirty
4	Masculine—Feminine	14	Beautiful—Ugly
5	Happy—Sad	15	Simple—Complex
6	Fresh—Stale	16	Full—Empty
7	Kind—Cruel	17	Strong—Weak
8	Large—Small	18	Serious—Humorous
9	Modern—Classical	19	Cool—Warm
10	Safe—Dangerous	20	Like—Dislike

IMAGING SCALES AFFECTED BY SHAPES

In order to find out the effect of image scales due to shape, the data were divided into 3 shapes (square, circle, and triangle). The principal component analysis was used to categorise these scales into different components. The results are summarised in Table 4 in terms of the 1st, 2nd or 3rd component numbered as 1, 2 or 3, respectively and the number in the bracket is the correlation coefficient between the image scale and component.

It can be seen in Table 4 that the scales categorised in the first component are the same for the three shapes studied except the inclusion of the large-small scale for the circle shape. It was also found that the image scales of the square samples exactly agreed with the results of Ou *et al* [5], who were also used the same shape. This indicates high repeatable experimental results in this type of study even with quite different groups of subjects. However, for the second and third components, the scales in circle and triangle shapes do not agree well with those in square shape. For the third component, there is a large difference between different shape groups, i.e. only Masculine-Feminine scale for circle shape, Masculine-Feminine and Angular-Rounded scales for triangle shape, and 4 scales (Warm-Cool, Safe-Dangerous, Simple-Complex and Angular-Rounded) for square shape.

Table 4. Principal components of mental image for the 3 shapes studied

Image scale	Square	Circle	Triangle
Fresh—Stale	1(0.98)	1(0.99)	1(0.98)
New—Old	1(096)	1(0.97)	1(0.96)
Beautiful—Ugly	1(0.94)	1(0.93)	1(0.95)
Happy—Sad	1(0.94)	1(0.97)	1(0.96)
Clean—Dirty	1(0.94)	1(0.95)	1(0.93)
Active—Passive	1(0.91)	1(0.92)	1(0.94)
Like—Dislike	1(0.90)	1(0.95)	1(0.96)
Modern—Classical	1(0.90)	1(0.96)	1(0.96)
Kind—Cruel	1(0.89)	1(0.86)	1(0.87)
Serious—Humorous	1(-0.76)	1(-0.67)	1(-0.80)
Strong—Weak	*2(0.94)*	*2(0.94)*	*2(0.72)*
Hard—Soft	*2(0.86)*	*2(0.76)*	**3(0.77)**
Full—Empty	*2(0.81)*	*2(0.86)*	*2(0.82)*
Heavy—Light	*2(0.80)*	*2(0.82)*	*2(-0.67)*
Masculine—Feminine	*2(0.62)*	**3(0.91)**	*3(0.7)*
Large—Small	*2(0.56)*	1(0.73)	*2(0.48)*
Cool—Warm	**3(0.88)**	*2(-0.66)*	*2(-0.84)*
Safe—Dangerous	**3(0.61)**	*2(-0.72)*	*2(-0.67)*
Simple—Complex	**3(0.54)**	*2(-0.69)*	*2(-0.71)*
Angular—Rounded	**3(-0.32)**	*2(0.37)*	**3(0.69)**

Note: the numbers are in italic and bold for the scales in the 2nd and 3rd components respectively.

In order to find out impact of shapes on scales, the average of the weighted mean for all the shades in a shape group was calculated and plotted in Figure 1. For a perfect agreement between three shapes, the three points in each scale should overlap. The results showed that only 4 scales had large discrepancies between shapes, i.e. Angular—Rounded, Large—Small, Hard—Soft, and Serious—Humorous. It is expected that the circle appears to be 'rounder' than the other two shapes. However, it is also found that the square is 'larger' than the other two shapes (even though the real areas of the three shapes are 100cm^2, 78.5cm^2 and 57.8cm^2 for the square, circle and triangle respectively calculated), and the circle is softer and more humour than the other two shapes.

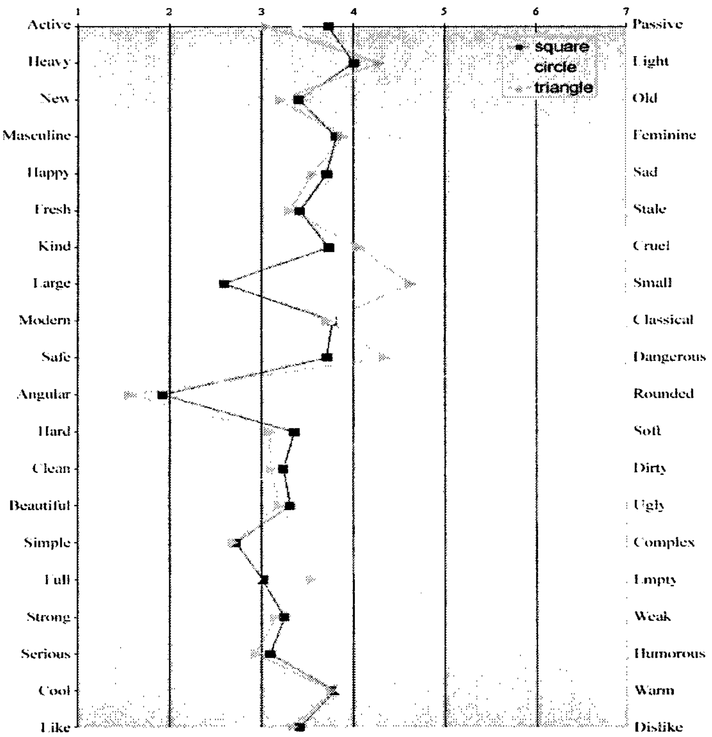

Figure 1. Mental image profiles amongst the three shapes studied

MODELLING THE LIKE-DISLIKE IMAGE SCALE

The Like-Dislike scale has been extensively studied. Some models were also developed based upon two approaches, one from the other image scales and the other from the colorimetric values. Both approaches are also used in this study. Firstly, coefficient of correlation *(r)* were calculated between the data of Like—Dislike and the other scales. It was found an *r* value of 0.963 between the Like-Dislike and Beautiful—Ugly scales. To include this scale to develop a preference model would make the other scales too insignificant. Therefore, this scale was excluded. A stepwise multiple regression analysis was performed to predict preference using the other scales except the Beautiful—Ugly. This results in a model as given in equation 1.

$$\underline{\textit{Like-Dislike}} = -0.365+0.388\,\underline{\textit{Modern-Classical}} + 0.154\,\underline{\textit{Cool-Warm}} - 0.066\,\underline{\textit{Angular-Rounded}} + 0.273\,\underline{\textit{Clean-Dirty}} + 0.247\,\underline{\textit{Kind-Cruel}} \qquad (1)$$

Equation 1 also shows that Like-Dislike scale is not strongly affected by the shape because only Angular—Rounded scale is associated with shape as found earlier.

The second approach to model the Like-Dislike scale was based on the colorimetric values as given in Table 1. Again, this was done by multiple regression analysis. Equation 2 shows the newly derived model.

$$\textit{Like-Dislike} = -7.081+0.02L^*-0.005a^* -0.03\,b^*+0.06\,\Delta E_B +0.52\,\textit{Circle} \qquad (2)$$

Equation 2 implies that a preferred colour is a light green or blue circle colour together with a high contrast against a background. It was also found that the three colorimetric parameters *(ΔE_B, L^* and b^*)* have equally high importance, followed by circle shape and a^* gives the smallest effect. When using equation 2, the term (circle) should be one and zero for the circle and the other samples respectively.

The performance of the image based (equation 1) and colorimetry based (equation 2) models are shown in Figures 2a and 2b respectively. Each figure shows the visual data plotted against the model's predictions. It can be seen that the both models accurately predicted the visual results with r of 0.91 and 0.96 respectively.

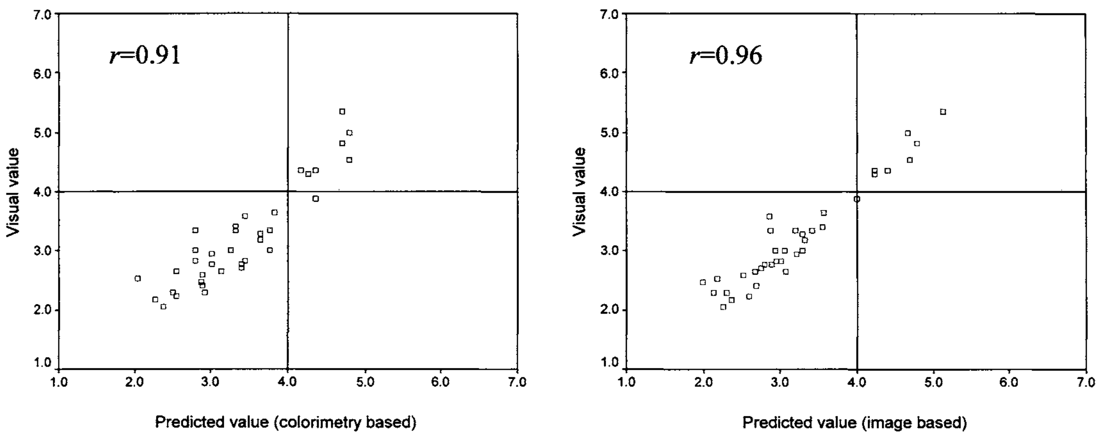

Figure 2. The visual data of Like-Dislike scale are plotted against those predicted by a) equation 1 and b) equation 2.

To use equation 1 requires the experimental data from the other four image scales. However, only colorimetric values are required for equation 2 so that equation 2 is easier than equation 1 for practical applications. However, individual colorimetric models can be derived for the four image scales included in equation 1.

CONCLUSION

This study investigates the image scales affected by 36 colour—shape combinations. A psychophysical experiment was carried out, in which each combination was assessed by 17 observers. Twenty image scales were evaluated. The major findings are given below.

- The image scales categorised in the first component are almost the same amongst the three shapes studied, but not for the other two components. The scales for the square in each component agree exactly with those obtained by Ou *et al.* This implies that the method employed here are highly repeatable.

- There are four image scales clearly influenced by shape, i.e. Angular—Rounded, Large—Small, Hard—Soft, and Serious—Humorous.
- Preferred colours have the tendency of clean, rounded, modern, cool and kind, in which Modern is the most important factor.
- Preferred colours also tend to have high lightness, high contrast with the background with green or blue hues and circle shape. The most important parameter on preference is high contrast.
- Two models based on image scale and colorimetry respectively were successfully developed. Both models can fit the visual data quite well.

REFERENCE

1. Mary Ann Spencer Pulaski. Understanding Piaget—An Introduction to Children`s Cognitive Development. 1980 NY: Harper & Row.
2. John T.E. Richardson. Imagery. 1999 Psychology Press Ltd.
3. Hogg J. Aprincipal Component Analysis of Semantic Differential Judgements of Single Colours and Colour Pairs. Journal of General Psychology 1969; 80:129-140.
4. Kobayashi S. The Aim and Method of Color Image Scale. Colour R&A 1981; 6:93-107.
5. Li-Chen Ou, M. Ronnier Luo, Andree Woodcock, Angela Wright. A Study of Colour Emotion and Colour Preference Part 1: Colour Emotions for single Colours. Submitted to Colour R&A 2003 000-000.
6. Wright B, Rainwater L. The Meaning of Colour. Journal of General Psychology 1962; 67:89-99.
7. Berlin, B. and Kay, P. Basic Colour Terms: Their Universality and Evolution. 1969. Berkeley and Los Angeles, University of California Press.
8. H. Lin, M. R. Luo, W. W. MacDonald, A. W. S. Tarrant. A Cross-Cultural Colour-Naming Study: Part II—Using a constrained Method. Colour R&A2001; 26:193-208.
9. Osgood CE, Suci GJ, Tannenbaum PH. The Measurement of Meaning. University of Illinois Press. 1957.

Goethe in Me (Goethe's Esthetic and Visual Impact on My Emotional Art)

Hee Sook Lee-Niinioja, Artist, Designer, Journalist

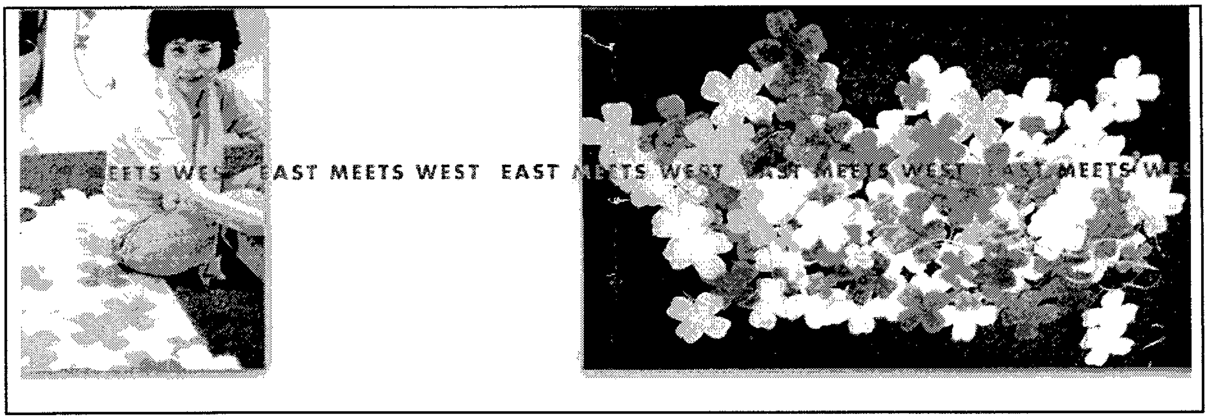

INTRODUCTION

According to the classification of arts, Hegel starts from the groundwork of the natural toward the spiritual and compares them to his symbolic, classical, and romantic theory series. (1) Architecture, in which the material is necessarily present, is for the symbolic. (2) Sculpture, which is a step towards ideality, is for the classical. (3) Painting, an art which represents life in form and color, is for the romantic, and is still further trained (4) in Music, the most subjective of the arts; and (5) in Poetry, the most universal and spiritual of them all. Hegel says that Goethe was one of most successful lyric poet because he could discover material for a song easily during his life.

Throughout histories, many philosophers have tried to identify the term 'esthetic and visual'. But, for me, they seem to be a kind of sublime expressions, such as purity, tranquility, translucence, and splendor, whose words have contributed tremendously to my emotional art. And, to fulfill these noble expressions, Goethe, a German poet, has had the greatest impact on me through his words, sounds, and colors since my youth.

In other words, Goethe possesses these three main elements which I have been pursuing for my art. The first element is his poetical words. His words put me into an action to set up esthetic and visual atmosphere around my emotion. The second one is his lyrical sounds. They can be originated from him directly, or indirectly from several composers who were influenced by his words. His sounds encourage me to execute a visualization of these selected words on the process of my art work. The last one is his symbolic colors. They affect me in the same way as sounds, consciously from him or unconsciously from different artists. His colors enforce me to fulfill these chosen words and sounds on my emotional art. Words, sounds and colors are an inseparable unity, but without passion and meditation between Goethe and me in a Gothic cathedral where the Divine Light blesses us, these three elements cannot affect my emotion perfectly.

As a matter of fact, many writers, composers, and artists had impressed me through their esthetic and visual expressions, for instance, Heine, Hesse, Mann (words), Beethoven, Mozart, Schubert (sounds), Turner, Matisse, Kandinsky (colors). However, all of them are also influenced by Goethe, as I mentioned above. That is my determination to attach to Goethe.

MY ENCOUNTER WITH GOETHE

Johann Wolfgang von Goethe is recognized as the greatest writer of the German culture during the Romantic period in the late eighteenth and early nineteenth centuries. Born in Frankfurt am Main in 1749, he studied in Strasbourg, where he found his identity as German. His meeting with Herder was of decisive importance for the preparation of his 'Sturm and Drang' movement with Schiller later. His poems were new standards for the genre in Germany, which later was set to music by Beethoven and Schubert. In 1775, Goethe was employed to the ducal court of Karl August in Saxe-Weimar. He achieved a knight title and made the small town of Weimar as a cultural center. He died in 1832.

Before my presentation of Goethe's words, sounds, and colors, for a better understanding of my emotional art, I am going to describe my general background in South Korea during the student life at universities. Two phenomena of groups existed. The one was intellectual and philosophical type who felt self as Faust, whom they learned from Goethe's "Faust". The other was sensitive and emotional youths who visualized themselves as Werther, whose origin was from Goethe's "The Sorrows of Young Werther". Whether they were either intellectual or emotionalist, they admired Goethe absolutely, and I was no exception.

Nevertheless, in parallel with this symptom, I believed that my real happiness could only be found through a man with whom I should share my life until my death. As I was tamed by the society, I searched for the man all around the world, while I had to struggle against cultural conflicts between the West and myself. I studied Christianity and became Christian.

Through this long and painful process for 20 years' wandering, I finally understood the meaning of life. Namely, it is to make others happy with talents which God has given to me. Besides, I also learned that my happiness had nothing to do with the man. It was my vanity and illusion.

Consequently, I re-established my talent of color and yearned for homage to God for this bliss. But the image of God was too abstract to illustrate for me, instead, I chose a human being who brought me in front of God. It was Goethe, once my idol, but forgotten. Surprisingly, Goethe was waiting for me in a Gothic cathedral with passion and meditation. Since then, through his esthetic and visual expressions, my emotional art was enabled to tribute to God and my viewers. It was my turning point into a new life.

GOETHE AND WORDS

I have allergy to words. On hearing a beautiful word, I feel my being transcended; on the other hand, bad words take me from my meaning to exist in this world. Words are both happiness and misery. With words, I can visualize all the experiences in an abstract form. Words of symbolical concept or natural phenomenon or spiritual existence add to my emotion more intensively.

For instance, an English phrase of "a splendor in the grass and glory of flower" was expressed by Wordsworth's "Ode". This phrase endows me pure heart and power to describe all the Nature around Wordsworth and me. So, it is an impact from Wordsworth's esthetic and visual expression into my emotional art. Moreover, whenever I accord myself with my German favorite phrase, Hesse's. "Das Jugend ist schö.n.' (The youth is beautiful), I sense splendid and my art works involve much stronger emotion.

However, nobody can compete with Goethe's words, particularly, his novel of "The Sorrows of Young Werther", which made sensation among the young generation in a whole Europe and brought suicide fever in the nineteenth century. Even, Napoleon read it seven times and took it to his battlefield. More I touch it, more I discover Goethe's esthetic and visual impressions on my emotional art.

It is a story that Werther traces in a series of letters the course of his love for Lotte, who is already engaged to a young official when he meets her. Misled by the warmth of her friendship but most of all by his own intense imagination, he gradually loses contact with the world around him (Lotte and Nature), and finally commits suicide. The event is between May 1771 and December 1772.

"A wondrous serenity has taken possession of all my soul, like the sweet spring mornings which I enjoy with all my heart. I am alone and I rejoice in my life in this region which is meant for such souls as mine. I am so happy, of best of friends, so immersed in a feeling of tranquil existence that my art suffers because of it. I could not draw now - not a single line, and I have never been a greater painter than in these moments. When the lovely valley breathes its mists around me and the high sun rests on the impenetrable darkness of my forest and only solitary rays of light steal into the inner sanctuary, and I then lie in the tall grass by the tumbling river and being closer to the earth, I find that thousand manifold grasses catch my eye." (10 May 1771)

"She liked towards heaven and then at me, I saw her eyes fill with tears, she laid her hand on mine and said: 'Klopstock'. I immediately recalled the splendid ode which was in her thoughts, and I sank into a torrent of feeling which she had poured out over me with this password. I could bear it no longer, I bent over her hand and kissed it, shedding the most blissful tears. And I liked into her eyes again - Oh noble man!" (16 June 1771)

Every time I read Goethe's these expressions, my spirit is immensely enhanced. It implies that Goethe's esthetic and visual impact on my emotional art is huge through his words.

GOETHE AND SOUNDS

Words need sounds for their transcendence. With sounds I can develop ideas of these selected words. Sounds encourage me to engage to my visual world. They are a mediator between words and colors. Sounds are both tranquilizer and agitator for my emotional art. They are a direct message to my esthetic experience. Like words, sounds are my other nourishment. Without sound, life is meaningless.

Though Goethe played piano, I would rather introduce a few of composers who got influenced by Goethe, such as Schubert, Beethoven, Brahms, and so on.

For instance, when I hear Schubert's 'Heidenröslein' (Wild rose) which was derived from Goethe's poem, not only I can suffer Goethe's painful mood from deserting his first woman, Friderike Brion, but also I can share my affection with Schubert, so that my emotional status became more powerful than just Goethe's words.

Beethoven's 'Egmond' was composed from Goethe's lyrical words. Beethoven explained that Goethe's poems attracted him because they harbored within a theme the 'secret of harmony.'

"Goethe's poems have great power over me, not only through their content, but also through their rhythm. This language, which seems designed by spirits for a higher order and which carries already the secret of harmony within itself, excites and exalts me to write music."

Brahms went further. To him, Goethe's poems were so perfect that no music could improve them. "They are so complete, music has nothing to add."

What Brahms and Beethoven sensed in Goethe's lyrics was precisely that inherent harmony of the "Sprachmusik" (Language-music) that Goethe's verses sound as if they were born with a melody inside them. Anybody who recites his poem can hear the inner melody. His verses are likely to compose of beautiful sound, gentle echoes reverberating between nature and the human soul, between the poet and the realm of ultimate peace.

However, the composer whose music came the nearest to Goethe's theoretical and practical ideals was Mozart. His music contains all the elements that fulfilled the poet's philosophical, scientific, and personal requirements of art. Goethe said about Mozart:

"A phenomenon like Mozart will always remain a miracle that cannot be explained. But how else can the divinity create miracles if not through extraordinary individuals whom we behold in awe and wonder but cannot grasp when they come."

Therefore, when I hear sounds of those composers, especially lyrical sounds from Goethe's poems, my mood pushes me into creativity. In other words, esthetic and visual impact of those composers on my emotional art is vast.

GOETHE AND COLORS

Colors fulfill my emotional art with those selected words and sounds. In colors, I am fully alive and am ready to tribute to God. By colors, I see my future. With colors, I can rebuild my identity. Colors are my last nourishment for my art work. Through colors, Goethe's esthetic and visual impact on my emotional art is at its zenith.

Despite my favorite violet color, impressive colors provide me with a positive esthetic approach to visualizing pictures, while expressive ones lead me to experiment my creativity. For example, when I see Matisse's colors, his vivid and designed-color, or when I am absorbed by Nolde's sun-setting red and Kandinsky's abstract yellow and blue, their influences on my emotion are beyond description. But behind them, there is Goethe, for these artists were also influenced by Goethe's "Color Theory".

Goethe's opposition with Newton's theory of color started with the classic Aristotelian notion of "cool" and "warm" colors (blues and reds). Blues represent a lightening of black; while reds do darkening of white. But his conception is expressed poetically: "colors are the deeds and sufferings of light." Though his theory was never recognized by physicists, his insight on the perception of color was powerful to scientist and public to a range of physical and psychological color-phenomena. Goethe argued that light was homogeneous, that it created color only when disturbed by darkness. The two extreme tonal hues of yellow and blue interacted by a process to form the third principal color, red (Purpur), named 'augmentation' (Steigerung).

Goethe demonstrated how color was specific, characteristic, and significant, unlike light: plus/minus, yellow/blue, action/negation, light/shadow, force/weakness, brightness/darkness, warmth/coldness, proximity/distance, repulsion/attraction, affinity with acids/affinity with alkalis. He also made a distinction between allegorical, symbolic and mystical color, where, - "the meaning of the sign must be first communicated to us before we know what it is to signify"- with a belief that colors had a direct effect on the mind and feelings.

It is well known that Turner was concerned with the interrelation of light and color and attempted to suit the scheme of three primary colors into the times of day: the red of dawn and sunset, and the yellow of morning. His instinct was to stress the polarities of light and dark and to arrange the scale of colors in a tonal order. What Turner's application of Goethe's polarities meant that he had a sense of the moral force of color.

Goethe's Theory also affected Gogh and Gauguin whose main concern was these 'moral harmonies' of color, and Matisse's after-image. Matisse's extraordinary sensitivity to psychological effect was mentioned by his experience when he saw the sun filtering through the design of leafage in the windows of Vence which were glazed with yellow, green and blue, but no red. So his experience was a negative after-image.

> "That effect of color has real power. So much power that, in certain lights, it seems to become a substance. Once when I found myself in the chapel, I saw on the ground a red of such materiality that I had the feeling that the color was not the effect of light falling through the window, but that it belonged to some substance. This impression was reinforced by a particular circumstance: on the floor in front of window there was some sand in a little pile that the red color was resting on. That gave the effect of a red power so magnificent that I have never seen the like in my life."

Nonetheless, the most interest in Goethe's principles was German Expressionist. Kandinsky's access to Goethe was through the theosophist Steiner, and he was describing a psychological drama from "On the Spiritual in Art", 1912.

So, when I face colors, especially musical colors from Goethe's Theory, my emotion is extremely stimulated. It means that esthetic and visual impact of artists on my emotional art is ultimate.

A GOTHIC CATHEDRAL

I expressed earlier that without passion and meditation between Goethe and me in a Gothic cathedral where Divine Light blesses us, these three elements of words, sounds and colors do not affect my emotion perfectly. In other terms, I have to encounter Goethe personally for our mutual communication. And if it happens in the Strasbourg Cathedral of which Goethe praised so highly, it could be the most impressive place. Whatsoever, from the beginning, both Goethe and I can be engaged with our thoughts, but when time flows, when purity, tranquility, translucence and splendor take place, we start to look for each other and become in unison by the blessing of God. Then, I am no longer myself. Goethe is with me in this given space. As soon as I feel Goethe is in me, I farewell to him in a hurry, in order to continue my solitary journey through his words, sounds, and colors. My emotion is boundless and my art is born.

EPILOGUE

The world of nature is one of constant renewal. As Goethe observed of plant life, everything is undergoing metamorphosis. Everything in the cosmos evolves in accordance with the Logo - the Divine Reason - which creates every moment, day after day and year after year from the creation until the end of time. All life and all nature follow this ever- continuing Reason.

And I know that I cannot avoid this procedure. In addition, I am aware that the meaning of life is to make others happy. So, at least on this earth, my life has three phases (an idea, its plan, and its realization). Goethe's words are my departure, his sounds are my transit, and his colors are my destination. By happen, if I were renewed in this earth, then who could I be? Once more, I am enforced to applause Goethe for his esthetic and visual impact on my emotional art.

Visualization of Color Combination of "Kasane," Japanese Ancient Court Costume

KOBAYASI, Mituo*,** and OKABE, Megumi*
*The University of Electro-Communications
**National Museum of Japanese History

Keywords : "kasane-irome", costume, color combination, visualization, software

1. INTRODUCTION

"Kasane" is a set of layered garments worn by the women in the aristocracy of Heian-era (794-1185) in Japan. Figure 1 illustrates a woman in "kasane" attire. The variations of the color combination of layered garments, called "kasane-irome", are one of the expressions of Japanese aesthetics. Color samples of "kasane-irome" made of dyed silk cloths have been published by researchers of Japanese traditional textiles.

Colorimetric measurements of such color samples were performed and the obtained data were compiled to publish a database of "Japanese traditional colors reproduced in dyed cloths" [1]. This database was already applied to analyze distinctive features of color combination in "kasane-irome"[2].

This time, from the above database, one of the most reliable data by S.Nagasaki [3] was referred to make a software system for multilateral visualization of "kasane-irome". The software leads to analytic comprehension and synthetic utilization of the structure of color combination in "kasane-irome". The paper first presents the structure of "kasane-irome", and then introduces our visualization system.

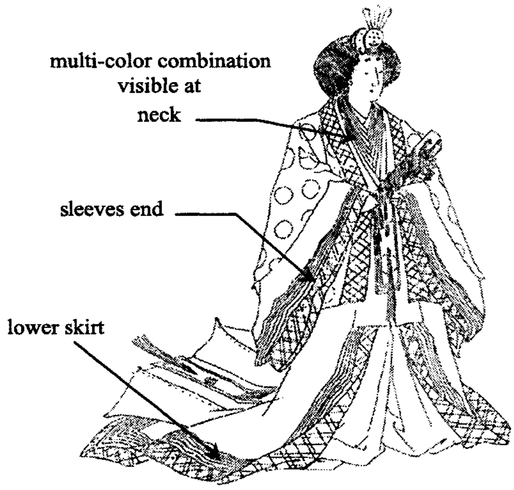

Figure 1. woman in "kasane" attire

2. STRUCTURE OF "KASANE-IROME"

2.1. Two types of "kasane-irome"

(a) Color combination of a robe (two-color or three-color combination)

One type of "kasane-irome" is a combination of two or three colors of a robe "Utiki". "Utiki" is made of two cloths, one for the right side and the other for the reverse side. The color of the reverse cloth appears as a thin line on the edge of the right cloth. Sometimes "Utiki" is made of three cloths to represent three-color combination on the edge of a robe.

(b) Color combination of layered garments (multi-color combination)

Another type of "kasane-irome" is a multi-color combination of layered garments, which is visible at neck, sleeves ends and lower skirt (Figure 1). The kind and the number of garments vary according to formal occasion or informal occasion. In the formal occasion, the garments consist of an undergarment "Hitoe", several inner robes "Utiki", an outer robe "Uwagi" and an outer jacket "Karaginu". In the informal occasion, they consist of a "Hitoe", several "Utiki", an "Uwagi" and an outer jacket "Koutiki". "Uwagi", "Karaginu" and "Koutiki" are made of two or three cloths like "Utiki". "Hitoe", unlike the other robes, is made of only one cloth. As the number of "Utiki" is mostly five, a set of "Utiki" is called "Itutuginu" meaning five robes. The number of "Utiki" might change according to the season. Especially the garments in summer consist of three robes, an "Utiki", an outer robe and an outer jacket. Table 1 shows typical examples of color combination in "kasane-irome".

---

* The University of Electro-Communications, 1-5-1 Chofugaoka, Chofu-shi, Tokyo 182-8585, JAPAN.
** National Museum of Japanese History, 117 Jônai-chô, Sakura-shi, Chiba 285-8502, JAPAN.

Table 1. examples of color combination in "kasane-irome"

(a) two-color combination of a robe: "Kôbai"(an apricot flower)

side	color
right side	purplish pink
reverse side	purplish red

(b) three-color combination of a robe: "Yukinosita"(an apricot flower under snow)

side	color
right side	white
in between	purplish pink
reverse side	purplish red

(c) multi-color combination of garments: "Kôbai-Nioi"(gradation of purplish pink)

Abr.	name of robe	two-color combinations		
		name	color of right side	color of reverse side
k	Koutiki(outer jacket)	"Ebizome"	deep purplish red	strong greenish blue
u	Uwagi(outer robe)	"Moegi"	spring green	spring green
i1	Itutuginu(inner robe)	"Kôbai"(deep)	deep purplish pink	deep purplish red
i2	Itutuginu	"Kôbai"	purplish pink	purplish red
i3	Itutuginu	"Kôbai"	purplish pink	purplish red
i4	Itutuginu	"Kôbai"(light)	light purplish pink	light purplish red
i5	Itutuginu	"Kôbai"(pale)	pale purplish pink	pale purplish red
h	Hitoe(undergarment)	——	deep purplish red	

2.2. Several attributes of "kasane-irome"

(1) Name of a color combination and name of a color

As a color is identified by its color name, a color combination of garments and a color combination of a robe are identified by their name. These names come from flower, plant, natural phenomena, and so on. Some names of color combination of garments often contain a word indicating the type of the color combination (Table 2).

Table 2. word indicating the type of a color combination

word	meaning
"Nioi"	gradation
"Usuyô"	gradation to white
"Murago"	variation of depth of a color
"Iroiro"	variety of colors

(2) Season

A certain "kasane-irome" is considered to be appropriate for a particular season. For example, a color combination name of a robe "Kôbai" shown in Table 2(a) is used in spring, while "Ebizome" and "Moegi" are used through all seasons. A color combination name of layered garments "Kôbai-nioi" shown in Table 2(c) is used in spring too.

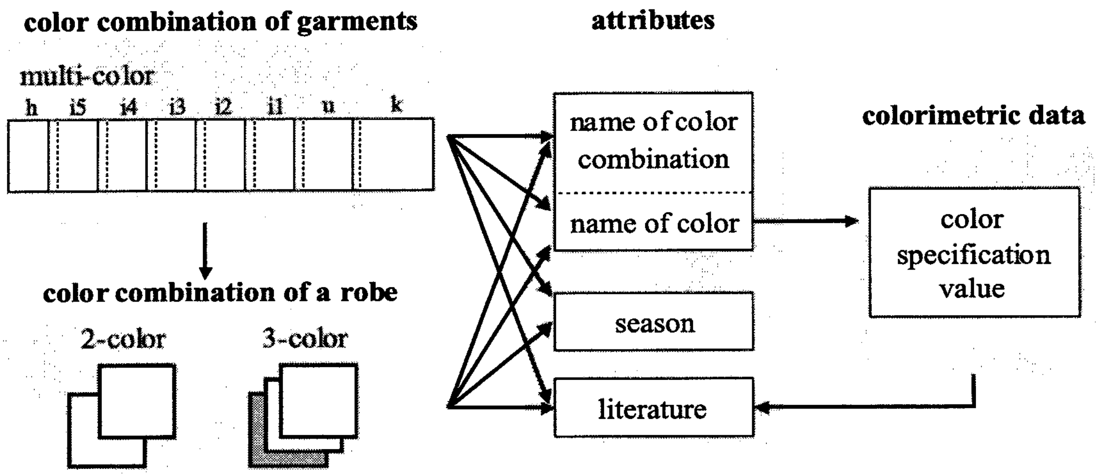

Figure 2. data structure of "kasane-irome"(a → b means "a refers b")

(3) Literature

Variations of "kasane-irome" are described and preserved in several literature in terms of color names or color combination names. One "kasane-irome" may have several color combinations depending on its sources.

2.3. Data structure of "kasane-irome"

Summarizing the above description we can illustrate the whole data structure of "kasane-irome" in Figure 2.

3. VISUALIZATION SYSTEM

Based on the above data structure, a visualization system of color combinations in "kasane-irome" was designed and implemented in an environment with operating system "Windows". For simplicity, design and texture (gloss, transparency, etc.) were disregarded.

3.1. Visualization mode

Several modes of visualization are available in the system.

(1) Simplified representation by means of color chips

Two-color or three-color combination of a robe can be visualized in the form of layered rectangle color chips. Multi-color combination of garments can be visualized in the form of a color-bar. See Figure 3.

(2) Simplified illustration of a robe or layered garments

The color combination of "ksane-irome" appears on the edges (Figure 4).

(3) Illustration of a woman in "kasane" attire

There are several variations: a standing form, a sitting form, a front side, a back side, etc. See Figure 1 and Figure 7.

(4) Illustration of women in "kasane" attire in a scene

We can use a copy of historical art works illustrating women in "kasane". Figure 5 is an example, a scene in spring of four women in the court. The type of color combination of women should match the season of the scene. This is a copy of one scene from the picture scroll of "Genji" tales, one of the most famous stories in Heian-era.

(5) Visualization of a color combination in several color spaces

A color combination of "kasane-irome" can be visualized in several color spaces: NCS, Munsell, CIELAB, CIELUV, and so on. According to user's request the 3D color space can be rotated and can be projected to a 2D plane (Figure 6).

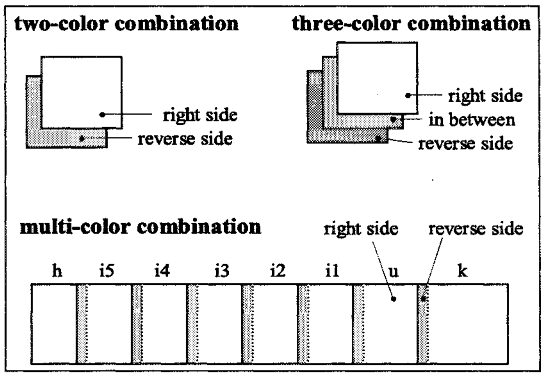

Figure 3. representation by color chips

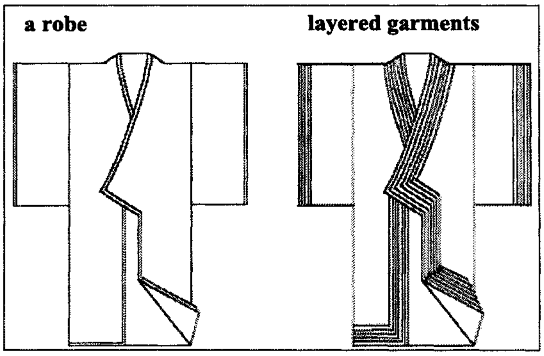

Figure 4. simplified illustration of a robe or layered garments

Figure 5. picture scroll of "Genji" tales

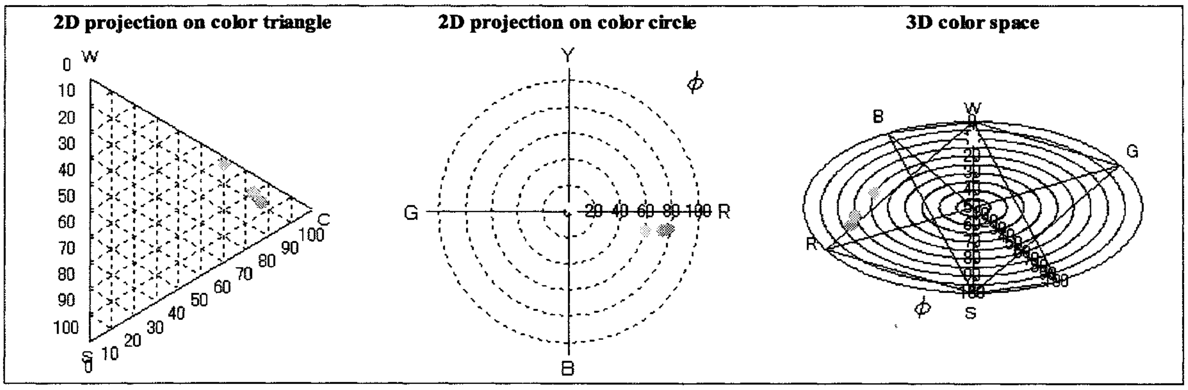

Figure 6. a color distribution of "kasane" in NCS color space

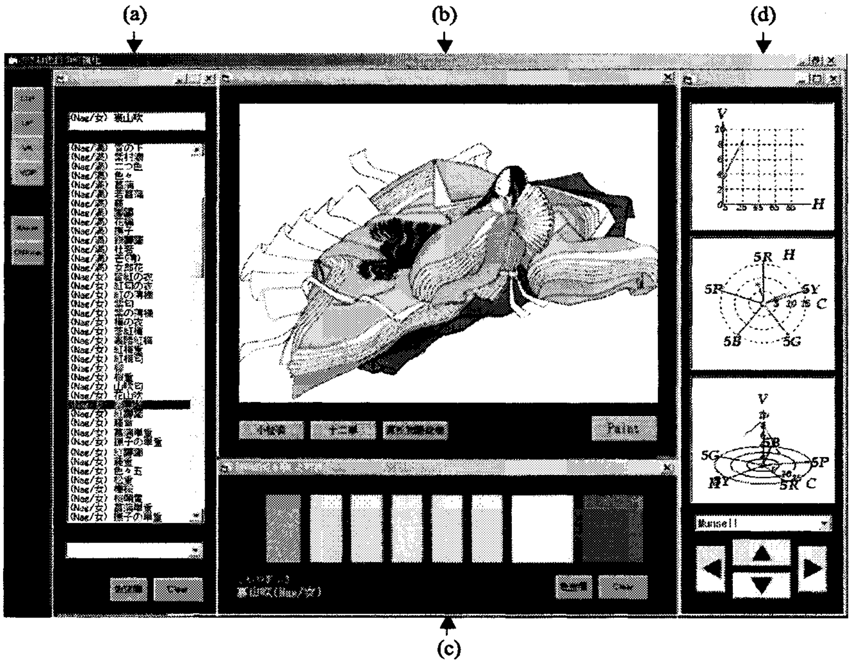

Figure 7. an example of execution on a display

3.2. Example of execution of the system

Figure 7 is a typical image of execution on a display. The left side window (a) shows a list of names of "kasane-irome". From this list we can search and select the desired "kasane-irome" to visualize it in the center window (b). The window (b) displays the illustration of mode 3 in section 3.1. The window (c) under the center window (b) includes a color bar expressing the color combination of "kasane" in the window (b). We can see a color combination in an arbitrary color space in the window (d). In the present case the color space Munsell is selected. If we press the button with a triangle sign, we can rotate the color space.

As the system allows us to edit the data-set of "kasane-irome", we can change a color or change a color combination to make our own "kasane-irome".

4. CONCLUSION

A software for visualization of a splendid color combination system "kasane-irome" in Japanese ancient time was devised. This software is applicable to simulate historical color combinations described in a literature, which have never been realized by real cloths. It will be useful not only for research but also for education. Further possibilities of this system are production of a new color design based on "kasane-irome", and utilization for restoration of ancient art works.

ACKNOWLEDGEMENT

Our thanks to Mr.SAWADA Kazuto(National Museum of Japanese History) and Ms.TAKAHASHI Minori(The University of Electro-Communications) for helpful discussion in advancing the study, and to Mr.TAKAHASHI Ryo(The University of Electro-Communications) for advice on programming.

REFERENCES

1. KOBAYASI Mituo and SUZUKI Takuzi : Database for Japanese Traditional Colors Reproduced in Dyed Cloths. Bulletin of the National Museum of Japanese History (to be published in 2003, in Japanese).
2. KOBAYASI Mituo, TAKAHASI Minori, and SUZUKI Takuzi : A Computational Analysis of Color Combination in "Kasane-Irome", Japanese Ancient Court Costume. Proceedings of AIC Color 2001 SI, Color & Textiles, pp.134-141, Maribor, Slovenia, 2002.
3. NAGASAKI Seiki: A study on Color Combination in "Kasane-Irome". Kyoto-shoin, 1987 (in Japanese).

Thai and Japanese Colour Emotion Words and their Comparison

Pontawee Pungrassamee, Aran Hansuebsai, O.Promsaka Na Sakolnakorn,
Tetsuya Sato*, Taeko Nakamura**
Chulalongkorn University, *Kyoto Institute of Technology, **Nara Saho College

1. Introduction

Colour gives us various emotions and impressions. It is very important to know the characteristics of colour emotion words which are expressed the emotions. Because emotion words are the output of colour cognition in our brain. Emotion induced by colour can be expressed by various emotion words and each emotion word is connected with an area of a colour space usually. In general, a word is not corresponding to only a word in a foreign language, but also a few or several words. Therefore, understanding the colour emotion phenomena and cross-cultural comparison of colour emotion have been the important topics of colour research.

On the other hand, many colour users are seeking some contribution of a colour emotion research to solve their communication problems. Going to 'globalization', it will be more important to know more objectively about meanings of emotion words and the differences of the meanings between different languages.

In this study, we tried to know the relationship between colours and emotion words in Thailand and Japan. Especially, the frequency categorising was conducted to find out the contribution of emotion words for a given colour and vice versa. With the results obtained by the frequency categorising, Thai and Japanese results were also compared.

2. Experiment

2-1. Colour sample

A set of dyed polyester colour samples were used to carry out visual assessments. The colour samples were generated using the SCODTDIC PLUS 2000 polyester system manufactured by Kensaikan Co. Ltd. The samples were rectangular (1.5cm x 1.2cm) and colours were chosen from all over colour space, selected by the hue-tone dividing method[1,2] that allowed colour space to be split along the lines of appearance attributes. A total of 212 colour samples were used in the study. Colour tone and tone number used in this study shows in Table 1. For example, '5GY3' means that the colour has 5GY Munsell hue and light greyish tone.

Table 1 Colour tone and tone number used in this study

Tone No.	Colour tone
1	pale greyish
2	pale
3	light greyish
4	light moderate
5	light
6	greyish
7	moderate
8	bright
9	dark greyish
10	dark
11	deep
12	strong
13	vivid

2-2. Visual assessment

In order to know relationship between colour emotion words and real colours, 2 kinds of visual assessments were carried out in both of Thailand and Japan. One was to choose colour samples reminded from emotion words (Experiment A). Another was to choose emotional words reminded from sample colours (Experiment B). The emotion words used in this study have been gathered in previous studies[3-5] already. The numbers of the words gathered in Thailand and Japan were 69 and 151, respectively. The visual assessments were carried out under D65 light condition with a viewing cabinet in Thailand and under a north facing window in Japan. Each sample was covered with a light grey surround to provide uniform surround viewing conditions. 30 Thai observers, who use colours such as dressmakers, graphic designers and architectures, were asked as observers to choose plural colours or emotion words in the experiments. 34 and 43 Japanese female students were respectively asked to choose only one colour and an emotion word in the experiments A and B.

3. Result

3-1. Colour reminded from word (Experiment A)

Each emotion word was connected with an area of a colour space. The connected colour areas were various. Roughly speaking, the influence of colour tone in Thai results was larger than that in Japanese results, and the influence of hue in Thai results was smaller than that in Japanese results.

An example of the influences is given in Table 2. In English-Thai and English-Japanese dictionaries, the emotion words corresponding to *warm* and *cool* in English were *ron* and *yen* in Thai, *atatakai* and *tsumetai* in Japanese. Colour reminded from Thai *ron* was vivid red, and colour reminded from Japanese *atatakai* was vivid yellowish red. Thai *ron* and Japanese *atatakai* colours were not the same, but similar. Thai *yen* colour was pale tone colour, and it did not have so much hue influence. But Japanese *tsumetaii* colour was blue, and it had hue influence.

By the way, we need to pay attention about that this paper is written in English. We can not correctly explain in English about the meanings of Thai and Japanese emotion words, because a word in Thai or Japanese is not completely the same to a word in English.

Table 2 Colours reminded from emotion words translated as warm and cool in English

warm (English)				*cool* (English)			
Thailand		Japan		Thailand		Japan	
ron (Thai)		*atatakai* (Japanese)		*yen* (Thai)		*tsumetai* (Japanese)	
Colour	Frequency	Colour	Frequency	Colour	Frequency	Colour	Frequency
5R12	22	10R12	9	10R2	23	5PB12	6
10R12	19	5R12	6	10BG2	22	10B5	4
10RP12	17	10R8	5	10Y2	20	5PB11	3
		10R5	5	5B2	20	5B4	2
		5YR8	3	10B2	19	10B8	2
		5YR11	3	10RP2	18	10B10	2
				5GY2	17	5PB5	2
				10GY2	17	5PB8	2
				5BG2	17	5PB10	2
				5Y2	16		

In this study, one of the most popular emotion words reminded from colours by Thai observers was *sod*. Table 3 shows the colour samples reminded from *sod* and from *fresh-na* in Japanese, which were translated from *fresh* in English. The remarkable point is that *sod* was connected with bright tone colour in almost all hue. This means that *sod* depends on tone but not on hue. On the other hand, *fresh-na* in Japanese was connected with vivid yellow green colours. This means that *fresh-na* depends on hue. Only two colours, bright yellow colour 10Y8 and bright blue colour 5PB8, were chosen by both of Thai and Japanese observers as *sod* or *fresh-na* colour.

Table 3 Colous reminded from sod in Thai and fresh-na in Japanese

fresh (English)			
Thailand		Japan	
sod (Thai)		*fresh-na* (Japanese)	
Colour	Frequency	Colour	Frequency
5RP8	27	5GY8	4
10YR8	26	10GY11	2
10Y8	26	5GY11	2
10RP12	26	5GY12	2
5R12	24	10G11	2
10B8	24	5PB8	2
10PB8	24	10Y5	2
10R12	23	10Y8	2
5PB8	22		
5P8	22		
5BG7	21		
10R8	20		

3-2. Word reminded from colour (Experiment B)

The influence of tone in Thai results was larger than that in Japanese results, and the influence of hue in Thai results was smaller than that in Japanese results, as well as the case of the experiment A.

An example of the influences is given in Table 4. For bright tone colours 5YR8 and 10B8, which are located at hue opposite coordinates in a colour space, Thai observers chose *sod* translated as *fresh* in English. But Japanese observers did not choose the same word for the two colours. In addition, Thai and Japanese observers chose similar words translated as *fresh* and *clear* in English for 10B8. This similarity between Thai and Japanese results was not found out only in the assessments for many colour samples in this experiment B, and also for many emotion words in the experiment A.

Comparing the results of experiment A with those of experiment B, the relationships between colours and emotion words were not the same in all comparisons. Table 5 shows as an example of discrepancy. 5R12 and 10R2 are the warmest and coolest colours in Thai results. But Thai observers did not reminded Thai *warm*

Table 4 Emotion words reminded from 5YR8 and 10B8

Colour	Thailand			Japan		
	Thai	English	Frequency	Japanese	English	Frequency
5YR8	*sod*	fresh	18	*azayakana*	vivid/bright	4
	paed	gaudy	16	*youkina*	cheerful	4
				genkina	spirited/cheerful	3
				akarui	light/bright	3
10B8	*sod*	fresh	20	*sawayakana*	fresh/cool	3
	sai	clear	20	*seiryouna*	clear	3
				sugasugashii	fresh/cool	3
				clear-na	clear	3

Table 5 Emotion words reminded from warm and cool colours

Colour	Thailand			Colour	Japan		
	Thai	English	Frequency		Japanese	English	Frequency
5R12	*sawang*	light	13	10R12	*azayakana*	vivid	3
					mabushii	dazzling/glaring	3
					atatakai	warm	2
10R2	*nual*	creamy	17	5PB12	*azayakana*	vivid	7
	sai	clear	16		*shizenna*	natural	4
	sawang	light	15		*sugasugashii*	fresh/cool	3
					sukkirishita	neat/pat	3
					spoty-na	sporty	3

and *cool* words, *ron* and *yen*, from the two colours. 10R12 and 5PB12 are the warmest and coolest colours in Japanese results. Japanese observers reminded Japanese *warm* and *cool* words, *atatakai* and *sugasugashii* (similar to *tsumetai*), from the two colours.

4. Summary

We tried to know the relationship between colours and emotional words and to compare the experimental results obtained in Thailand and Japan. Consequently, we had some information in the relationships, and we also found out some similarities and discrepancies between the Thai and Japanese assessments.

The obtained results will contribute to the standardisation for Thai and Japanese emotion words. In addition, the emotion word tables and/or diagrams, which are put emotion words onto a colour space through the obtained results, will serve as guidelines for the quantitative analysis of colour communication, particularly for cross culture comparison.

But, as experimental conditions carried out in Thailand and Japan were a little different, we can not come to a conclusion if our results are correct. Therefore, we need to carry out more experiments with same conditions in Thailand and Japan, and same experiment in a country using English.

Reference

1. Kazushige Teraji, Omoshiroi Iro no Hanashi (*in Japanese*), Nikkan Kogyo Shinbun-sha, p.146 (1991)
2. T Sato and K Teraji, Study on the Dividing of Iso-hue Plane from the Standpoint of Color Appearance (*in Japanese*), Journal of the Color Science Association of Japan, Vol.13, p.60 (1989)
3. Pontawee Pungrassamee, Aran Hansuebsai, O.Promsakha-na-Sakonnakorn, Tetsuya Sato, Taeko Nakamura, The Arrangement of Thai Color Emotion Words into Color Spaces, Proceedings of the International Conference on Colour Emotion Research and Application, Bangkok Thailand, p.24 (2002, 7)
4. Taeko Nakamura, Tetsuya Sato, Kazushige Teraji, Tamotsu Fukuda, Arrangement of Color Image Words into the Non-Luminous Object Color Space (*in Japanese*), Journal of the Color Science Association of Japan, Vol.18, p.10, (1994)
5. Iro no Imeiji Jiten (*in Japanese*), Nihon Ryukoshoku Kyokai, p.181 (1991)

Colour as Perception: Reflection on a Magritte Painting

Danthong Breen
Mahanakorn University of Technology, Thailand

"The Palace Curtains" is one of the simplest compositions of the Surrealist painter, Rene Magritte. It treats of the most basic aspect of colour; that while light is a physical entity, colour is a perception.

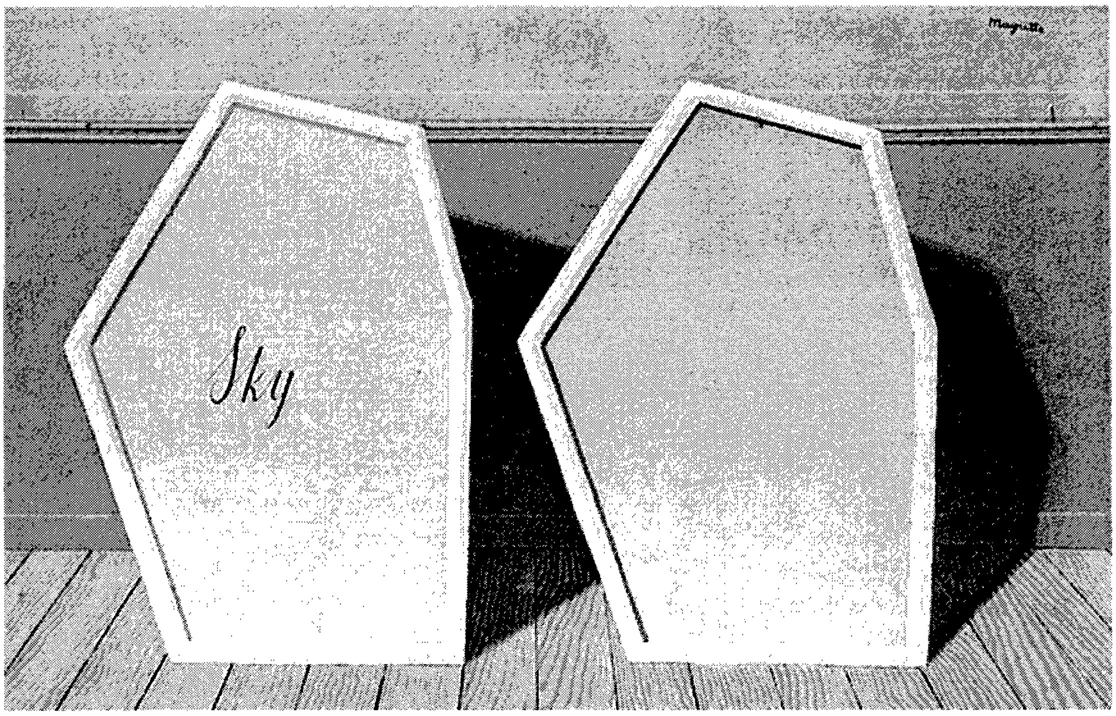

Figure 1. The Palace of Curtains

One may analyze the composition into four elements, as follows:

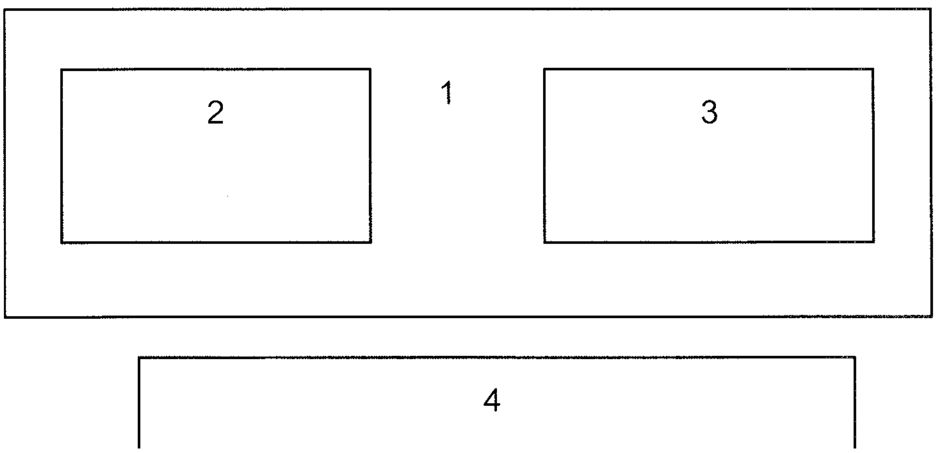

1. **Background**: Two framed panels are shown in a background of muted brown colours. The panels rest on floorboards against a paneled wall. The drawing is meticulous and completely realistic to emphasize the ordinariness of the setting. Brown is the least assertive of colours and draws little attention to itself. This background is a device portraying the content as the statement of an artist. By presenting a picture within a picture the artist informs viewers that they are viewing an artifact, an artistic statement.
2. **To the left of the composition** a polygonal frame encloses the word "Sky" written in what has been called "convent" script, on a plain background. The script implies didactic purpose. This panel is a painting of the word 'Sky'.
3. **A similarly shaped** frame encloses a pale blue colour without variation. In another picture bearing the same title, the blue panel has traces of white cloud. This panel is a painting of blue.
4. **Title** "The Palace of Curtains". The titles of Magritte's paintings are enigmatic. They were chosen by friends at gatherings to select names for new paintings. Suggestions and proposals were discussed until the appropriate name emerged to the agreement of all.

Magritte's painting is completely realist, each element executed with a draughtman's precision.

Mystery arises from an unusual juxtaposition of elements.

Begin by noting the aspect of the two frames which are similar but not identical. They contrast with the static Cartesian background, the polygonal shapes suggesting movement. The two frames incline to the left, one following the other in a slow tango. Their shadows highlight a differing distance from the back wall, enhancing a dynamic effect. Shadows within the frames themselves draw attention to their art work content.

It is the differing content of the frames which challenges thought

. **What is the relationship between sky blue and the word Sky?**

This is the wrong question. The format of paintings within a painting would have us ask **What is the relationship between our perception of a painted blue and a painted word Sky?**

Magritte raises issues identified by Foucault as the ruling principles of Western painting; the relationship between plastic representation and linguistic reference; what is the relationship between a painting of sky blue and a painting of the word Sky? (1)

It is said that a picture is worth a thousand words. This is not so. A picture is irreplaceable by words. One could discourse on "The Palace of Curtains" in many thousand words and draw no nearer to Magritte's mystery. Of course the mind must ponder the mystery and one may clarify what Magritte is about from others of his paintings.

It is said that a picture is worth a thousand words. This is not so. A picture is irreplaceable by words. One could discourse on "The Palace of Curtains" in many thousand words and draw no nearer to Magritte's mystery. Of course the mind must ponder the mystery and one may clarify what Magritte is about from others of his paintings.

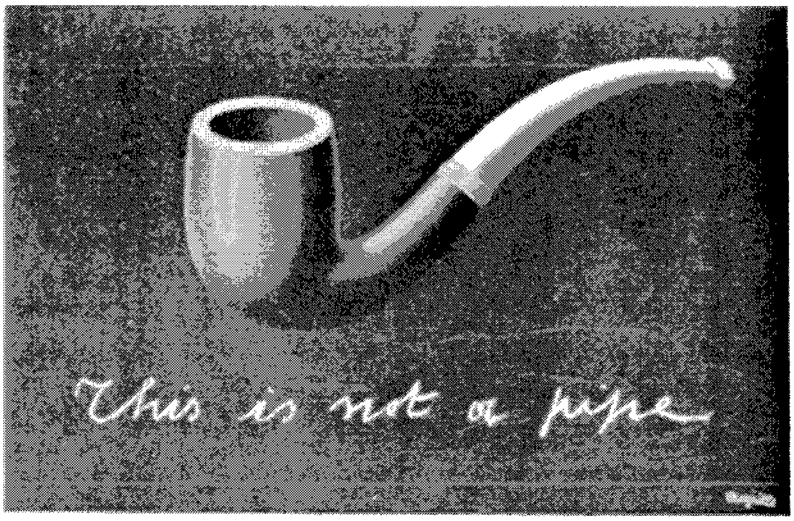

Figure 2. **The Treason of the Pictures**

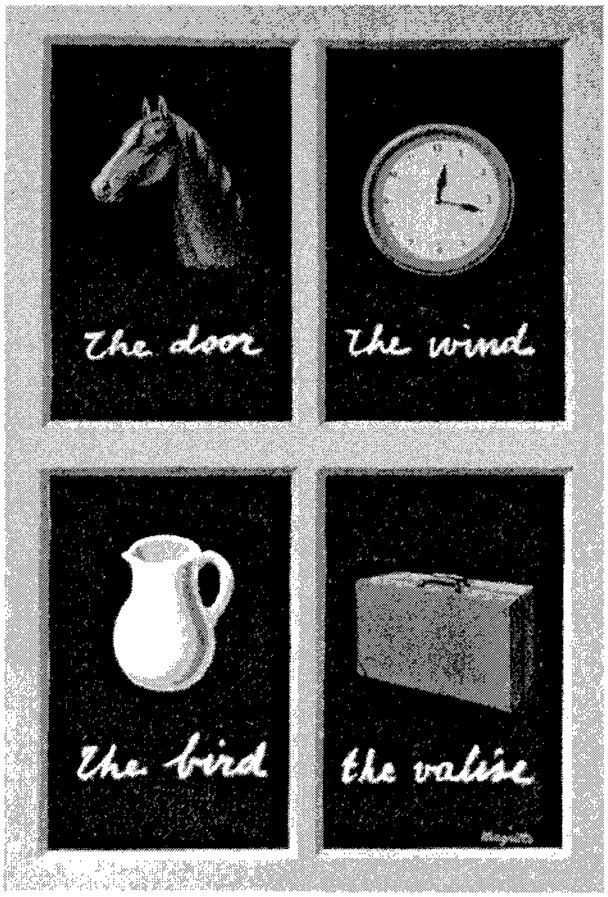

Figure 3..**The Key to Dreams**

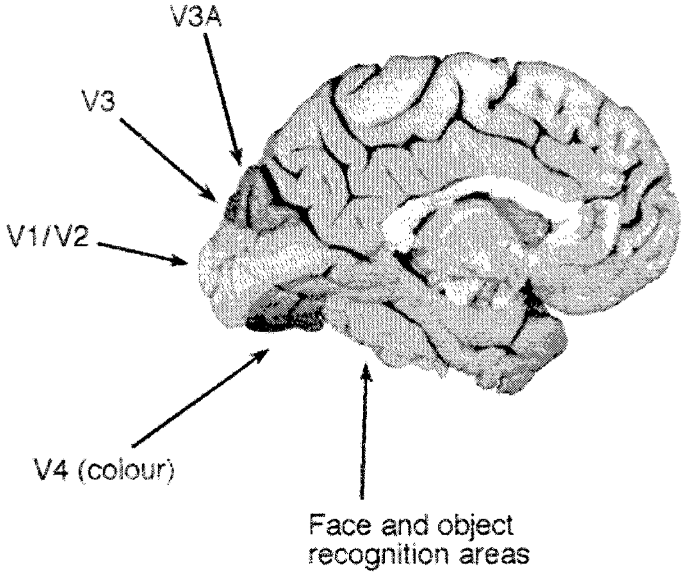

Figure 4. **Activated areas in the cerebral cortex**

We may also consult recent findings of neurophysiology locating areas of the human cortex where colour (sky blue) is perceived and object recognition (Sky) is achieved.

Perhaps both panels excite both areas equally. Or not.

Return to Magritte's image. Our eye follows the dance from blue to Sky and back. That this exercise enlightens us more than discourse may be a result of our evolution: "The reason is perhaps to be found in the greater perfection of the visual system, which has evolved over many more millions of years than the linguistic system, it is able to detect a great deal more in a fraction of a second……. By contrast, language is a relatively recent evolutionary acquisition, and it has yet to catch up with and match the visual system in its capacity to extract essentials so efficiently." (2)

Or perhaps colour and word are different. Just as artists knew the realities of colour long before the physics and the physiology of colour perception were expressed , so Magritte's picture suggests the reality of colour perception which cannot now, and may never, be stated in words..

"In a painting, words are of the same cloth as images. Rather one sees images and words differently in a painting" (Magritte quoted by Foucoult.) (3)

Finally the title: Palace of Curtains. The titles of Magritte appear to be clues of a cryptic crossword. But like his pictures they are clues having no verbal solution. The titles are "verbal lightening flashes" that streak and shatter the drawings. The curtains of Magritte do not hide reality but reveal it as the curtains drawn in a theatre reveal the stage. The angled edges of the frames symbolize curtains, revealing sky blue and Sky.

"The World is Full of Curtains" Magritte.

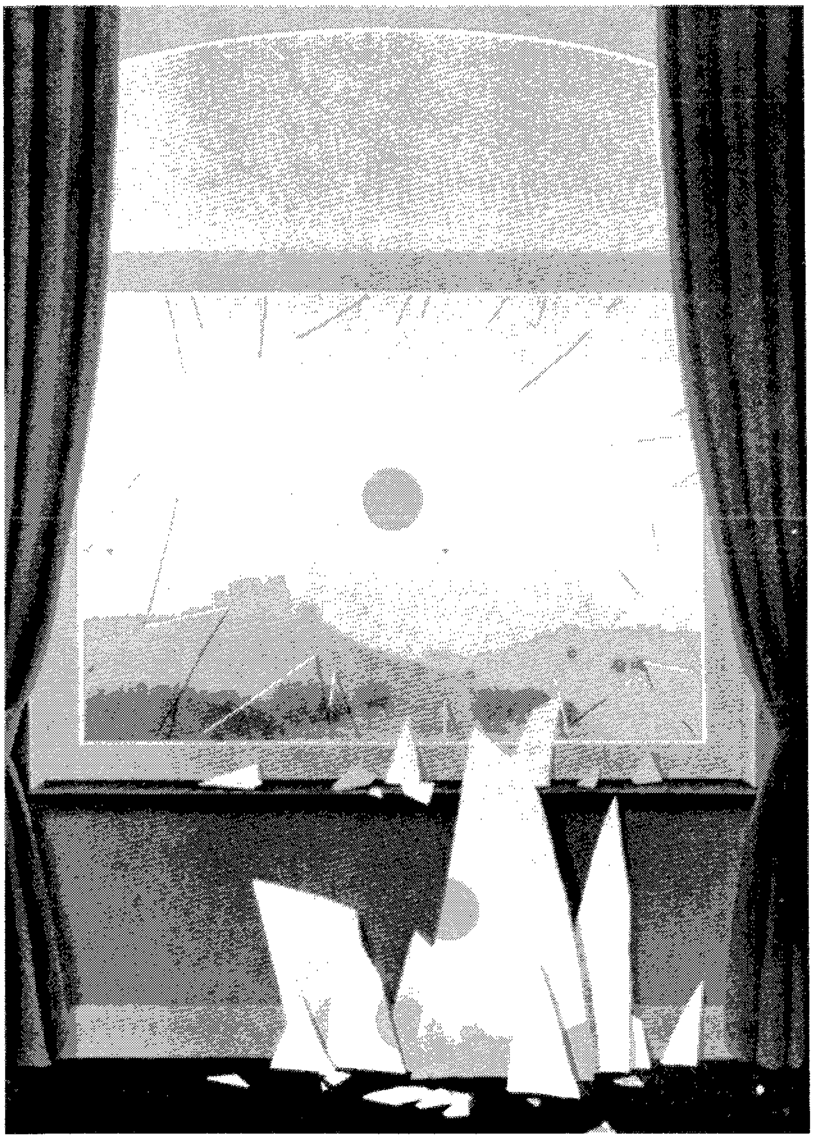

Figure 5. **Evening Falls**

References

(1) Foucault, Michel: "This is not a pipe", 1983, University of California Press

(2) Zeki, Semir: "Inner Vision" , 1999, Oxford University Press

Renormalization of Color Mechanisms Across the Life Span

John S. Werner,[1] Peter Delahunt,[1] Lei Ma[1] and Michael A. Webster[2]

[1]Departments of Ophthalmology, and Neurobiology, Physiology & Behavior, University of California, Davis
[2]Department of Psychology, University of Nevada, Reno

ABSTRACT

Throughout the life span, there is reduction in retinal illuminance, particularly at short wavelengths. Concurrently, there is a reduction in sensitivity of the photoreceptors and numerous morphological changes in the visual pathways. As a result, there is a great deal of age-related change in the retinal stimulus and the signals leaving the retina for perceptual analysis. Nevertheless, we have found that there is a remarkable degree of stability in color perception across the life span. Color naming of broad-band reflective samples, the wavelengths of unique blue and yellow, saturation and the achromatic locus are all relatively invariant with normal aging. Stability of color perception despite many changes in the retinal stimulus implies that the visual system continuously renormalizes itself to maintain constancy of perception. Thus, an elderly person may call the same stimulus "white" as he or she did 70 years ago, even though it must be based upon a markedly different retinal stimulus and mechanism sensitivities. To characterize the renormalization implicit in these findings, we measured the chromaticity of the achromatic point before and after cataract surgery. There was a shift following cataract surgery (removal of a brunescent lens) that was initially toward yellow in color space, but over the course of months, it drifted back in the direction of the achromatic point before surgery. This long-term renormalization is as it should be; otherwise, the white of the young would be the yellow of the old. Such adjustments may occur by calibrating the average responses in color mechanisms according to the average color in scenes (similar to the processes of von Kries adaptation) and the consequent changes in white may be particularly useful as an internal reference for color constancy.

1. INTRODUCTION

What are the consequences for the average 70-year old who, compared to the average 25 year-old, receives less than one-third the retinal illuminance due to a more dense lens and smaller pupil,[1] a substantially greater loss of S- than M- or L-cone stimulation due to the selective absorption changes in the lens,[2] sustains an additional factor of four loss in the sensitivity of each class of photoreceptor[3] and has about 30% fewer retinal ganglion cells[4]? Most studies of aging have considered this question in relation to thresholds (see reviews by Weale[5], 1992, Knau and Werner[6]) and discrimination,[7,8] but have seldom considered the consequences for how subjects actually experience the world. The results of recent studies on color appearance in the elderly are surprising in that they reveal a remarkable degree of stability across the life span, as summarized in the next sections. To achieve this stability, however, raises new questions about how it may be accomplished when much of the visual system is changing. The problem is partly that of color constancy whereby the system must compensate for changing illumination, but it is more complex, for not only is the stimulus changing with age, but so too is the system used to analyze it.

2. STABILITY OF HUE PERCEPTION WITH AGING

We[9] began by asking whether color terms were applied to natural broadband stimuli in the same manner by younger and older observers. Fifteen stimuli were selected from the Optical Society of America (OSA) Uniform Color Scales and presented as 2° test surfaces in a middle gray ganzfeld-like hemisphere with an illuminant having a correlated color temperature of 6200 K. Scaling data were obtained using 15 younger (mean age = 21 years) and 15 older (mean age = 72 years) subjects. Five stimuli were presented at three lightness levels (in OSA space); one set was equal to the surround lightness while the other two sets of stimuli were four steps above and four steps below the surround lightness. Each lightness level included samples chosen so that one pair plotted along a tritan axis in MacLeod-Boynton receptor-excitation space[10] and another pair plotted approximately on an axis of constant S-cone stimulation. The chromatic and achromatic components were scaled for each stimulus using the 4+1 categories method.[11] The appearance of each test stimulus was first scaled in terms of the percentage of each fundamental hue, red, green, yellow, and blue. In a second series of trials the subjects described the proportion of overall chromatic and achromatic content.

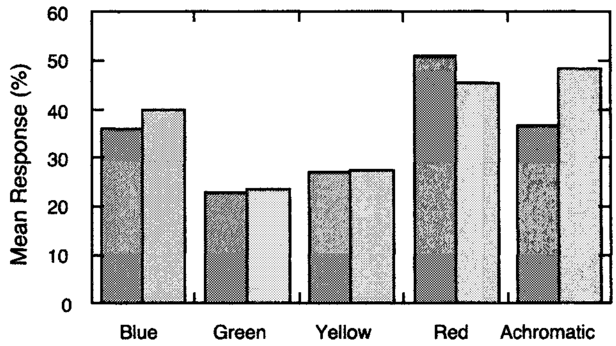

Fig. 1. Mean percentages assigned by younger (dark bars) and older (light bars) observers to 15 broadband surfaces from the OSA Uniform Color Samples. (From Schefrin and Werner.[9])

Color-naming percentages averaged across stimuli in which a particular hue name was assigned by either group are presented in Figure 1. Also shown by the bars on the far right are the mean achromatic (black/white) proportions for the two age groups. Not only were the same hue names assigned to the same stimuli by each group, but younger and older means did not differ by more than about 5% for each hue. Statistical analyses failed to reveal any significant overall differences between younger and older subjects' hue-naming percentages. The achromatic proportion assigned to the stimuli was, however, significantly different for younger and older observers. In general, older subjects perceived the colors of all stimuli to have more achromatic content (less chromatic content) than demonstrated by younger observers. Differences between the two age groups in perceived chromatic content of the test stimuli progressively increased as the lightness and luminance levels of the test stimuli decreased. In other words, the two groups differed primarily for darker colors. These results are similar to those reported by Okajima, Tsuchiya and Yamashita[12] using 75 chips. Essentially no difference between young and old were found when the subjects chose one of 11 color names for each stimulus. When the task involved assigning percentages to each hue term, there were small differences that depended on saturation.

Control experiments by Schefrin and Werner[9] with young observers were conducted using a neutral density filter and a broadband yellow filter that simulated the effects of smaller pupils in the elderly[13] and the senescent lens,[14,15] respectively. These tests showed that following 15 minutes of adaptation with the yellow filter, younger subjects' performance was not shifted to that of elderly subjects, perhaps implying a long-term adaptation process or senescent changes at some level of processing for the latter group.

The relative stability of hue perception across the life span is further supported by measurements of the wavelengths of the spectral unique hues. Figure 2 shows results obtained from 50 observers with 1° diameter stimuli presented at one of the three (7.1 cd·m^{-2}) luminance levels tested.[16] Similar results were obtained at other luminance levels for unique blue and unique yellow as well as in a separate study of 50 observers using Maxwellian-view.[17] Thus, unique blue and yellow are relatively constant across luminance level and observer age. Unique green was neither constant with luminance level nor with observer age, presumably because photoreceptor signals are combined non-linearly by the yellow-blue chromatic process.[18,19] The change in unique green with age may thus be secondary to a reduction in physical intensity of the stimuli resulting from lenticular senescence or secondary to the effective intensity of signals from aging cone photoreceptors.[3]

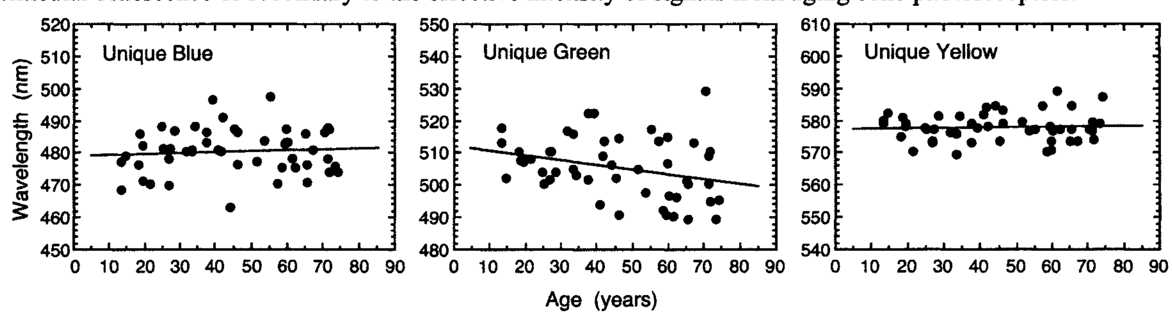

Fig. 2. Wavelengths of unique blue, green and yellow plotted as a function of age for 50 observers. Solid lines are fitted by least squares regression. (Date from Schefrin and Werner.[16])

3. STABILITY OF SPECTRAL BRIGHTNESS AND SATURATION WITH AGING

To explore whether the perception of brightness for spectral lights is predictable from age-related changes in ocular media density, Kraft and Werner[20] measured heterochromatic flicker-photometry and heterochromatic brightness-matching functions using a 1.2° foveally-viewed stimulus with 50 observers, ranging in age from 19 to 85 years. (See also Sagawa and Takahashi.[21]) As expected from earlier work by Verriest,[22] heterochromatic flicker-photometry sensitivity was similar for all observers at long wavelengths, but decreased at shorter wavelengths with increasing observer age. These changes are consistent with age-related changes in ocular media density and show that there is no compensation or normalization of relative sensitivity for lenticular senescence in the heterochromatic flicker photometry function which is mediated by an achromatic mechanism. Indeed, this function can be used to estimate individual observer's ocular media density, if one makes reasonable assumptions about the M- and L-cone action spectra.

Heterochromatic brightness-matching sensitivity data were also similar across observers at long wavelengths, on average, but declined at short wavelengths as a function of increasing age. However, the decline in sensitivity at short wavelengths was substantially less than for the heterochromatic flicker photometry functions. By using ocular media density estimates from the heterochromatic flicker photometry functions, heterochromatic brightness-matching functions could be specified at the retina. Linear regression of brightness sensitivity at each wavelength and age, which fitted the retinally-equated heterochromatic brightness-matching functions well, were used to estimate the change in heterochromatic brightness-matching sensitivity per decade. This analysis showed that heterochromatic brightness-matching sensitivity actually *increases* as an increasing function of age, but only over the range of about 420 to 560 nm where it is needed to compensate for lenticular senescence. The average increase of ≈ 0.05 per decade implies that sensitivity at the retina would double for the average person between ages 10 and 70 years. Of course, this compensation is not spectrally perfect because the ocular media density spectrum is different from the spectral response of any single cone type or their various postreceptoral combinations. As a result, the compensation in the heterochromatic brightness-matching data is too low at some wavelengths and too high at others relative to what would be needed for perfect compensation for lenticular senescence.

To determine whether similar processes influence age-related changes in saturation scaling, we measured colorimetric purity (Pc) discrimination[23] and saturation scaling[24] for 21 observers ranging from 22 to 88 years (18 individuals were the same for both tasks). Test stimuli of 1.2° diameter were presented in Maxwellian view. Discrimination was measured using a temporal 2AFC procedure in which the subject was asked to signal which of two primarily broadband white (CIE x,y = 0.33,0.35) stimuli also contained a chromatic component derived from a superposed monochromatic light (420-680 nm). Retinal illuminances (250 td and 10 td) were equated on the basis of individual heterochromatic flicker photometry (HFP) functions. Measured Pc discrimination sensitivity was lower in the older group than in the younger group at both retinal illuminances, and the performance difference between the age groups was approximately constant across the spectrum after corrections for ocular media light losses were applied. The difference between discrimination at 10 td and 250 td was relatively small for the younger group, but larger for the older group, indicating a selective

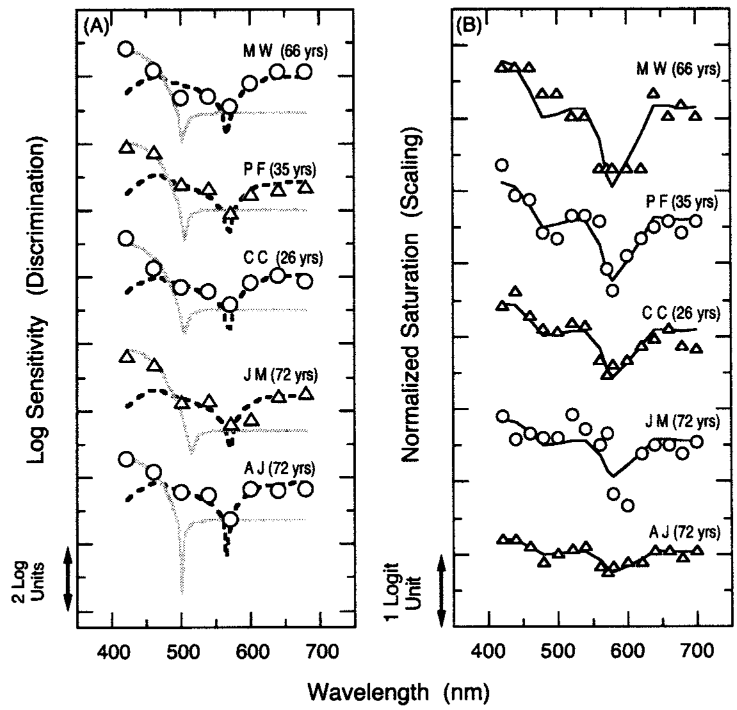

Figure 3. Panel A shows colorimetric purity discrimination functions for 5 observers plotted as a function of wavelength. The functions have been shifted arbitrarily along the ordinates, but for any one observer, higher points indicate better discrimination. The two curves show S-(L+M) (light, solid) and L-M (dark, dashed) mechanisms used to fit the data. Panel B shows scaling data, with individual subjects shifted arbitrarily along the ordinates. Smooth curves represent model fits. (From Kraft and Werner.[24])

performance decrement for older observers at low light levels. The data were modeled as a Euclidean sum of differential weighted responses from S-(L+M) and L-M opponent mechanisms. Figure 3A presents data from 5 observers and model fits showing the contributions of the S-(L+M) and L-M opponent mechanisms represented by the solid and dashed curves, respectively. Regression analyses using all subjects indicate similar age-related losses of sensitivity in the two chromatic mechanisms, perhaps secondary to receptoral sensitivity losses.

In the main scaling experiment, two sets of stimuli were used, one equated at the cornea by a luminosity function for a standard observer and the other equated in retinal illuminance by individual HFP functions. Observers were asked to assign percentages to indicate the proportion of a desaturated stimulus that appeared chromatic. Fig. 3B shows saturation scaling data for 5 observers chosen to illustrate the variation in dynamic ranges of the functions, which are known to vary substantially between observers.[25] The symbols show logit-transformed saturation plotted as a function of wavelength. Comparing the corneally-equated and retinally-equated stimuli reveals that the visual system of the elderly observer can compensate for age-related changes in ocular media density over a certain range values. In other words, their scaled saturation is more similar to that of a young person despite large changes in the retinal stimulus due to lenticular senescence and losses of receptor sensitivity. There is a limit, however, as might be expected, and compensation is less complete for individuals with more extreme lens density. There is also a limit when the field sizes are small. Knau and Werner[26] obtained saturation scaling for 58 observers (18 to 83 years of age) using nine field sizes and three retinal locations. Older observers require larger stimuli to reach the asymptote of the function relating saturation to field size, although the critical size is still small. Overall, these and other data from our lab show that despite substantial senescent losses in sensitivity of cone mechanisms and poorer chromatic discrimination, color appearance is relatively less affected by aging.

4. STABILITY OF THE ACHROMATIC POINT WITH AGING

The previous sections described the stability of color appearance over various regions of color space, but not at its theoretical center, the achromatic or white point. This point is important in color theory because it depends on the balance of all chromatic mechanisms, and is potentially a sensitive indicator of color appearance changes with age in any direction.

Age-related shifts in the locus of the average achromatic point might be expected due to senescent changes in the ocular media, as well as changes in receptoral and postreceptoral processes. The arrows in Figure 4 show theoretically predicted shifts in the chromaticity of a light mixture that appears achromatic. If the intersection of all arrows represents a theoretical observer at age 10 years, it is straightforward to calculate the expected shift due to lenticular changes for an average observer at age 80. This is shown by the solid arrows, with different arrows derived from different additive mixtures of short and long-wave pairs of lights. Because age-related increases in ocular media density will cause less short-wave light to reach the retina, an older observer would be expected to compensate by adding more short-wave light in the mixture to restore the retinal stimulus to be metameric at the retina for a younger observer. As a result, aging of the lens is predicted to shift the mixture perceived as achromatic to short wavelengths as shown by the solid arrows. The dashed arrows show additional shifts *if* there were selective losses in S-cone sensitivity.

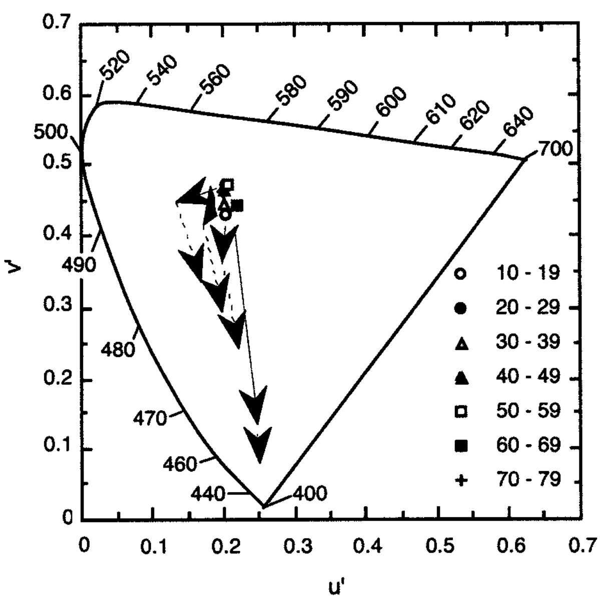

Fig. 4. The intersection of all arrows represents the location of a theoretical achromatic point for a 10-year-old observer plotted in CIE 1976 u',v' chromaticity coordinates. Arrows show the expected shift in this point resulting from changes in the ocular media from age 10 to 80. Different arrows are associated with different pairs of monochromatic lights. Dashed arrows represent additional age-related changes in the achromatic point expected from selective losses in S cones. Data points, several of which are occluded due to overlap, represent average achromatic loci of different age groups. [Data from Werner and Schefrin.[17])

The data points in Figure 4 show that the predictions do not agree with the data. Each datum represents the mean chromaticity of the achromatic point for each age group. 50 observers were tested by asking them to vary the ratio of a short- and long-wave light (their unique blue and yellow for convenience) to find a balance that appeared achromatic. Contrary to expectations, there was no significant shift in the achromatic point with observer age. Because the loss in short-wave light reaching the retina is certain, a constant achromatic point with age must imply that one or more processes renormalize or recalibrate the visual system to maintain constancy across the life span. Werner and Schefrin[17] described a simple quantitative model whereby the visual system adjusts the relative response of the three classes of cone photoreceptors so that it is constant with respect to an arbitrary "white" (equal-energy was used as an example). This is reminiscent of long-term von Kries adaptation in a "gray world" and is similar to processes suggested in other contexts by Pokorny and Smith[27] and Mollon.[28] The next section describes a more direct test of the hypothesis that the stability of color perception is due to renormalization in response to age-related changes in the ocular media.

5. TESTS OF RENORMALIZATION FOLLOWING CATARACT SURGERY

The results in the previous sections are consistent with the hypothesis that the visual system renormalizes itself so that stimuli specified at the cornea appear similarly even though they change at the level of the retina over the life span. Relevant direct tests of this idea are lacking as most previous research has been concerned with short-term (e.g., Kraft and Brainard[29]) changes in the illuminant. There is some evidence that the visual system may require a number of days to recover from medium-term adaptation.[30,31] For example, the recent work by Neitz et al.[31] reports that unique yellow settings can shift by about +/- 4 nm after subjects adapt to 'red' or 'green' light for a number of hours per day over several days, and that the visual system can take about 10 days to return to the pre-adaptive state.

We have tested the locus of the achromatic point in observers before cataract surgery and for up to one year after cataract surgery to determine the time course of renormalization following the removal of a cataractous lens to which the person has presumably adapted over a number of years. Stimuli were presented on a calibrated CRT and chromaticity was adjusted in CIE u'v' color space with luminance fixed at 30 cd·m^{-2}. The 9.5° test stimulus flashed on and off at 3 s intervals to reduce adaptation to the stimulus. The starting chromaticity of the stimulus was selected randomly. Settings were made before surgery and at various intervals after surgery up to one year. The stimuli were viewed monocularly.

The settings for one observer (age 71) are shown in Figure 5. After surgery, there is a large shift in the achromatic point in the yellow direction, from a to b in the figure. Much of this effect is expected from removal of the cataractous lens and the change in the retinal stimulus. However, the achromatic point slowly drifts back in the direction of the achromatic point before surgery, reaching a fairly stable value at about three months after surgery. Figure 5 shows the locus of the achromatic point after one year. Tests on other subjects show a similar pattern of results.

Neitz et al.[31] found inter-ocular transfer of color appearance shifts and suggested that the changes they recorded were due to cortical processes. We did not find this to be the case in our study. For example, the subject presented in Figure 5 was tested in her fellow eye which had a cataractous lens removed 8 months prior to the 'test' eye. There was little change in the settings over the same period as the 'test' eye. This suggests most of the long-term adaptation effects studied here, and by inference associated with normal aging, occur at a site prior to binocular combination.

The post-surgery settings for the subject presented in Figure 5 were converted to cone responses using Smith-Pokorny fundamentals.[32] Most of the differences in achromatic settings can be accounted for by changes in S-cone response which might be expected in view of normal lens aging having its greatest effect on S-cone stimulation and also for various phases of daylight.[2]

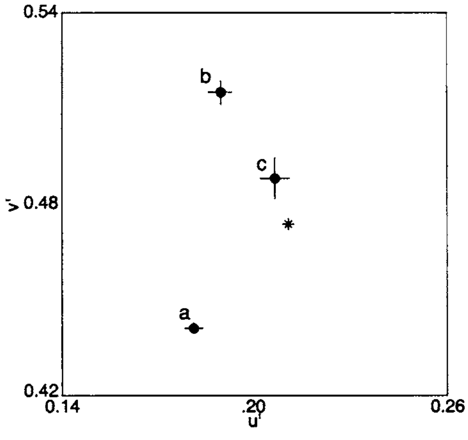

Fig. 5. Locus of average achromatic setting in CIE u'v' chromatic coordinates for one observer (a) before cataract removal, (b) 1 day post-surgery and [c] 12 months post-surgery. Asterisk is equal-energy white.

6. CONCLUSIONS

Color appearance was probed in different regions of color space and using several different methods, but in all cases the stability of perception across the life span is remarkable. Because the retinal stimulus is continually changing with age and there are losses in sensitivity of the receptors with age, stability across the life span would only seem possible if the visual system compensated for the changed inputs by renormalizing itself. This occurs over a much more protracted time scale than classical color constancy. Renormalizing the achromatic point, or the balance of chromatic mechanisms, seems to require as long as three months following removal of a cataractous lens.

The ability of the visual system to maintain stable color perception despite the large physiological variations with aging has a number of important implications. First, measures of visual sensitivity may be poor predictors of perceptual experience, and thus direct measures of appearance are important for characterizing the consequences of visual aging. Second, the compensations considered here are not restricted to color vision or aging, but probably reflect a general design principle in visual coding. For example, sensitivity varies dramatically with retinal eccentricity, yet the world does not appear to depend on where we fixate, and analogous processes of normalization may compensate for sensitivity differences between the fovea and periphery (e.g. owing to differences in macular pigment). Similarly, aging and eccentricity alter most aspects of vision, and these may be normalized in similar ways. For example, visual acuity declines with both senescence and peripheral viewing, yet threshold contrast sensitivity fails to predict the contrast constancy observed in suprathreshold patterns,[33] or the stable perception of image focus across eccentricity.[34] Finally, the fact that these adjustments are calibrating the visual system for properties of the physical world implies that they not only maintain perceptual constancy within observers, but also across observers. That is, if a young and old individual agree on the stimulus they call white, then this is because they both are normalized for a common "ageless" stimulus in their environment.

Supported by the National Institutes of Health (EY10834 and AG04058) and a Jules and Doris Stein Research to Prevent Blindness Professorship.

REFERENCES

1. Weale, R.A. *The Aging Eye* (London, H.K. Lewis, 1963).
2. Werner, J.S. Visual problems of the retina during ageing: Compensation mechanisms and colour constancy across the life span. In N.N. Osborne and J. Chader (Eds.), *Progress in Retinal and Eye Research. Vol. 15/2* (Oxford: Pergamon Press, pp. 621-645, 1996).
3. Werner, J.S., Bieber, M.L. and Schefrin, B.E. Senescence of foveal and parafoveal cone sensitivities and their relations to macular pigment density. *Journal of the Optical Society of America A,* **17**, 1918-1932 (2000).
4. Curcio, C.A. and Drucker, D.N. Retinal ganglion cells in Alzheimer's disease and aging. *Annals of Neurology,* **33**, 248-257 (1993)
5 Weale, R.A. *The Senescence of Human Vision* (Oxford: Oxford University Press, 1992).
6. Knau, H. and Werner, J.S. Senescence of the human cone photoreceptor pathways. In V. Lakshminarayanan (Ed.), *Trends in Optics and Photonics, 35, Vision Science and Its Applications.* (Washington, DC: Optical Society of America, pp. 382-392, 2000).
7. Knoblauch, K., Saunders, F., Kusuda, M., Hynes, R., Podgor, M., Higgins, K.E. and deMonasterio, F.M. Age and illuminance effects in the Farnsworth-Munsell 100-hue test. *Applied Optics,* **26**, 1441-1448 (1987).
8. Shinomori, K., Schefrin, B.E. and Werner, J.S. Age-related changes in wavelength discrimination. *Journal of the Optical Society of America A,* **18**, 310-318 (2001).
9. Schefrin, B.E. and Werner, J.S. Age-related changes in the color appearance of broadband surfaces. *Color Research and Application,* **18**, 380-389 (1993).
10. MacLeod, D.I.A. and Boynton, R.M. Chromaticity diagram showing cone excitation by stimuli of equal luminance. *Journal of the Optical Society of America,* **69**, 1183-1186 (1979).
11. Gordon, J. and Abramov, I. Scaling procedures of specifying color appearance. *Color Research and Application,* **13**, 146-152 (1988).
12. Okajima, K., Tsuchiya, N. and Yamashita, K. Age-related changes in colour appearance depend on unique-hue components. *Proceedings of SPIE,* **4421**, 259-262 (2002).
13. Loewenfeld, I.E. Pupillary changes related to age. In H.S. Thompson, R. Daroff, L. Frisén, J.S. Glasen and M.D. Sanders (Eds.), *Topics in Neuro-Ophthalmology.* (Baltimore, Williams and Wilkins, Baltimore, pp. 124-150, 1979).
14. Werner, J.S. Development of scotopic sensitivity and the absorption spectrum of the human ocular media. *Journal of the Optical Society of America,* **72**, 247-258 (1982).
15. Weale, R.A. Age and the transmittance of the human crystalline lens. *Journal of Physiology (London),* **395**, 577-587 (1988)

16. Schefrin, B. and Werner, J.S. Loci of spectral unique hues throughout the life span. *Journal of the Optical Society of America A,* **7**, 305-311 (1990).
17. Werner, J.S. and Schefrin, B.E. Loci of achromatic points throughout the life span. *Journal of the Optical Society of America A,* **10,** 1509-1516 (1993).
18. Larimer, J., Krantz, D.H. and Cicerone, C.M. Opponent-process additivity--II. Yellow/blue equilibria and nonlinear models. *Vision Research,* **15**, 723-731 (1975).
19. Werner, J.S. and Wooten, B.R. Opponent-chromatic mechanisms: Relation to photopigments and hue naming. *Journal of the Optical Society of America,* **69**, 422-434 (1979).
20. Kraft, J.M. and Werner, J.S. Spectral efficiency across the life span: flicker photometry and brightness matching. *Journal of the Optical Society of America A,* **11**, 1213-1221 (1994).
21. Sagawa, K. and Takahashi, Y. Spectral luminous efficiency as a function of age. *Journal of the Optical Society of America,* **18**, 2659-2667 (2001).
22. Verriest, G. La variation de la courbe spectrale photopique d'efficacité lumineuse relative chez les sujets normaux. *Nouvelle Revue d'Optique appliquée,* **1**, 107-126 (1970).
23. Kraft, J.M. and Werner, J.S. Aging and the saturation of colors: 1. Colorimetric purity discrimination. *Journal of the Optical Society of America A,* **16**, 223-230 (1999).
24. Kraft, J.M. and Werner, J.S. (1999) Aging and the saturation of colors: 2. Scaling of color appearance. *Journal of the Optical Society of America A,* **16**, 231-235 (1999).
25. Kaiser, P.K., Comerford, J.P. and Bodinger, D.M. Saturation of spectral lights. *Journal of the Optical Society of America,* **66**, 818-826 (1976).
26. Knau, H. and Werner, J.S. Senescent changes in parafoveal color appearance: Saturation as a function of stimulus area. *Journal of the Optical Society of America A,* **19**, 208-214 (2002).
27. Pokorny, J. and Smith, V.C. Evaluation of single-pigment shift model of anomalous trichromacy, *Journal of the Optical Society of America,* **67**, 1196-1209 (1977).
28. Mollon, J.D. Color vision. *Annual Review of Psychology,* **33**, 41-85 (1982).
29. Kraft, J.M. and Brainard, D.H. Mechanisms of color constancy under nearly natural viewing. *Proceedings of the National Academy of Sciences USA,* **96**, 307-312 (1999).
30. Eisner, A. and Enoch, J. M. Some effects of 1 week's monocular exposure to long-wavelength stimuli. *Perception & Psychophysics,* **31**, 169-174 (1982).
31. Neitz, J., Carroll, J., Yamouchi, Y., Neitz, M. and Williams, D. R. Color perception is mediated by a plastic neural mechanism that is adjustable in adults. *Neuron,* **35**, 783-792 (2002).
32. Smith, V. and Pokorny, J. Spectral sensitivity of the foveal cone photopigments between 400 and 500 nm. *Vision Research,* **15**, 161-171 (1975).
33. Georgeson, M. A. and G. D. Sullivan. Contrast constancy: Deblurring in human vision by spatial frequency channels. *Journal of Physiology,* **252**, 627-656 (1975).
34. Galvin, S. J., R. P. O'Shea, Squire, A.M., Govan, D.G. Sharpness overconstancy in peripheral vision. *Vision Research,* **37**, 2035-2039 (1997).

Color Perception of the Elderly
- *Basic Researches and Applications* -

Katsunori Okajima
Imaging Science and Engineering Laboratory, Tokyo Institute of Technology,
4259 Nagatsuda, Midori-ku, Yokohama 226-8503, Japan
(email:okajima@isl.titech.ac.jp)
Department of Applied Physics, National Defense Academy, 1-10-20
Hashirimizu, Yokosuka 239-8686, Japan
(email:okajima@nda.ac.jp)

ABSTRACT

It is important to know the visual characteristics of the elderly and to develop the color design tools for aging and aged societies. Visual characteristics of older people can be classified in terms of the aging effects on the ocular system, retina, optic nerve and brain stages. In particular the age-related change of the crystalline lens produces a modification of the spectral characteristic of the light arriving at the retina of older people. In the present review, I will introduce summaries of our researches on age-related changes of human color vision such as an experiment on color appearance with young and older subjects. Next, I will introduce special filters which can simulate human crystalline lens of the elderly for young people and the validity of the filters by referring some experimental results. Finally, I will propose an aging-color simulator to transform color images for young designers taking color constancy of the elderly and some age-related changes of ocular system into account.

Keywords: age-related changes, color perception, optical filter, color image simulator

1. INTRODUCTION

The population ratio of the elderly to young is increasing quite rapidly (Tuljapurkar, 2000) and the technical establishment of color design so that the elderly can live a safe and a comfortable life, is an important object. Visual characteristics of older people can be classified in terms of the aging effects on the ocular system, retina, optic nerve and brain stages (Werner, 1990, 1996). In particular the age-related change of the crystalline lens in the human ocular system produces a modification of the spectral characteristic of the light arriving at the retina of older people (Xu, 1997). It would be expected that color appearance seen by older people is different from that seen by young people (Okajima, 2001a). In the present review, I discussed the age-related changes of vision and color appearance of the elderly. To compare color appearance as seen by older and young people quantitatively, we conducted experiments where the subjects responded to the color appearance of 75 color chips using a categorical color naming method and an elemental color scaling method. The results showed that categorical color naming between elderly and young subjects is almost the same for most color chips though a few differences between two-age groups were noticed. In addition, I developed an aging-color simulator to transform color images for use by young designers, taking such color constancy of the older people and some age-related changes of ocular system into account. By using the simulation software, young people can quickly and easily experience the color appearance as seen by the elderly on any PC screen and can check the visibility of the color designs for the elderly. In particular it is expected that this tool would be convenient for young people designing, for example, colorful product packages and Homepages on the Internet for older people. These results are useful in considering color designs for the elderly people as well as for all ages.

2. AGE-RELATED CHANGES OF OCULAR SYSTEM

Visual characteristics of older people can be classified in terms of the aging effects on the ocular system, retina, optic nerve and brain stages. For example, as crystalline lens becomes cloudy the passage light decreases and the scattered light increases. The dynamic range of pupil aperture and the sensitivity of visual pigments decrease with age, so elderly people have a difficulty in dark environment. In addition, noise in the optic nerve and the receptive field size increase with age, causing deteriorations in color discrimination (Knoblauch, 1987) and spatial resolution (Iwata, 2001). The age-related change of the crystalline lens in the human ocular system produces a modification of the spectral characteristic of the light arriving at the retina of older people. The spectral transmittance curves of crystalline lens for several ages can be derived with the "two-factor model" spectral transmittance curves of crystalline lens for several ages can be derived with the "two-factor model" (Pokorny, 1987). The model was mainly derived from the color matching data (Stiles, 1955). In this model, the spectral optical density of human lens L as a function of wavelength λ and age A is expressed using two components, TL_1 and TL_2 as follows:

$$L(\lambda, A) = [1.00 + 0.02(A - 32)]TL_1(\lambda) + TL_2(\lambda) \quad \text{for } 20 \leqq A \leqq 60$$

$$L(\lambda, A) = [1.56 + 0.0667(A - 60)]TL_1(\lambda) + TL_2(\lambda) \quad \text{for } A > 60. \qquad (1)$$

The first component TL_1 is a function of the change in optical density with age but the second component TL_2 is a constant factor which is independent of age. Notice that the coefficients of TL_1 in the model depend on whether the person is above or below the age of 60 because of the differential ratio of the optical density changes for a 60-year-old in this model. Although the two-factor model originally provides relative values of the spectral optical density, it has been shown that, in fact, we can treat the values as absolute density values. There is a relationship between intensities of the incident light $I(\lambda)$ and the transmitted light $I'(\lambda)$ by human lens:

$$L(\lambda) = \log_{10}(I(\lambda)/I'(\lambda)) \qquad (2)$$

Therefore, the spectral transmittance of human lens τ can be expressed as the following:

$$\tau(\lambda, A) = 10^{-L(\lambda, A)} \qquad (3)$$

Figure 1 shows the spectral transmittances of human lens calculated using Eq.(3). The transmittance ratio for short wavelength light significantly declines with increasing age in comparison with for long wavelength light. By dividing the transmittance ratio of older people by the ratio of younger one, we can derive the differential transmittance ratio between the two ages.

A filter whose transmittance is $F(\lambda, A_2, A_1)$ represented as Eq.(4) can be useful in simulating the lens transmittance of an elderly person of age A_2 as seen by a younger subject of age A_1:

$$F(\lambda, A_2, A_1) = \tau(\lambda, A_2)/\tau(\lambda, A_1) \qquad (4)$$

Demonstrations and simulations of aging vision using yellow filters for young people have recently been performed. The transmittance of the yellow filter should be quantitatively simulated with the lens transmittance of the target age of elderly being divided by that of the young observer. However, this generally has not been taken into consideration. It is important to use filters whose transmittance has modified the transmittance of the subject's lens in order to produce precise demonstrations and simulations.

In addition, the decrease of pupil size with increasing age is also a critical phenomenon for color appearance in the elderly. Figure 2 shows the age-related changes of pupil size as a function of the log illuminance level (Winn, 1994). Each symbol indicates the average size of pupil at each age group. In this figure, only small differences of pupil size among age groups are found at high illuminance levels whereas there are large differences at low illuminance levels.

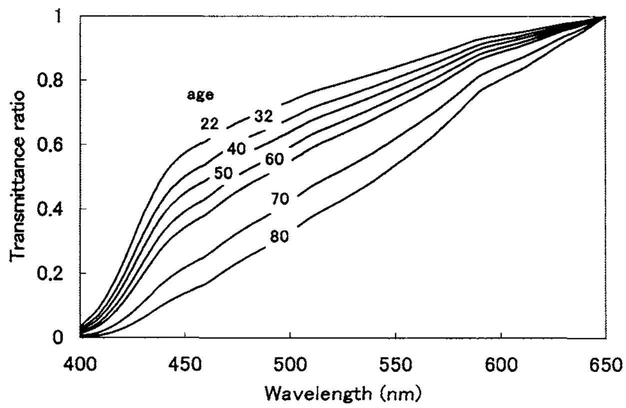

Fig.1 Spectral transmittances of the human lens for several ages calculated from the two-factor model.

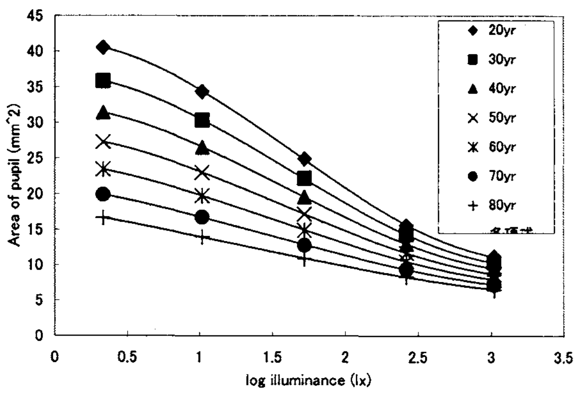

Fig.2 Age-related changes of pupil size as a function of the log illuminance level.

3. COLOR PERCEPTION

We examined age-related changes in color appearance at two illumination levels. To compare color appearance as seen by older and young people, we conducted experiments where the subjects responded to the color appearance of 75 color chips using a categorical color naming and an elemental color scaling methods (Okajima, 2001b). Six elderly subjects and six young subjects participated as volunteers, all the subjects having normal color vision and no eye defects. Both age groups included three men and three females. All subjects were naive; none of them having previously been in any psychophysical experiment like the present one. We used 75 color chips selected from a color set made by Toyo Ink company which distributed widely and uniformly in the a*b* chromaticity diagram. Twenty-four fluorescent lights whose color temperature was D65 white were set in the roof of a booth. The illumination level was set at 500 lx or 50 lx during one session by controlling brightness of the lights. One session consisted of 75 trials for all the color ships. Three sessions were repeated at each illumination level for another three days. Subjects observed the test color chip on an N5 gray background with binocular natural viewing. The distance between the eye and the chip was around 45cm, and the visual size of test chips was approximately 2.1 and 6.4 degrees. The subjects first adapted to the illumination level for 10 minutes. The test color chips were presented in random order and the subjects were asked color component ratios according to elemental color scaling method. First of all, subjects were asked for the ratio of the achromatic and chromatic components in the test color chip and then ratio of whiteness and blackness in the achromatic components and the ratio of the four unique-hue components in the chromatic components. Continuously, the subjects were asked to choose one color name out of 11 basic color terms (RED, GREEN, YELLOW, BLUE, ORANGE, PURPLE, PINK, BROWN, WHITE, BLACK and GRAY) to describe the chip's color. This method is generally called categorical color naming (Okajima, 2002). One session took between 1 and 2 hours depending on the subject and day. Figure 3 shows the method of elemental color scaling. The results showed that categorical color naming between elderly and young subjects is almost the same for most color chips though a few differences between two-age groups were derived. However, saturation and hue perception systematically change with age.

4. SIMULATIONS

To experience these age-related changes of color vision by young people, observing through a yellow filter or a spectacle with yellow filters has been proposed as a method for aging-simulation (Okajima, 2000). However, two critical issues are involved in the simulation method. First, although the transmittance of the yellow filter must be quantitatively simulated, the lens transmittance of the target age of older people relating to the young subject has generally not been taken into consideration. Second, the colors seen through such yellow filters appear quite yellowish even though the transmittance of the filters has been correctly designed. The second reason indicates that we cannot simulate the color appearance of the elderly by young people with only optical method but that we need to use a sort of computer generated color image processing method. So we developed a computer software to simulate the color appearance of the elderly (70- and 80-year-olds) as seen by the 20-year-old people on a PC screen. As mentioned above, we have to consider the changes of spectral transmittance by the age-related change

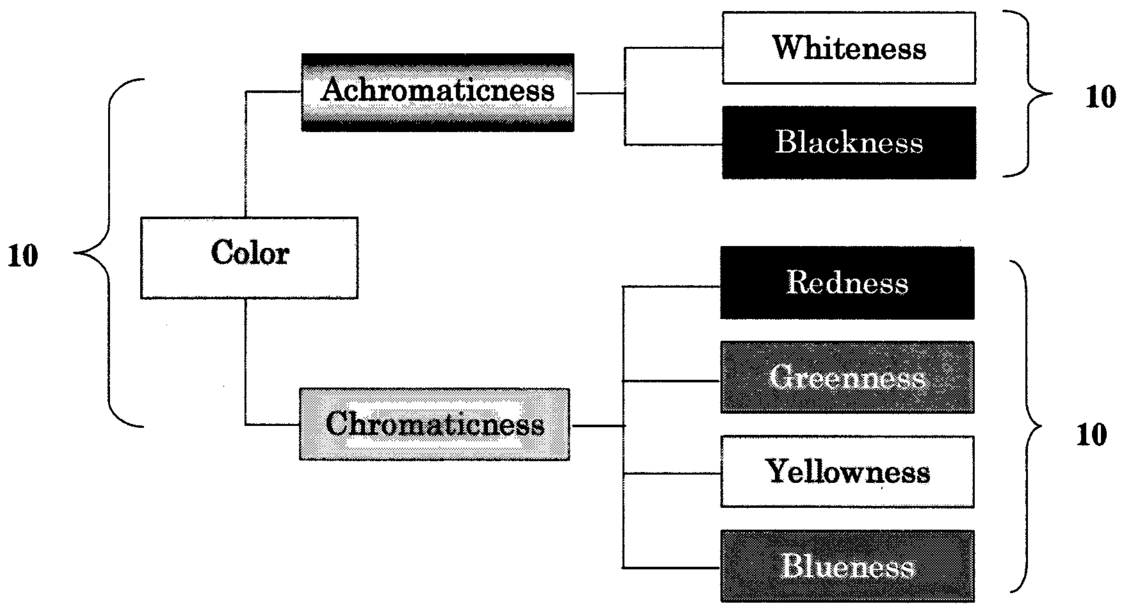

Fig.3 Method of the elemental color scaling.

of human lens and of the decrease of pupil size with increasing age. First of all, the photometric values of all pixels on the PC screen are transformed from RGB values and each luminance value of R, G and B phosphors is also calculated. By keeping the xy-chromaticity values of the pixels constant for the elderly, only the luminance values are changed to allow the decline of the transmittance of the aged human lens and of the pupil size of the elderly. Finally, the translated values are transformed to RGB values, and then the results are presented back on the PC screen as the simulated image. The general impression of the simulated image is darker than the original image. However, the changes of the brightness depend on the color. Blue colors appear much darker in the simulated image in comparison with red or yellow (Okajima, 2000). As a result, the visibility of the color pattern depends on the color scheme. For example, blue characters on a black background generally provide a poor visibility for the elderly because blue becomes darker and then the contrast becomes low. On the contrary, dark blue characters on a white background will be good combination for the elderly because the effective contrast for the elderly is higher than that for the young. Since there are innumerable color combinations, it is impossible to calculate and to consider visibility for the elderly in all situations of color pattern as seen by the elderly. However, by using the software we proposed, young people can easily and directly experience the appearance and check the visibility of any color pattern as seen by the elderly.

5. CONCLUSIONS

Categorical color perception appears to be independent of aging but saturation and hue perception change with age. The results show the characteristics of a color constancy mechanism in human color vision so as to compensate for the age-related change of the crystalline lens (Okajima, 2001c). In addition, we developed a color simulator for use by young designer and demonstrated that the tool readily enables young people to experience the color appearance as seen by the elderly and to check the visibility the color designs as seen by the elderly. Our results will be useful in considering color designs for the elderly as well as for all ages.

REFERENCES

Iwata, M., Okajima, K. and Ujike, H. 2001. "Age-Related Change of Contrast Sensitivity Function Depends on Illumination Level". *In* Proceedings of International Workshop for Gerontechnology 87-88. Tsukuba, Japan.

Knoblauch, K. et al. 1987. "Age and illuminance effects in the Farnsworth-Munsell 100-hue test". Appl.Opt. 26 1441-1448.

Okajima, K., Yoshida, H. and Ujihara, A. 2000. "Test Methods of Color Visibility for Old People Based on Age-Related Change of Luminance Contrast". J. Color Science Association of Japan 24(3) 164-170. *(in Japanese)*

Okajima, K. and Takase, M. 2001a. "Computerized simulation and chromatic adaptation experiments based on a model of aged human lens". Optical Review 8 64-70.

Okajima, K., Tsuchiya, N. and Yamashita, K. 2001b. "Age-Related Changes in Color Appearance Depend on Unique-Hue Components". *In* Proceedings of the 9th Congress of the International Colour Association (AIC Color 01) 259-262.

Okajima, K., Tsuchiya, N. and Yamashita, K 2001c. "Age-Related Nonlinear Compensation in the Color Vision Mechanism". *In* Proceedings of the First Asian Conference on Vision 65.

Okajima, K., Robertson, A.R. and Fielder, G.H. 2002. "A Quantitative Network Model for Color Categorization". Color Research and Application 27(4) 225-232.

Pokorny, J., Smith, V.C. and Lutze, M.1987. "Aging of the Human Lens". Appl. Opt. 26 1437-1440.

Stiles, W.S. and Burch, J.M. 1955. "Interium Report to the CIE, Zurich, 1955, on the National Physical Laboratory's Investigation of Colour-Matching". Opt.Acta 2 168-181.

Tuljapurkar, S., Li, N. and Boe, C. 2000. "A universal pattern of mortality decline in the G7 countries". Nature 405(6788) 789-792.

Werner, J.S., Peterzell, D.H. and Scheetz, A.J. 1990. "Light, vision and aging". Optometry and Visual Science 67 214-229.

Werner, J.S. 1996. "Visual problems of the retina during ageing: compensation mechanisms and colour constancy across the life span". Progress in Retinal and Eye Research 15 621-645.

Winn, B., Whitaker, D., Elliott, D.B. and Phillips, N.J. 1994. "Factors Affecting Light-Adapted Pupil Size in Normal Human Subjects". Invest.Ophthalmol.Vis.Sci. 35 1132-1137.

Xu, J., Pokorny, J. and Smith, V.C. 1997. "Optical density of the human lens". J.Opt.Soc.Am. A14 953-960.

Color appearance of color charts observed with a cataract experiencing goggle

Mitsuo Ikeda＊, Tomoko Obama＊＊, Azusa Kusumi＊, Hiroyuki Shinoda＊
＊Faculty of Science and Engineering, Ritsumeikan University
＊＊Panasonic Mobile Communications Co., Ltd.

ABSTRACT

Color appearance of color charts observed with a cataract experiencing goggle composing of two kinds of filters, a haze filter and a colored filter, was investigated by three different experiments. Color charts that appeared same in color with and without the goggle indicated that the saturation of color charts decreased with the goggle. Color appearance region for a same color category on a JIS Colour Standards sheet decreased with the goggle except for hue 5Y so that the border of the region moved toward higher saturation. Finally the luminance of color charts to match with a reference N8 in brightness had to be increased with the goggle. All the three experimental results indicated desaturation of color with the goggle and it was hypothesized that the desaturation was caused by light coming from environmental illumination and scattered by the haze filter to enter into the subject's eyes. It was suggested that a similar desaturation takes place in elderlies with cataract.

Keywords; cataract, goggle, color appearance, elderlies, color region, brightness

1. INTRODUCTION

The population of elderlies is increasing rapidly in Japan and it is becoming important for manufacturers to make products and for self-governing bodies to design public spaces that can be used comfortably by elderlies. Various goggles have been developed to simulate the visual system of elderleis so that young engineers and designers can experience the ways that elderlies see in the works of designing the products suitable for elderlies. When one of the authors MI used one such goggle[1)] commercially available after his eyes were operated for cataract and implanted with IOL, he felt the visual perception was very similar to that he experienced before the operation. The cataract experiencing goggle was developed to simulate a weak cataract eye and is composed of a haze filter to scatter light and a color filter to absorb more light at short wavelengths. Although the data from 48 elderlies who were operated for cataract were used in choosing the color filter, the data were mere subjective reports about color impression before and after the operation. It was thought therefore important to quantitatively investigate the property of the goggle about color appearance and we did three different experiments; to find out two color patches that appear same in color with and without the goggle, to decide the color regions that appear same on the Book of JIS Colour Standards, and to measure the luminance of color charts that appear same in brightness with an achromatic reference chart.

2. EXPERIMENT 1
A PAIR OF COLOR CHARTS OF A SAME APPEARANCE

2.1 Experiment and Procedure

This experiment is to know how the color appearance of a color chart changes with the cataract experiencing goggle. A color chip on a hue sheet of the Book of JIS Colour Standards was observed with the goggle and a corresponding color chip on the hue sheet, or on neighboring hue sheets if needed, was decided without the goggle such that it appeared same as the color appearance with the goggle. To save time for the experiment we modified the goggle so that its filters for right eye were removed off from the goggle. Two same hue sheets were placed on a desk side by side with an appropriate distance. A subject first observed a reference color chip on the left sheet with his/her left eye with goggle and then observed the right sheet without goggle to find a color chip that appeared same in color with that perceived by the left eye. The search was done by moving around a mask by subject himself placed over the hue sheet. He could return to the left sheet at any time to confirm the color appearance through the goggle. The subject covered one eye by his left hand when it was not used and could not see two color chips of the left and the right at a same time. Each sheet was covered with a black mask so that the subject could see only one color chip on the sheet.

Seventeen colors were employed as the reference color chip to be presented on the left side; 5R5/12、5YR7/14、5Y8/12、5GY7/10、5G6/10、5BG6/8、10B6/10、5P6/8、5R5/6、5YR7/6、5Y8/6、5GY7/4、5G6/4、5BG6/4、10B6/4、5P6/4, and N6. The experiment was done in a normal room of which illuminance was adjustable. Illuminance of 10 and 1000 lx were employed.

Four subjects participated in the experiment, TK (22years old, male), AK (25, female), KT (35, female), and MI (69, male). The subject MI was operated for both eyes and implanted with IOL. His visual acuity was over 1.5 in both eyes. All the subjects were normal in color vision in both eyes when tested with 100 hue test.

2.2 Results of Experiment 1

Color appearance change is shown in Fig.1 by the Munsell notation graph for the subject KT. Along the circumference the Hue is taken and along the radius the Chroma, the circle corresponding to 14. The open circle indicates a reference color that was observed by the left eye with the goggle, and an arrowhead the color chart that appeared same as the reference color when judged by the right eye without the goggle. In other words if the chart shown by an open circle is observed by the eye with the goggle it appears same color as the color chart

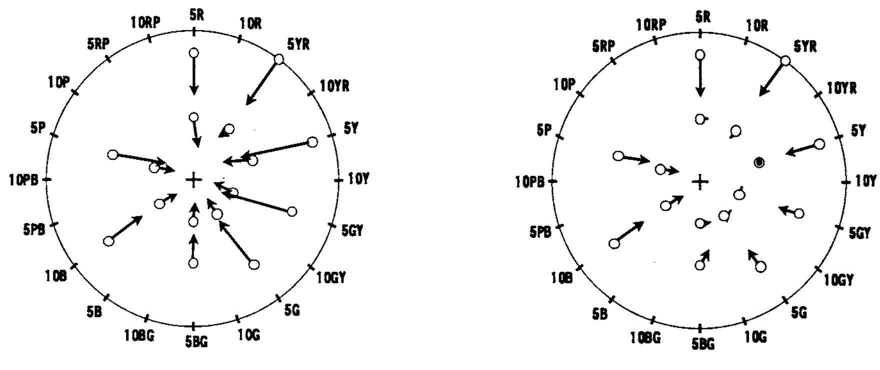

Fig.1 A pair of color charts that appeared same with and without the goggle; left, 10 lx and right, 1000 lx. Subject, KT.

shown by an arrowhead. The longer the length of arrow the larger the change in the color appearance with the goggle. In this subject the length is longer when the room illuminance was low at 10 lx compared to 1000 lx. The most significant property of the arrows is their direction. Almost all arrows direct towards the center to imply that the chroma reduced. That is, all the colors desaturated when the subject used the goggle. This property was found in all other subjects.

We expected that the arrows might direct towards right, namely towards yellow, because the color filter was slightly yellow, but the expectation was not fulfilled. On the contrary, even the yellowish color charts as 5YR7/14、5Y8/12 and 5GY7/10 changed to the opposite direction from the expectation. All the color charts lost their saturation large and small.

3. EXPERIMENT 2
SAME COLOR APPEARANCE REGION

3.1 Experiment and Procedure

This experiment is to know how the same color appearance region changes with the cataract experiencing goggle. The same experimental room as for Experiment 1 was used but with a regular two eyes goggle. One hue sheet of the Book of JIS Colour Standards was placed on the desk and a subject determined the region in which all the color chips belonged to the color category that he decided for the color chips of high chroma in the sheet. No suggestion was given to the subject about the appearance. The color category was solely determined by the subject himself. The subject showed the region by tracing the boundaries between the color chips to belong to the category and others. The determination was carried out with and without the goggle.

Eight hues were employed; 5R, 5YR, 5Y, 5GY, 5G, 5BG, 10B and 5P. The room illuminance 10, 80 and 1000 lx were employed. The 80 lx represents a typical illuminance level for home appliances in residence. The same subjects as for Experiment 1 participated in this experiment also.

3.2 Results of Experiment 2

Results are shown in Fig.2 for three hues 5Y, 5G and 10B, for 10 and 1000 lx, and for the subject KT. The abscissa indicates the Munsell Chroma and the ordinate the Munsell Value. Thick solid lines show the

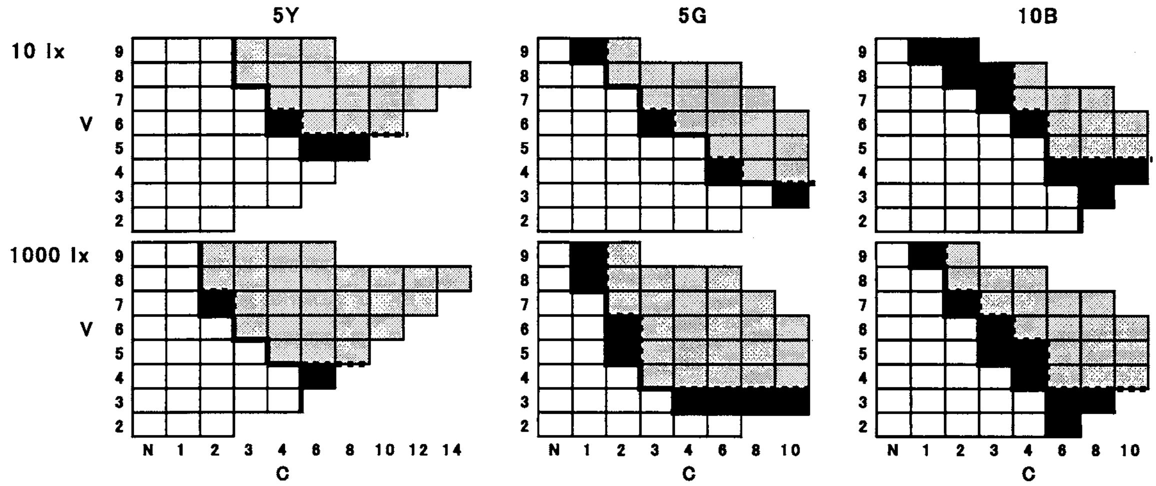

Fig.2 Same color appearance regions for Y5、 G5 and B10 sheets. Subject, KT

boundaries without the goggle and thick dotted lines with the goggle. The same color appearance region is almost always smaller with the goggle and the black chips show the narrowed area. There was found difference in the narrowing effect of the goggle among hues. It is big in 10B, but small in 5Y. Other subjects showed similar tendency.

4. EXPERIMENT 3
LUMINANCE OF COLOR CHARTS FOR A SAME BRIGHTNESS

4.1 Experiment and Procedure

This is to know difference in luminance to give a same brightness perception with or without the goggle. A different experimental room from the previous two experiments was used, which was composed of two rooms, a subject room and a test stimulus room. On the front wall of the subject room a reference stimulus of N8 of the size 22 x 22 mm was pasted and a hole of the same size was opened at the immediate right side of the reference. Behind the hole a color chart was placed as a test stimulus and it was illuminated by lamps. The intensity was controlled by the subject and the luminance of the test stimulus was changed. When the subject looked at the reference and the test stimulus they appeared as if they were just pasted on the wall side by side.

Thus subject's task was to adjust the luminance of the test stimulus to make the brightness matching between the test stimulus and the reference stimulus. This task was carried out with and without the goggle. Sixteen color charts were employed as the test stimulus; 10RP4/10, 5RP4/10, 10P4/10, 5P4/10, 10PB4/10, 5PB4/10, 5B4/9, 10BG4/9, 5BG4/9, 10G5/10, 10GY6/10, 5GY6/9, 10Y7/10, 10YR6/10, 5YR5/10, and 10R4/10. The room illuminance was 10 and 1000 lx. The same subjects as previous experiments also participated to the present experiment.

4.2 Results of Experiment 3

Results of the subject KT are shown in Fig.3 for 10 and 1000 lx. Test charts are taken along the abscissa and their luminance at the brightness matching with the reference N8 is taken along the ordinate in logarithmic unit. The horizontal dashed line shows the luminance of the reference stimulus N8. The open circles were obtained without the goggle and filled circles with the goggle. Both of the open and the filled circles came below the dashed line to imply less luminance was needed to match the achromatic reference N8 in brightness. It is well known that color contributes to brightness[2] and we can understand the lowered luminance of any color chart is

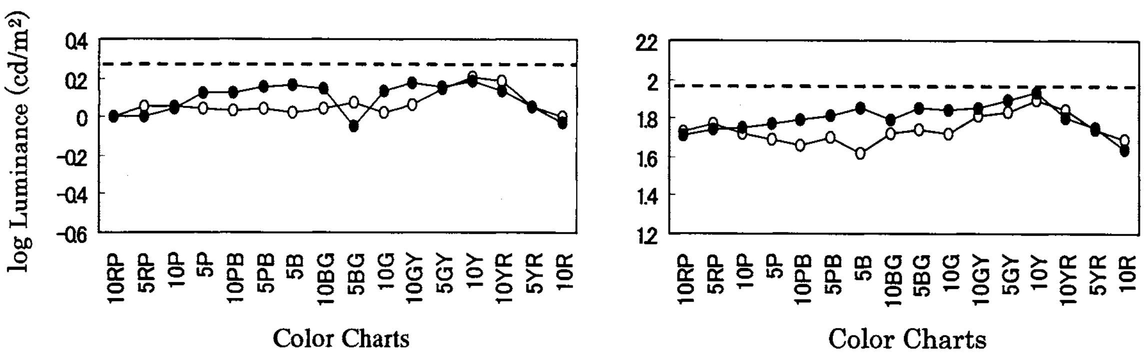

Fig.3 Luminance of various color charts to have the same brightness as N8. Subject, KT.

because of the contribution. It is also well known that yellow color is most inefficient for brightness[3,4] and the present results confirm it by showing the highest luminance with 10Y among all the color charts. The most significant result here is the elevation of the filled circles from the open circles. We can suppose that the elevation was because of the desaturation of color charts when viewed through the goggle.

5. DISCUSSION

All the results suggest us that the effect of the cataract experiencing goggle for the color perception is to desaturate colors. We hypothesized the cause for the desaturation as follows. Light from surrounding environment coming to the eyes is scattered by the haze filter of the goggle, enters the eyes, and overlays the retinal image of a colored chart. As the environment light is considered achromatic in general, it desaturates the color of the chart. In a supplementary experiment we measured the colors of various color charts by a colorimeter under various illuminance levels of the surrounding environment. The measurement clearly showed the desaturaiton of the color and the desaturation was stronger with higher levels of illumination. The property of the color filter used for the cataract experiencing goggle was low in its transmittance at short wavelengths, which should affect the color of charts to shift towards yellow. The effects of color filter and haze filter cooperate to desaturate blue color, but they oppose with each other for yellow color. The effect of the haze filter of the goggle used in the present experiment must be overwhelming compared with the effect of the color filter. The scattering of the incoming light from the environment will take place in the actual crystalline lens of cataract eye and the desaturation of color of the outside world should occur.

REFERENCES

1) Cataract experiencing goggle, a product of Matsushita Electric Industrial Co., Ltd.

2) M. Ikeda and S. Ashizawa; Equivalent lightness of colored objects of equal Munsell Chroma and of equal Munsell Value at various illuminances, Col. Res. Appl. 16 (1991) 72-80.

3) M. D. Fairchild and E. Pirrotta; Predicting the lightness of chromatic object colors using CIELAB, Col. Res. Appl. 16 (1991) 385-393.

4) M. Ikeda, S. Ashizawa and H. Kobayashi; Hue coefficient of equivalent lightness formulas, J. Illum. Engng. Inst. Jpn. 78 (1994) 511-515. (in Japanese).

---

*Correspondence; ro003974@se.ritsumei.ac.jp, Department of Photonics, Faculty of Science and Engineering, Ritsumeikan University, Nojihigashi, Kusatsu-shi, 525-8577 Japan

Duality of Color Perception with Colored Eyeglass for Different Color Appearance Modes

Azusa Kusumi*, Mitsuo Ikeda and Hiroyuki Shinoda
Department of Photonics, Faculty of Science and Engineering
Ritsumeikan University

ABSTRACT

Color appearance of a test patch presented in a room was investigated by the elementary color naming method when it was observed through the eyeglass simulating the elderly crystalline lens. The luminance of the test patch and the illuminance of the room were set at different levels to present the object, unnatural and light source color for the test patch. For the object color mode of the test patch, its color remained unchanged, but for the light source color, the color changed toward the color of the eyeglass. The duality of the color perception was observed. We suggest that the duality also takes place in the elderlies whose crystalline lenses changed in the spectral transmittance in time, although the phenomenon should be confirmed with actual elderly observers in the future.

Keywords: color appearance, color appearance mode, color constancy, color filter, the recognized visual space of illumination, crystalline lens, elderlies, eyeglass

1. INTRODUCTION

Yellow glasses to simulate the crystalline lens of elderlies were developed by Okajima et al.[1] and we made an eyeglass by using one of their glasses which simulate 70 years old eyes when worn by a normal 20 years old person. When we see the outside world with the eyeglass the scene should appear almost same as before in color impression because of the color constancy. But when one of the authors AK used the glasses at night the color impression for the scene was quite different from that with her naked eyes. Street lamps, lit windows of houses and lighting signs of stores changed toward yellow, though colors of other objects remained same as usual. The object color did not change in its apparent color but the light source color changed toward the color of the eyeglass at night. The color constancy held for the object color but not for the light source color. We called this phenomenon the duality of color perception.

We can explain this experience by the concept of the recognized visual space of illumination, RVSI[2-6]. When one comes to a space he/she immediately understands how the space is illuminated. We define this understanding or recognition as RVSI and express it by a circle as shown in Fig.1. Its color property is expressed by the direction of axis and the brightness perception for the space by the size of the circle. Any objects in

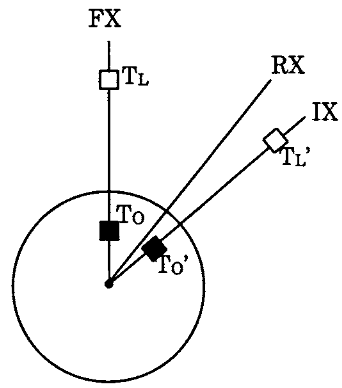

Fig.1 Scheme of RVSI.

these spaces are plotted within the circle such as T_O and T_O'. Their positions are determined by their lightness and the brightest object such as a white paper comes on the circumference. Let us suppose we see an achromatic object T_O in a space with and without eyeglass. We perceive them achromatic because of the color constancy[7]. When we wear the eyeglass, the outside world changes as if it is illuminated by light of color given by the eyeglass. The illumination axis of RVSI rotates to IX and the object T_O comes on the axis as shown by T_O'. The recognition axis RX is pulled by the IX so that the angle between the two axes becomes small. As the apparent color of any object is determined by the angle from the RX to the direction of the object plotted in the RVSI circle, the appearance of T_O' remains almost same as T_O.

If the object T_O is illuminated locally by an additional light, its luminance becomes higher than the white paper and its position goes outside the RVSI circle. The color appearance should become in the RVSI theory unnatural as an object in the space. For a further increase of the luminance the position comes far from the circle as shown by T_L or T_L' and the surface of the object finally begins to appear to radiate light or to shine itself, of which color appearance is called the light source color or the self-luminous color. Because the position is way out the RVSI its color appearance is not determined in relation to the recognition axis RX but in relation to the fundamental axis FX. The T_L moves to T_L' with the eyeglass and its color appearance is yellowish as the angle from FX to T_L' is large toward yellow.

In this experiment, we will confirm the color appearance of T_O remains same but T_L changes toward yellow when a subject wears the eyeglass by measuring the color by the elementary and categorical color naming methods in an experimental room.

2. EXPERIMENT

We constructed an experimental room shown in Fig.2. The room is illuminated by ceiling fluorescent ramps of the daylight type with the correlated color temperature 6500K. Artificial flowers, books, a PC, and other objects were placed on shelves and a mask, a calendar and a small vase were hung on the walls to simulate a normal room. On one of the shelves a test patch box of the size 26cm x 22.5cm was placed. It was made of acrylic boards and a fluorescent lamp was installed inside. At the center of the surface a hole of 3cm x 3cm was opened to serve as the test patch. All other parts were covered with a black paper to caulk the light coming from inside except the test patch hole. In this way we could adjust the luminance of the test patch independently from the ceiling light.

To present various colors of the test patch we inserted colored filters over the hole of the test patch box. We employed 15 colors for the test patch to include deep color, tint color and various hues. A subject sat on a chair and looked at the front wall from the distance 150cm binocularly. He first judged the apparent color mode of the test patch and reported by one of three modes, the object color, the unnatural color as an object in the room, and the light source color. Then he selected one color from basic 11 colors, red, yellow, green, blue, orange, purple, pink, brown, white, gray and black. After that

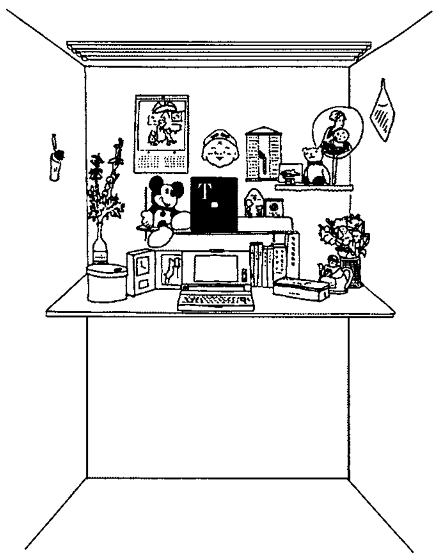

Fig.2 View of front walls. T, test patch.

he reported the amount of blackness, whiteness and chromaticness and the hue by the elementary color naming method by using four unique hues R, Y, G and B. These judgments were all done with and without the eyeglass. The room illuminance of 5 and 1500 lx were employed. We set up the test patch luminance at three levels so that the subject could see the object color, the unnatural color and the light source color under respective room illuminance. The chromaticity coordinates of the test patches at the level of the light source color under the room illuminance 5 lx are shown in Fig.3 for both cases of the with- and without-eyeglass.

Five young subjects participated in the experiment, RY (26 years old, female), AK (24, female), YS (23, male), TK (23, male) and YI (22, male).

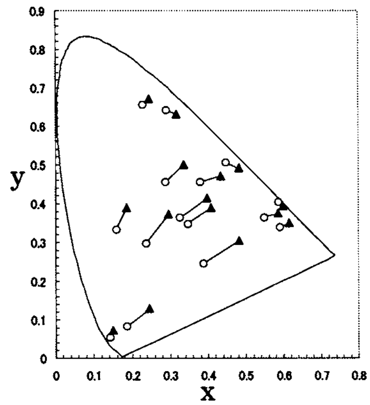

Fig.3 Chromaticities of test patches.

○*, without eyeglass;* ▲*, with eyeglass.*

3. RESULTS

The results of the elementary color naming are shown in Fig.4 for the subject AK. The amount of chromaticness is taken along the radius where the outmost circle represents 100%. The hue is shown along the arc. The left column shows the results for 5 lx and the right for 1500 lx. The upper two graphs show the results for the test patch at the level of the object color mode, the middle the unnatural color and the bottom the light source color.

Arrows correspond to test patches. The origin of an arrow represents the color appearance of the test patch without the eyeglass and the arrowhead with the eyeglass. Some colors did not change much and the arrows were not drawn.

The results of the upper right with the combination of the object color mode and 1500 lx show that the length of arrows is either almost zero or very short if any, indicating that there was practically no change in color in all the test patches whether the subject wore the eyeglass or not. The results confirm the subject AK's experience outdoors at daytime with the eyeglass. The results of the lower left with the combination of the light source color and 5 lx show that the length is large with most test patches. The color changed with the eyeglass. Again the results confirm her experience outdoors at night. The tendency is most clearly indicated by the achromatic test patch plotted at the center of diagram. The arrow length is practically null in the combination of the object color and 1500 lx, but it is long and its

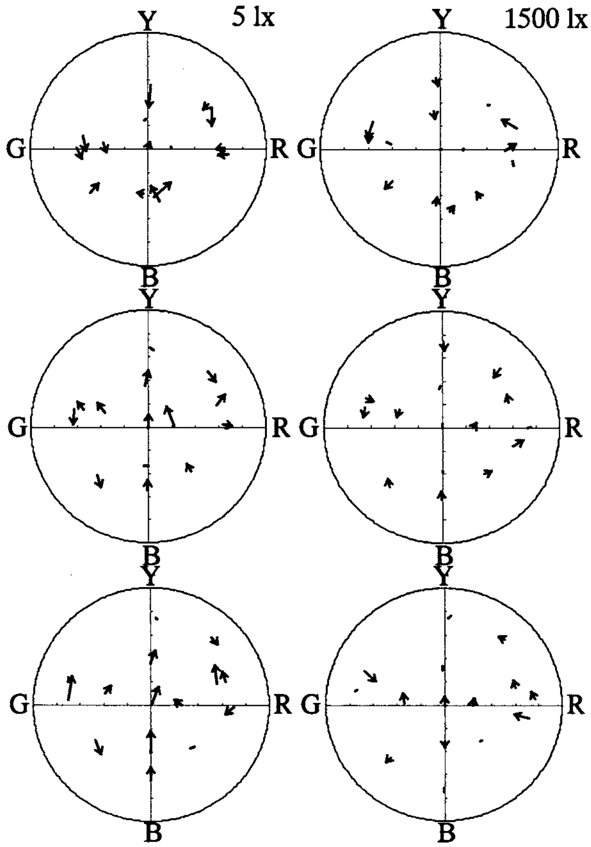

Fig.4 Results of elementary color naming for test patches. Subject, AK. Arrowheads, with eyeglass; Origin of allow, without eyeglass.

direction is toward yellow, or toward the color of the eyeglass in the combination of the light source color and 5 lx. The color constancy did hold in the former case and did not in the latter case, thus the duality of the color perception with the colored eyeglass.

The result from the categorical color naming confirmed this tendency. The achromatic test patch remained achromatic with the eyeglass for the condition of the object color and 1500 lx, but it changed to yellow with the eyeglass for the condition of the light source color and 5 lx.

Most of arrows obtained for the room illuminance 5 lx shown at the left column in Fig.4 are long, but their directions are different depending on the color appearance mode. When the test patches appeared the light source color, the most arrows direct toward yellow implying the direct effect of the color of the eyeglass as shown at the left bottom. When the test patches appeared the object color, the arrows direct toward the center implying no change of hues. The color constancy holds here.

When we compare two figures at the bottom of Fig.4, the arrows under the room illuminance 1500 lx are shorter although in both cases the test patches appeared the light source color. The reason for this difference lies in the ratio of the luminance of test patch to the brightness size of the RVSI. It is much smaller under 1500 lx than under the 5 lx. The appearances of test patch are still affected by the RVSI in the case of 1500 lx but they are no longer determined in relation to the RVSI in the case of 5 lx. The color constancy holds in 1500 lx, but not in 5 lx.

References

1) Katsunori Okajima and Masanori Takase: Effect of wearing filter spectacles to simulate the aging of the human lens in the color naming of Munsell color chips. J. Illum. Engng. Inst. Jpn. Vol.84 No.11 (2000) 838.

2) Mitsuo lkeda: Appearance of colours in environment and their use in life. Abstract Volume, AIC 7th Congress, Budapest (1993) 257.

3) Yoko Mizokami, Mitsuo Ikeda and Hiroyuki Shinoda: Lightness judgment in relation to the size of the recognized visual space of illumination controlled by lightness and color saturation of objects. Proc. AIC 8th Congress, Kyoto (1997) 167.

4) Mitsuo Ikeda, Hiroyuki Shinoda and Yoko Mizokami: Three dimensionality of the recognized visual space of illumination proved by hidden illumination. Opt. Rev. 5 (1998) 200.

5) Mitsuo Ikeda, Hiroyuki Shinoda and Yoko Mizokami: Phenomena of apparent lightness interpreted by the recognized visual space of illumination, RVSI. Opt. Rev. 5 (1998) 380.

6) Yuko Hattori, Mitsuo Ikeda and Hiroyuki Shinoda: Method of displaying exact colored scenes perceived by the aged. Proc. AIC Midterm Meeting, Warsaw (1999) 109.

7) Mitsuo Ikeda, Azusa Kusumi and Hiroyuki Shinoda: Color appearance seen through a colored filter of various sizes. Opt. Rev. 8 (2001) 480.

---

*Correspondence; ro003974@se.ritsumei.ac.jp, Department of Photonics, Faculty of Science and Engineering, Ritsumeikan University, Nojihigashi, Kusatsu-shi, 525-8577 Japan

Age-related changes in temporal characteristics of achromatic and chromatic channels.

Keizo Shinomori
Department of Information Systems Engineering,
Kochi University of Technology,
Tosayamada-town, Kami-gun, Kochi 782-8502, Japan (shinomori.keizo@kochi-tech.ac.jp)

ABSTRACT

Temporal characteristics of color vision change with age, as with color appearance and discrimination. Luminous and chromatic impulse response functions (IRFs) were measured for 70 (luminous IRF) and 30 (chromatic IRF) normal observers ranging in age from 16 to 86 years, because theoretical responses to any temporally-modulated visual stimulus can be predicted with use of these functions. In this research, chromatic IRFs were measured in response to S-cone stimulation.

Thresholds were measured for a series of double-flashes separated by intervals from 6.7 to 180 msec for luminous pulses and from 20 to 720 msec for chromatic pulses. The subject's task was to press a button corresponding to one of four quadrants in which the stimulus (a white or chromatic test spot) was detected on a white background (10 cd/m^2). For chromatic pulses, the test spot was changed from white to bluish along an individually determined tritan line. The retinal illuminance was equated across observers.

The calculated luminous IRFs were characterized by an initial positive phase (excitation) followed by a negative phase (inhibition) but there was no negative phase for S-cone IRFs. In general, there were no significant changes in the time to the peak or duration of the excitatory phase. The luminous IRF of some observers over 60 years of age, however, had a reduced or absent inhibitory phase, causing their excitatory phase to be long (Shinomori & Werner, 2003). The duration of chromatic IRFs was much longer than the achromatic IRFs.

PURPOSE

Recently, traffic accidents among elderly people have become a serious problem in Japan. Not only those extreme cases, it is well known that physical activities become slower with age. Although these problems are caused largely by slower motor actions, as well known, it may partially be caused by slower information processing in visual system. Senescent losses in sensitivity have been demonstrated for all three cone-pathways and have been shown to be due to both optical and neural factors. Age-related changes in temporal contrast sensitivity and resolution have also been demonstrated, but they are subtle when retinal illuminance is controlled (Kim & Mayer, 1994; Tyler, 1989).

The impulse response function (IRF) is a theoretical response to an infinitely short flash. The temporal CSF is commonly used for inferring the IRF, however, it only provides information about amplitude and does not preserve phase (Victor, 1989). The shape of the IRF can be derived more accurately using this double-pulse method because an auto-correlation function of the IRF can be obtained. Chromatic IRFs were obtained in previous study but mostly measured with red and green isoluminant pulses (Uchikawa and Yoshizawa, 1993; Burr and Morrone,1993). Previously measured chromatic (blue) IRFs were obtained using short-wave stimuli to which not only S-cones, but also M- and/or L-cones may have been sensitive (Uchikawa and Ikeda,1986).

This study addresses two questions in relation to these previous findings:

* *Is the amplitude of the impulse response lower with age?*
* *Is the impulse response slower with age?*

My colleague, (Dr.) John S. Werner in UC Dacis, and I sought to measure the chromatic IRF of an isolated human S-cone pathway (S-cone IRF) with the double-pulse method. We have already measured the luminous IRF presented in our previous work (Shinomori & Werner, 2003).

METHODS

Stimulus : We used a double pulse method to measure the impulse response function (IRF). Each pulse was presented in a single frame on a CRT display (SONY GDM-200PS) operating at a 150 Hz frame rate controlled by a video board (Cambridge Research Systems Inc. VSG2/3). Inter stimulus intervals (ISIs) are set by changing a number of blank flames between pulses from 6.7 to 180 msec for luminous pulses and from 20 to 720 msec for chromatic pulses.

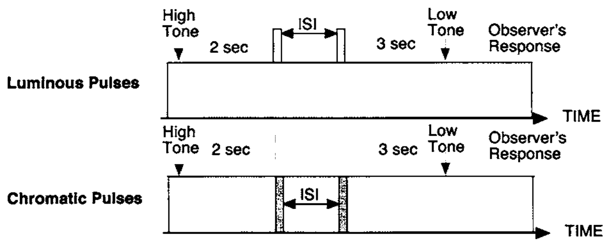

Figure 1. Temporal profile of the double pulses.

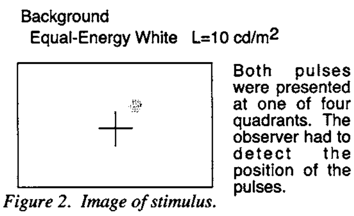

Figure 2. Image of stimulus.

The luminous pulses had a spatial Gaussian shape (±1 SD =2.3 deg. diameter) presented as an increment on a 10 cd/m2 background, having the same chromaticity as the pulse. The chromatic pulses had the same shape presented as a chromatic change from a white background to a bluish color on an individual tritan line. Step size of the chromatic change was defined in terms of S-cone Td. Luminance was always kept constant (10 cd/m2) in the chromatic pulses.

Observers : We employed 70 observers for the measurement of the luminous IRF and 30 observers for chromatic IRF ranging in age from 17 to 86 years. We used only the data form observers who had passed eye exams. The observers used for the analysis in chromatic IRF were 3 males and 3 females in each observer group (16~29, 30~44, 45~59, 60~74, 75~90 years old).

Retinal illuminance and Individual Tritan line : To minimize age-related changes in retinal illuminance, the stimuli were viewed through a 2.1 X telescope that created a 1.5 mm exit pupil conjugate with the eye pupil to eliminate effects of age-related changes in pupil diameter. Retinal illuminance was equated approximately across observers using heterochromatic flicker photometry (18Hz) whereby the intensity of the blue and green phosphors was adjusted to the red phosphor. Lenticular absorption of the red phosphor varies negligibly across this age range. Individual Tritan lines were measured by using metameric matching of two bipartite fields (2deg*2deg square) superimposed on a blue adaptation light (420 nm in Maxwellian view).

Procedure : To control for possible changes of criterion with age, a spatial 4-alternative forced-choice (4AFC) method was combined with a staircase procedure in which the luminance or S-cone Td of both pulses was changed simultaneously to obtain a contrast threshold. After 5minutes dark adaptation, the observer looked at the screen with a white background in 5 minutes. After 10 minutes adaptation, stimuli were presented on the screen after a high tone. The observer had to answer the place where the pulses were presented by pressing one of four buttons after a low tone. In one session, 14 ISI settings were tested with 14 different staircases in a random order. Each subject participated in three to four sessions.

MODEL ANALYSIS

We used the IRF model by Burr and Morrone (1993) and the model of detection threshold by Watson (1979) to calculate IRFs from the threshold data. This model does not assume a minimum phase.

Model of Impulse Response Function (Burr and Morrone, 1993)

Impulse Response Function I(t); $I(t) = a_0 H(t)\, t \sin\{2\pi[a_1 t (t+1)^{-a_2}]\} \exp(-a_3 t)$

$(\text{where } H(t) = 0 \quad (t < 0); \quad H(t) = 1 \quad (t >= 0))$

**** Model of Detection Threshold with Probability Summation over Time (Watson, 1979)***

Visual Response Function R(t, τ); $R(t, \tau) = K[I(t) + H(t-\tau) I(t-\tau)]$

$(\text{where } H(t-\tau) = 0 \quad (t < \tau); \quad H(t-\tau) = 1 \quad (t \geq \tau))$

Proportion correct p; $$p = 1 - (1 - r)e^{\left[-\left(\int_0^T |R(t,\tau)|^\beta dt\right)\right]}$$

(where r = probability by chance level; r =1/4 (4AFC), $p =$ ‑ 2 2(Two down one up staircase), T = Reasonably-long time (3.18 sec in this experiment, $\beta = 4$.)

Four parameters in the model equation were changed to get the best fit to the threshold data with a leastsquares method.

RESULTS

Figures 3 and 4 show threshold data (left panel) and model IRFs (right panel) for a 36.3 year-old observer (#1) measured by luminous and chromatic pulses, respectively.

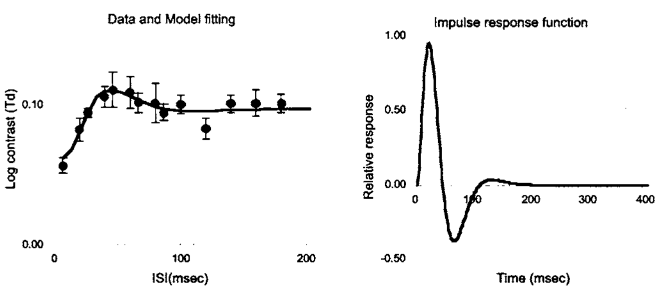

Figure 3. Luminous IRF

Left: Contrast thresholds and model fits plotted as a function of ISI for observer #1 (36.3 years old). Error bars denote Standard Error of the mean (SEM). Right: IRF calculated from the model for the same observer.

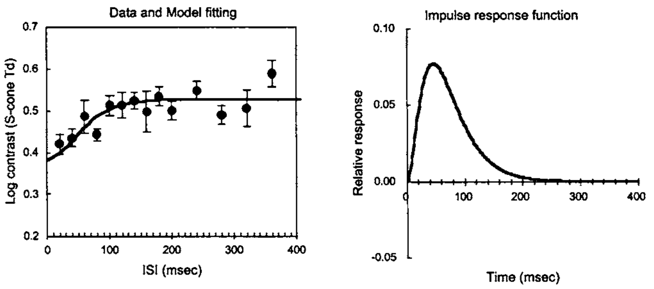

Figure 4. S-cone IRF

Same with figure 3 except the data for the S-cone IRF (for the observer #1).

As expected from previous works, only the luminous IRF has the secondary negative phase and is much faster than the chromatic (S-cone) IRF. Both in luminous and chromatic IRFs, there is an observer's variation. Figures 5 shows the luminous IRFs (left panel) and chromatic IRFs (right panel) for the observer #1 denoted by sold curves and the other observer #2 (59.7 years old) denoted by gray curves.

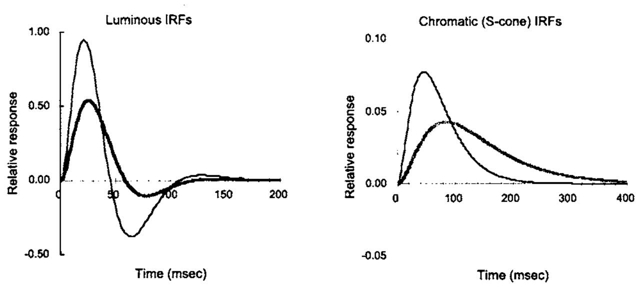

Figure 5.
Observers' variation

Left: Luminous IRFs for one young (36.3 yrs. old) observer denoted by a solid curve and one old (59.7 yrs. old) observer denoted by a gray curve.

Consistent with these examples, younger observers typically have IRFs with higher amplitude. But the temporal features are relatively similar to that of older observers (See Discussion).

DISCUSSION

We analyzed two aspects of the IRF data in relation to age.

Temporal characteristics of IRFs

First, we analyzed the temporal characteristics of IRFs. Figure 6 shows the duration of the first (excitatory) phase in luminous IRFs as a function of age (Left panel) and the duration of the chromatic (S-cone) IRF measured from 0 to the time when the amplitude is 5% of the peak amplitude.

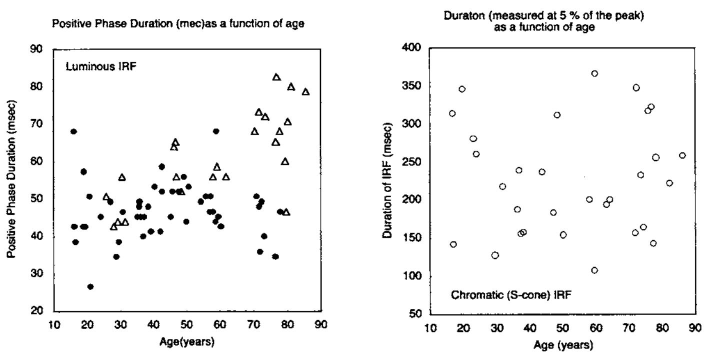

Figure 6. Duration of IRF as a function of age

Left: Positive Phase Duration of Luminous IRF. Triangles denote the IRFs which have low signal level.

Right: Duration of Chromatic IRF measured at 5 % of the peak ampllitude.

The luminous IRF can be slower with age but it happens only for observers whose IRFs have little or no inhibitory phase. The speed of the IRF decreases little with normal aging (Shinomori & Werner, 2003). On the contrary, this tendency could not be found in chromatic IRF.

Strength (Gain) of IRFs

Second, we also analyzed the data in terms of peak amplitude of IRFs. Figure 7 shows peak amplitude of calculated IRFs as the function of age.

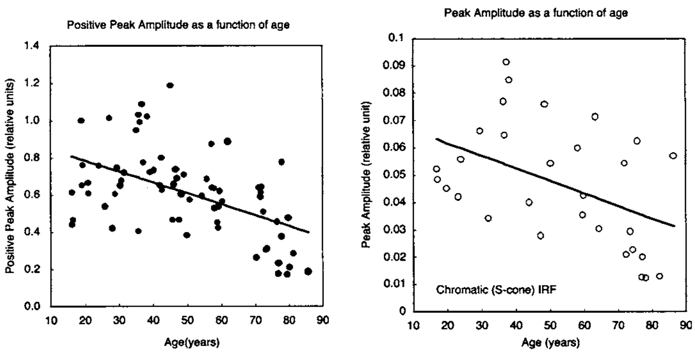

Figure 7. Peak Amplitude of IRF as a function of age

Left: Positive Peak Amplitude of Luminous IRF. Black line denotes the linear regression line.

Right: Peak Amplitude of Chromatic IRF. Black line denotes the linear regression line.

The amplitude reduces with age both in luminous and chromatic IRFs.

Age-related change in IRFs

These results suggest that the human visual system maintains a stable speed of response to a flash until about 80 years of age; even while the response signal level decreases with age. It is reasonable to ignore the age-related reduction of signals, especially caused by change in cones, if possible, because the IRFs is the basic information for processing temporal feature of visual stimuli. If the IRFs would be slower, some visual processing like estimate the speed of stimuli might be affected.

ACKNOWLEDGMENTS

This study was funded by the High-Tech Research Center Grant to the Kochi University of Technology, the National Institute on Aging (grant AG04058), the National Eye Institute (Core grant EY12576), and a Jules and Doris Stein Professorship from research to Prevent Blindness.

REFERENCES

Burr, D.C. & Morrone, M.C. (1993) J. Opt. Soc. Am., **10**, 1706-1713.
Kim, C.B.Y. & Mayer, M.J. (1994) J. Opt. Soc. Am., **11**, 1958-1969.
Shiomori, K. & Werner, J.S. (2003) Vision Res., **43**, 617-627.
Tyler, C.W. (1989) J. Opt. Soc. Am., **6**, 481-490.
Uchikawa, K. & Ikeda, M. (1986) J. Opt. Soc. Am. A, **3**, 2109-2115.
Uchikawa, K. & Yoshizawa, T. (1993). J. Opt. Soc. Am. A, **10**, 1697-1705.
Victor, J.D. (1989) J. Opt. Soc. Am. A, **6**, 1302-1303.
Watson, A.B. (1979) Vision Res.,**19**, 515-522.

AGE-RELATED LUMINANCE AND SPAN OF CATEGORICAL COLOURS FOR DESIGNING VISUAL SIGNS FOR OLDER PEOPLE

Ken Sagawa

National Institute of Advanced Industrial Science and Technology, Japan

ABSTRACT

Two age-related changes in human color vision, spectral sensitivity function and spans pf categorical colors, were investigated. Spectral sensitivity function showed gradual sensitivity loss in the short-wave region (blue lights) with age, which should be taken into account in designing visual sign using blue colors. Span of categorical colors were determined for younger and older observers to show the age-related difference in size and shape of the span, which also should be taken into account in color combinations used in visual signs.

1. INTRODUCTION

National Institute of Advanced Industrial Science and Technology (AIST) in Japan has launched a number of projects to develop human technology that meets for the aging society providing safe and comfort life environment for older people. Fundamental Research on Standardization is one of them in which physical and psychological database of human functions are being developed for social and industrial use. In this paper, two age-related changes of human color vision are to be shown together with examples of how to use those data in designing visual signs seen by older people.

2. AGE-RELATED LUMINANCE DEFINED BY SPECTRAL SENSITIVITY AS A FUNCTION OF AGE

Human eye becomes less and less sensitive to the short-wave light due to the transmittance change of lens of the eye. Quantitative data on how much the sensitivity decreases with age across the visible spectral range was

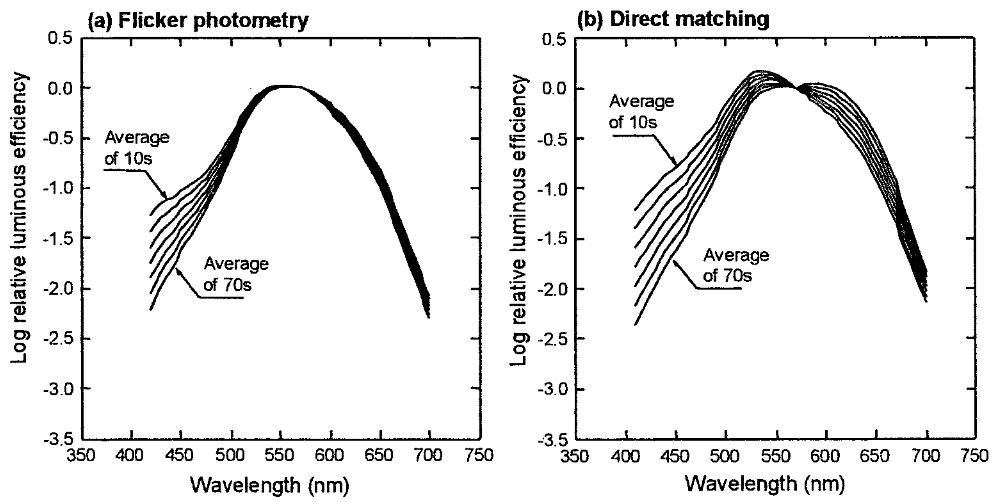

Figure 1(a) and 1(b): Spectral luminous efficiency functions for seven age groups. (a): Flicker photometry. (b): Direct brightness matching.

reported by Kraft and Werner (1994), but more data are needed for developing a standard data that should be used in photometric system. In AIST the spectral sensitivity function of the eye was measured by flicker photometry (FP) and by direct brightness matching (BM) for 91 and 97 observers respectively with different age from 11 to 78 years old (Sagawa and Takahashi, 2001). The summarized data for 7 age group divided in decades are shown in Figure 1(a) and 1(b). Each function of different age groups is based on the data of about 10 observers or a bit more except for the function for the 20s and the 60s group for which more than 20 observers were participated. All data are normalized at 570 nm. It is obvious that in the short-wave region the sensitivity decreases gradually with age and the difference between the 10s and the 70s function is about one log unit at most both for the FP and BM data. It should be noted that the similar but less extent sensitivity reduction is observed for the long-wave region for the BM data, which is considered due to the contribution of chromatic signals to brightness that changes with age.

The FP data can be directly applied to the photometric system with efficacy of 683 lm/w at the 540 Thz spectral light by definition, i.e.:

$$L_{(a)} = K_m \int L_{e,\lambda} V(\lambda)_{(a)} d\lambda \qquad (1)$$

where $L_{(a)}$ is the age-related luminance and $V(\lambda)_{(a)}$ is the sensitivity function of the age group a, while K_m is maximum efficacy and $L_{e,\lambda}$ means the spectral radiance.

Figure 2 illustrates how the age-related luminance should be used. The example of a visual sign constitutes blue characters on dark yellow background, spectral radiance of which being virtually defined as shown in the figure (Sagawa, 2002). With these given spectral radiance data for the sign and the background, it is possible to calculate the age-related luminance by using equation (1) with an appropriate choice of sensitivity function $V(\lambda)_{(a)}$. Two calculation examples are shown in Figure 2, one by usuing the 20s function and the other one by the 60s

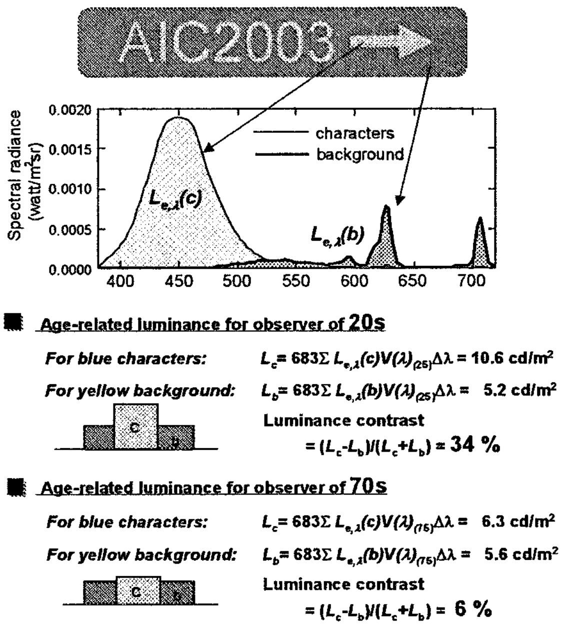

Fig. 2: Calculation examples of age-related luminance and contrast specification by using the luminance for the younger (20s) and older person (70s).

function. By calculating this age-related luminance for both background and characters the luminance contrast can be obtained directly and the visibility of the sign can be evaluated. The contrast is 34% for the younger (20s) observer showing high contrast enough to be seen clearly, but the contrast is 6% for the older (60s) observer which shows slightly over the threshold meaning not good visibility. Therefore, the sign as shown in Figure 2 appears very differently to the younger and the older observer, which should be taken into account in designing visual signs seen by people of different age.

3. SPAN OF CATEGORICAL COLORS

There is a need for creating color combination with easy identification as well as easy discrimination to be used in visual signs such as traffic and emergency signs. In order to provide a guideline of such color combination, the span of color category was measured for a total of 13 fundamental colors, selected as red, orange, yellow, green-yellow, green, blue-green, blue, purple-blue, purple, purple-red, white, grey, and black.

The measurement was based on similarity of colors judged by the observers between a fundamental color chosen from the 13 colors above mentioned and a test color chosen from a total of 286 Munsell color chips. Percentage of observers who judged as "similar" for each pair of colors was the measure for the span of category. A total of 50 older observers (60-78 years old) and of 50 younger observers were participated (18-26 years old). A photopic (500 lx) and a mesopic (0.5 lx) lighting condition were employed.

Figures 3 shows two examples of the span of fundamental color, red and green, expressed in the Munsell color space at the Value 5 plane for younger people (solid lines) as well as for older people (dashed lines) for

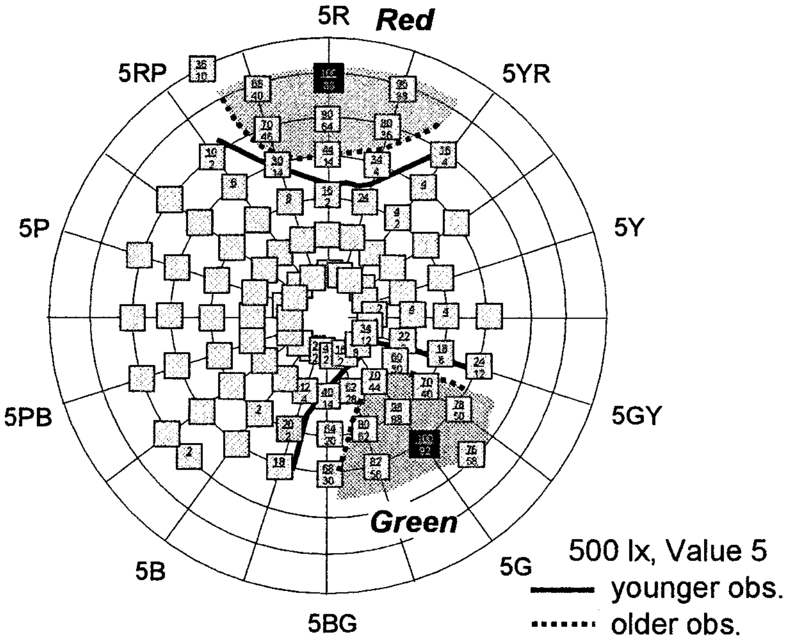

Fig.3: Two examples of the similarity data at around red and green colors and span of categorical colors obtained by the experiment.

comparison. In the figure test color patches used are also shown. The reddish area ranges from the red-purple (5RP) to the orangish red (5YR) forming so to say the red family. Similarly, the greenish area spans from the green-yellow to blue-green forming the green family. Each area can be surrounded by the boundary of certain level of "percent similar" that gives the span of color category for a corresponding fundamental color. In this figure, similarity of 30 % is taken to draw the boundary of color category for both younger and older observers.

Figure 4 shows the spans of all the fundamental colors used in the experiment both for younger and older observers. Generally speaking, the span is larger for younger observers (solid line) than for older observers (dashed line) in the photopic level. One reason for this might be that the colors are desaturated for older people

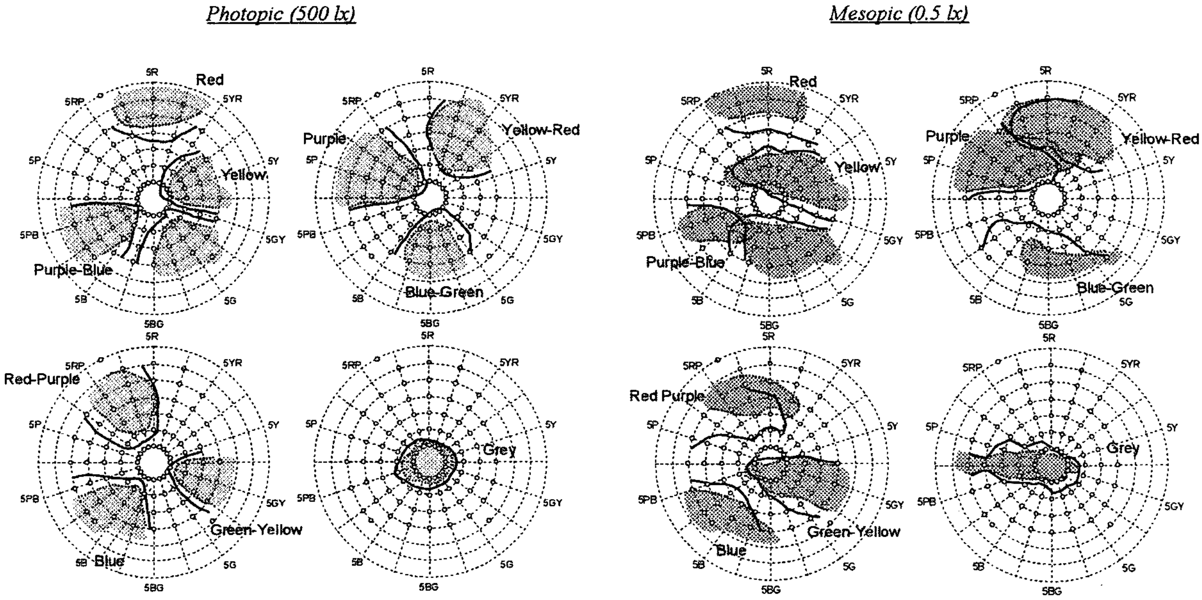

Fig.4: Spans of categorical colors expressed in Munsell value 5 plane for photopic (500 lx) and mesopic (0.5 lx) conditions. Solod and dashed carves mean the data for younger and older observers respectively.

than the younger. Despite of these quantitative differences, it can be said no basic difference is seen in the shape of the category area between the older and younger observers throughout all the data obtained in the color space. For the mesopic condition, however, the difference between older and younger observers is quite large, not only in quantitative aspect but in qualitative aspect, too. The reason for this is not clear yet, but may be due to the difference in absolute level of light intensity between older and younger observers.

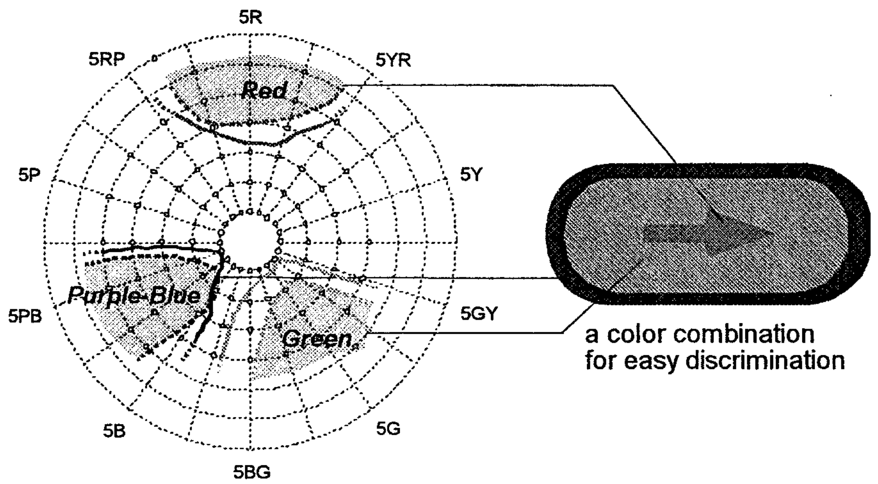

Figure 5: An example of color combination for easy discrimination based on different color categories.

It should be noted that the area of each of fundamental colors defined here is not the just noticeable difference of small color difference but an area that forms a family of similar colors with much larger color difference. This means that different colors belonging to the difference categories are not easily confused when they are used in combination. Being based on this idea, an example is shown in Figure 5 how to use these spans of categorical colors. A visual sign that is formed by the colors picked up from different categories as shown in the Figure should be easily detected or discriminated. In Figure 5 the arrow sign is composed of three colors of difference categories, i.e. red, green, and purple-blue defined in the present study and is expected to be seen in high discrimination not only by older people but by the younger people as well. Other examples of color combination are also possible which are as equally discriminable as the example as long as colors are selected from those three categories. This flexiblily in color choice is also a merit of color combination based on color category.

4. SUMMARY

Human color vision changes with aging were shown for two major color functions in this paper, spectral sensitivity function and span of color category, together with experimental data obtained for a large number of observers including the elderly. These quantitative data, and hopefully more for other color vision functions, are being required for designing visual signs that can be seen clearly by people at any age.

REFERENCES

1) Kraft, J.M. and Werner, J.S. (1994). Spectral efficiency across the life span: flicker photometry abd brightness matching, J. Opt. Soc. Am., **A 11**, 1213-1221.
2) Sagawa, K. and Takahashi, Y. (2001). Spectral Luminous efficiency as a function of age, Journal of the Optomological Society of America, **A 18**, 2659-2667.
3) Sagawa, K. (2002). Visual finctions of older people and visibility of traffic signs, J. Gerontechnology **Vol 1** June 2002, 296-299.
4) Ishida, T. (2002). Color Identification Data Obtained from Photopic to Mesopic Illuminance Levels, Color Res. and Appl., 27, 252-259.

Change of color appearance of elderly observer through human lens and intraocular lens

Miyoshi Ayama*, Kohei Narisada**, Noriyuki Suda*

* Graduate School of Engineering, Utsunomiya University, Japan

** Faculty of Psychology, Chukyo University, Japan

ABSTRACT

Hue and saturation evaluation, subjective blackness and categorical color naming experiments were conducted for one elderly observer whose left eye is a crystalline lens eye while the right one is implanted an intraocular lens. Stimuli were presented either in a surface-color mode or in a self-luminous mode using the Munsell charts and CRT. Measurements were done one year and two years after the implant surgery. The color matching between the two eyes was carried out in the second experiment. All the results showed the tendency explained mainly by the deterioration of the spectral transmittance of the lens in the short wavelength region. The results of the first and the second experiments showed similar tendency. It is indicated that the color appearance through the crystalline-lens eye and through the intraocular-lens eye does not fuse after two years adaptation to visual environment in everyday life.

Keywords: Color appearance, Elderly observer, Intraocular lens

1. INTRODUCTION

Intraocular lens helps to regain visual functions of people who suffers from crystalline lens browning by severe cataract. However, it has often been pointed out that patients with intraocular implants complain glare and chromatopsia. Little information has been indicated in the literature on the presice measurement comparing color appearance through the intraocular-lens eye with that through human crystalline-lens eye.

In this study, psychophysical experiments were carried out to measure color appearance of a number of color stimuli, presented either in a surface-color mode or in a self-luminous mode, using Munsell charts and CRT, for a male observer whose right eye is an intraocular-lens implanted while his left eye is a human crystalline lens. The results measured with monocular vieing condition, with the left eye or the right eye, and with binocular viewing condition are compared.

2. EXPERIMENT

2.1 Observer

Observer in this study is a male, age 69 at the surgery. Eye decease was age-related cataract and macula fibrosis. He had the operation to extract the crystalline lens and implant the intraocular lens for his right eye in August 1998. The first and the second experiments were carried out in September 1999, and October 2000, about one and two years after the surgery, respectively. At the time of experiments, visual acuity was corrected to 1.0 and 0.9 for his right and left eye, respectively, using the glasses.

2.2 Color Appearance Evaluation Experiment

In the experiment to evaluate the color appearance of the stimuli, 20 Munsell charts and 25 CRT color stimuli were prepared for monocular measurement, whereas 10 Munsell charts and 13 CRT stimuli were employed for the binocular measurement. The size of the test stimulus was 2 deg $\times$2 deg square and presented at the center of either a gray surround (surface-color mode) or a dark surround (self-luminous mode). Luminance of the Munsell chart test stimuli was set at about 35 cd/m^2, while that of the CRT test stimuli was set about 28 to 37 cd/m^2. Luminance of the gray surround in the surface-color mode setting is about 64 cd/m^2. Experimental conditions were indicated in Fig.1.

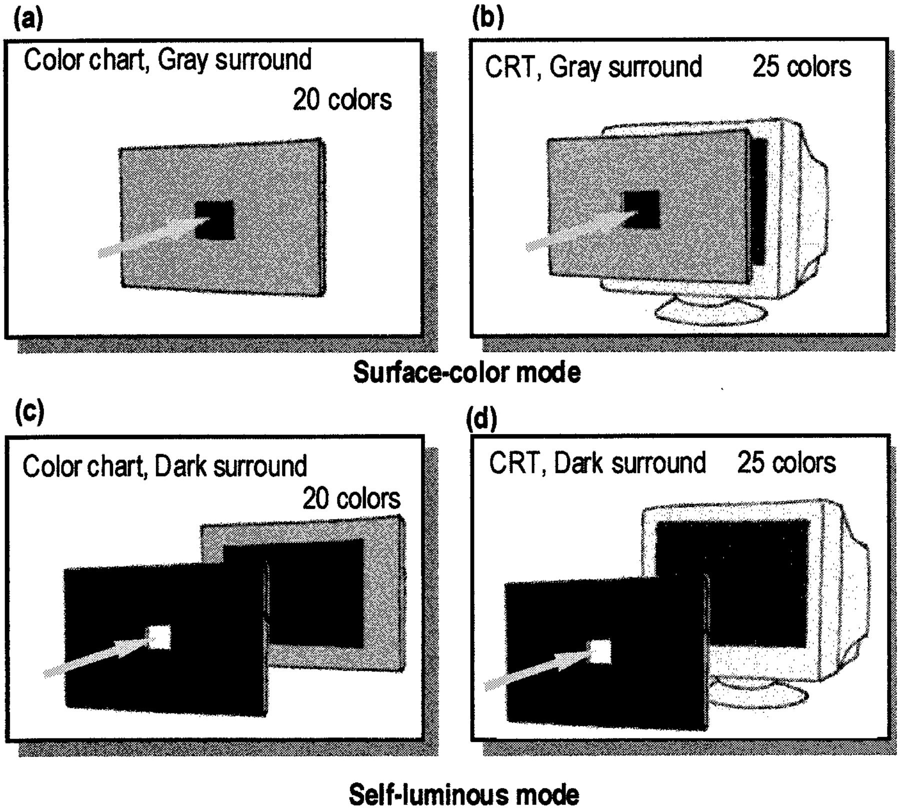

Figure 1. Experimental conditions.

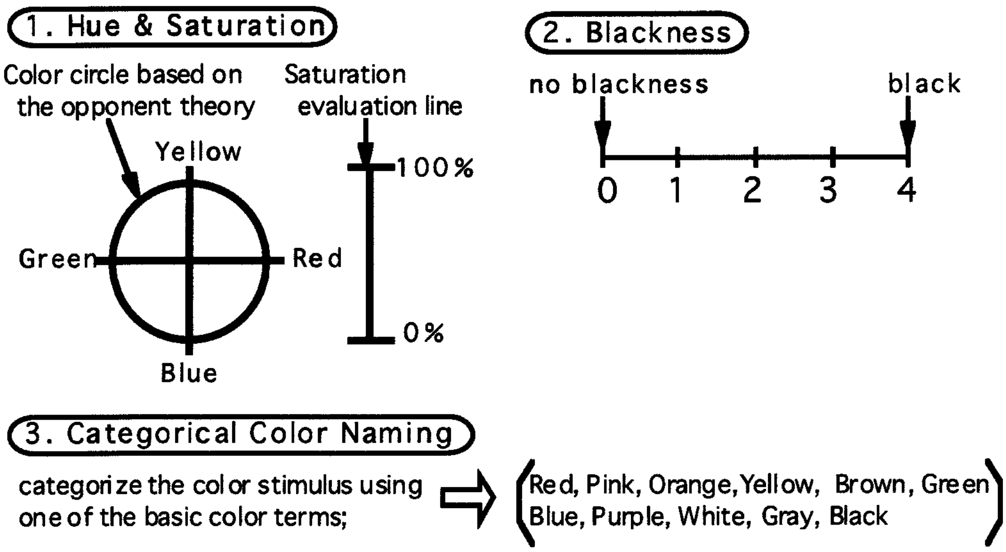

Figure 2. Experimental procedures in the color appearance evaluation.

Each session was preceded by 5 min of dark adaptation. Then observer began to judge color appearance of the stimulus in the way shown in Fig.2. First, hue and saturation were evaluated using the opponent-colors type color evaluation [1]. Instead of oral response, we employed a pointing technique using a figure shown in the top left of Fig.2. The vertical line on the right is the saturation-evaluation line, the circle on the left is a hue circle where four unique hues are placed at the 3, 6, 9, and 12 o'clock positions, respectively. This figure was attached on the digitizer placed in front of the observer. The observer was instructed to respond to the perceived hue and saturation in the test stimulus by pointing to the corresponding positions on the hue circle and saturation evaluation line. The positions indicated by the observer were entered into a computer. Next, perceived blackness is evaluated using magnitude estimation where 0 corresponds to no blackness while 4 corresponds to a full of blackness, i.e. black. Finally, categorical color naming using eleven basic color terms was done.

2.3 Color Matching Experiment

In the second experiment, color-matching experiment was also conducted. Thirteen CRT test stimuli employed in the color appearance evaluation experiment for binocular observation were used. The observation box that has two small square windows on the wall opposite to the observer and was divided by a perpendicular plate to achieve dichoptic-viewing condition was constructed. Two CRTs, one was used in the color appearance evaluation experiment, and another one for the color matching were placed at the back of the observation box, and the test color stimuli were presented for the right and left eye through small windows with the size of 2 deg X 2 deg. Without any illumination in the box, the stimuli were appeared in a self-luminous mode. The chin rest with forehead stopper was used. Luminance of the test stimuli was lowered to 14 to 18 cd/m^2 to obtain sufficient range of luminance in the color matching adjustments. Four sessions were done for the condition that the test and variable stimuli were presented to the right and left eye, respectively. Another four sessions were repeated in the vice-versa condition.

3. RESULTS

From the hue and saturation judgement, values of saturation and unique hue components (abbreviated as UHC in the following portion) for red, yellow, green, and blue were obtained. UHC, a product of the saturation value and percentage of one unique hue in the hue judgment, was employed as a measure of the perceived strengths of redness, yellowness, greenness, and blueness. For example, with a saturation of 70% and a hue of a mixture of 80% blue and 20% green, the score of the unique blue component (abbreviated as UBC) would be 56%. Simultaneously, the score of the unique green component would be 14%. Thus, if the hue response is not a unique hue, two kinds of UHC are obtained for a single stimulus.

Results in the dark surround (self-luminous mode) condition are more stable than those in the gray surround (surface-color mode) condition. Thus the results in the former conditions are shown here. Fig.3 shows the results of difference of UBC between the right and the left eyes. Dark gray circles denote that the UBC value is higher in the right intraocular lens eye than the left crystalline-lens eye. Pale gray circles, though only a few points are seen in Fig.3, indicate vice versa. Fig.3 (a) and (b) are the results using the Munsell chart and CRT stimuli, respectively, in the first experiment, and Fig.3 (c) and (d) are their counterparts in the second experiment.

As clearly shown in the figure, UBC is higher in the intraocular-lens eye than natural crystalline-lens eye in bluish region. Increase of UBC is brought mainly by the increase of saturation in these stimuli [2], while in some of the green-blue and red-blue stimuli, hue shift toward blue was also observed. Therefore the striking increase of UBC shown in Fig.3 is a net effect of saturation and hue judgements. This tendency is commonly observed in the Munsell chart and CRT stimuli. Furthermore, the results in the first and second experiments show similar property despite a yearlong period between the two measurements. In the results of unique hue component for other hues, i.e., red, yellow, and green, the opposite tendency are often observed that values are higher in the left (crystalline lens) eye than the right (intraocular lens) eye. These results are consistent with that the intraocular lens has higher transmittance in the short wavelength region of the spectrum than that of the aged crystalline lens, so that more bluish light reaches to the retina through the intraocular lens eye resulting a marked increase of UBC [3-6]. In the results of binocular viewing condition, saturation value is higher than that in the right and the left eyes in most of the stimuli, although the results show some variability.

The results in the categorical color naming, the change of the color term most frequently observed was that the stimuli named as 'red', 'orange', 'brown', 'yellow', 'pink', or undefined, in the crystalline-lens eye, were named as 'purple'

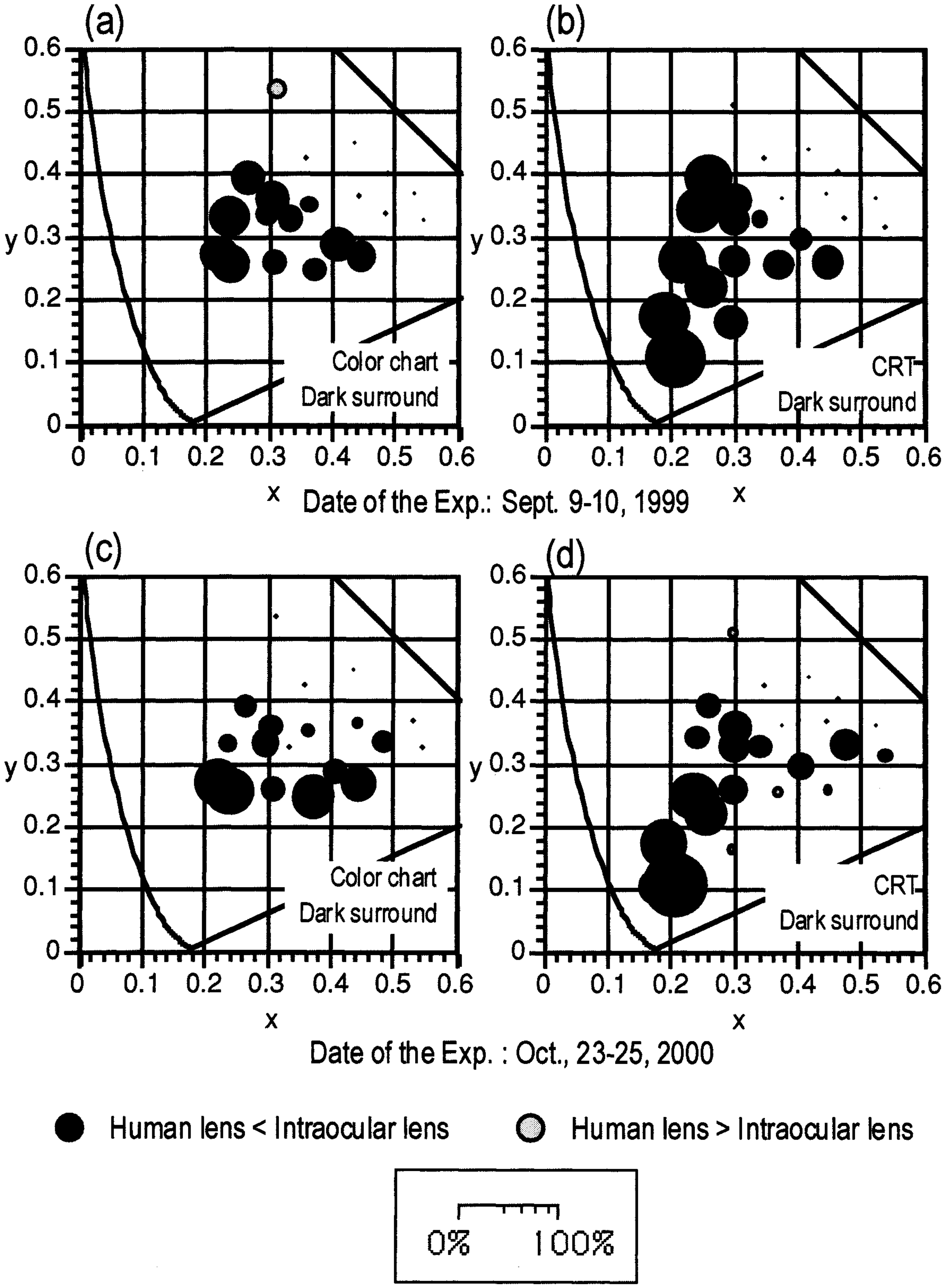

Figure 3. Difference of the unique blue component between the human crystalline-lens eye and intraocular-lens eye. (a) and (b) : the first experiment, a year after the surgery. (c) and (d) : the second experiment, two years after the surgery.

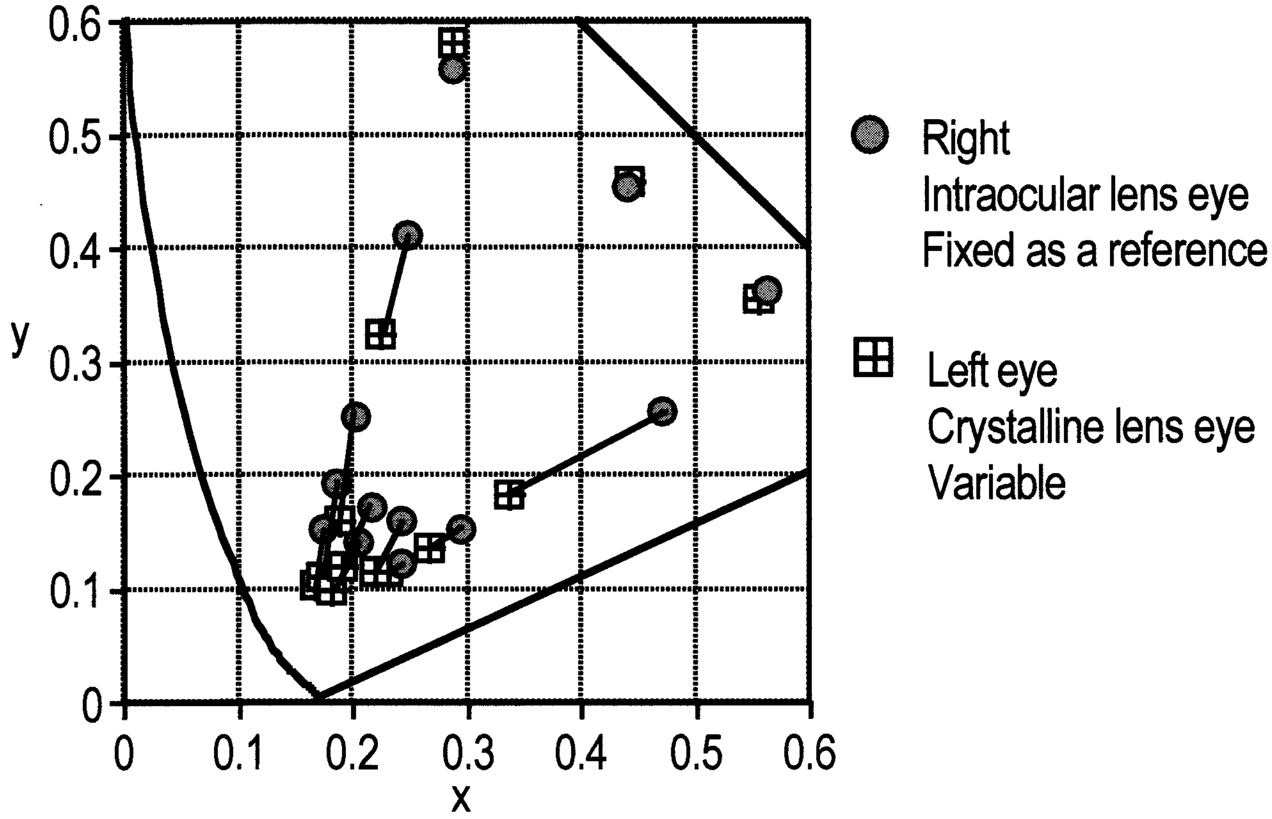

Figure 4. Results of the color matching experiment between the human crystalline-lens eye and intraocular-lens eye.

in the intraocular-lens eye. The change from 'green', 'purple', 'yellow', or undefined in the left eye, to 'blue' in the right eye was also often occurred. Although the observer in this study did not complain the chromatopsia even at the time of the first experiment, the results in this study prove that the color appearance of the stimuli through his right and left eyes are quite different.

These results of color appearance evaluation are consistent with the two pictures of the same scene painted by Claude Monet, famous French painter of Impressionism. One was painted with yellow and orange pallet, whereas the other one was painted with blue, green, and purple pallet [7]. These paintings are believed to be painted with only one eye (crystalline lens eye) or the other (aphakic eye).

The result of the color matching experiment is indicated in Fig.4. The condition here is that the stimuli presented to the right intraocular-lens eye were fixed in chromaticity and luminance as reference stimuli, and those presented to the left crystalline-lens eye were variable. As expected, chromaticity of the matching points of the variable moves toward the short-wavelength region of the spectrum from the reference points except those on the line connecting the red and green phosphors of the CRT. The results are consistent with the color matching results between phakic and aphakic eyes [8]. We calculated the chromaticities of the variable points assuming that the deviation of the chromaticity is caused by the difference between the spectral transmittance curves of the aged crystalline lens [5] and the intraocular lens implanted to his eye. The estimated results are agreed well with the experimental results indicating that difference in the ocular media is the most effective cause for the chromaticity difference in the color matching between the the crystalline-lens eye and the intraocular-lens eye.

4. SUMMARY

Color appearance of the stimuli, presented either in a surface mode or in a self-luminous mode using Munsell charts and CRT, are investigated for one elderly observer whose left eye is a human crystalline-lens eye while the right one is implanted an intraocular lens. Hue and saturation were evaluated using the opponent-colors type color evaluation method. Subjective blackness and categorical color name were also responded. The first and second measurements were done one year and two years after the surgery, respectively. The color matching between the two eyes was conducted in the second experiment. All the results, higher scores of saturation and unique blue component for bluish stimuli in the intraocular-lens eye, higher scores of saturation for other stimuli in the crystalline-lens eye, change of color name from 'green', 'yellow', or 'orange' in crystalline-lens eye to 'blue' or 'purple' in the intraocular-lens eye, chromaticity shifts in the color matching, are explained mainly by difference in the spectral transmittance of the lenses. The results in the surface-color mode and the self-luminous mode, no matter which device, Munsell chart or CRT, is used, showed no significant difference except blackness evaluation. Furthermore, the results in the first and second experiments show similar property despite a yearlong period between the two measurements. It is interesting that chromatic information via intraocular-lens and crystalline-lens eyes does not fuse in higher level of visual pathway after a year span of adaptation

REFERENCES

[1] M. Ayama and M. Sakurai, "Changes in hue and saturation of chromatic lights presented in the peripheral visual field",Color Res. Appl., (in the press).

[2] M. Ayama, N. Suda, and K. Narisada, "Color appearance of elderly observer with and without intraocular lens", in *Proceedings of the International Workshop on Gerontechnology*, AIST, Tsukuba, 2001, pp.81-82.

[3] R.A. Weale, "Age and the transmittance of the human crystalline lens", Journal of Physiology, 1988, 395, pp. 577-587.

[4] J.S. Werner and F.E. Hardenbergh, "Spectral sensitivity of the pseudophakic eye", Arch. Ophthalmol. 1983, Vol. 101, pp. 758-760.

[5] J. Pokorny, V.C. Smith, and M. Lutze, "Aging of the human lens", Applied Optics, 1987, Vol. 26, No.8, pp1437-1440.

[6] K. Sagawa and Y.Takahashi, "Spectral luminous efficiency as a function of age", J. Opt. Soc. Am. A, 2001, Vol. 18, No. 11, pp. 2659-2667.

[7] J.S. Werner, "Aging through the eyes of Monet", in *Color Vision*, Water de Gruyter, 1998, pp. 1-41.

[8] L. Mori, K. Kohmoto, J. Akiyama, K. Hijikata, and T. Azuma, "A psychophysical measurement of the perceived color change by the crystalline lens browning", J. Col. Sci. Assoc. Jpn., Vol. 7, No.3, pp. 11-18 (in Japanese).

Authors

Miyoshi Ayama and Noriyuki Suda
Department of Information and Systems Control Science,
Graduate School of Engineering, Utsunomiya University
7-1-2 Yoto, Utsunomiya 321-8585 Japan
Phone: +81-28-689-6263, e-mail nakatsue@is.utsunomiya-u.ac.jp

Kohei Narisada
Faculty of Psychology, Chukyo University
101-2 Yagoto honmachi, Showa-ku, Nagoya, 466-8666 Japan

Comparison of Response Speed to Color Stimuli between Elderly and Young Adults with and without Filters Simulating an Aged Human Lens

T. Suzuki, Q. Yi, S. Sakuragawa, H. Tamura and K. Okajima* **

Shizuoka Industrial Research Institute of Shizuoka Prefecture, 2078 Makigaya, Shizuoka-City, 421-1298, Japan
* Department of Applied Physics, National Defense Academy, 1-10-20 Hashirimizu, Yokosuka 239-8686, Japan
** Imaging Science and Engineering Laboratory, Tokyo Institute of Technology, 4259 Nagatsuda, Midori-ku, Yokohama 226-8503, Japan

ABSTRACT

In order to examine whether filters simulating an aging human lens are effective tools for evaluating the visibility of elderly adults, we conducted a visibility test in elderly and young subjects with and without filters simulating an aging human lens. In the test, we measured response speed for color stimuli on a CRT display. The results indicate that the response speeds of the elderly subjects are distinctly slower than those in the young for gray and blue stimuli with a gray color background. In addition, the results for the young subjects with the filters, showed that a similar tendency as those of the elderly subjects. It was shown that the filters for young adults can properly simulate the visibility of the elderly for color stimuli.

Keywords: color vision, aging vision, age-related change, visibility, simulation filter, crystalline lens

1 INTRODUCTION

The age-related change of crystalline lens in human ocular system produces a modification of the spectral characteristic of the light arriving at the retina of the elderly adults [1,2]. This decreases visibility depending on the color scheme perceived [3-6]. As one method of color scheme design for elderly adults, young adults evaluate elderly visibility by using filters that simulate an aging human lens [7]. The filters are produced based on the two-factor model [1,2]. Considering the actual status of products in use, it is important to evaluate the smooth processing of a series of operations consisting of looking, recognizing, and acting in order to improve product usability. Therefore, to confirm the effectiveness of the filters, it is necessary to examine the adaptability of the filters for changing response speed due to aging.

In the present study, we examined the response speed evaluation as indices of visibility. The response speeds among elderly adults, young adults, and young adults with filters simulating an aging human lens were compared.

2 METHOD

2.1 Filters Simulating an Aging Human Lens

The filters are designed to make the spectral transmittance of the crystalline of a 20-year-old adult equivalent to that of a 70-year-old adult [7]. Figure 1 shows the theoretical values and measured values of the spectral transmittance of the filters. In the experiment, the filters were attached to a regular spectacle frame and worn by young subjects as necessary.

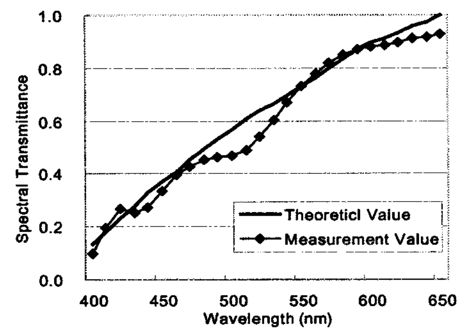

Figure 1. Spectral transmittance values of the filters. The theoretical value is based on the two-factor model and the measured value of a simulation filter.

2.2 Apparatus

Figure 2 shows the apparatus. A subject sat on a chair in an experiment room and observed the CRT display (SONY CPD-G520). The screen was placed 1 meter in front of the subject, and the screen was fitted with a hood to prevent invading projections. Stimuli were presented on the CRT display controlled by a computer. The subject held a push-button in his hand and responded by pressing the button when a target stimulus was presented. The responses and response times were recorded automatically. The experiment was carried out under the illumination of popular fluorescent lamps (Matsushita E.W. FLR40SWMX36). The horizontal illuminance of the lamps at the subjects' head level was approximately 500 lx.

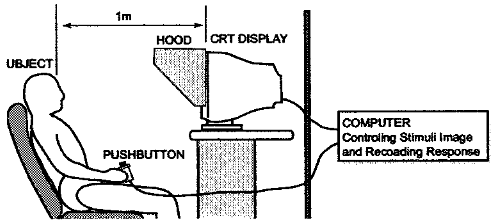

Figure 2. Apparatus Arrangement.

2.3 Subjects

All the subjects had normal color vision. Some of the subjects used vision correction devices (glasses or contact lenses) that they used in daily life. The numbers of subjects participating, their average age, and average visual acuities for 3 meters from their eyes are shown in Table 1.

Table I. Numbers, average ages, and average visual acuities (include use of vision correction device) of subjects.

			Visual Acuity	
	N	Age	Right	Left
Young Subjects	8	22.3	1.1	1.1
Elderly Subjects	8	65.9	0.7	0.7

2.4 Stimuli

Stimuli were Landolt-Cs and their colors were handled as test colors. The Landolt-C sizes were equivalent to a visual acuity of 0.1 at 1 meter from their eyes. The size figures on the screen had a height of 15 mm, thickness of 3 mm, and an opening width of 3 mm. There were 5 test colors: gray, red, yellow, green, and blue. The background color for the stimulus image was gray, and the stimuli (Table II) were as follows:

i) The luminance contrast values of the stimuli were nearly constant (approximately 0.05). The luminance contrast C was defined as $C = (L - L_b) / (L + L_b)$, where L and L_b represents the luminance value of a test color and the background.

ii) The color differences between the test colors and the background on the CIE1976UCS chromaticity diagram were nearly constant (approximately 0.65).

iii) A yellow color darker than the background color was chosen in order to reduce the effective luminance contrast by using filters that simulated the elderly adult luminance contrast on the retina through crystalline.

Table II. Luminance;L, contrast;C, chromaticity ;(u',v') and (x,y).

Color	L (cd/m^2)	C	CIE1976UCS u'	v'	CIE1931 x	y
Gray	6.616	0.050	0.178	0.481	0.298	0.358
Red	6.627	0.051	0.241	0.494	0.391	0.357
Yellow	5.392	-0.052	0.184	0.544	0.376	0.495
Green	6.647	0.052	0.142	0.529	0.291	0.482
Blue	6.647	0.052	0.173	0.420	0.246	0.266
Background	5.984		0.179	0.481	0.300	0.358

2.5 Procedure

Stimuli were randomly presented one after another on the CRT display. Subjects were asked to press the button in the way of odd ball task when a Landolt-C appeared with the instructed opening direction (target stimulus). The duration of the stimulus presentation was 800 ms and the presentation interval varied at random between 2200 ms and 2800 ms. There were 60 presentations including 15 of the target stimuli. Measurements were carried out for 5 kinds of test colors. The responses and response time were measured. These procedures were done for elderly and young subjects. In case of young subjects, they wore glass frames with filers and did not ware.

3 RESULTS AND DISSCUSSION

In order to evaluation the visibility of the stimuli, the response speed was calculated as reciprocal of the measured response time. When there was no response from the subject, the response speed was defined as 0 since the response time was infinite. Figure 3 shows the average values of the response speeds and the standard deviations for each test color. In order to investigate i) the differences of young subjects with and without filters, and ii) the differences by categories of the subjects (elderly, young with filters, and young without filters), the results of the response speeds were examined with the Wilcoxon signed-ranks test method.

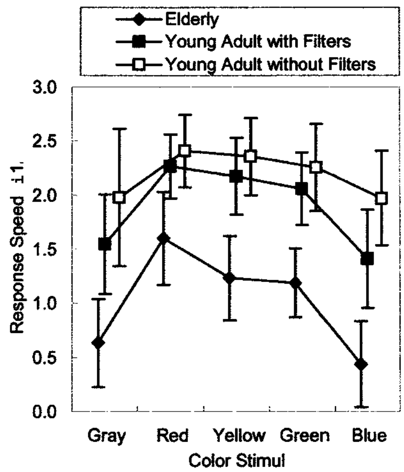

Figure 3. Response speed for color stimuli.

i) Change in response speed of young subjects with and without filters

Table III shows the p-values obtained by examining the difference of the response speeds of young subjects with and without filters for each test color. For blue, they indicate that the response speed with filters is significantly slower with than that without filters. ($p<0.027$)

Table III. Significance probability p on the response speed of young subjects with and without the filters: Smaller p values (p<0.05) are shown in italics.

Color	Gray	Red	Yellow	Green	Blue
p	0.115	0.248	0.345	0.345	*0.027*

ii) Change in response speed of subjects by categories for color stimuli

Table IV shows p-values obtained by examining the difference of the response speeds by categories of the subjects for color stimuli. The response speeds of the young subjects without filters (TABLE IV (a)) for gray and blue stimuli are slower than for red stimuli ($p<0.035$). The response speeds of the young subjects with filters (TABLE IV (b)) for gray and blue stimuli are slower than for red, yellow, and green stimuli ($p<0.036$). The response speeds of the elderly subjects for gray and blue stimuli are slower than for red, yellow, and green stimuli ($p<0.016$), showing the same tendency as the young subjects with filters. This means that the colors that make the response speeds of the young adults with filters slower are consistent with those of the elderly.

Table IV. Significance probability p on the response speed for difference of color stimuli: Smaller p values ($p<0.05$) are shown in italics.

(a) Young subjects without filters

	Gray	Red	Yellow	Green	Blue
Gray	-	-	-	-	-
Red	***0.035***	-	-	-	-
Yellow	0.074	0.674	-	-	-
Green	0.172	0.293	0.528	-	-
Blue	0.916	***0.015***	0.115	0.141	-

(b) Young subjects with filters

	Gray	Red	Yellow	Green	Blue
Gray	-	-	-	-	-
Red	***0.005***	-	-	-	-
Yellow	***0.027***	0.529	-	-	-
Green	***0.036***	0.172	0.600	-	-
Blue	0.529	***0.003***	***0.008***	***0.012***	-

(c) Elderly subjects

	Gray	Red	Yellow	Green	Blue
Gray					
Red	***0.002***				
Yellow	***0.009***	0.142			
Green	***0.016***	0.059	0.834		
Blue	0.248	***0.001***	***0.003***	***0.002***	

The reason for obtaining these results is that the effective luminance contrast of stimuli formed on the retinas of young and elderly subjects is equalized due to applying the filters designed to make the spectral transmittance of crystalline lens of 20-year-old adults equal to that of 70-year-old adults [3]. We can see that young subjects observing presented color stimuli through the filters have their visibility effected by the spectral transmitting characteristics of the filters, and the effective luminance contrast of the stimuli images varies by colors. In particularly, blue indicated the lowest effective luminance contrast because of the lower transmittance of the filter at shorter wavelengths. It suggests that the lowered effective luminance contrast on the retina caused difficulty in discriminating blue with a gray color background. On the other hand, the effective luminance contrast of the gray was not lowered significantly. It is suggested that the small color difference with the background made the response speed slower than for other colors.

Considering the actual application of the filters for evaluating the visibility of signs and devices for elderly adults that need to be judged and controlled in a limited time, it should be pointed out that these signs and devices are usually designed by young engineers and designers. Reviewing the results of the experiment, it is possible to make designing and development more efficient by easily and quantitatively using the estimated visibility (response speed) of elderly adults.

4 CONCLUSIONS

To confirm the effectiveness of the filters, we measured the response time for presented color Landolt-Cs of elderly adults, young adults with the filters simulating an aging human lens, and young adults without the filters. The response speeds of the elderly adults were slower than young adults without the filter, particularly with gray and blue with a gray color background. The responses speeds of the young adults, who were fitted with the filters for the color stimuli, showed a similar tendency to the responses of the elderly adults. The reason for these results is considered that the crystalline lens of elderly subjects reduces the transmittance of the short wavelength component of visible light due to aging and the effective luminance contrast of color stimuli on the retina and the background is decreased, and this in turn causes the decrease in visibility.

The filters that simulate the spectral transmittance of the crystalline lens of elderly adults indicated their significant effectiveness as a tool for evaluating the visibility of elderly adults. The filters particularly proved their simulating the visibility of elderly adults by qualitatively slowing the response speed according to the colors.

REFERENCES

1. J. Xu, J. Pokorny, V. C. Smith, Optical Density of the Human Lens. J. Opt. Soc. Am. 1997;A-14:953-960
2. J. Pokorny, V. C. Smith, M. Lutze, Aging of the Human Lens. Applied Optics 1987;26:1437-1440
3. K.Okajima, M.Takase, Computerized Simulation and Chromatic Adaptation Experiments Based on a Model of Aged Human Lens. Optical Review 2002; 8 No.1: 64-70.
4. R. A. Weale, Age and transmittance of the human crystalline lens. J of Physiology 1988;395:577-587
5. J. S. Werner, V. G. Steele, Sensitivity of Human Foveal Color Mechanisms Throughout the Life Span. J. Opt. Soc. Am. 1988:A-12:2122-2130
6. K.Okajima, N.Tsuchiya and K.Yamashita, Age-Related Changes in Color Appearance Depend on Unique-Hue Components. Proceedings of the 9th Congress of the International Colour Association (AIC Color 01): 2001:: 259-262
7. K. Okajima, M. Takase, Effect of Wearing Spectacles to Simulate the Aging of the Human lens in the Color Naming of Muncell Color Chips. J. Illum. Engng. Inst. Jpn. 2000:84-11:839-842 (in Japanese)

Color perception of a cataract left eye compared to his right eye with an interocular lens.

Mitsuo Ikeda*, Azusa Kusumi*, Tomoko Obama** and Hiroyuki Shinoda*
*Ritsumeikan University
**Panasonic Mobile Communications Co., Ltd.

ABSTRACT

Three experiments were conducted in one subject to compare the color perception of his cataract left eye and his right eye operated and implanted with an interocular lens. In Experiment 1 seventeen reference color charts were observed with the left cataract eye and the corresponding color charts that appeared same to the right operated eye were determined. It was found that most of the color charts appeared desaturated with the cataract eye. In Experiment 2 the region of a same color appearance on a hue sheet of the Book of JIS Colour Standards was determined with his right and left eye respectively. The region was smaller with the cataract eye than with the normal eye to imply desaturation and lowered lightness of color charts with the cataract eye. In Experiment 3 the heterochromatic brightness matching between a reference N8 and sixteen color charts was carried out with right and left eye respectively before and after the cataract operation. Luminance of the color charts had to be higher with the cataract eye implying less contribution of the color to brightness. All the three experiments indicated that the saturation of color charts decreased with the cataract eye. We interpreted the desaturation caused by the haze of crystalline lens which scattered incoming light from environment over the retinal image of color charts.

Keywords; cataract, color appearance, elderlies, brightness, color region

INTRODUCTION

Soon or later the eyes of elderlies become cataract, light or heavy, and experience different visual perception from and often inferior to their youth. It is important to know about the properties of their visual functioning such as the color perception so that the visual environment can be designed to suit them. There are two ways to know the properties. One is to derive the properties by statistically comparing data collected from many young people and elderlies[1)]. The other is to compare data from respective eyes of an elderly subject whose one eye is implanted with an IOL and the other eye is of cataract. The latter case became possible as one of the authors MI was operated for his cataract eyes, but with one month interval. During the interval three different color appearance experiments were conducted so that the data from his right eye with an IOL can be compared with the data from his left eye with cataract. He was 70 years old when operated. After the operation the visual acuity became 1.5 or better. His inherent color vision is normal.

EXPERIMENT 1

PAIR OF COLOR CHARTS OF SAME APPEARANCE

This is to find a pair of color charts that appear same to both eyes. Seventeen reference colors to be observed by the left cataract eye were chosen from the Book of JIS Colour Standards; 5R5/12、5YR7/14、5Y8/12、5GY7/10、5G6/10、5BG6/8、10B6/10、5P6/8, 5R5/6、5YR7/6、5Y8/6、5GY7/4、5G6/4、5BG6/4、10B6/4、5P6/4 and N6. Same two pages of the Book that included a reference color chart were placed side by side and a reference color chart was presented by masking all the color charts but the reference on the left side sheet. The subject observed it only by his left eye by covering his right eye by his left hand. Then he covered the left eye to observe the right hand sheet by his right eye. By moving a mask with an aperture by his right hand he searched for a color chart that appeared same in color appearance as the reference observed by his left eye a moment ago. He could observe two sheets in turn as many times as he wished until he finally decided the color chart on the right hand sheet. During these observations the left eye could see only the reference chart and the right eye could not see the reference chart but a color chart in the right sheet. All seventeen colors were investigated in one session and three such sessions were conducted.

The two color sheets were placed on a table in a normal room of which illuminance was adjustable. The room was decorated by interior decorations such as books, dolls, artificial flowers and so on to simulate a normal room. The subject sat down on a chair during the experiment. Two illuminance levels, 10 and 1000 lx, were employed.

The results are shown in Fig.1 for 10 lx at the left and 1000 lx at the right. The Munsell Hue is specified along the circumference and the Munsell Chroma along the radius, the outer edge corresponding to 14. Open circles represent the reference colors and the arrowheads the color charts that matched the reference colors in color appearance. Numbers attached to arrows show difference of the Munsell Value in the matched color charts by the left eye. For example, the reference color chart 5YR7/14 locating at the upper right appeared as 4.2YR6.6/11.3 when it was observed by the cataract left eye.

Let us first look at the results of 1000 lx. Most of arrows on the left side direct towards right and the highly saturated blue colors desaturate greatly. The fact of this desaturation agrees with the subject's experience after the eye operation that he was very much impressed by vivid blue objects. The arrows of colors at the extreme

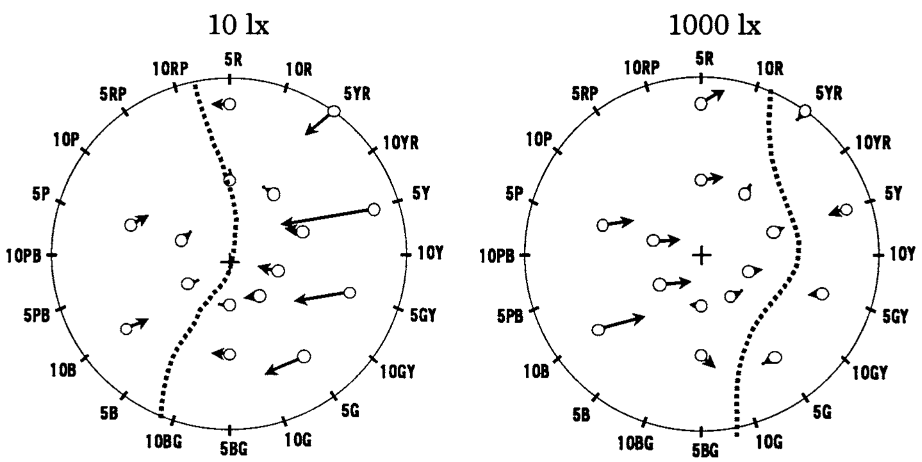

Fig.1 Change of color with the cataract eye.

right side direct towards left. They also desaturate in a sense, though a little. The dotted curve is drawn in regions where color appearance seems unchanged. The dotted curve shifts toward left when the room illuminance was low at 10 lx. At this dim surrounding it is yellow color that desaturates greatly.

EXPERIMENT 2
REGION OF A SAME COLOR CATEGORY

This is to investigate the region of a same color category on a hue sheet of the Book of JIS Colour Standards. The subject was asked to decide the extent in a sheet for a same color as that seen for the upper right color chips. The subject was not suggested any specific color name for the chips and had to decide himself the color for the chips. He traced by a stick on a sheet a boundary to include all chips that he thought to belong to the color that he decided. This was done by his operated right eye and by his cataract left eye, respectively. Eight sheets of different hues were investigated; 5R、5YR、5Y、5GY、5G、5BG、10B and 5P. The same room used for Experiment 1 was also used in this experiment. Three illuminance levels, 10, 80 and 1000 lx were employed. The 80 lx level was to represent illumination for a space in a residence where home electric machines such as a washing machine are normally used. Three sessions were conducted for each illuminance level.

Results are shown in Fig.2 for three hues 5YR, 5G and 10B and two illumination levels 10 and 1000 lx. Thick solid lines indicate borders drawn with the operated right eye and thick dotted lines borders with the cataract left eye. Each line is the average of three lines, but it is not a mathematical mean. Three lines of raw data were superposed and a line of the average was drawn by visual inspection to trace borders of color chips. The regions determined by the cataract eye is almost always smaller than those determined by the operated eye. The dark areas are the difference between the two.

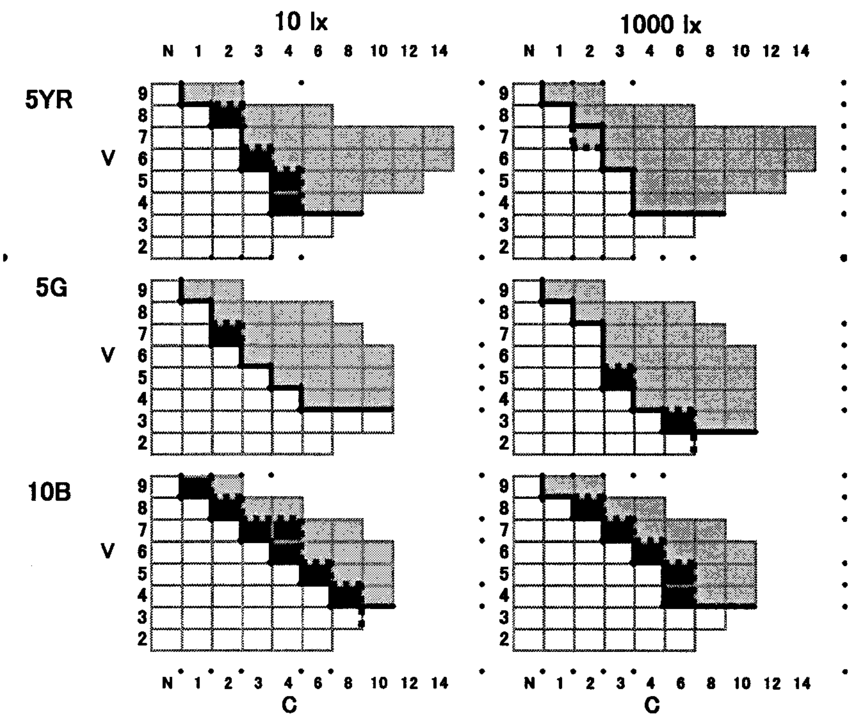

Fig.2 Region of a same color category with and without cataract.

For all the three levels of illumination the cataract eye chose much narrower regions, particularly for hues 10B and 5P, but the cause for the reduction seems different depending on illumination level. It was shown in Fig.1 that at 1000 lx the colors of those hues desaturate with the cataract eye, but at 10 lx their lightness goes down with the eye. The reduction of the same color regions at 1000 lx is because of the desaturation of colors with the cataract eye, while at 10 lx it is because of lowered lightness with the cataract eye. In case of 5YR the desaturation did not take place with the cataract eye at 1000 lx as shown in Fig.1 and the reduction did not occur in the same color region as seen in Fig.2. For this hue the reduction is observed at 10 lx and the cause is the desaturation of color as shown in Fig.1.

Colors are often used as code such as traffic signs. The present results suggest us that the saturation and lightness should be raised up by one or two steps in the Munsell notation even for weak cataract eyes when compared with normal young eyes.

EXPERIMENT 3
LUMINANCE FOR EQUI-BRIGHTNESS OF COLOR CHARTS

This is to investigate the luminance of color charts that appear same in brightness as a reference chart N8. Sixteen color charts, 10RP4/10、5RP4/10、10P4/10、5P4/10、10PB4/10、5PB4/10、5B4/9、10BG4/9、5BG4/9、10G5/10、10GY6/10、5GY6/9、10Y7/10、10YR6/10、5YR5/10 and 10R4/10 were employed. A different from the previous experiments but a similar and normal room was again used for the present experiment. The reference chart N8 of the size 22x22 mm was pasted on the front wall of the subject who observed it at the distance 170 cm. At the immediately right hand side of the reference an aperture with the same size was opened and behind it a test color chart was placed and illuminated independently from the subject's room. The illuminance was adjusted by the subject to change the luminance of the test chart. When the subject looked the aperture he felt as if the color chart was also pasted on the front wall.

The subject's task was to match the test color chart with the reference in brightness by adjusting the luminance of the test color chart. Both eyes were investigated respectively on different days before and after the cataract operation. Illuminance of 10 and 500 lx were employed for the subject room.

The results are shown in Fig.3 for 500 lx, left section for the left eye and right for the right eye. Test color charts are taken along the abscissa and luminance along the ordinate. Horizontal dotted lines indicate the luminance of the reference N8. Filled symbols are for the cataract eyes and open symbols for the operated eyes. Both curves

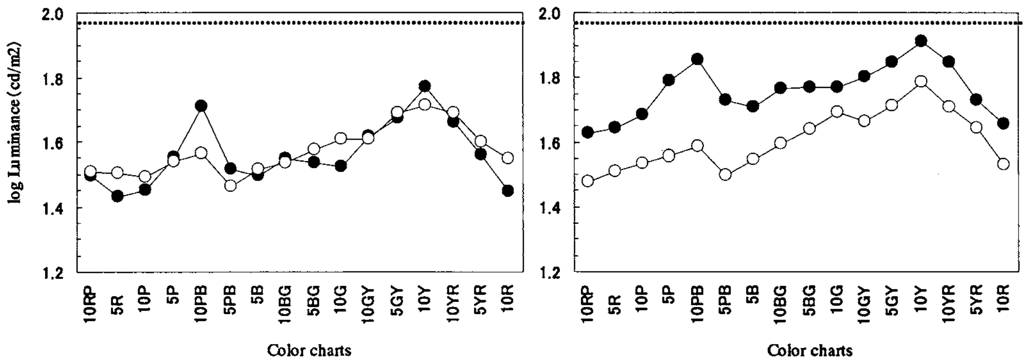

Fig.3 Luminance of test charts for the same brightness of N8.

of open circles locate much lower than the dotted lines to indicate color contribution to the brightness perception. Two curves almost perfectly overlap with each other to indicate a same functioning of both eyes with implanted IOL after operation. The curves with filled circles differ in vertical position. The curve of the left eye is almost identical with the curve after operation, but that of the right eye is much higher than the curve after operation coming closer to the dotted line. The subject noticed before the operation that his right eye suffered more from the cataract than from his left eye. The stronger cataract must be the cause for the elevation of the curve, or in other words the right cataract eye showed less contribution of color to the brightness perception. In our separate experiment where a cataract experiencing goggle was used with young subjects[2] we found that the environment light goes into the eye by being scattered by the haze filter and desaturates the color of test charts. We can interpret the elevation of the curve from the right cataract eye by less contribution of color to the brightness because of the desaturation by environment light.

DISCUSSION

The most distinct feature of the cataract eyes in perceiving color was the desaturation of the color and it occurred in any color if the cataract proceeded as in the right eye of the present subject. It is well known that the spectral transmittance of the crystalline lens declines at short wavelengths with age[3,4] and the much emphasize is given to the effect of the yellowed lens in the studies of the color perception of elderlies. From the present experiments we note that the emphasis also should be given to the effect of light scattering caused by the illuminated environment when the eyes get even a weak cataract. The effect of the environment illumination should be seriously considered for elderlies when we design daily living spaces for them.

REFERENCES

1) Data base is available at http://www.hql.or.jp/gpd/jpn/www/13web2000/2000top.htm
2) M. Ikeda and S. Ashizawa: Equivalent lightness of colored objects of equal Munsell Chroma and of equal Munsell Value at various illuminances. Col. Res. Appl. 16-2(1991)72-80.
3) J. Pokorny, V. C. Smith, and M. Lutze: Aging of the human lens, Appl. Opt. 26-8(1987)1437-1440.
4) K. Okajima and M. Takase: Computerized simulation and chromatic adaptation experiments based on a model of aged human lens, Opt. Rev. 8-1(2001)64-70.

*Correspondence; ro003974@se.ritsumei.ac.jp, Department of Photonics, Faculty of Science and Engineering, Ritsumeikan University, Nojihigashi, Kusatsu-shi, 525-8577 Japan

Author Index